STRESS ANALYSIS MANUAL

Air Force Flight Dynamics Laboratory
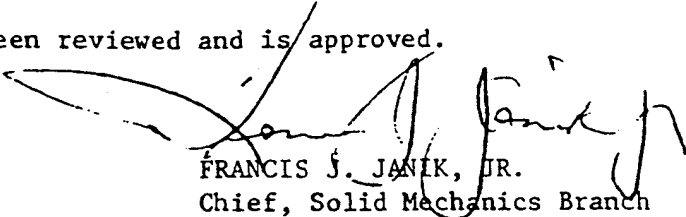Wright-Patterson AFB, OH

Oct 86
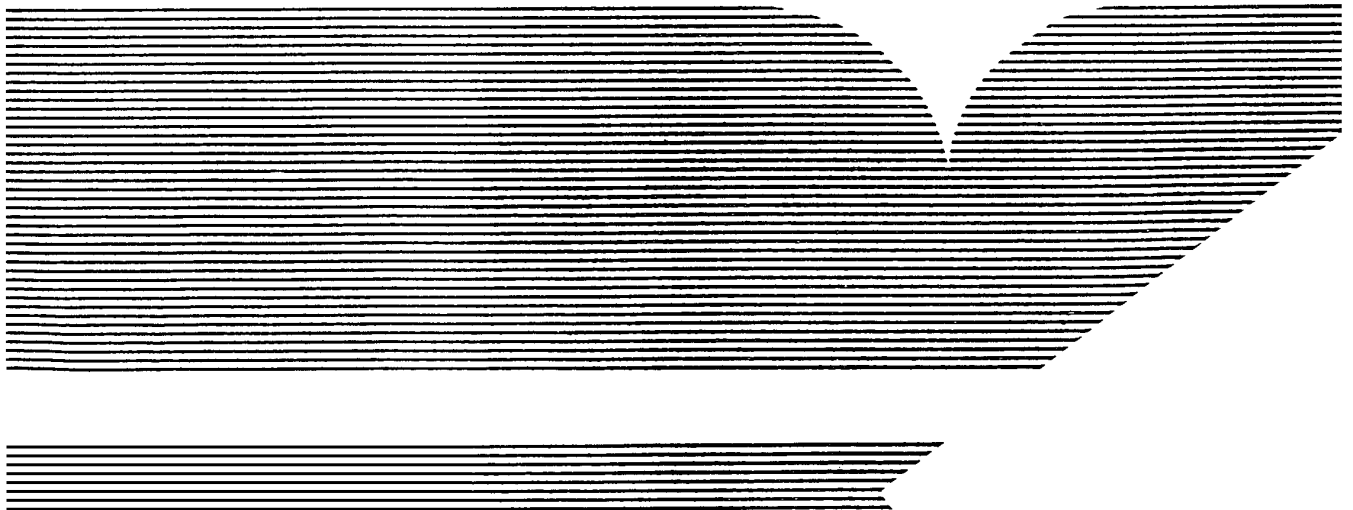
AFFDL-TR-69-42

FOREWORD

This report is the result of a combined in-house and contract effort. Under Project 1467, "Structural Analysis Methods" and Task 146702 "Thermoelastic Stress Analysis Methods" an in-house effort collected and categorized available analysis and design techniques. This collection was further reduced and through an automated search technique a comparison of approaches and references was made under Contract F33615-67-C-1538 which was initiated and sponsored by the USAF Flight Dynamics Laboratory. This contract with Technology Incorporated, Dayton, Ohio, covered the time period 30 April 1967 to 30 April 1969.

Mr. Gene E. Maddux, of the Flight Dynamics Laboratory, served as the Air Force contract monitor. For Technology Incorporated, Mr. Dudley C. Ward, manager of the Aeromechanics Department, was the project director; and Mr. Leon A. Vorst, senior research engineer, was the project engineer.

The authors are grateful for the assistance and the contributions of other Technology Incorporated personnel, particularly Mr. Robert R. Yeager, junior research engineer; Mr. Thomas J. Hogan, scientific programmer; and Mr. Harold P. Zimmerman, scientific programmer.

This technical report has been reviewed and is approved.

FRANCIS J. JANIK, JR.
Chief, Solid Mechanics Branch
Structures Division
Air Force Flight Dynamics Laboratory

TABLE OF CONTENTS

TABLE OF CONTENTS

KEYWORD INDEX

Introduction

This Keyword Index is based on the headings in Chapters 1 through 11. In the preparation of this index, first all significant words in these headings were extracted and arranged alphabetically. Words closely related such as "loads," "loading," and "load" were denoted by the single word "loading." The resultant significant words are presented on this page. Second all headings with significant words were grouped alphabetically under each significant word. The following pages present the grouped headings, each with its number identification, under the respective significant words.

INTRODUCTION

This introduction serves a threefold purpose: (1) it summarizes the eleven chapters making up this manual; (2) it references several publications which contain related information; and (3) it lists the nomenclature most commonly used in the chapters.

CHAPTER SUMMARIES

Chapter 1 - Beams

Section 1.3 of this chapter presents the method of analysis for simple, shear web, and partial-tension-field beams in bending, as well as methods of determining the reactions on statically indeterminate beams. Section 1.4 treats beam columns, and Section 1.5 covers beams in torsion including helical springs.

Chapter 2 - Column Analysis

Section 2.2 of this chapter treats primary bending and torsional failure as well as crippling failure of columns of uniform cross section. Stepped and tapered columns are treated in Section 2.3, and the material on beam columns is in Chapter 1.

Chapter 3 - Bar Analysis

This chapter treats bars in tension with emphasis upon the effect of stress raisers.

Chapter 4 - Trusses

Section 4.3 of Chapter 4 gives methods of determining the stresses and deflections of statically determinate trusses, and Section 4.4 treats statically indeterminate trusses.

Chapter 5 - Frames and Rings

This chapter gives a general treatment of frames composed of straight elements of uniform cross section, in addition to particular solutions for various simple frames and circular rings under several types of loadings.

Chapter 6 - Plates

Methods for determining the critical buckling stress of both flat and curved plates with and without stiffeners and having various loadings are given. Charts and curves covering most common loadings and supports facilitate analysis.

Chapter 7 - Membranes

Circular, square, and rectangular membranes under uniform pressure are treated in this chapter.

Chapter 8 - Pressure Vessels

Section 8.3 treats thin pressure vessels both with and without stiffeners. Stresses due to supports as well as membrane and discontinuity stresses are considered for thin pressure vessels without stiffeners. The analysis of thick pressure vessels is considered in Section 8.4, and glass fiber pressure vessels are briefly discussed in Section 8.5.

Chapter 9 - Lug Analysis

This chapter presents methods of analyzing lugs and their pins and bushings under various loading angles.

Chapter 10 - Shafts

The analysis of power transmission shafting is presented for circular shafts. Methods for treating discontinuities such as keyways, grooves, holes, and steps are given. A general design equation is presented to facilitate analysis.

Chapter 11 - Bearing Stresses

This chapter treats bearing stresses in riveted joints as well as those between elastic bodies of various shapes. Formulas are also given for the deformations of elastic bodies in contact.

REFERENCES

The following references are given to aid the reader in finding other treatments of the work contained in this manual. It is evident that a work of this nature owes a great deal to previous works. In particular, the editors wish to acknowledge the kind permission of the Frederick Ungar Publishing Company, 250 Park Avenue South, New York, N.Y. for the use of material from the volume "Handbook of Formulas for Stress and Strain" (1966) by William Griffel. Much of the data in Chapters 6 and 8 was derived from this handbook.

Abraham, Lewis H., Structural Design of Missiles and Spacecraft, McGraw-Hill Book Company, Inc., 1962.

Aluminum Company of America, Alcoa Aluminum Handbook, 1967.

Aluminum Company of America, Alcoa Structural Handbook, 1960

Becker, Herbert, Handbook of Structural Stability, Part II - Buckling of Composite Elements, NACA TN 3782, 1957.

Bruhn, E. F., Analysis and Design of Flight Vehicle Structures, Tri-State Offset Company, 1965.

Faires, Virgil M., Design of Machine Elements, Fourth Edition, The Macmillan Company, 1965.

Faupel, Joseph H., Engineering Design, John Wiley and Sons, Inc., 1964.

Gerard, George and Becker, Herbert, Handbook of Structural Stability, Part I - Buckling of Flat Plates, NACA TN 3781, 1957.

Gerard, George, Handbook of Structural Stability, Part IV - Failure of Plates and Composite Elements, NACA TN 3784, 1957.

Gerard, George, Handbook of Structural Stability, Part V - Compressive Strength of Flat Stiffened Panels, NACA TN 3785, 1957.

Griffel, William, Handbook of Formulas for Stress and Strain, Frederick Ungar Publishing Company, 1966.

Niles, Alfred S. and Newell, Joseph S., Airplane Structures, Third Edition, John Wiley and Sons, Inc., 1943.

Peery, David J., Aircraft Structures, McGraw-Hill Book Company, Inc., 1950.

Roark, Raymond J., Formulas for Stress and Strain, Fourth Edition, McGraw-Hill Book Company, 1965.

Seeley, Fred B., and Smith, James O., Advanced Mechanics of Materials, Second Edition, John Wiley and Sons, Inc., 1952.

Singer, Ferdinand L., Strength of Materials, Second Edition, Harper and Brothers, 1962.

Timoshenko, Stephen P., and Gere, James M., Theory of Elastic Stability, Second Edition, McGraw-Hill Book Company, Inc., 1961.

Timoshenko, S. and Goodier, J. N., Theory of Elasticity, Second Edition, McGraw-Hill Book Company, Inc., 1951.

Timoshenko, S., and MacCullough, Gleason H., Elements of Strength of Materials, Second Edition, D. Van Nostrand Company, Inc., 1940.

NOMENCLATURE

    The most commonly used nomenclature is presented here. Complete lists of nomenclature are available at the beginning of each chapter.

A	area
a	1/2 the major diameter of an ellipse
a	plate length
a	linear dimension as indicated in diagrams
a	subscript, allowable
all	subscript, allowable
ax	subscript, axial
B	ductility factor for lugs with less than 5% elongation
b	1/2 the minor diameter of an ellipse
b	plate width
b	linear dimension as indicated in diagrams
b	effective bearing width
b	subscript, bending
br	subscript, bearing
C	centroid
C	coefficient of constraint for columns
C	numerical constant
C_{BT}	torsion - bending coefficient
C_r	rivet factor
c	1/2 the minor diameter of an ellipse
c	distance from neutral axis to extreme fiber
c	linear dimension as indicated in diagrams
c	subscript, compression
cc	subscript, crippling
cr	subscript, critical
D	diameter
DF	distribution factor
d	mean diameter
d	linear dimension as indicated in diagrams
E	modulus of elasticity
E_r	reduced modulus
E_s	secant modulus
E_t	tangent modulus
e	eccentricity
e	strain
F	allowable stress
F_{acol}	allowable stress for concentrically loaded column
F_b	allowable bending stress
F_{br}	allowable bearing stress
F_{bru}	allowable ultimate bearing stress

F_{bry}	allowable yield bearing stress
F_c	allowable compressive stress
F_{cc}	allowable crippling stress
F_{col}	allowable column stress (upper limit of column stress for primary failure)
F_{cp}	proportional limit in compression
F_{cr}	critical stress
F_{cy}	compressive yield stress
F_s	allowable web shear stress
F_{scc}	crippling stress in shear
F_{scr}	critical buckling stress
F_{su}	allowable ultimate shear stress
F_{sy}	yield stress in shear
F_{ty}	yield stress in tension
FEM	fixed-end moment
FS	factor of safety
f	calculated stress
f_b	calculated bending stress
f_{br}	calculated bearing stress
f_c	calculated compressive stress
f_s	calculated shear stress
f_t	calculated tensile stress
G	modulus of elasticity in shear
H	horizontal reaction
h	height
hp	horsepower
I	moment of inertia
I_p	polar moment of inertia
i	subscript, inside
J	torsion constant
J	polar moment of inertia
K	a constant, generally empirical
k	radius of gyration
k	diagonal tension factor
k	a constant, generally empirical
L	length
L′	effective length
M	moment
M	empirical constant in straight line column equation
N	number of cycles
N	empirical constant in straight line column equation
n	number of elements
n	factor of safety
n	empirical constant
o	subscript, outside
P	applied concentrated load
P	axial load
P_a	allowable load

P_a	alternating load
P_{sc}	crippling load
P_{cr}	critical load
p	pressure or pressure difference
p	rivet spacing
$_p$	subscript, polar
$_p$	subscript, pressurized
Q	statical moment of a cross section
q	shear flow
q	notch sensitivity factor
R	reaction force
R	radius or radius of curvature
R	stress ratio - f/F
r	radius
r	cylindrical or polar coordinate
$_r$	subscript, radial
$_r$	subscript, ring
$_r$	subscript, rivet
S	tension force per inch on the edge of a membrane
s	distance measured along a curved path
$_s$	subscript, shear
$_s$	subscript, skin
$_{st}$	subscript, stringer
T	torque
T	tensile force
T	thickness of pressure vessel head
t	thickness
$_t$	subscript, tension
$_{tr}$	subscript, transverse
$_u$	subscript, ultimate
$_u$	subscript, upright
V	shear force
V	vertical reaction
V	velocity
W	applied concentrated load
W	total load
W	potential energy
w	applied distributed load
w	width
$_w$	subscript, web
X	force in redundant member of a truss
x	rectangular coordinate
y	rectangular coordinate
y	deflection
$_y$	subscript, yield
z	rectangular coordinate
α	empirical constant
α	angle

β	empirical constant
β	angle
Δ	increment or difference
δ	deflection
ϵ	strain
η	plasticity coefficient
θ	cylindrical coordinate
θ	angle or angular deflection
λ	empirical constant
λ	half wavelength of buckling
μ	Poisson's ratio
μ	torsional spring constant
μ_e	elastic Poisson's ratio
μ_p	plastic Poisson's ratio
ν	Poisson's ratio
ν_e	elastic Poisson's ratio
ν_p	plastic Poisson's ratio
ρ	radius of gyration
ρ	density
Σ	summation
φ	angle or angular deflection
ψ	angular deflection
Ω	empirical constant
ω	angular velocity

1. BEAMS

1.1 Introduction to the Analysis of Beams

Beams under various loadings are considered in this chapter. Section 1.3 treats beams in bending while beams under combined axial and transverse loads and beams in torsion are treated in Sections 1.4 and 1.5, respectively.

1.2 Nomenclature for the Analysis of Beams

A	=	cross-sectional area
A	=	area of moment diagram
A	=	constant of integration
A	=	width of the larger leg of an angle section
A_f	=	cross-sectional area of tension or compression flange
A_u	=	cross-sectional area of upright or stiffener
A_{ue}	=	effective cross-sectional area of upright or stiffener
a	=	1/2 the major diameter of an ellipse
a	=	linear dimension
a	=	$\int \frac{ds}{t}$
a	=	$\sqrt{EIy\,h^2/4\,GJ}$ for an I beam of depth h
$\bar{a}$	=	distance from the left end of a span to the centroid of its moment diagram
B	=	width of the smaller leg of an angle section
B	=	constant of integration
b	=	1/2 the minor diameter of an ellipse
b	=	width of section
b	=	developed length of thin section
b	=	linear dimension
b	=	subscript, bending
$\bar{b}$	=	distance from the right end of a span to the centroid of its moment diagram
C	=	centroid of moment diagram
C_1, C_2, C_3	=	stress concentration factors
C_r	=	rivet factor $\left(\frac{\text{rivet spacing - rivet diameter}}{\text{rivet spacing}}\right)$
c	=	distance from neutral axis to extreme fiber
c	=	linear dimension
c_f	=	distance from neutral axis of flange to the extreme fiber of flange
cr	=	subscript, critical
D	=	diameter
D_i	=	inside diameter
D_o	=	outside diameter
d	=	linear dimension
d	=	stiffener spacing

1 - 1

E = modulus of elasticity

e = distance from centroid of upright to web

e = subscript, effective

F_{cc} = allowable crippling stress of upright

F_{co} = column yield stress (allowable column stress at $L'/\rho = 0$)

F_{col} = allowable column stress

F_{max} = ultimate allowable compressive stress for natural crippling

F_o = ultimate allowable compressive stress for forced crippling

F_o' = reduced ultimate allowable compressive stress for forced crippling

F_s = allowable web shear stress

F_s' = reduced allowable web shear stress

F_{scoll} = collapsing shear stress for solid unstiffened webs

F_{scr} = critical (or initial) buckling stress

F_{st} = torsional modulus of rupture

F_{su} = ultimate stress in pure shear

F_{sy} = yield stress in pure shear

F_{tu} = ultimate tensile stress

f = subscript, flange

f_b = calculated primary bending stress

f_{cent} = calculated compressive stress at the centroidal axis of the upright

f_{cr} = calculated critical compressive stress

f_f = calculated stress in flange due to the horizontal component of diagonal tension in a partial tension field beam

f_s = calculated shear stress

f_{sb} = secondary bending moment in flange

f_u = calculated average compressive stress in upright

f_{umax} = calculated maximum compressive stress in upright

G = modulus of elasticity in shear

h = height or depth - height of shear web beam between centroids of flanges

I = moment of inertia

I_f = average moment of inertia of beam flanges

I_p = polar moment of inertia

I_s = required moment of inertia of upright or stiffener about its base

I_u = moment of inertia of upright or stiffener about its base

i = subscript, inside

J = torsion constant

K = a constant

k	=	diagonal tension factor
L	=	length
L'	=	effective length of beam
M	=	applied bending moment
M_{cr}	=	critical moment
M_{fp}	=	fully plastic bending moment
M_{sb}	=	secondary bending moment in flange
M_t	=	bending moment due to transverse loads alone
M_y	=	bending moment at the onset of yielding
m	=	coefficient given by Figure 1-8
n	=	number of active spring coils
n	=	constant given in Section 1.3.1.6
o	=	subscript, outside
P	=	applied concentrated load
P	=	axial load
P_u	=	upright end load
p	=	rivet spacing
p	=	pressure
Q	=	statical moment of cross section - $\int_{A_1} y\,dA$
q	=	shear flow
q'	=	beam shear at a distance of $2h/3$ from the beam end
q_r	=	shear load of web to flange rivets (lb/in.)
q_t	=	tension load on web to upright rivets (lb/in.)
q_t'	=	increased tension load on web to upright rivets (lb/in.
R	=	reaction
r	=	radius
r	=	subscript, rivet
r_i	=	inside radius
r_o	=	outside radius
S	=	tension force on edge of membrane (lb/in.)
s	=	distance measured along curved path
s	=	distance from centroidal axis to point of application of load
s	=	subscript, shear
T	=	torque
T_{max}	=	maximum allowable torque
t	=	thickness
t	=	subscript, tension
t_e	=	effective thickness
t_f	=	flange thickness
t_s	=	skin thickness
t_{st}	=	thickness of closed stiffener
t_u	=	upright thickness
t_w	=	web thickness
U	=	$L\sqrt{\dfrac{P}{EI}}$ for beam column

U	=	developed length of elongated section
u	=	subscript, ultimate
u	=	subscript, upright
V	=	shear force
W	=	concentrated transverse load
w	=	distributed transverse load
w	=	subscript, web
x, y, z	=	rectangular coordinates
y	=	deflection of beam due to bending
y	=	subscript, yield
α	=	angle of diagonal tension
α	=	coefficient given by Table 1-14
β	=	coefficient given by Table 1-14
δ	=	spring deflection
δ_s	=	portion of spring deflection due to direct shear
η	=	plasticity coefficient
ρ	=	radius of gyration
θ	=	slope of beam
Σ	=	summation

1.3 Introduction to Beams in Bending

For the purposes of discussion, beams in bending are divided here into simple beams (Section 1.3.1) and shear web beams (Section 1.3.2). Shear web beams are further subdivided into shear resistant beams and partial tension field beams. If a beam is statically indeterminate, Section 1.3.4 must be consulted in order to determine the reaction forces and moments. Otherwise, the equations of statics may be used to determine the reactions.

1.3.1 Simple Beams in Bending

Simple beams in elastic and plastic bending are treated in Sections 1.3.1.1 and 1.3.1.3, respectively, while the possibility of lateral instability of deep beams in bending is treated in Section 1.3.1.5.

1.3.1.1 Simple Beams in Elastic Bending

This section treats simple beams in bending for which the maximum stress remains in the elastic range.

The maximum bending stress in such a beam is given by the formula

$$f_b = \frac{Mc}{I} \tag{1-1}$$

while the shear flow is given by

$$q = \frac{VQ}{I} \tag{1-2}$$

where $Q = \int_{A_1} y\,dA$. The use of these equations is illustrated in Section 1.3.2.2.

The vertical and angular displacements of a simple beam in elastic bending are given by Equations (1-3) and (1-4), respectively, where A and B are constants of integration.

$$y = \iint \frac{M}{EI}\,dx^2 + Ax + B \tag{1-3}$$

$$\theta = \frac{dy}{dx} = \int \frac{M}{EI}\,dx + A \tag{1-4}$$

1.3.1.2 Sample Problem - Simple Beams in Elastic Bending

Given: The cantilever beam shown in Figure 1-1.

1 in. square aluminum bar
$I = 0.0833$

50 lb.

20
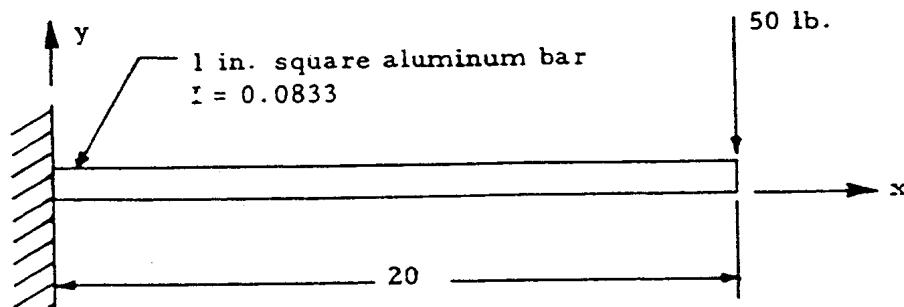
Figure 1-1. Cantilever Beam in Bending

Find: The maximum bending and shear stresses.

Solution: From the equations of statics, the shear and moment diagrams in Figure 1-2 may be obtained.

$V = 50$

$M = 50x - 1000$
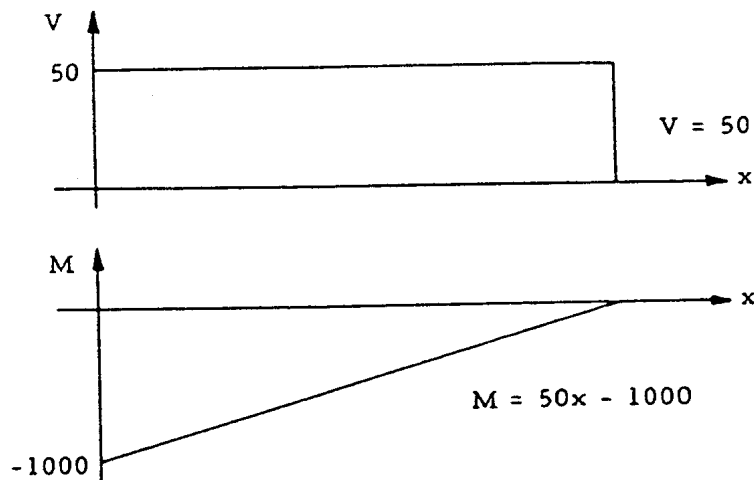
Figure 1-2. Shear and Moment Diagrams for the Beam in Figure 1-1

1 - 5

Since c and I are constant along the beam, the maximum bending stress occurs at the point of maximum bending moment; and from Equation (1-1),

$$f_b = \frac{Mc}{I} = \frac{-1000(0.5)}{0.0833} = 6,000 \text{ psi}$$

Q may be computed at a distance y_1 from the neutral axis by considering the beam cross section shown in Figure 1-3:

$$Q = \int_{A_1} y dA = \int_{y_1}^{1} y (1) dy = \frac{1}{2} - \frac{y_1^2}{2}$$

Q is maximum at $y_1 = 0$ where $Q = 1/2$. Thus, the maximum shear flow occurs at the neutral axis and is given by Equation (1-2) as

$$q = \frac{VQ}{I} = \frac{50(0.5)}{0.0833} = 300 \text{ lb/in.}$$

The maximum shear stress is thus,

$$\frac{300 \text{ lb/in.}}{1 \text{ in.}} = 300 \text{ lb/in.}^2$$
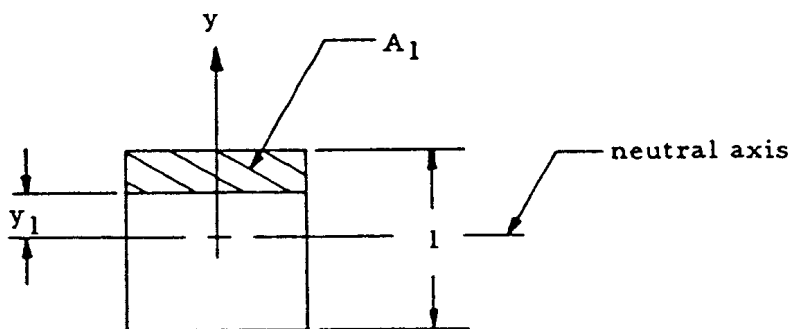
Figure 1-3. Cross Section of Beam
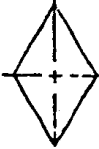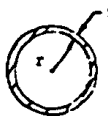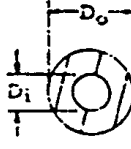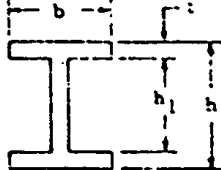
1.3.1.3 Simple Beams in Plastic Bending

In some cases, yielding of a beam in bending is permissible. If the beam material may be considered to be elastic-perfectly plastic, the bending moment at failure is given by

$$M_{fp} = k M_y \tag{1-5}$$

where M_{y1} is the moment that causes initial yielding of the extreme fibers and K is the shape factor given in Table 1-1.

1 - 6

Values of the Shape Factor, K

Section				thin walled		
K	1.0^*	1.5	2.0	1.70	$1.27\left(1-\dfrac{t}{r}\right)$	$\dfrac{32D_0(D_0^3-D_i^3)}{3\pi(D_0^4-D_i^4)}$	$\dfrac{3\pi}{2}\left(\dfrac{bh^2-2b_1h_1^2}{bh^3-2b_1h_1^3}\right)$

* All mass is assumed to be concentrated at the centroids of the flanges.

1.3.1.4 Sample Problem - Simple Beams in Plastic Bending

Given: The simply supported beam shown in Figure 1-4.

2 x 1 C1045 Annealed Steel Bar
F_y = 55,000 psi, I = 0.666 in.^{4}
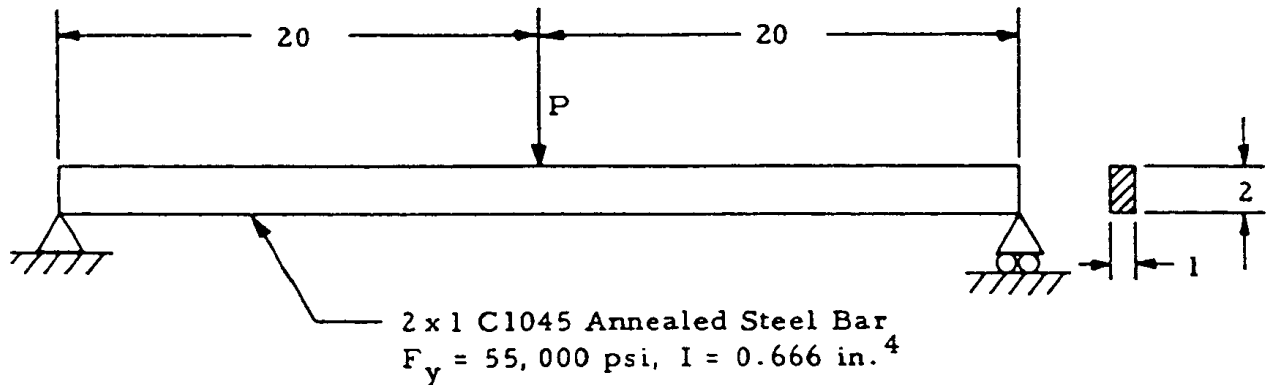
Figure 1-4. Simply Supported Beam in Bending

Find: The load, P, that causes fully plastic bending.

Solution: Rearranging Equation (1-1) and replacing the bending stress with the yield stress gives

$$M_y = \frac{F_yI}{c} = \frac{55000(0.666)}{1.0} = 36,600 \text{ in./lb.}$$

Inserting the value of K from Table 1-1 into Equation (1-5) gives

$$M_{fp} = K M_y = 1.5(36,600) = 54,900 \text{ in./lb.}$$

From statics, the maximum moment on the bar is 10P. Thus, for fully plastic bending,

$$P = \frac{M_{fp}}{10} = 5,490 \text{ lb.}$$

1.3.1.5   Introduction to Lateral Instability of Deep Beams in Bending

Beams in bending under certain conditions of loading and restraint can fail by lateral buckling in a manner similar to that of columns loaded in axial compression. However, it is conservative to obtain the buckling load by considering the compression side of the beam as a column since this approach neglects the torsional rigidity of the beam.

In general, the critical bending moment for the lateral instability of the deep beam, such as that shown in Figure 1-5, may be expressed as

$$M_{cr} \quad \frac{K\sqrt{EI_y\,GJ}}{L} \tag{1-6}$$

where J is the torsion constant of the beam and K is a constant dependent on the type of loading and end restraint. Thus, the critical compressive stress is given by

$$f_{cr} = \frac{M_{cr}\,c}{I_x} \tag{1-7}$$

where c is the distance from the centroidal axis to the extreme compression fibers. If this compressive stress falls in the plastic range, an equivalent slenderness ratio may be calculated as

$$\left(\frac{L'}{\rho}\right) = \pi\sqrt{\frac{E}{f_{cr}}} \tag{1-8}$$
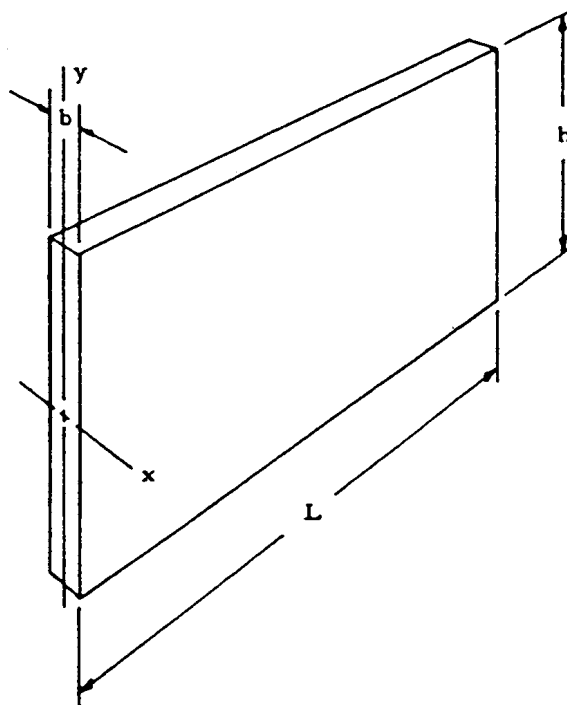
Figure 1-5.   Deep Rectangular Beam

The actual critical stress may then be found by entering the column curves of Chapter 2 at this value of (L'/ρ). This value of stress is not the true compressive stress in the beam, but is sufficiently accurate to permit its use as a design guide.

1.3.1.6 Lateral Instability of Deep Rectangular Beams in Bending

The critical moment for deep rectangular beams loaded in the elastic range loaded along the centroidal axis is given by

$$M_{cr} = 0.0985\, K_a E \left(\frac{b^3 h}{L} \right) \qquad (1-9)$$

where K_a is presented in Table 1-2, and b, h, and L are as shown in Figure 1-5. The critical stress for such a beam is

$$f_{cr} = K_f E \left(\frac{b^2}{Lh} \right) \qquad (1-10)$$

where K_a is presented in Table 1-2.

If the beam is not loaded along the centroidal axis, as shown in Figure 1-6, a corrected value K_f' is used in place of K_f in Equation (1-10). This factor is expressed as

$$K_f' = K_f\, (1-n) \left(\frac{s}{L} \right) \qquad (1-11)$$

where n is a constant defined below:

(1) For simply supported beams with a concentrated load at mid-span, $n = 2.84$.

(2) For cantilever beams with a concentrated end load, $n = 0.816$.

(3) For simply supported beams under a uniform load, $n = 2.52$.

(4) For cantilever beams under a uniform load, $n = 0.725$.

Note: s is negative if the point of application of the load is below the centroidal axis.
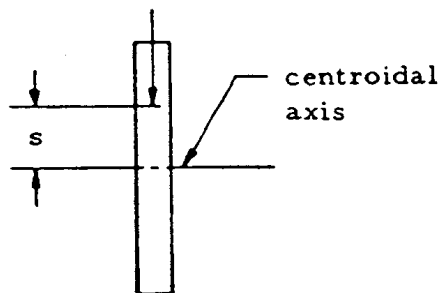
Figure 1-6. Deep Rectangular Beam Loaded at a Point Removed from the Centroidal Axis

TABLE 1-2

Constants for Determining the Lateral Stability of Deep Rectangular Beams in Bending
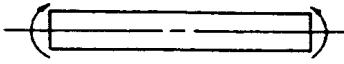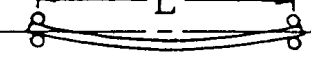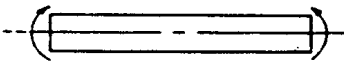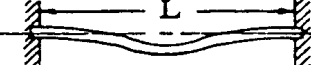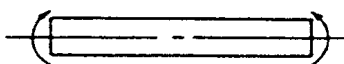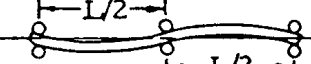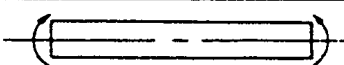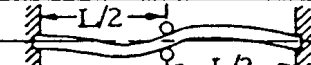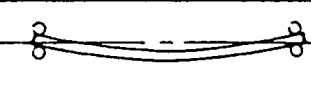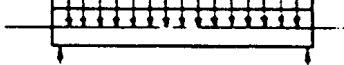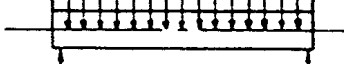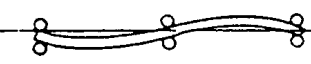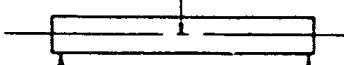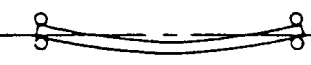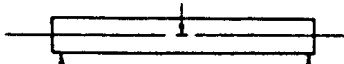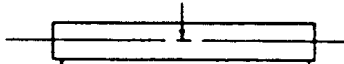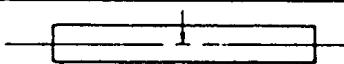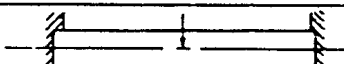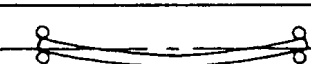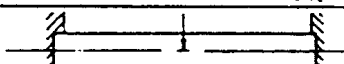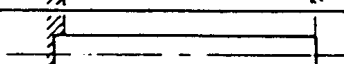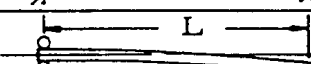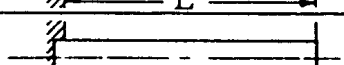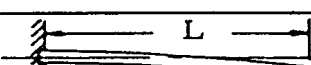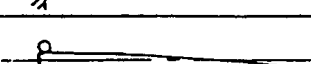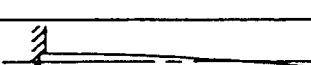
Case	Type of Loading and Constraint		K_f	K_m
	Side View	Top View		
1			1.86	3.14
2			3.71	6.28
3			3.71	6.28
4			5.45	9.22
5			2.09	3.54
6			3.61	6.10
7			4.87	8.24
8			2.50	4.235
9			3.82	6.47
10			6.57	11.12
11			7.74	13.1
12			3.13	5.29
13			3.48	5.88
14			2.37	4.01
15			2.37	4.01
16			3.80	6.43
17			3.80	6.43

TABLE 1-2

Constants for Determining the Lateral Stability of Deep Rectangular Beams in Bending (concluded)
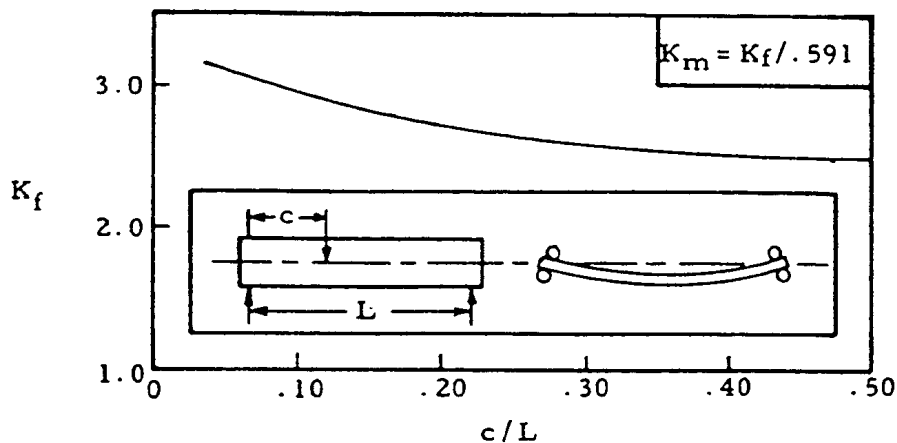
1.3.1.7   Lateral Instability of Deep I Beams

Figure 1-7 shows a deep I beam.
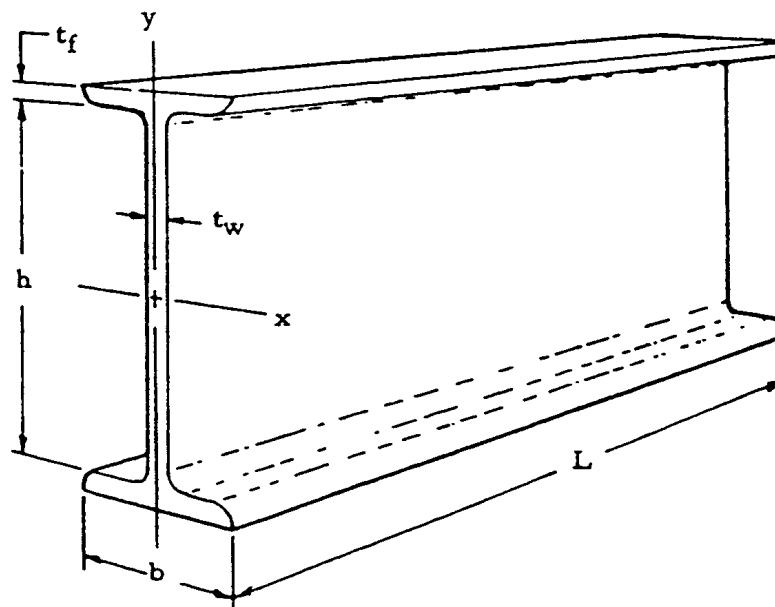
Figure 1-7.   Deep I Beam

The critical stress of such a beam in the elastic range is given by

$$f_{or} = K_I \left(\frac{L}{a} \right) \left(\frac{h}{L} \right)^2 \frac{I_y}{I_x} \qquad (1-12)$$

where K_I may be obtained from Table 1-3, and a is given by

$$a = \sqrt{EI_y h^2/4 \, GJ} \qquad (1-13)$$
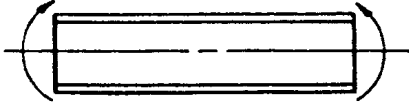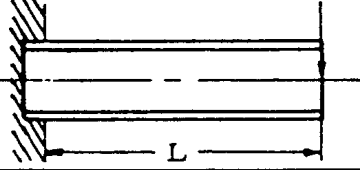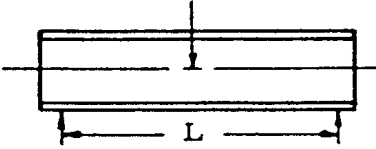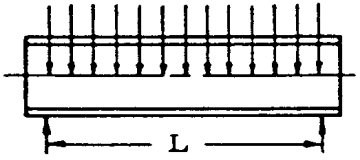
where J is the torsion constant of the I beam. This constant may be approximated by

$$J = 1/3 \left(2b \, t_f{}^3 + h \, t_w{}^3\right) \qquad (1\text{-}14)$$

This method can be applied only if the load is applied at the centroidal axis.

TABLE 1-3

Constants for Determining the Lateral Stability of I-Beams

Case	Type of Loading and Constraint		K_I *
	Side View	Top View	
1			$\dfrac{m_1}{4}(E)$
2			$\dfrac{m_2}{4}(E)$
3			$\dfrac{m_3}{16}(E)$
4			$\dfrac{m_4}{32}(E)$

* Use Figure 1-8 to obtain m
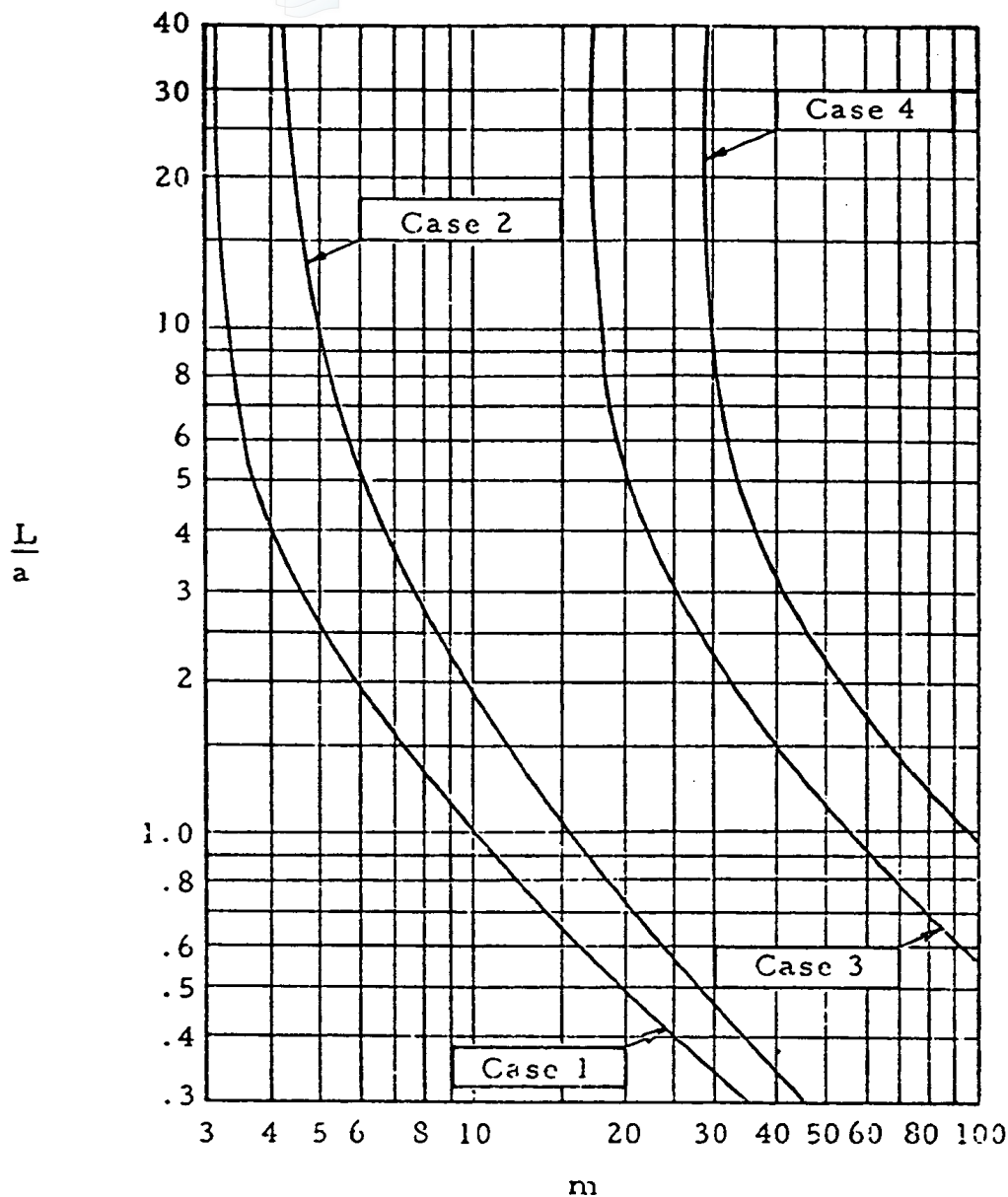
Figure 1-8.   Values of m for Table 1-3

1.3.2   Introduction to Shear Web Beams in Bending

The most efficient type of beam is one in which the material resist-
ing bending is concentrated as near the extreme fiber as possible and the
material resisting shear is a thin web connecting tension and compression
flanges.   The simplifying assumption that all the mass is concentrated at the
centroids of the flanges may be made for such beams, thus reducing the
simple beam formulas to $f_b = M/A_f h$ for bending and to $f_s = V/ht$ for shear.
The flanges resist all bending and the web resists all shear.

These beams are divided into two types, shear resistant and partial
tension field beams.   The webs of shear resistant beams resist the shear load

without buckling, and the webs of partial tension field beams buckle at less than the maximum beam load.

If $\sqrt{V}/h$ is less than seven, the use of a partial tension beam is recommended on the basis of weight economy; and the use of a shear resistant beam is recommended if $\sqrt{V}/h$ is greater than eleven. If $7 < \sqrt{V}/h < 11$, factors other than weight will determine the type of beam used.

1.3.2.1 Introduction to Shear Resistant Beams in Bending

If the web of a shear resistant beam is sufficiently thin, the simplifying assumption that all the mass is concentrated at the centroids of the flanges may be made. This reduces the simple beam formulas to

$$f_b = \frac{M}{A_f h} \tag{1-15}$$

for bending, and

$$f_s = \frac{V}{ht} = \frac{q}{t} \tag{1-16}$$

for shear. The flanges resist all of the bending and the webs resist all of the shear. Unstiffened shear resistant beams are discussed in Section 1.3.2.2 while stiffened shear resistant beams are treated in Section 1.3.2.3.

1.3.2.2 Unstiffened Shear Resistant Beams in Bending

Both the web and flanges of an unstiffened shear resistant beam must be checked for failure. The flange is generally considered to have failed if the bending stress in it exceeds the yield stress of the material, although bending in the plastic range may be used if some permanent set can be permitted.

The web must be checked for ultimate load as well as for collapse. If the web is not subject to collapse, the allowable average stress at ultimate load, F_s, will be either 85% of the ultimate strength in shear or 125% of the yield strength in shear. Figure 1-9 gives the collapsing stress for two aluminum alloys. It should be noted that for thinner webs ($h/t > 60$), initial buckling does not cause collapse.

In conclusion, the required thickness of a thin unstiffened web is given by

$$t = \frac{V}{hF_s} \tag{1-17}$$

or

$$t = \frac{V}{hF_{scoll}} \tag{1-18}$$

whichever is larger.
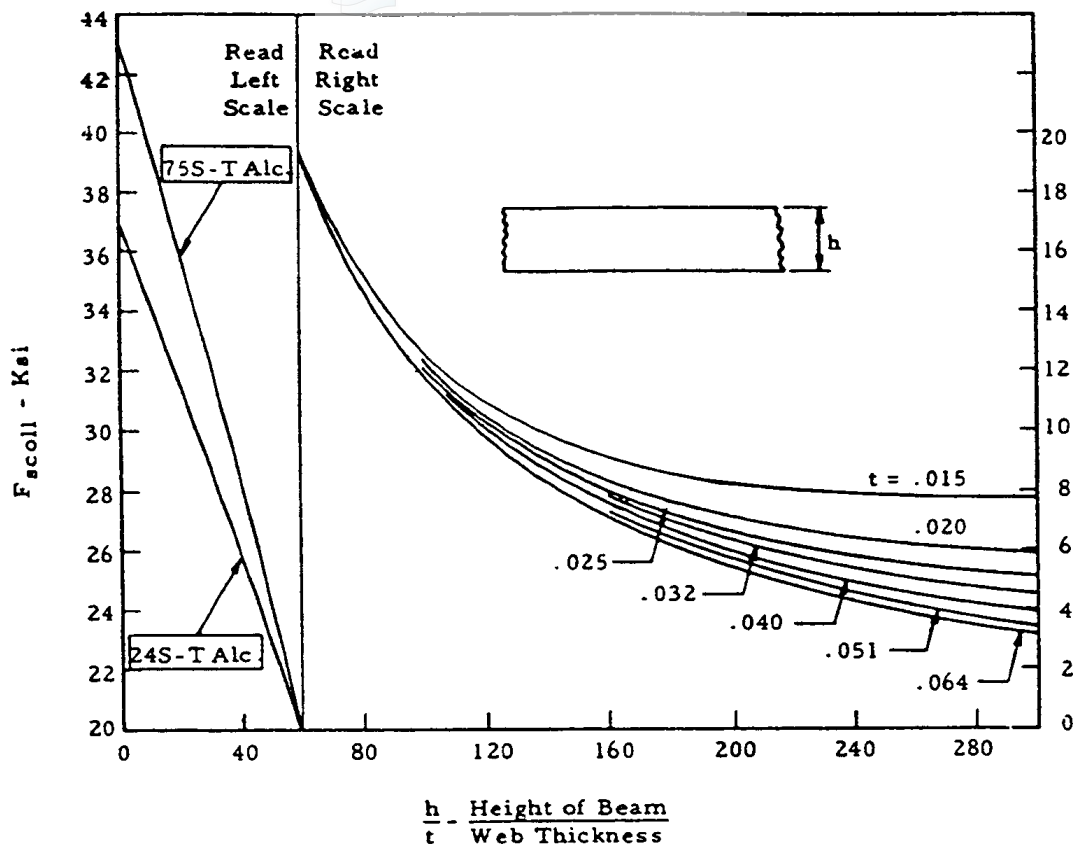
Figure 1-9.   Collapsing Shear Stress, F_{scoll}, for Solid Webs of 24S-T and 75S-T Alclad Sheet

1.3.2.3   Stiffened Shear Resistant Beams in Bending

The vertical stiffeners in a shear resistant beam resist no compressive load, as is the case for tension field beams, but only divide the web into smaller unsupported rectangles, thus increasing the web buckling stress. The flange web and rivets of such a beam must be analyzed.

1.3.2.4   Flanges of Stiffened Shear Resistant Beams

The flanges of a stiffened shear-resistant beam must be checked for yielding or ultimate strength by means of Equation (1-15) as in the case of unstiffened shear resistant beams.

1.3.2.5   Webs of Stiffened Shear Resistant Beams

The web panel of a stiffened shear-resistant beam must be checked for strength as well as for stability.

The strength of such a web may be checked by Equation (1-16) as in the case of unstiffened shear resistant beams, and the stability of such a beam may be checked by Equation (1-19) in conjunction with Figures 1-10 through 1-16.
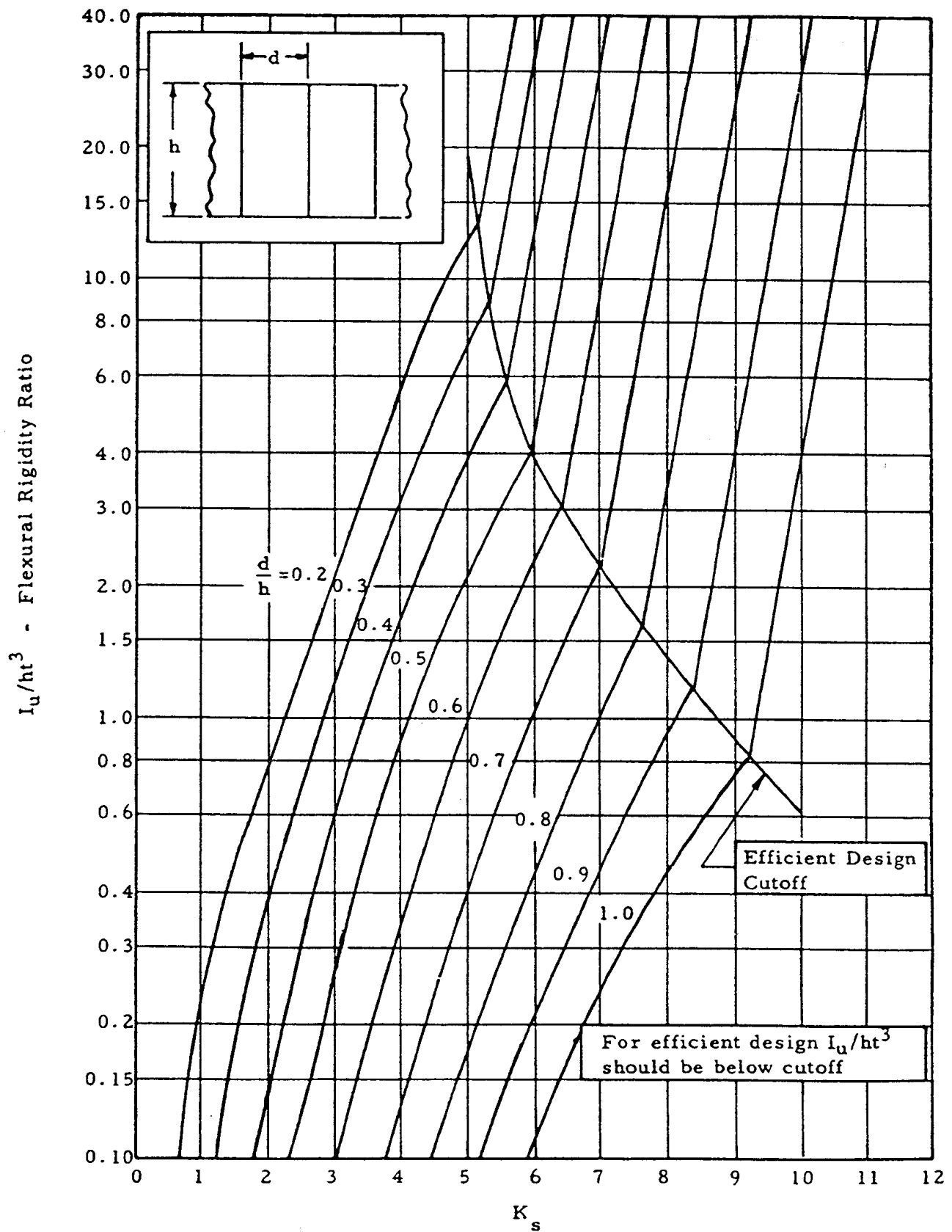
Figure 1-10. Critical Shear Stress Coefficient, K_s

$$\frac{F_{scr}}{\eta} = K_s E \left(\frac{t}{d}\right)^2$$

SAMPLE PROBLEM 1.3.2.7

$K_s = 6.9$

$t = 081$ in.

$E = 10 \times 10^6$ psi

$d = 6$ in.

$$\frac{F_{scr}}{\eta} = 12,500 \text{ psi}$$
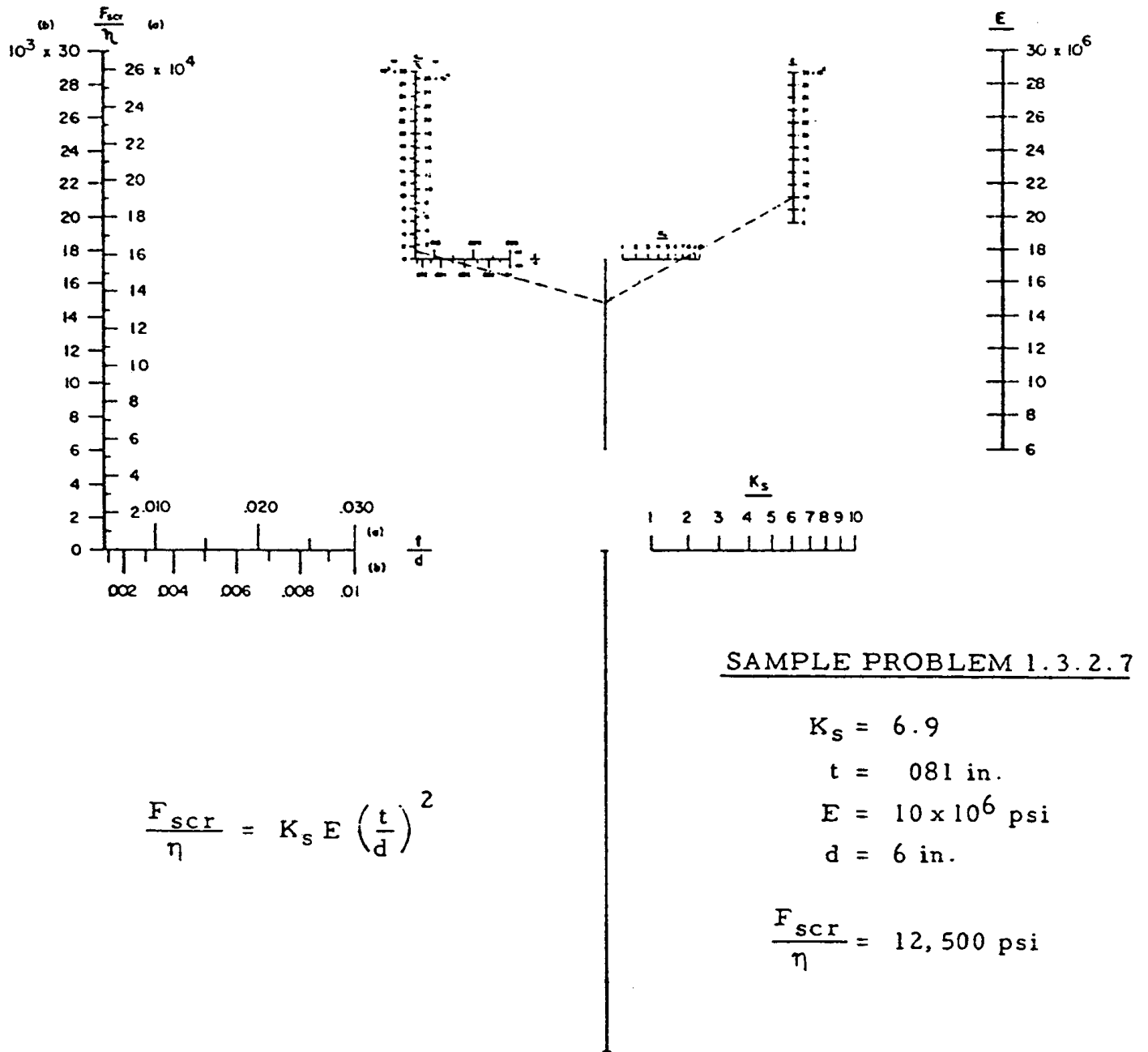
Figure 1-11. Nomograph for Critical Buckling Stress (Equation 1-19)
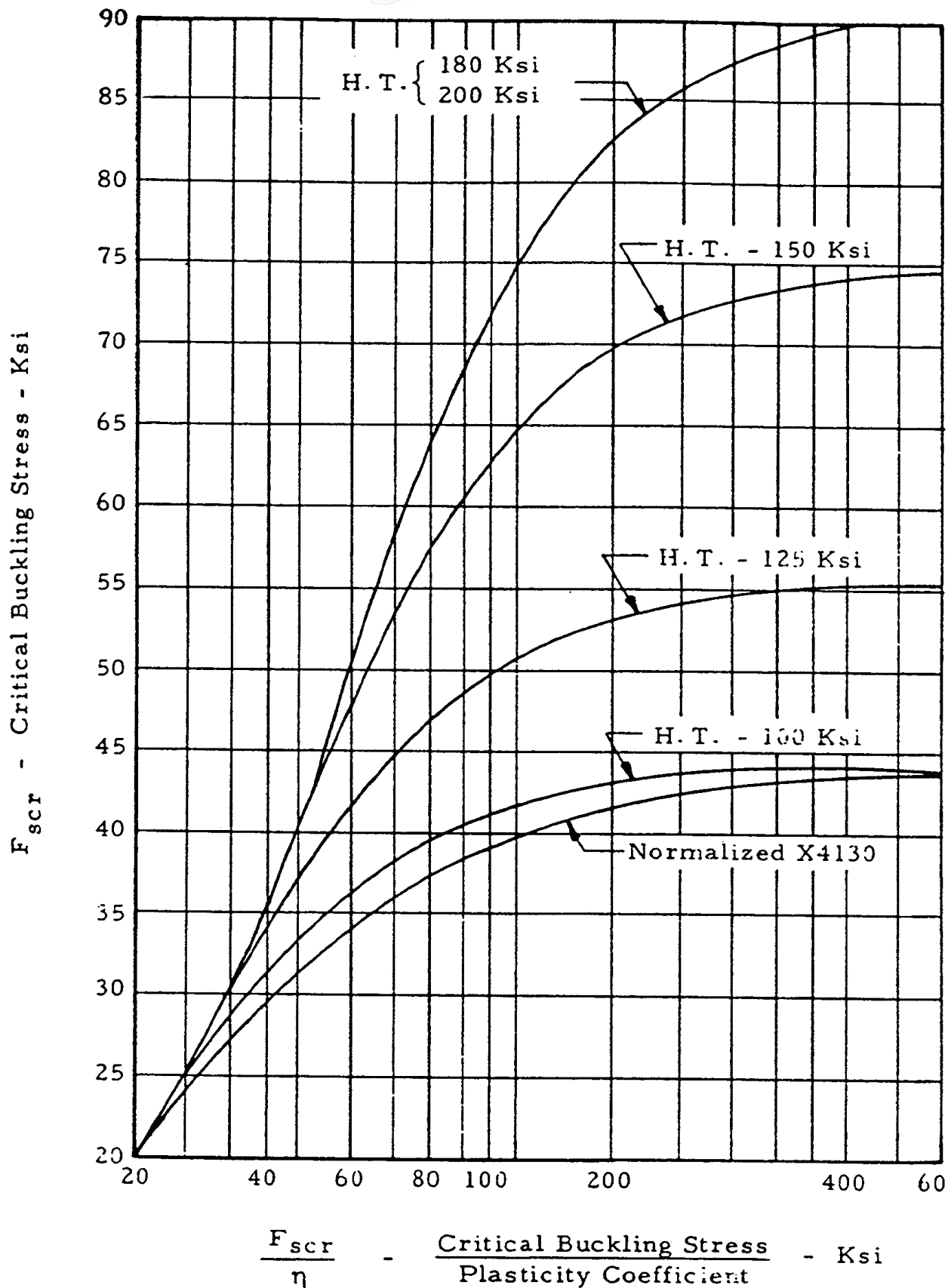
Figure 1-12. F_{scr} versus F_{scr}/η for Alloy Steel

$$\frac{F_{scr}}{\eta} - \frac{\text{Critical Buckling Stress}}{\text{Plasticity Coefficient}} - Ksi$$

1 - 18

$$\frac{F_{scr}}{\eta} - \frac{\text{Critical Buckling Stress}}{\text{Plasticity Coefficient}} - \text{Ksi}$$
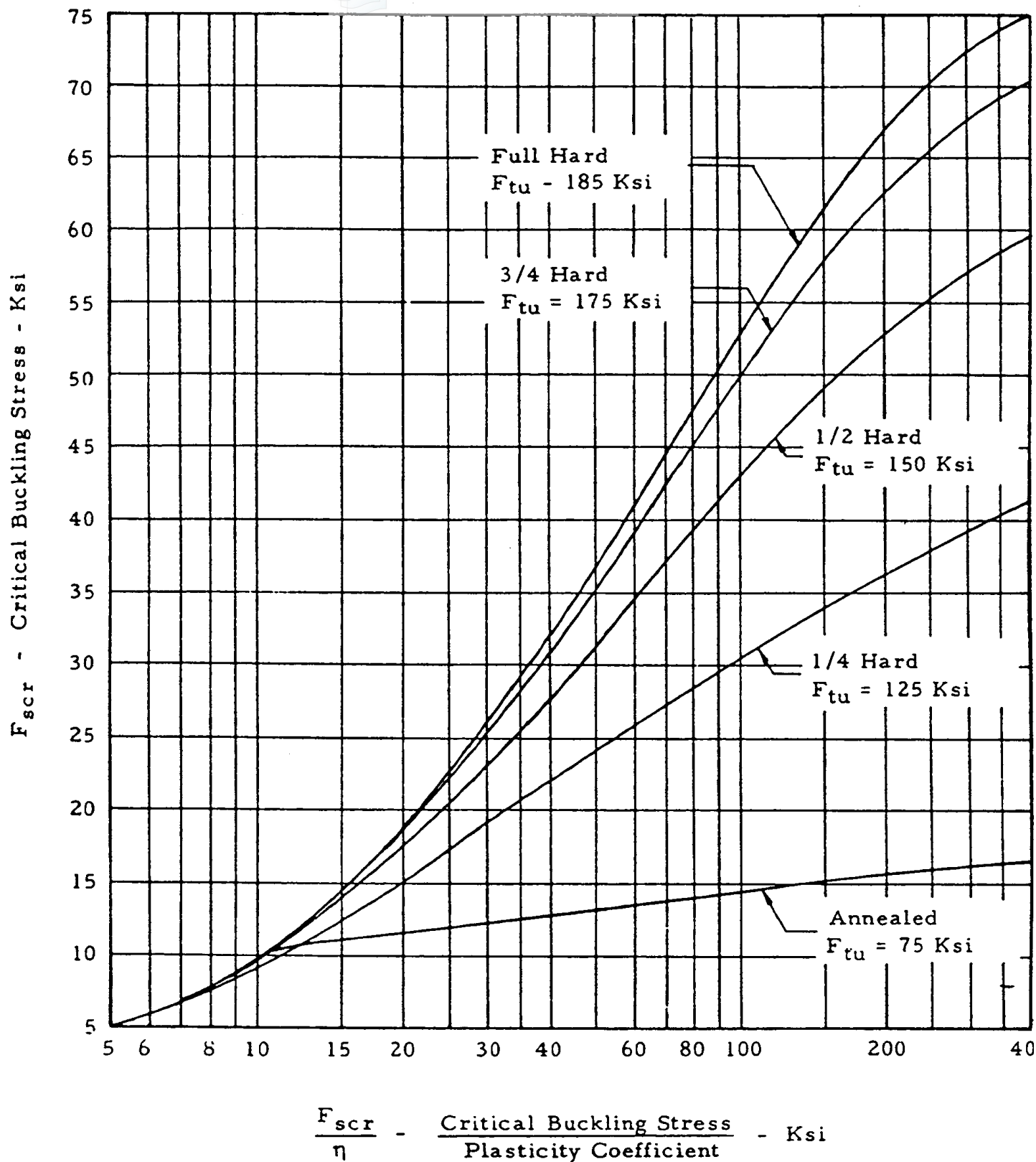
Figure 1-13 F_{scr} versus F_{scr}/η for Stainless Steel
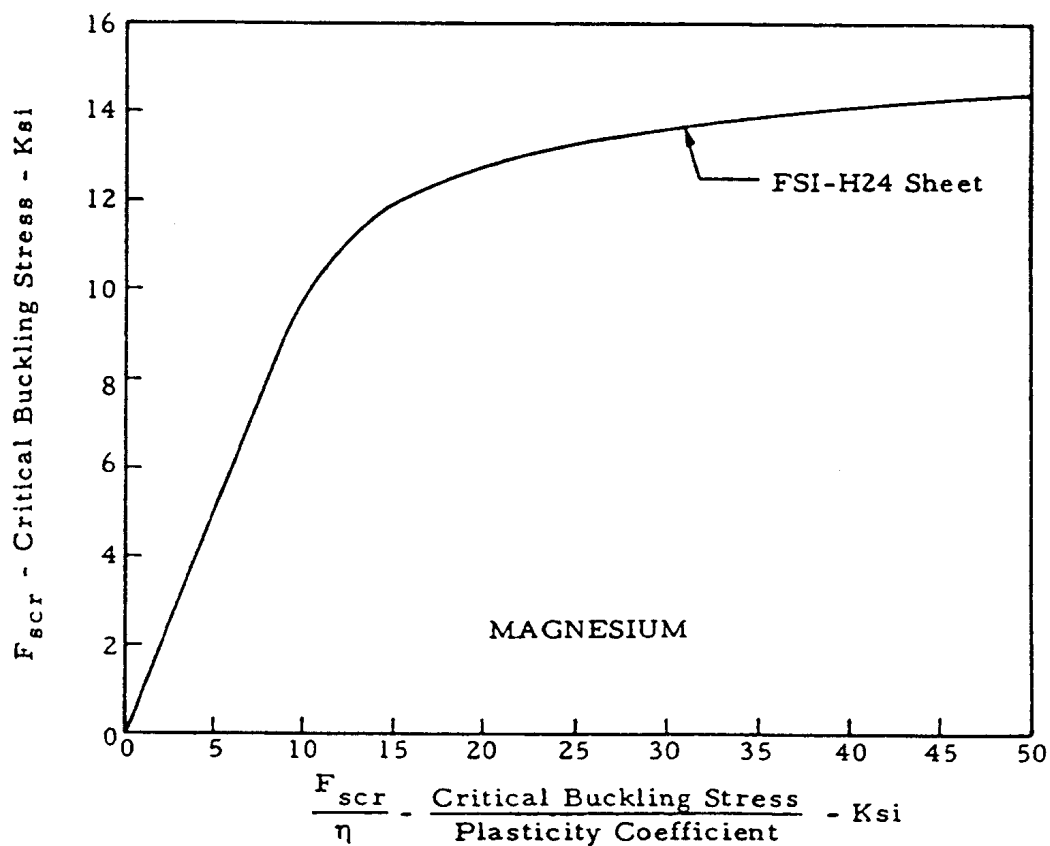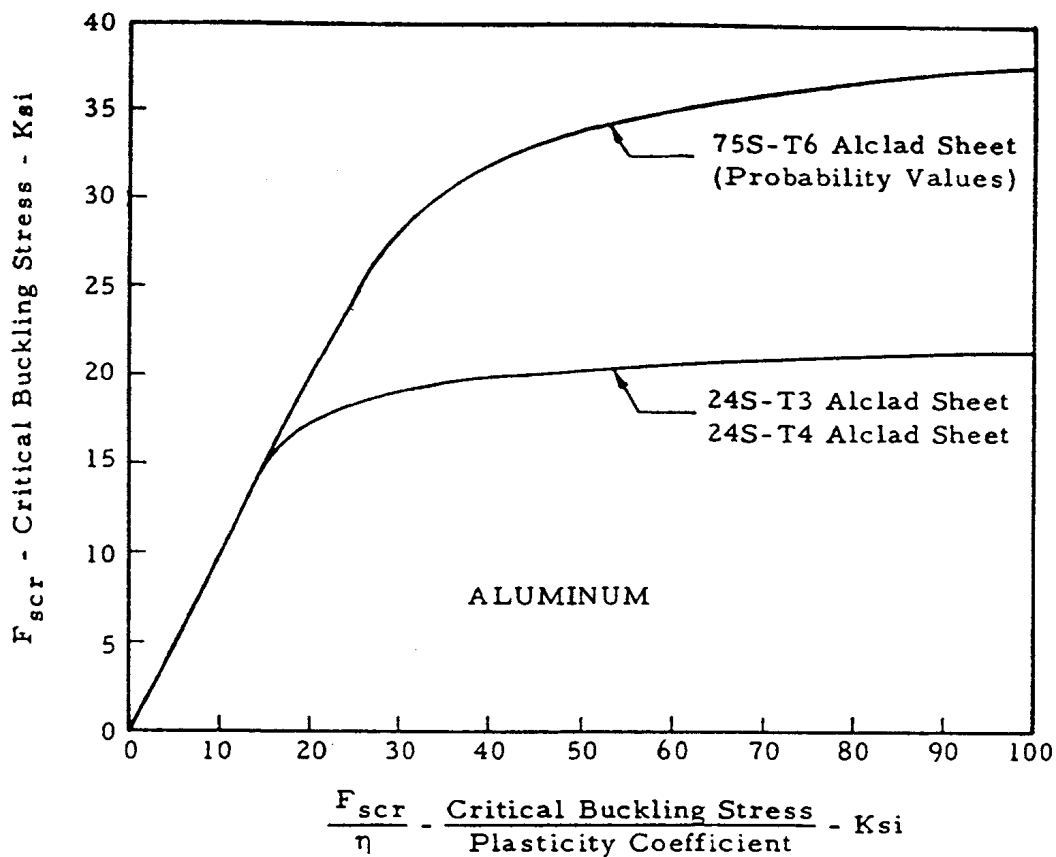
Figure 1-14. F_{scr} versus F_{scr}/η for Aluminum and Magnesium

$$\frac{F_{scr}}{\eta} - \frac{\text{Critical Buckling Stress}}{\text{Plasticity Coefficient}} - \text{Ksi}$$
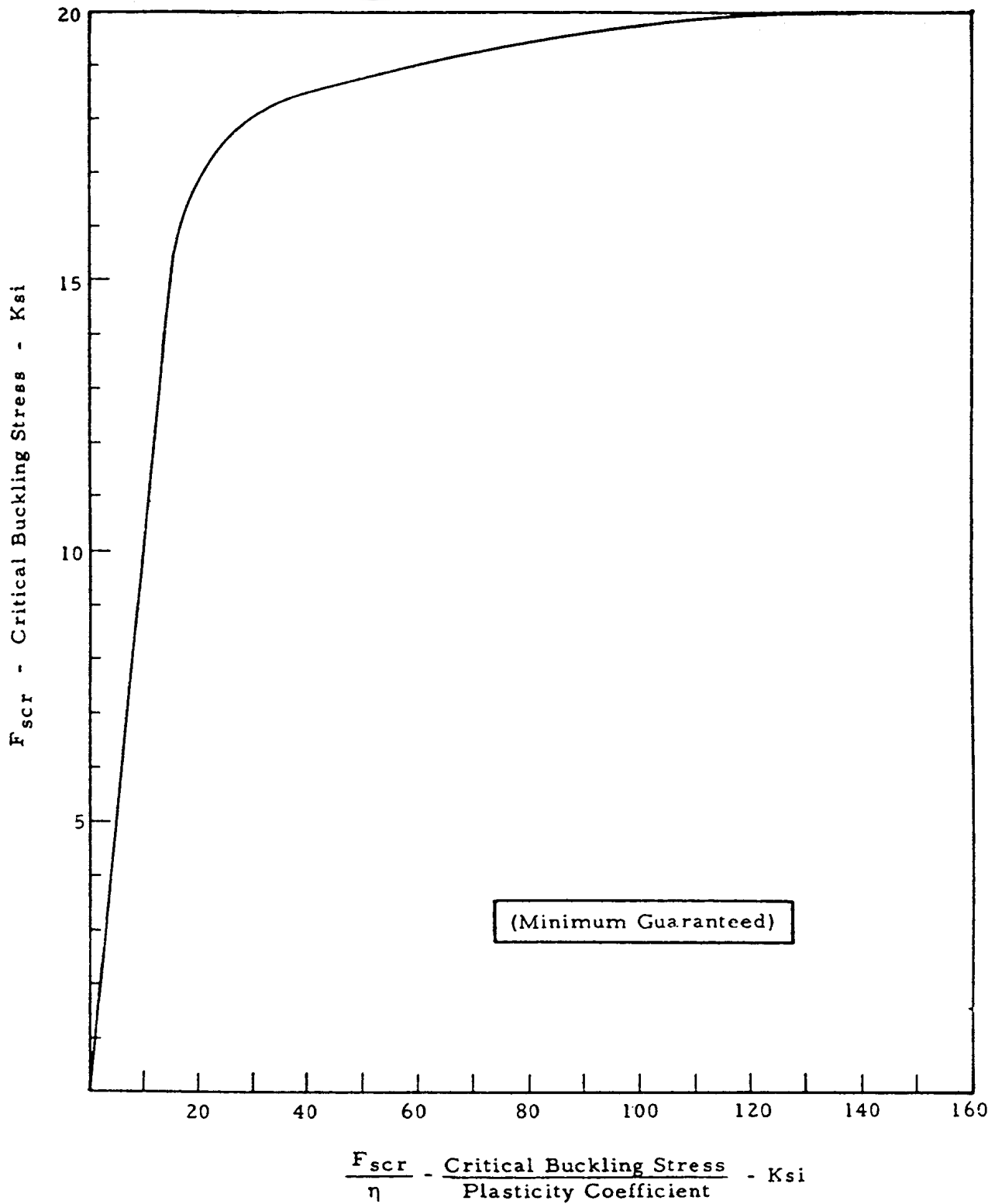
Figure 1-15. F_{scr} versus F_{scr}/η for 6061-T6 Sheet and Plate
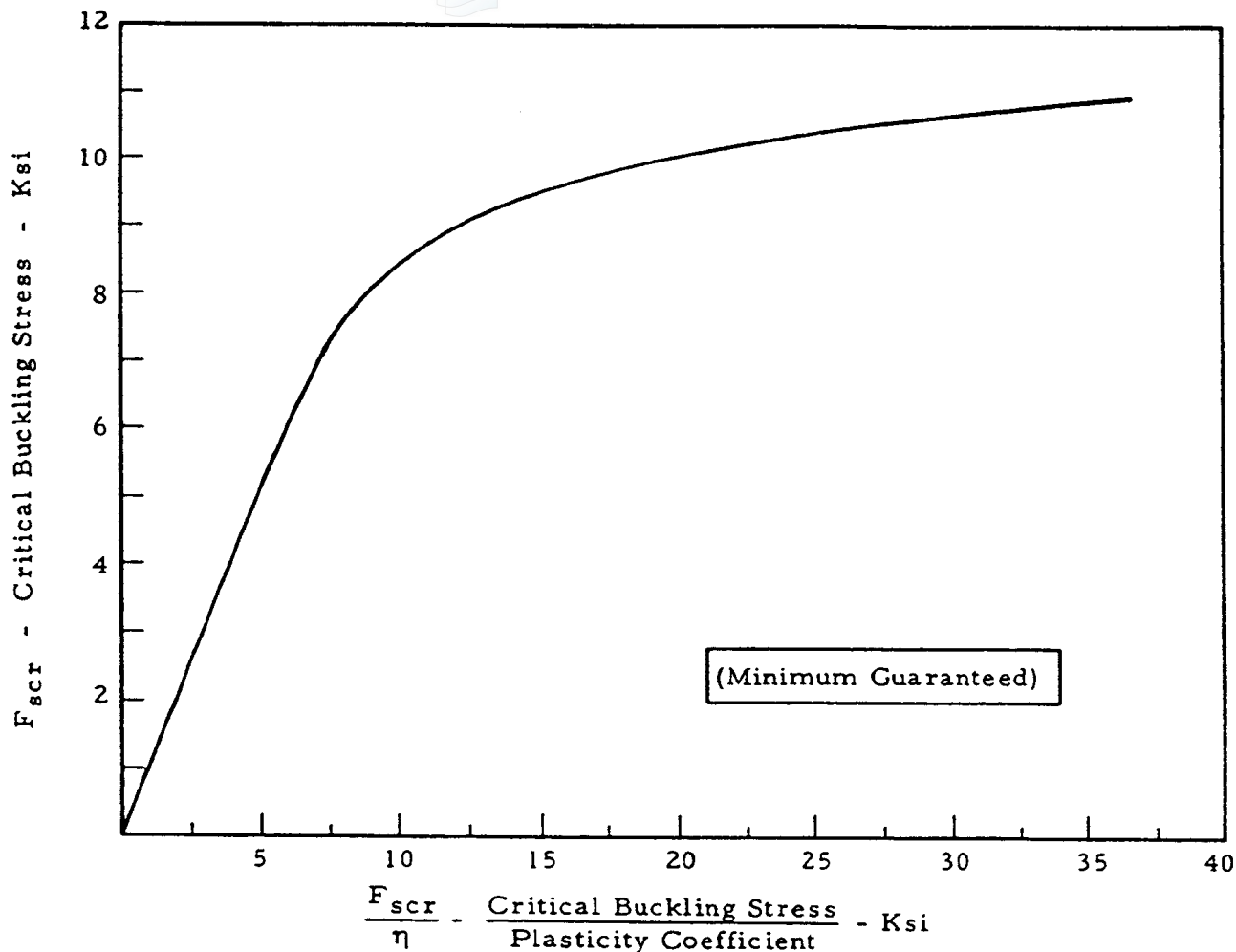
Figure 1-16. F_{scr} versus F_{scr}/η for 356-T6 Sand Casting

The critical buckling stress of a web panel of height h, width d, and thickness t, is given by

$$\frac{F_{scr}}{\eta} = K_s E \left(\frac{t}{d} \right)^2 \qquad (1-19)$$

In this equation, K_s is a function of d/h and the edge restraint of the web panel. Figure 1-10 relates K_s to d/h and I_u/ht^3. Once K_s has been found, F_{scr}/η may be obtained from the nomogram in Figure 1-11. F_{scr} may then be found from Figures 1-12 through 1-16. It should be noted that the moment of inertia of the stiffener, I_u, for Figure 1-10 should be calculated about the base of the stiffener (where the stiffener connects to the web). Also, the modulus of elasticity of the web has been assumed to be equal to that of the stiffeners.

1.3.2.6   Rivets in Shear Resistant Beams

Rivets are required to fasten the web to flange in shear resistant beams. In addition, rivets are used to fasten the web to the stiffener and the stiffeners to the flange in stiffened shear resistant beams.

1.3.2.6.1   Web-to-Flange Rivets in Shear Resistant Beams

The spacing and size of web-to-flange rivets should be such that the rivet allowable (bearing or shear) divided by q x p (the applied web shear flow times the rivet spacing) gives the proper margin of safety. The rivet factor, C_r (rivet spacing - rivet diameter/rivet spacing), should not be less than 0.6 for good design and in order to avoid undue stress concentration.

1.3.2.6.2   Web-to-Stiffener Rivets in Shear Resistant Beams

No exact information is available on the strength required of the attachment of stiffeners to web in shear resistant beams. The data in Table 1-4 is recommended.

TABLE 1-4

Recommended Data for Web-to-Stiffener Rivets
in Shear Resistant Beams

Web Thickness, in.	Rivet Size	Rivet Spacing, in.
.025	AD 3	1.00
.032	AD 4	1.25
.040	AD 4	1.10
.051	AD 4	1.00
.064	AD 4	.90
.072	AD 5	1.10
.081	AD 5	1.00
.091	AD 5	.90
.102	DD 6	1.10
.125	DD 6	1.00
.156	DD 6	.90
.188	DD 8	1.00

1.3.2.6.3   Stiffener-to-Flange Rivets in Shear Resistant Beams

No information is available on the strength required of the attachment of the stiffeners to flange. It is recommended that one rivet the next size larger than that used in the attachment of stiffeners to web or two rivets the same size be used whenever possible.

1.3.2.7   Sample Problem - Stiffened Shear Resistant Beams

Given: The beam shown in Figure 1-17 made of 75S-T6 Alclad.
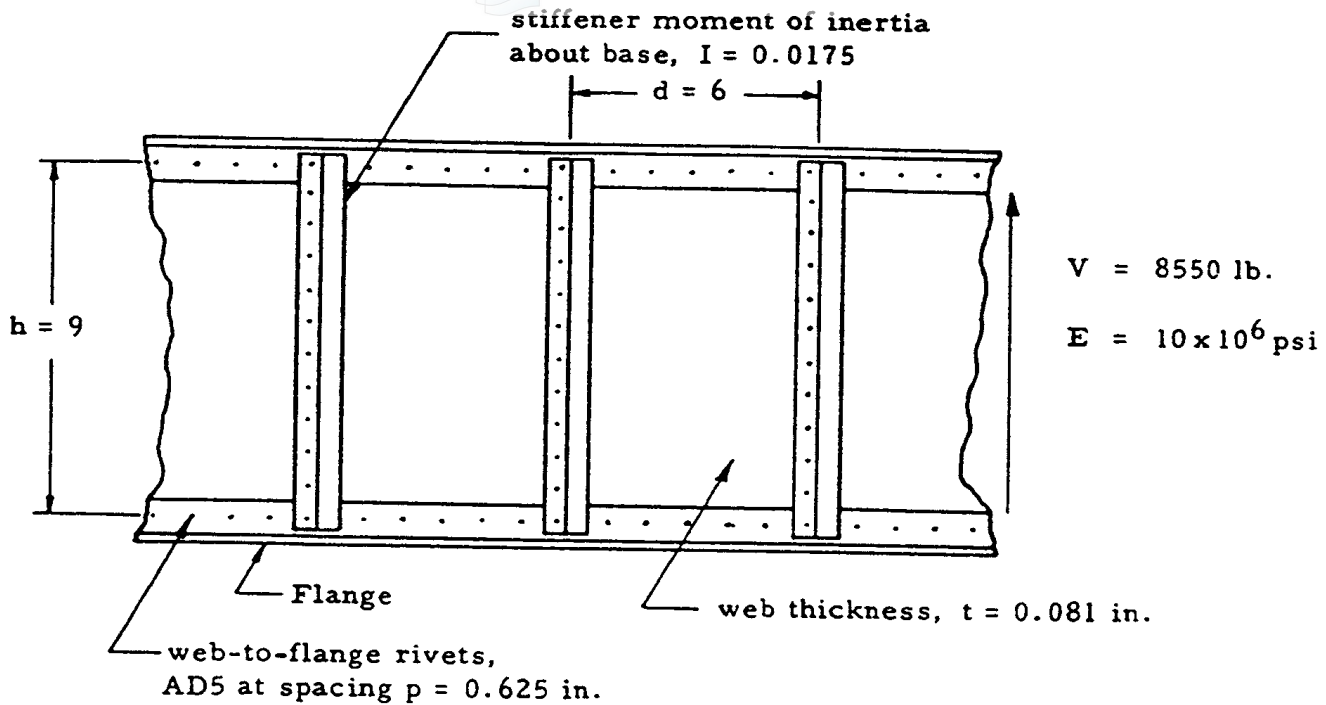
Figure 1-17.   Stiffened Shear Resistant Beam

<u>Find:</u> The margin of safety of the web and the load on each web to flange rivet.

<u>Solution:</u> From Equation (1-16) the web shear stress is given by

$$f_s = \frac{V}{ht} = \frac{8550}{9(0.081)} = 11,720 \text{ psi}$$

$$\frac{d}{h} = \frac{6}{9} = 0.667$$

and

$$\frac{I_u}{ht^3} = \frac{0.0175}{9(0.081)^3} = 3.66$$

From Figure 1-10, $K_s = 6.9$. From Figure 1-11, $F_{scr}/\eta = 12,500$ psi.
From Figure 1-14, $F_{scr} = 12,500$ psi.

Since the critical buckling stress of the web is less than the yield stress, the most likely type of failure is buckling. Thus, the margin of safety of the web may be given by

$$M.S. = \frac{F_{scr}}{f_s} - 1 = \frac{12500}{11720} - 1 = 0.06$$

The load per web-to-flange rivet is

$$q \times p = \frac{V}{h} \, p = \frac{8550}{9} (0.625) = 594 \text{ lb}.$$

1.3.3 Introduction to Partial Tension Field Beams in Bending

A tension field beam is defined to be one for which the web is incapable of supporting any compressive load, and thus buckles upon application of any load, and the web of a stiffened shear resistant beam is designed so that it will not buckle. The web of a partial tension field beam is capable of resisting compressive loads, but buckles at a load less than the ultimate beam load. The vertical stiffeners in a partial tension field beam serve to resist a compressive load and also increase the web buckling stress by dividing the web into smaller unsupported rectangles.

The curves given for partial tension field beams give reasonable assurance of conservative strength predictions provided that normal design practices and proportions are used. The most important points are:

(1) The ratio of the thickness of the uprights to that of the web, t_u/t, should be greater than 0.6.

(2) The upright spacing, d, should be in the range $0.2 < d/h < 1.0$.

(3) The method of analysis presented here is applicable only to beams with webs in the range $115 < h/t < 1500$.

In the following presentation, it is considered sufficiently accurate to take the distance between flange centroids, h, as the web height and upright length.

The methods of analysis of the web, uprights, flanges, and rivets of partial tension field beams are given in the following sections. The end of a partial tension field beam must be treated differently and is covered in Section 1.3.3.9. If a partial tension field beam has access holes, it should be treated according to Section 1.3.3.14.

1.3.3.1 Webs of Partial Tension Field Beams

The web shear flow and shear stress of a partial tension field beam are given to a close degree of approximation by Equations (1-20) and (1-21):

$$q = \frac{V}{h} \tag{1-20}$$

$$f_s = \frac{q}{t} = \frac{V}{ht} \tag{1-21}$$

1 - 25

The diagonal tension field factor, k, of a partial tension field beam specifies the portion of the total shear that is carried by the diagonal tension action of the web. This factor can be found from Figure 1-18 as a function of the web shear stress, f_s, and the ratios d/t and d/h. This curve is based on the assumption that the shear panel has simply supported edges. The accuracy, however, is sufficient for tension field beams whose webs have varying degrees of edge restraint. It is recommended that the diagonal tension factor at ultimate load satisfy the following inequality:

$$k < 0.78 - (t - 0.012)^{1/2} \qquad (1-22)$$

This criterion is presented in tabular form in Table 1-5.

TABLE 1-5

Tabular Presentation of Equation (1-22)

t	.020	.025	.032	.040	.051	.064	.072	.081	.091	.102	.125	.156	.188	.250
$.78-(t-0.012)^{1/2}$	.69	.67	.64	.61	.58	.55	.53	.52	.50	.48	.44	.40	.36	.29

The allowable web shear stress, F_s, can be obtained from Figure 1-19 for 75S-T6 or 24S-T4 aluminum sheet. These values are based on tests of long webs subjected to loads approximating pure shear and contain an allowance for the rivet factor, C_r. The allowance for rivet factor is included because the ultimate allowable shear stress based on the gross section is almost constant in the normal range of the rivet factor ($C_r > 0.6$). The values of F_s are given as a function of the stress concentration factor, C_2, which can be found from Figure 1-20 as a function of h/t, d, and I_f. The higher values of C_2 are largely theoretical, but a few scattered tests indicate that the values of C_2 become increasingly conservative in the higher ranges.

1.3.3.2 Effective Area of the Upright of a Partial Tension Field Beam

The total cross-sectional area of the uprights for double or single uprights is designated as A_u. In order to make the design charts apply to both single and double uprights, the following effective upright areas, A_{ue}, are to be used in the analysis.

For double uprights, symmetrical with respect to the web,

$$A_{ue} = A_u \qquad (1-23)$$
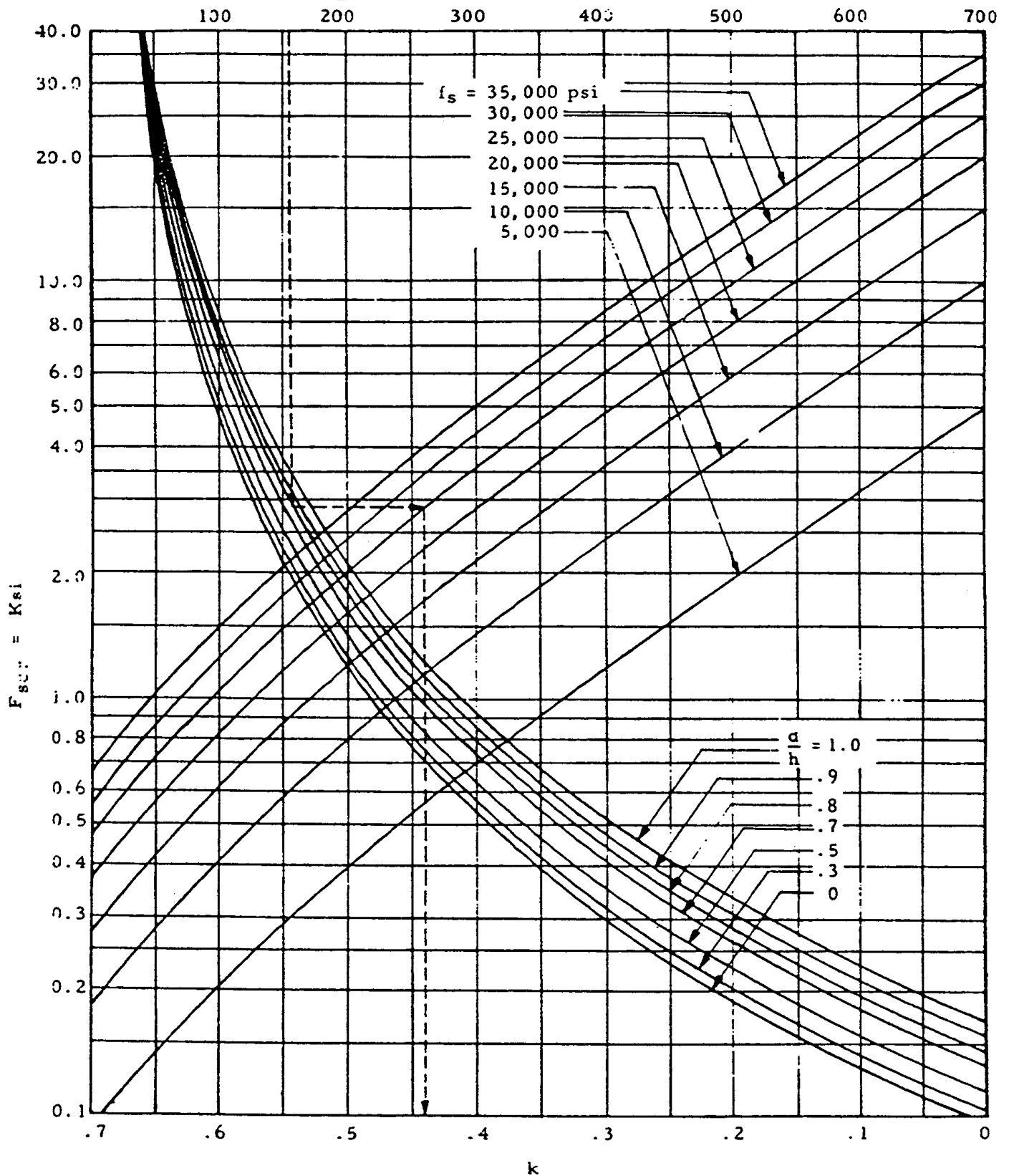
Figure 1-18. Diagonal Tension Factor, k, and Initial Buckling Stress, F_{scr}, for Shear Webs with Simply Supported Edges, $E = 10 \times 10^6$ psi

Figure 1-19. Allowable Web Shear Stress

ALCLAD 75S-T6

F_{tu} = 72 ksi

Note: For bare 75S-T6
multiply by 1.07

BARE 24S-T4

F_{tu} = 62 ksi

Note: For Alclad 24S-T4
multiply by 0.98

| C_2 - - - | 0 | .1 | .2 | .3 | .4 | .5 | .6 | .7 | .8 | .9 | 1.0 |
| C_3 - - - | 1.00 | .96 | .92 | .89 | .87 | .85 | .82 | .79 | .77 | .74 | .72 |
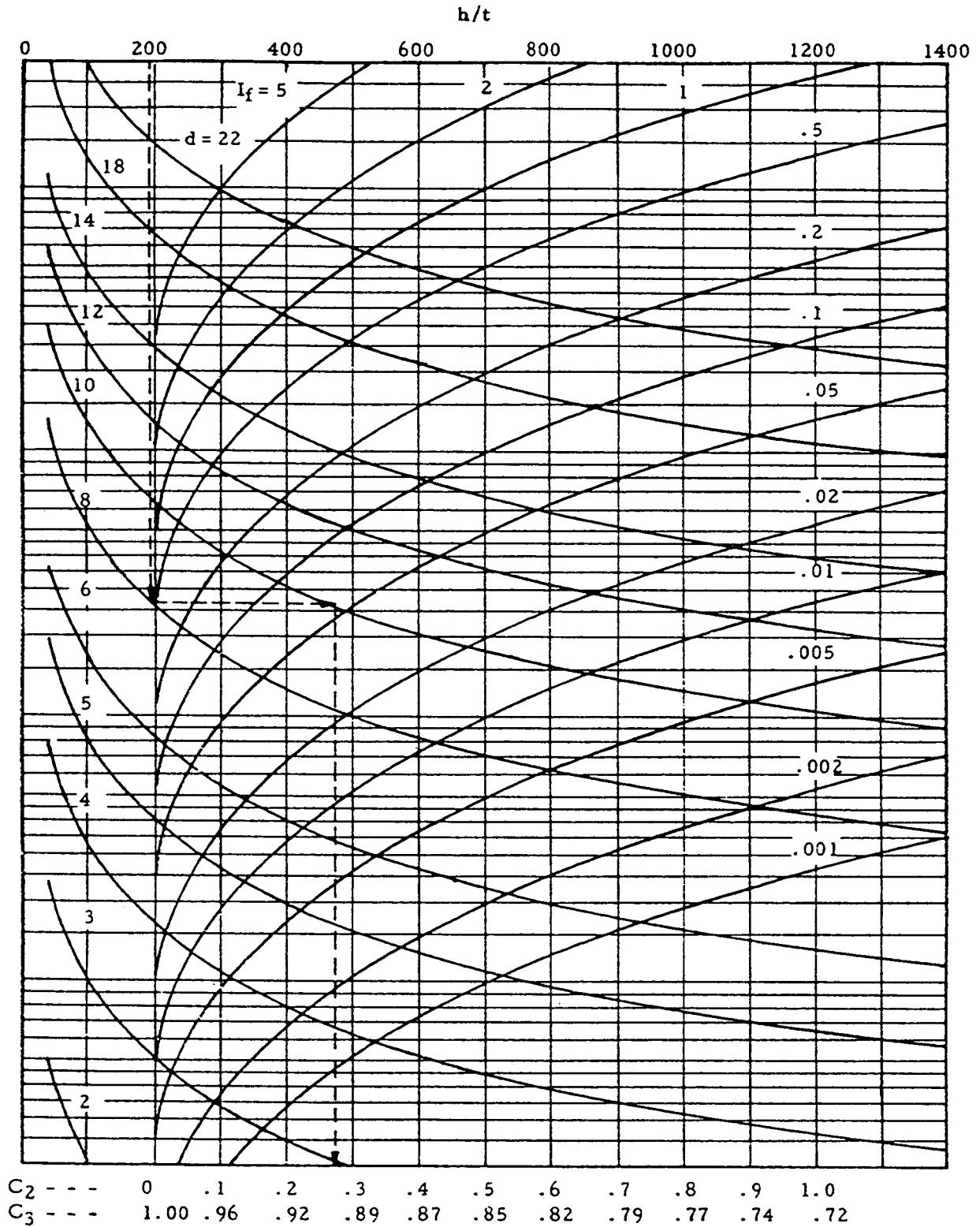
Figure 1-20. Stress Concentration Factors, C_2 and C_3

For single uprights,

$$A_{ue} = \frac{A_u}{1 + \left(\dfrac{e}{\rho}\right)^2} \qquad (1\text{-}24)$$

where ρ is the radius of gyration of the stiffener and e is the distance from the centroid of the stiffener to the center of the web. If the upright itself has a very deep web, A_{ue} should be taken to be the sum of the cross-sectional area of the attached leg and an area $12\,t_u^2$ (i. e. , the effective width of the outstanding leg is 12 times t_u).

The properties of standard extruded angles commonly used as uprights may be obtained from Table 1-6.

1.3.3.3   Design Criteria for the Uprights of a Partial Tension Field Beam

The uprights or web stiffeners of a partial tension field beam must have a sufficient moment of inertia to prevent buckling of the web system as a whole before formation of the tension field, as well as to prevent column failure under the loads imposed on the upright by the tension field. The upright must also be thick enough to prevent forced crippling failure caused by the waves of the buckled web. This forced crippling failure is almost always the most critical.

1.3.3.4   Moment of Inertia of the Uprights of a Partial Tension Field Beam

The required moment of inertia of the upright about its base (the surface attached to the web) is given in Figure 1-21 as a function of ht^3 and d/h. These curves are essentially derived by equating the critical buckling stress of the sheet between the stiffeners to the general instability stress of the web as a whole.

1.3.3.5   Computed Stresses in the Uprights of a Partial Tension Field Beam

The lengthwise average stress in the upright at the surface of attachment to the web, f_u, may be obtained from Figure 1-22 as a function of k, A_{ue}/td, and f_s as

$$f_u = f_s(f_u/f_s) \qquad (1\text{-}25)$$

The upright stress varies from a maximum at the neutral axis of the beam to a minimum at the ends of the upright. The maximum stress, f_{umax}, may be obtained from Figure 1-22 as a function of k, d/h, and f_u as

$$f_{umax} = f_u(f_{umax}/f_u) \qquad (1\text{-}26)$$

1 - 30

TABLE 1-6

Properties of Standard Extruded Uprights

$$(A_{uc})_y = \frac{A_u}{1 + (\bar{x}/\rho_{0_y})} \qquad (A_{uc})_x = \frac{A_u}{1 + (\bar{y}/\rho_{0_x})}$$
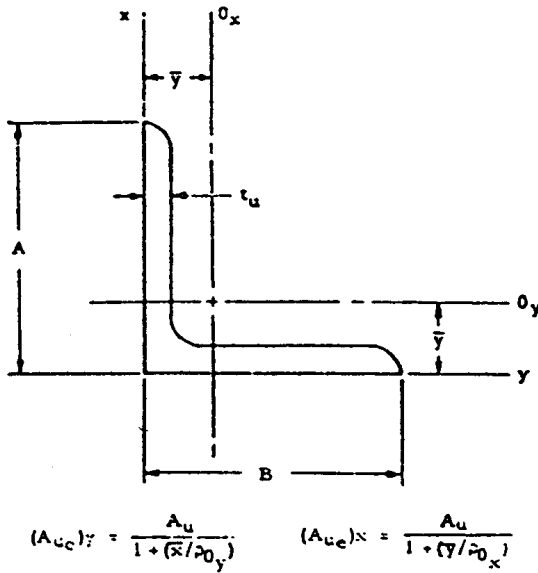
Angle - Equal Leg, Extruded

A	t_u	A_u	ρ_{0_x} or ρ_{0_y}	I_x or I_y	A_{uc}
.500	.063	.0582	.147	.0025	.0297
.625	.063	.0749	.186	.0049	.0400
	.078	.0908	.185	.0060	.0467
	.094	.1068	.181	.0071	.0525
.750	.063	.0908	.227	.0085	.0498
	.094	.130	.220	.0123	.0665
	.125	.167	.216	.0163	.0802
.875	.063	.107	.265	.0135	.0597
	.094	.154	.262	.0179	.0819
	.125	.198	.256	.0259	.0999
1.000	.063	.128	.302	.0205	.0735
	.094	.183	.296	.0296	.0989
	.125	.235	.293	.0373	.121
1.250	.063	.159	383	.0399	.0932
	.094	.230	.379	.0588	.129
	.125	.298	.373	.0773	.160
	.188	.427	.362	.1139	.210
1.500	.063	.191	.464	.0693	.113
	.094	.277	.460	.1024	.158
	.125	.360	.454	.1343	.199
	.188	.521	.443	.1989	.268
1.750	.094	.330	.536	.1627	.198
	.125	.429	.532	.2154	.249
	.188	.621	.521	.3180	.329
2.000	.094	.377	.617	.2440	.222
	.125	.491	.612	.3217	.288
	.188	.715	.601	.4768	.383
	.250	.924	.591	.6267	.479
2.500	.125	.616	.774	.6324	.359
	.188	.903	.762	.9399	.507
	.250	1.17	.751	1.2345	.628
3.000	.188	1.09	.924	1.6334	.621
	.250	1.42	.912	2.1476	.788
	.313	1.73	.900	2.6665	.932

Angle - Unequal Leg, Extruded

A	B	t	A_u	ρ_{0_y}	I_y	$(A_{uc})_y$	ρ_{0_x}	I_x	$(A_{uc})_x$
.625	.500	.050	.0535	.193	.0039	.0276	.146	.00195	.0397
.750	.500	.063	.0739	.235	.0085	.0357	.159	.00246	.0423
	.625	.063	.0818	.232	.0084	.0427	.181	.00484	.0454
.875	.625	.063	.0922	.274	.0136	.0470	.177	.00497	.0537
	.750	.063	.100	.270	.0136	.0539	.221	.00851	.0575
		.125	.184	.258	.0259	.0872	.211	.01639	.0920
1.000	.625	.063	.100	.316	.0202	.0494	.170	.00486	.0576
		.125	.184	.304	.0388	.0807	.165	.00971	.0945
	.750	.063	.108	.313	.0203	.0565	.217	.00852	.0648
		.125	.200	.302	.0389	.0937	.208	.01652	.1044
	.875	.063	.116	.310	.0203	.0637	.262	.01351	.0680
		.094	.167	.305	.0297	.0872	.257	.01992	.0924
1.250	.750	.063	.124	.400	.0398	.0616	.209	.00854	.0795
		.094	.179	.393	.0586	.0845	.203	.01257	.1052
		.125	.231	.387	.0767	.104	.200	.01678	.1270
	1.000	.063	.139	.394	.0398	.0756	.298	.02034	.0846
		.094	.202	.389	.0587	.105	.291	.02973	.1162
		.125	.262	.382	.0769	.130	.286	.03921	.1434
1.500	.750	.094	.204	.476	.1019	.0927	.194	.01266	.1239
		.125	.264	.465	.1337	.114	.191	.01697	.1495
	1.000	.094	.228	.474	.1020	.114	.282	.03006	.1379
		.125	.295	.468	.1341	.142	.276	.03944	.1686
		.156	.361	.463	.1656	.169	.271	.04798	.1994
	1.250	.094	.251	.468	.1021	.135	.372	.05882	.1481
		.125	.327	.462	.1343	.170	.365	.0773	.1844
		.156	.400	.457	.1662	.201	.360	.0956	.2168
1.750	1.000	.125	.327	.553	.2140	.153	.269	.0397	.1945
	1.250	.125	.358	.549	.2141	.180	.360	.0787	.2113
	1.500	.125	.389	.542	.2140	.208	.447	.1347	.2243
		.156	.478	.537	.2655	.248	.441	.1666	.2664
2.000	1.000	.125	.358	.637	.3212	.162	.261	.0399	.2190
		.156	.439	.631	.3970	.193	.256	.0498	.2535
	1.250	.125	.392	.643	.3217	.195	.348	.0778	.2386
		.156	.480	.629	.3978	.229	.343	.0963	.2807
		.188	.568	.622	.4747	.263	.336	.1154	.3161
	1.500	.125	.423	.629	.3213	.221	.437	.1348	.2531
		.156	.519	.623	.3979	.263	.431	.1672	.2995
		.188	.615	.618	.4756	.304	.426	.1997	.3433
	1.750	.125	.454	.625	.3215	.249	.526	.2147	.2656
		.156	.558	.617	.3983	.298	.520	.2661	.3167
		.188	.662	.611	.4761	.344	.514	.3181	.3641
2.500	1.250	.156	.558	.796	.7822	.252	.326	.0971	.3411
		.188	.662	.790	.9369	.292	.321	.1170	.3865
	1.500	.156	.597	.795	.7827	.288	.414	.1677	.3642
		.188	.709	.789	.9371	.334	.409	.2009	.4183
	1.750	.156	.636	.791	.7828	.324	.503	.2667	.3836
		.188	.756	.785	.9378	.376	.497	.3196	.4420
	2.000	.156	.681	.783	.7843	.363	.590	.3997	.4037
		.188	.809	.777	.9391	.421	.584	.479	.467
	2.250	.156	.720	.776	.7841	.398	.679	.572	.418
		.188	.856	.770	.9392	.462	.674	.684	.487
3.000	1.500	.188	.809	.956	1.6306	.367	.391	.202	.495
		.250	1.050	.943	2.1344	.458	.381	.269	.595
	2.000	.188	.903	.950	1.6309	.451	.576	.480	.553
		.250	1.17	.938	2.1394	.564	.556	.629	.672
	2.500	.250	1.30	.927	2.1471	.676	.734	1.239	.734
		.313	1.60	.915	2.6647	.803	.722	1.537	.867
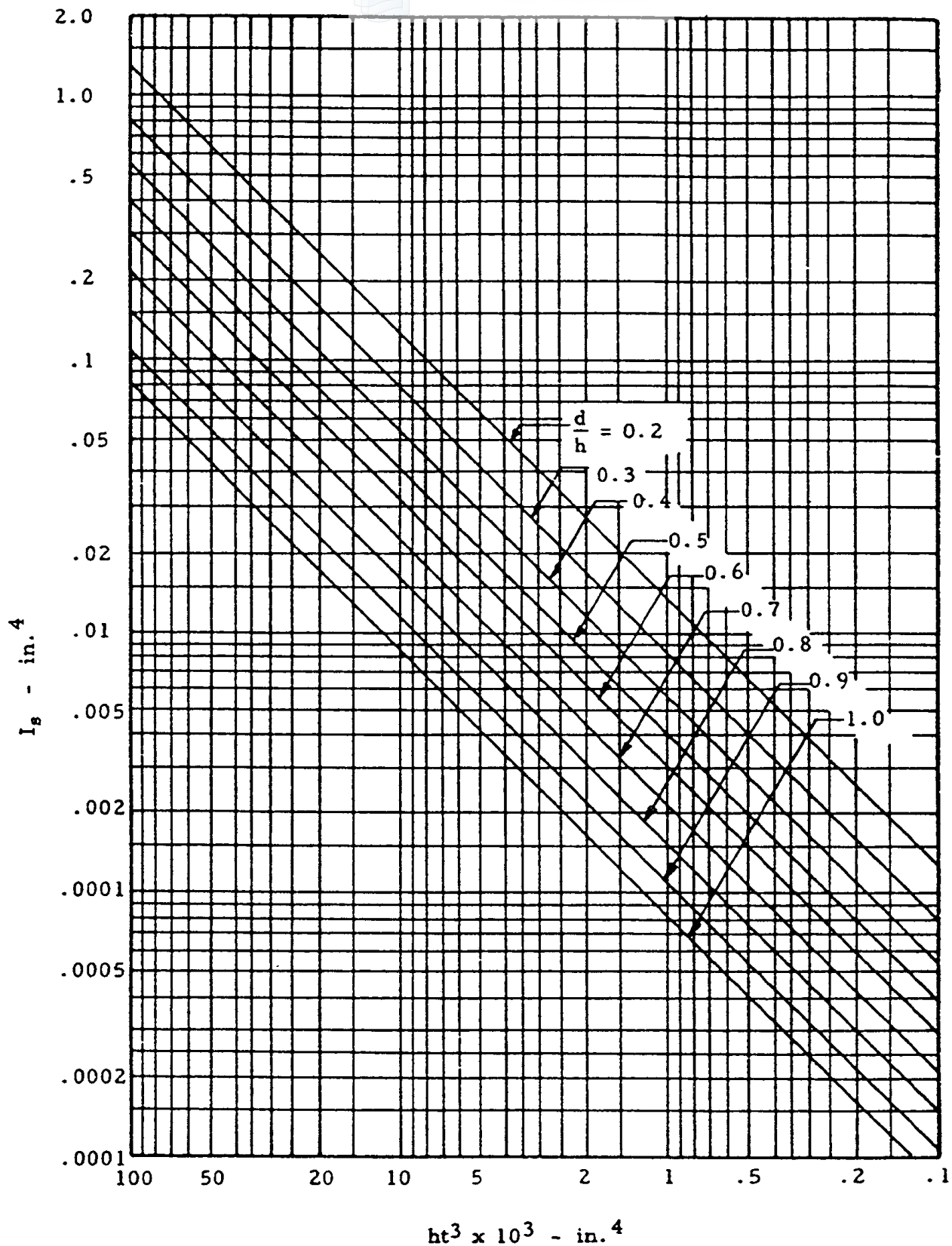
Figure 1-21.   Minimum Moment of Inertia Required for Tension Field
Beam Uprights Assuming Simply Supported Panels

$$\frac{A_{u_e}}{dt} = 0 \qquad .1$$
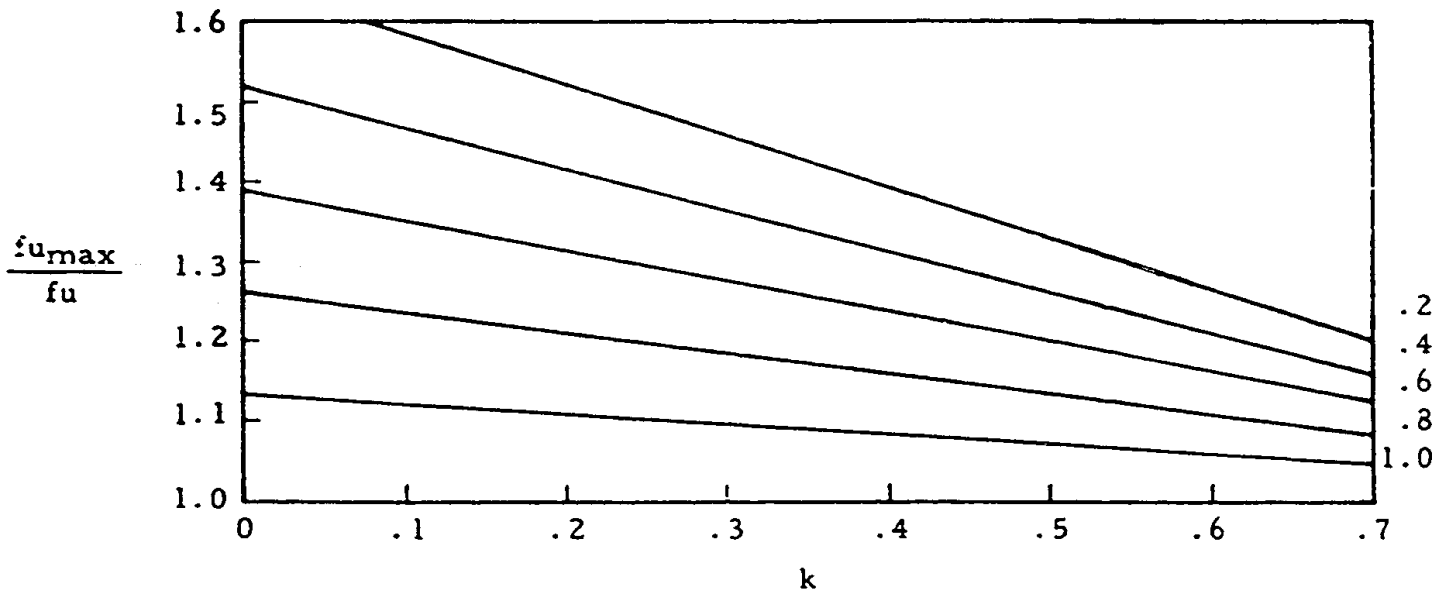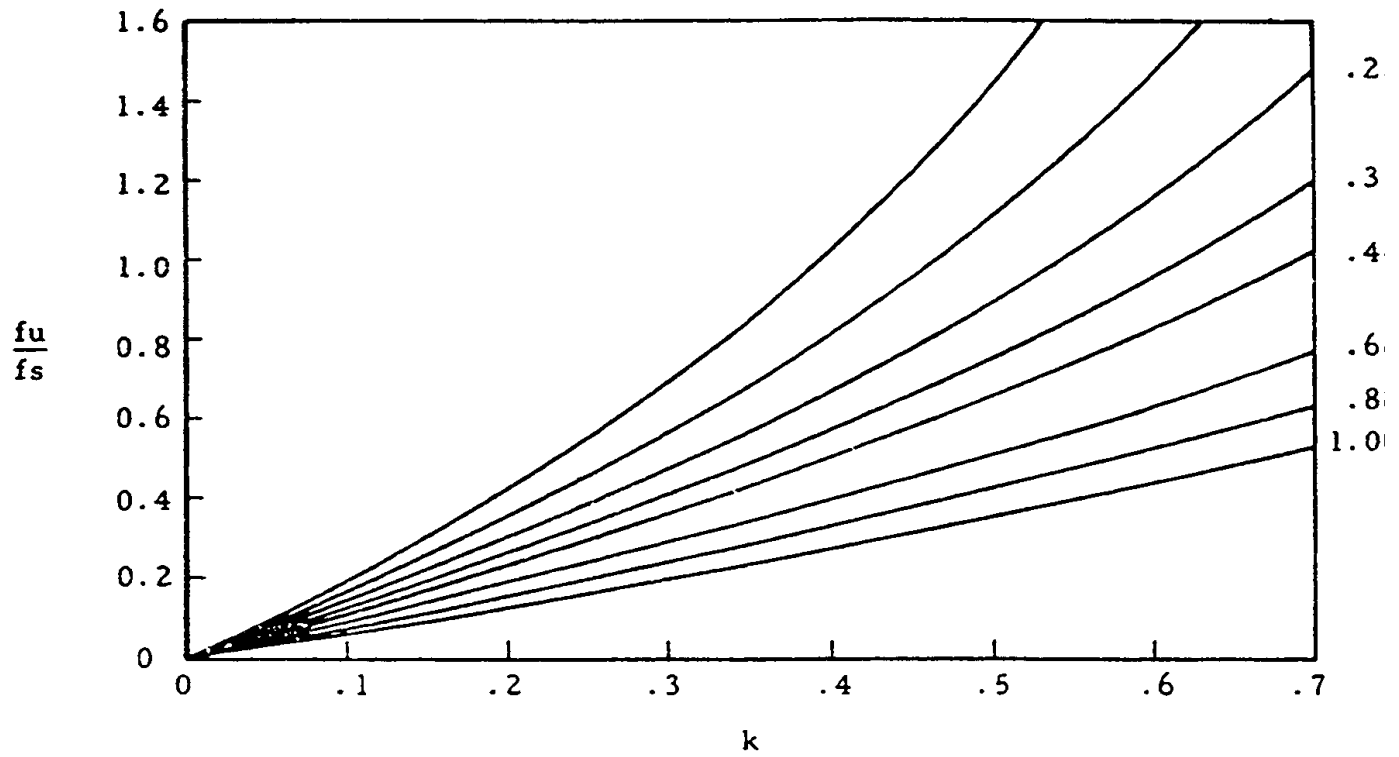
Figure 1-22.   Upright Stress Ratios

1 - 33

1.3.3.6   Allowable Stresses in the Uprights of a Partial Tension Field Beam

The maximum upright stress, f_{umax}, should be checked against an allowable forced crippling stress, F_0, which is obtained from Figure 1-23. If the upright has legs of unequal thickness, the thickness of the leg attached to the web should be used to determine the ratio t_u/t. In the case of double uprights, f_{umax} should also be checked against the allowable natural crippling stress of the flange.

The stress, f_u, should be no greater than the column yield stress, F_{co} (the stress at $L'/\rho = 0$). The centroidal upright stress, $f_{cent} = f_u A_{ue}/A_u$, should be checked against an allowable column stress, F_{col}. F_{co} and F_{col} can be found from the column curves in Chapter 2.

For simplicity, the effective column length of the upright, h', may be taken as h, since this effect is rarely critical. However, the following values of h' may be used if necessary:

$$h' = \frac{h}{\sqrt{1 + k^2 \left(3 - \frac{2d}{h}\right)}} \qquad (1-27)$$

for double uprights, and

$$h' = \frac{h}{2} \qquad (1-28)$$

for single uprights.

1.3.3.7   Flanges of Partial Tension Field Beams

The total stress in the flanges of a partial tension field beam is the result of the superposition of three individual stresses: the primary beam stress, f_b, the compressive stress, f_f, caused by the horizontal component of the diagonal tension in the web, and the secondary bending stress, f_{sb}, caused by the distributed vertical component of the diagonal tension.

The primary beam stress is given by

$$f_b = \frac{M}{A_f h} \qquad (1-29)$$

The compressive stresses due to the horizontal component of diagonal tension is given by

$$f_f = \frac{kqh}{2A_f + 0.5(1-k)\,th} \qquad (1-30)$$

24S-T ALUMINUM ALLOY

$F_o = 26,000 \ k^{2/3} \ (tu/t)^{1/3}$ — Single Uprights

$F_o = 21,000 \ k^{2/3} \ (tu/t)^{1/3}$ — Double Uprights

75S-T6 ALUMINUM ALLOY

$F_o = 32,500 \ k^{2/3} \ (tu/t)^{1/3}$ — Single Uprights

$F_o = 26,000 \ k^{2/3} \ (tu/t)^{1/3}$ — Double Uprights
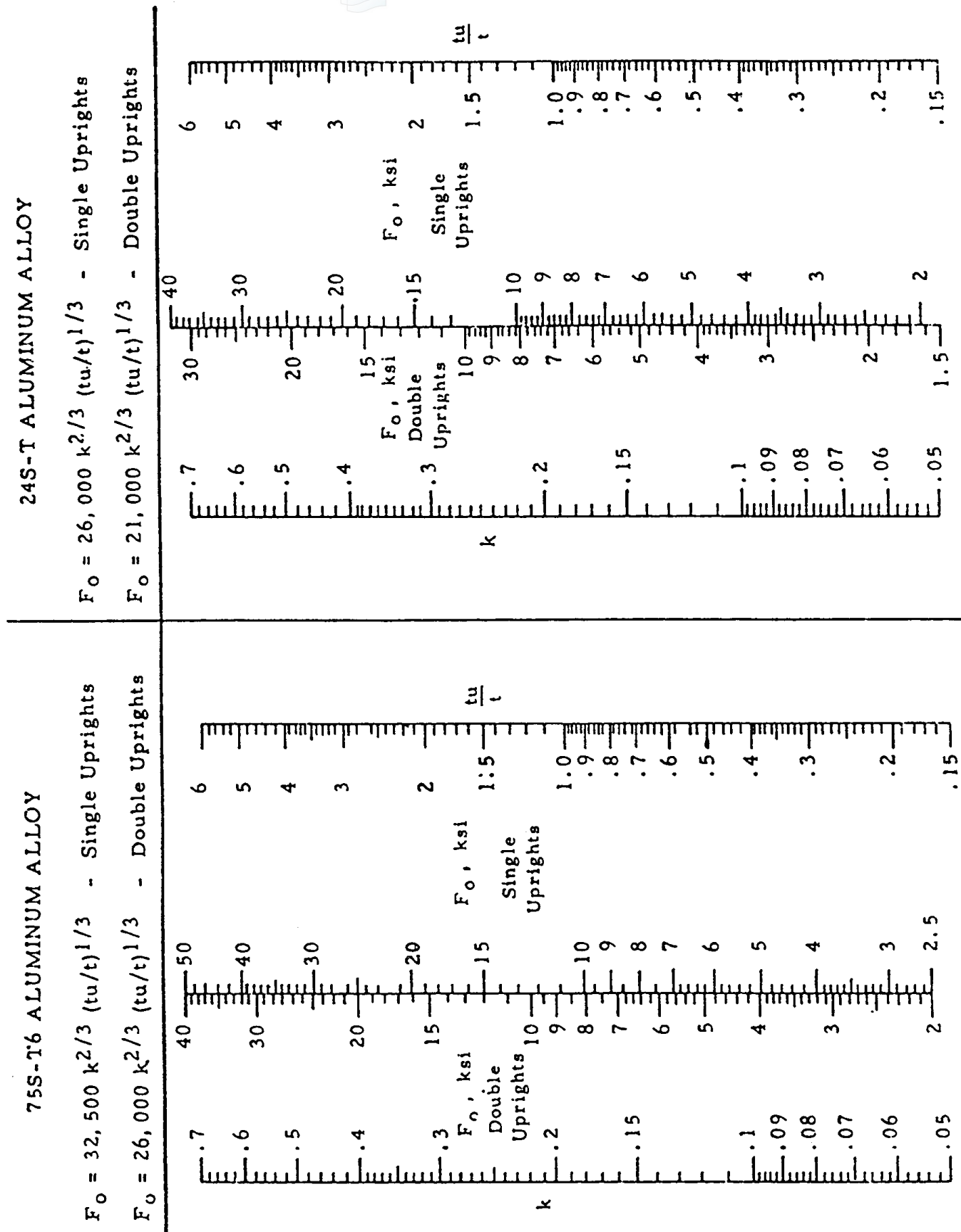
Figure 1-23.   Nomograms for Upright Forced Crippling Allowable Stress

where k is the diagonal tension field factor which may be found by referring to Figure 1-18. The secondary bending moment due to the distributed vertical component of diagonal tension is given by

$$M_{sb} = \frac{1}{12} kf_s td^2 C_3 \qquad (1-31)$$

where C_3 is given in Figure 1-20. M_{sb} is the maximum moment in the flange and exists in the portion of the flange over the uprights. If C_3 and k are near unity, the secondary bending moment in the flange midway between the uprights is half as large as that given and of opposite sign. The secondary bending stress is then

$$f_{sb} = \frac{M_{sb}}{\left(\dfrac{I_f}{C_f}\right)} \qquad (1-32)$$

where (I_f/c_f) is the section modulus of the flange. The total stress in the flange is equal to $f_b + f_s + f_{sb}$.

1.3.3.8   Rivets in Partial Tension Field Beams

Three types of rivets must be analyzed in partial tension field beams. These are web-to-flange rivets, web-to-upright rivets, and upright-to-flange rivets.

1.3.3.8.1   Web-to-Flange Rivets in a Partial Tension Field Beam

The shear load per inch acting on the web-to-flange rivets in partial tension field beams is given in Figure 1-24. The rivet factor, C_r, should be greater than 0.6 to justify the allowable web stresses used in Section 1.3.3.1 and to avoid undue stress concentration.

1.3.3.8.2   Web-to-Upright Rivets in Partial Tension Field Beam

The tensile load per inch acting on the web-to-upright rivets is given in Figure 1-25. This tensile load is a result of the prying action of the buckled web. Although these loads reflect time-tested practice, they should be considered only tentative because of the limited test data presently available. The tensile load criteria is believed to insure a satisfactory design as far as shear strength is concerned.

1.3.3.8.3   Upright-to-Flange Rivets in a Partial Tension Field Beam

The shear load on the upright-to-flange rivets in a partial tension field beam is given by

$$P_u = f_u A_{ue} \qquad (1-33)$$

where f_u is the average compressive stress in the upright and A_{ue} is the effective area of the upright as given in Section 1.3.3.2.
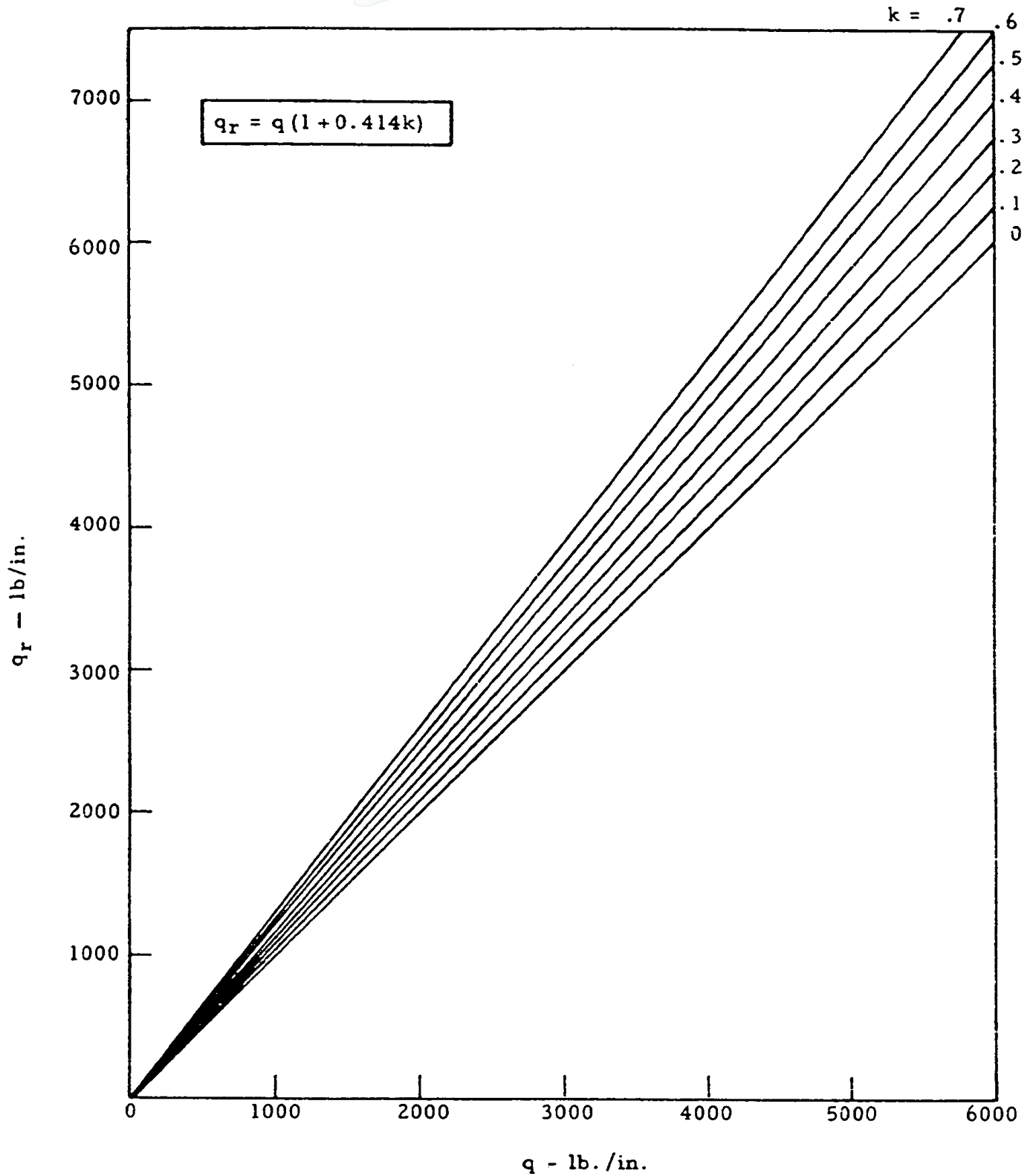
Figure 1-24. Rivet Loads—Web-to-Flange and Web Splices

$$q_r = q(1 + 0.414k)$$

$k =$ .7

$q_r - lb./in.$

$q - lb./in.$
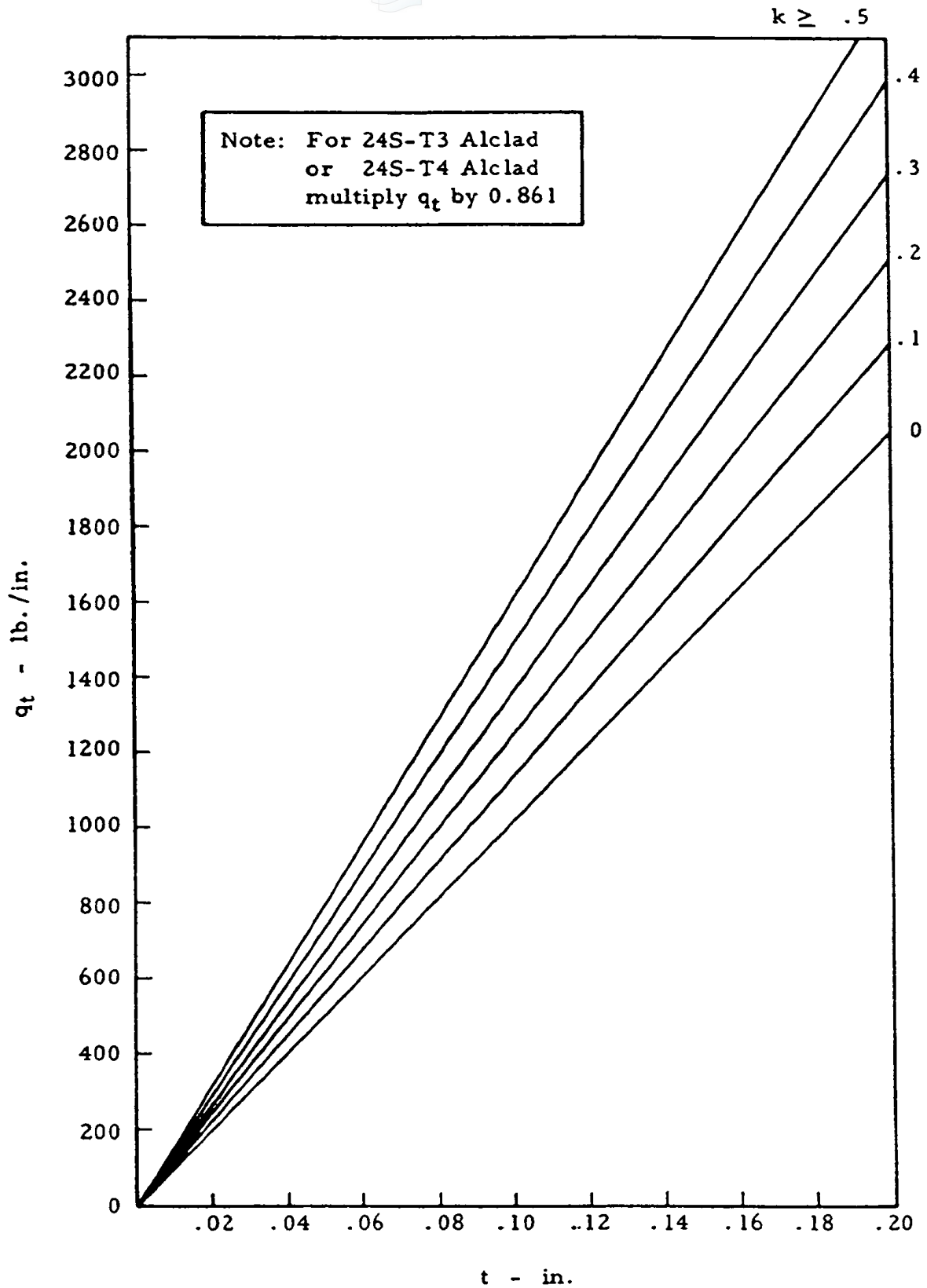
Figure 1-25. Rivet Tension Loads—Web-to-Upright 75S-T6 Alclad

1.3.3.9   Ends of Partial Tension Field Beams

The end of a partial tension field beam must be specially handled since the web is discontinuous at the end and the tension component of web stress must be transferred to the flanges in the end panel.

The following treatment is based on the assumption that the basic beam shear, q, is constant over a length $2h/3$ from the end of the beam. When the basic beam shear, q, varies over this length, the terms $(q + 1.5kq)$, $(q + 1.0 kq)$, and $(q\ kh/4A_u)$ should be replaced by the terms $(q + 1.5 kq')$, $(q + 1.0 kq')$, and $(q'kh/4A_u)$, respectively, where q is the actual beam shear at the point being considered, and q' is the beam acting at a distance $2h/3$ from the end of the beam.

1.3.3.10   Webs at the Ends of Partial Tension Field Beams

The web in one corner must carry a shear flow of $q + 1.5 kq$. If reinforcement is necessary, a doubler of the dimensions shown in Figure 1-26 should be added to the web, resulting in a combined shear strength of $q + 1.5 kq$. This is usually necessary in one corner only. If the applied shear flow is opposite to that shown in Figure 1-26, the doubler should be attached to the lower corner of the web. The shear flow in the web in the corner not reinforced is $q - 1.5 kq$, where q is the shear flow in the web at points removed from the end.
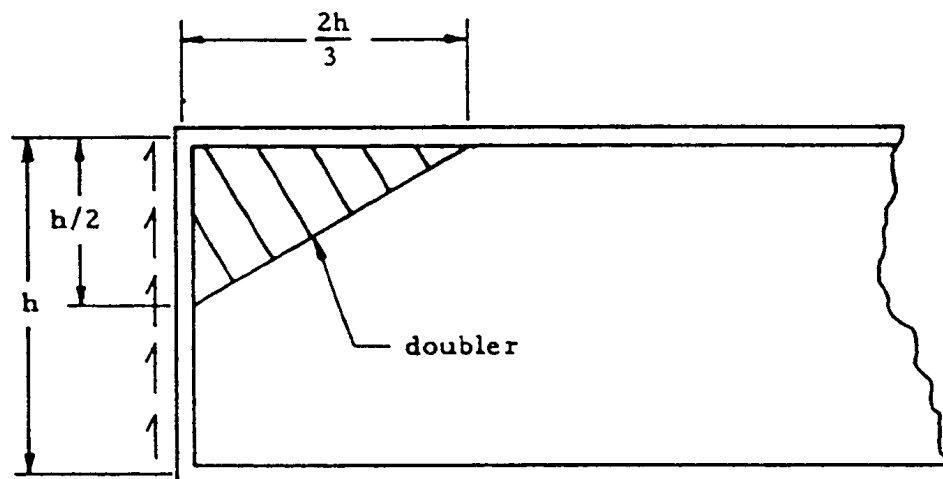
Figure 1-26.   Doubler at the End of a Partial
Tension Field Beam

If the shear can act in either direction, double reinforcement may be necessary. In general, the basic web is capable of carrying about a 60% reversal of shear without double reinforcement.

1.3.3.11   Uprights at the Ends of Partial Tension Field Beams

The following stresses act simultaneously on the end stiffener of a partial tension field beam:

1. A compressive stress due to the vertical component of web diagonal tension. This compressive stress varies from $(f_u - f_{umax}/2)$ at either end to $f_{umax}/2$ at the midpoint of the stiffener.

2. A compressive stress due to the variable shear flow along the end stiffener. The equivalent shear flow distribution curve is assumed to vary linearly from $(q - 1.0 kq)$ at one corner to $(q + 1.0 kq)$ at the other corner. This compressive stress builds up from zero at either end of the stiffener to $kqh/4A_u$ at the midpoint of the stiffener.

Thus, the maximum compressive stress in the end stiffener (exclusive of additional external loads acting) is equal to

$$\frac{f_{umax}}{2} + \frac{qkh}{4 A_u}$$

(1-34)

This stress should be compared with the lower of F_s or F_{cc} for the upright in computing the margin of safety.

1.3.3.12 <u>Rivets at the Ends of Partial Tension Field Beams</u>

The doubler should be attached to the web in accordance with Table 1-7. The diagonal edge of the doubler should be attached with a minimum of two rows of rivets with a minimum distance between rows of four rivet diameters. The strength of this attachment in lb/in. should be equal to the thickness of the doubler times 30,000 psi.

TABLE 1-7

Doubler-to-Web Rivets

Doubler Gage	Rivet Size	Rivet Spacing
.020 - .032	AD-4	1.5 in. on centers
.040 - .051	AD-5	2.0 in. on centers
.064 & greater	DD-6	2.5 in. on centers

1 - 40

The web-to-flange attachment adjacent to the doubler must be strong enough to carry a shear flow of $(q + 1.5q)(1 + 0.414k)$ lb/in. The other flange attachment must carry a shear flow of $q(1 + 0.414k)$ lb/in.

The attachment of the end stiffener of a partial tension field beam to the web must be strong enough to carry a shear flow of $(q + 1.5kq)(1 + 0.414k)$ lb/in. in the region of the doubler and $q(1 + 0.414k)$ elsewhere.

1.3.3.13 Sample Problem - Partial Tension Field Beams

Given: The partial tension field beam shown in Figure 1-27.

web - 0.051 75S-T6 Alclad

d = 8

q = 1250 lb./in.

h = 10

Flanges - 1.25 x 1.25 x 0.188
75S-T6 angle

upright - 0.75 x 0.75 x 0.094
75S-T6 angle
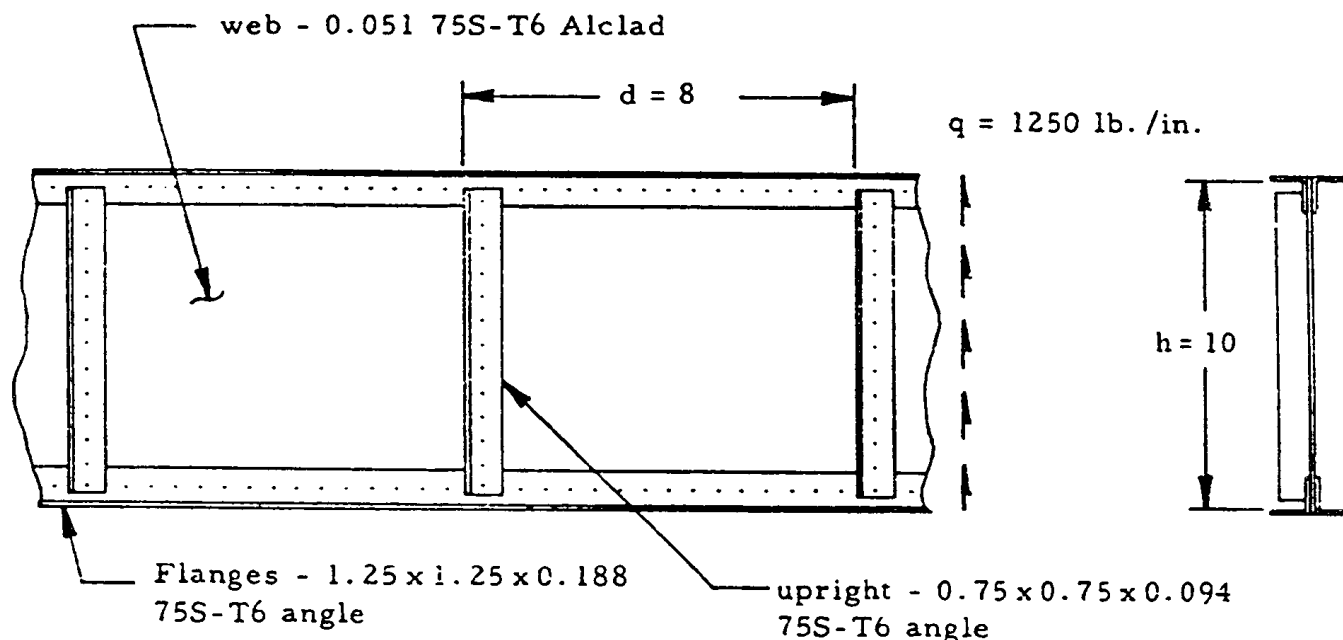
Figure 1-27.   Partial Tension Field Beam with Single Uprights

Find: The margins of safety of web and uprights and the rivet loads.

Solution: The method of obtaining the desired quantities is summarized in Table 1-8.

TABLE 1-8

Solution of Sample Problem - Partial Tension Field Beams

Quantity	Symbol	Reference	Value	Row
Shear Flow	q, lb/in.		1250	1
Web Thickness	t, in.		0.051	2
Beam Depth	h, in.		10	3
Upright Spacing	d, in.		8	4
Upright Thickness	t_u, in.		0.094	5
Upright Area	A_u, in.^{2}	Table 1.7	0.130	6
Upright Radius of Gyration	ρ, in.	Table 1.7	0.220	7
Upright Moment of Inertia	I_u, in.^{4}	Table 1.7	0.0123	8
Upright Effective Area	A_{uc}, in.^{2}	Table 1.7	0.0665	9
Web Shear Stress	f_s, psi	Equation (1-21)(①/②)	24,500	10
Parameters	d/t	④/②	157	11
	d/h	④/③	0.80	12
	h/t	③/②	196	13
	A_{uc}/td	⑨/(④②)	0.163	14
	$ht^3 \times 10^3$, in.^{4}	1000 ③②^3	1.33	15
	t_u/t	⑤/②	1.84	16
	h/ρ	③/⑦	45.5	17
Diagonal Tension Factor	k	Figure 1.19	0.435	18
Ratio - Upright-to-Web Stresses	f_u/f_s	Figure 1.20	0.81	19
Ratio - Upright Stresses	f_{umax}/f_u	Figure 1.21	1.15	20
Stress Concentration Factor - Flange Flexibility	C_2	Figure 1.21	0.27	21
Moment of Inertia Required for Upright	I_s, in.^{4}	Figure 1.22	0.00205	22

TABLE 1-8

Solution of Sample Problem - Partial Tension Field Beams (concluded)

Quantity	Symbol	Reference	Value	Row
ANSWER - Rivet Shear Load - Web-to-Flange	q_r, lb./in.	Figure 1.23	1470	23
ANSWER - Rivet Tensile Load - Web-to-Upright	q_t, lb./in.	Figure 1.24	780	24
Upright Allowable - Column Yield Stress	F_{co}, psi	Section 1.3.3.6 and Figure 2.5	79,000	25
Upright Allowable - Forced Crippling	F_{col}, psi	Section 1.3.3.6 and Figure 2.5	52,000	26
Allowable Web Stress	F_o, psi	Figure 1.25	23,000	27
Allowable Web Stress	F_s, psi	Figure 1.26	25,200	28
Upright Stress, Average	f_u, psi	Equation (1-25) (⑩)(⑲)	19,830	29
Upright Stress, Centroidal	f_{cent}, psi	Section 1.3.3.6 (㉙)(⑨)/(⑥)	10,150	30
Upright Stress, Maximum	f_{umax}, psi	Equation (1-26)(㉙)(⑳)	22,800	31
ANSWER - Rivet Load - Upright-to-Flange	P_u, lb.	Equation (1-33)(㉙)(⑨)	1,320	32
ANSWER - Margin of Safety - Web		$\left(\frac{㉘}{⑩}\right) - 1$	0.03	33
ANSWER - Margin of Safety - Uprights		*	0.01	34

* $\left(\dfrac{⑧}{㉒} - 1\right)$, $\left(\dfrac{㉕}{㉙} - 1\right)$, $\left(\dfrac{㉖}{㉚} - 1\right)$, or $\left(\dfrac{㉗}{㉛} - 1\right)$ whichever is least

1.3.3.14 Partial Tension Field Beams with Access Holes

Figure 1-28 shows a partial tension field beam with access holes of diameter, D. Such a beam may be analyzed in the same manner as one without access holes except that the substitutions described in Sections 1.3.3.15, 1.3.3.16, and 1.3.3.17 must be made.
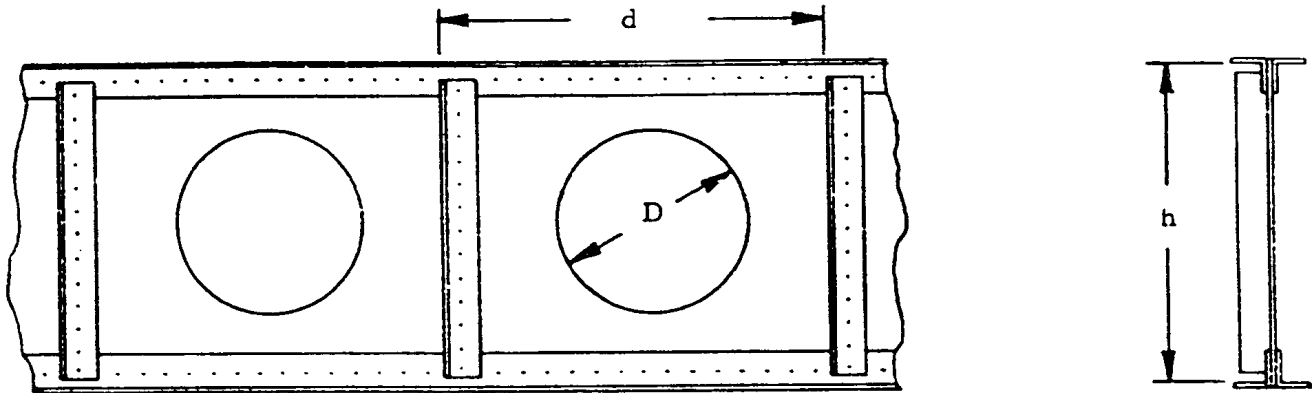
Figure 1-28. Partial Tension Field Beam with Access Holes

1.3.3.15 Webs of Partial Tension Field Beams with Access Holes

The method of analyzing webs, given in Section 1.3.3.1, should be used for partial tension field beams with access holes except that the allowable web shear stress, F_s, must be replaced by a reduced allowable web shear stress given by

$$F_s{}' = F_s \left[\frac{td(d-D) + A_u D C_4}{C_5 td^2} \right] \tag{1-35}$$

where the design reduction factors, C_4 and C_5, are given in Figure 1-29. This method gives good correlation with tests if beam parameters are in the following ranges:

$$0.020 \text{ in.} < t < 0.132 \text{ in.}$$
$$0.040 \text{ in.} < t_u < 0.079 \text{ in.}$$
$$7.4 \text{ in.} < h < 19.4 \text{ in.}$$
$$7.0 \text{ in.} < d < 18.0 \text{ in.}$$
$$2.375 \text{ in.} < D < 5.875 \text{ in.}$$

1.3.3.16 Uprights of Partial Tension Field Beams with Access Holes

The method of analyzing uprights, given in Sections 1.3.3.2 through 1.3.3.6, may be used for partial tension field beams with access holes except that the forced crippling allowable, F_o, should be replaced by a reduced forced crippling allowable given by

$$F_o{}' = \frac{F_o}{1 + \dfrac{D}{d}} \tag{1-36}$$

1 - 44
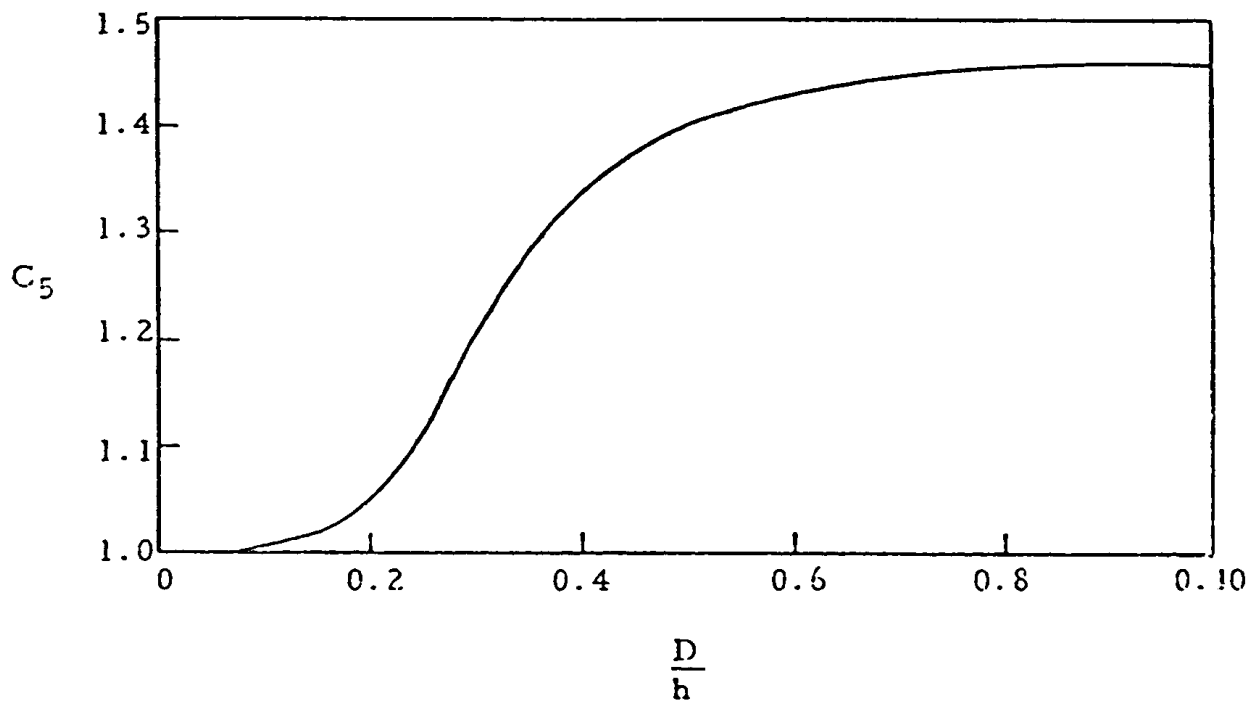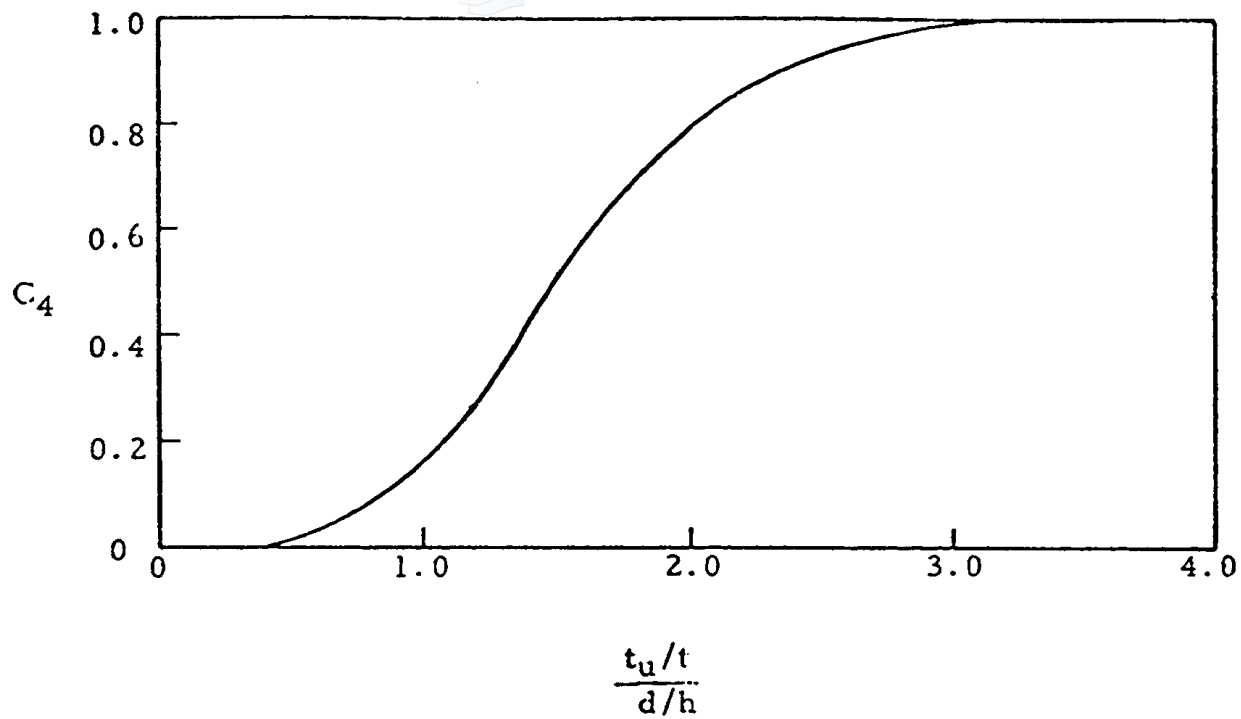
Figure 1-29.   Design Reduction Factors Due to Access Hole

1.3.3.17 Rivets in Partial Tension Beams with Access Holes

The method given in Section 1.3.3.8 for analyzing rivets may be used for partial tension field beams with holes except that the tensile load on the web-to-upright rivets, q_t, should be replaced by an increased load given by

$$q_t' = q_t \left(1 + \frac{D}{d}\right) \qquad (1-37)$$

1.3.4 Introduction to Reaction Forces and Moments on Beams Under Transverse Loading.

Figure 1-30 shows a beam under transverse loading. Two equations of equilibrium may be applied to find the reaction loads applied to such a beam by the supports. These consist of a summation of forces in the vertical direction and a summation of moments. If a beam has two reaction loads supplied by the supports, as in the case of a cantilever beam or a beam simply supported at two points, the reaction loads may be found by the equilibrium equations and the beam is statically determinate. However, if a beam has more than two reaction loads, as in the case of a beam fixed at one end and either pinned or fixed at the other end, it is statically indeterminate and beam deflection equations must be applied in addition to the equations of statics to determine the reaction loads.
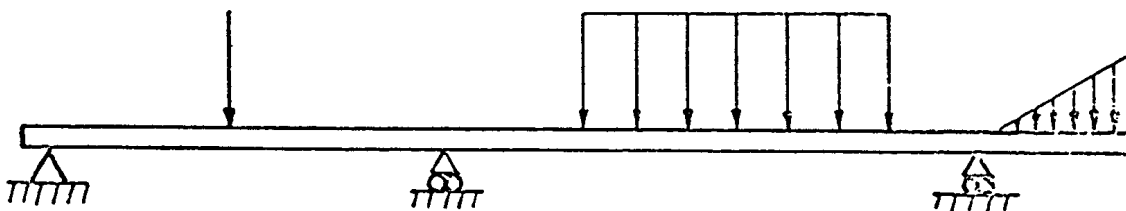
Figure 1-30. Beam Under Transverse Loading

Section 1.3.4.1 presents a method for determining reaction loads on beams fixed at one end and pinned at another point, and Section 1.3.4.3 treats reaction loads for beams fixed at both ends. Beams on three or more supports are treated in Section 1.3.4.5.

1.3.4.1 Reaction Forces and Moments on Beams with One Fixed End and One Pinned Support

Figure 1-31(a) shows a uniform beam with one fixed and one pinned support. The following procedure may be used to determine the support reactions on such a beam if its stresses are in the elastic range.

1. Split the beam at the pinned support as in Figure 1-31(b) and find M_A from the equations of statics.

2. Consider the right section of the beam as a single beam simply
    supported at both ends as in Figure 1-31(b). Find the moment
    diagram for this beam as in Figure 1-31(c). A is the area of
    this moment diagram and C is the centroid of this area.
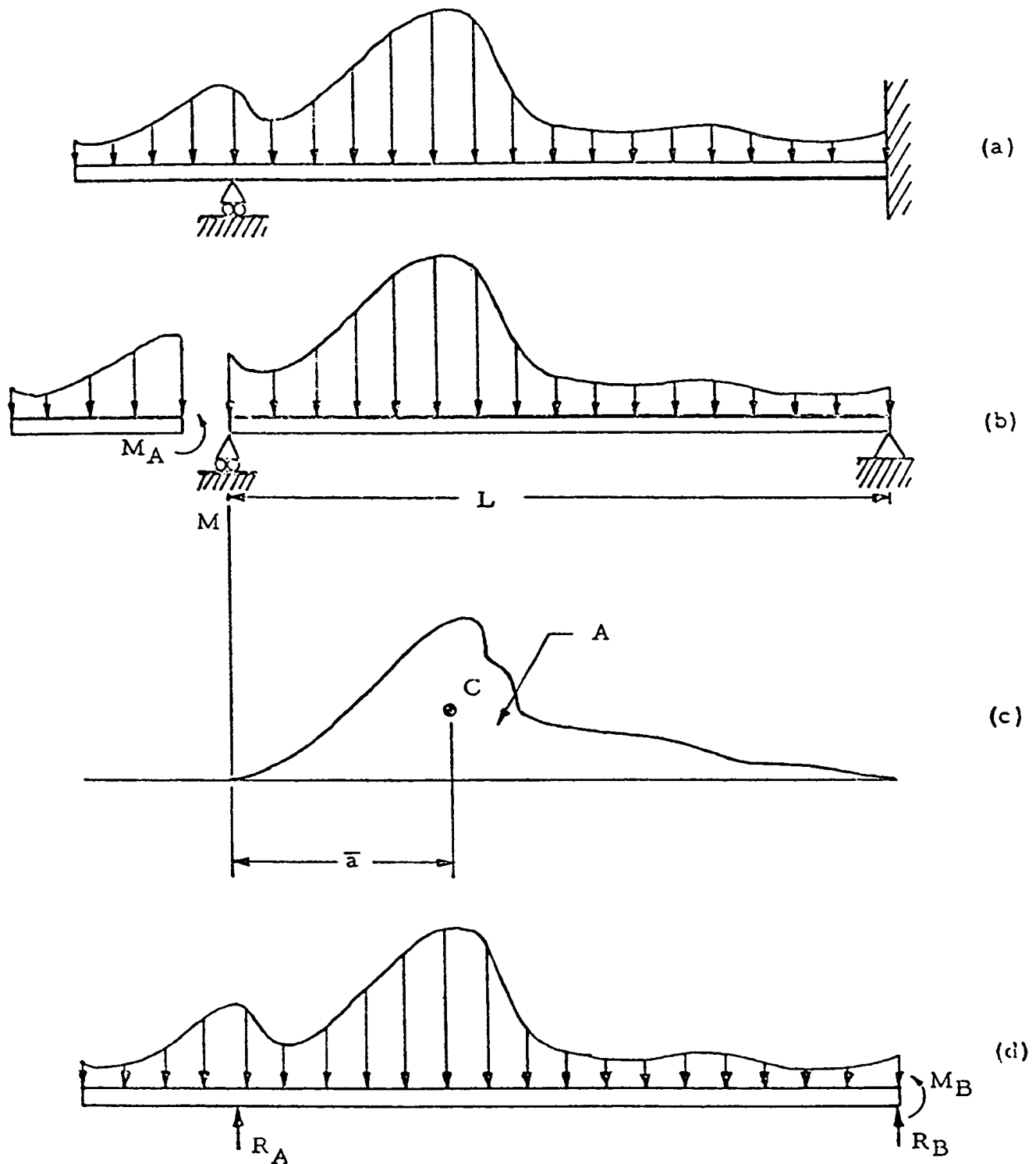
Figure 1-31.   Method of Determining Reaction Forces and Moments
               on a Beam Fixed at One End and Pinned at One Point

1 - 47

3. Find M_B by the equation

$$M_B = \frac{-3A\overline{a}}{L^2} - \frac{M_A}{2} \qquad (1-38)$$

The evaluation of the first term of this equation may be facilitated by the use of Table 1-10.

4. Evaluate R_A and R_B by applying the equations of statics to Figure 1-31(d).

Once the support reactions have been determined, the moment and shear diagrams may be constructed for the beam. If the pinned support is at the end of the beam, M_A may be set equal to zero.

1.3.4.2 Sample Problem - Reactions on Beam with One Fixed and One Pinned Support

Given: The beam shown in Figure 1-32.
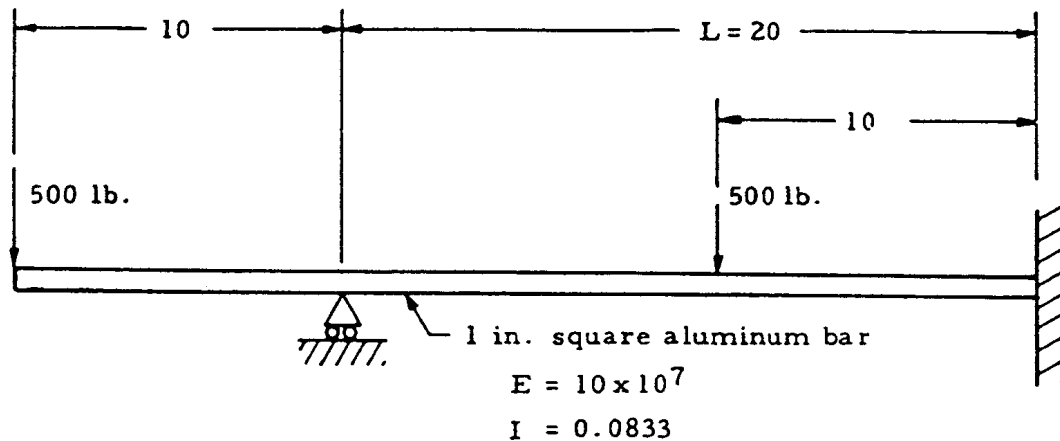
Figure 1-32. Beam with One Fixed End and One Pinned Support

Find: The reaction moments and forces on the beam.

Solution: Figure 1-33(a) may be obtained by redrawing the beam as in Figure 1-31(b). The moment diagram may then be drawn for the right portion; and A, $\overline{a}$, and M_A may be determined as in Figure 1-33(b).

From Equation (1-38),

$$M_B = \frac{-3A\overline{a}}{L^2} - \frac{M_A}{2} = \frac{-3(25000)(10)}{(20)^2} - \frac{5000}{2} = -4,375 \text{ in. lb.}$$

1 - 48

Now that M_B is known, R_A and R_B may be found by applying the equations of statics to Figure 1-33(c). Doing this gives $R_A = 781$ lb. and $R_B = 219.0$ lb.

500 lb.   500 lb.   (a)

$M_a = 5000$ in.lb.

$A = \dfrac{2500 \times 20}{20} = 25000$ in.^{2}lb.

C   (b)

20 in.

$\bar{a} = 10$

500 lb.   500 lb.   (c)

                                                    M_B

R_A R_B
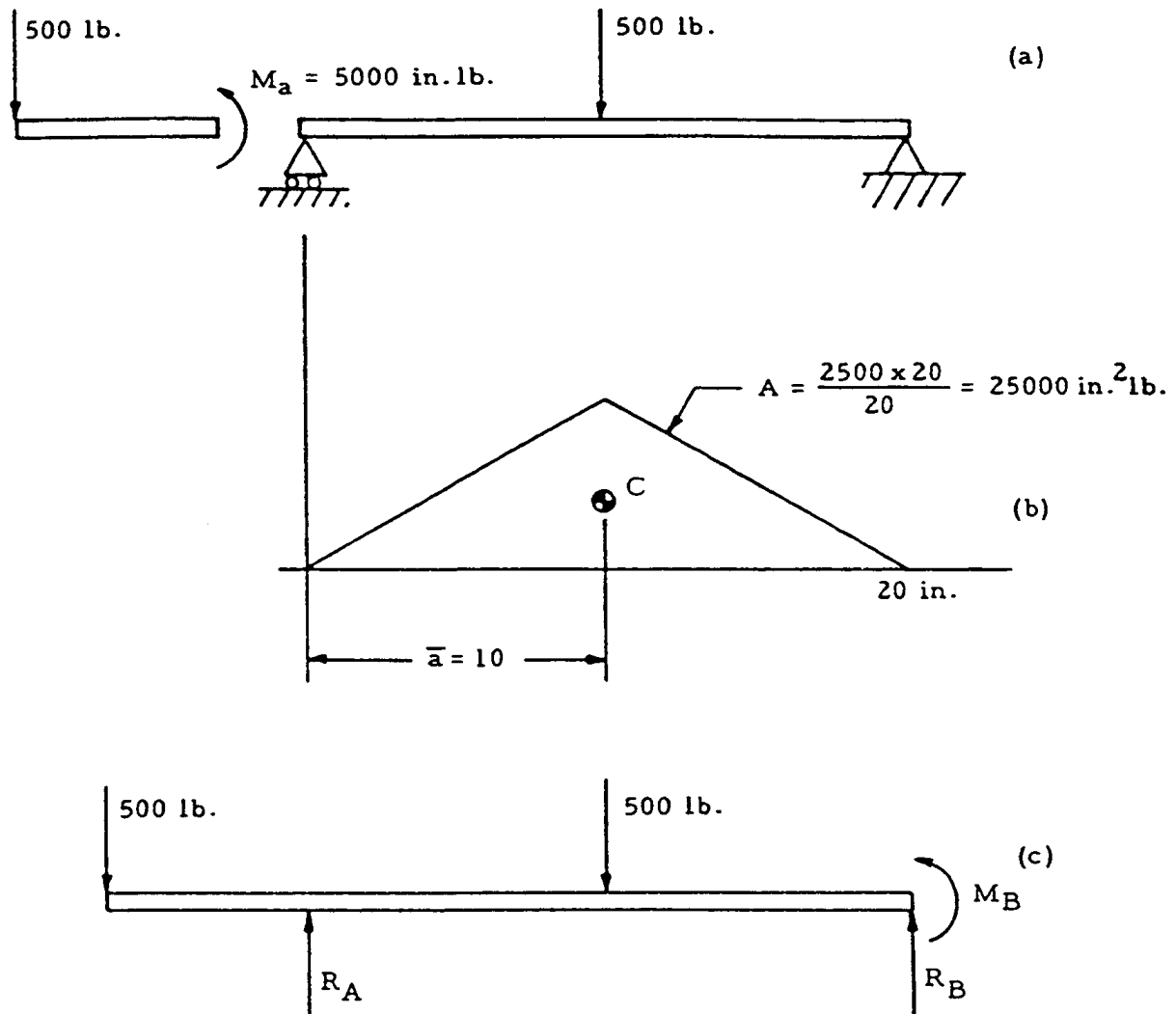
Figure 1-33. Solution for the Reaction Forces and Moments on the Beam in Figure 1-31

1.3.4.3 Reaction Forces and Moments on Beams with Both Ends Fixed

Figure 1-34(a) shows a uniform beam with both ends fixed. The following procedure may be used to determine the support reactions on such a beam if its stresses are in the elastic range.

1. Consider the beam to be simply supported as in Figure 1-34(b).

2. Find the moment diagram for this simply supported beam as in Figure 1-34(c). A is the area of the moment diagram and C is the centroid of this area.

1 - 49
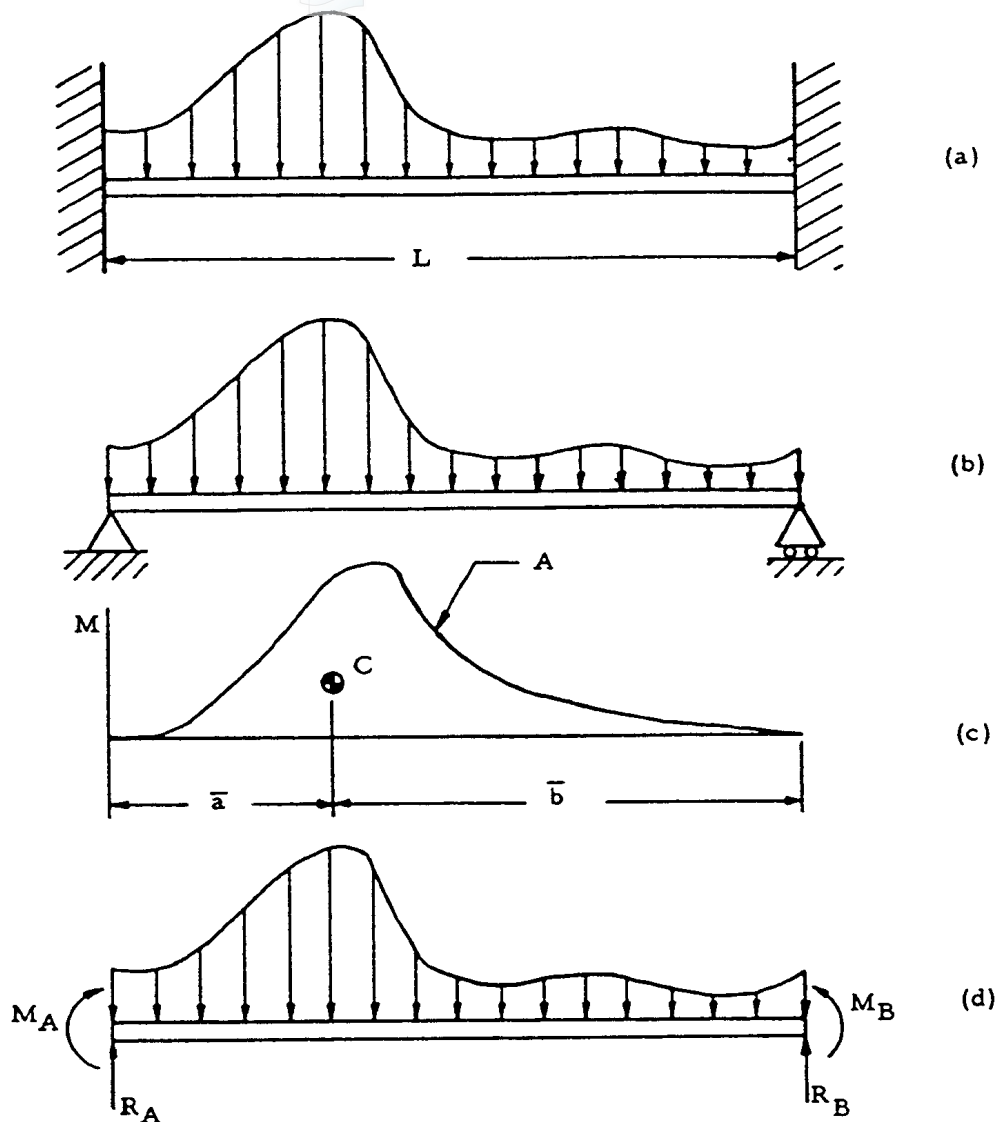
Figure 1-34.   Method of Determining Reaction Forces and Moments
on a Beam Fixed at One End and Pinned at One Point

3.   Find M_A and M_B by the equations

$$M_A = \frac{2A}{L^2} (2\overline{b} - \overline{a}) \tag{1-39}$$

$$M_B = \frac{2A}{L^2} (2\overline{a} - \overline{b}) \tag{1-40}$$

The evaluation of the terms in these equations may be facilitated
by the use of Table 1-10.

4.   Evaluate R_A and R_B by applying the equations of statics to
Figure 1-34(d).

Once the end reactions have been determined, the moment and shear diagrams
may be constructed for the beam.

1 - 50

The above procedure may be avoided by using Table 1-9 which gives equations for the reaction moments for beams fixed at both ends under various loadings. The sign convention for this table are as shown in Figure 1-34(d).

TABLE 1-9

End Moment Reactions for Beams with Both Ends Fixed Under Various Loadings
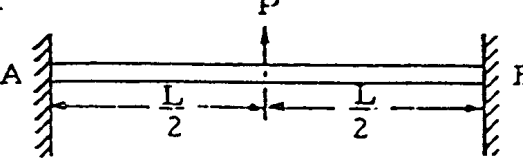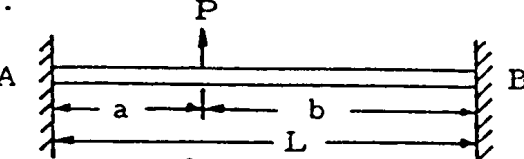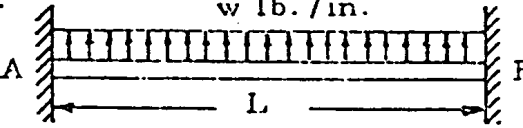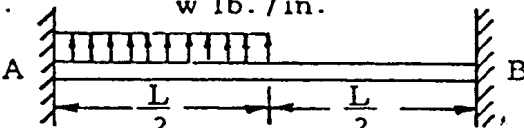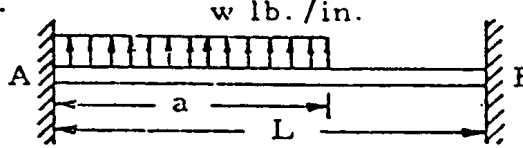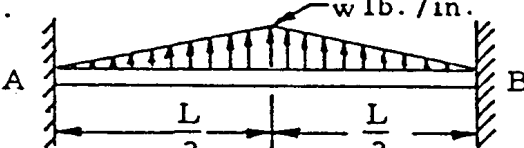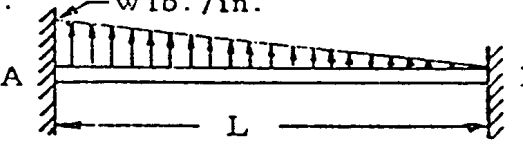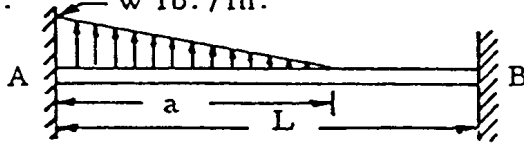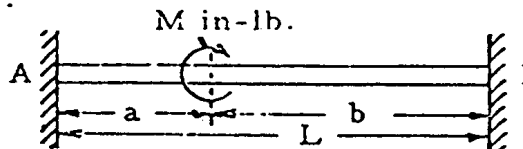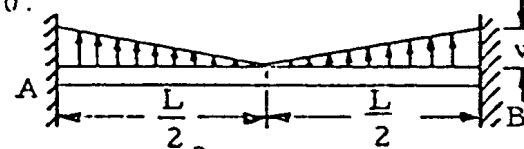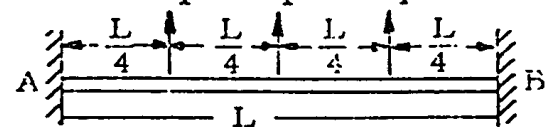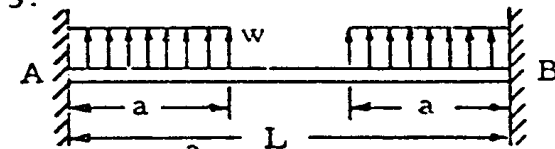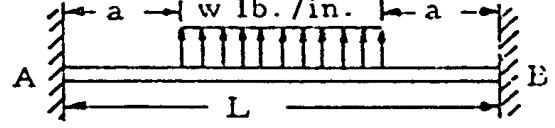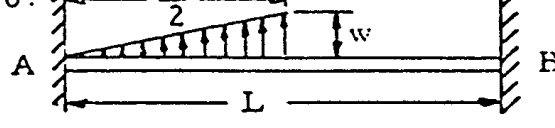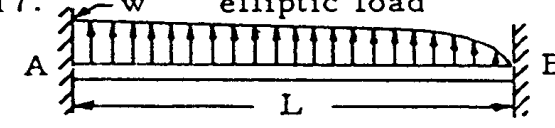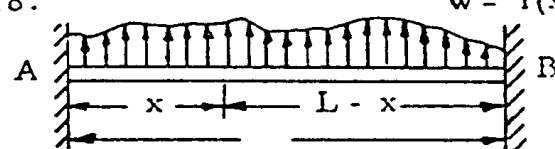
1.

$$M_A = \frac{PL}{8} \qquad M_B = \frac{PL}{8}$$

2.

$$M_A = \frac{Pab^2}{L^2} \qquad M_B = \frac{Pa^2 b}{L^2}$$

3.

$$M_A = \frac{wL^2}{12} \qquad M_B = \frac{wL^2}{12}$$

4.

$$M_A = \frac{11wL^2}{192} \qquad M_B = \frac{5wL^2}{192}$$

5.

$$M_A = \frac{wa^2}{12L^2}(6L^2 - 8aL + 3a^2)$$

$$M_B = \frac{wa^2}{12L^2}(4aL - 3a^2)$$

6.

$$M_A = \frac{5wL^2}{96} \qquad M_B = \frac{5wL^2}{96}$$

7.

$$M_A = \frac{wL^2}{20} \qquad M_B = \frac{wL^2}{30}$$

8.

$$M_A = \frac{wa^2}{60L^2}(10L^2 - 10aL + 3a^2)$$

$$M_B = \frac{wa^3}{60L^2}(5L - 3a)$$

9.

$$M_A = \frac{Mb}{L}\left(3\frac{a}{L} - 1\right), \quad M_B = \frac{Ma}{L}\left(3\frac{b}{L} - 1\right)$$

10.

$$M_A = \frac{wL^2}{32} \qquad M_B = \frac{wL^2}{32}$$

1 - 51

TABLE 1-9

End Moment Reactions for Beams with Both Ends Fixed
Under Various Loadings (concluded)

11. $M_A = Pa(1 - \frac{a}{L})$ $M_B = M_A$	12. $M_A = \frac{15PL}{48}$ $M_B = M_A$
13. $M_A = \frac{wa^2}{6L}(3L-2a)$ $M_B = M_A$	14. $M_A = \frac{w}{12L}(L^3 - a^2L + 4a^3) M_B = M_A$
15. $M_A = \frac{wa^2}{30}(10 - 15\frac{a}{L} + 6\frac{a^2}{L^2})$ $M_B = \frac{wa^2}{20}(5 - 4\frac{a}{L})$	16. $M_A = \frac{wL^2}{30}$ $M_B = \frac{3wL^2}{160}$
17. elliptic load $M_A = \frac{wL^2}{13.52}$ $M_B = \frac{wL^2}{15.86}$	18. $w = f(x)$ $M_A = \frac{1}{L^2} \int_0^L x(L-x)^2 f(x)dx$ $M_B = \frac{1}{L^2} \int_0^L x^2(L-x)f(x)dx$

1.3.4.4   Reaction Forces and Moments on Continuous Beams

A continuous beam is one with three or more supports. Such a beam is statically indeterminate and deflection equations must be applied to find the support reactions. The three-moment equation is such an equation.

1.3.4.5   Application of the Three Moment Equation to Solving for the Reactions on Continuous Beams

Figure 1-35(a) shows a uniform beam that is simply supported at three colinear points, A, B, and C. In order to obtain the reactions, the beam is broken into two simply supported sections with no end moments, as shown in Figure 1-35(b). The moment diagrams are then found for these sections and the area A and centroid C of these diagrams are found as shown in Figure 1-35(c). The quantities found may now be substituted into the three-moment equation:

$$M_A L_1 + 2M_B (L_1 + L_2) + M_C L_2 = \frac{-6A_1 \bar{a}_1}{L_1} - \frac{6A_2 \bar{b}_2}{L_2} \qquad (1-41$$

If M_A and M_C are known, this equation may be solved for the moment at B, M_B. Knowing this moment, the support reactions at A, B, and C may be found by applying the equations of statics.

The terms to the right of Equation (1-41) may be found for various simple loadings by use of Table 1-10.
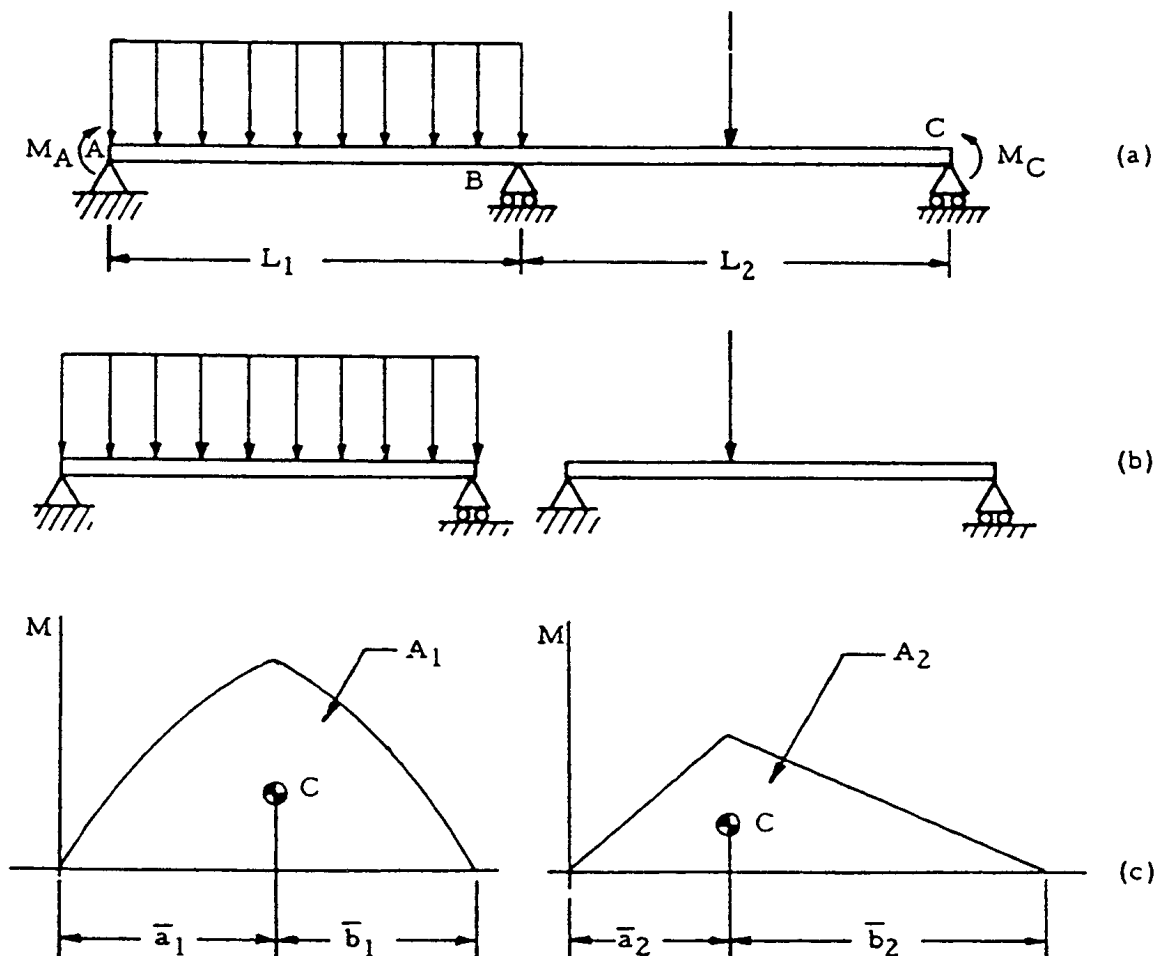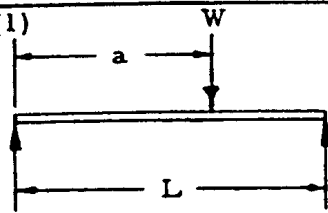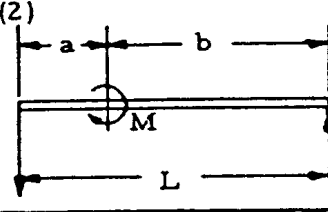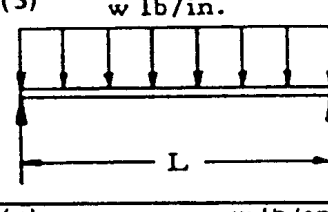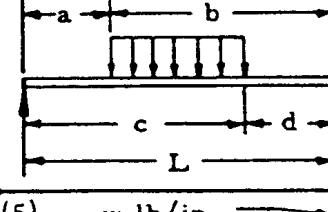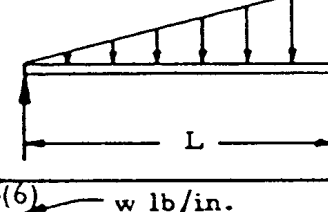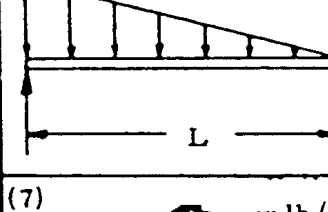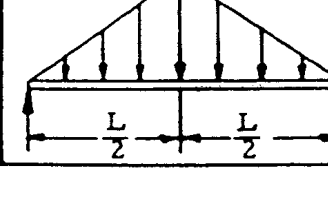
Figure 1-35.   Beam Simply Supported at Three Points

TABLE 1-10

Values of $\dfrac{6A\bar{a}}{L}$ and $\dfrac{6A\bar{b}}{L}$

Type of Loading on Span	$\dfrac{6A\bar{a}}{L}$	$\dfrac{6A\bar{b}}{L}$
(1)	$\dfrac{Wa}{L}(L^2 - a^2)$	$\dfrac{W}{L}(L-a)(2a-a^2)$
(2)	$-\dfrac{M}{L}(3a^2 - L^2)$	$+\dfrac{M}{L}(3b^2 - L^2)$
(3)	$\dfrac{wL^3}{4}$	$\dfrac{wL^3}{4}$
(4)	$\dfrac{W}{4L}\left[c^2(2L^2 - c^2) - a^2(2L^2 - a^2)\right]$	$\dfrac{W}{4L}\left[b^2(2L^2 - b^2) - d^2(2L^2 - d^2)\right]$
(5)	$\dfrac{8}{60}wL^3$	$\dfrac{7}{60}wL^3$
(6)	$\dfrac{7}{60}wL^3$	$\dfrac{8}{60}wL^3$
(7)	$\dfrac{5}{32}wL^3$	$\dfrac{5}{32}wL^3$

If a beam has a number of concentrated loads as shown in Figure 1-36, Equation (1-42) becomes

$$M_A L_1 + 2M_B (L_1 + L_2) + M_C L_2 = -\sum \frac{P_1 a_1}{L_1} (L_1^2 - a_1^2) - \sum \frac{P_2 b_2}{L_2} (L_2^2 - b_2^2) \quad (1-42)$$

where P_1 denotes any one of several concentrated loads which may act on the left span at a distance a_1 from support A. Similarly, P_2 denotes any load in the right span at a distance from support C.
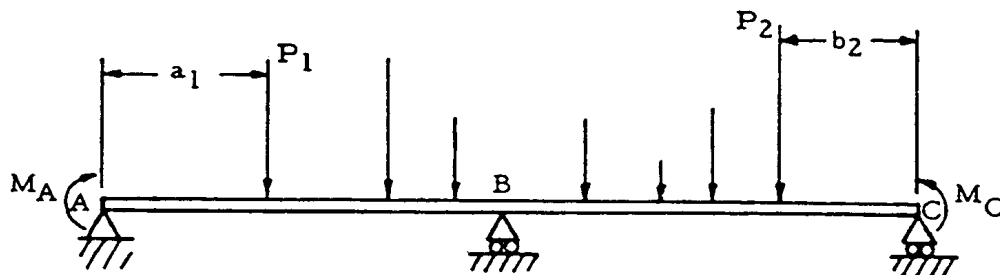
Figure 1-36. Continuous Beam Under Several Concentrated Loads

If a beam is simply supported at more than three points, the three-moment equation may be written for each intermediate support. The equations may then be solved simultaneously to obtain the moments at each support. This procedure is illustrated by the sample problem in Section 1.3.4.6.

1.3.4.6 Sample Problem - Reactions on Continuous Beams by the Three
Moment Equation

Given: The continuous beam shown in Figure 1-37.
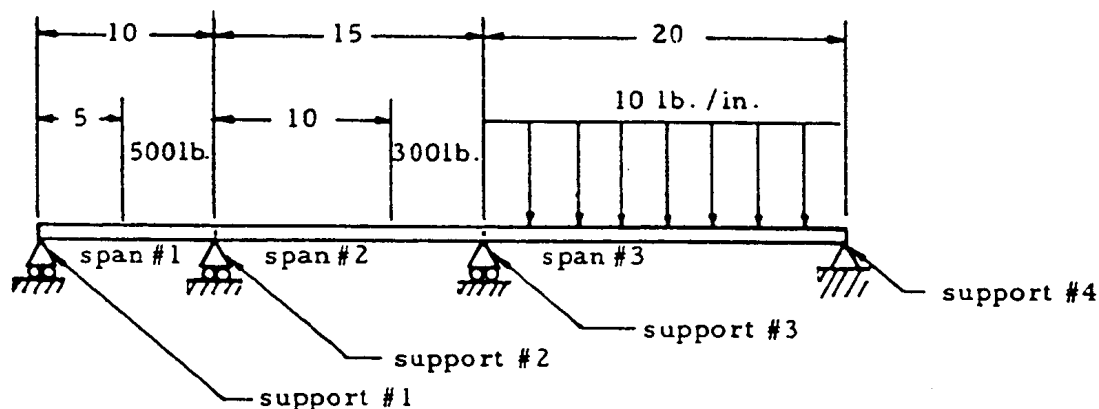
Figure 1-37. Continuous Beam on Four Supports

1 - 55

<u>Find</u>: The support reactions.

<u>Solution</u>: The three-moment equation may be written for spans 1 and 2. Since only concentrated loads are present, the special case given by Equation (1-42) may be used. Thus,

$$M_1 L_1 + 2M_2 (L_1 + L_2) + M_3 L_3 = \frac{-P_1 a_1}{L_1} (L_1^2 - a_1^2) - \frac{P_2 b_2}{L_2} (L_2^2 - b_2^2)$$

Inserting numerical values gives

$$0(10) + 2M_2 (10 + 15) + M_3(20) = \frac{-500(5)}{10} (10^2 - 5^2) - \frac{300(5)}{15} (15^2 - 5^2)$$

Simplifying gives $5M_2 + 2M_3 = 3875$.

The more general form of the three-moment equation given by Equation (1-41) may now be written for spans 2 and 3 with the aid of cases one and three of Table 1-10.

$$M_2(15) + 2M_3(15 + 20) = \frac{-300(10)}{15} (15^2 + 10^2) - \frac{10(20)^3}{4}$$

Simplifying gives $3M_2 + 14M_3 = -15,000$.

The two equations in M_2 and M_3 that were just obtained may be solved simultaneously to find that $M_2 = -376$ and $M_3 = -990$.

The equations of statics may now be applied as illustrated in Figure 1-38 to find the reaction forces.

(1)
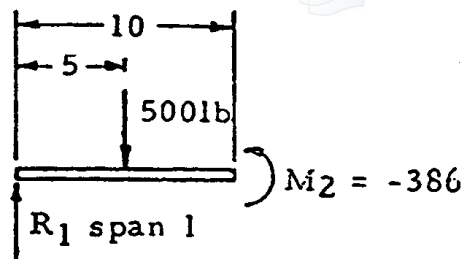
$$10\,R_1 - 5(500) = -386$$

Therefore, $R_1 = 211.4$ lb

(2)
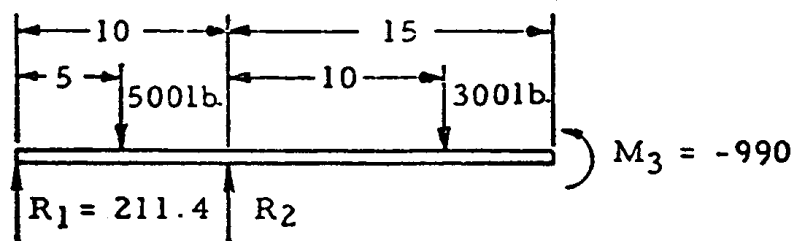
$$25(211.4) - 20(500) + 15\,R_2 - 5(300) = -990$$

Therefore, $R_2 = 348$ lb.

(3)
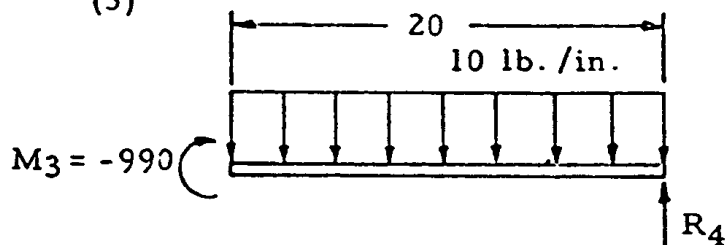
$$20\,R_4 - 10(200) = -990$$

Therefore, $R_4 = 50.5$ lb.

(4) Summing the vertical forces gives

$$R_1 + R_2 + R_3 + R_4 - 500 - 300 - 200 = 0$$
$$211.4 + 348 + R_3 + 50.5 - 500 - 300 - 200 = 0$$

Therefore, $R_3 = 390.1$ lb.

Figure 1-38.   Solution for Reaction Forces

The beam may now be drawn as in Figure 1-39.
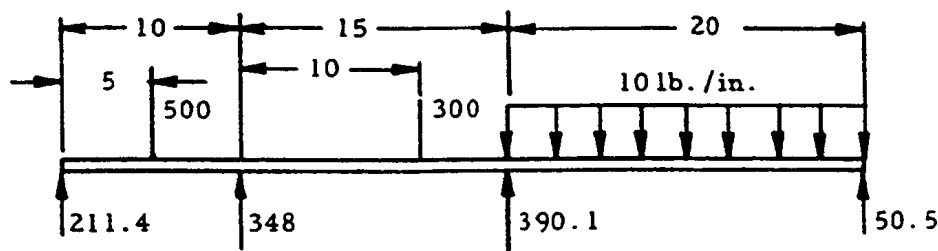
Figure 1-39. Continuous Beam on Four Supports with Reaction Forces

1.4 Introduction to Beams Under Combined Axial and Transverse Loads - Beam Columns

A beam under combined axial and transverse loads cannot be analyzed by simply superposing the effects of the two types of loading. The method of solution must take into account the simultaneous effect of these loads, and may thus become quite complex. Axial tension tends to straighten the beam, thus counteracting the bending moments produced by the transverse load. On the other hand, since axial compression may greatly increase the bending moment and the slope and deflection of the beam, it is the more serious type of axial load.

Two methods of analysis may be used to determine the total fiber stress in members under combined axial and transverse loads. The first method, which is approximate in nature, assumes that the elastic curve of the deflected member is similar in form to the curve for a like member under the action of transverse loads alone. The moment due to deflection is estimated on this assumption and combined with the moment due to transverse loads. This approximate method is treated in Section 1.4.1. The other method, which is the exact one, makes use of the differential equation of the elastic curve and is treated in Section 1.4.2. The criteria for the use of these methods is given in these sections.

1.4.1 Approximate Method for Beams Under Combined Axial and Transverse Loads - Beam Columns

For any condition of combined axial and transverse loading, the maximum stress in the extreme fiber is given by

$$f_{max} = \frac{P}{A} \pm \frac{M}{I/c} \qquad (1-43)$$

where P is the axial load and M is the maximum bending moment due to

the combined effect of axial and transverse loads. (The plus sign is for fibers in which the direct stress and the bending stress are in the same direction, the minus sign for fibers in which they are in opposite directions.) If a column is comparatively stiff so that the bending moment due to the axial load is negligible, M may be set equal to the maximum moment due to transverse loads M_t alone. This may be done with an error of less than five percent if $P < 0.125\ EI/L^2$ for cantilever beams, $P < 0.5\ EI/L^2$ for beams with pinned ends, or $P < 2EI/L^2$ for beams with fixed ends.

If $0.125\ EI/L^2 < P < 0.8\ EI/L^2$ for cantilever beams and $0.5\ EI/L^2 < P < 3\ EI/L^2$ for beams with fixed ends, the value of M for Equation (1-43) may be given by *

$$M = \frac{M_t}{\left(1 + K\ \dfrac{PL^2}{EI}\right)} \qquad (1\text{-}44)$$

for an error of less than five percent where K is given in Table 1-11 for various manners of loading and end support. The plus sign is used in the denominator if P is a tensile load and the minus sign is used if P is a compressive load. Equation (1-44) is appropriate only for beams in which the maximum bending moment and maximum deflection occur at the same section.

TABLE 1-11

Values of α for Equation (1-44)

Manner of Loading and Support	K
Cantilever, end load	1/3
Cantilever, uniform load	1/4
Pinned ends, center load	1/12
Pinned ends, uniform load	5/48
Equal and opposite end couples	1/8
Fixed ends, center load	1/24
Fixed ends, uniform load	1/32 (for end moments)
	1/16 (for center moments)

1.4.2 Exact Method for Beams Under Combined Axial and Transverse Loads - Beam Columns

Table 1-12 gives exact formulas for the bending moment, M, deflection, y, and end slope, θ, in beams which are subjected to

* Griffel, William, Handbook of Formulas for Stress and Strain

1 - 59

TABLE 1-12

Formulas for Beams Under Combined Axial and Transverse Loading
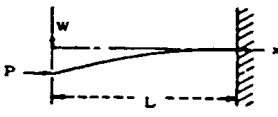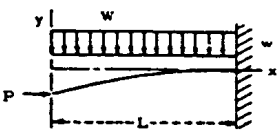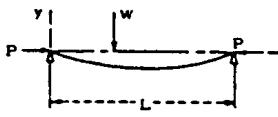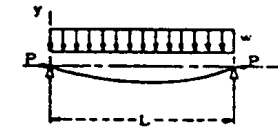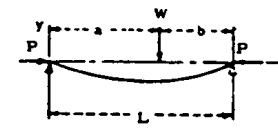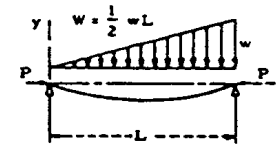
Case	Formulas
1.	Max M = -WL tan U/U at x = L Max y = $-\frac{W}{P}$ (L tan U/U - L) at x = 0 $\theta = \frac{W}{P}\left(\frac{1-\cos L/U}{\cos L/U}\right)$ at x = 0
2.	Max M = $-\frac{wL}{U}\left[L(1-\sec U)/U + L\tan U\right]$ at x = L Max y = $-\frac{wL}{PU}\left[\frac{L}{U}\left(1+\frac{1}{2}U^2 - \sec U\right) + L(\tan U - U)\right]$ at x = 0 $\theta = \frac{wL}{P}\left[\frac{1}{\cos U} - \frac{1-\cos 2U}{U\sin 2U}\right]$
3.	Max M = $\frac{WL}{2U}\tan\frac{1}{2}U$ at x = $\frac{1}{2}L$ Max y = $\frac{1}{2}\frac{WL}{PU}\left(\tan\frac{1}{2}U - \frac{1}{2}U\right)$ at x = $\frac{1}{2}L$ $\theta = -\frac{W}{2P}\left(\frac{1-\cos\frac{1}{2}U}{\cos\frac{1}{2}U}\right)$ at x = 0
4.	Max M = $wL^2(\sec\frac{1}{2}U - 1)/U^2$ at x = L/2 Max y = $\frac{wL^2}{PU^2}\left(\sec\frac{1}{2}U - 1 - \frac{1}{8}U^2\right)$ at x = $\frac{1}{2}L$ $\theta = -\frac{wL}{PU}\left[-\frac{1}{2}U + \frac{1-\cos U}{\sin U}\right]$ at x = 0
5.	Moment equation: x = 0 to x = a: M = $\frac{\frac{WL}{U}\sin\frac{bU}{L}\sin\frac{xU}{L}}{\sin U}$; Max M at x = $\frac{\pi L}{2U}$ if $\frac{\pi L}{2U} < a$ Moment equation: x = a to x = L: M = $\frac{\frac{WL}{U}\sin\frac{aU}{L}\sin\frac{(L-x)U}{L}}{\sin U}$; Max M at x = $\left(L - \frac{\pi L}{2U}\right)$ if $\left(L-\frac{\pi L}{2U}\right) > a$ if $\frac{\pi L}{2U} > a$ and $\left(L - \frac{\pi L}{2U}\right) < a$, Max M is at x = a Deflection equation: x = 0 to x = a: y = $\frac{WL}{PU}\left(\frac{\sin\frac{bU}{L}\sin\frac{xU}{L}}{\sin U} - \frac{bxU}{L^2}\right)$ Deflection equation: x = a to x = L: y = $\frac{WL}{PU}\left(\frac{\sin\frac{aU}{L}\sin\frac{(L-x)U}{L}}{\sin U} - \frac{aU(L-x)}{L^2}\right)$ $\theta = -\frac{W}{P}\left(\frac{b}{L} + \frac{\sin\frac{aU}{L}}{\tan U} - \cos\frac{aU}{L}\right)$ at x = 0; $\theta = \frac{W}{P}\left(\frac{a}{L} - \frac{\sin\frac{aU}{L}}{\sin U}\right)$ at x = L
6.	Moment equation: x = 0 to x = L: M = $\frac{WL^2}{U^2}\left(\frac{\sin\frac{Ux}{L}}{\sin U} - \frac{x}{L}\right)$ Max M at x = $\frac{L}{U}\arccos\left(\frac{\sin U}{U}\right)$ Deflection equation: x = 0 to x = L: x = $-\frac{w}{P}\left(\frac{x^3}{6L} + \frac{\frac{L^2}{U^2}\sin\frac{Ux}{L}}{\sin U} - \frac{Lx}{U^2} - \frac{1}{6}Lx\right)$ $\theta = -\frac{w}{P}\left(\frac{L}{U\sin U} - \frac{L}{U^2} - \frac{1}{6}L\right)$ at x = 0 $\theta = \frac{w}{P}\left(\frac{L}{U\tan U} + \frac{L}{U^2} - \frac{1}{3}L\right)$ at x = L

1 – 60

TABLE 1-12

Formulas for Beams Under Combined Axial and Transverse Loading (continued)
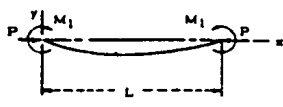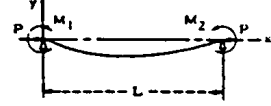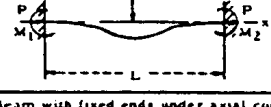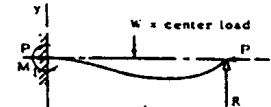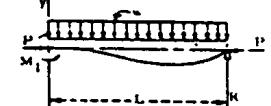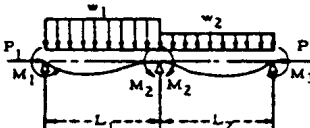
Case	Formulas
7.	$\text{Max } M = M_1 \sec \frac{1}{2}U \text{ at } x = \frac{1}{2}L$ $\text{Max } y = -\frac{M_1}{P}\left(\frac{1-\cos\frac{1}{2}U}{\cos\frac{1}{2}U}\right) \text{ at } x = \frac{1}{2}L$ $\theta = -\frac{M_1 U}{PL}\tan\frac{1}{2}U \text{ at } x = 0$
8.	Moment equation: $x = 0$ to $x = L$: $M = \left(\frac{M_2 - M_1\cos U}{\sin U}\right)\sin\frac{xU}{L} + M_1\cos\frac{xU}{L}$ $\text{Max } M \text{ at } x = \frac{L}{U}\arctan\left(\frac{M_2 - M_1\cos U}{M_1\sin U}\right)$ Deflection equation: $x = 0$ to $x = L$: $y = \frac{1}{P}\left[M_1 + (M_2-M_1)\frac{x}{L} - (M_2-M_1\cos U)\frac{\sin\frac{xU}{L}}{\sin U} - M_1\cos\frac{xU}{L}\right]$ $\theta = \frac{1}{P}\left[\frac{M_2-M_1}{L} - \frac{U(M_2-M_1\cos U)}{L\sin U}\right] \text{ at } x = 0$ $\theta = \frac{1}{P}\left[\frac{M_2-M_1}{L} - \frac{U(M_2-M_1\cos U)}{L\sin U}\cos U + \frac{M_1 U}{L}\sin U\right] \text{ at } x = L$
9. Beam with fixed ends under axial compression and transverse center load 	$M_1 = M_2 = \frac{WL}{2U}\left(\frac{1-\cos\frac{1}{2}U}{\sin\frac{1}{2}U}\right)$ At $x = \frac{L}{2}$ $M = \frac{WL}{2U}\left(\tan\frac{1}{2}U - \frac{1-\cos\frac{1}{2}U}{\sin\frac{1}{2}U\cos\frac{1}{2}U}\right)$ $\text{Max } y = \frac{WL}{2PU}\left[\tan\frac{1}{2}U - \frac{1}{2}U - \frac{(1-\cos\frac{1}{2}U)^2}{\sin\frac{1}{2}U\cos\frac{1}{2}U}\right]$
10. Beam with fixed ends under axial compression and uniform transverse load 	$M_1 = M_2 = \frac{wL^2}{U^2}\left(1 - \frac{\frac{1}{2}U}{\tan\frac{1}{2}U}\right)$ At $x = \frac{L}{2}$ $M = \frac{wL^2}{U^2}\left(\frac{\frac{1}{2}U}{\sin\frac{1}{2}U} - 1\right)$ $\text{Max } y = \frac{wL^2}{PU^2}\left[-\left(1 - \frac{U}{\tan U}\right)\left(\frac{1-\cos\frac{1}{2}U}{\cos\frac{1}{2}U}\right) + \sec\frac{1}{2}U - \frac{1}{8}U^2 - 1\right]$
11. Beams with one end fixed, other end pinned under axial compression and transverse center load 	$\text{Max } M = M_1 = \frac{WL}{2U}\left[\frac{\tan U(\sec\frac{1}{2}U-1)}{L\tan U - L}\right]$ $R = \frac{1}{2}W - \frac{M_1}{L}$ Moment equation $x = \frac{L}{2}$ to $x = L$: $M = M_1\left(\frac{\sin\frac{Ux}{L}}{\tan U} - \cos\frac{Ux}{L}\right) + \frac{WL}{U}\left(\sin\frac{1}{2}U\cos\frac{Ux}{L} - \frac{\sin\frac{1}{2}U\sin\frac{Ux}{L}}{\tan U}\right)$ Deflection equation $x = \frac{L}{2}$ to $x = L$: $y = -\frac{1}{P}\left\{M_1\left(1 - \frac{x}{L} + \frac{\sin\frac{Ux}{L}}{\tan U} - \cos\frac{Ux}{L}\right) + \frac{WL}{U}\left[\frac{(L-x)U}{2L} + \frac{\sin\frac{1}{2}U\sin\frac{Ux}{L}}{\tan U} - \sin\frac{1}{2}U\cos\frac{Ux}{L}\right]\right\}$
12. Beams with one end fixed, other end supported, under axial compression and uniform transverse load 	$\text{Max } M = M_1 = \frac{wL^2}{U^2}\left[\frac{\tan U(\tan\frac{1}{2}U - \frac{1}{2}U)}{\tan U - U}\right]$ $R = \frac{1}{2}wL - \frac{M_1}{L}$ Moment equation: $x = 0$ to $x = L$: $M = M_1\left(\cot U\sin\frac{Ux}{L} - \cos\frac{Ux}{L}\right) - w\frac{L^2}{U^2}\left[\frac{\sin\frac{Ux}{L}}{\sin U}(1-\cos U) - \cos\frac{Ux}{L} + 1\right]$ Deflection equation $x = 0$ to $x = L$: $y = -\frac{1}{P}\left\{M_1\left(1 - \frac{x}{L} - \cot U\sin\frac{Ux}{L} - \cos\frac{Ux}{L}\right) - w\frac{L^2}{U^2}\left[\cot U\sin\frac{Ux}{L} - \frac{\sin\frac{Ux}{L}}{\sin U} - \cos\frac{Ux}{L} - \frac{(Lx-x^2)U^2}{2L^2} + 1\right]\right\}$
13. Same as Case 1 (cantilever with end load) except that P is tension	$\text{Max } M = -WL\tanh U/U \text{ at } x = L$ $\text{Max } y = \frac{W}{P}\left(L - \frac{L}{U}\tanh U\right) \text{ at } x = 0$
14. Same as Case 2 (cantilever with uniform load) except that P is tension	$\text{Max } M = -wL\left[L\tanh U - \frac{L}{U}(1-\operatorname{sech} U)\right]/U \text{ at } x = L$ $\text{Max } y = -\frac{wL}{PU}\left[\frac{L}{U}\left(1 - \frac{1}{2}U^2 - \operatorname{sech} U\right) - L\tanh(U-U)\right] \text{ at } x = 0$
15. Same as Case 3 (pinned ends, center load) except that P is tension	$\text{Max } M = \frac{WL}{U}\tanh\frac{1}{2}U \text{ at } x = \frac{1}{2}L$ $\text{Max } y = -\frac{W}{P}\left(\frac{1}{4}L - \frac{L}{2U}\tanh\frac{1}{2}U\right) \text{ at } x = \frac{1}{2}L$
16. Same as Case 4 (pinned ends, uniform load) except that P is tension	$\text{Max } M = wL^2(1-\operatorname{sech}\frac{1}{2}U)/U^2$ $\text{Max } y = -\frac{w}{P}\left[\frac{1}{8}L^2 - \frac{L^2}{U^2}\left(1 - \operatorname{sech}\frac{1}{2}U\right)\right]$
17. Same as Case 9 (fixed ends, center load) except that P is tension	$M_1 = M_2 = \frac{WL}{2U}\left(\frac{\cosh\frac{1}{2}U - 1}{\sinh\frac{1}{2}U}\right)$, $\qquad \text{Max } M = \frac{WL}{2U}\left(\frac{1-\cosh U}{\sinh\frac{1}{2}U\cosh\frac{1}{2}U} - \tanh\frac{1}{2}U\right) \text{ at } x = \frac{1}{2}L$ $\text{Max } y = \frac{WL}{2PU}\left[\frac{1}{2}U - \tanh\frac{1}{2}U - \frac{(1-\cosh\frac{1}{2}U)^2}{\sinh\frac{1}{2}U\cosh\frac{1}{2}U}\right]$

TABLE 1-12

Formulas for Beams Under Combined Axial and Transverse Loading (concluded)

Case	Formulas
18. Same as Case 10 (fixed ends, uniform load) except that P is tension	$M_1 = M_2 = \dfrac{wL^2}{U^2}\left(\dfrac{\frac{1}{2}U - \tanh\frac{1}{2}U}{\tanh\frac{1}{2}U}\right)$, Max $+ M = \dfrac{wL^2}{U^2}\left(1 - \dfrac{\frac{1}{2}U}{\sinh\frac{1}{2}U}\right)$ at $x = \frac{1}{2}L$) Max $y = -\dfrac{wL^2}{8PU^2}\left[\dfrac{4U(1-\cosh\frac{1}{2}U)}{\sinh\frac{1}{2}U} - U^2\right]$ at $x = \frac{1}{2}L$
19. Beam with ends pinned to rigid supports so horizontal displacement is prevented. Uniform transverse load and unknown axial tension.	$\dfrac{E^2 A^2 k^6}{w^2 l^8} U^9 = \dfrac{1}{24}U^3 - \dfrac{5}{4}U + \dfrac{5}{2}\tanh\dfrac{U}{2} + \dfrac{U}{4}\tanh^2\dfrac{U}{2}$ where $k = \sqrt{\dfrac{I}{A}}$ This equation is solved for U, and P determined therefrom When $C = \dfrac{wL^4}{16EAk^3}$ is small (less than 4), $P = \dfrac{68}{630}\dfrac{EIC^2}{L^2}\left(1 - \dfrac{\cdot 62}{2835}C^2\right)$ When C is large (greater than 15), $P = \dfrac{4EI}{L^2}\left[\left(\dfrac{C^2}{6}\right)^{\frac{2}{3}} - 2\right]$ When P has been found by one of the above formulas, M and y may be found by the formulas of Case 16
20. Continuous beam, spans 1 and 2 unequal and unequally loaded	$\dfrac{M_1 L_1}{I_1}\left(\dfrac{U_1 \csc U_1 - 1}{U_1^2}\right) + \dfrac{M_3 L_2}{I_2}\left(\dfrac{U_2 \csc U_2 - 1}{U_2^2}\right)$ $- M_2\left[\dfrac{L_1}{I_1}\left(\dfrac{1 - U_1 \cot U_1}{U_1^2}\right) + \dfrac{L_2}{I_2}\left(\dfrac{1 - U_2 \cot U_2}{U_2^2}\right)\right]$ $= \dfrac{w_1 L_1^3}{I_1}\left(\dfrac{\tan\frac{1}{2}U_1 - \frac{1}{2}U_1}{U_1^3}\right) + \dfrac{w_2 L_2^3}{I_2}\left(\dfrac{\tan\frac{1}{2}U_2 - \frac{1}{2}U_2}{U_2^3}\right)$ (Theorem of Three Moments: Subscripts with P, L, w, I, and U refer to first and second spans. M_2 acts on span 1, M_2' on span 2)

combined axial and transverse loading. Although these formulas should be used if $P > 0.125\ EI/L^2$ for cantilever beams, $P > 0.5\ EI/L^2$ for beams with pinned ends, or $P > 2\ EI/L^2$ for beams with fixed ends, they may be used for beams with smaller axial loads. In these formulas, $U = L\sqrt{P/EI}$. The quantity U may be found rapidly through the use of the nomogram in Figure 1-40. The formulas for beams under a compressive axial load may be modified to hold for a tensile axial load by making the following substitutions: $-P$ for P; $U\sqrt{-1}$ for U; $\sqrt{-1}\sinh U$ for $\sin U$; and $\cosh U$ for $\cos U$. This has been done for some of the more common loadings and the resulting formulas given in cases 13 to 18 of Table 1-12.
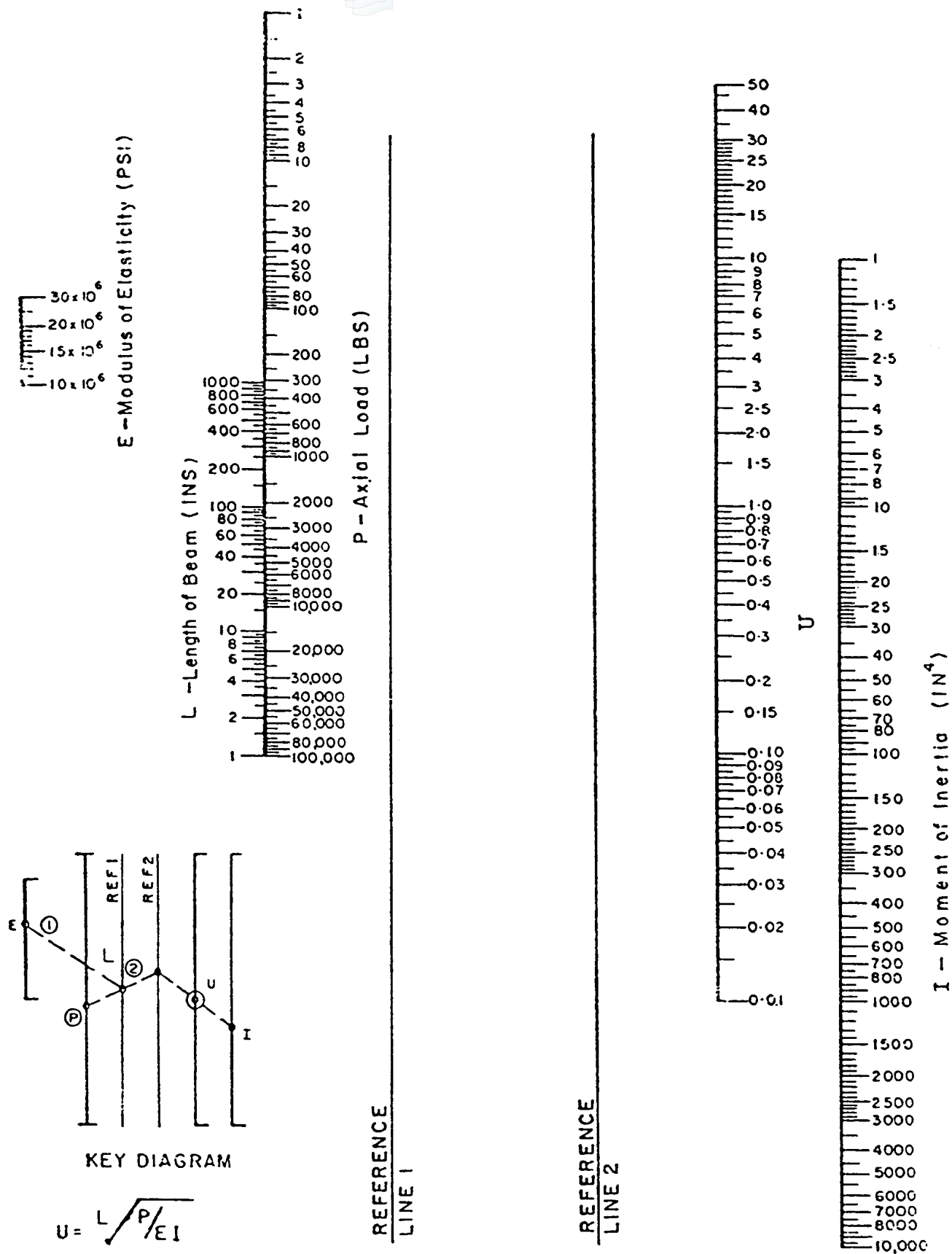
Figure 1-40. Nomogram for Determining U *

* Griffel, William, Handbook of Formulas for Stress and Strain

$$U = {}^L\!\sqrt{P/EI}$$

KEY DIAGRAM

1.4.3   Sample Problem - Beams Under Combined Axial and Transverse
Loads - Beam Columns

Given: The beam column shown in Figure 1-41.
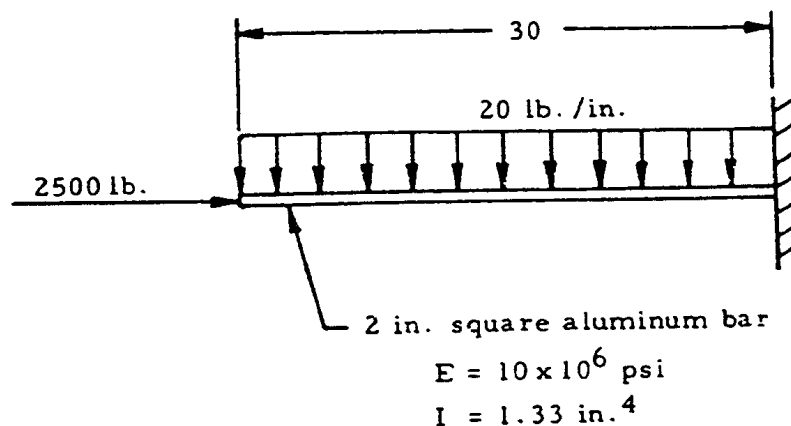
Figure 1-41.   Cantilever Beam Under Combined Axial and
Transverse Loads

Find: The maximum bending moment, M, vertical deflection,
y, and angular deflection, θ, of the bar.

Solution:

$$0.125 \frac{EI}{L^2} = 0.125 \frac{(10 \times 10^6)(1.33)}{(30)^2} = 1,850 \text{ lb.}$$

According to Section 1.4.2, the exact method must be used
for cantilever beams if $P < 0.125 \, EI/L^2$ as is true in this
case. From Figure 1-40,

$$U = L \sqrt{\frac{P}{EI}} = 30 \sqrt{\frac{2500}{(10 \times 10^6)(1.33)}} = 0.41$$

From Table 1-12, Case 2,

$$\text{Max } M = \frac{-wL}{U} \left[\frac{L}{U} \left(1 - \sec U \right) + L \tan U \right]$$

$$= \frac{-20 (30.0)}{0.41} \left[\frac{30.0 (1 - \sec 0.41)}{0.41} + 30 \tan 0.41 \right] = 8200 \text{ in. lb.}$$

1 - 64

$$\text{Max } y = \frac{-wL}{PU}\left[\frac{L}{U}\left(1 + \frac{1}{2}U^2 - \sec U\right) + L(\tan U - U)\right]$$

$$= \frac{=20(30.0)}{2500(0.40)}\left\{\left[\frac{30}{0.41}\left(1 + \frac{0.41^2}{2} - \sec 0.41\right)\right]\right.$$

$$\left. + \left[30(\tan 0.41 - 0.41)\right]\right\} = 2.92 \text{ in.}$$

$$\theta = \frac{w}{P}\left[\frac{L}{\cos U} - \frac{L}{U}\left(\frac{1-\cos 2U}{\sin 2U}\right)\right]$$

$$= \frac{20}{2500}\left[\frac{30}{.915} - \frac{30}{0.41}\left(\frac{1-\cos 0.82}{\sin 0.82}\right)\right] = 0.0095 \text{ rad}$$

$$= 0.55°$$

1.5 Introduction to Beams in Torsion

For purposes of discussion, beams in torsion are broken into two categories: circular beams, which are treated in Section 1.5.1, and non-circular beams, which are treated in Section 1.5.2. Circular beams are further divided into those with uniform cross sections (Section 1.5.1.1) and those with nonuniform cross sections (Section 1.5.1.2). Noncircular beams are divided into open noncircular beams (Section 1.5.2.1) and closed or hollow ones (Section 1.5.2.2), and the effect of end restraint on non-circular beams is treated in Section 1.5.2.3.

Section 1.5.3 treats the membrane and sandheap analogies for beams in torsion. Since the loading of the wires of helical springs is primarily torsional, they are listed under beams in torsion and treated in Section 1.5.4.

1.5.1 Circular Beams in Torsion

This section considers the torsion of solid or concentrically hollow circular beams.

1.5.1.1 Uniform Circular Beams in Torsion

Figure 1-42 shows a uniform circular beam in pure torsion. If the stresses in such a beam are in the elastic range, the stress distribution at a cross section is as shown in Figure 1-43.
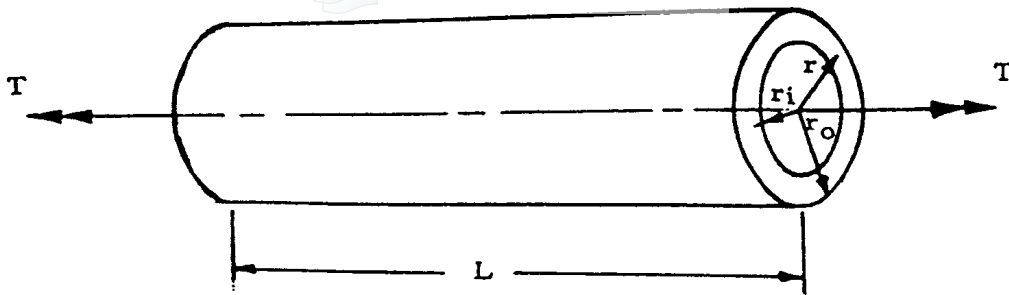
Figure 1-42.   Uniform Circular Beam in Torsion
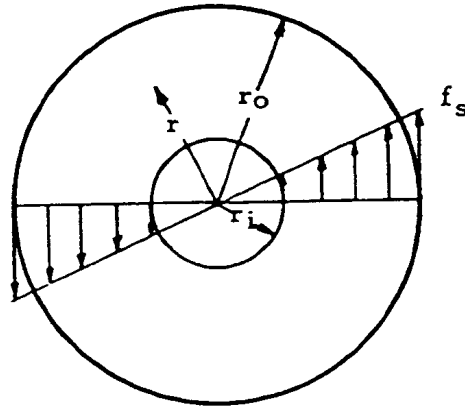
Figure 1-43.   Stress Distribution of Circular Beam in Torsion

The shear stress at a distance r from the center is given by

$$f_s = \frac{Tr}{I_p}$$
(1-45)

The angle of twist of the beam is

$$\theta = \frac{TL}{GI_p}$$
(1-46)

Inserting the value of I_p for a circular cross section into Equations (1-45) and (1-46) gives

$$f_s = \frac{2\,Tr}{\pi\,(r_o^{\,4} - r_i^{\,4})}$$
(1-47)

and

$$\theta = \frac{2\,TL}{\pi\,(r_o^{\,4} - r_i^{\,4})G}$$
(1-48)

1 - 66

In order to treat solid circular shafts, r_i may be set equal to zero in Equations (1-47) and (1-48).

It should be noted that Equations (1-47) and (1-48) apply only to beams with circular cross sections.

The maximum shear stress occurs at the outside surfaces of the beam and may be computed by setting r equal to r_0 in Equation (1-47). The maximum tensile and compressive stresses also occur at the outside surface and both are equal in magnitude to the maximum shear stress.

If a circular beam is twisted beyond the yield point until the outer portions are at the ultimate torsional stress, a stress distribution such as that shown in Figure 1-44 is obtained. The maximum torque that such a beam may sustain in static loading is given by

$$T_{max} = \frac{F_{st} I_p}{r_o} \qquad (1-49)$$

where F_{st} is designated as the torsional modulus of rupture. This torsional modulus of rupture is shown graphically for steel beams in Figure 1-45.
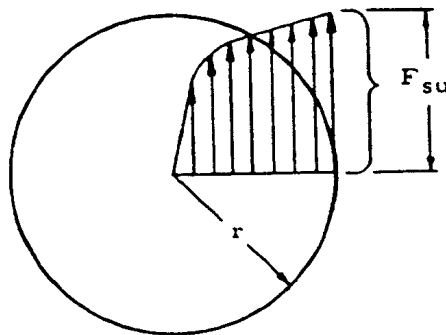
Figure 1-44. Plastic Stress Distribution of Circular Beam in Torsion
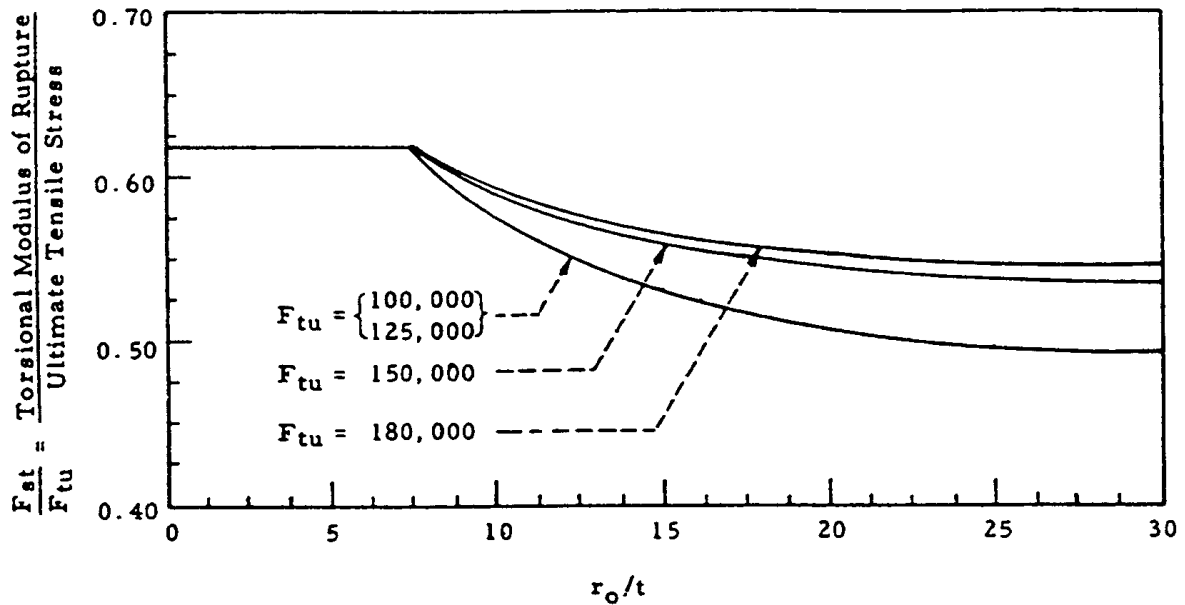
Figure 1-45. Torsional Modulus of Rupture for Steel Beams

In many cases, the torsional modulus of rupture of a material may not be available. These may be treated by assuming the uniform shear stress distribution shown in Figure 1-46.
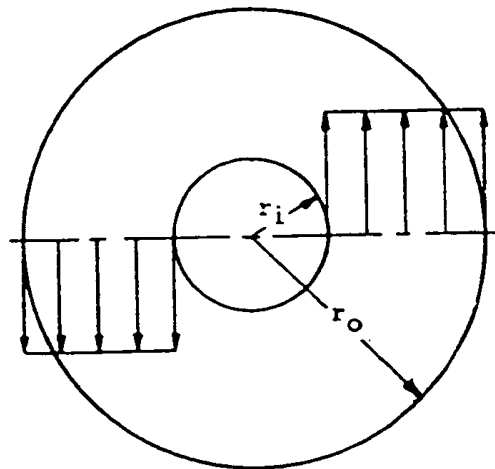
Figure 1-46. Assumed Plastic Stress Distribution
of Circular Beam in Torsion

The magnitude of the uniform shear stress may be assumed to be equal to the yield shear stress (F_{sy}) for conservative results or the ultimate shear stress (F_{su}) for nonconservative results. In the first case, the maximum torque in the beam may be expressed as

1 - 68

$$T_{max} = \frac{4}{3} \frac{F_{sy} I_p}{r_o} \tag{1-50}$$

and in the second case, the maximum torque in the beam may be expressed as

$$T_{max} = \frac{4}{3} \frac{F_{su} I_p}{r_o} \tag{1-51}$$

It should be noted that the possibility of crippling in thin-walled tubes was not considered in the previous discussion. Crippling of circular tubes is treated in Chapter 8. This tubes should be checked for crippling.

1.5.1.2   Nonuniform Circular Beams in Torsion

When a circular beam of nonuniform cross section is twisted, the radii of a cross section become curved. Since the radii of a cross section were assumed to remain straight in the derivation of the equations for stress in uniform circular beams, these equations no longer hold if a beam is non-uniform. However, the stress at any section of a nonuniform circular beam is given with sufficient accuracy by the formulas for uniform bars if the diameter changes gradually. If the change in section is abrupt, as at a shoulder with a small fillet, a stress concentration must be applied as explained in Chapter 10.

Figure 1-47 shows a nonuniform circular beam in torsion.
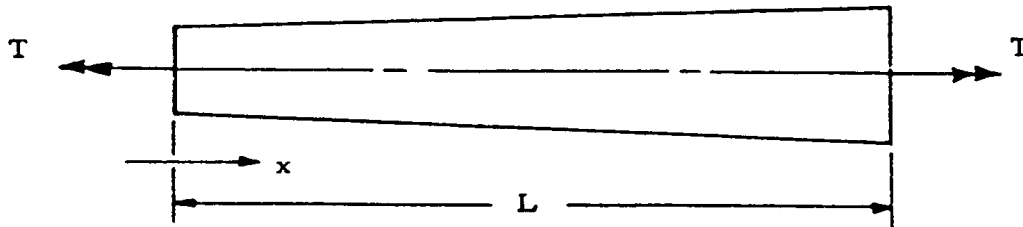
Figure 1-47.   Nonuniform Circular Beam in Torsion
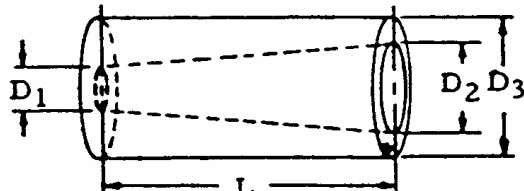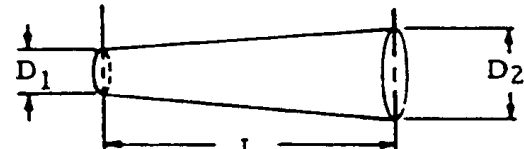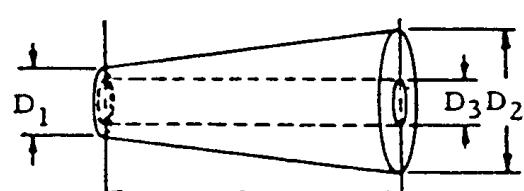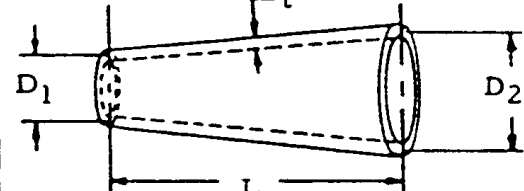
If its diameter changes gradually, its angle of twist is

$$\theta = \frac{T}{G} \int_o^L \frac{dx}{I_p} \tag{1-52}$$

This equation is used to obtain the formulas for θ for various beams of uniform taper that are shown in Table 1-13.

TABLE 1-13

Formulas for the Angle of Twist of Nonuniform Circular Beams in Torsion*

Type of Beam	Angle of Twist
inside taper, outside uniform	$\theta = \dfrac{8TL}{\pi G(D_2 - D_1)D_3^3}\left\{ 2\arctan\left(\dfrac{D_2}{D_3}\right) - 2\arctan\left(\dfrac{D_1}{D_3}\right) + \text{Log}_e\left[\left(\dfrac{D_3 + D_2}{D_3 - D_2}\right)\left(\dfrac{D_3 - D_1}{D_3 + D_1}\right)\right]\right\}$
solid beam, outside taper	$\theta = \dfrac{32TL}{3\pi G D_1 D_2}\left(\dfrac{1}{D_1^2} + \dfrac{1}{D_1 D_2} + \dfrac{1}{D_2^2}\right)$
inside uniform, outside taper	$\theta = \dfrac{8TL}{\pi G(D_2 - D_1)D_3^3}\left\{ 2\arctan\left(\dfrac{D_2}{D_3}\right) - 2\arctan\left(\dfrac{D_1}{D_3}\right) + \text{Log}_e\left[\left(\dfrac{D_3 + D_2}{D_3 - D_2}\right)\left(\dfrac{D_3 - D_1}{D_3 + D_1}\right)\right]\right\}$
thin tapered tube with uniform wall thickness	$\theta = \dfrac{2TL(D_1 + D_2)}{\pi G t D_1^2 D_2^2}$

* Griffel, William, Handbook of Formulas for Stress and Strain

1 - 70

1.5.1.3   Sample Problem - Circular Beams in Torsion

Given: The circular beam shown in Figure 1-48.

Aluminum - G = 4×10^6 psi

Figure 1-48.   Tapered Circular Solid Beam in Torsion

Find: The angle of twist and maximum stress in the beam.

Solution: From Table 1-13.

$$\theta = \frac{32\,TL}{3\pi\,GD_1D_2}\left(\frac{1}{D_1^2} + \frac{1}{D_1D_2} + \frac{1}{D_2^2}\right)$$

$$= \frac{32(10000)(20)}{3\pi(4\times10^6)(2.5)(3)}\left(\frac{1}{2.5^2} + \frac{1}{2.5(3)} + \frac{1}{3^2}\right) = 0.0091 \text{ rad.}$$

$$= 0.52°$$

Applying Equation (1-47) to the outside of the thin end of the beam

$$f_{smax} = \frac{2\,Tr}{\pi(r_o^4 - r_i^4)} = \frac{2(10000)(1.25)}{\pi(1.25^4 - 0^4)} = 3,260 \text{ psi}$$

1.5.2   Noncircular Beams in Torsion

In the derivation of formulas for circular beams in torsion, it was assumed that plane sections remain plane and radii remain straight in the deformed configuration. Since these assumptions no longer hold for noncircular sections, the equations for circular sections do not hold. The warping of plane sections of a square bar under torsion is illustrated in Figure 1-49.

Figure 1-49.   Warping of the Sections of a Square Bar in Torsion

1.5.1.3 Sample Problem - Circular Beams in Torsion

Given: The circular beam shown in Figure 1-48.

Aluminum - $G = 4 \times 10^6$ psi

Figure 1-48. Tapered Circular Solid Beam in Torsion

Find: The angle of twist and maximum stress in the beam.

Solution: From Table 1-13.

$$\theta = \frac{32\,TL}{3\pi\,GD_1 D_2} \left(\frac{1}{D_1^{\,2}} + \frac{1}{D_1 D_2} + \frac{1}{D_2^{\,2}} \right)$$

$$= \frac{32(10000)(20)}{3\pi(4 \times 10^6)(2.5)(3)} \left(\frac{1}{2.5^2} + \frac{1}{2.5(3)} + \frac{1}{3^2} \right) = 0.0091 \text{ rad.}$$

$$= 0.52°$$

Applying Equation (1-47) to the outside of the thin end of the beam

$$f_{max} = \frac{2\,Tr}{\pi(r_o^{\,4} - r_i^{\,4})} = \frac{2(10000)(1.25)}{\pi(1.25^4 - 0^4)} = 3,260 \text{ psi}$$

1.5.2 Noncircular Beams in Torsion

In the derivation of formulas for circular beams in torsion, it was assumed that plane sections remain plane and radii remain straight in the deformed configuration. Since these assumptions no longer hold for non-circular sections, the equations for circular sections do not hold. The warping of plane sections of a square bar under torsion is illustrated in Figure 1-49.

Figure 1-49. Warping of the Sections of a Square Bar in Torsion

The angle of twist of an elliptical beam of length, L, is

$$\theta = \frac{T(a^2 + b^2)L}{\pi a^3 b^3 G}$$

(1-56)

1.5.2.1.2 Rectangular Beams in Torsion

Figure 1-51 shows a rectangular beam in torsion. The maximum stress in such a beam occurs at the center of the long side and is given by

$$f_{smax} = \frac{T}{a b t^2}$$

(1-57)

where α is a constant given in Table 1-14. The angle of twist of a rectangular beam in tension is

$$\theta = \frac{TL}{\beta bt^3 G}$$

(1-58)

where β is given in Table 1-14.
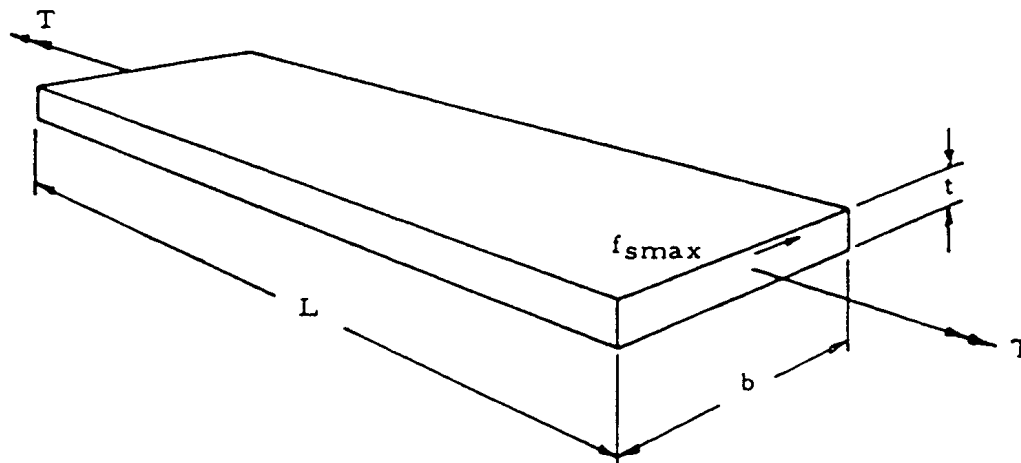
Figure 1-51. Rectangular Beam in Torsion

TABLE 1-14

Constants for Equations (1-57) and (1-58)

b/t	1.00	1.50	1.75	2.00	2.50	3.00	4	6	8	10	∞
α	0.208	0.231	0.239	0.246	0.258	0.267	0.282	0.299	0.307	0.313	0.333
β	0.141	0.196	0.214	0.229	0.249	0.263	0.281	0.299	0.307	0.313	0.333

The maximum stress and angle of twist of a rectangular beam in torsion may also be computed with satisfactory accuracy (error less than 4%) from the following equations:

$$f_{s_{max}} = \frac{T}{bt^3} \left(3 + 1.8 \frac{t}{b} \right) \tag{1-59}$$

$$\theta = \frac{3\,TL}{bt^3 \left[1 - \frac{0.63t}{b} \left(1 - \frac{t^4}{12\,b^4} \right) \right]} \tag{1-60}$$

1.5.2.1.3   Noncircular Beams with Thin Open Sections in Torsion

If a rectangular beam is very thin relative to its length (b>>t) Equations (1-59) and (1-60) become

$$f_{s_{max}} = \frac{3T}{bt^2} \tag{1-61}$$

and

$$\theta = \frac{3\,TL}{bt^3\,G} \tag{1-62}$$

From Table 1-14, it can be seen that these expressions are correct within 10 percent if b/t = 8.

Although Equations (1-61) and (1-62) have been developed for rectangular beams, they can be applied to the approximate analysis of shapes made up of thin rectangular members such as those in Figure 1-52. If sharp corners exist, however, large stress concentrations may result so that Equation (1-61) is not valid. The effect of sharp corners is explained by the membrane analogy in Section 1.5.3.1. Equations (1-61) and (1-62) may be applied directly to sections such as those at the top of Figure 1-52 if b is taken to be the developed length of the cross section as shown.

If a thin section is composed of a number of thin rectangular sections as are those at the bottom of Figure 1-52, the following equations may be applied:

$$\theta = \frac{3\,TL}{G\Sigma\,bt^3} = \frac{3\,TL}{G(b_1 t_1^3 + b_2 t_2^3 + \dots)} \tag{1-63}$$

$$f_{s_{max_1}} = \frac{3\,T\,t_1}{\Sigma\,bt^3} = \frac{3\,T\,t_1}{b_1 t_1^3 + b_2 t_2^3 + \dots} \tag{1-64}$$

1 - 74

$$f_{smax_2} = \frac{3\,T\,t_2}{\Sigma\,bt^3} = \frac{3\,T\,t_2}{b_1 t_1^3 + b_2 t_2^3 + \ldots} \qquad (1\text{-}65)$$

$$f_{smaxn} = \frac{3\,T\,t_n}{\Sigma\,bt^3} = \frac{3\,T\,t_n}{b_1 t_1^3 + b_2 t_2^3 + \ldots} \qquad (1\text{-}66)$$

In the above equations, f_{smaxn} is the maximum stress in the nth rectangular portion of the section, L is the beam length, and T is the applied torque.

If a section is composed of thick rectangular sections, the equations in Section 1.5.2.1.5 should be used. The advantage of the equations in this section is that they may be applied to specific shapes for which a more exact formula may not be available.
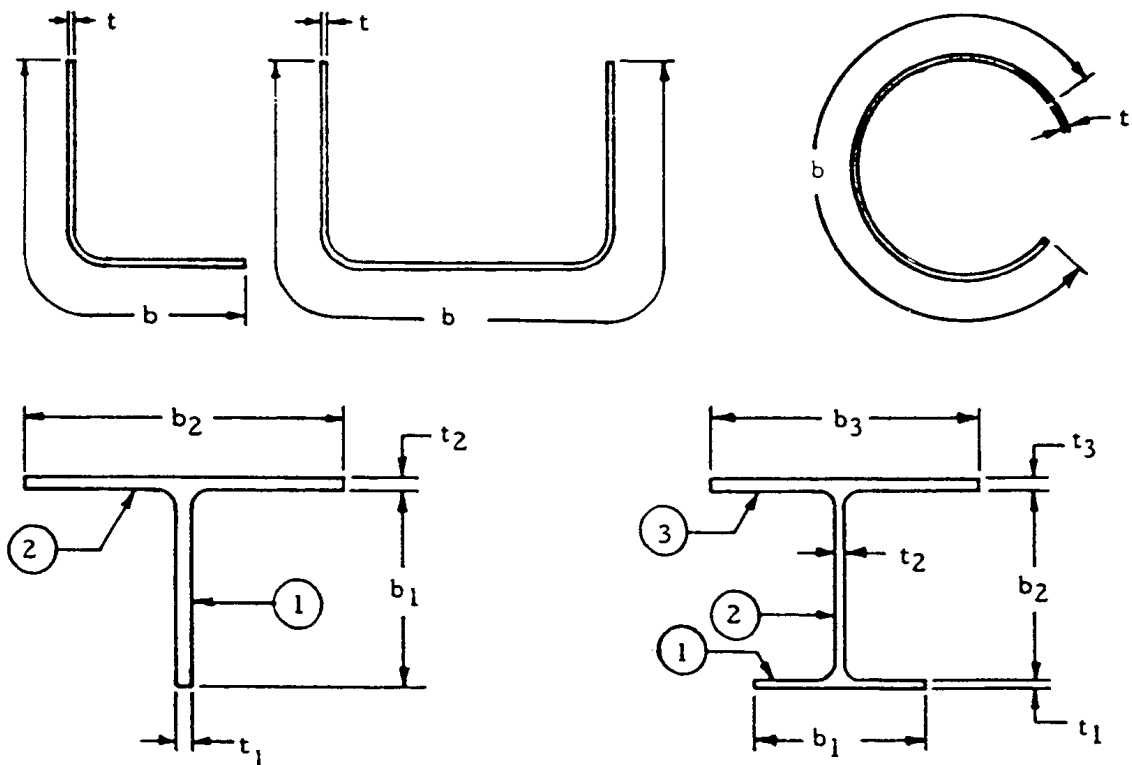
Figure 1-52.   Beams Composed of Thin Rectangular Members

1.5.2.1.4   Sample Problem - Noncircular Beams with Thin Open Sections in Torsion

Given: A 50-in.-long beam with a cross section such as that shown in Figure 1-53 under a torsional load of 500 in. lb.

1 - 75

$t = 0.125$ $G = 4 \times 10^{-6}$ psi

$r = 1$
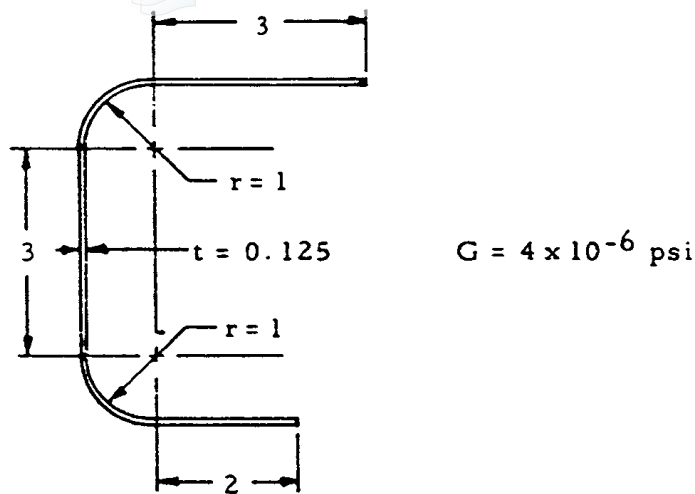
Figure 1-53.   Thin Open Section

Find: The maximum shear stress and the angle of twist of the beam.

Solution: The developed length of the section is

$$b = 3 + 3 + 2 + \pi = 11.14 \text{ in.}$$

Equations (1-61) and (1-62) may now be applied to obtain

$$f_{max} = \frac{3\,T}{b\,t^2} = \frac{3(500)}{(11.14)(0.125)^2} = 8,610 \text{ psi}$$

and

$$\theta = \frac{3\,TL}{b\,t^3\,G} = \frac{3(500)(50)}{11.14(0.125)^3(4 \times 10^6)} = 0.86 \text{ rad.} = 49°$$

1.5.2.1.5   Noncircular Open Beams with Various Cross Sections in Torsion

Table 1-15 gives formulas for the deformation and stress of open noncircular beams with various cross sections in torsion. The formulas for Case 1 are based on rigorous mathematical analysis, and the remaining formulas are obtained either by approximate mathematical analysis or the membrane analogy and are normally accurate within 10 percent.

1 - 76

TABLE 1-15

Formulas for Deformation and Stress of Various Open Section in Torsion
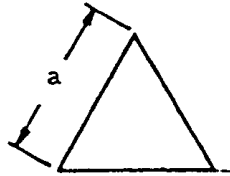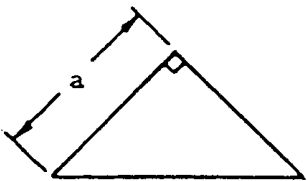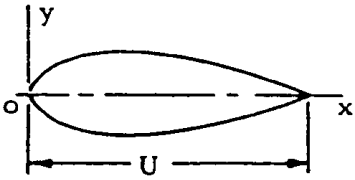
Form of Cross Section	Angle of Twist	Magnitude and Location of Maximum Shear Stress
(1) Equilateral Triangle	$\theta = \dfrac{80\,TL}{3\,G\,a^4}$	$f_{smax} = \dfrac{20\,T}{a^3}$ at the mid- point of each side
(2) Right Isosceles Triangle	$\theta = \dfrac{38.31\,TL}{G\,a^4}$	$f_{smax} = \dfrac{18.05\,T}{a^3}$
(3) 	$\theta = \dfrac{TL\left(1 + \dfrac{16\,I_x}{A\,U^2}\right)}{4\,I_x\,G}$	For cases (3) to (9) inclusive, f_{smax} occurs at or very near one of the points where the largest inscribed circle touches the boundary, unless there is a sharp reentrant angle at some other point on the boundary causing high local stress. Of the points where the largest inscribed circle touches the boundary, f_{smax}

1 - 77

TABLE 1-15

**Formulas for Deformation and Stress of
Various Open Sections in Torsion (continued)**
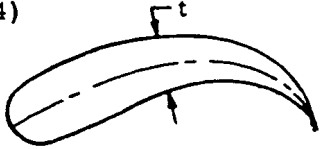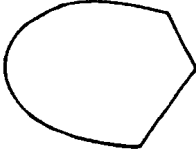
Form of Cross Section	Angle of Twist	Magnitude and Location of Maximum Shear Stress
(4) Any elongated section or thin tube. dU = elementary length along median line t = thickness normal to median line A = area of section	$\theta = \dfrac{3\left(1 + \dfrac{4F}{3AU^2}\right)TL}{GF}$ where $F = \int_0^U t^3\, dU$	occurs at the one where the boundary curvature is algebraically least. (Convexity represents positive, concavity negative, curvature of the boundary. At a point where the curvature is positive (boundary of section straight or convex) the maximum stress is given approximately by $f_{smax} = \dfrac{G\theta c}{L}$ where $c = \dfrac{D}{1 + \dfrac{\pi^2 D^4}{16 A^4}}\left[1 + 0.15\left(\dfrac{\pi^2 D^4}{16 A^2} - \dfrac{D}{2r}\right)\right]$ where D = diameter of largest inscribed circle r = radius of curvature of boundary at the point (positive for this case) A = area of the section
(5) Any solid, fairly compact section without reentrant angles. I_p = polar moment of inertia about centroidal axis A = area of the section	$\theta = \dfrac{40\,TL\,I_p}{GA^4}$	

TABLE 1-15

Formulas for Deformation and Stress of
Various Open Sections in Torsion (continued)
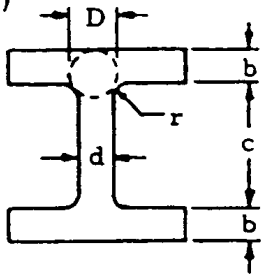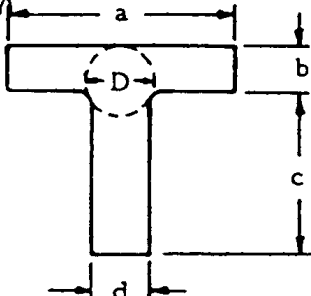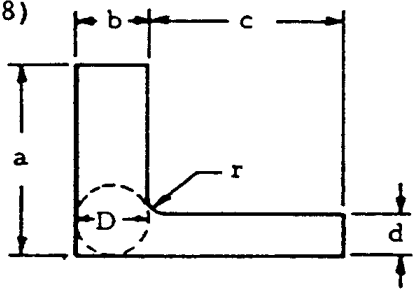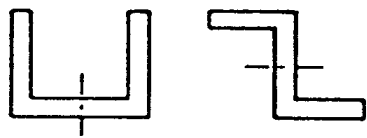
Form of Cross Section	Angle of Twist	Magnitude and Location of Maximum Shear Stress
(6) I section, flange thickness. r = fillet radius D = diameter of largest inscribed circle t = b if b < d, t = d if d < b, t_1 = b if b > d, t_1 = d if d > b	$\theta = \dfrac{TL}{G(2K_1 + K_2 + 2\alpha D^4)}$ where $K_1 = ab^3 \left[\dfrac{1}{3} - 0.21 \dfrac{b}{a} \left(1 - \dfrac{b^4}{12a^4} \right) \right]$ $K_2 = \dfrac{1}{3} cd^3$ and $\alpha = \dfrac{t}{t_1} (0.15 + 0.1 \dfrac{r}{b})$	At points where the boundary of a section is concave or re-entrant, the maximum stress is given approximately by $f_{smax} = \dfrac{G\theta c}{L}$ where $C = \dfrac{D}{1 - \dfrac{\pi^2 D^4}{16 A^4}} \left[1 + 0.118 \, Log_e \left(1 - \dfrac{D}{2r} \right) \right.$ $\left. - \dfrac{0.238 D}{2r} \right\} \tanh \dfrac{2\phi}{\pi} \right]$
(7) T section, flange thickness uniform: r, D, t and t_1 as for Case (6)	$\theta = \dfrac{TL}{G(K_1 + K_2 + \alpha D^4)}$ where $K_1 = ab^3 \left[\dfrac{1}{3} - 0.21 \dfrac{b}{a} \left(1 - \dfrac{b^4}{12a^4} \right) \right]$ $K_2 = cd^3 \left[\dfrac{1}{3} - 0.105 \dfrac{d}{c} \left(1 - \dfrac{d^4}{192c^4} \right) \right]$ $\alpha = \dfrac{t}{t_1} (0.15 + 0.10 \dfrac{r}{b})$	where D, A and r have the same meaning as before and ϕ = angle through which a tangent to the boundary rotates in turning or traveling around the re-entrant portion, measured in radians. (Here r is negative.)

TABLE 1-15

Formulas for Deformation and Stress of Various Open Sections in Torsion (concluded)

Form of Cross Section	Angle of Twist	Magnitude and Location of Maximum Shear Stress
(8) L section r and D as for Cases (6) and (7)	$$\theta = \frac{TL}{G(K_1 + K_2 + \alpha D^4)}$$ where $$K_1 = ab^3\left[\frac{1}{3} - 0.21\frac{b}{a}\left(1 - \frac{b^4}{12a^4}\right)\right]$$ $$K_2 = cd^3\left[\frac{1}{3} - 0.105\frac{d}{c}\left(1 - \frac{d^4}{192c^4}\right)\right]$$ and $$\alpha = \frac{d}{b}\left(0.07 + 0.076\frac{r}{b}\right)$$	
(9)	$$\theta = \frac{TL}{G\Sigma(K_1 + K_2 + \alpha D^4)}$$ where the summation is for the constituent L sections computed as for case (8)	

1.5.2.2   Noncircular Closed Beams in Torsion

Closed beams have one or a number of hollow portions in their cross section. This type of beam is much more efficient in torsion than open beams.

Section 1.5.2.2.1 treats single cell closed or box beams in torsion, and Section 1.5.2.2.7 treats multicell closed beams in torsion.

1.5.2.2.1   Single Cell Noncircular Closed Beams in Torsion

This section treats box beams with a single hollow portion in their cross section. Section 1.5.2.2.2 treats such beams having uniform cross section, and Section 1.5.2.2.3 treats tapered box beams. The effect

1 - 80

of stiffeners and cutouts in box beams are treated in Sections 1.5.2.2.4 and
1.5.2.2.6, respectively.

1.5.2.2.2   Single Cell Noncircular Closed Beams with Uniform Cross
Section in Torsion

Figure 1-54 shows a cross section of a thin box beam. The
angle of twist of such a beam of length, L, due to an applied torque, T, is
given by

$$\theta = \frac{TL}{4A^2 G} \int \frac{dU}{t} \qquad (1\text{-}67)$$

In this equation, A is the area enclosed by the median line, t is the thickness
at any point, and U is the length along the median line. The shear flow in
such a tube is uniform at all points and is given by

$$q = \frac{T}{2A} \qquad (1\text{-}68)$$

If the shear stress is assumed to be uniform across any thickness, it is
given by

$$f_s = \frac{q}{t} = \frac{T}{2At} \qquad (1\text{-}69)$$

From this expression, it can be seen that the maximum shear stress occurs
where the thickness is minimum.
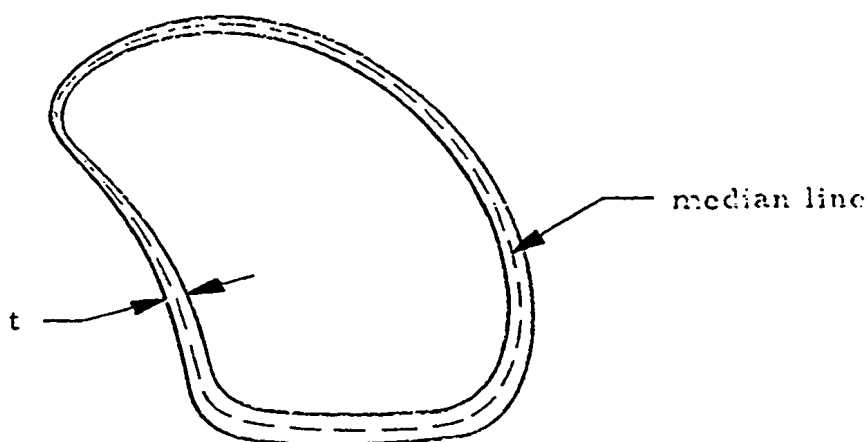
Figure 1-54.   Cross Section of a Single Cell Closed Beam

1 - 81

If the thickness of the tube is uniform, Equation (1-67) becomes

$$\theta = \frac{TLU}{4A^2 Gt} \qquad (1-70)$$

and Equations (1-68) and (1-69) remain the same.

1.5.2.2.3   Single Cell Noncircular Tapered Closed Beams in Torsion

Figure 1-55 shows a tapered box beam under a torsional load, T. Since all four sides are tapered in such a way that the corners of the box would intersect if extended, the equations in Section 1.5.2.2.2 may be applied to this beam if A is taken to be the area at the cross section in question.
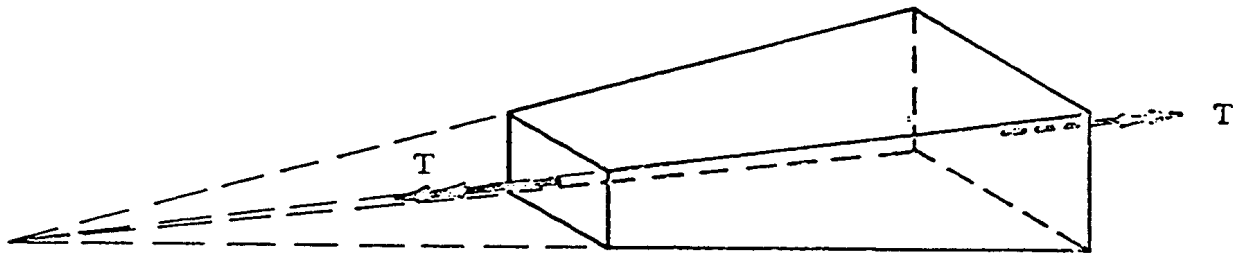
Figure 1-55.   Tapered Box Beam in Torsion

However, these equations no longer apply for box beams for which the taper ratio of the horizontal webs is not the same as that of the vertical webs since the shear flows will not have the same distribution for all webs.   Such a beam is shown in Figure 1-56.   Although the equations in Section 1.5.2.2.2 are not valid for a box beam such as that shown in Figure 1-56, they are quite accurate for the common airplane wing structure with closely spaced ribs.   The ribs divide the web into several smaller webs and serve to distribute shear flows so that they are approximately equal in the horizontal and vertical webs.
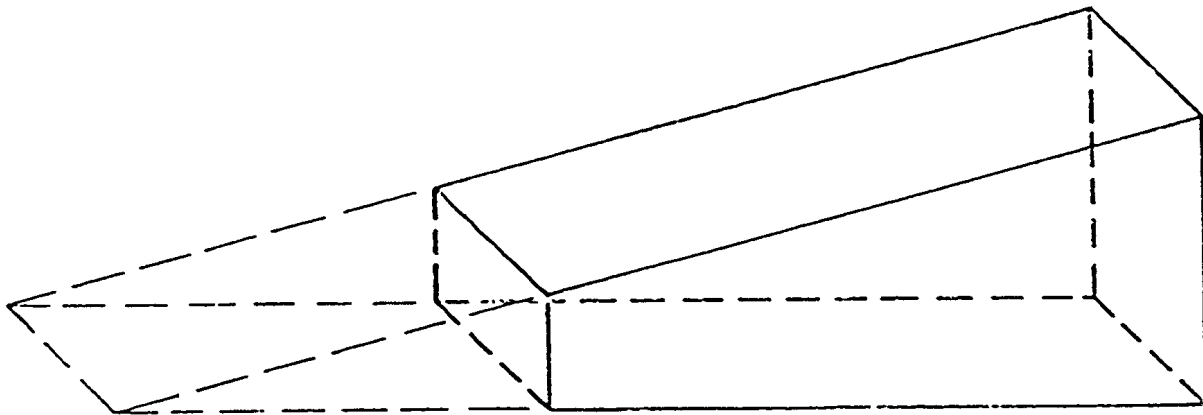
Figure 1-56.   Box Beam with Nonuniform Taper

1.5.2.2.4   Effect of Stiffeners on Noncircular Closed Beams in Torsion

Thin-walled airplane structures usually contain longitudinal stiffeners spaced around the outer walls as shown in Figure 1-57. If the open-type stiffener, as shown to the left in Figure 1-57, is used, the torsional rigidity of the individual stiffeners is so small compared to the torsional rigidity of the thin-walled cell that it is negligible. However, a closed-type stiffener is essentially a small tube and its stiffness is thus much greater than that of an open section of the same size. Thus, a cell with closed-type stiffeners attached to its outer walls could be treated as a multicell closed beam with each stiffener forming an additional cell. Since the analysis of a beam with a large number of cells is difficult and, in general, the torsional stiffness provided by the stiffeners is small compared to that of the overall cell, an approximate simplified procedure may be used with sufficient accuracy.
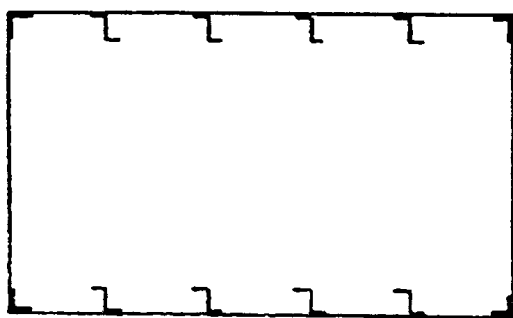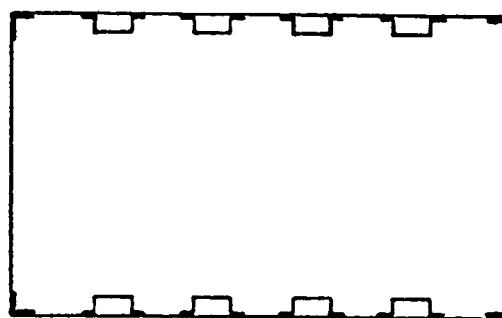
Open-Type Stiffener   Closed-Type Stiffener

Figure 1-57.   Types of Stiffeners

In the approximate method, the thin-walled tube and closed stiffeners are converted into an equivalent single thin-walled tube by modifying the closed stiffeners by one of two procedures. This equivalent tube is then analyzed according to the material in Section 1.5.2.2.2. The two procedures for modifying the closed stiffeners are:

1. Replace each closed stiffener by a doubler plate having an effective thickness given by

$$t_e = t_{st} \; s/d \qquad\qquad (1-71)$$

This procedure and the necessary nomenclature are illustrated in Figure 1-58.

2. Replace the skin over each stiffener by a "liner" having a thickness given by

$$t_e = t_s \; d/s \qquad\qquad (1-72)$$

This method and the necessary nomenclature are illustrated in Figure 1-59. The first of these procedures slightly over-estimates the stiffness effect of the stiffeners, whereas the second procedure slightly underestimates this effect.
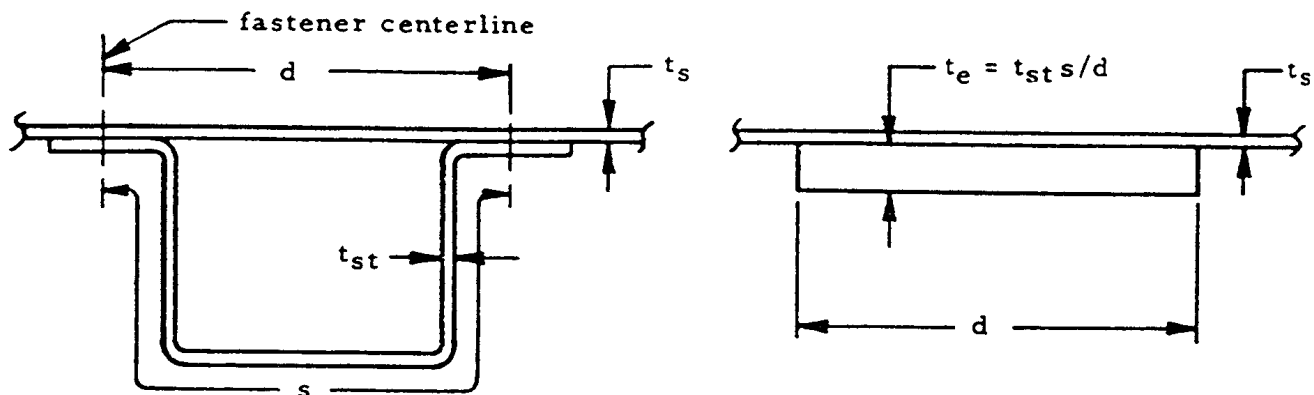
Figure 1-58. First Method of Transforming Closed Stiffeners

Original Stiffener   Transformed Stiffener
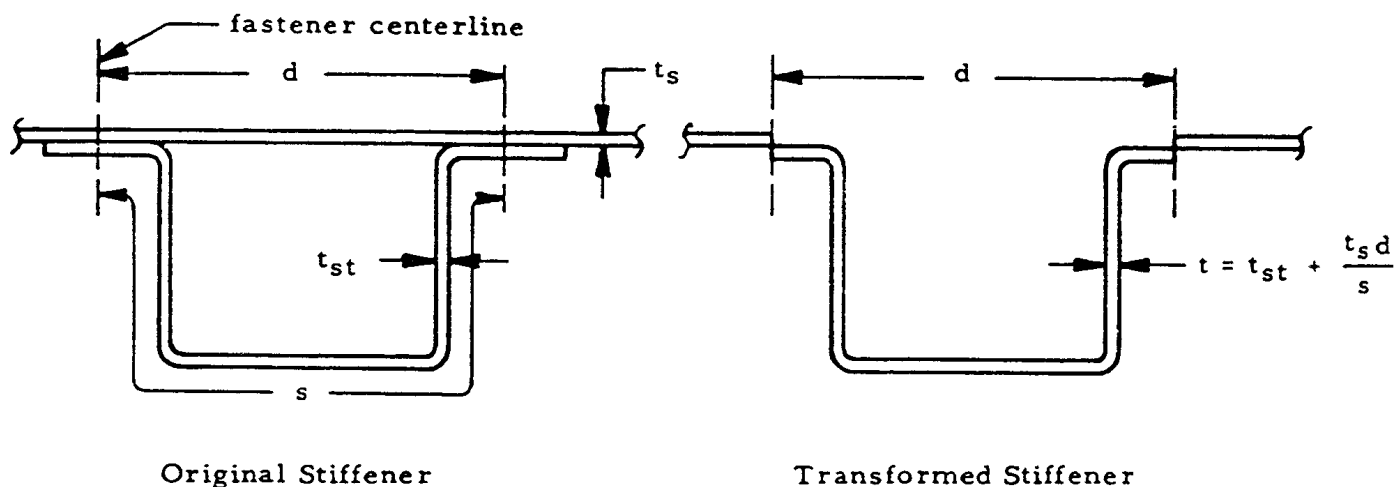
Figure 1-59. Second Method of Transforming Closed Stiffeners

Since the corner members of a stiffened cell are usually open or solid sections such as those shown in Figure 1-57, their torsional re-sistance can be simply added to the torsional stiffness of the thin-walled overall cell.

1.5.2.2.5   Sample Problem - Noncircular Closed Stiffened Uniform Section Beam in Torsion

Given: A 120-in.-long beam under an applied torque of 10,000 in.lb. with a cross section as shown in Figure 1-60.

Find: The angle of twist and maximum shear stress in the beam.

1 - 84

Stiffener Detail

1 x 1 x 1/8 angles at corners

$$G = 4 \times 10^6$$
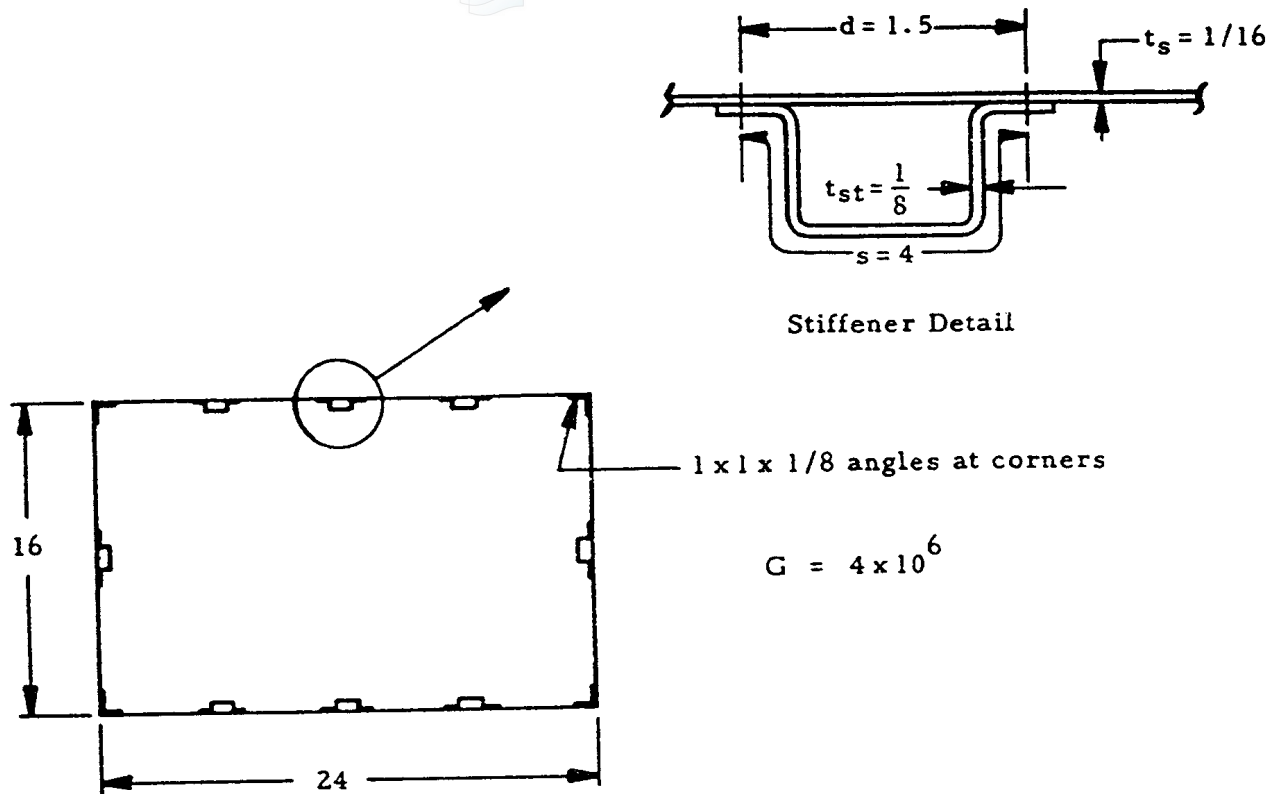
Figure 1-60. Cross Section of Stiffened Single Cell Open Beam
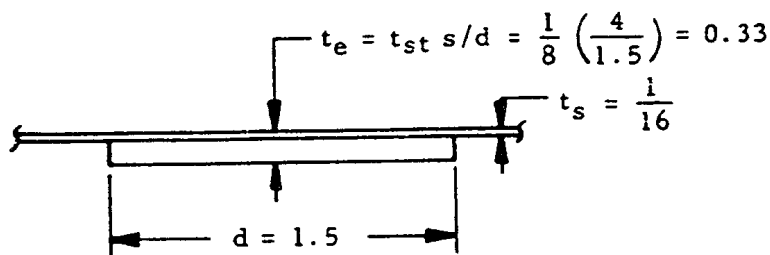
Figure 1-61. Doubler Equivalent to Beam Stiffeners

Solution: From Section 1.5.2.2.4, a doubler plate equivalent
to a stiffener may be drawn as shown in Figure 1-61. The
area enclosed by the median line of the transformed section
is thus

$$A = (24 \times 16) - 8 \left(\frac{t_e}{2} \right) (d) - 4 \left(\frac{1}{16} \right) (2)$$

where the last term takes into account the effect of the corner
angles. Thus,

$$A = (24 \times 16) - 8 \left(\frac{0.33}{2} \right) (1.5) - 4 \left(\frac{1}{16} \right) (2) = 381.5$$

Applying Equation (1-67) to the equivalent beam gives

1 - 85

$$\theta = \frac{TL}{4A^2 G} \int \frac{dU}{t} = \frac{10^4(120)}{4(381.5^2)(4 \times 10^6)} \left\{ \frac{8d}{t_\bullet + t_\bullet} \right.$$

$$+ \frac{4(2)}{t_s + \frac{1}{8}} + \left. \frac{2(24+16) - [8d + 4(2)]}{\frac{1}{16}} \right\}$$

where the terms in the parenthesis represent integration over the doubler, angles and skin, respectively. Thus

$$\theta = \frac{10^4(120)}{4(3815^2)(4 \times 10^6)} \left\{ \frac{8(1.5)}{(0.33 + 0.0625)} + \frac{4(2)}{(0.0625 + 0.125)} \right.$$

$$+ \left. \frac{2(24+16) - [8(1.5) + 4(2)]}{0.0625} \right\} = 5.35 \times 10^{-4} \text{ rad} = 0.0306°$$

From Equation (1-69)

$$f_s = \frac{T}{2At} = \frac{10^4}{2(381.5)t} = \frac{13.1}{t}$$

Thus, the maximum shear stress occurs at the point of minimum thickness and

$$f_s = \frac{13.1}{0.0625} = 210 \text{ psi}$$

1.5.2.2.6   Effect of Cutouts on Closed Single Cell Beams in Torsion

Typical aircraft structures consist of closed boxes with longitudinal stiffeners and transverse bulkheads. It is necessary to provide many openings in the ideal continuous structure for wheel wells, armament installations, doors, windows, etc. These cutouts are undesirable from a structural standpoint but are always necessary. A closed torque box is necessary for most of the span of an airplane wing but may be omitted for a short length such as the length of a wheel well opening. When a portion of the skin is omitted for such a region, the torsion is resisted by differential bending of the spars, as indicated in Figure 1-62, since the open section has low torsional rigidity. If the torsion is to be assumed to be resisted by the two side webs acting independently as cantilever beams, as shown in Figure 1-62(b), one end must be built in as shown in Figure 1-62(a).

$$P = \frac{TL}{bh}$$

$$q = \frac{T}{bh}$$

Note: Bottom Skin
Removed   (a)

(b)
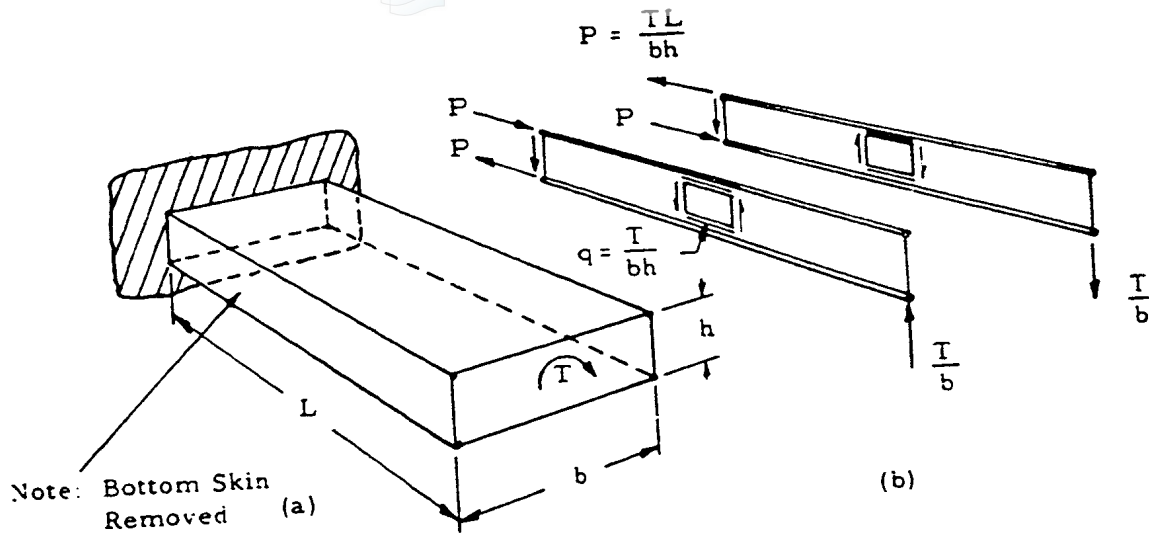
Figure 1-62.   Illustration of the Effect of a Cutout

The existence of a cutout and the resultant axial loads in the flanges also increase the shear flow in closed portions of the box adjacent to the cutouts.

1.5.2.2.7   Multicell Closed Beams in Torsion

Figure 1-63 shows the internal shear flow pattern on a multicell tube consisting of n cells under a pure torsional load, T. The torque applied to this tube is given by

(1-73)

$$T = 2q_1 A_1 + 2q_2 A_2 + \ldots + 2q_n A_n$$

where A_1 through A_n are the areas enclosed by the medium lines of cells 1 through n. The line integral, ds/t, where s is the length of the median of a wall and t is the wall thickness, may be represented by a. Then a_{KL} is the value of this integral along the wall between cells K and L, where the area outside the tube is designated as cell (0). Using this notation, the following equations may be written for cells (1) through (n):

(1-74)

$$\text{cell (1)} \quad \frac{1}{A_1} \left[q_1 a_{10} + (q_1 - q_2) a_{12} \right] = 2G\theta$$

(1-75)

$$\text{cell (2)} \quad \frac{1}{A_2} \left[(q_2 - q_1) a_{12} + q_2 a_{20} + (q_2 - q_3) a_{23} \right] = 2G\theta$$

(1-76)

$$\text{cell (3)} \quad \frac{1}{A_3} \left[(q_3 - q_2) a_{23} + q_3 a_{30} + (q_3 - q_4) a_{34} \right] = 2G\theta$$

cell (n-1) $\dfrac{1}{A_{n-1}}$ $[(q_{n-1} - q_{n-2}) a_{n-2, n-1} + q_{n-1} a_{n-1, 0}$

$$+ (q_{n-1} - q_n) a_{n-1, n}] = 2 G\theta \qquad (1-77)$$

cell (n) $\dfrac{1}{A_n}$ $[(q_n - q_{n-1}) a_{n-1, n} - q_n a_{n0}] = 2 G\theta \qquad (1-78)$

The shear flows, q_1 through q_n, may be found by solving Equations (1-73) through (1-78) simultaneously. From these shear flows, the shear stress distribution may be found since $f_s = q/t$.

Figure 1-63. Multicell Tube in Torsion

1.5.2.2.8 Sample Problem - Multicell Closed Beams in Torsion

Given: A multicell beam with the cross section shown in Figure 1-64 under a torsional load of 5,000 in.lb.

Figure 1-64. Two Cell Closed Beams

Find: The shear stress in each of the walls.

Solution: Assuming the cell corners to square gives

$$A_1 = (2.5)(6.5) = 16.25 \text{ in.}^2$$

$$A_2 = (2.5)(4) = 10 \text{ in.}^2$$

$$a_{10} = [2(6.5) + 2.5]/0.1875 = 77.3$$

$$a_{12} = 2.5/0.250 = 10$$

$$a_{20} = [2(4) + 2.5]/0.125 = 84$$

Applying Equations (1-73), (1-74), and (1-75) to the given beam gives

$$T = 2q_1 A_1 + 2q_2 A_2,$$

$$\frac{1}{A_1} [q_1 a_{10} + (q_1 - q_2) a_{12} = 2 G\theta,$$

and

$$\frac{1}{A_2} [(q_2 - q_1) a_{12} + q_2 a_{20}] = 2 G\theta.$$

Inserting numerical values into these equations gives

$$5000 = 2q_1(16.25) + 2q_2(10),$$

$$\frac{1}{16.25} [q_1(77.3) + (q_1 - q_2)(10)] = 2(4 \times 10^6)\theta,$$

and

$$\frac{1}{10} [(q_2 - q_1)(10) + q_2(84)] = 2(4 \times 10^6)\theta.$$

Solving these equations simultaneously gives

$$q_1 = 78 \text{ lb/in.}, \quad q_2 = 123 \text{ lb/in. and}$$

$$\theta = 1.345 \times 10^{-4} \text{ rad} = 0.0077°$$

The shear stress in wall (1) is

$$f_s = \frac{q_1}{t_1} = \frac{78}{0.1875} = 415 \text{ psi}$$

The shear stress in wall (2) is

$$f_s = \frac{q_2}{t_2} = \frac{123}{0.125} = 984 \text{ psi}$$

1 - 89

The shear stress in wall (1.2) is

$$f_s = \frac{q_1 - q_2}{t_{1.2}} = \frac{123 - 78}{0.250} = 180 \text{ psi}$$

1.5.2.3 Effect of End Restraint on Noncircular Beams in Torsion

The equations for noncircular beams in torsion in previous sections assumed that cross sections throughout the length of torsion members were free to warp out of their plane and thus there could be no stresses normal to the cross sections. In actual structures, restraint against the free warping of sections is often present at the point of attachment of a beam. For example, the airplane wing cantilevers from its attachment to a rather rigid fuselage structure and is restrained against warping at its point of attachment. The effect of end restraint is greater at points close to the restraint than those further removed. Sections such as I-beams are more effected by end restraint than compact sections such as circles and squares.

Figure 1-65 shows an I-beam with one end restrained under a torsional load, T. The maximum flange bending moment is

$$M_{max} = \frac{T}{h} \, a \tanh \frac{L}{a} \qquad (1\text{-}79)$$

where

$$a = \frac{h}{2} \sqrt{\frac{2 \, Iy \, E\theta}{TL}} \qquad (1\text{-}80)$$

and θ is the angle of twist of an I-beam with unrestrained ends given in Table 1-15. The angle of twist of such an I-beam with restrained ends is

$$\theta_r = \theta \left(1 - \frac{a}{L} \tanh \frac{L}{a} \right) \qquad (1\text{-}81)$$

From this equation, it can be seen that the end restraint has a stiffening effect on the beam.

1.5.3 Analogies for Beams in Torsion

Two analogies for beams in torsion are useful both for visualization of stress distributions and magnitudes and for experimental work. The membrane analogy, which is described in Section 1.5.3.1, is valid for open beams for which the shear stress is in the elastic range. The sand heap analogy (Section 1.5.3.2) may be used to treat open beams under torsional loads for which the plastic shear stress is the same at all points on the cross section.
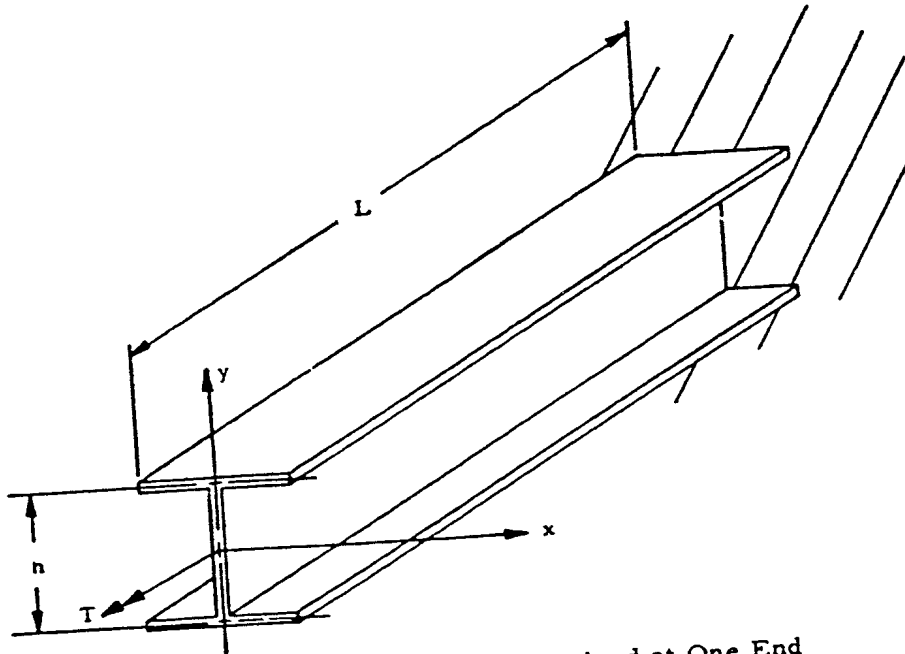
Figure 1-65. I-Beam Restrained at One End

1.5.3.1   Membrane Analogy for Beams in Elastic Torsion

The equation for the torsion of a beam in the elastic range is analogous to that for small deflections of a membrane under uniform pressure. Figure 1-66 shows such a membrane. The pressure on the membrane is designated as p, and S is the uniform tension per unit at its boundary. The membrane analogy gives the following relationships between the deflected membrane and a beam of the same cross section in torsion:

(1) Lines of equal deflection on the membrane (contour lines) correspond to shearing stress lines of the twisted bar.

(2) The tangent to a contour line at any point on the membrane surface gives the direction of the resultant shear stress at the corresponding point on the cross section of the bar being twisted.

(3) The maximum slope of the deflected membrane at any point with respect to the edge support plane is proportional to the shear stress at the corresponding point on the cross section of the twisted bar. Thus, the shear stress is greatest where the contour lines are closest.

(4) The applied torsion on the twisted bar is proportional to twice the volume included between the deflected membrane and a plane through the supporting edges. If $p/S = 2 G\theta$, this torque is equal to twice the volume.

1 - 91
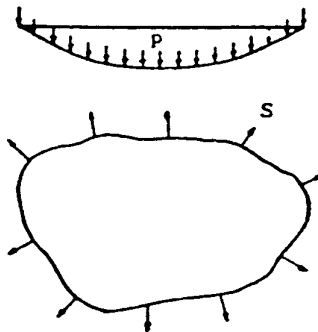
Figure 1-66. Membrane Under Pressure

The membrane analogy may be used to experimentally measure quantities for beams in torsion. However, possibly the main advantage of the membrane theory is that it provides a method of visualizing to a considerable degree of accuracy how stress conditions vary over a complicated cross section of a bar in torsion. For example, consider the bar with rectangular cross section shown in Figure 1-67(a). A membrane may be stretched over an opening of the same shape and deflected by a uniform pressure. Equal deflection lines for the deflected membrane will take the shape as shown in Figure 1-67(b). These contour lines tend to take the shape of the bar boundary as it is approached as does the direction of shearing stress. The shear stress is maximum where the contour lines are closest (center of long side). Since the applied torsion is proportional to the membrane volume, the more elongated of two rectangular bars of equal area has the smaller torsional rigidity. Also, it is obvious that bending a long thin rectangular section will not appreciably change the membrane volume and, thus, the torsional rigidity of a bar of this shape.

(a)   (b)
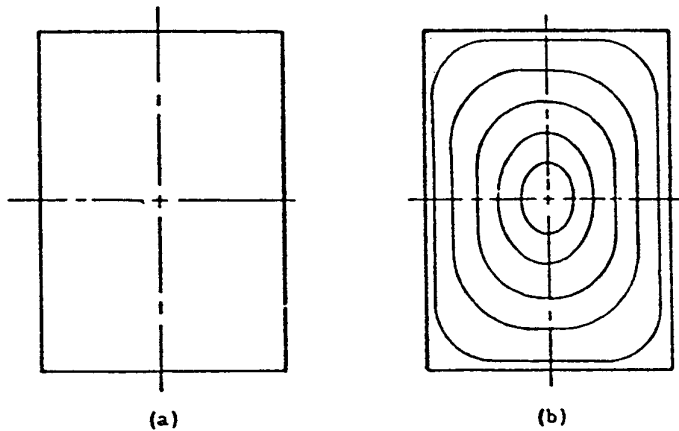
Figure 1-67. Rectangular Bar in Torsion

The membrane analogy also makes it apparent that stresses are very low at the ends of outstanding flanges or protruding corners and very high where the boundary is sharply concave. For example, Table 1-16 gives the stress concentration factor for the concave side of the shape in Figure 1-68. Multiplying the maximum stress obtained from the formula for thin rectangular sections in torsion by this factor gives the maximum stress on the concave side of a thin bent section.

TABLE 1-16

Stress Concentration Factor for Thin
Sections in Torsion

r/t	1/8	1/4	1/2	1
Factor	2-1/2	2-1/4	2	1-3/4
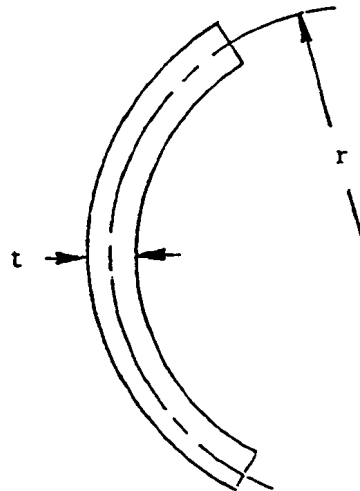
Figure 1-68. Thin Curved Section

1.5.3.2 Sand Heap Analogy for Beams in Plastic Torsion

The maximum ultimate torque that an open beam may withstand in torsion is given by

$$T = 2V \, F_{su} \tag{1-82}$$
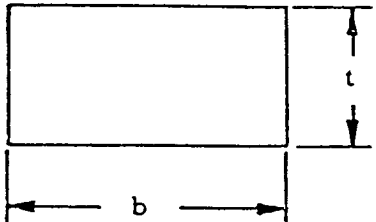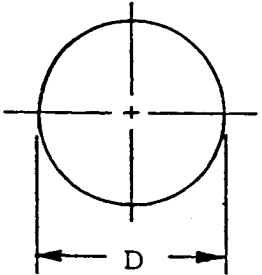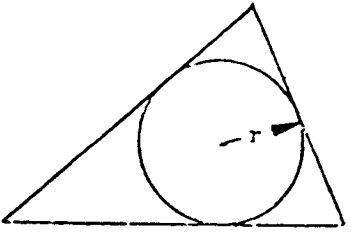
where V is the volume of a sand heap with a maximum slope of unity, piled on a plate having the same shape as the beam cross section. Table 1-17 gives the volume of sand heaps with various bases of various shapes.

1.5.4 Helical Springs

The primary stresses in the wire of a helical spring are due to torsion. Section 1.5.4.1 treats helical springs composed of round wire, and those composed of square wire are treated in Section 1.5.4.2.

TABLE 1-17

Sand Heap Volumes for Equation (1-82)

Type Section	Sand Heap Volume
Rectangle	$V = \dfrac{t^3(3b-t)}{12} \quad b \geq t$
Circle	$V = \dfrac{\pi D^3}{24}$
Triangle	$V = \dfrac{Ar}{3}$

A = area of triangle

r = radius of inscribed circle

1.5.4.1   Helical Springs of Round Wire

Figure 1-69 shows a helical spring made of round wire under an axial load, P. If the spring radius (r) is much greater than the wire diameter (D), the wire may be treated as a straight round beam under a torsional load, Pr, as indicated in Figure 1-69. Superposing the stress due to torsion of the wire on the uniform shear stress due to direct shear $(4P/\pi D^2)$, the following equation for the maximum shear stress in the spring may be obtained:

$$f_{smax} = \frac{16\ Pr}{\pi\ D^3}\left(1 + \frac{D}{4r}\right) \qquad (1-83)$$

In the cases of heavy coil springs composed of wire with a relatively large diameter, D, in comparison to r, the initial curvature of the spring must be accounted for. This is done in the following equation:

$$f_{smax} = \frac{16\ Pr}{\pi\ D^3}\left(\frac{4m-1}{4m-4} + \frac{0.615}{m}\right) \qquad (1-84)$$

where

$$m = \frac{2r}{D} \qquad (1-85)$$

This equation reduces to Equation (1-83) as r/D becomes large.

The total deflection (δ) of a round spring of n free coils is given by

$$\delta = \frac{64\ Pr^3 n}{GD^4} \qquad (1-86)$$

This equation neglects the deflection due to direct shear which is given by

$$\delta_s = \frac{8\ PRn}{Gd^2} \qquad (1-87)$$

This portion of the deformation, however, is generally negligible compared to the value of δ given by Equation (1-86) and is thus generally ignored.

All of the equations in this section apply to both compression and tension springs, and in both cases the maximum shear stress occurs at the inside of the wire.

1 - 95
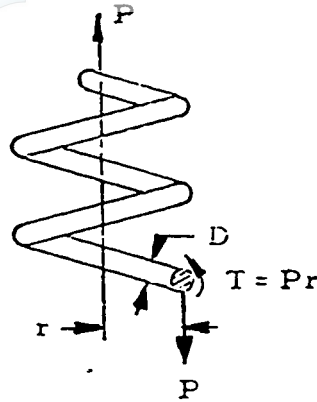
Figure 1-69. Helical Spring of Round Wire

1.5.4.2   Helical Springs of Square Wire

Figure 1-70 shows a helical spring made of square wire under an axial load, P. The maximum shear stress in the square wire is given by

$$f_{smax} = \frac{4.80\,Pr}{b^3}\left(\frac{4m-1}{4m-4} + \frac{0.615}{m}\right) \tag{1-88}$$

where

$$m = \frac{2r}{b} \tag{1-89}$$

The total deflection of such a spring is given by

$$\delta = \frac{44.5\,Pr^3 h}{Gb^4} \tag{1-90}$$

where n is the number of active or free coils in the spring. This equation neglects the deflection due to direct shear as did Equation (1-86). However, the deflection due to direct shear is normally negligible compared to that given by Equation (1-90).
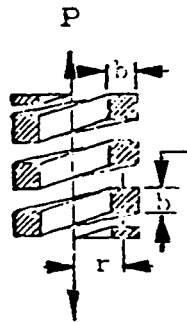
Figure 1-70. Helical Spring of Square Wire

1 - 96

2. COLUMN ANALYSIS

2.1 Introduction to Column Analysis

The stresses that a structural element can sustain in compression are functions of several parameters. These parameters are:

(1) the length of the element along its loading axis,
(2) the moment of inertia of the element normal to its loading axis,
(3) the cross-sectional variation of the element with length,
(4) the eccentricity of the applied load,
(5) the continuity of the integral parts of the element,
(6) the cross-sectional characteristics of the element,
(7) the homogeneity of the element material,
(8) the straightness of the element, and
(9) the end fixity of the element.

The effects of these parameters can be categorized by first establishing certain necessary assumptions. For the following analysis, it is assumed that the material is homogeneous and isotropic. It is further assumed that the element is initially straight and, if it is composed of several attached parts, that the parts act as integral components of the total structural configuration.

The remainder of the previously mentioned parameters dictate more general classifications of compression elements. If a compression element is of uniform cross section and satisfies the previously mentioned assumptions, it is referred to as a simple column and is treated in the first part of this chapter. On the other hand, compression members having variable cross-sectional properties are called complex columns and are covered in the latter part of this chapter. Stepped and latticed columns are included in the treatment of complex columns.

The possible basic types of failure defined for columns are primary and secondary failure. Primary failure occurs when a column fails as a whole and may be defined by the fact that cross sections of the element retain their original shape although they may be translated and/or rotated with respect to their original position. If cross sections are translated but not rotated, the primary failure is of the bending type. Failures for which cross sections of a column are either rotated or rotated and translated are treated in the section on torsional instability.

If a column experiences a failure due to lateral bending at a stress level below the elastic limit of the material, it is defined to be a long column while failures at a maximum stress greater than the elastic limit are characteristic of short columns.

Secondary failures occur when buckling or crippling occur in sections of a column before it is loaded enough to produce a primary failure.

A column failure of a selected element is influenced by the eccentricity of the applied load and by the end fixity of the element. Both of these dictate boundary conditions that modify the solutions to the differential equations governing column response.

In general, a column must be designed to prevent both the bending and torsional types of primary failure as well as crippling. Crippling is likely to occur in columns having thin portions in their cross sections. The torsional type of primary failure is likely to occur at a lower load than the bending type in columns having cross sections of relatively low torsional stiffness. Closed sections have enough torsional stiffness to insure that any primary failure will be of the bending type so they must only be designed against this and crippling.

2.2   Nomenclature for Column Analysis

A	= area
a	= linear dimension as indicated in diagrams
a	= subscript, allowable
b	= linear dimension as indicated in diagrams
b'	= $b + h/2$ in Section 2.3.2.4
C	= coefficient of constant $\equiv (L/L')^2$
C_{BT}	= torsion – bending constant
C	= distance from neutral axis to the concave side of loaded column
cr	= subscript, critical
D	= diameter
E	= modulus of elasticity
E_r	= reduced modulus of elasticity
E_s	= secant modulus of elasticity
E_t	= tangent modulus of elasticity
e	= eccentricity of loading
e	= strain
e	= subscript, for Euler's equation
ec/ρ^2	= eccentric ratio
F_{acol}	= working concentrically loaded column stress
F_b	= working bending stress
F_c	= allowable compressive stress
F_{cb}	= working compressive stress in bending
F_{cc}	= allowable crippling stress
F_{co}	= empirical constant in Johnson parabolic equation (column yield stress)
F_{col}	= maximum fiber stress for primary failure of a column
F_{cp}	= proportional limit in compression
F_{cy}	= compressive yield stress
FS	= factor of safety
f	= calculated stress

f_c	= calculated compressive stress
f_1	= stress at which the secant modulus of elasticity is equal to 0.7
G	= modulus of elasticity in shear
h	= height
I	= moment of inertia
I_p	= polar moment of inertia
J	= torsion constant
K	= spring constant
K	= empirical constant
k	= empirical constant
L	= length
L'	= effective length = $L/\sqrt{C}$
L/ρ	= slenderness ratio
L'/ρ	= effective slenderness ratio
$(L'/\rho)_{cr}$	= critical effective slenderness ratio
M	= empirical constant in straight line column equation
N	= empirical constant in straight line column equation
n	= empirical constant in Ramberg-Osgood equation
P	= axial load
P_a	= allowable load
P_{cc}	= crippling load
P_{cr}	= critical load
P_e	= Euler critical load
r	= radius
T	= torque
t	= thickness
x, y, z	= rectangular coordinates
ϵ	= Ee/f_1 where e is strain
μ	= Poisson's ratio
μ	= torsional spring constant
ρ	= radius of gyration = $\sqrt{I/A}$
Σ	= summation
σ	= f_c/f_1
θ	= angular deflection
φ	= angular deflection

2.3 Simple Columns

A simple column acts as a single unit and has a uniform cross section along its length. Such columns are treated in the following material.

2.3.1 Primary Failure of Simple Columns

A simple column has a primary failure when its cross sections are translated and/or rotated while retaining their original shape, that is, when the column fails as a whole without local instability. If the column cross

2 - 3

sections are translated but not rotated as shown to the left of Figure 2-1, it is said to fail by bending while pure rotation or a combination of rotation and translation are characteristic of torsional failures.
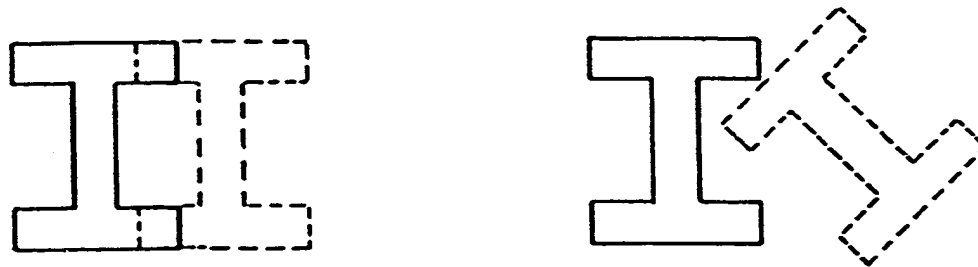
Figure 2-1.   Modes of Primary Failure

2.3.1.1   Column Data Applicable to Both Long and Short Columns

A stable section (not subject to crippling) testing for various lengths will generate data of the form shown in Figure 2-2.   The stress F_{col} is the stress at failure, and L'/ρ is the ratio of the effective column length to the radius of gyration of the section.   This L'/ρ ratio is called the effective slenderness ratio of the column.
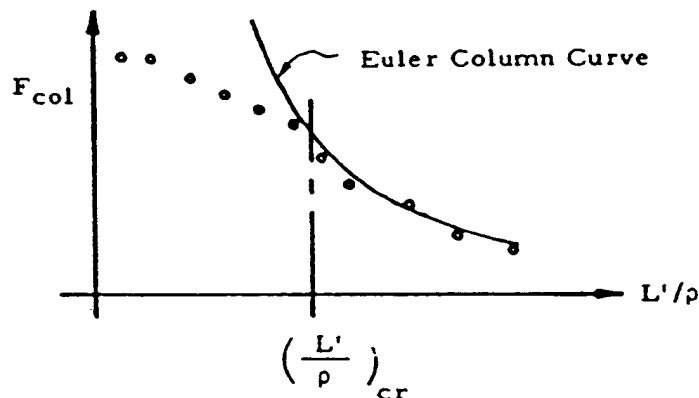
Figure 2-2.   Typical Column Failure Curve

From the figure, it is apparent that the Euler column curve is quite accurate beyond a critical L'/ρ which defines the separation between long and short columns.   A great amount of test data, collected for particular materials, is available and eliminates the need to determine whether a long or a short column curve is applicable.   A summary of column allowable curves that are applicable to both long and short columns is outlined and presented on the following pages.   These curves are based upon the tangent modulus equation which is discussed in Section 2.3.1.11.1.   The column allowables are based on minimum guaranteed properties, Basis A, or probability properties, Basis B, if the latter are available.   The pertinent basis is indicated in the figures.

2 - 4

INDEX OF COLUMN ALLOWABLE CURVES

INDEX OF COLUMN ALLOWABLE CURVES (Cont'd.)

2014 AND 7075 EXTRUSIONS

Curve	Designation	Thickness and Area	Basis
1	2014-T6	.125-.499	B
2	2014-T6	.500-.749	B
3	2014-T6	$\geq$ .750, A$\leq$25	B
4	2014-T62	$\geq$ .125, A$\leq$32	A
5		< .250, .750-1.499	B
6	7075-T6510	.250-.499	B
7	and -T6511	.500-.749	B
8		1.500-2.999	B

1, 2, 3, & 4

Figure 2-3.   Column Allowable Curves

2024 BARE SHEET AND PLATE

Curve	Material Designation	Thickness	Basis
1	2024-T42	< .250	A
2	2024-T4	501-2.00	B
	2024-T3	≤ .250	B
3	2024-T36	≤ .500	B
4	2024-T6	≤ 2.00	A
5	2024-T86	< .063	A
6	2024-T86	≥ .063, < .5	A

Figure 2-4. Column Allowable Curves

Curve	Material Designation	Thickness	Basis
1	2024-T42	.250-3.00	A
2	2024-T4	.250-.500	B
3	7075-T6	.016-.039	B
4	7075-T6	.040-.249	B
5	7075-T6	.501-1.00	B
6	7075-T6	.250-.500	B
		1.001-2.00	B

2024 BARE PLATE
7075 BARE SHEET AND PLATE

Figure 2-5.   Column Allowable Curves

2 - 9

2024 EXTRUSION

Curve	Material Designation	Thickness and Area	Basis
1	2024-T4	<.250	B
2	2024-T4	.250-.749	B
3	2024-T4	.750-1.499	B
	2024-T4	$\geq 1.50, A \leq 25$	B
4	2024-T42	$\geq .250, A \leq 32$	A
5	2024-T62	All	A
6	2024-T81	<.750	A

Figure 2-6.   Column Allowable Curves
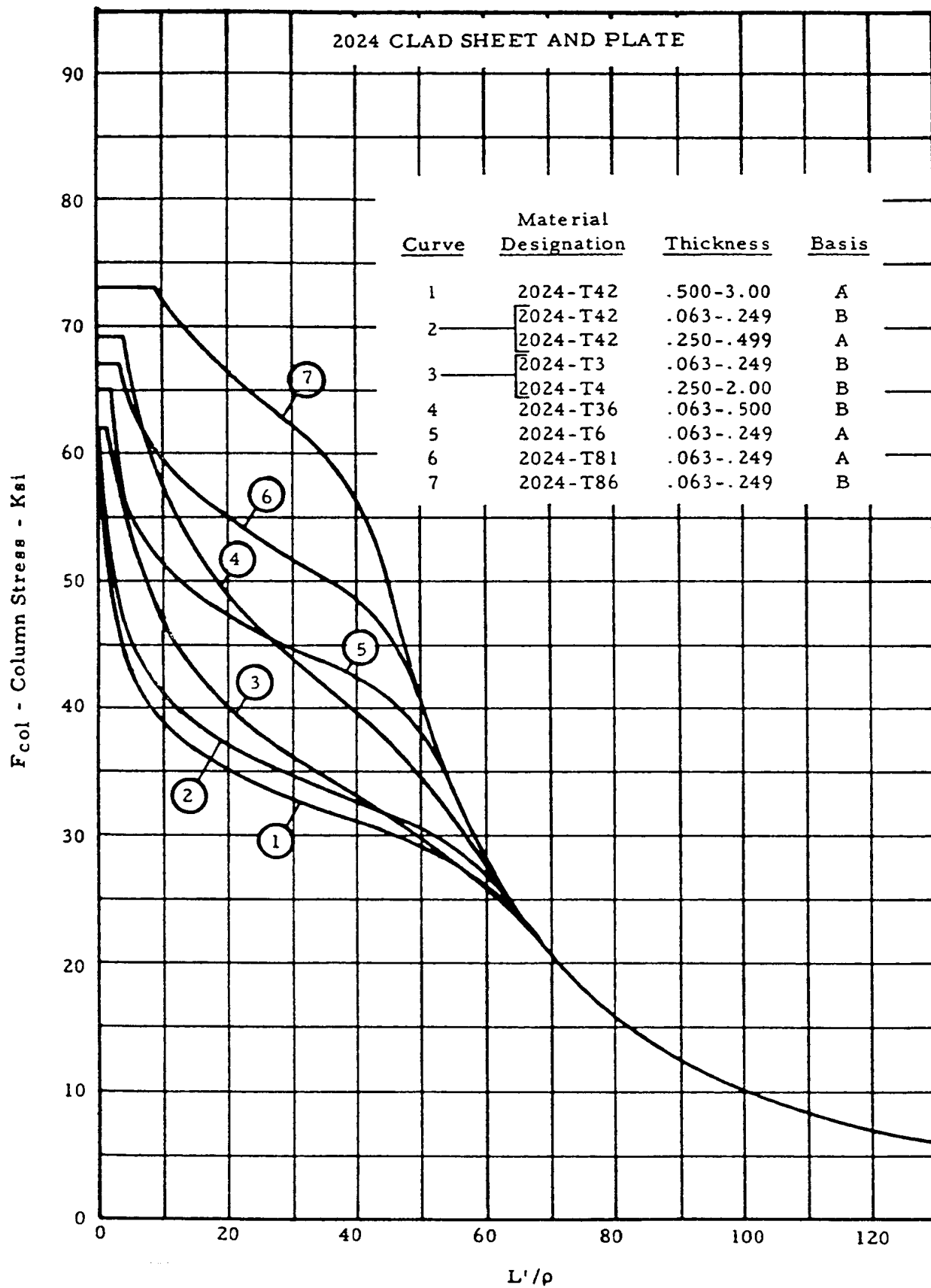
Figure 2-7. Column Allowable Curves

2 - 11

2024 CLAD SHEET
7075 CLAD SHEET

Curve	Material Designation	Thickness	Basis
1	2024-T42	<.063	B
2	2024-T3	<.063	B
3	2024-T36	<.063	B
4	2024-T6	<.063	A
5	2024-T81	<.063	A
6	2024-T86	<.063	B
7	7075-T6	.016-.039	B
8	7075-T6	.040-.062	B
9	7075-T6	.063-.187	B
10	7075-T6	.188-.249	B

F_{col} - Column Stress - Ksi

L'/ρ
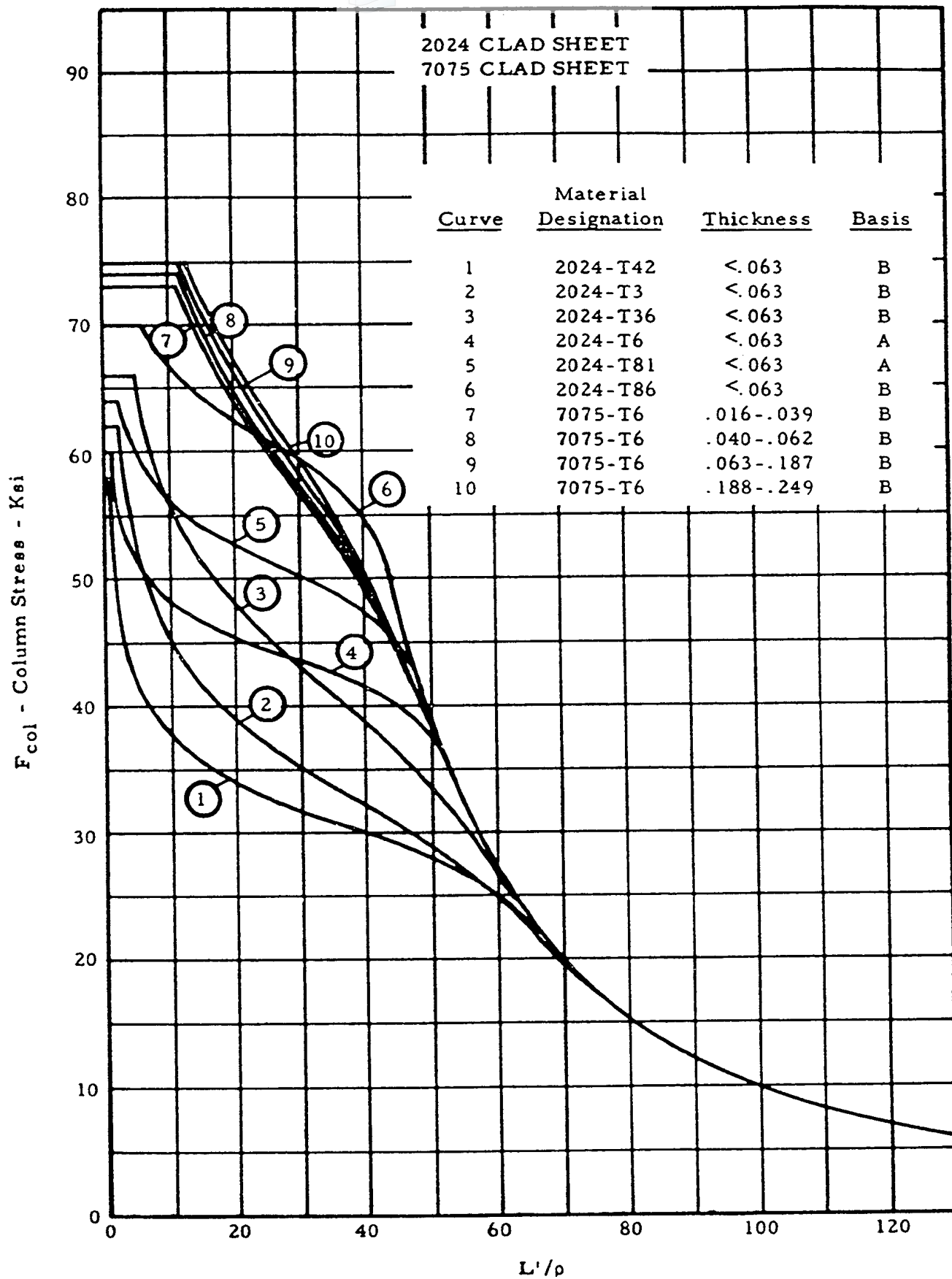
Figure 2-8.   Column Allowable Curves

2 - 12
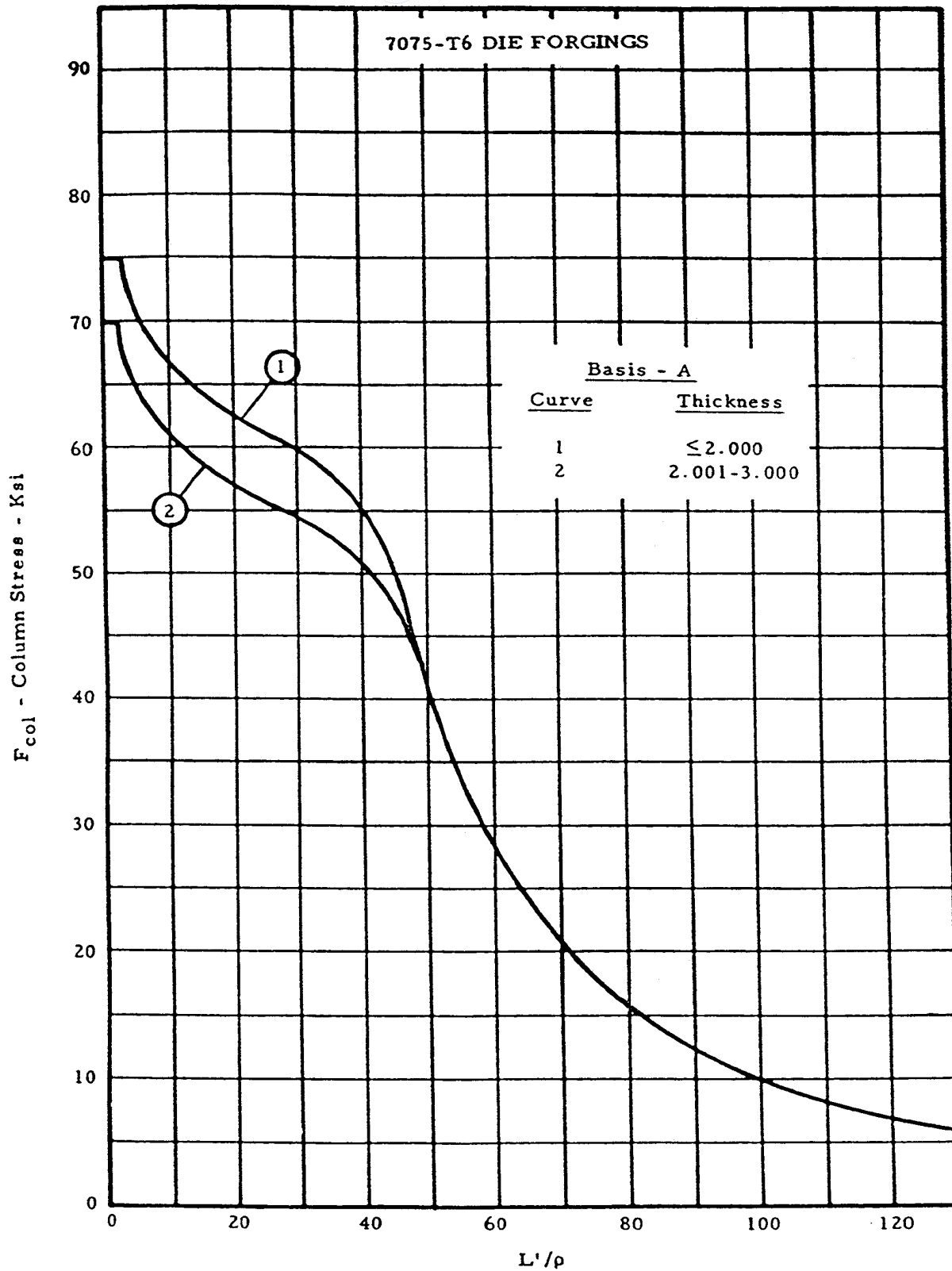
Figure 2-9.   Column Allowable Curves
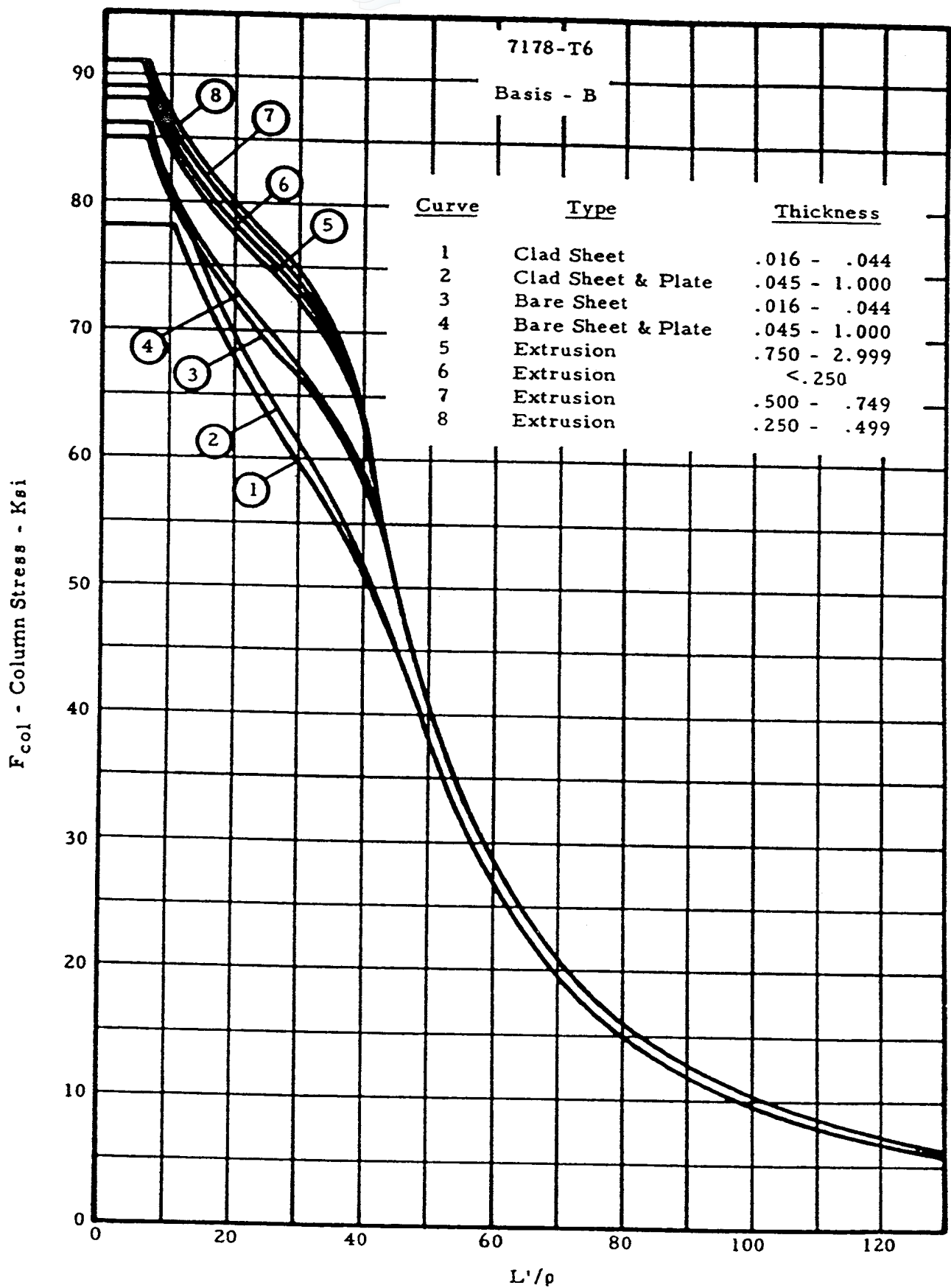
Figure 2-10.   Column Allowable Curves

The chart is titled **7178-T6**, **Basis - B**, with the vertical axis labeled F_{col} - Column Stress - Ksi and the horizontal axis labeled L'/ρ.

Curve	Type	Thickness
1	Clad Sheet	.016 - .044
2	Clad Sheet & Plate	.045 - 1.000
3	Bare Sheet	.016 - .044
4	Bare Sheet & Plate	.045 - 1.000
5	Extrusion	.750 - 2.999
6	Extrusion	< .250
7	Extrusion	.500 - .749
8	Extrusion	.250 - .499
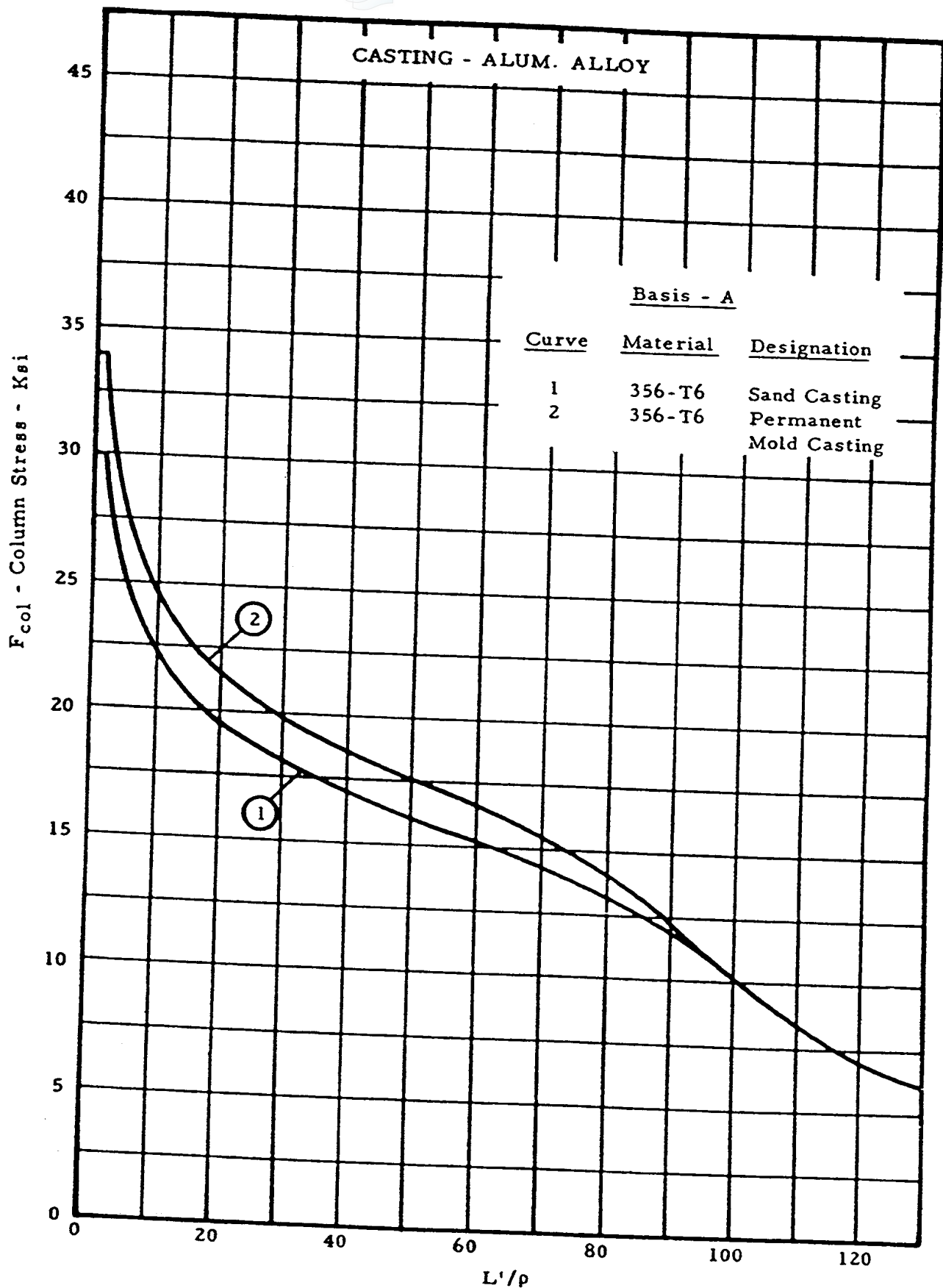
Figure 2-11.   Column Allowable Curves
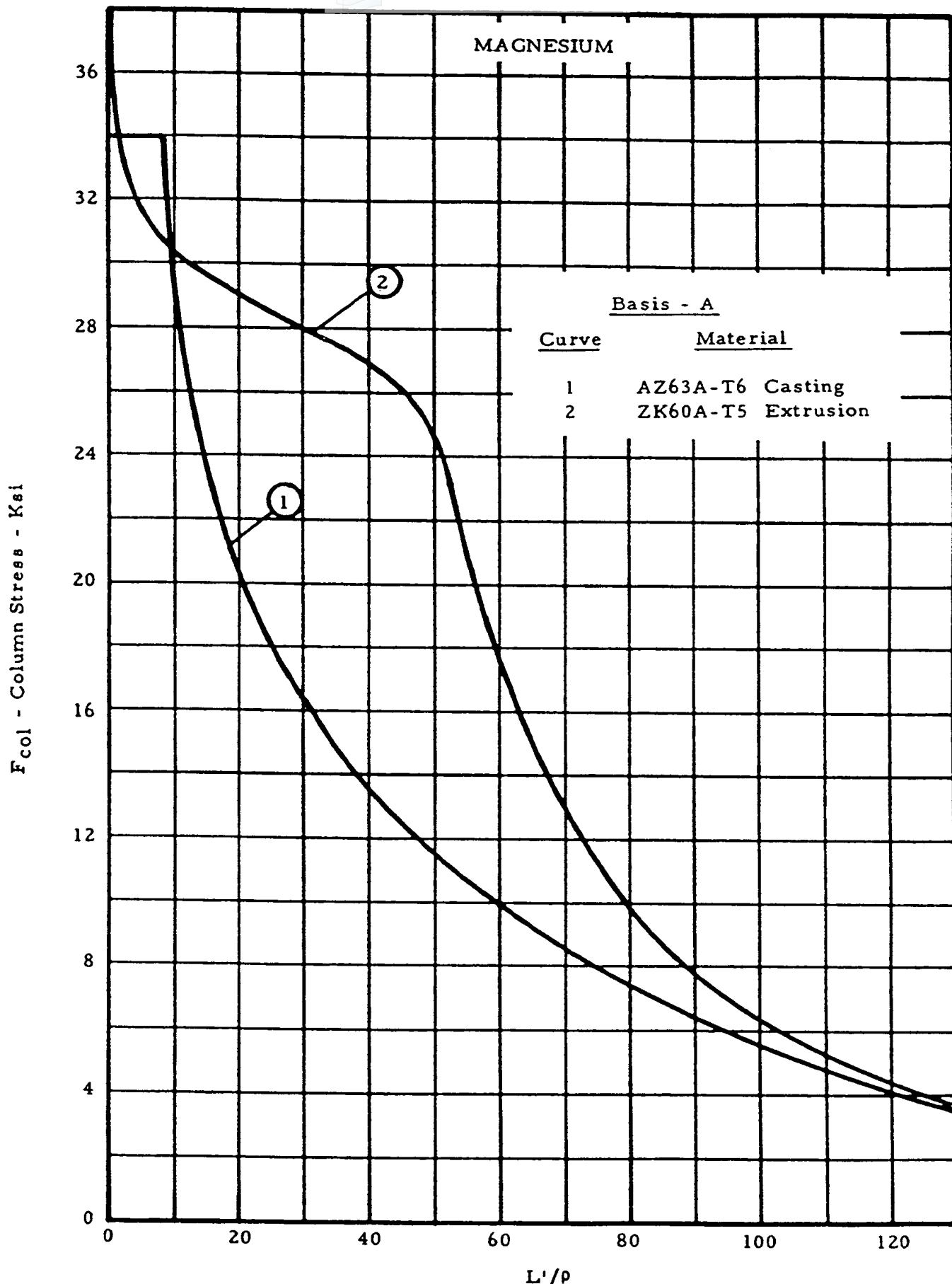
Figure 2-12. Column Allowable Curves
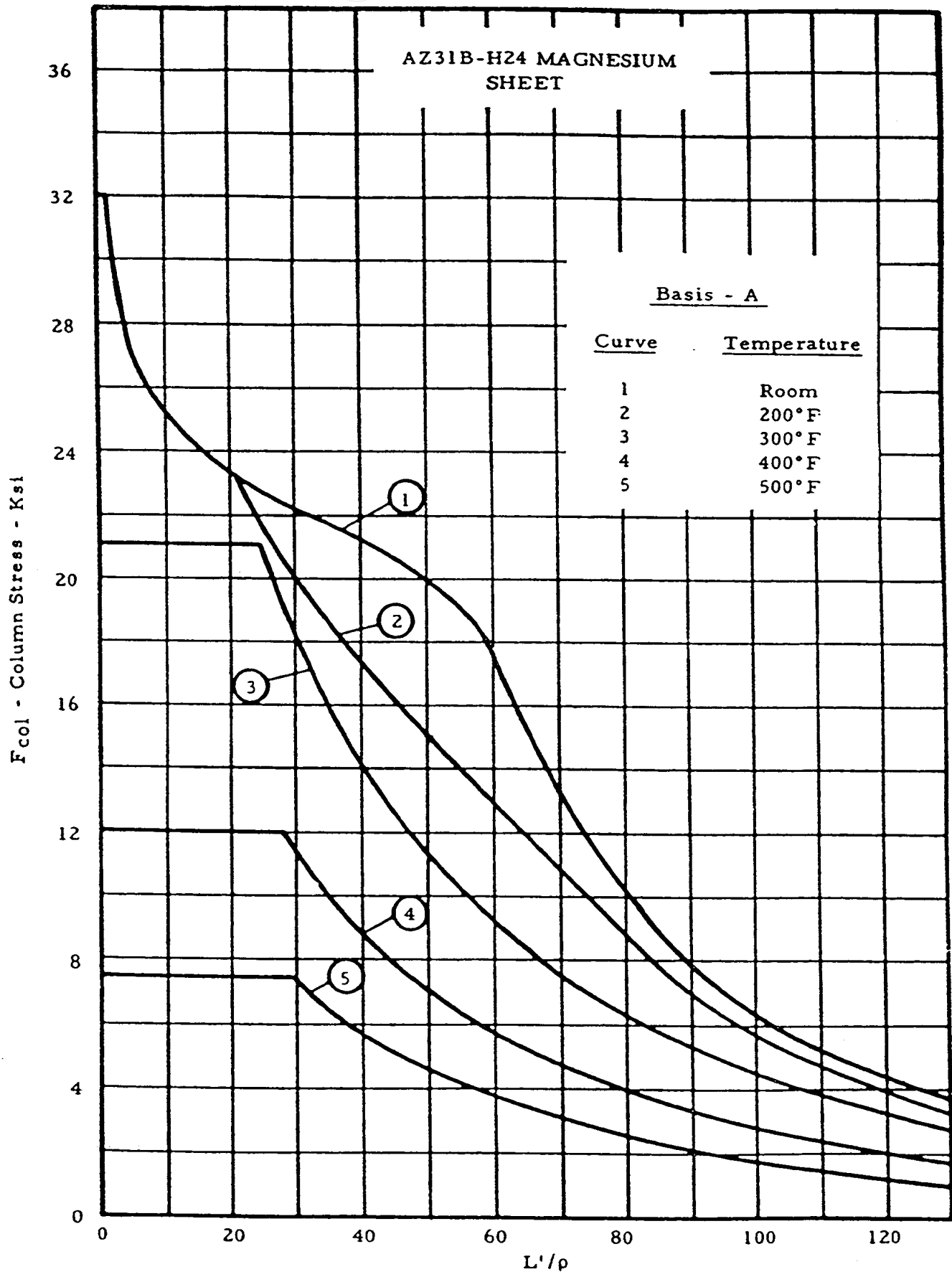
Figure 2-13.   Column Allowable Curves
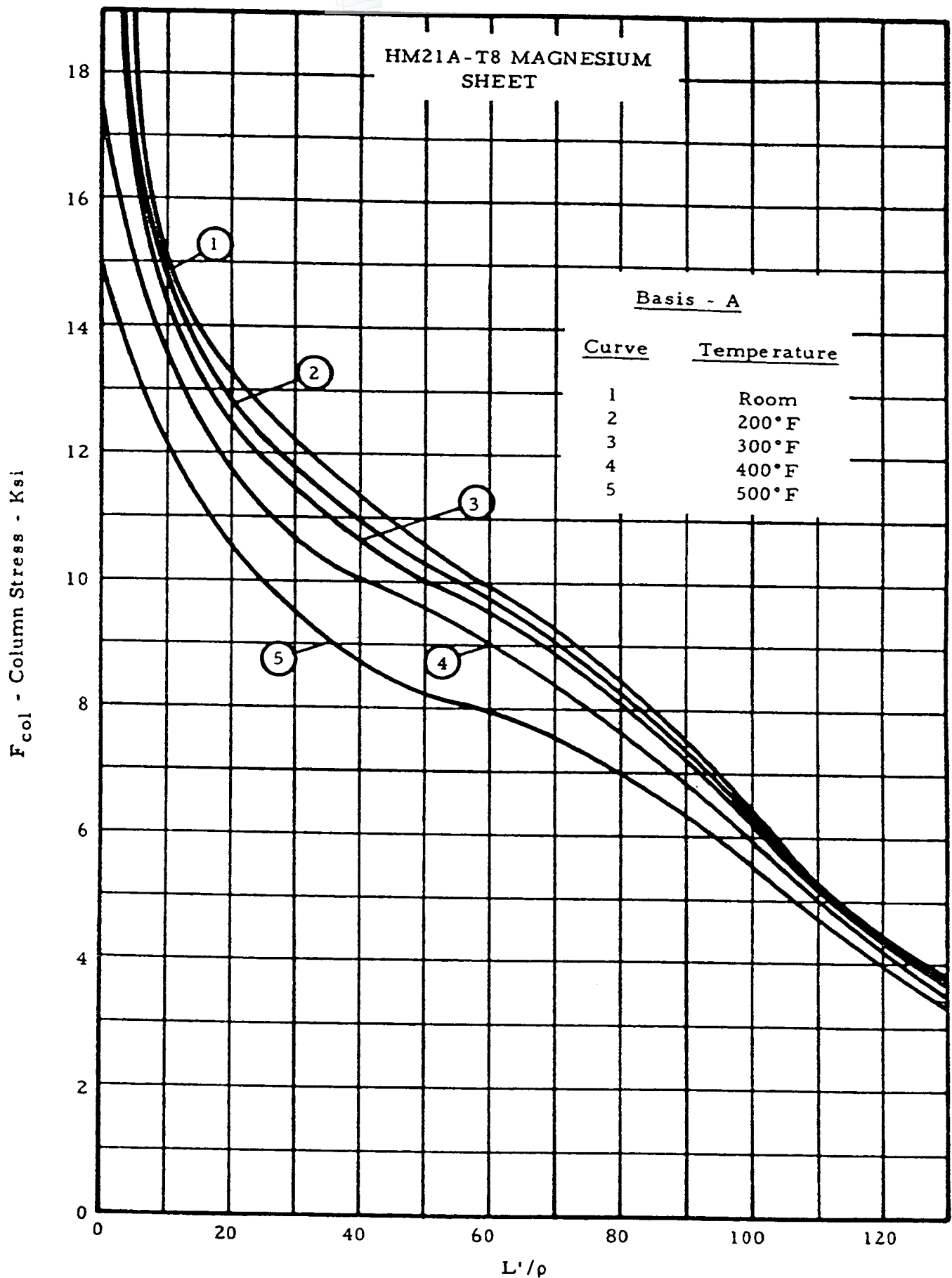
Figure 2-14.   Column Allowable Curves

2 - 18
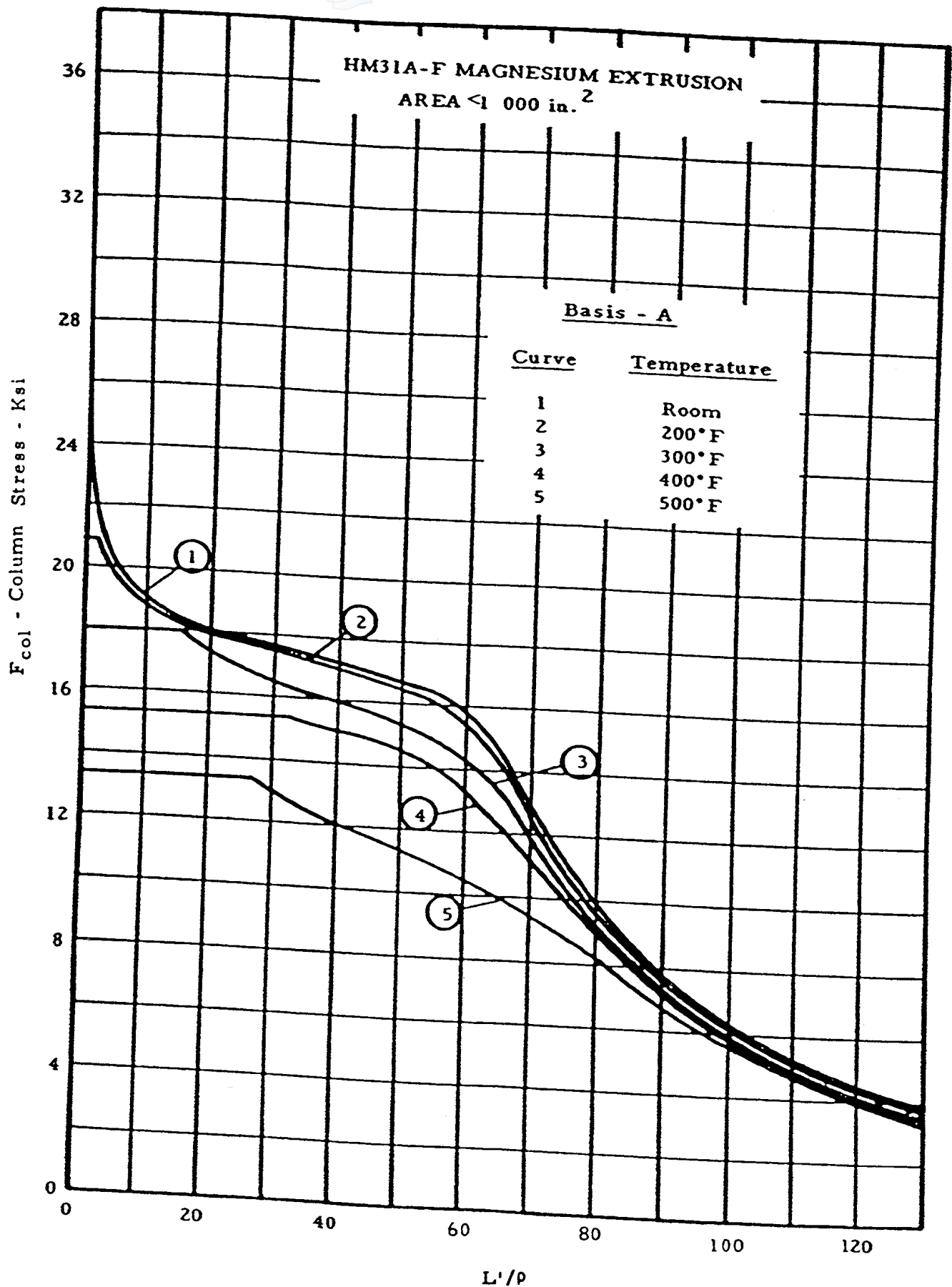
Figure 2-15.   Column Allowable Curves
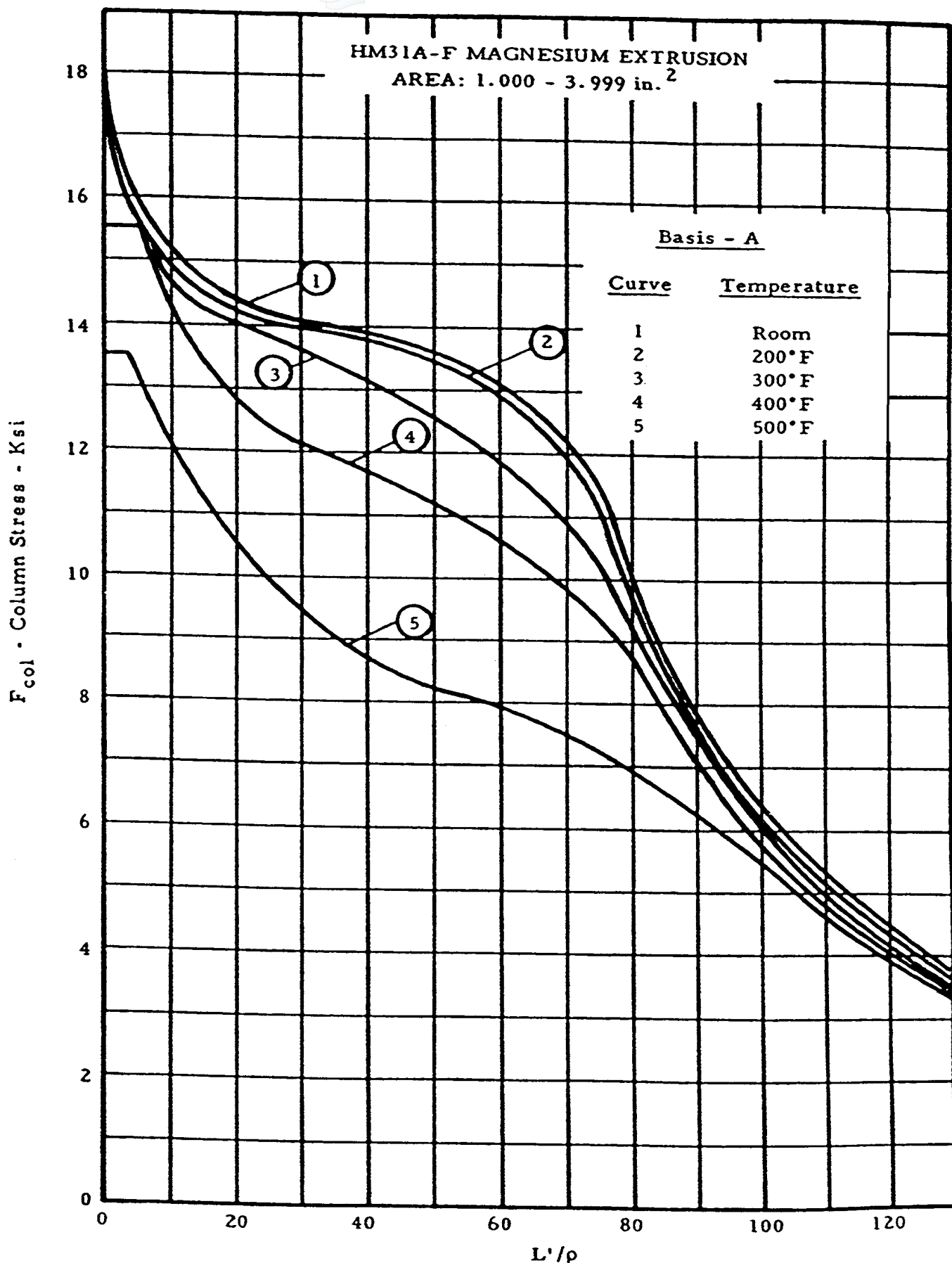
Figure 2-16.   Column Allowable Curves
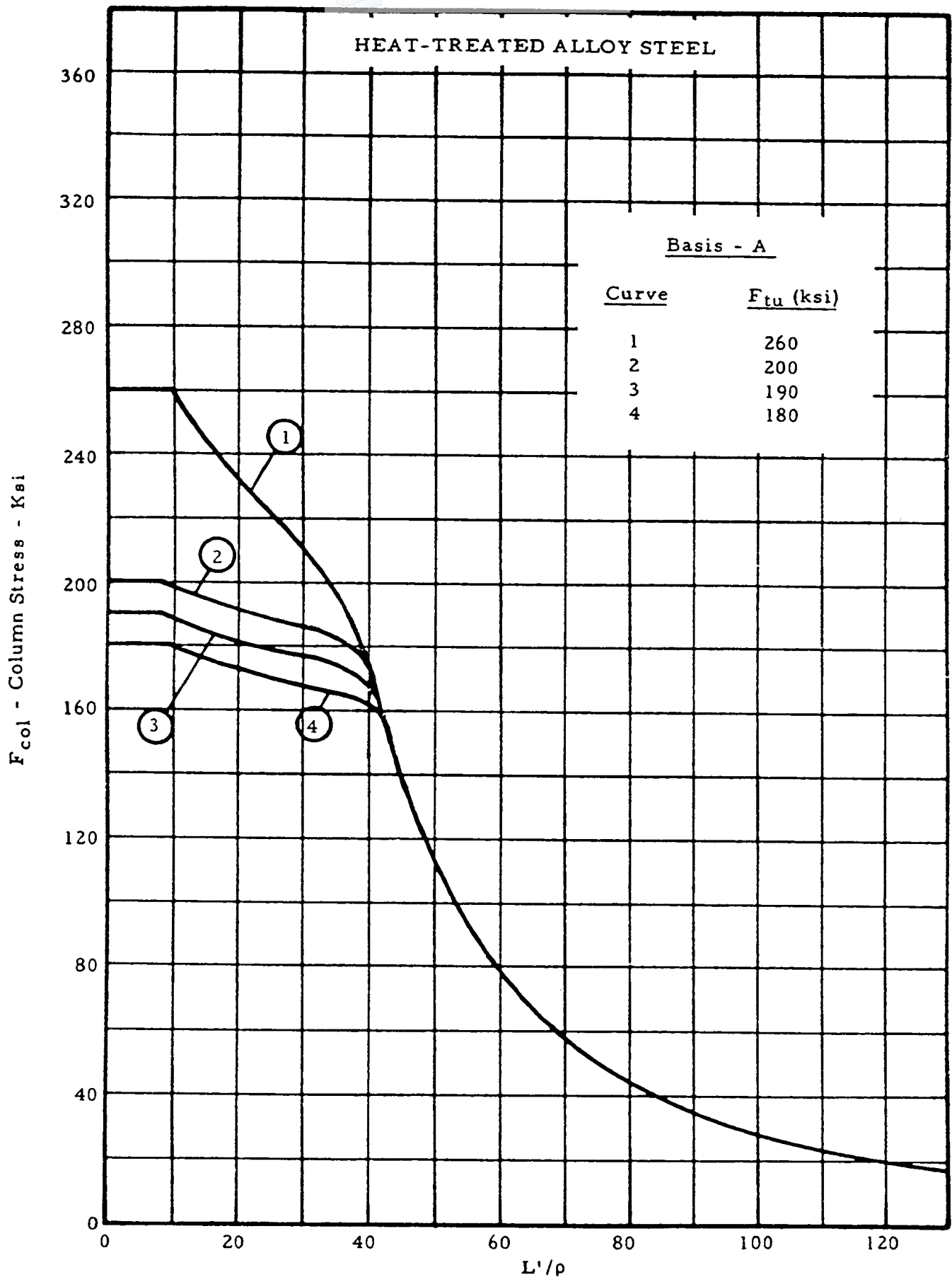
Figure 2-17.   Column Allowable Curves
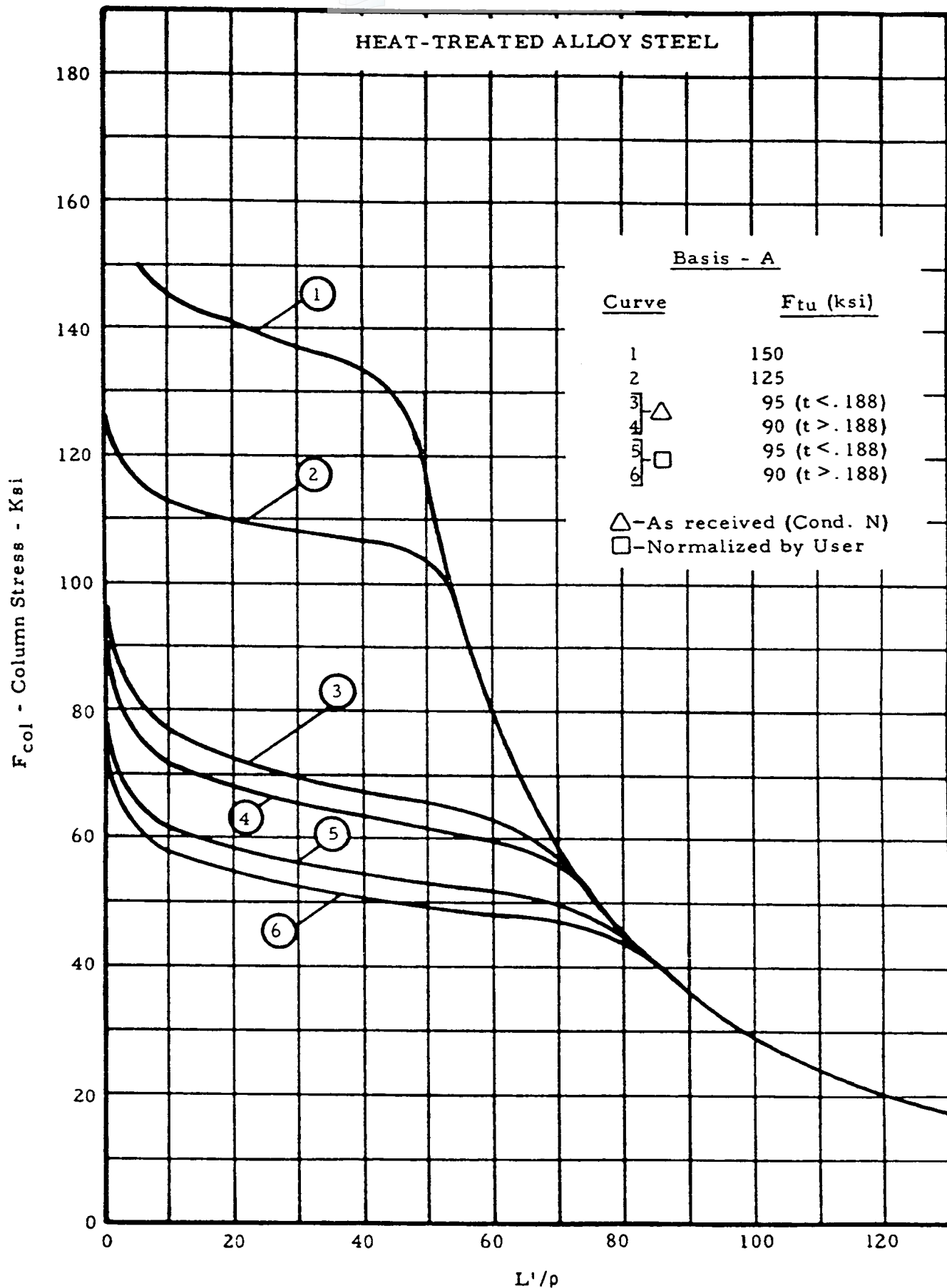
Figure 2-18. Column Allowable Curves
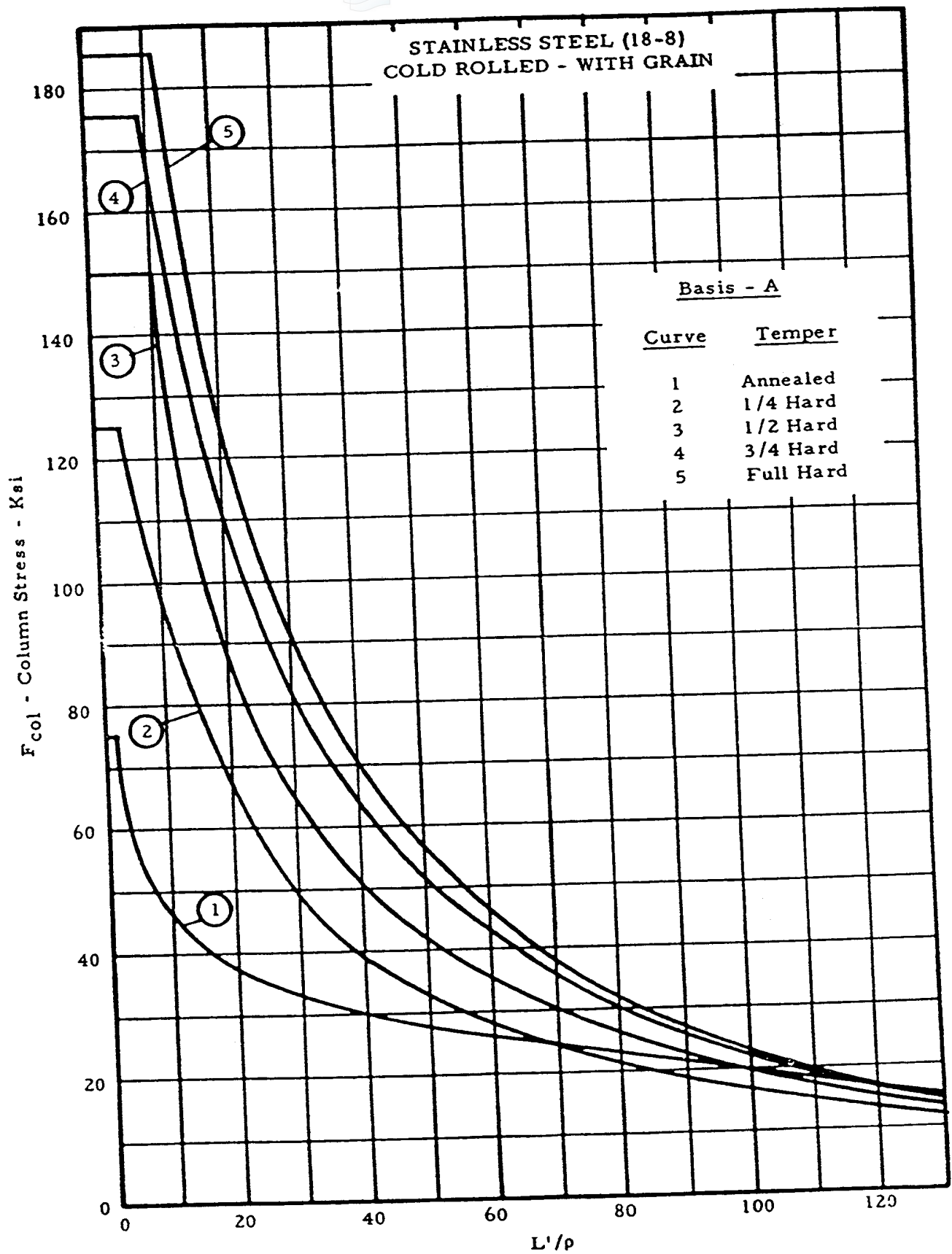
Figure 2-19.   Column Allowable Curves
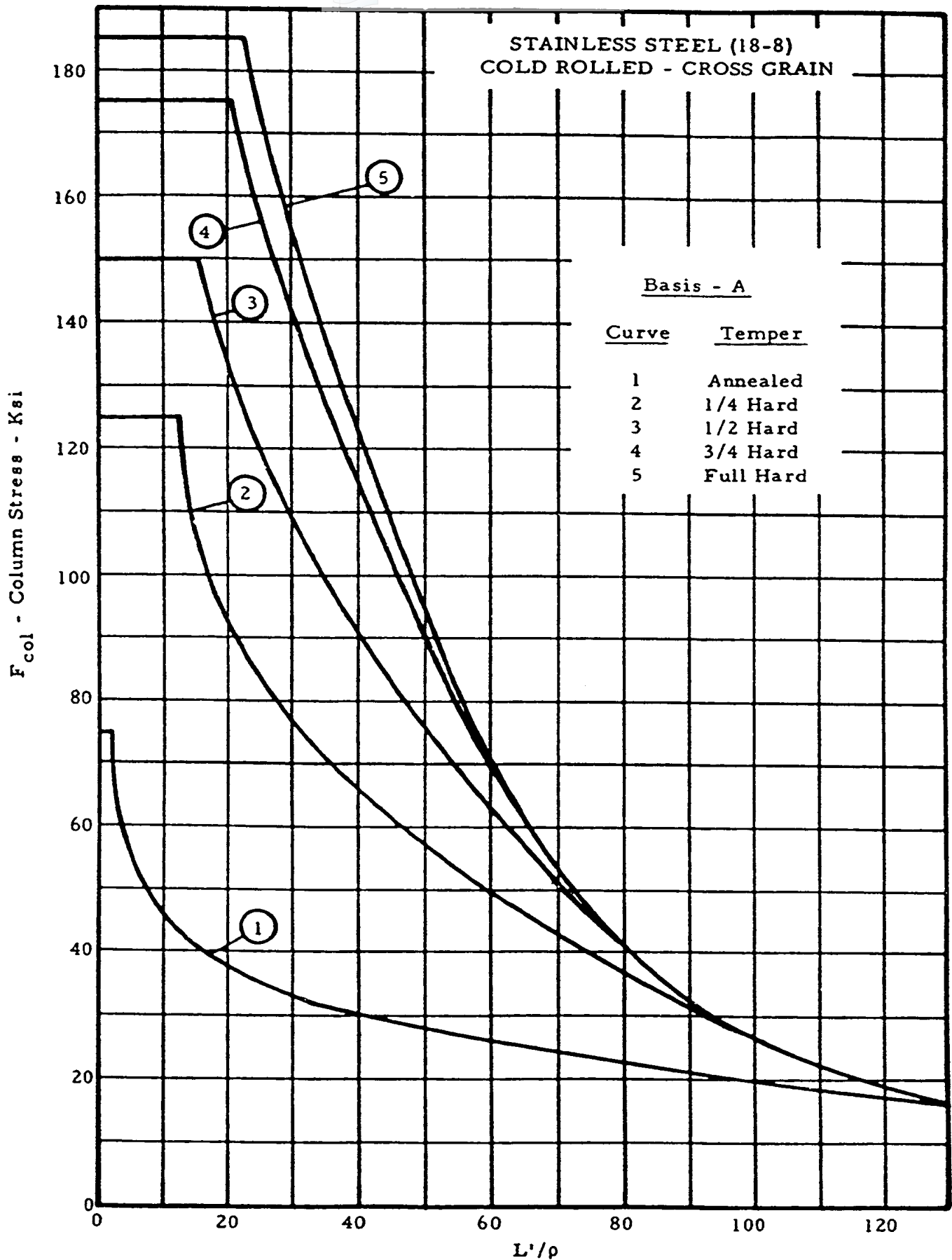
Figure 2-20.   Column Allowable Curves

2 - 24
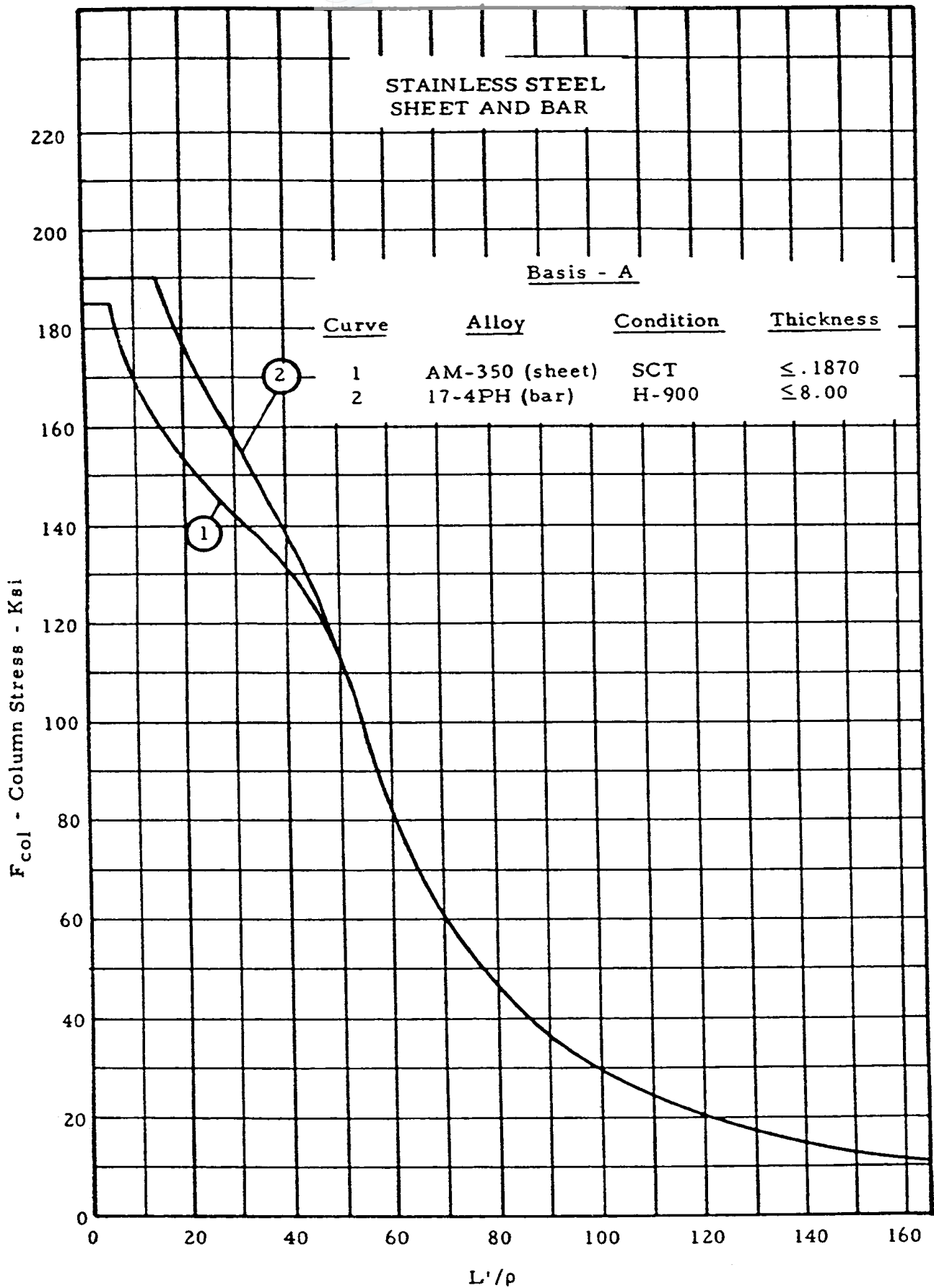
Figure 2-21. Column Allowable Curves
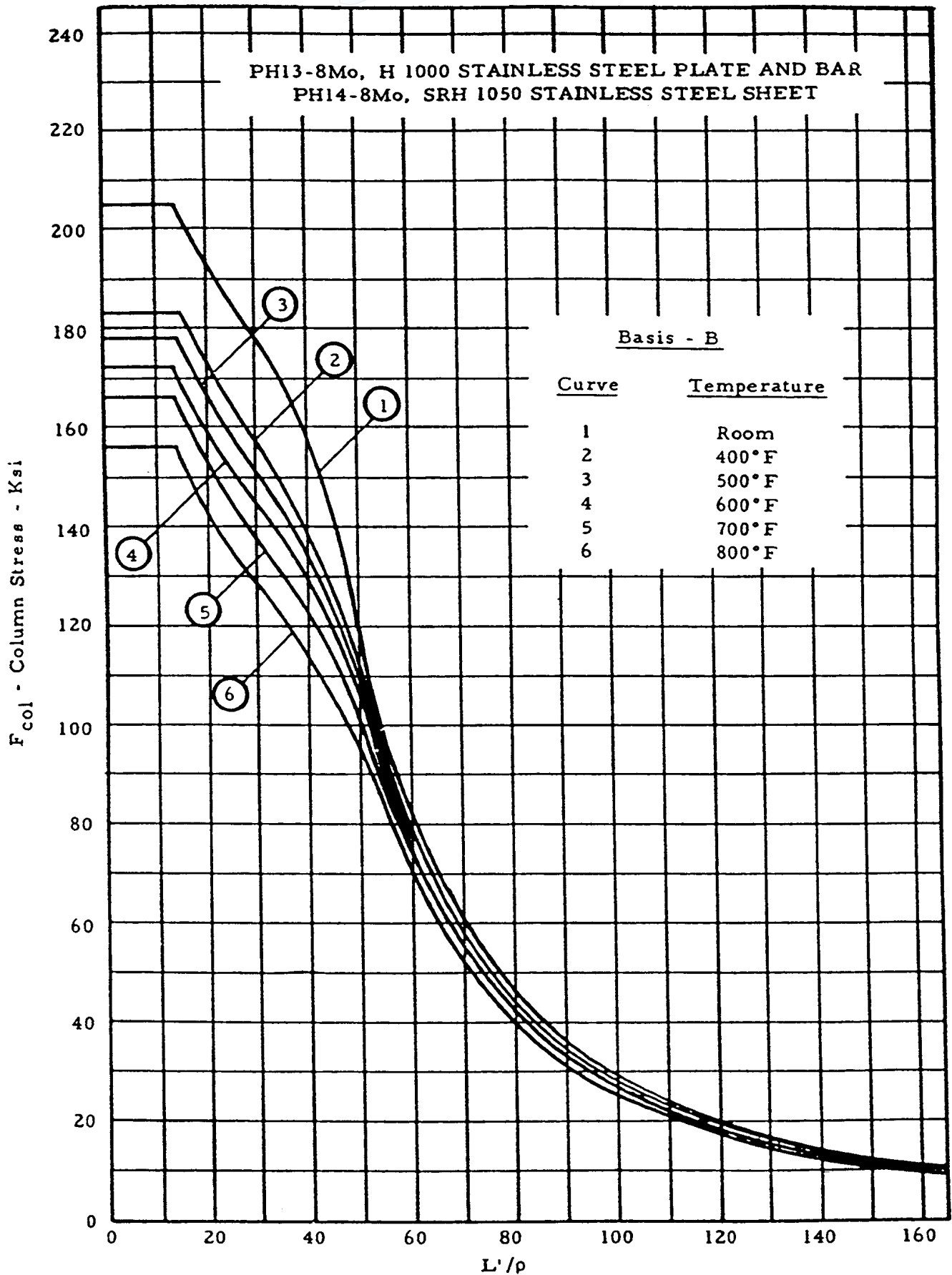
Figure 2-22. Column Allowable Curves

PH15-7Mo STAINLESS STEEL SHEET AND PLATE

F_{col} - Column Stress - Ksi

L'/ρ

	Basis - A	
Curve	Condition	Thickness
1	TH-1050	≤ .500
2	RH-950	≤ .125
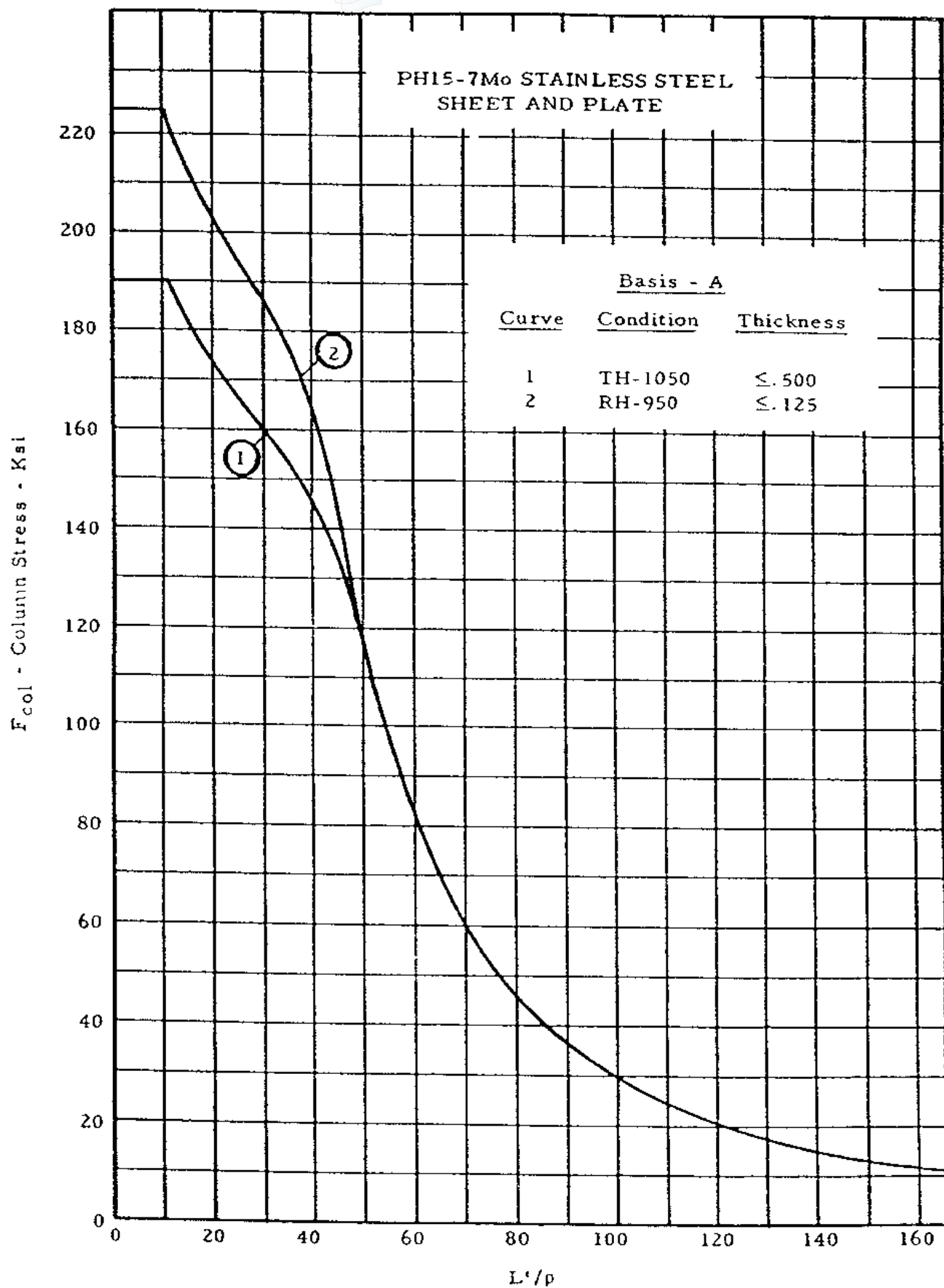
Figure 2-23.   Column Allowable Curves
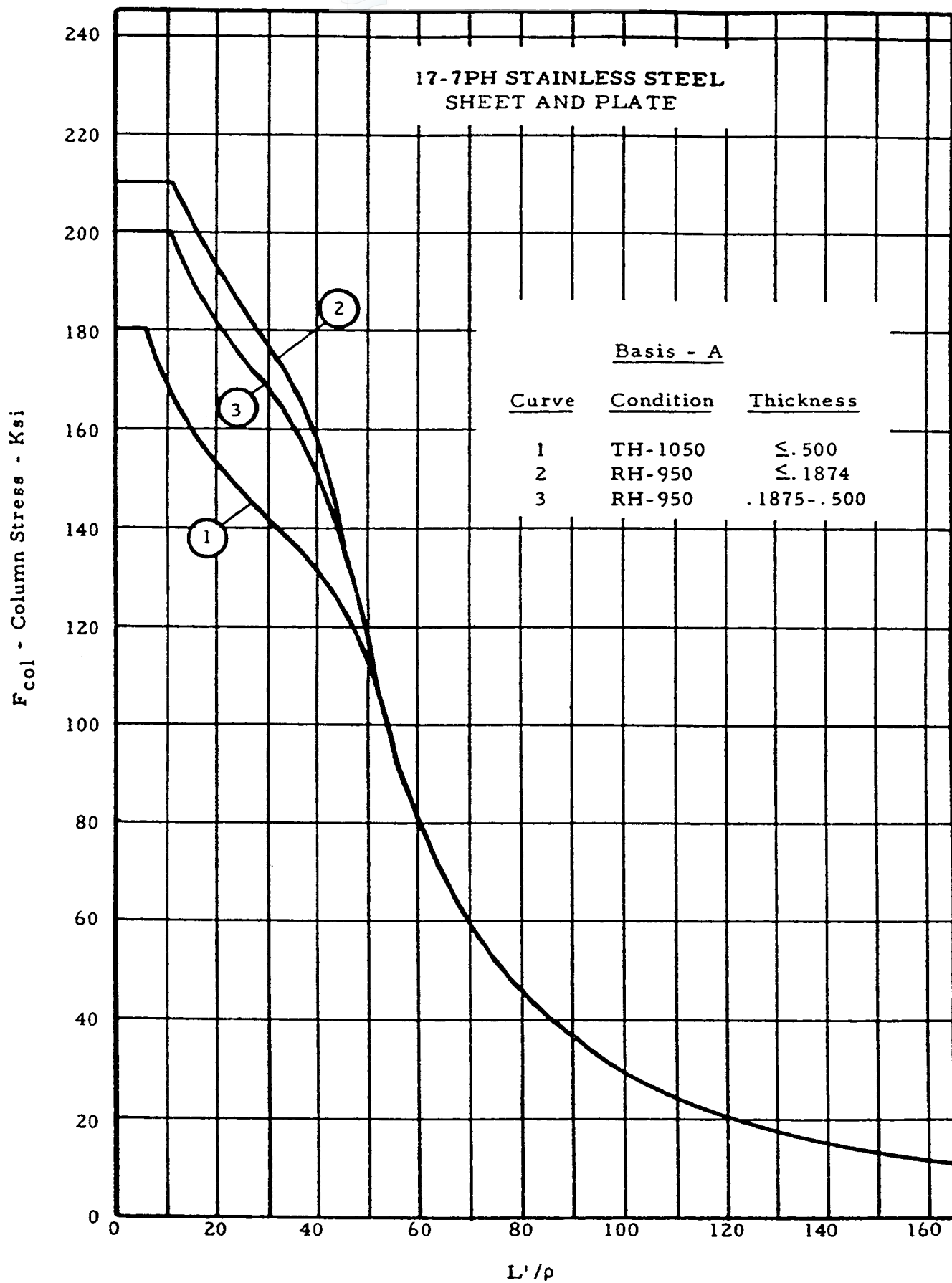
Figure 2-24.   Column Allowable Curves
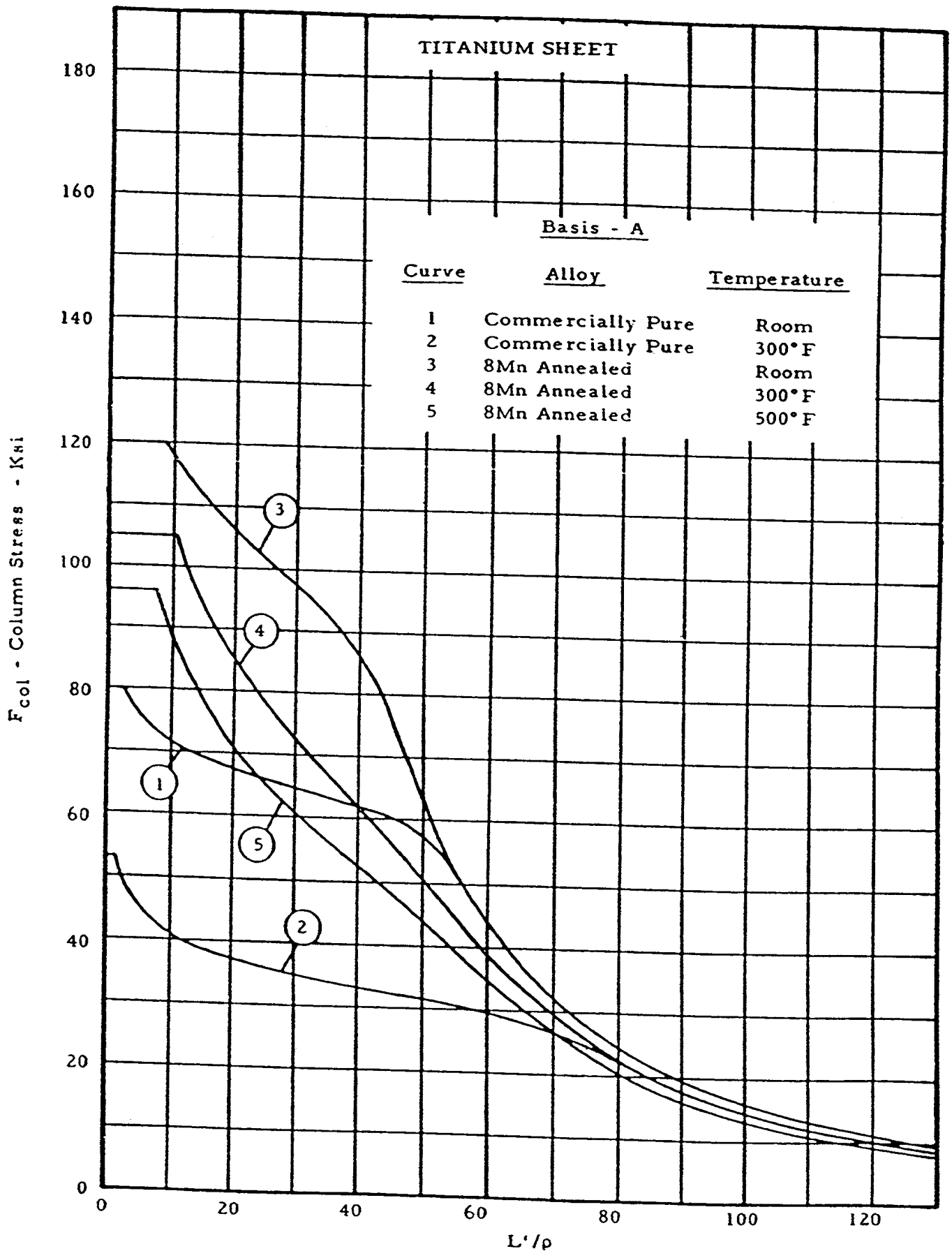
Figure 2-25.   Column Allowable Curves

2 - 29

4Al-3Mo-1V TITANIUM ALLOY
SOLUTION TREATED AND AGED SHEET AND PLATE
$t \leq .250$

Basis - B

Curve	Temperature
1	Room
2	300° F
3	400° F
4	500° F
5	600° F
6	700° F

F_{col} - Column Stress - Ksi

L'/ρ
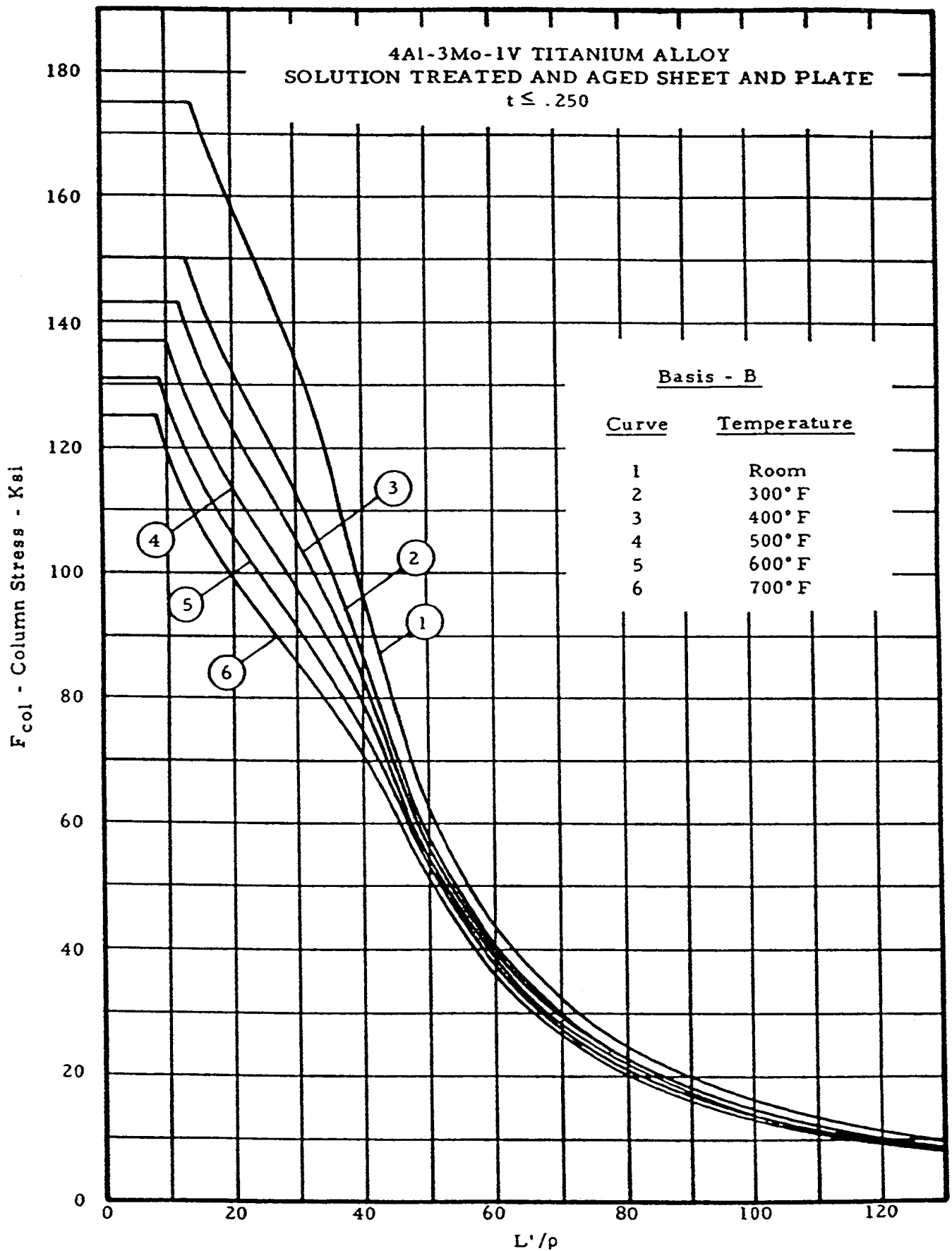
Figure 2-26   Column Allowable Curves

2 - 30
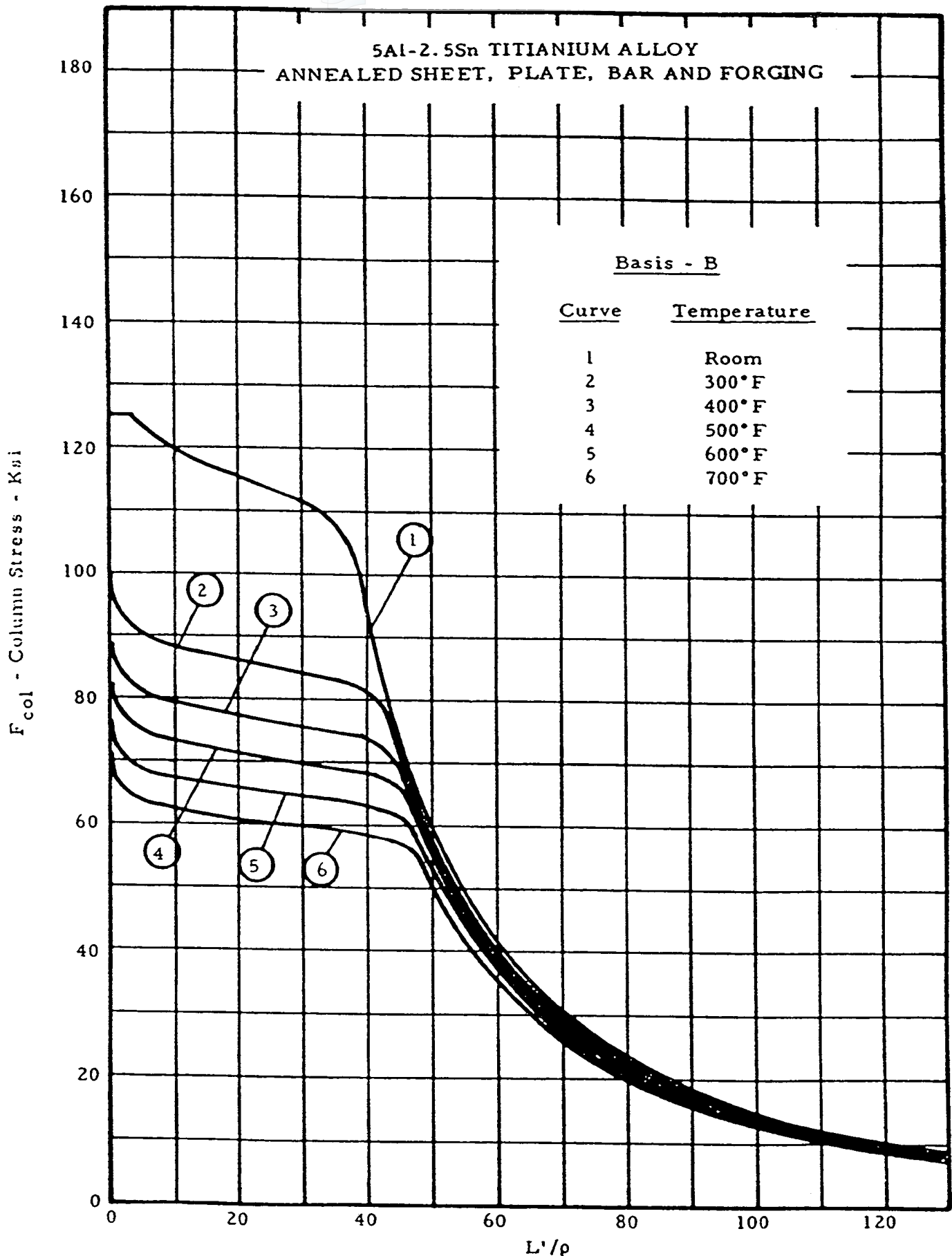
Figure 2-27. Column Allowable Curves

2 - 31
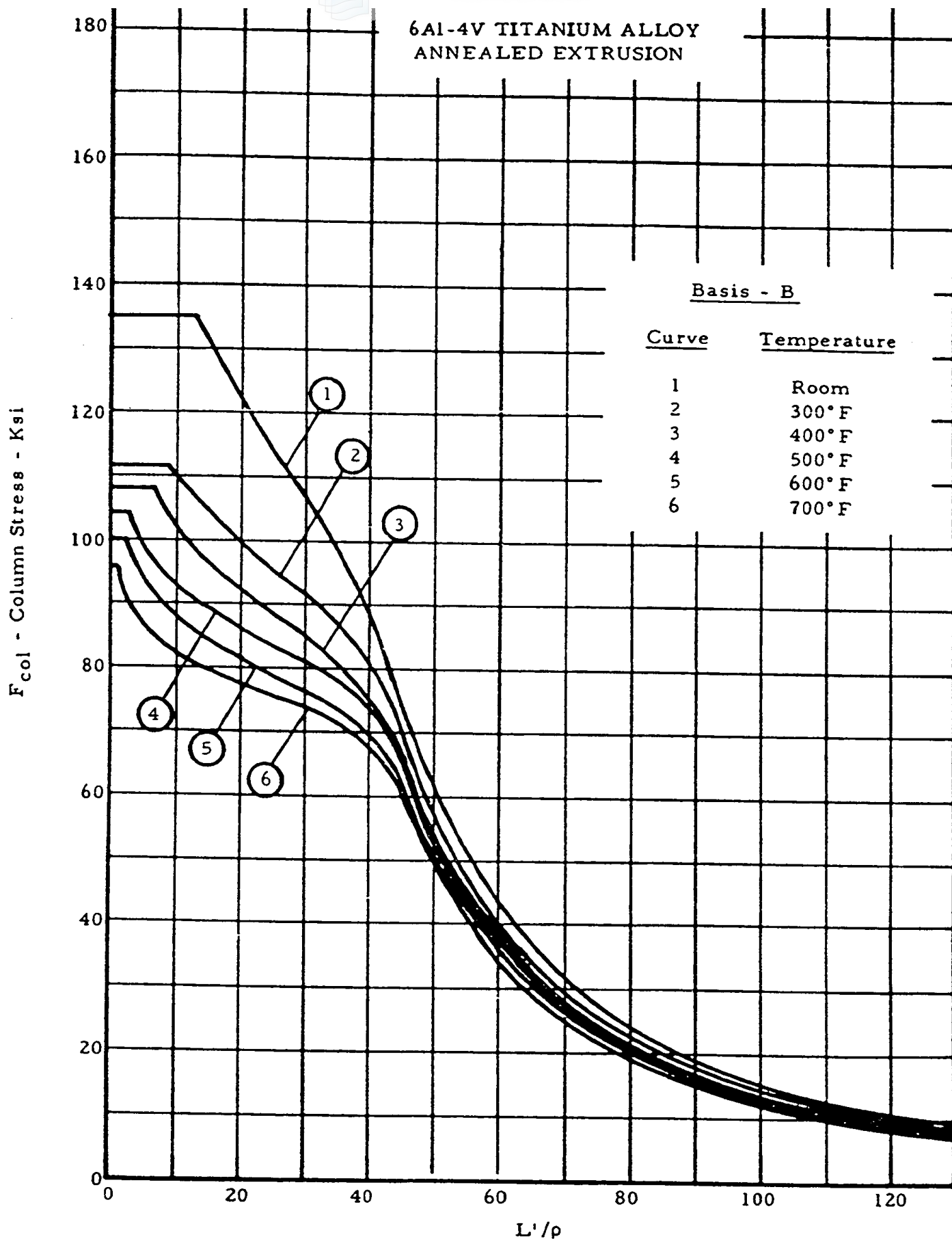
Figure 2-28.   Column Allowable Curves
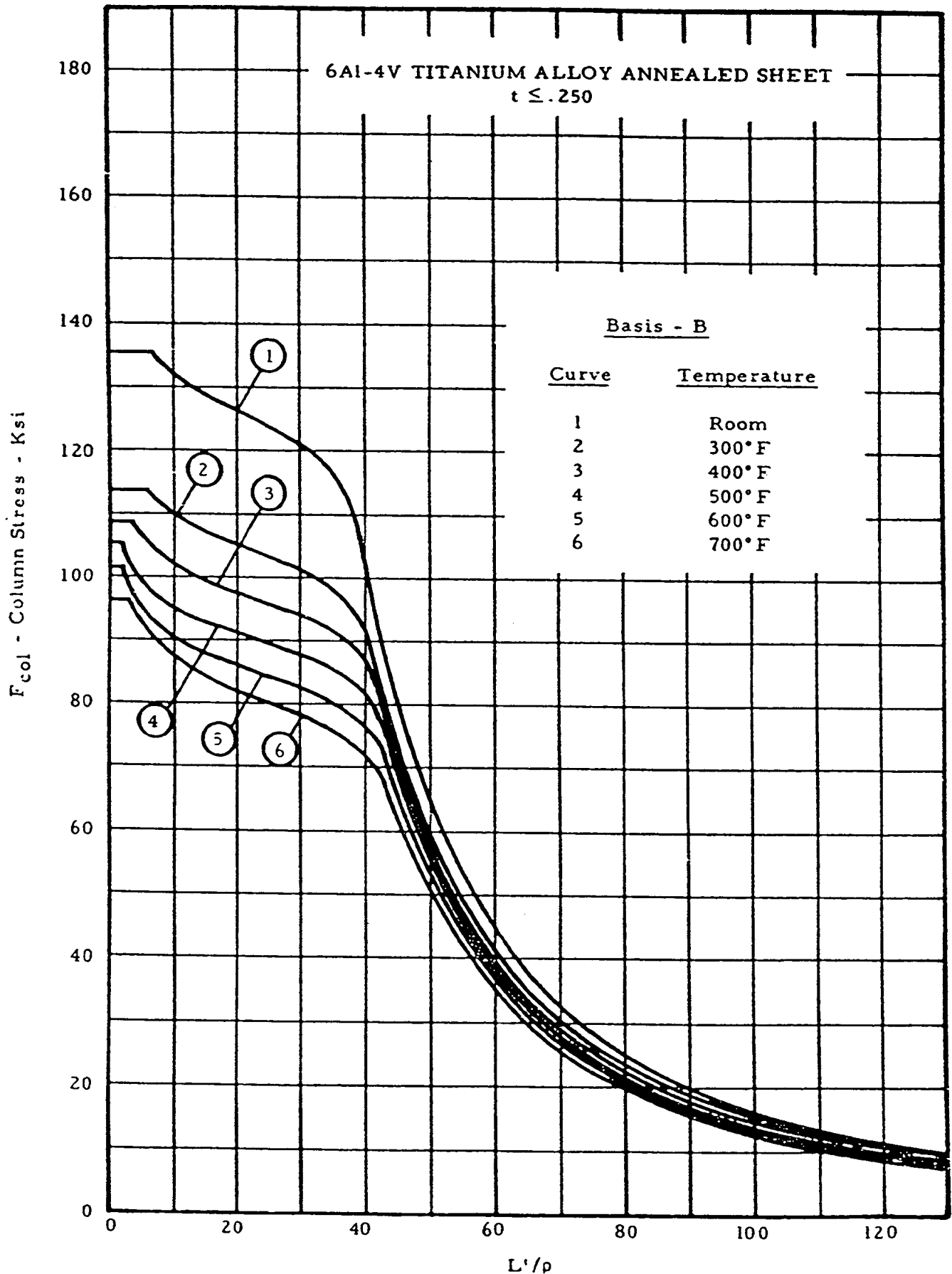
Figure 2-29. Column Allowable Curves
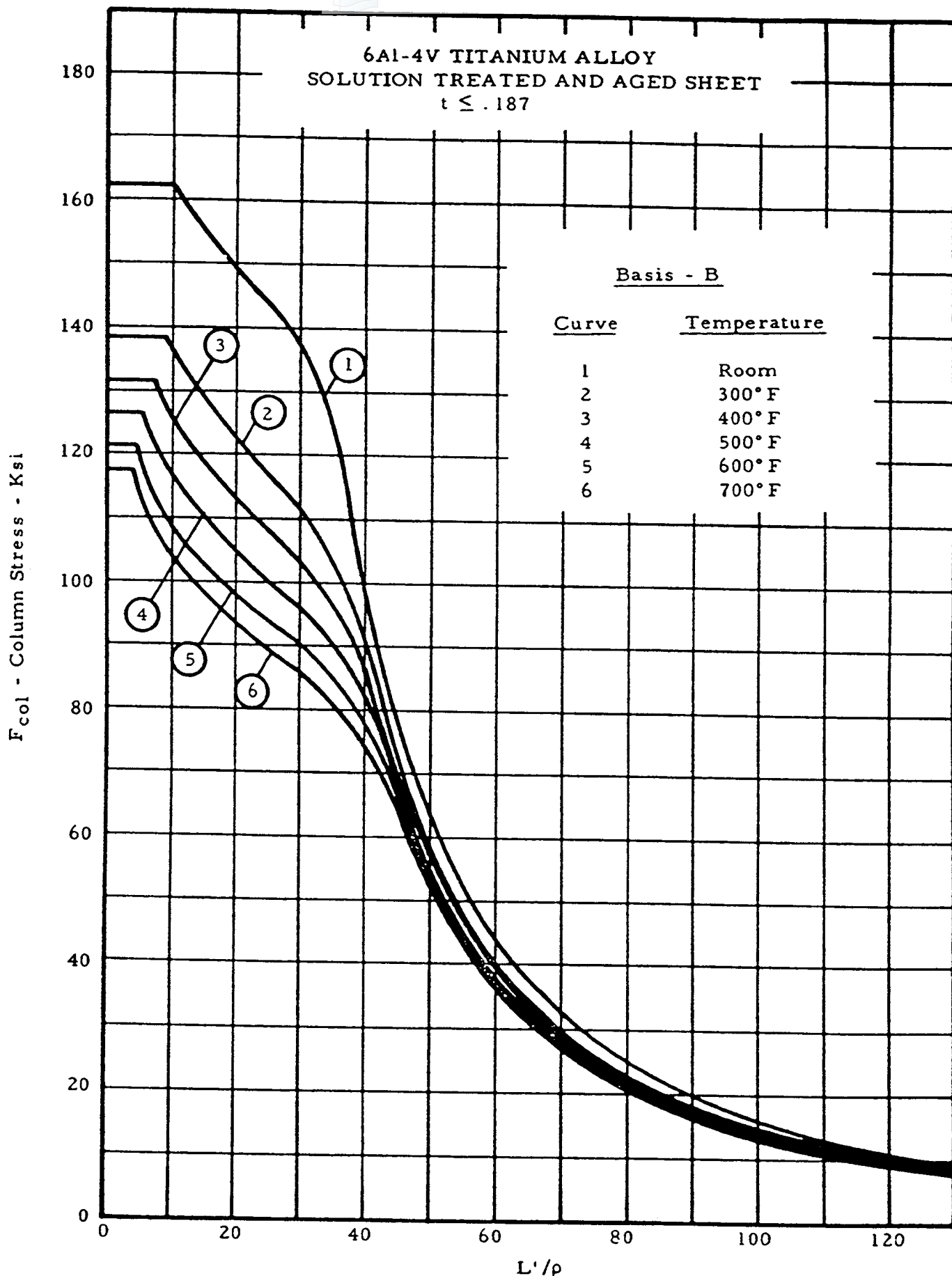
Figure 2-30. Column Allowable Curves

2 - 34

6Al-4V TITANIUM ALLOY
SOLUTION TREATED AND AGED EXTRUSION
$t \leq .500$

Basis - B

Curve	Temperature
1	Room
2	300°F
3	400°F
4	500°F
5	600°F
6	700°F

F_{col} - Column Stress - Ksi

L'/ρ
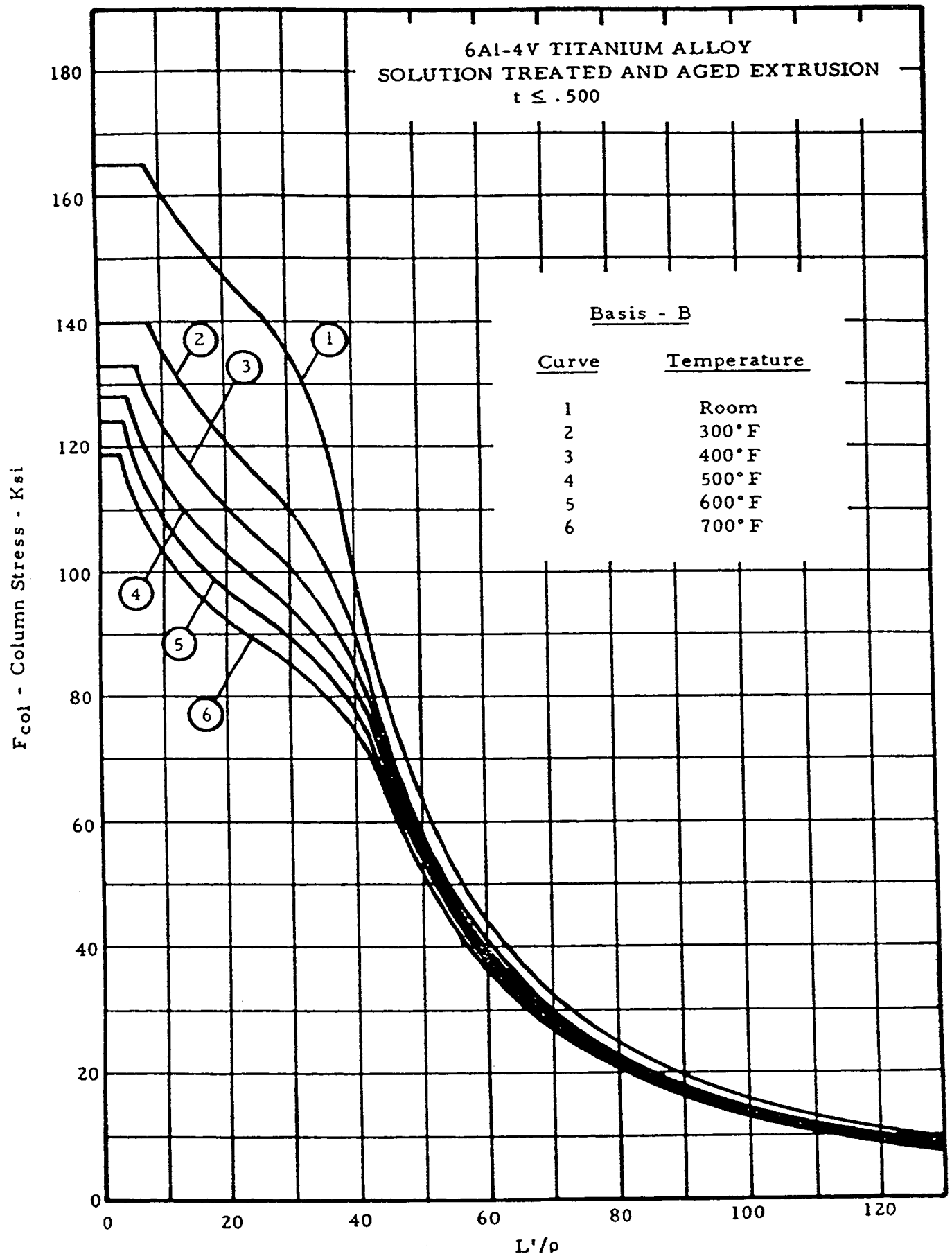
Figure 2-31. Column Allowable Curves

2 - 35

8Al-1Mo-1V TITANIUM ALLOY
SINGLE ANNEALED SHEET AND PLATE
$t \leq .500$

Basis - B

Curve	Temperature
1	Room
2	300°F
3	400°F
4	500°F
5	600°F
6	700°F

F_{col} - Column Stress - Ksi

L'/ρ
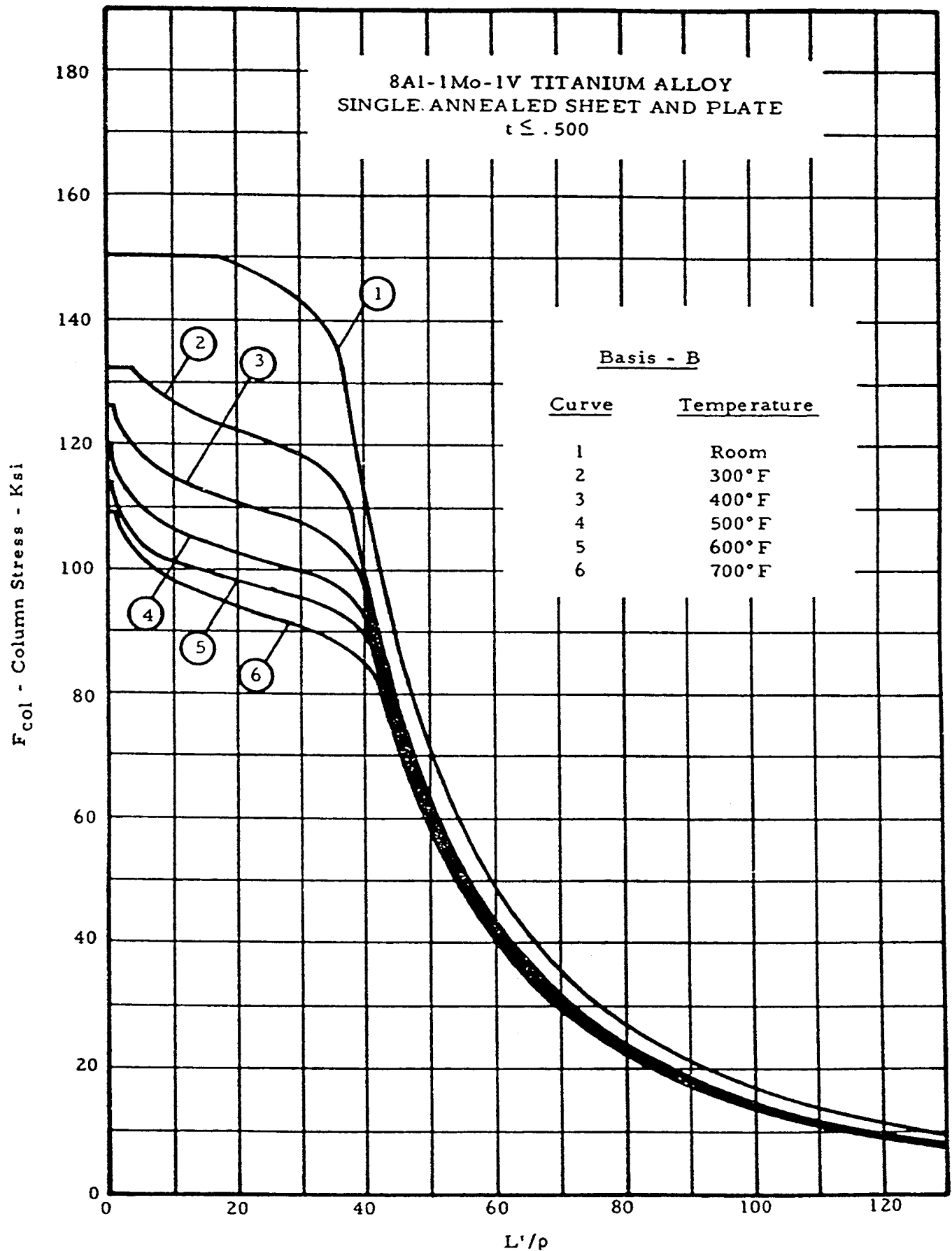
Figure 2-32.   Column Allowable Curves

2 - 36
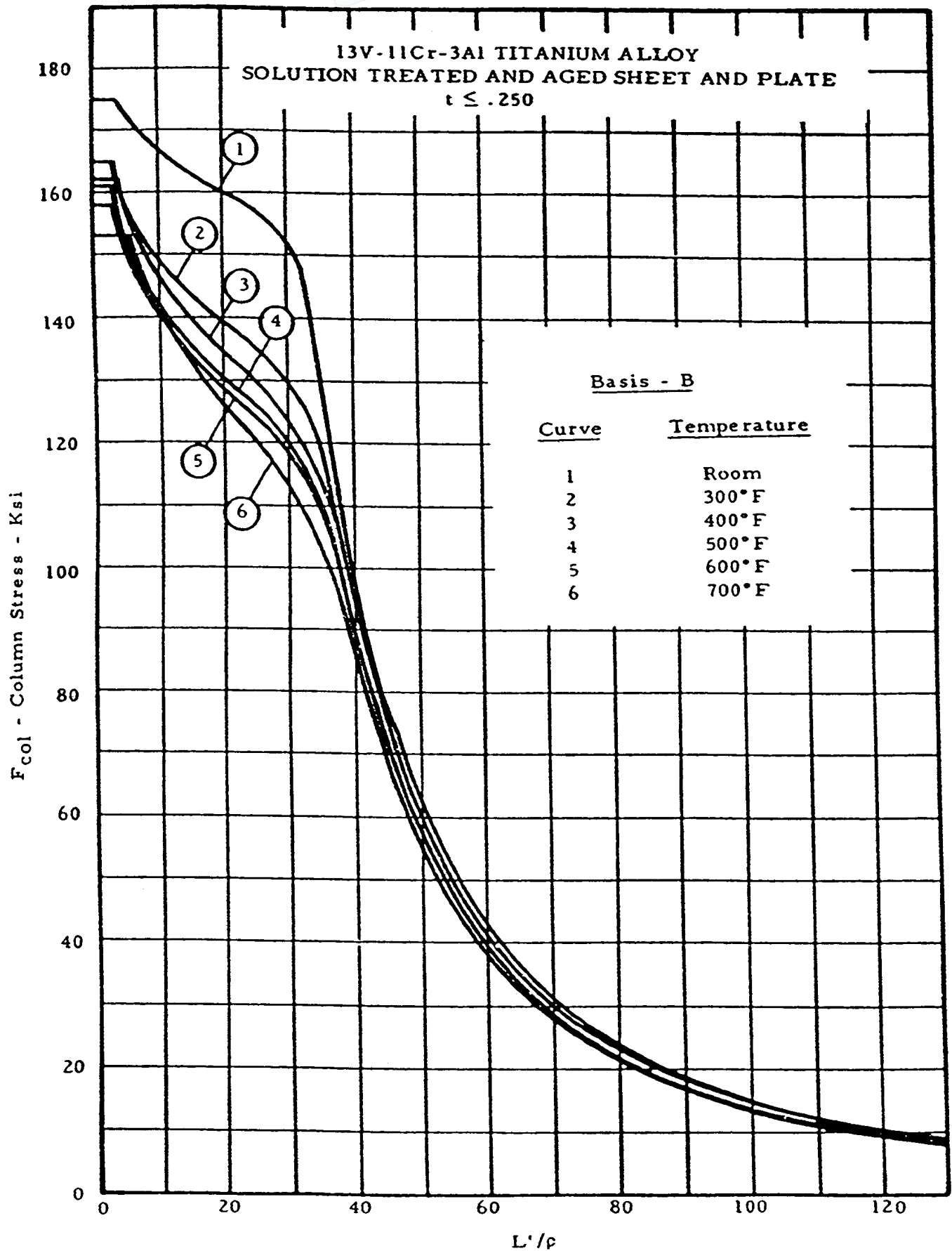
Figure 2-33.   Column Allowable Curves
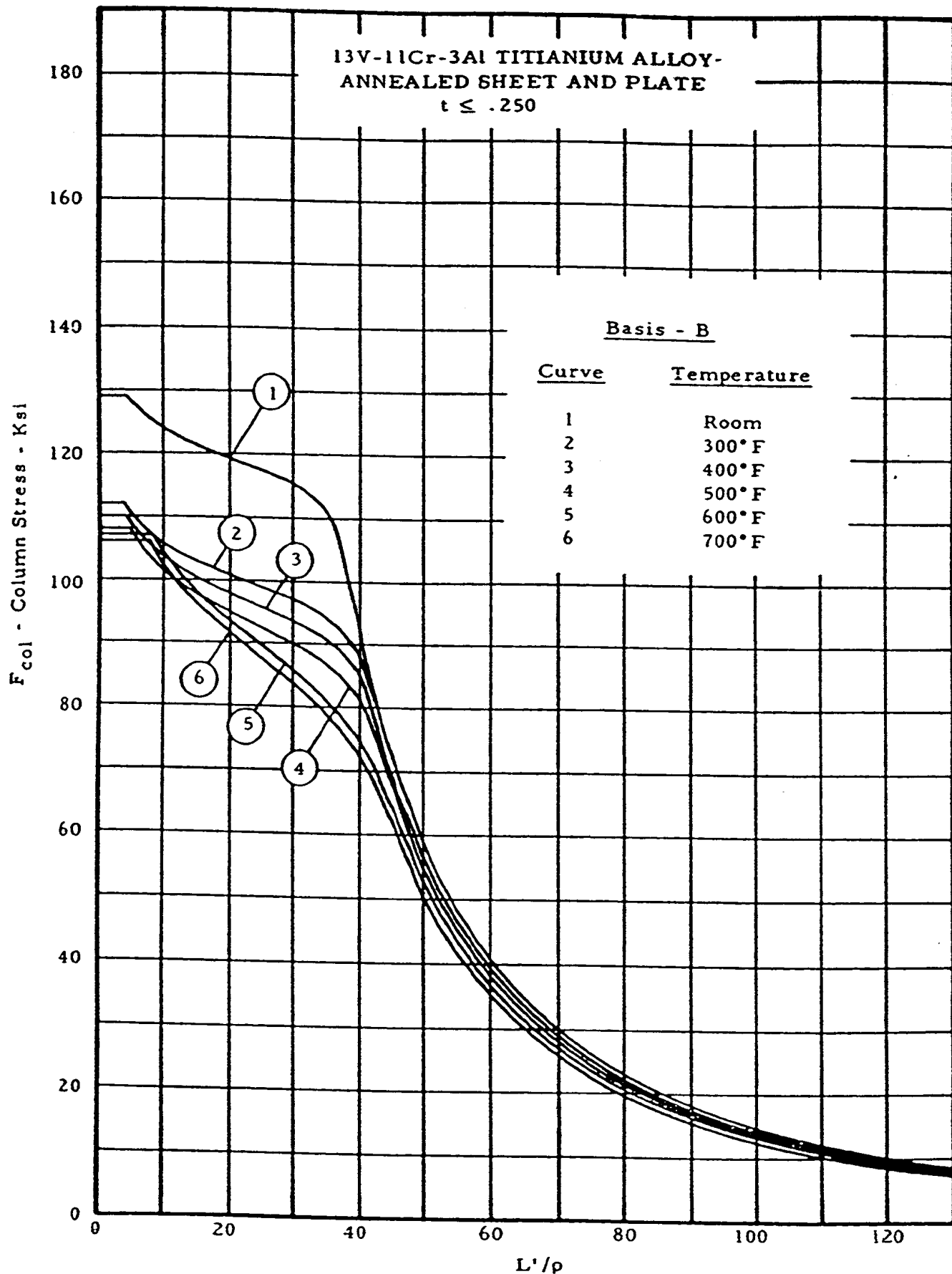
Figure 2-34. Column Allowable Curves

2.3.1.2 Sample Problem - Column Data Applicable to Both Long and Short Columns

Given: The 0.6 in. square concentrically loaded column shown in Figure 2-35.

2014-T6 aluminum alloy extrusion
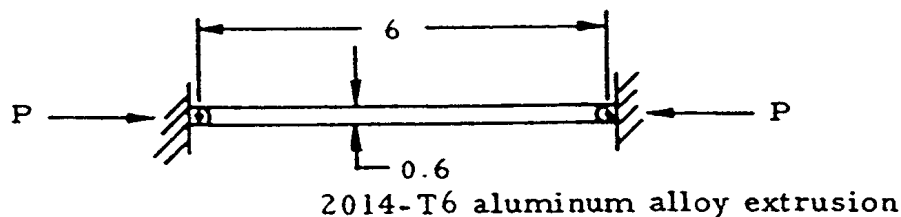
Figure 2-35. Pinned End Column in Axial Load

Find: The critical load, P_{cr}, by using column curves applicable to both long and short columns.

Solution: Since the column is pinned at both ends, $L' = L = 6$ in. For a square, $I = b^4/12$ and $A = b^2$. Thus,

$$\rho = \sqrt{\frac{I}{A}} = \sqrt{\frac{b^2}{12}} = \sqrt{\frac{(.6)^2}{12}} = 0.173 \text{ in.}$$

$$\frac{L'}{\rho} = \frac{6 \text{ in.}}{0.173 \text{ in.}} = 34.6$$

From Figure 2-3, curve 2, find $F_{col} = 56,200$ psi. Thus,

$$P_{cr} = F_{col}A = 56,200 \ (.6)^2 = 20,200 \text{ lb.}$$

2.3.1.3 Bending Failure of Concentrically Loaded Long Columns

In the process of describing column behavior in this chapter, the simplest cases are covered first and then various complications are covered. Historically, the first type of column to be successfully studied was the long concentrically loaded one for which Euler developed an equation giving the buckling load in terms of column parameters. This is also the simplest case.

The Euler formula, which is perhaps the most familiar of all column formulas, is derived with the assumptions that loads are applied concentrically and that stress is proportional to strain. Thus, it is valid for concentrically loaded columns that have stable (not subject to crippling) cross sections and fail at a maximum stress less than the proportional limit, that is, concentrically loaded long columns. The form of the Euler formula is

$$\frac{P_{cr}}{A} = \frac{C\pi^2 E}{\left(\frac{L}{\rho}\right)^2} \quad \text{or} \quad \frac{P_{cr}}{A} = \frac{\pi^2 E}{\left(\frac{L'}{\rho}\right)^2} \tag{2-1}$$

Here, P/A is the ratio of the axially applied load at failure to the cross-sectional area of the column. E is the modulus of elasticity of the column and L/ρ is the ratio of the column length to the least radius of gyration of its section. The radius of gyration is defined to be equal to $\sqrt{I/A}$, where I is the moment of inertia of the section. The constant, C, which is called the coefficient of constraint, is dependent upon end restraints and is discussed in Section 2.3.1.4 . In the second form of Equation (2-1), L' is an effective length which takes into account end restraint conditions.

2.3.1.4   Coefficient of Constraint for End Loaded Columns

In the discussion of columns, the coefficient of constraint C often occurs. As was mentioned before, this coefficient depends upon the manner in which the ends of a column are restrained, which, in turn, determines the boundary conditions that must be satisfied by the equations describing the column.

Sometimes, the use of a coefficient is avoided by using an effective length L' instead of the actual length L in formulas derived for a column with both ends pinned of length L. The term L' is then the distance between points of inflection of the loaded column curve. For example, the effective length of a column of length L that is rigidly supported at both ends is L/2 as can be seen in Figure 2-36.
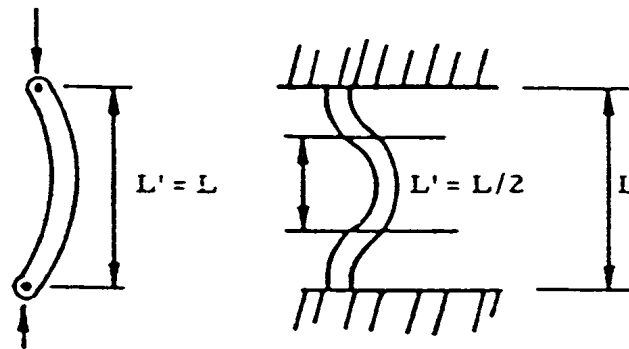
Figure 2-36.   Example of Effective Length
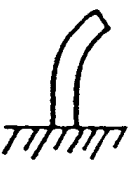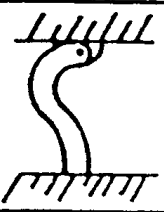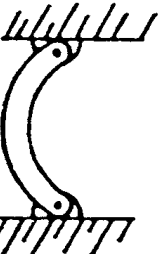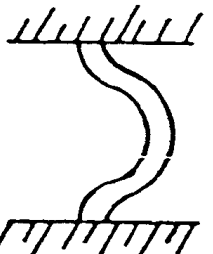
The relationship between L' and L, and C is

$$\left(\frac{L}{L'}\right)^2 = C \tag{2-2}$$

2 - 40

By assuming various combinations of idealized end restraints, a table of theoretical end constraint factors may be constructed. This is shown in Table 2-1.

TABLE 2-1

Coefficients of Constraint for Idealized End Conditions

Type of Fixity	C	Type of Fixity	C
	.25		2.05
	1.00		4.00

The end restraints of an actual column are never exactly equivalent to pinned or fixed ends, but lie somewhere between the two extremes. This discrepancy is due to the fact that a pinned joint is never entirely frictionless and a member to which a column is fixed is never perfectly rigid.

Cases for which one or both of the ends of a column are fixed to nonrigid members may be treated by considering these ends to be restrained by a torsional spring of spring constant μ. The constant μ is defined to be $dT/d\theta$ where T is a torque applied to the support at the point where the column is attached and θ is the angle of twist at this point. Given this definition, μ may be calculated by applying formulas from strength of materials to the member to which the column is attached before attachment. For example, consider the column shown in Figure 2-37. The torsional spring constant for the end is found by considering the beam supporting the column and calculating $dT/d\theta$ where T and θ are as shown in the middle diagram. $dT/d\theta$ is a constant for small deflections so T/θ may be found from beam formulas. The column is then redrawn with the attached beam replaced by an equivalent torsional spring.

$$\mu = \frac{dT}{d\theta}$$
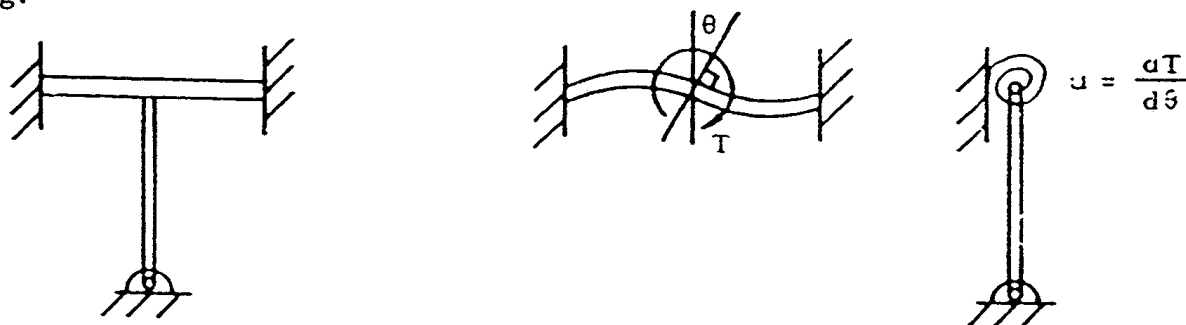
Figure 2-37.   Example of Equivalent Torsional Spring

2 - 41

Equations have been developed that give the end fixity coefficient, C, as a function of μ, L, E, and I for columns equally elastically restrained at both ends and for those pinned at one end. These equations are given and plotted in Figure 2-38. From these plots, it can be seen that C approaches the value corresponding to a fixed end rather than an elastically restrained end as μ increases. Likewise, C approaches the value corresponding to a pinned end as the spring constant approaches zero.

For $u = \infty$, C = 4.0

Both Ends Equally Restrained

$$\frac{uL}{EI} = \pi \sqrt{C} \, \cot \frac{\pi \sqrt{C}}{2}$$

C = fixity coefficient
E = modulus of elasticity
I = moment of inertia
L = length of column
u = bending restraint coefficient - spring constant (in-lb/rad)

One End Restrained

$$\frac{uL}{EI} = \frac{(\pi)^2 C}{\pi \sqrt{C} \, \cot \pi \sqrt{C} - 1}$$

For $\mu = \infty$, C = 2.05
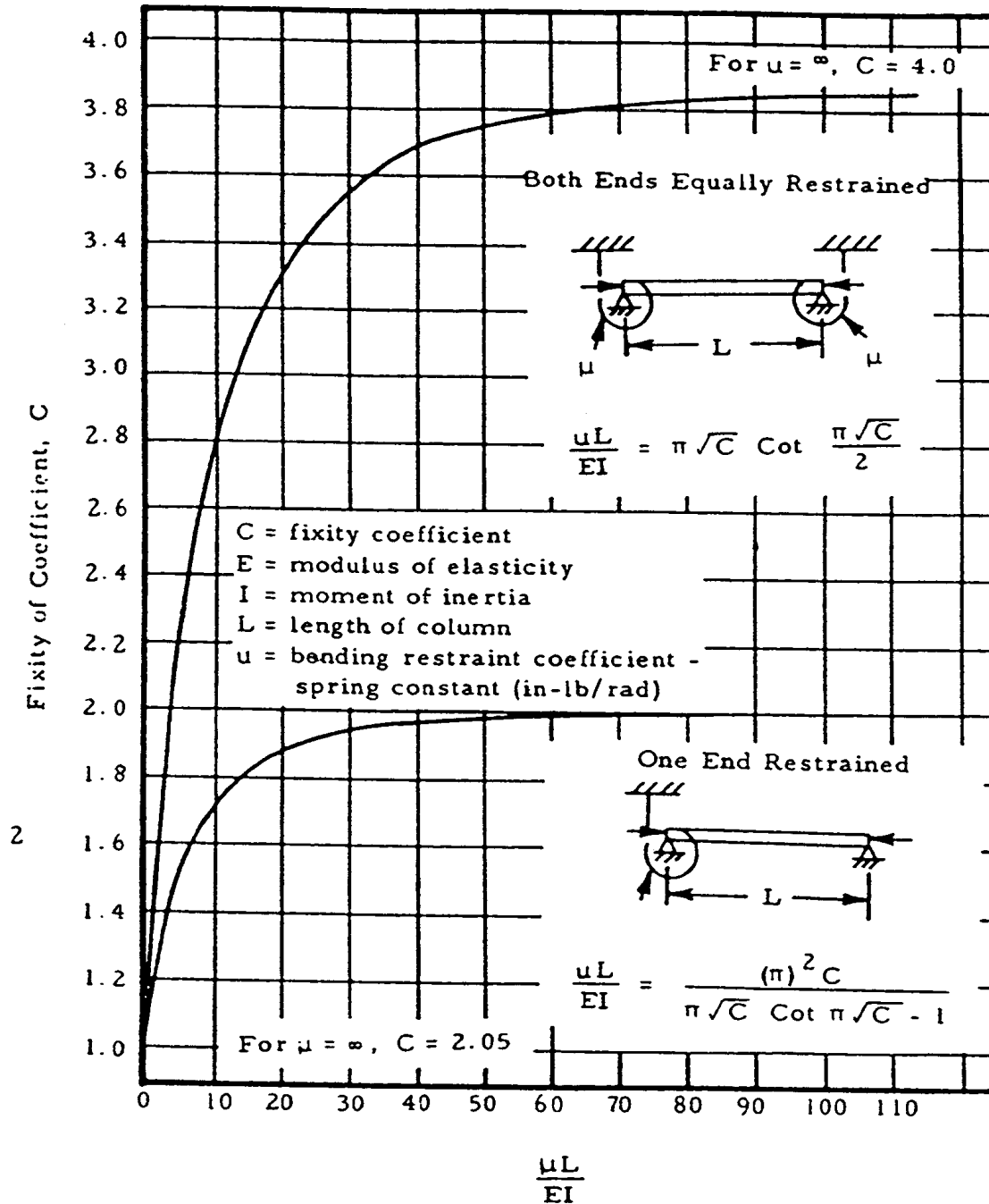
Figure 2-38. Fixity Coefficient for a Column with End Supports Having a Known Bending Restraint

At times, a column may be supported along its length as well as at the ends. For example, the column shown in Figure 2-39 is supported at its midsection by another member.
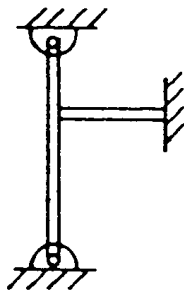
Figure 2-39. Simply Supported Column with Intermediate Support

In order to treat such a case, namely that illustrated in Figure 2-39, we may consider the member supporting the column at its midsection to be a spring of spring constant K lbs/in. which may be found by applying strength of materials to the support. Charts that give the coefficients of restraint of a pinned column with a single lateral support along its midsection or two lateral supports symmetrically placed on its midsection are available. Figure 2-40 shows a simply supported column with one lateral restraint and gives the coefficient of constant of such a column as a function of column parameters. Figure 2-41 shows a simply supported column with two symmetrically placed lateral restraints and gives the coefficient of constraint as a function of column parameters.

The previous discussion of coefficients of constraint was limited to relatively simple cases. At times, however, a column may be attached to members for which an equivalent torsional spring constant is not easily found or it may be attached in more complicated ways than those previously discussed. In such cases, certain general rules may be applied.

In normal practice, the coefficient of constraint is less than two and the effect of end fixity is smaller for short columns than for long ones.

2 - 43
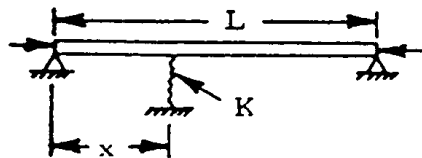
Note:

A center support behaves
rigidly if $q \geq 16 \pi^2$

$$E = \text{Modulus of Elasticity}$$

$$q = \frac{K L^3}{EI}$$
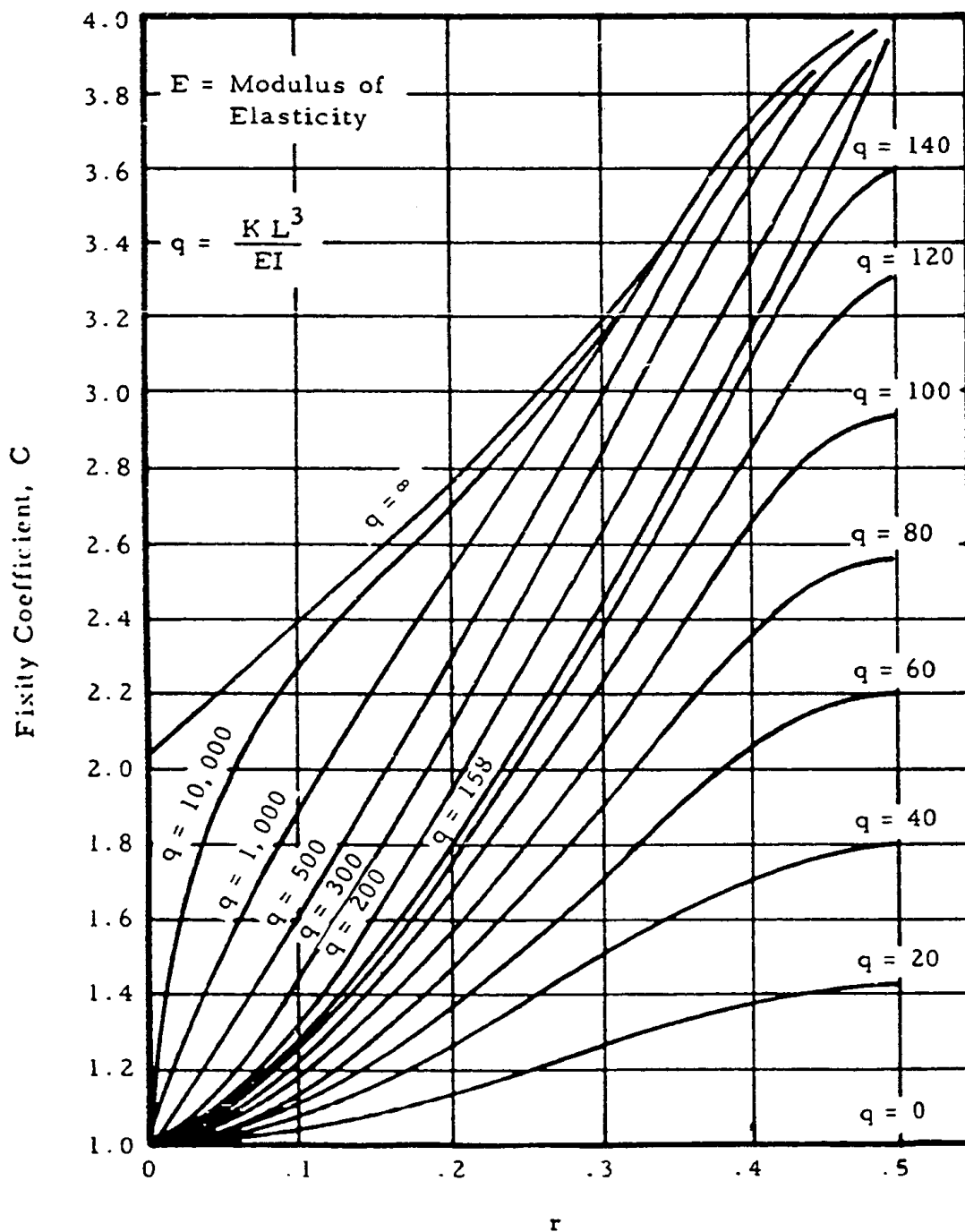
Figure 2-40.   Fixity Coefficient for a Column with Simply Supported Ends
and an Intermediate Support of Spring Constant, K

$$q = \frac{K L^3}{8 EI}$$

where K = spring constant lb/in
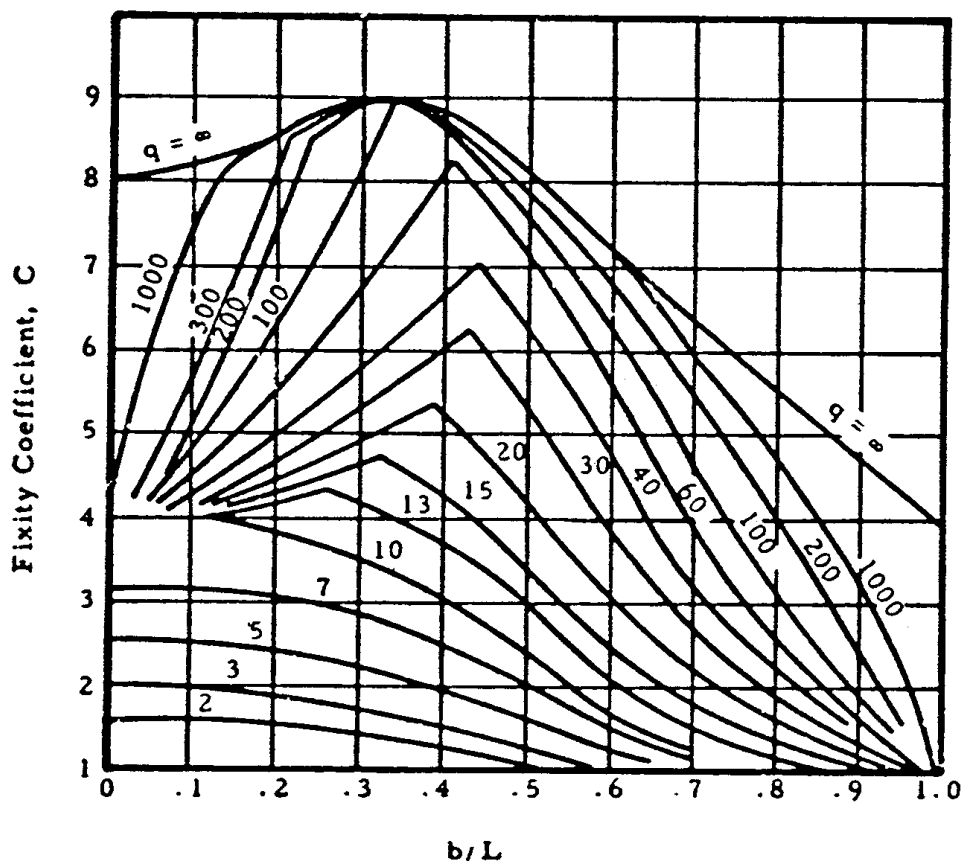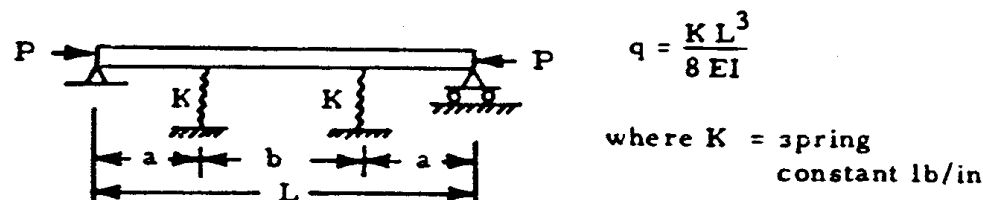
Figure 2-41.   Fixity of a Column with Two Elastic, Symmetrically
Placed Supports Having Spring Constants, K

The ends of a compression member in a welded truss of steel tubes,
like those that are often used in aircraft structures, cannot rotate without
bending all of the other members at the end joints.   Such a truss is shown
in Figure 2-42.   It is difficult to obtain the true end fixity of a compressive
member in such a truss since the member may buckle either horizontally or
vertically and is restrained by the torsional and bending rigidity of many
other members.   It is usually conservative to assume C = 2.0 for all mem-
bers.   A smaller coefficient of constraint might be used for a heavy com-
pressive member restrained by comparatively light members.   Likewise, a
larger coefficient of constraint may hold for a light compressive member
restrained by heavier members.   A coefficient of constraint of one should be
used if all of the members at a joint are in compression.   Steel tube engine
mounts are usually designed with the conservative assumption of a coefficient
of constraint of unity.
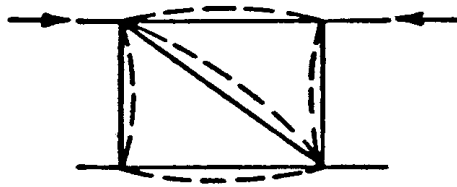
Figure 2-42.   Welded Truss

Stringers which act as compression members in semimonocoque
wing or fuselage structure, such as that shown in Figure 2-43, are usually
supported by comparatively flexible ribs or bulkheads.   The ribs or bulk-
heads are usually free to twist as shown so that their restraining effect may
be neglected and the value of C is taken to be unity, where L is the length
between bulkheads.   If the bulkheads are rigid enough to provide restraint
and clips are provided to attach the stringers to the bulkheads, a value of 1.5
is sometimes used for C.
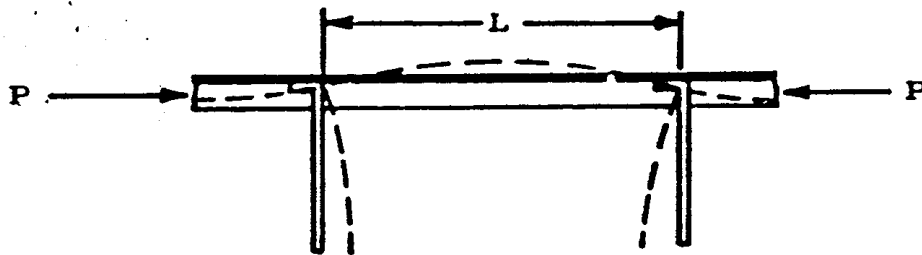
Figure 2-43.   Semimonocoque Structure

2.3.1.5   Distributed Axial Loads

Columns subjected to distributed axial loads may be treated by
formulas developed for end loaded columns if a coefficient of constraint is
used that takes into account both the load condition and end fixities.   Fig-
ure 2-44 shows columns under a uniformly distributed axial load of P/L
lbs/in. with various end restraints and their corresponding coefficients of
constraint.   The values P, L, and C are used in the formulas for end loaded
columns.

| C = 3.55 | C = 7.5 | C = 1.87 | C = .794 |
| P/L lb/in | P/L lb/in | P/L lb/in | P/L lb/in |
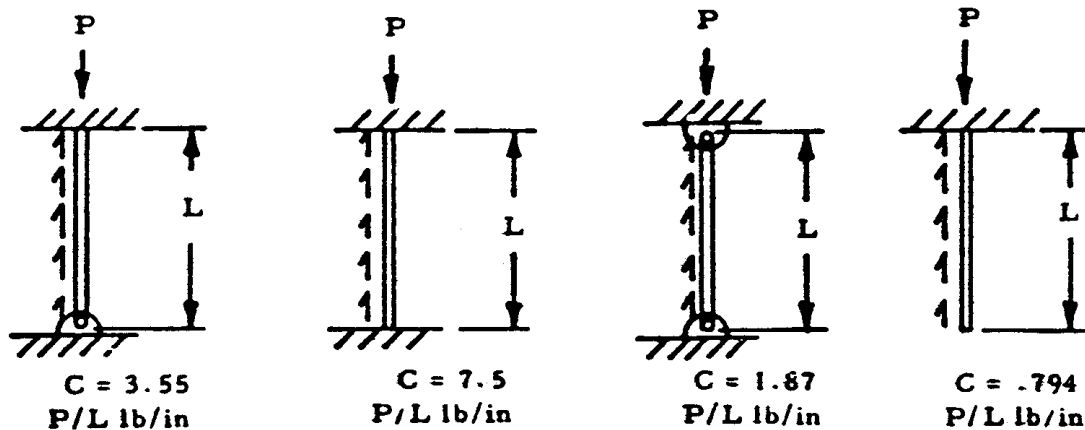
Figure 2-44.   Coefficients of Constraint for Columns Under a Uniformly
Distributed Axial Load

2 - 46

3.1.6 <u>Sample Problem – Concentrically Loaded Long Columns in Bending</u>

<u>Given</u>: The concentrically loaded rectangular bar shown in Figure 2-45 is fixed at one end and attached to a round bar at the other end. Both bars are made of steel for which $E = 30 \times 10^6$ psi and $G = 11.5 \times 10^6$ psi.
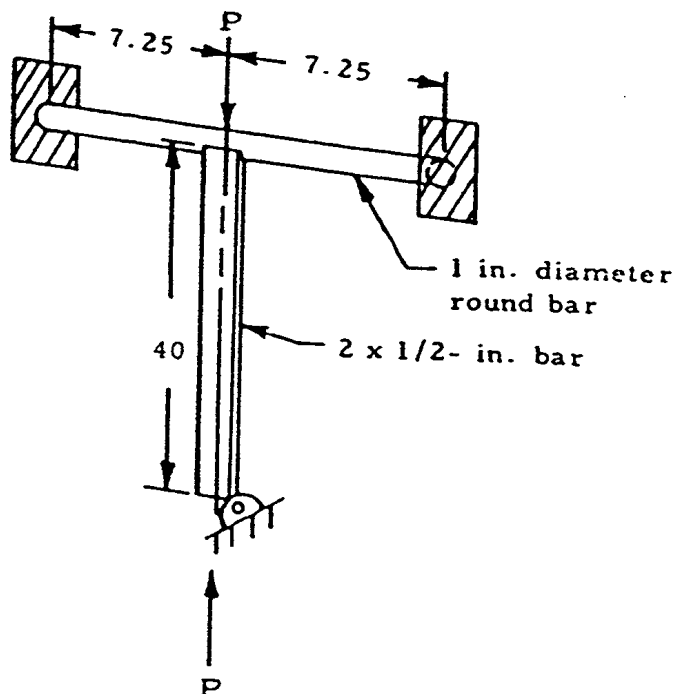
Figure 2-45. Example of Constrained Column

<u>Find</u>: P_{cr}

<u>Solution</u>: From elementary strength of materials, $\theta = TL/I_pG$ for a torsion bar. In effect, there are two 7.25-in.-long bars attached to the end of the column so that the equivalent torsional spring constant is

$$\mu = 2 \frac{T}{\theta} = \frac{2JG}{L}$$

Substituting the appropriate values into the expression for μ gives

$$\mu = \frac{(2) \frac{\pi(1)^4}{32} (11.5 \times 10^6)}{7.25} = 3.12 \times 10^5 \text{ in.-lb/rad}$$

The column may now be redrawn as Figure 2-46.
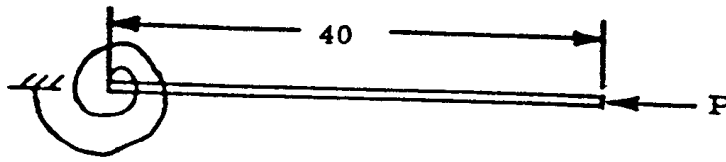
Figure 2-46.   Free Body Diagram of Constrained Column

$$\frac{\mu L}{EI} = \frac{(3.12 \times 10^5)(40)}{(30 \times 10^6)\left[\frac{2(.5)^3}{12}\right]} = 20$$

From Figure 2-38, we find that C = 1.88. Solving Equation (2-2) for L' gives

$$L' = \frac{L}{\sqrt{C}} = \frac{40}{\sqrt{1.88}} = 29.2 \text{ in.}$$

The radius of gyration of the bar is

$$\sqrt{I/A} = \sqrt{\frac{2(.5)^3}{12} / 2(.5)} = 0.144 \text{ in.}$$

The slenderness ratio

$$\frac{L'}{\rho} = \frac{30.5}{0.144} = 212$$

From Section 2.3.1.11.7, it is found that a steel column for which L/ρ is greater than 120 is a long column. Thus, the Euler formula, Equation (2-2), becomes

$$P_{cr} = \frac{A \pi^2 E}{\left(\frac{L'}{\rho}\right)^2}$$

Substituting the values for the given column into this equation gives

$$P_{cr} = \frac{(.5 \times 2)\pi^2 (30 \times 10^6)}{150^2} = 13,100 \text{ lb.}$$

2 - 48

In general, a column such as this must also be checked for buckling in the plane through the bar and the column. In this case, however, the column will not fail by this mode.

2.3.1.7 Bending Failure of Eccentrically Loaded Long Columns

A theoretically correct formula that holds for eccentrically loaded columns is the secant formula:

$$\frac{P}{A} = \frac{F_{col}}{1 + \frac{ec}{\rho^2} \sec\left[\frac{L'}{2\rho} \sqrt{\frac{P}{AE}}\right]} \tag{2-3}$$

In this formula, P, A, ρ, L, C, and E are defined as before, and e is the eccentricity of the load. The distance between the central axis and the concave side of the loaded column is designated as c. In the case of a long eccentrically loaded column, F_{col} may be taken to be the value of P_{cr}/A found from the Euler formula in Section 2.3.1.3. If a factor of safety, FS, is applied, the corresponding formula for allowable load, P_a, becomes

$$\frac{(FS)P_a}{A} = \frac{F_{col}}{1 + \frac{ec}{\rho^2} \sec\left[\frac{L'}{2\rho} \sqrt{\frac{(FS)P_a}{AE}}\right]} \tag{2-4}$$

The secant formula may also be used for short columns by finding F_{col} differently as will be shown in the material on short columns.

All physical columns have some accidental initial curvature due to imperfections and some eccentricity of loading. In these cases, an equivalent eccentricity may be used to approximate the effects of the imperfections. Data may also be found for the equivalent eccentric ratio which is the ec/c^2 term in the secant formula. Values for these may be found in Section 2.3.1.8.

The secant formula applies when the eccentricity is in the plane of the bending.

Unfortunately, the secant formula is difficult to solve and must be solved by either trial and error or charts.

2.3.1.8 Equivalent Eccentricity for Imperfect Columns

As was mentioned previously, no column is perfectly straight and concentrically loaded. In order to allow for these initial imperfections in a column whose loads are concentrically applied, an equivalent eccentricity of

loading may be asssumed. The column may then be treated by methods used for an eccentrically loaded column.

Opinion is divided as to whether the equivalent eccentricity assumed for imperfections is dependent upon or independent of the length of a column. If we assume that it is independent of column length, an equivalent eccentric ratio ec/ρ^2 ranging from 0.1 to 0.25 may be used. The mean value of such an eccentric ratio is approximately equal to 0.2. We may also assume that the equivalent eccentricity, e, is proportional to the effective length of the column. If this procedure is used, e may be taken to be equal to KL where K is a constant. Values of K ranging from 0.001 to 0.0025 may be used with the latter yielding conservative results.

2.3.1.9 Sample Problem - Long Eccentrically Loaded Columns and Equivalent Eccentricity

Given: The round column shown in Figure 2-47 with nominally concentric loading.

Steel - E = 30 x 10⁶ psi
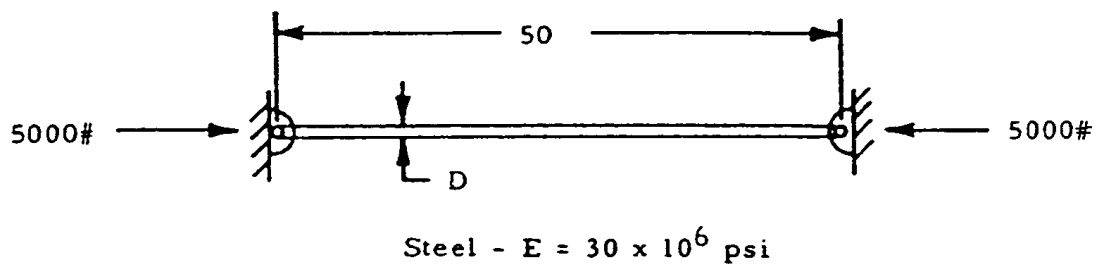
Figure 2-47. Column Loading for Study of Eccentricity

Find: The column diameter, D, for a factor of safety of 1.5, considering the initial imperfections of the column.

Solution: For a round section, $I = \pi D^4/64$ and $A = \pi D^2/4$. Thus, $\rho = \sqrt{I/A} = D/4$. Since the column is pin ended, $L = L' = 50$ in. Try D = 1.215.

$$\frac{L'}{\rho} = \frac{50}{\dfrac{1.215}{4}} = 164.5$$

According to Section 2.3.1.11.7, steel columns for which L'/ρ is greater than 120 may be treated as long columns. Thus F_{col} in the secant formula may be found by the Euler formula:

$$F_{col} = \frac{\pi^2 E}{\left(\dfrac{L'}{\rho}\right)^2} = \frac{\pi^2 (30 \times 10^6)}{(164.5)^2} = 10,950 \text{ psi}$$

2-50

The secant formula, Equation (2-4), may now be written as

$$\frac{(FS)P_a}{A} = \frac{F_{col}}{1 + \frac{ec}{o^2} \sec\left[\frac{L'}{2\rho} \sqrt{\frac{(FS)\,P_a}{AE}}\right]}$$

$$= \frac{10,950}{1 + \frac{ec}{o^2} \sec\left[\frac{L'}{2o} \sqrt{\frac{(FS)\,P_a}{AE}}\right]}$$

According to Section 2.3.1.8, equivalent eccentric ratio due to initial imperfections is between 0.1 and 0.25. To be on the conservative side, use an equivalent eccentric ratio of 0.25. Substituting this and column parameters into the secant formula, the expression below is obtained.

$$\frac{(1.5)(5000)}{\frac{\pi(1.215)^2}{4}} = \frac{10,950}{1 + .25 \sec\left[\frac{50}{\frac{2(1.215)}{4}} \sqrt{\frac{(1.5)(5000)}{\frac{\pi(1.215)^2}{4}}(30 \times 10^6)}\right]}$$

or 6450 = 6450

Thus, the original guess of D = 1.215 was correct. If this were not true, different values of D would have to be chosen until one was found that would make both sides of the secant formula equal.

2.3.1.10   Bending Failure of Short Columns

In the previous discussion of long columns, it was assumed that the column material was in the elastic range at the time of buckling. This assumption, however, is not true for columns having an effective slenderness ratio of less than a certain critical value for a given material. This value of the critical effective slenderness ratio, L'/o, is discussed in Section 2.3.1.11.7. Since the Euler formula no longer applies for short columns, one of the formulas used to fit short column data must be used to treat them.

2.3.1.11   Bending Failure of Concentrically Loaded Short Columns

Several formulas are available to treat short columns. These have o theoretical justification as did the Euler formula, but fit column data to a degree of accuracy depending upon the material and column parameters. The equations most commonly used for short columns are the tangent modulus, Johnson Parabolic, and straight-line equations.

2 - 51

2.3.1.11.1   <u>Tangent Modulus Equation</u>

If the slenderness ratio of a column is low enough that some of its fibers are no longer in the elastic range at the time of failure, the Euler formula no longer holds. However, this case may be treated by defining a tangent modulus of elasticity, E_t, to be the slope of the stress-strain curve at a given point. This tangent modulus of elasticity may then be substituted for the modulus of elasticity in the Euler equation to obtain the tangent modulus equation (modified Euler equation).

$$\frac{P}{A} = \frac{(\pi^2 E_T)}{\left(\frac{L}{\rho}\right)^2} \tag{2-5}$$

Since E_T is equal to E in the elastic range, the tangent modulus equation reduces to the Euler equation for long columns and is thus valid for both long and short columns.

The value of stress at which E_T is found is the maximum stress in the column. In the case of a concentrically loaded column, this is equal to P/A. Since E_T is a function of loading, the tangent modulus equation must be solved by trial and error if E_T is found from stress-strain diagrams or tables.

The tangent modulus equation has been solved for a number of different materials and these solutions are shown in Section 2.3.1.1.

The main disadvantage of the previously described procedure for solving the tangent modulus equation is the trial and error method required. This disadvantage may be eliminated if an equation for the stress-strain curve is available. Such an equation is the Ramberg-Osgood equation,

$$\epsilon = \sigma + \frac{3}{7} \sigma^n$$

Here, $\epsilon = Ee/f_1$ and $\sigma = f_c/f_1$ where e is the strain, f_c is the compressive stress, and f_1 is the stress at which the slope of a line from the origin to a point on the stress-strain curve is 0.7. E and n are constants determined experimentally for a given material. The Ramberg-Osgood equation may be used to obtain the following expression for the tangent modulus of elasticity.

$$E_t = \frac{E}{1 + 3/7 \, n\sigma^{n-1}} \tag{2-6}$$

This expression may in turn be substituted into the tangent modulus equation with f_c equal to F_{col} to obtain

$$F_{col} = \frac{\pi^2 E}{\left(\dfrac{L'}{\rho}\right)^2} \left(\frac{1}{1 + 3/7\, n\sigma^{n-1}}\right) \qquad (2\text{-}7)$$

In the case of a column under concentric loading, F_{col} is equal to P/A. A nondimensional plot of this equation is shown in Figure 2-48. Values of n, f_1, and E that are needed for the Ramberg-Osgood equation are shown in Table 2-2.
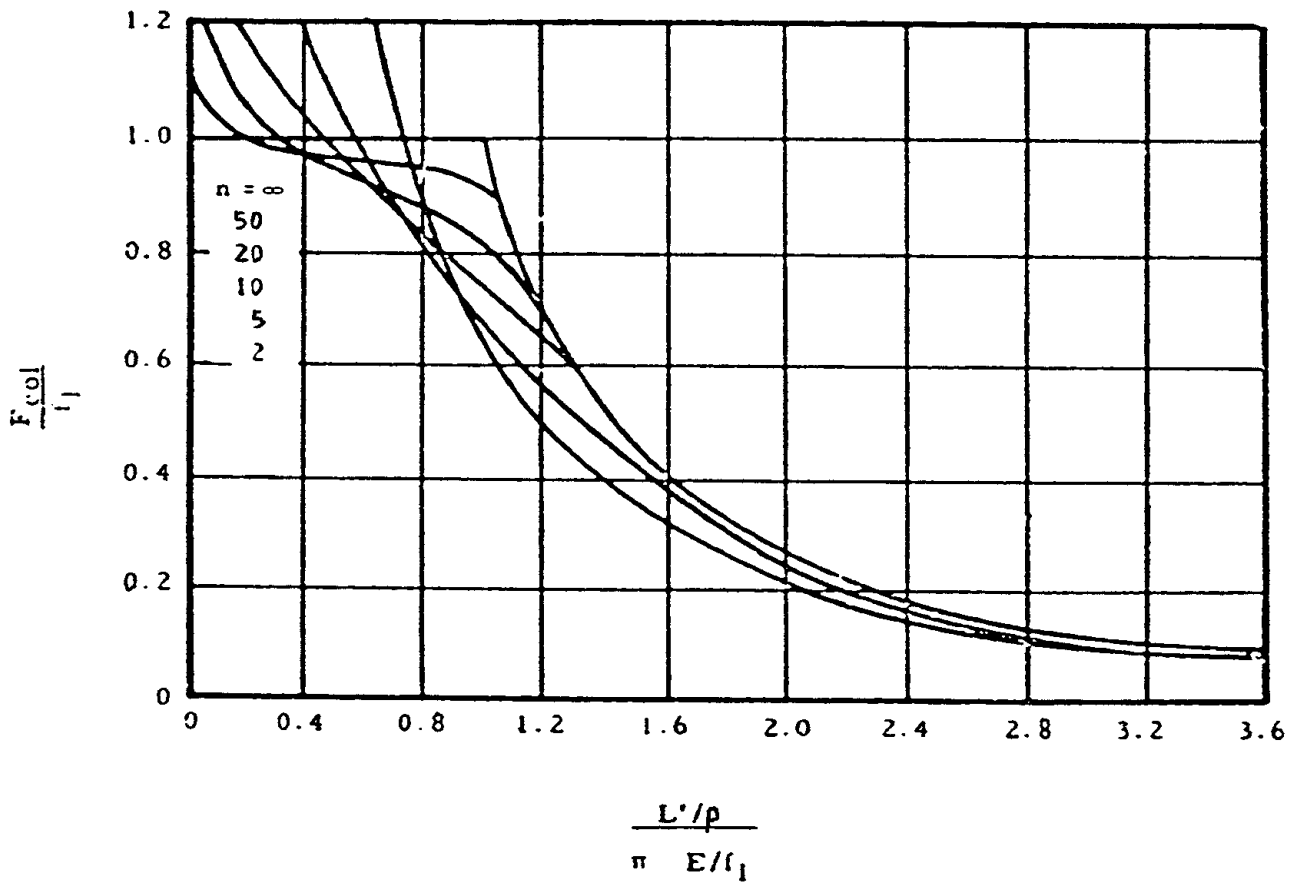
Figure 2-48. Nondimensional Plot of Tangent Modulus Equation with E_t Obtained from the Ramberg-Osgood Equation

TABLE 2-2

Properties of Various Materials for Ramberg-Osgood Equation

Material	E, Ksi	n	f_1 Ksi
Aluminum Alloys			
24 S-T Sheet	10,700	10	41
24 S-T Extrusion	10,700	10	37
75 S-T Extrusion	10,500	20	71
Clad 2024-T3 Longitudinal	10,000	10	38.1
Clad 2024-T4 Longitudinal	10,000	15	36.5
Steel			
Normalized	29,000	20	75
$F_{tu} = 100,000$	29,000	25	80
$F_{tu} = 125,000$	29,000	35	100
$F_{tu} = 150,000$	29,000	40	135
$F_{tu} = 180,000$	29,000	50	165
Titanium 6Al-4V Bar Stock, Longitudinal $F_{tu} = 145$ Ksi at room temp., 1/2 hr. exposure to temperature			
at room temperature	17,500	10	164
at 500°F	16,000	17	108
at 700°F	15,000	10	93.3
at 900°F	13,800	9	85.7

One great advantage of using the Ramberg-Osgood relation is that the necessary constants may be obtained for new materials without extensive testing.

In general, the tangent modulus theory will yield conservative results. However, this theory yields values for the critical load that are too high for very short columns for which E_t may be less than 0.2 at failure.

2.3.1.11.2   Sample Problem - Use of Tangent Modulus Equation for Concentrically Loaded Short Columns

Given: The 1-in. square concentrically loaded column shown in Figure 2-49.

Find: The maximum value of P by using the tangent modulus equation, with E_t obtained from the Ramberg-Osgood relation.
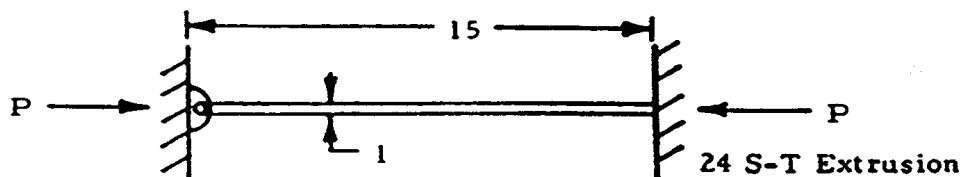
Figure 2-49.   Column Loading Used for Illustration of Tangent-
Modulus Equation

Solution: Ultimately, Equation (2-7) must be solved. This
equation is shown graphically in Figure 2-48. From Table 2-2,
find $E = 10.7 \times 10^6$ psi, $n = 10$, and $f_1 = 37,000$ psi for the
given material. Consulting Section 2.3.1.4, find that $C = 2.05$
for the given end constraints. Solving Equation (2-2), find that
$L' = L/\sqrt{C}$. In this case,

$$L' = \frac{15}{\sqrt{2.05}} = 10.55 \text{ in.}$$

For a square, $I = b^4/12$ and $A = b^2$.

$$\rho = \sqrt{\frac{I}{A}} = \sqrt{\frac{b^2}{12}}$$

In this case,

$$\rho = \sqrt{\frac{1}{12}} = .289$$

Thus,

$$\frac{L'/\rho}{\pi\sqrt{E/f_1}} = \frac{10.55/0.289}{\pi\sqrt{10.7 \times 10^6/3.7 \times 10^4}}$$

From Figure 2-48,

$$\frac{F_{col}}{f_1} = 0.88$$

Thus,

$$F_{col} = \frac{P_{cr}}{A} = 0.88 f_1$$

$$P_{cr} = 0.88 A f_1 = 0.88(1)(37,000)$$

$$P_{cr} = 32,600 \text{ lb.}$$

2.3.1.11.3   Reduced Modulus Equation

An equation that is theoretically more correct than the tangent modulus equation is the reduced modulus equation. In this case, a reduced modulus of elasticity, E_r, is used to replace E in the Euler equation. This reduced modulus is a value between E and E_t, one suggested value being

$$E_r = \frac{4 \, E \, E_t}{(\sqrt{E} + \sqrt{E_t})^2} \qquad (2-8)$$

It can be seen from this equation that E_r approaches E as E_t approaches E so that the reduced modulus equation reduces to the Euler equation for long columns as does the tangent modulus equation.

The reduced modulus equation is accurate for specimens in which extreme care in manufacturing and testing is used but yields high values of critical load for other columns. The more conservative tangent modulus equation is preferred to the reduced modulus equation for this reason as well as for its greater simplicity.

2.3.1.11.4   Johnson-Euler Equation

For many materials a parabola may be used to fit column test data in the short column range. The equation of such a parabola may be written as

$$F_{col} = F_{co} - K \left(\frac{L'}{\rho}\right)^2 \qquad (2-9)$$

where F_{co} and K are constants chosen to fit the parabola to test data for a particular material. The Johnson-Euler column curve consists of the Euler curve for high L'/ρ ratios combined with a parabola that is tangent to this curve and covers short column ranges. If Equation (2-9) is adjusted so that it is tangent to the Euler curve, we obtain the Johnson equation

$$F_{col} = F_{co} \left[1 - \frac{F_{co} \left(\frac{L'}{\rho}\right)^2}{4 \, \pi^2 E} \right] \qquad (2-10)$$

Here, F_{col} is the maximum column stress which is given as P/A for concentrically loaded long columns and by more complicated formulas for eccentrically loaded columns. The single experimentally determined constant, F_{cc}, is called the column yield stress but has little physical significance for columns with stable cross sections since very short columns for which L'/ρ is less than approximately 12 fail by block compression. In cases where local crippling and primary bending failure interact, F_{cc} may be taken to be equal

2 - 56

to the section crippling allowable. This case will be discussed more extensively in Section 2.3.2. A typical Johnson-Euler curve is shown in Figure 2-50. The coordinates that are marked show the point of tangency between the Johnson parabola and the Euler curve. Thus, the critical effective slenderness ratio separating long columns from short columns is $\sqrt{2}\pi\sqrt{E/F_{cc}}$ for the Johnson-Euler curve.
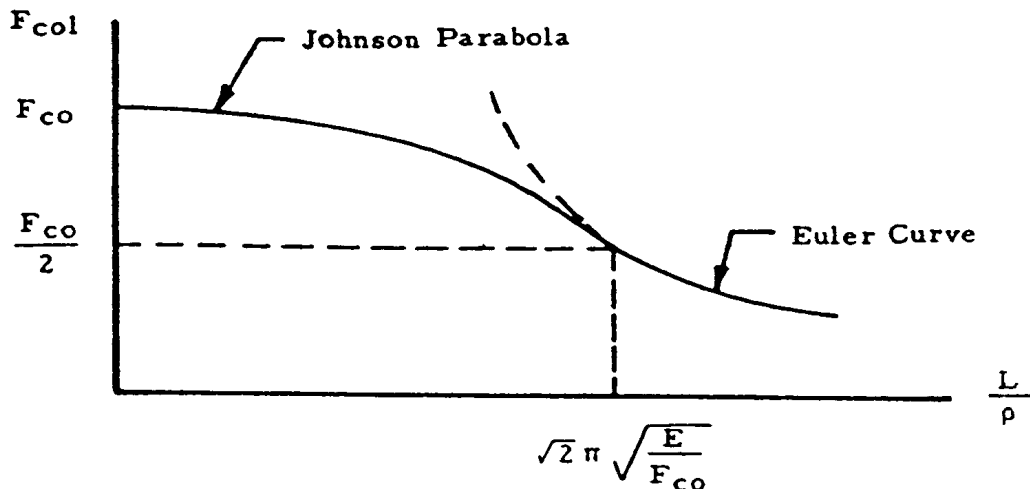
Figure 2-50. Typical Johnson-Euler Curve

The main advantages of the Johnson-Euler curve are its ability to fit data when there is an interaction between crippling and primary bending failure and simplicity of computation. For columns having stable cross sections, one of the other short column curves is normally perferred.

2.3.1.11.5   Straight Line Equation

Short column curves for most aluminum alloys and several other materials are best represented by straight lines. A typical straight line is shown in Figure 2-51.
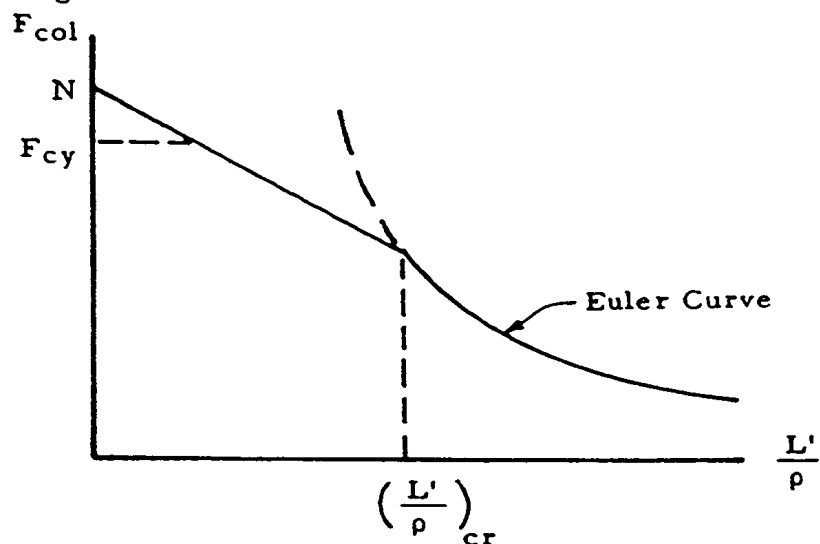
Figure 2-51. Typical Straight Line for Short Columns

2 - 57

As can be seen from Figure 2-51, the straight line is not necessarily tangent to the Euler curve as is the case for the Johnson parabola but this is often the case.   The straight line shown may be given by the equation

$$F_{col} = N - M\left(\frac{L'}{\rho}\right) \tag{2-11}$$

where N and M are constants chosen to best fit column data for a given material.   As in the case of the Johnson parabola, this straight line does not always hold for very short columns that fail by block compression so it is cut off at F_{cy} as shown in the figure.

The critical effective slenderness ratio may be found by equating F_{col} as found by the Euler formula to that value as found by Equation (2-11).   This procedure involves solving a cubic equation and will not be presented here since values of the critical slenderness ratio are tabulated in Table 2-3.

Values of the constants N, M and the corresponding critical slenderness ratio $(L'/\rho)_{cr}$ are available for a large number of aluminum alloys and manufacturing processes.   These values are shown in Table 2-3.

TABLE 2-3

Constants for Straight Line Equation

Extruded Rod, Bar and Shapes

Alloy and Temper	Thickness, In.	N(ksi)	M(ksi)	$\left(\frac{L'}{\rho}\right)_{cr}$
2014-O	All	9.9	0.037	160
2014-T4	All	35.2	0.251	89
2014-T6	Up thru 0.499	61.4	0.410	50
2014-T6	0.500-0.749	67.3	0.471	48
2014-T6	0.750 and over			
	Area 25 sq in. max.	69.7	0.496	47
	Area 25 to 32 sq in.	67.3	0.471	48
2024-O	All	9.9	0.037	160
2024-T4	Up thru 0.249	43.6	0.300	65
2024-T4	0.250-0.749	44.8	0.313	64
2024-T4	0.750-1.499	50.9	0.379	60
2024-T4	1.500-2.999			
	Area 25 sq in. max.	58.4	0.466	56
2024-T4	3.000 and over			
	Area 25 sq in. max.	58.4	0.466	56
2024-T4	1.500 and over			
	Area 25 thru 32 sq in.	53.4	0.407	59
3003-O	All	5.4	0.015	222
3003-H112	All	5.4	0.015	222
5454-O	Up to 5.000	13.3	0.058	142
5454-H112	Up to 5.000	13.3	0.058	142
5454-H311	Up to 5.000	20.4	0.111	121
5456-O	Up to 5.000 ③	21.6	0.120	111
5456-H112	Up to 5.000 ③	21.6	0.120	111
5456-H311	Up to 5.000 ③	25.3	0.153	106
6061-O	All	5.4	0.015	222
6061-T4	All	15.7	0.074	128
6061-T6	All	38.3	0.202	63
6061-T62	All	28.1	0.127	74
6062-O	All	5.4	0.015	222
6062-T4	All	15.7	0.074	128
6062-T6	All	38.3	0.202	63
6062-T62	All	28.1	0.127	74

TABLE 2-3

Constants for Straight Line Equation (Cont'd.)

Extruded Rod, Bar and Shapes (Cont'd.)

Alloy and Temper	Thickness In.	N(ksi)	M(ksi)	$\left(\frac{L'}{\rho}\right)_{cr}$
6063-T42	Up thru 0.500	11.0	0.043	149
6063-T5	Up thru 0.500	17.5	0.076	103
6063-T6	Up thru 0.124	28.0	0.155	81
6063-T6	0.125-0.500	28.0	0.155	81
7075-O	All	13.3	0.058	142
7075-T6	Up thru 0.249	79.3	0.602	44
7075-T6	0.250-0.499	87.8	0.859	46
7075-T6	0.500-1.499	87.8	0.859	46
7075-T6	1.500-2.999	81.7	0.629	43
7075-T6	3.000-4.499 ①	85.2	0.821	47
7075-T6	3.000-4.499 ②	79.3	0.602	44
7075-T6	4.500-5.000 ①	76.9	0.575	45
7178-T6	Up thru 0.249	86.5	0.686	42
7178-T6	0.250-2.999 ③	88.9	0.714	42

Rolled and Cold-Finished Rod and Bar

Alloy and Temper	Diameter or Thickness, In.	N(ksi)	M(ksi)	$\left(\frac{L'}{\rho}\right)_{cr}$
EC-O	All	3.2	0.006	241
EC-H12	Up to 1 in.	8.7	0.030	165
EC-H13	Up to 1 in.	13.3	0.058	142
EC-H17	Up to 1/2 in.	16.8	0.082	124
1100-O	All	4.3	0.010	221
1100-F	0.375 and over	7.6	0.025	186
2011-T3	0.125-1.500	45.4	0.368	79
2011-T3	1.501-2.000	40.3	0.308	85
2011-T3	2.001-3.000	35.2	0.251	89
2011-T8	0.125-3.250	48.0	0.400	77

TABLE 2-3

Constants for Straight Line Equation (Cont'd.)

Rolled and Cold-Finished Rod and Bar (Cont'd.)

Alloy and Temper	Diameter or Thickness, In.	N(ksi)	M(ksi)	$\left(\dfrac{L'}{\rho}\right)_{cr}$
2014-O	Up thru 8.000	9.9	0.037	160
2014-T4	Up thru 6.750	37.7	0.278	86
2014-T6	Up thru 6.750	64.7	0.543	54
2017-O	Up thru 8.000	9.9	0.037	160
2017-T4	Up thru 8.000	37.7	0.278	86
2024-O	Up thru 8.000	9.9	0.037	160
2024-T4	Up thru 6.500	48.0	0.400	77
3003-O	All	5.4	0.015	222
3003-H12	Up thru 0.374	12.2	0.051	148
3003-H14	Up thru 0.313	16.8	0.082	124
3003-H16	Up thru 0.250	22.8	0.131	112
3003-H18	Up thru 0.204	26.5	0.164	103
5052-O	All	11.0	0.043	149
5052-F	0.375 and over	12.2	0.051	148
6061-O	Up thru 8.000	5.4	0.015	222
6061-T4	Up thru 8.000	18.0	0.092	128
6061-T6	Up thru 8.000	38.3	0.202	63
7075-O	Up thru 8.000	12.2	0.051	148
7075-T6	Up thru 4.000	78.7	0.729	49

Standard Structural Shapes (Rolled or Extruded)

Alloy and Temper	Thickness, In.	N(ksi)	M(ksi)	$\left(\dfrac{L'}{\rho}\right)_{cr}$
2014-O	All	9.9	0.037	160
2014-T4	All	35.2	0.251	89
2014-T6	All	64.7	0.543	54

TABLE 2-3

Constants for Straight Line Equation (Cont'd.)

Standard Structural Shapes (Rolled or Extruded)

Alloy and Temper	Thickness, In.	N(ksi)	M(ksi)	$\left(\dfrac{L'}{\rho}\right)_{cr}$
5456-O	All	21.6	0.120	111
5456-H112	All	21.6	0.120	111
5456-H311	All	25.3	0.153	106
6061-O	All	5.4	0.015	222
6061-T4	All	15.7	0.074	128
6061-T6	All	38.3	0.202	63
6061-T62	All	28.1	0.127	74
6062-O	All	5.4	0.015	222
6062-T4	All	15.7	0.074	128
6062-T6	All	38.3	0.202	63

Die Forgings

Alloy and Temper	Thickness, In.	N(ksi)	M(ksi)	$\left(\dfrac{L'}{\rho}\right)_{cr}$
1100-F	Up to 4 in.	4.3	0.010	221
2014-T4	Up to 4 in.	35.2	0.251	89
2014-T6	Up to 4 in.	61.4	0.410	50
2018-T61	Up to 4 in.	48.0	0.400	77
2218-T61	Up to 4 in.	48.0	0.400	77
2218-T72	Up to 4 in.	33.9	0.237	91
3003-O	All	5.4	0.015	222
3003-F	All	5.4	0.015	222
4032-T6	Up to 4 in.	50.6	0.433	75
6061-T6	Up to 4 in.	38.3	0.202	63
6151-T6	Up to 4 in.	40.6	0.220	61
7075-T6	Up to 3 in.	73.3	0.535	46
7079-T6	Up to 6 in.	72.1	0.522	46

TABLE 2-3

Constants for Straight Line Equation (Cont'd.)

Drawn Tube

Alloy and Temper	Wall Thickness, In.	N(ksi)	M(ksi)	$\left(\dfrac{L'}{\rho}\right)_{cr}$
2024-O	All	8.7	0.030	165
2024-T3	0.018-0.500	50.6	0.433	75
3003-O	All	5.4	0.015	222
3003-H12	All	12.2	0.051	148
3003-H14	All	16.8	0.082	124
3003-H16	All	22.8	0.131	112
3003-H18	All	26.5	0.164	103
Alclad 3003-O	0.014-0.500	5.4	0.015	222
Alclad 3003-H12	0.014-0.500	12.2	0.051	148
Alclad 3003-H14	0.014-0.500	16.8	0.082	124
Alclad 3003-H16	0.014-0.500	22.8	0.131	112
Alclad 3003-H18	0.014-0.500	26.5	0.164	103
5050-O	All	6.5	0.019	185
5050-H34	All	20.4	0.111	121
5050-H38	All	25.3	0.153	106
5052-O	All	11.0	0.043	149
5052-H34	All	26.5	0.164	103
5052-H38	All	33.9	0.237	91
6061-O	All	5.4	0.015	222
6061-T4	0.025-0.500	18.0	0.092	128
6061-T6	0.025-0.500	38.3	0.202	63
6062-O	All	5.4	0.015	222
6062-T4	0.025-0.500	18.0	0.092	128
6062-T6	0.025-0.500	38.3	0.202	63
6063-T83	All	32.6	0.159	69
6063-T831	All	27.0	0.120	75
6063-T832	All	38.3	0.202	63

TABLE 2-3

Constants for Straight Line Equation (Cont'd.)

Extruded Tube

Alloy and Temper	Wall Thickness, In.	N(ksi)	M(ksi)	$\left(\frac{L'}{\rho}\right)_{cr}$
2014-O	All	9.9	0.037	160
2014-T4	0.125-0.499	30.2	0.200	100
2014-T4	0.500 and over	35.2	0.251	89
2014-T6	0.125-0.499	61.4	0.410	50
2014-T6	0.500-0.749	67.3	0.471	48
2014-T6	0.750 and over —			
	Area 25 sq in. max.	69.7	0.496	47
	Area 25 to 32 sq in.	67.3	0.471	48
2024-O	All	9.9	0.037	160
2024-T4	0.499 and less	41.1	0.275	67
2024-T4	0.500-1.499	50.9	0.379	60
2024-T4	1.500 and over —			
	Area 25 sq in. max.	53.4	0.407	59
	Area 25 to 32 sq in.	50.9	0.379	60
3003-O	All	5.4	0.015	222
3003-F	All	5.4	0.015	222
5154-O	All	12.2	0.051	148
6061-O	All	5.4	0.015	222
6061-T4	All	15.7	0.074	128
6061-T6	All	38.3	0.202	63
6062-O	All	5.4	0.015	222
6062-T4	All	15.7	0.074	128
6062-T6	All	38.3	0.202	63
6063-T42	Up to 0.500	11.0	0.043	149
6063-T5	Up to 0.500	17.5	0.076	103
6063-T6	Up to 0.500	28.0	0.155	81
7075-O	All	13.3	0.058	142
7075-T6	Up to 0.249	79.3	0.602	44
7075-T6	0.250-2.999	81.7	0.629	43
7178-T6	Up to 0.249	86.5	0.686	42
7178-T6	0.250-2.999	88.9	0.714	42

TABLE 2-3

Constants for Straight Line Equation (Cont'd.)

Pipe

Alloy and Temper	Size or Thickness, In.	N(ksi)	M(ksi)	$\left(\frac{L'}{\rho}\right)_{cr}$
3003-O	All	5.4	0.015	222
3003-H112	1 in. and over	6.5	0.019	185
3003-H18	Under 1 in. size	26.5	0.164	103
3003-F	1 in. and over	5.4	0.015	222
6051-T6	Under 1 in. size	38.3	0.202	63
6061-T6	1 in. and over	38.3	0.202	63
6063-T5	All	17.5	0.076	103
6063-T6	All	28.0	0.155	81
6063-T832	All	38.3	0.202	63

Sand Castings

Alloy and Temper	Thickness, In.	N(ksi)	M(ksi)	$\left(\frac{L'}{\rho}\right)_{cr}$
43-F		7.6	0.025	186
122-T61		35.2	0.251	89
142-T21		15.7	0.074	128
142-T571		35.2	0.251	89
142-T77		18.0	0.092	128
195-T4	The values to the right are based on tests of standard specimens individually cast.	15.7	0.074	128
195-T6		24.0	0.141	107
195-T62		33.9	0.237	91
195-T7		19.2	0.101	120
214-F		11.0	0.043	149
B214-F		12.2	0.051	148
F214-F		11.9	0.043	149
220-T4		15.9	0.076	131
319-F		11.5	0.047	163
319-T6		14.4	0.065	134

TABLE 2-3

Constants for Straight Line Equation (Cont'd.)

Sand Castings (Cont'd.)

Alloy and Temper	Thickness, In.	N(ksi)	M(ksi)	$\left(\frac{L'}{\rho}\right)_{cr}$
355-T51		12.2	0.051	148
355-T6		14.4	0.065	134
355-T61		23.4	0.136	109
355-T7		24.2	0.143	107
355-T71		15.9	0.076	131
356-T51	The values to the right are based on tests of standard specimens individually cast.	11.5	0.047	163
356-T6		13.7	0.061	144
356-T7		18.8	0.098	123
356-T71		13.0	0.056	143
A612-F		14.4	0.065	134

Permanent Mold Castings

Alloy and Temper	Thickness, In.	N(ksi)	M(ksi)	$\left(\frac{L'}{\rho}\right)_{cr}$
43-F		7.6	0.025	186
C113-F		24.0	0.141	107
122-T551		37.7	0.278	86
122-T65		35.2	0.251	89
F132-T5		---	---	---
142-T571	The values to the right are based on tests of standard specimens individually cast.	33.9	0.237	91
142-T61		44.1	0.352	80
B195-T4		16.8	0.082	124
B195-T6		25.3	0.153	106
B195-T7		18.0	0.092	128
A214-F		14.5	0.066	135

TABLE 2-3

Constants for Straight Line Equation (Cont'd.)

Permanent Mold Castings (Cont'd.)

Alloy and Temper	Thickness, In.	N(ksi)	M(ksi)	$\left(\dfrac{L'}{\rho}\right)_{cr}$
333-F		18.0	0.092	128
333-T5		25.3	0.153	106
333-T6		29.0	0.188	100
333-T7		26.5	0.164	103
355-T51	The values to the right are based on tests of standard specimens individually cast.	25.3	0.153	106
355-T6		26.5	0.164	103
355-T62		44.1	0.352	80
355-T7		31.4	0.212	98
355-T71		31.4	0.212	98
C355-T61[4]		35.2	0.251	89
356-T6		25.3	0.153	106
356-T7		24.0	0.141	107
A356-T61[4]		31.4	0.212	98
C612-F		15.7	0.074	128
750-T5		8.7	0.030	165
B750-T5		---	---	---

[1] Area up thru 20 sq in.

[2] Area 20 thru 32 sq in.

[3] Area up thru 30 sq in.

[4] The values shown for this alloy are valid for any location in the casting.

2.3.1.11.6   <u>Sample Problem - Use of Straight Line Equation for</u>
<u>Concentrically Loaded Short Columns</u>

<u>Given</u>: The concentrically loaded rectangular bar shown
in Figure 2-52.

6061-T4 Aluminum Alloy Extruded
Bar, Width = 1.0 in.
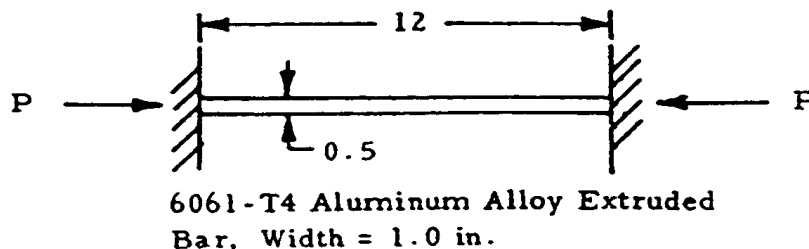
Figure 2-52.   Concentrically Loaded Short Column

<u>Find</u>: The critical load, P_{cr},

<u>Solution</u>: Since the column is made of aluminum alloy, a
straight-line equation should be accurate if the column is
short. From Section 2.3.1.4, C = 4 for columns having
both ends fixed. Since $C = (L/L')^2$, $L' = L/2$. The radius
of gyration,

$$\rho = \sqrt{\frac{I}{A}} = \sqrt{\frac{bh^3}{12}} \bigg/ bh$$

Thus,

$$\rho = \sqrt{\frac{h^2}{12}} = \sqrt{\frac{(.5)^2}{12}} = 0.144.$$

$$\frac{L'}{\rho} = \frac{6}{.144} = 41.6$$

From Table 2-3, we find that $(L'/\rho)_{cr} = 128$ for this material.
Since L'/ρ is less than this critical value, a straight line
equation may be applied. Substituting the values of N and M,
given for 6061-T4 extruded bars in Table 2-3, into Equation
(2-11), we obtain

$$F_{col} \left[15.7 - .074 \left(\frac{L'}{\rho} \right) \right] Ksi$$

2 - 68

Thus,

$$\frac{P_{cr}}{A} = F_{col} = [15.7 - .074(41.6)] \; Ksi$$

or

$$P_{cr} = 12.55A = 12.55(.5) = 6.27 \; kip$$

$$P_{cr} = 6,270 \; lb.$$

2.3.1.11.7   Critical Effective Slenderness Ratio

So far, long columns and concentrically loaded short columns have been discussed. It has been mentioned that a long column is one for which the Euler equation holds in the concentrically loaded case. This equation holds for columns having an effective slenderness ratio greater than a value called the critical effective slenderness ratio of the column. In some cases, this critical effective slenderness ratio need not be determined. For example, the tangent modulus equation, reduced modulus equation, or plotted data may be applied to either long or short columns. In other cases, this ratio must be known in order to decide which of two equations is to be applied to a column. A critical effective slenderness ratio must be found if the Johnson-Euler or a straight line equation is to be used.

The critical effective slenderness ratio is, in general, a function of the column material. If the Johnson-Euler formula is to be used, we obtain

$$\left(\frac{L'}{\rho}\right)_{cr} = \pi \sqrt{\frac{2E}{F_{co}}} \tag{2-12}$$

as our critical effective slenderness ratio. If a straight line formula is to be used, the critical slenderness ratio is the slenderness ratio for which the Euler curve and the straight line either intersect or are tangent. A general formula is not given here since the critical effective slenderness ratio for each straight-line equation whose parameters are given in Table 2-3 is also given there.

In general, a steel column having a critical effective slenderness ratio of greater than 120 or an aluminum column having one of greater than 220 may be immediately treated as a long column. Columns having lower effective slenderness ratios must be checked by Equation (2-12) or Table 2-3 or treated by a method applicable to both long and short columns. If Equation (2-12) is used, F_{co} may be assumed to be approximately equal to F_{cy} for a rough estimate of L'/ρ.

2.3.1.11.8 **Bending Failure of Eccentrically Loaded Short Columns**

The column formulas in the previous section do not apply if a column is eccentrically loaded or if initial imperfections are large enough to have the effect of an appreciable initial eccentricity. In such cases, either another formula must be used or adjustments must be made to existing equations.

The secant formula that was given in Section 2.3.1.7 may also be applied to short columns if its parameters are chosen correctly. This equation is given again below for convenient reference.

$$\frac{(FS)P_a}{A} = \frac{F_{col}}{1 + \frac{ec}{\rho^2} \sec\left[\frac{L'}{2\rho}\sqrt{\frac{(FS)P_a}{AE}}\right]}$$

(2-13)

F_{col} is the maximum fiber stress at failure as before. Different references suggest various ways of choosing F_{col}. Reasonable results may be obtained for very short columns if F_{col} is assumed to be equal to the compressive yield point for steel or the compressive yield stress for light alloys. In the case of intermediate length columns, F_{col} should be taken to be the stress obtained from one of the formulas for a concentrically loaded short column. If the formula used for this purpose is the tangent modulus equation, E should be replaced by E in the secant equation. The secant equation must either be solved by trial and error or through use of a chart such as that shown in Figure 2-53.

Unfortunately, the secant formula is inconvenient for computation. A simpler approach may be used if the column deflection is small compared to the eccentricity of loading. This assumption is true for very short columns and to a lesser extent for intermediate length columns.

Using the previously mentioned assumption, the basic design equation for an eccentrically loaded short column becomes

$$\frac{F_{col}}{FS} = \frac{P}{A} + \frac{P_a c}{I}$$

(2-14)

Here F_{col} is the maximum column stress as computed from one of the equations for a short concentrically loaded column.

A more refined design equation based on the assumption of a small column deflection relative to the eccentricity of loading is

$$1 = \frac{P}{A\,F_{scol}} + \frac{P_a c}{I\,F_b}$$

(2-15)

here F_{acol} is the working concentrically loaded column stress and F_b is the orking compressive stress in bending.

In conclusion, the secant formula is theoretically more correct and yields better results for eccentrically loaded short columns. However, due to the difficulty of applying this formula, Equation (2-14) or (2-15) may at times be applied, especially for shorter columns.

$$F_{col} = \frac{(FS)P_a}{A} \left(1 - \frac{ec}{2} \sec \frac{L}{2} \sqrt{\frac{(FS)P_a}{AE}} \right)$$
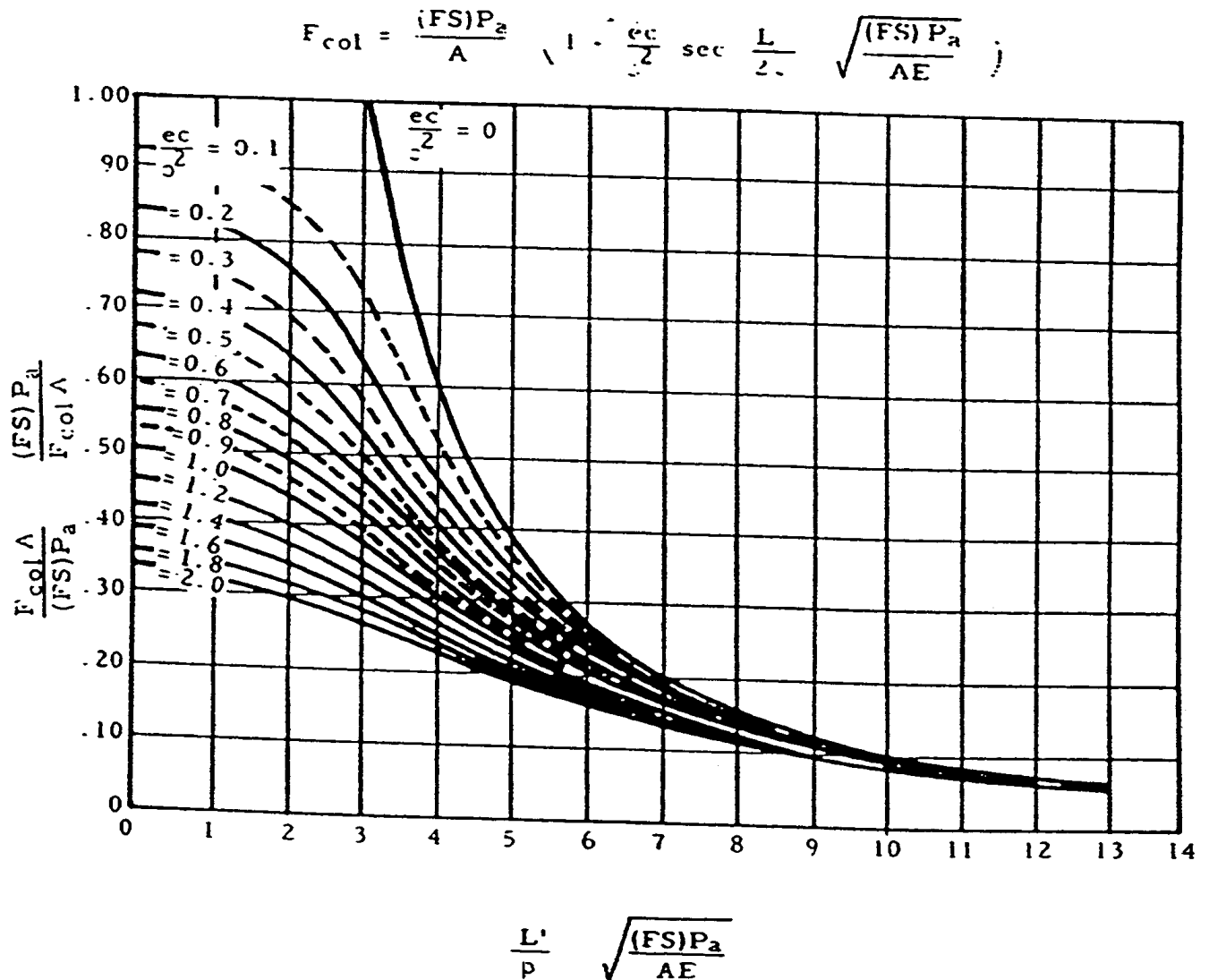
Figure 2-53. Graphical Presentation of the Secant Column Formula

2.3.1.11.9   Sample Problem – Eccentrically Loaded Short Column
in Bending

Given: The eccentrically loaded round column shown in
Figure 2-54.
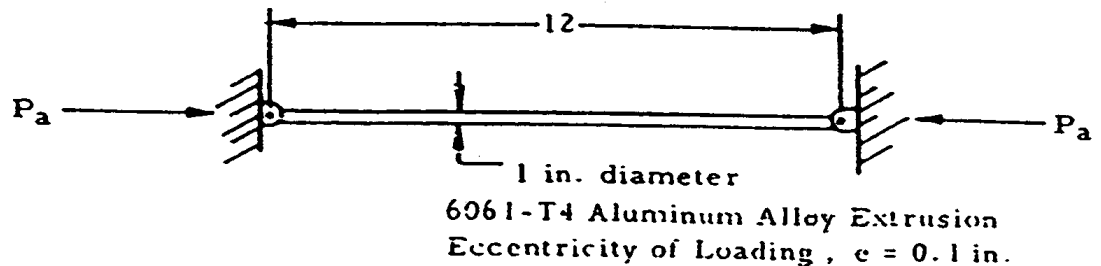
Figure 2-54.   Column Loading Used for Illustration of Secant-
Modulus Equations

Find: The allowable load, P_a, if a factor of safety of 1.3
is used.   Use (a) the secant modulus equation, and (b)
Equation (2-14).

Solution: (a) The secant modulus equation may be written as

$$\frac{(FS)\,P_a}{A} = \frac{F_{col}}{1 + \dfrac{ec}{\rho^2}\,\sec\left[\dfrac{L'}{2\rho}\sqrt{\dfrac{(FS)\,P_a}{AE}}\right]}$$

Since the column is made of aluminum alloy, the straight-line
column Equation (2-11) may be used to find F_{col} if it is short.
From Table 2-3, find that B, D, and $(L'/\rho)_{cr}$ for this material
are 15,700 lb, 15 lb, and 128 respectively.   Thus,

$$F_{col} = 15,700 - 15\left(\frac{L'}{\rho}\right)$$

Since the column is pin ended, $L' = L = 12$ in.   For a circular
section, $\rho = D/4 = 0.25$.   Inserting these values into the above
equation gives $F_{col} = 14,980$ psi.   Since L'/ρ is equal to 48
and $(L'/\rho)_{cr}$ is equal to 128, the assumption of a short column
is valid.   All of the parameters for the secant formula are now
known except P_a.   Inserting these values in the secant modulus
equation gives

$$\frac{1.3\,P_a}{\dfrac{\pi(1)^2}{4}} = \frac{14,980}{1 + \dfrac{.1(.5)}{(.25)^2}\,\sec\left[\dfrac{12}{2(.25)}\sqrt{\dfrac{1.3\,P_a}{\dfrac{\pi(1)^2}{4}}(10\times10^6)}\right]}$$

Simplifying this gives

$$P_e = \frac{9,090}{1 + .8 \sec [0.00975 \sqrt{P_a}]}$$

Try P_a = 5,000 lb. Substituting this value, we find that it solves this equation. Thus, P_a = 5,000. If our original guess was incorrect, other values of P_a would have to be tried until a value was found that solved the equation.

(b) Inserting the equation for F_{col} from part (a) into Equation (2-14) gives

$$\frac{15,700 - 15 (L'/\rho)}{FS} = \frac{P}{A} \div \frac{P_{ec}}{I}$$

or

$$\frac{15,700 - 15 (12/0.25)}{1.3} = \frac{P}{\pi/4} + \frac{P(0.1)(0.5)}{\pi/64}$$

Solving this for P gives P_{cr} = 6,540 lb. Notice that although this procedure eliminates the trial and error methods used with the secant equation, it yields less conservative results.

2.3.1.12 <u>Torsional Failure of Simple Columns</u>

The previous sections discussed the failure of long and short columns by bending. It was assumed throughout this treatment that the sections of the column are translated but not rotated as it fails. However, primary failure may occur at loads lower than those predicted in the section on bending failure if the sections should rotate as well as translate as shown in Figure 2-55.
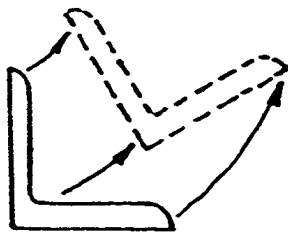
Figure 2-55.   Section Subject to Translation and Rotation

In general, columns whose cross sections have a low torsional rigidity, GJ, must be examined for torsional instability. Columns having closed sections or solid ones, such as round or square sections, have such a high torsional rigidity that there is little possibility of them failing by torsional instability. However, torsional instability must be considered in the case of columns composed of thin sections. Failure by twisting is unlikely for flanged columns whose cross sections are symmetrical about a point such as I, H, and Z sections. Twisting-type failures are most apt to occur in the case of torsionally weak sections that are unsymmetrical or have only one axis symmetry such as angles, tees, and thin-walled channels.

The basic equation for a column that fails by a combination of bending and twisting gives the critical stress as

$$F_{col} = \frac{GJ}{I_p} + \frac{C_{BT} \pi^2 E}{I_p (L')^2} \tag{2-16}$$

In this case, C_{BT} is a sectional property defined below and the parameters are defined as usual.

The torsion bending constant is dependent upon the axis of rotation and defined as

$$C_{BT} = \int_A w^2 \, dA - \frac{1}{A} \left[\int_A w \, dA \right]^2 \tag{2-17}$$

where

$$w = \int_o^u r_t \, d_u \tag{2-18}$$

The parameters used above are shown on an arbitrary cross section in Figure 2-56. Values of the torsional bending constant are given in graphical form for various cross sections in Figures 2-57 through 2-60. The torsion constant, J, may be obtained in Figures 2-61 for bulb angles or from the following equation for formed sections:

$$J = st^3/3 \tag{2-19}$$

Here, s is the developed length of the median line.
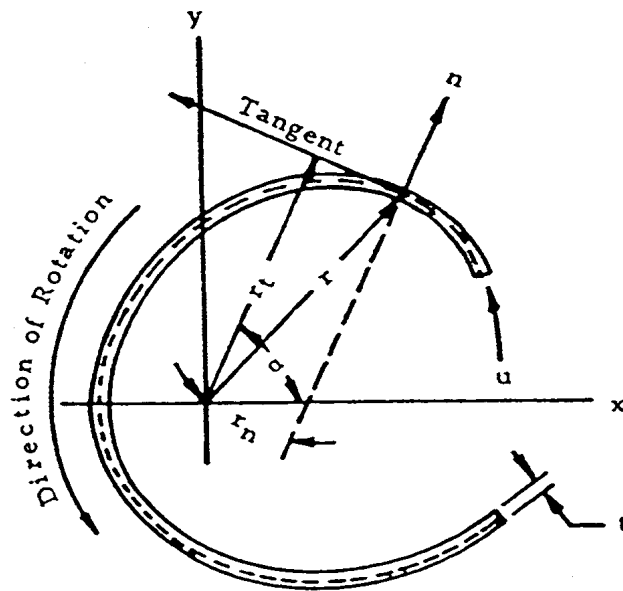
Figure 2-56.   Parameters Used to Define the Torsion Bending Constant

If a column is not attached to a sheet, the twisting failure is by rotation of sections about shear center of cross section.   In this case, I_p and C_{BT} are taken about this shear center.   If the column is attached to a sheet, sections may be assumed to rotate about a point in the plane of the sheet.   This procedure gives rough results but unfortunately little specific information is available on this subject.   In general, columns are stronger when they are used as stiffeners than when they stand free.   However, a column having an unsymmetrical cross section may be weaker when it is attached to a sheet.
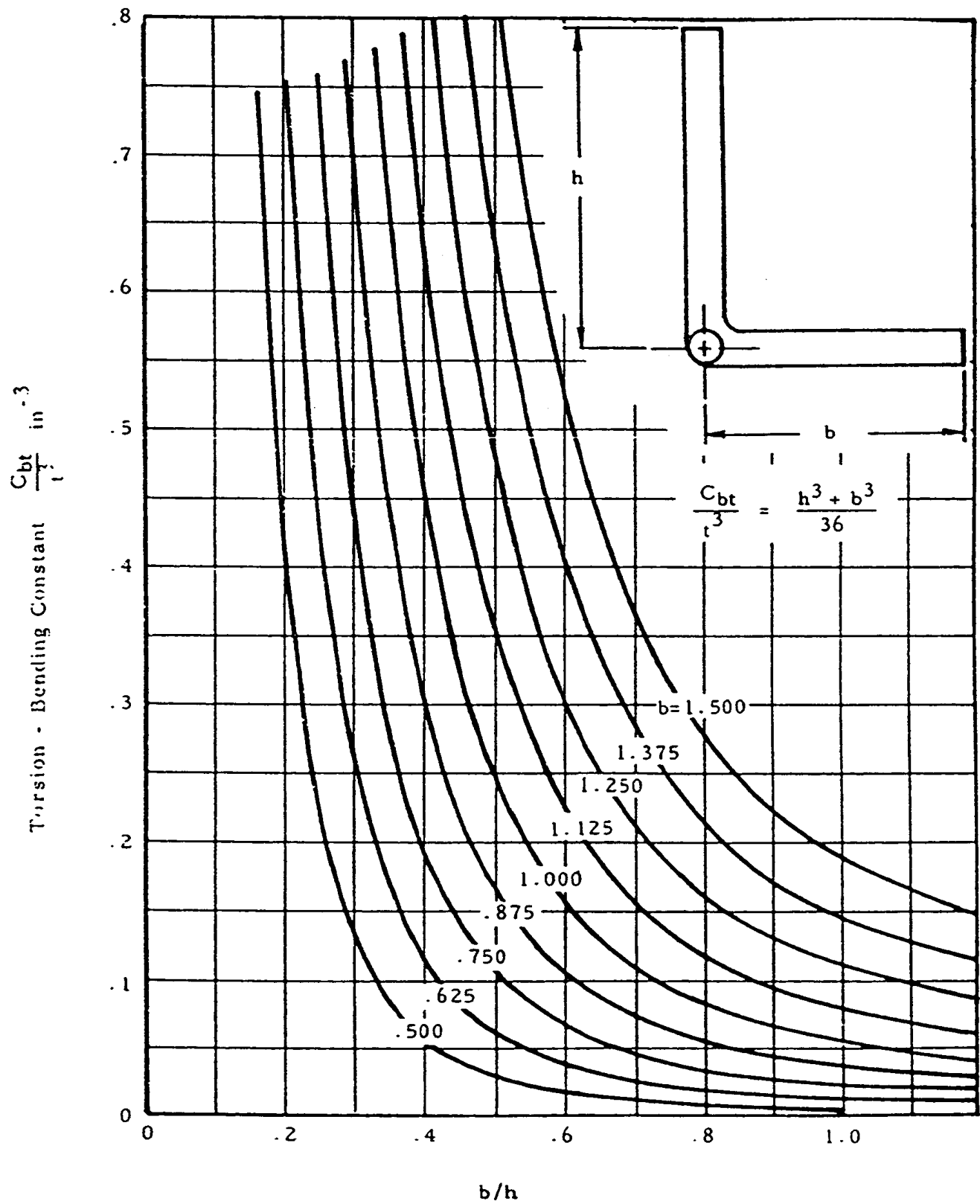
Figure 2-57.   Torsion - Bending Constant of Angle - About Its Shear Center
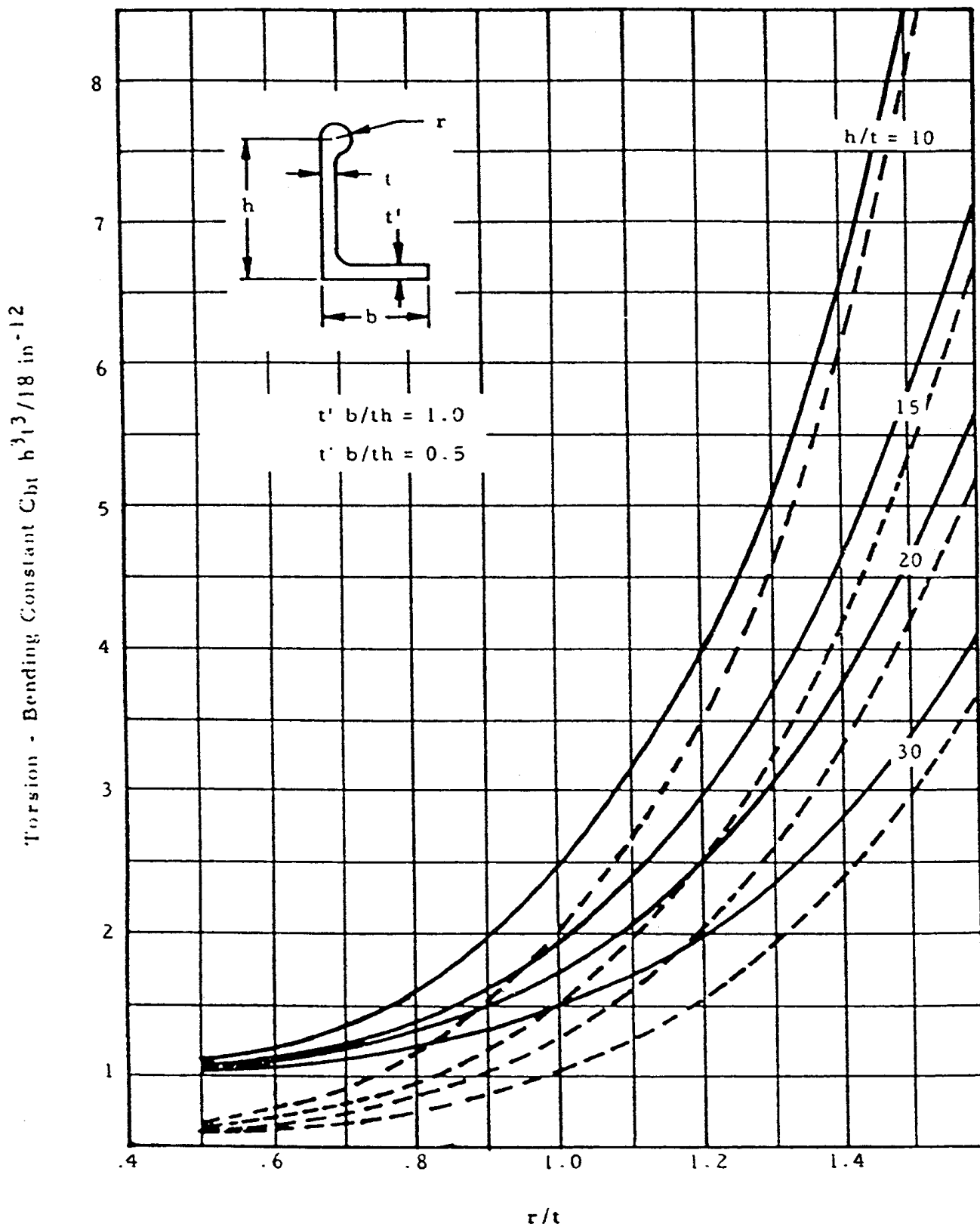
Figure 2-58.   Torsion - Bending Constant of Bulb Angle - About Shear Ce

$$\frac{C_{bt}}{t^3} = \frac{h^3}{36} \left[1 + 1/4 \left(\frac{b}{h} \right)^3 \right]$$
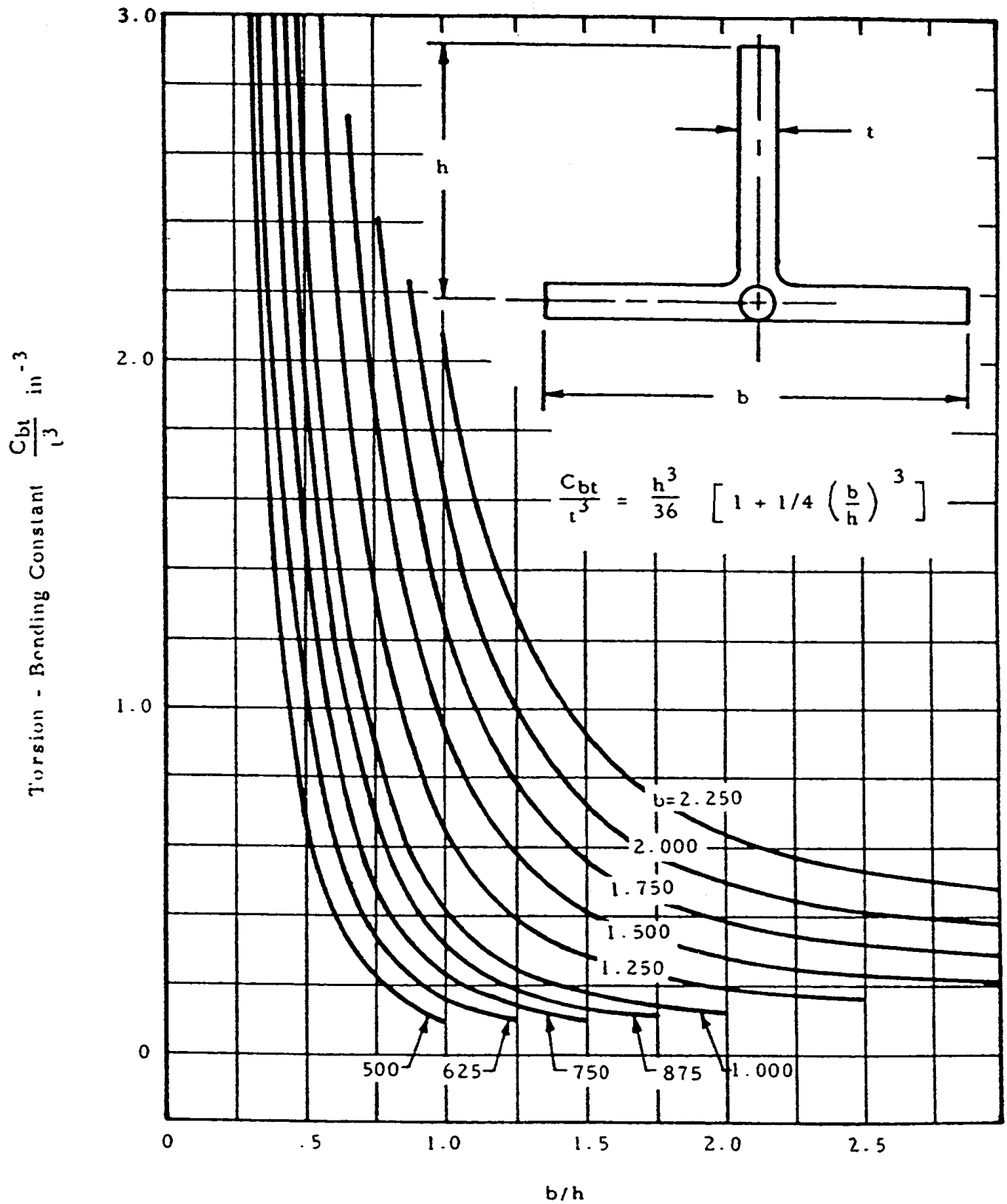
Figure 2-59.   Torsion - Bending Constant of Tee - About Shear Center

$$\frac{C_{bt}}{t} = \frac{h^2}{12} \left[e^2(h-6b) + 2b^2(b-3e) \right]$$

$$e = \frac{b}{2(1+h/6b)}$$
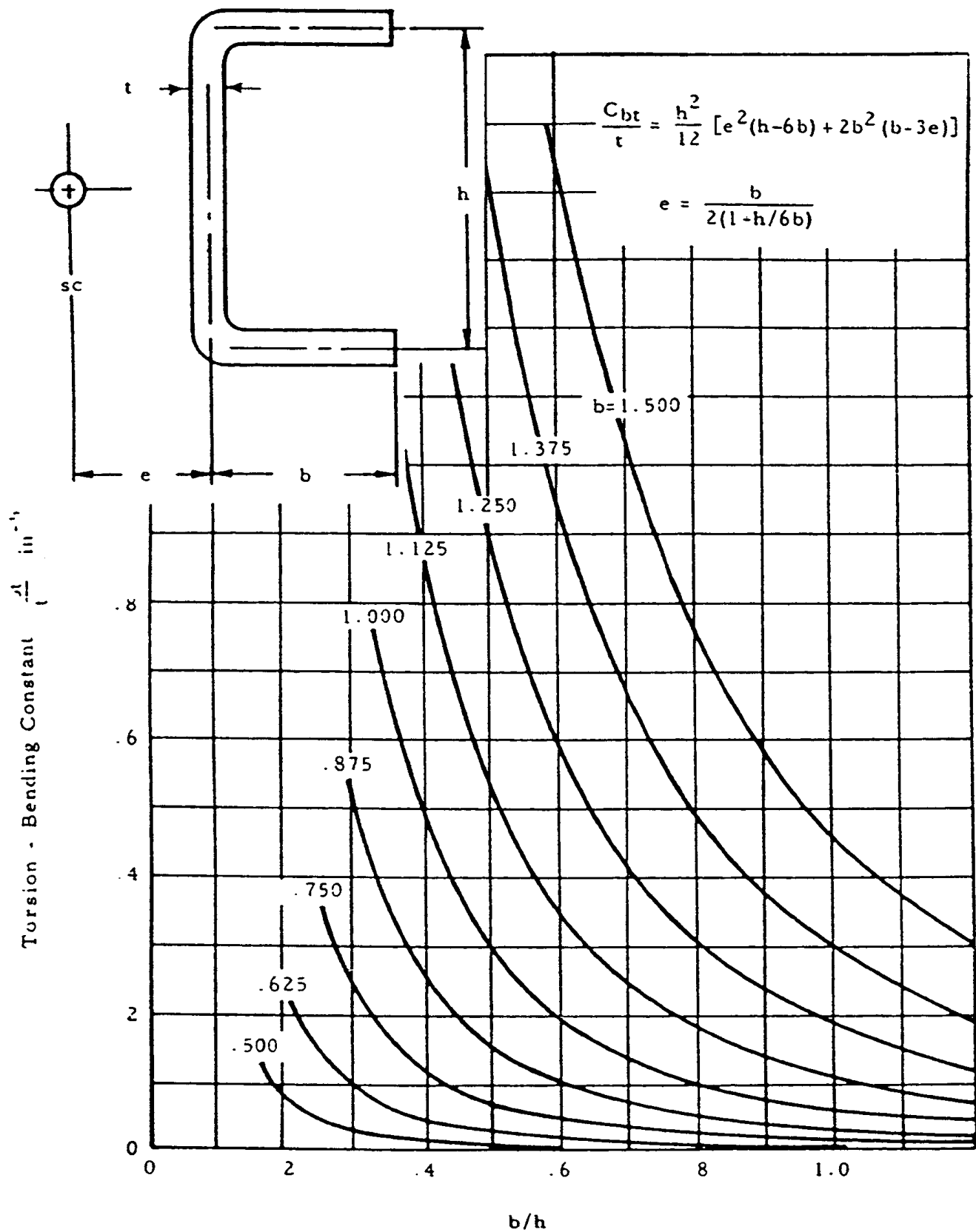
Figure 2-60.   Torsion – Bending Constant of Channel – About Shear Center
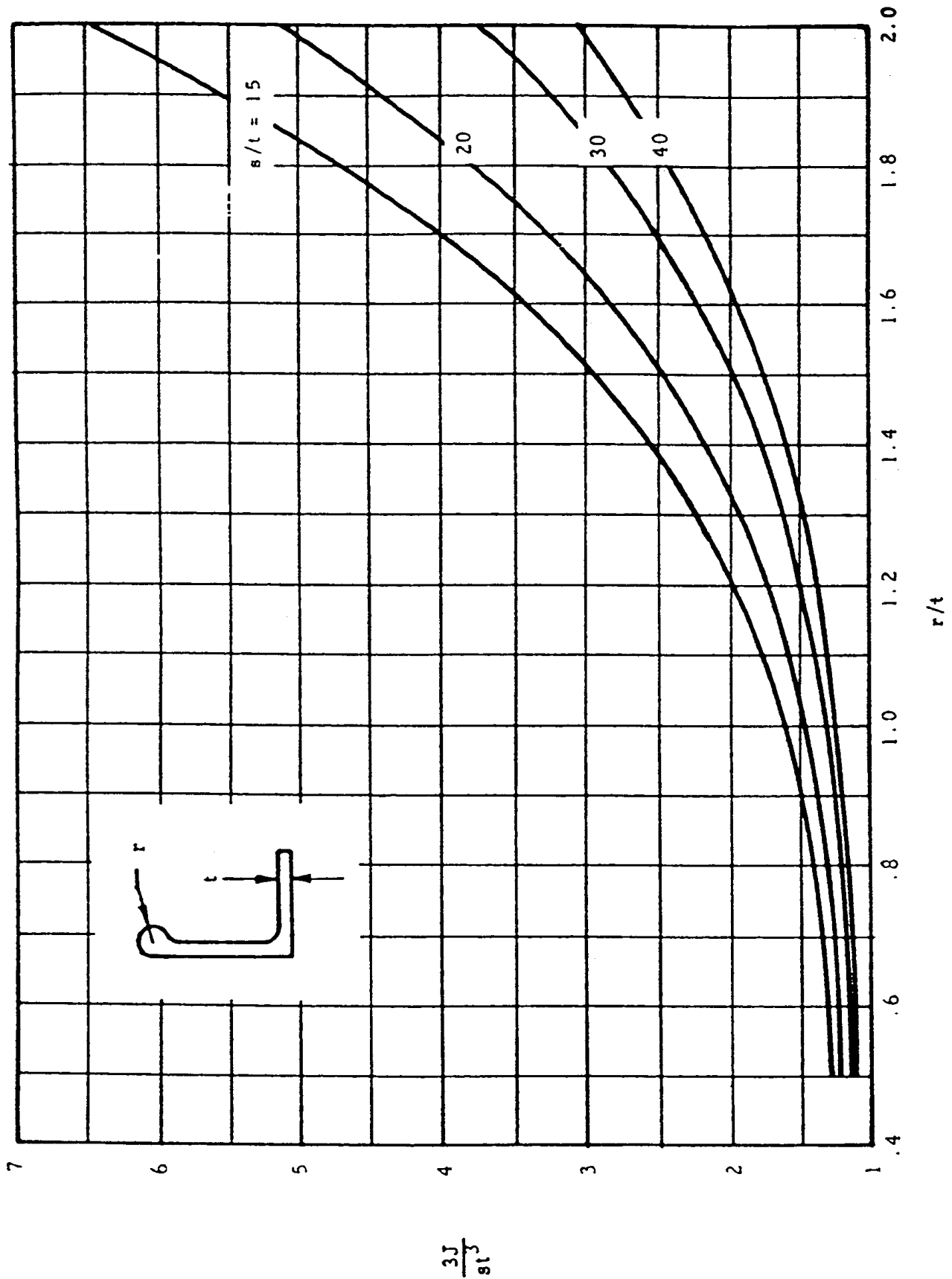
Figure 2-61. Torsion Constant of Bulb Angle

2.3.1.13 Sample Problem - Torsional Failure of Simple Columns

Given: A column with cross section and material properties as shown in Figure 2-62.

$$G = 3.85 \times 10^6$$
$$E = 10 \times 10^6 \text{ psi}$$
$$L' = 100$$
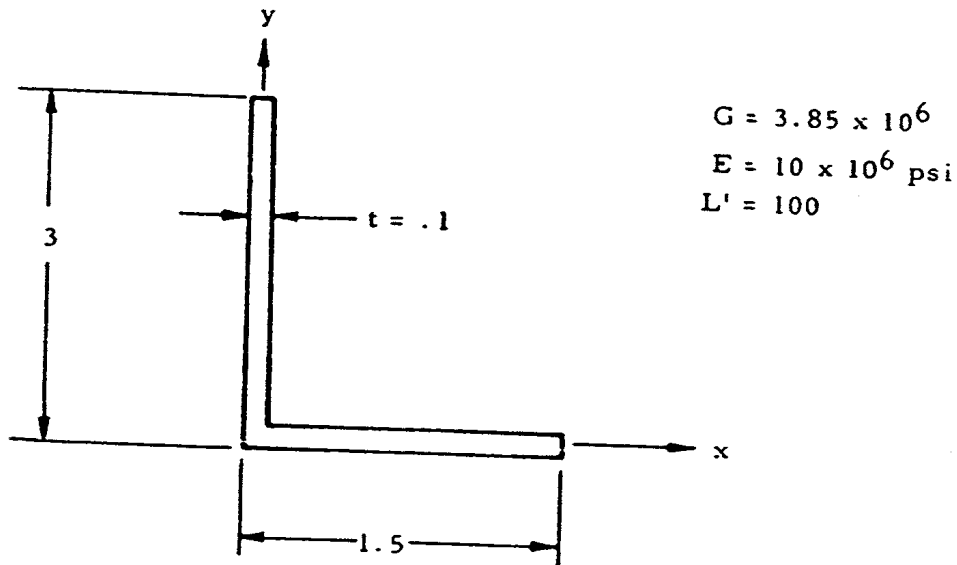
Figure 2-62. Cross Section of Column Used for Illustration of Torsional Failure

Find: F_{col} for failure by a combination of bending and twisting.

Solution: Since t is small, the shear center may be assumed to be at the corner of the angle.

The polar moment of inertia about the shear center is given by

$$I_p = I_x + I_y$$

or

$$I_p = \left\{ \left[\frac{1.5(.1)^3}{12} \right] + \left[\frac{(.1)(3)^3}{12} + (.1)(3)(1.5)^2 \right] \right\} = .9$$

From Equation (2-19)

$$J = \frac{st^3}{3} = \frac{4.5(0.1)^3}{3} = 1.5 \times 10^{-3}$$

From Figure 2-57,

$$C_{bt} = \frac{t^3(h^3 + b^3)}{36} = \frac{(0.1)^3(27 + 3.48)}{36} = 8.46 \times 10^{-4}$$

Inserting these values into Equation (2-16) gives

$$F_{col} = \frac{(3.85 \times 10^6)(1.5 \times 10^{-3})}{0.9} + \frac{(8.46 \times 10^{-4})\pi^2 (10 \times 10^6)}{(0.9)(10^4)}$$

Thus, $F_{col} = 6,419$ psi.

2.3.2   Introduction to Crippling Failure of Columns

In the previous sections, the primary failure of simple columns was considered. However, if a column has thin sections, it may fail at a load well below the critical load predicted for primary failure. Thus, a column must, in general, be checked for both primary failure and crippling. Primary failure may be assumed to be independent of crippling effects, in which case, a failure curve such as that shown in Figure 2-63 may be used. The right-hand portion of the curve describes the stress required for primary failure of the column at various effective slenderness ratios. This curve is cut off at the crippling stress level by the flat portion to the left.
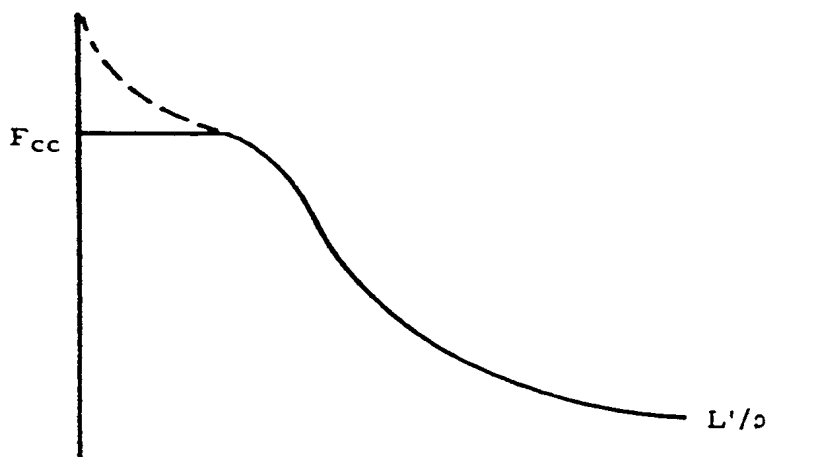
Figure 2-63.   Failure Curve Based on the Assumption of No
Interaction Between Primary Failure and Crippling

If the interaction between crippling and primary failure is to be taken into account, the constant F_{co} in the Johnson-Euler equation may be set equal to the crippling stress F_{cc}. Although this procedure is more correct, it also introduces added complications, and only works for columns having a crippling stress less than the primary failure stress as L'/ρ approaches zero. Figures 2-64 and 2-65 show sets of Johnson-Euler curves for various materials. The curve used in a given case is the one that intercepts the ordinate at the value of F_{cc} for that column.

2 - 82

ALUMINUM ALLOYS

Johnson-Euler Formulas
For Aluminum Columns

Johnson Formula

$$F_{col} = F_{cc} - \frac{F_{cc}^2 \left(\frac{L}{\rho \sqrt{C}}\right)^2}{4 \pi^2 E}$$

Where:

C = restraint coefficient
$E = 10.3 \times 10^6$ psi

Euler Formula

$$F_{col} = \pi^2 E \left(\frac{\rho \sqrt{C}}{L}\right)^2$$

F_{col} - Allowable Column Stress - Ksi

$L'/\rho = L/\rho \sqrt{C}$
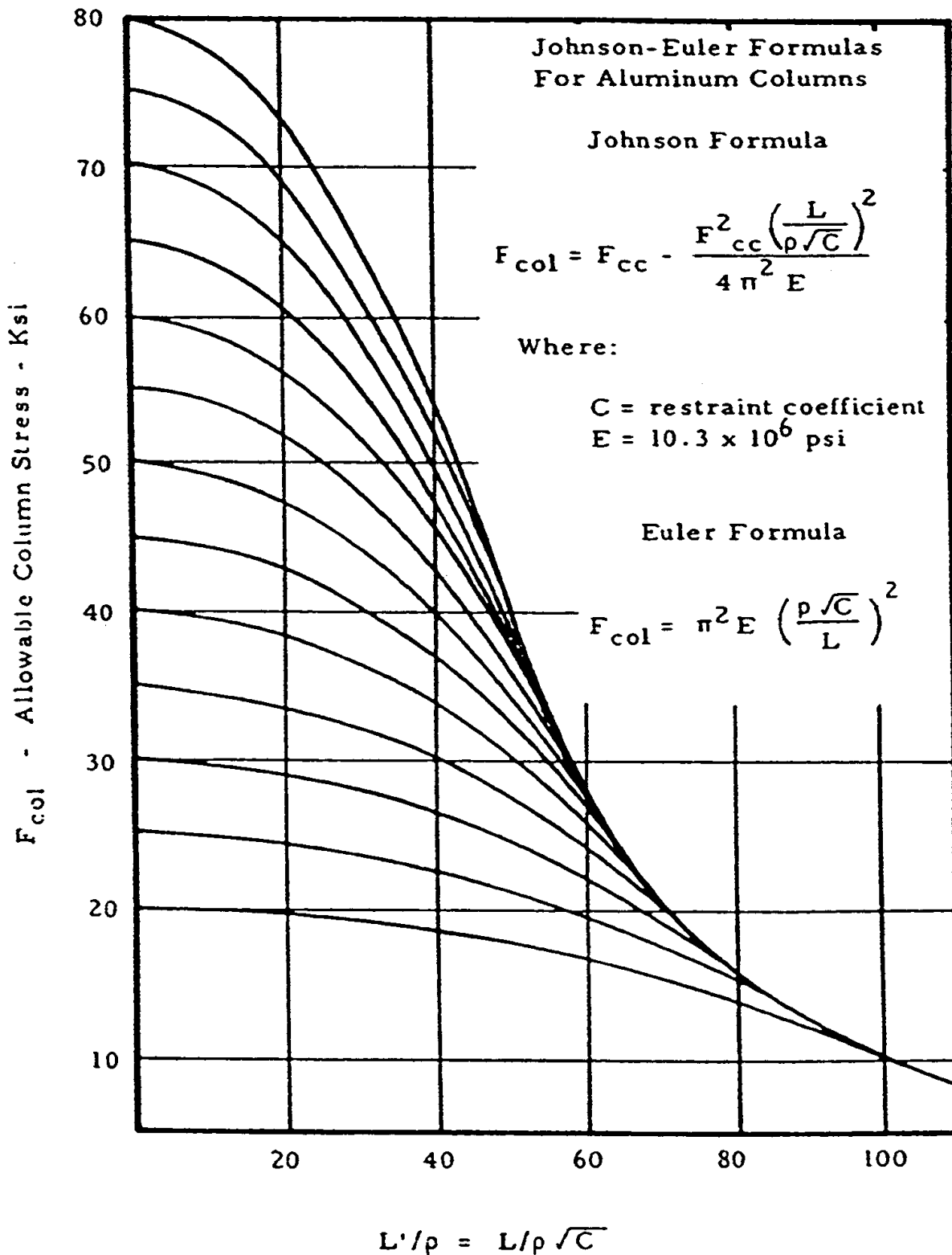
Figure 2-64a. Johnson-Euler Column Curve

MAGNESIUM ALLOYS

$$F_{ca} = F_{cc} - \frac{(F_{cc})^2}{4\pi^2 E} \left(\frac{L}{\rho\sqrt{C}}\right)^2$$

Where:

C = coefficient of restraint
E = modulus of elasticity = 6.5×10^6

$$F_{col} = \frac{\pi^2 E}{\left(\frac{L}{\rho\sqrt{C}}\right)^2}$$

$$L'/\rho = L/\rho\sqrt{C}$$
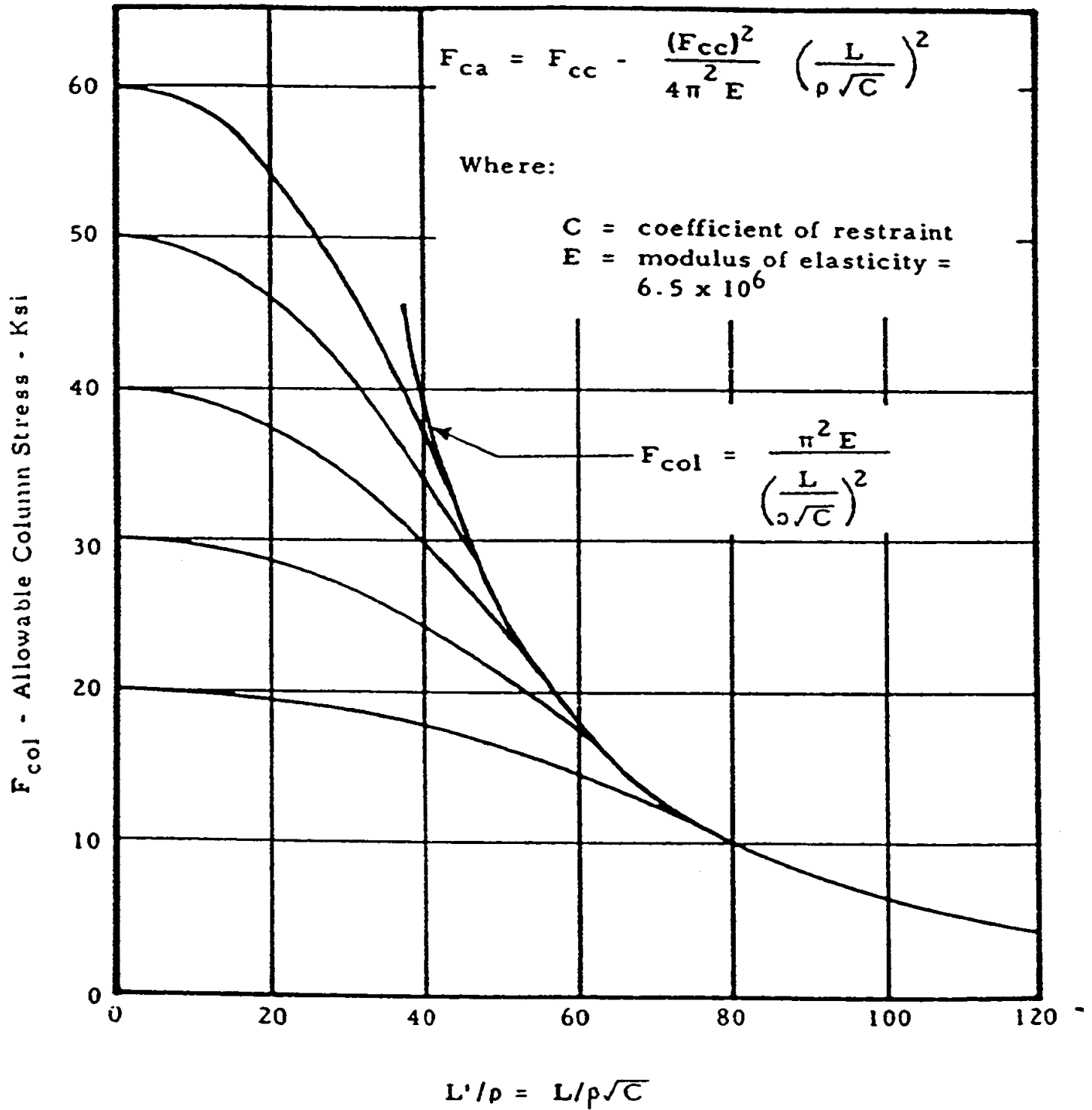
Figure 2-64b. Johnson-Euler Column Curve

STEELS

Steel Columns

Johnson Formula

$$F_{col} = F_{cc} - \frac{F^2_{cc}\left(\frac{L}{\rho\sqrt{C}}\right)^2}{4\pi^2 E}$$

Where C = restraint coefficient
E = 29,000,000

Euler Formula

$$F_{col} = \frac{\pi^2 E}{\left(\frac{L}{\rho\sqrt{C}}\right)^2}$$

Applies to Corrosion
and Non-Corrosion
Resisting Steels

$L'/\rho = L/\rho\sqrt{C}$
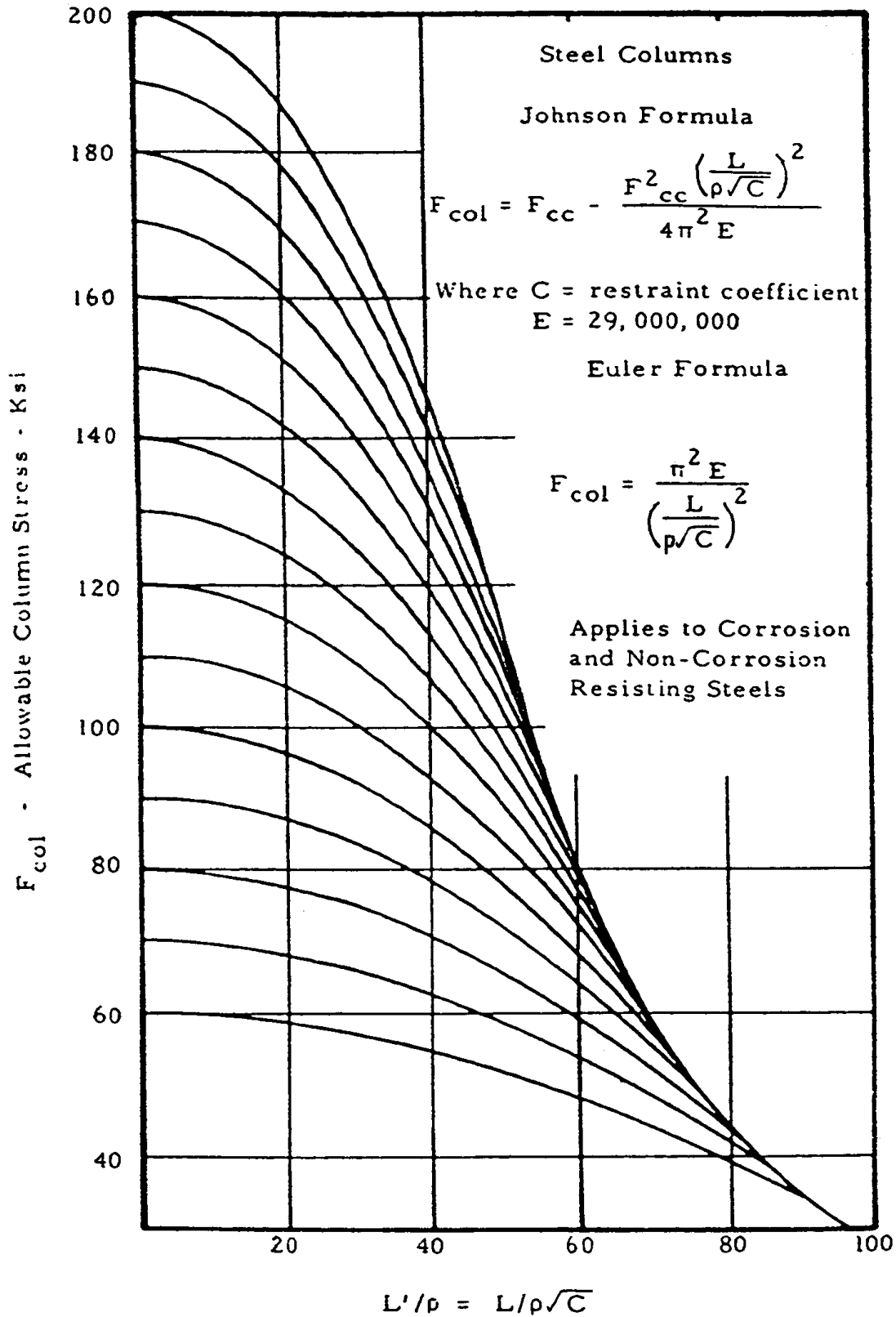
Figure 2-65a. Johnson-Euler Column Curve

2 - 85

$$F_{col} = F_{cc} - \frac{(F_{cc})^2}{4\pi^2 E} \left(\frac{L}{\rho\sqrt{C}}\right)^2$$

Where:

C = restraint coefficient

E = modulus of elasticity = 15.5×10^6

$$F_{col} = \frac{\pi^2 E}{\left(\frac{L}{\rho\sqrt{C}}\right)^2}$$

Commercially Pure Titanium

$L'/\rho = L/\rho\sqrt{C}$
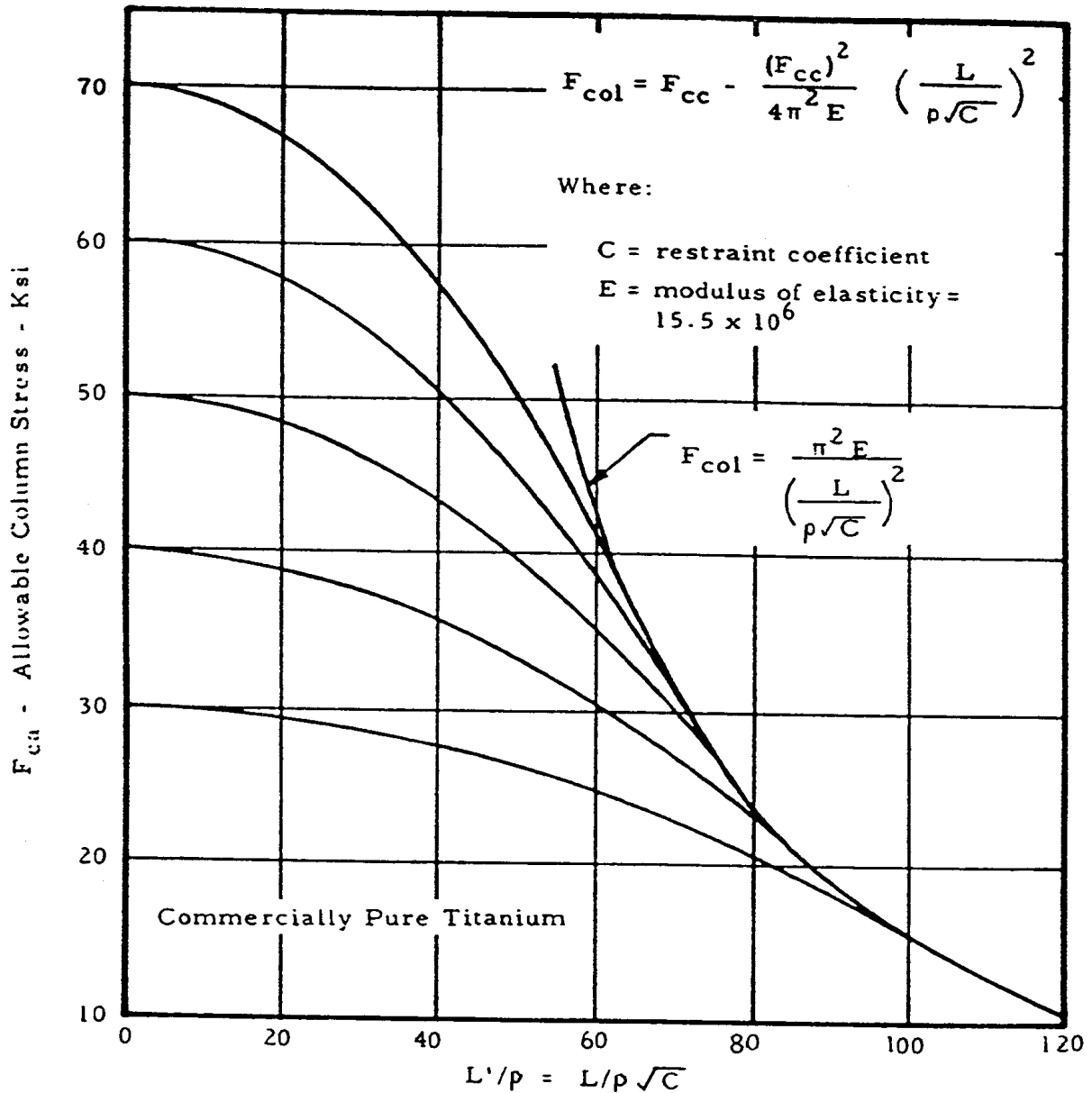
Figure 2-65b. Johnson-Euler Column Curve

2.3.2.1 Crippling Stress of Round Tubes

Steel tubes for which the diameter-to-wall thickness ratio is less than 50 need not be checked for crippling. This gives us some general idea of the thinness required if a tube is to fail by crippling rather than by primary instability. A theoretically correct formula for the crippling stress of a tube is

$$F_{cc} = \frac{1}{\sqrt{3(1-u^2)}} \frac{Et}{r} \tag{2-20}$$

where r is the mean radius and μ = Poisson's ratio. If μ is taken to be 0.3, is the case for steel and aluminum alloys, we obtain

2 - 86

$$F_{cc} = .605 \frac{Et}{r} \qquad (2\text{-}21)$$

This equation, however, is extremely unconservative for small values of t/r and should only be used for approximations in the early stages of design.

More conservative and accurate empirical methods are available for the treatment of tubular columns. If L/r is less than 0.75, use the equation

$$\frac{P_{cc}}{A} = F_{cc} = \frac{2K\pi^2 r}{L^2 t} \qquad (2\text{-}22)$$

where the critical stress coefficient, K, is given in Figure 2-66.

$$Z = \frac{L^2}{rt} \sqrt{1-\mu^2}$$
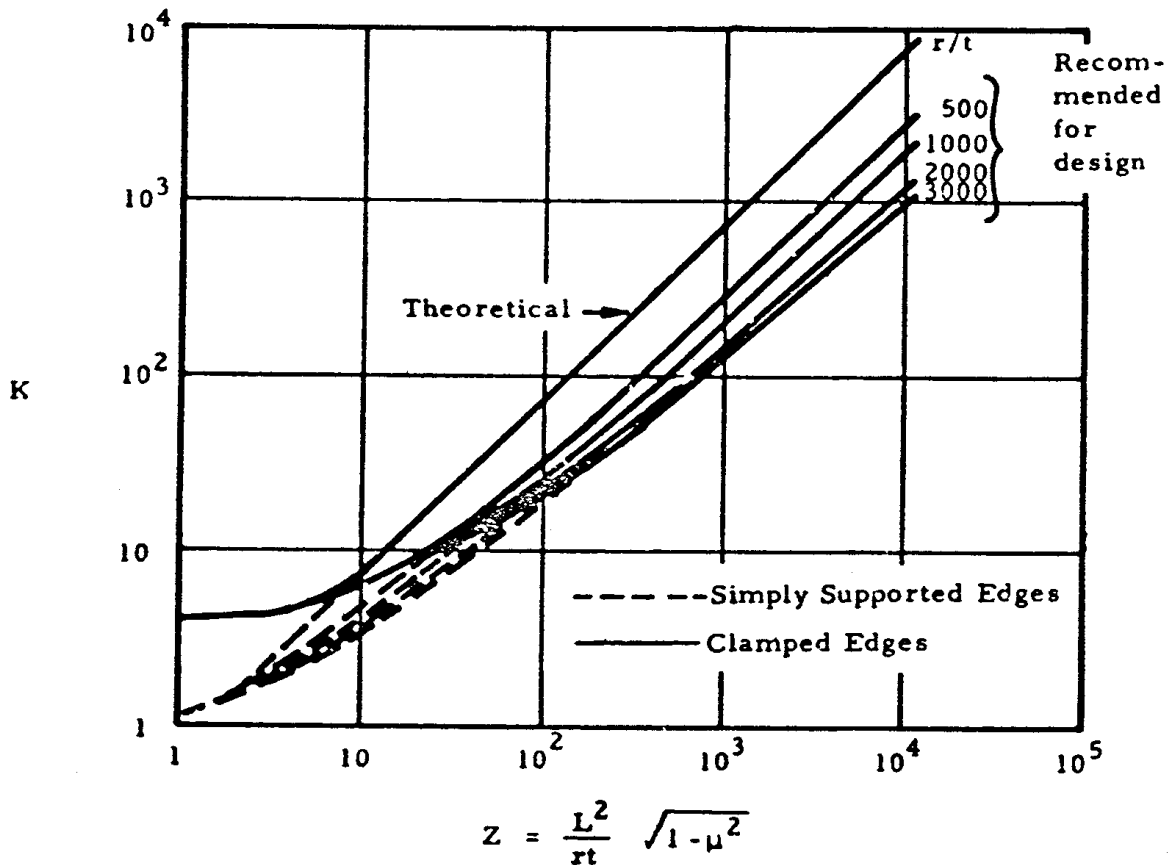
Figure 2-66. Critical Stress Coefficients for Thin-Walled Short Circular Cylinders Subjected to Axial Compression

If L/r is greater than 0.75, use the equation

$$\frac{P_{cc}}{A} = F_{cc} = CE \frac{t}{r} \qquad (2\text{-}23)$$

where C is given in Figure 2-67.

2 - 87
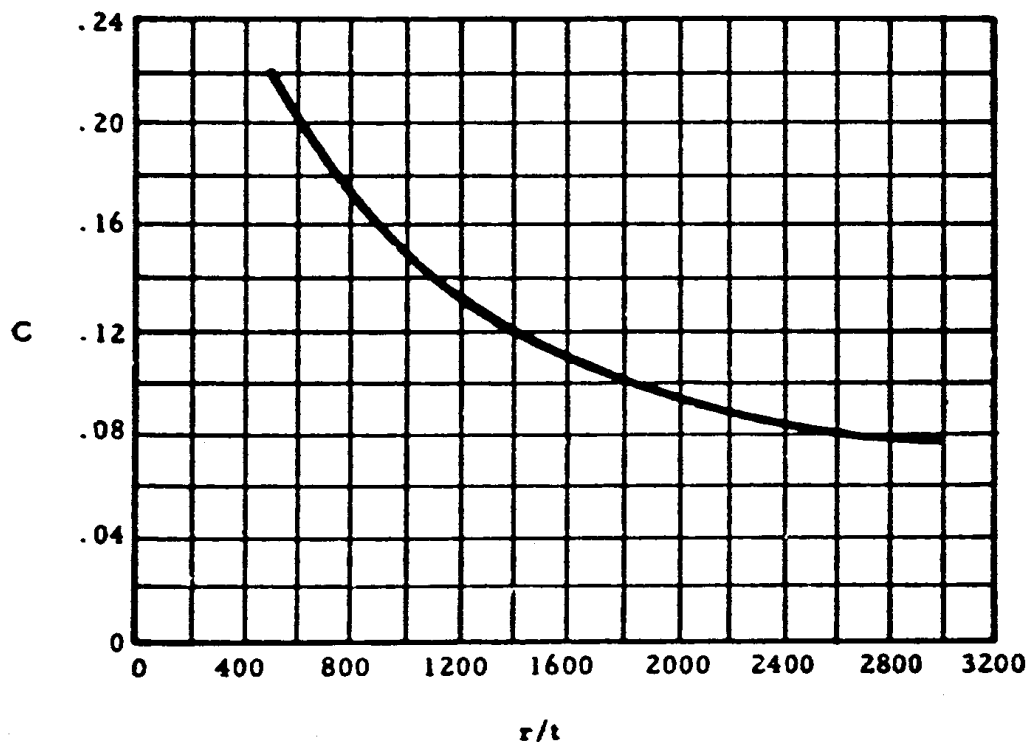
Figure 2-67.   Coefficient for Computing Critical Axial Compressive
Stresses of Indeterminate Length and Long Cylinders

2.3.2.2   Sample Problem - Crippling Stress of Round Tubes

Given: The tubular aluminum column shown in Figure 2-68.
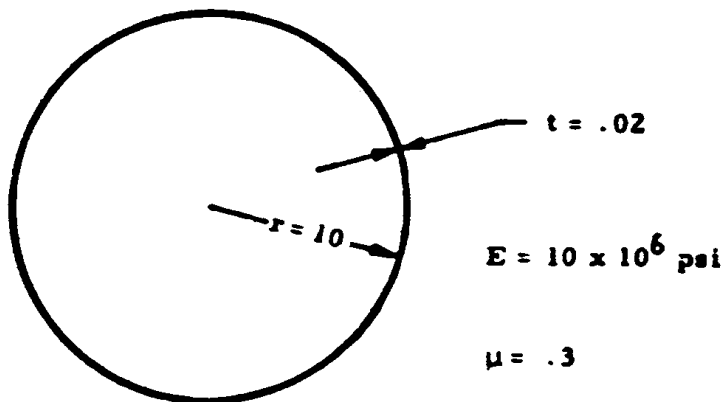
Figure 2-68.   Cross Section of Column Used for Illustration of
Crippling Failure of Round Tube

Find: The crippling stress if

  (a) L = 5 in.
  (b) L = 60 in.

Solution: (a) In this case, $L/r < 0.75$ so we may use Equation (2-22)

$$Z = \frac{L^2}{rt} \sqrt{1 - \mu^2} = \frac{(5)^2}{10(.02)} \sqrt{1 - (.3)^2} = 119.5$$

$$\frac{r}{t} = \frac{10}{.02} = 500$$

From Figure 2-66, $K = 11$. Substituting this value into Equation (2-22), we find that

$$F_{cc} = \frac{2K\pi^2 r}{L^2 t} = \frac{2(11)\pi^2(10)}{(5)^2(.02)} = 4,350 \text{ psi}$$

(b) If $L = 60$ in., $L/r > 0.75$ so that Equation (2-23) may be used

$$\frac{r}{t} = 500$$

From Figure 2-67, $C = 0.22$. Substituting this value into Equation (2-23), we obtain

$$F_{cc} = 0.22 \frac{Et}{r} = \frac{0.22(10 \times 10^6)(0.02)}{10} = 4,400 \text{ psi}$$

If the theoretically correct formula, Equation (2-20), is used for either of these two columns,

$$F_{cc} = 0.605 \frac{Et}{r} = 12,100 \text{ psi}$$

This value may be seen to be much greater than those obtained from the more accurate empirical formulas.

2.3.2.3 Crippling Stress of Outstanding Flanges

Two idealized cases of edge restraint of long flanges are shown in Figure 2-69. In case (a), the flange is fixed along its edge and the equation for its crippling stress is

$$F_{cc} = \frac{1.09E}{1 - \mu^2} \left(\frac{t}{b}\right)^2 \tag{2-24}$$

2 - 89

The flange shown in (b) is hinged along its edge and the equation for its crippling stress is

$$F_{cc} = \frac{.416E}{1-\mu^2} \left(\frac{t}{b}\right)^2 \qquad (2-25)$$

A column flange is neither rigidly fixed nor hinged along its edge so its crippling stress lies between those given by Equations (2-24) and (2-25), the latter giving more conservative results.
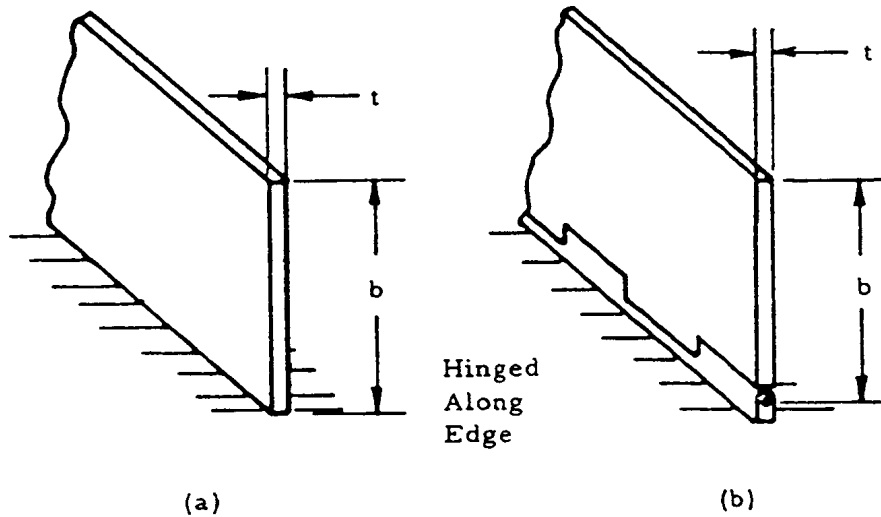
Figure 2-69.   Idealized Edge Constraints of Long Flanges

2.3.2.4   Crippling Stress of Angle Elements and Complex Shapes

The basic design equations for the crippling stress and load of the angle section shown in Figure 2-70 are

$$\frac{F_{cc}}{\sqrt{F_{cy}E}} = \frac{C_e}{\left(\frac{b'}{t}\right)^{0.75}} \qquad (2-26)$$

and

$$P_{cc} = \left[C_e \frac{\sqrt{F_{cy}E}}{\left(\frac{b'}{t}\right)^{0.75}}\right] A \qquad (2-27)$$

Here b´ is equal to (h+b)/2 as seen in Figure 2-69 and C_e is a constant dependent upon the fixity of the edges, as shown to the right of Figure 2-70.

2 - 90

Figure 2-70.   Angle Section
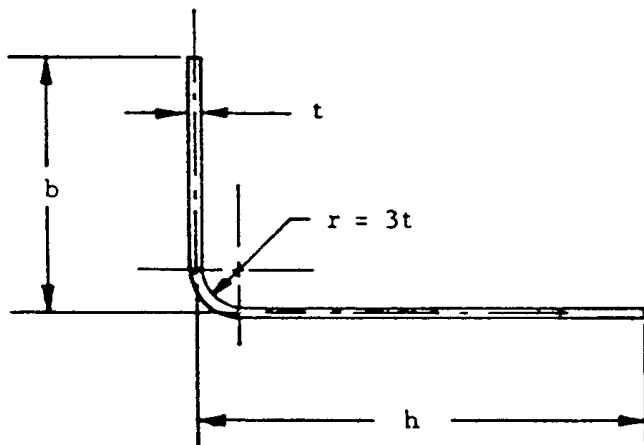
$$b' = \frac{h-b}{2}$$

$C_c = .316$ (two edges free)

$C_c = .342$ (one edge free)

$C_c = .366$ (no edge free)

The area of this angle is given by

$$A = \left[\left(\frac{b'}{t} \right) - 0.214 \left(\frac{r}{t} \right) \right] 2t^2 \qquad (2-28)$$

Nondimensional plots of Equations (2-26) and (2-27) are shown in Figures 2-71 and 2-72, respectively. These plots may be used to facilitate the solution of angle problems. It must be noted that Equations (2-26) and (2-27) have no significance when F_{cc} is greater than F_{cy}. These cutoffs are shown for two alloys in the following figures.

2 - 91
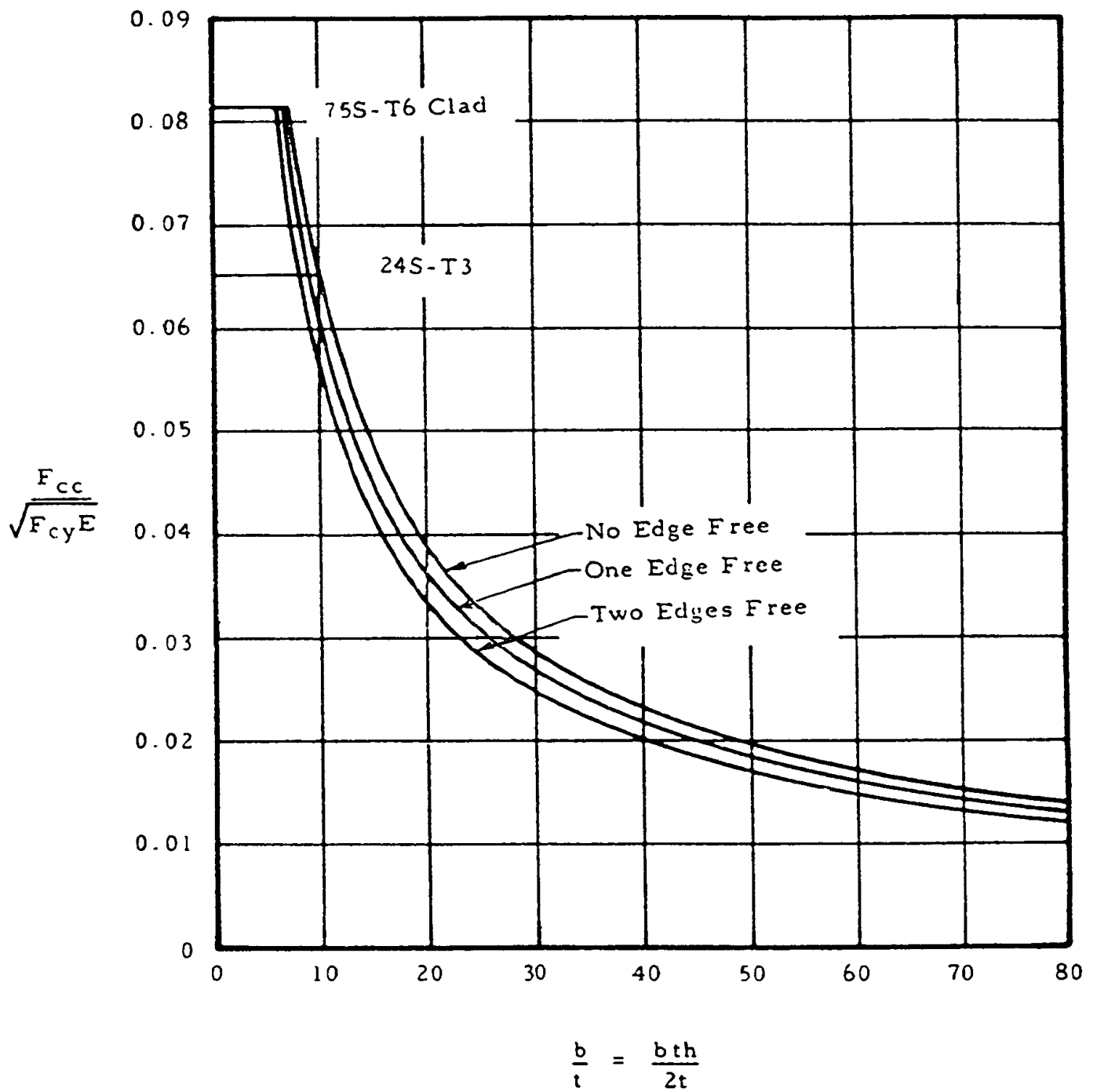
Figure 2-71. Dimensionless Crippling Stress of Angles vs. b'/t
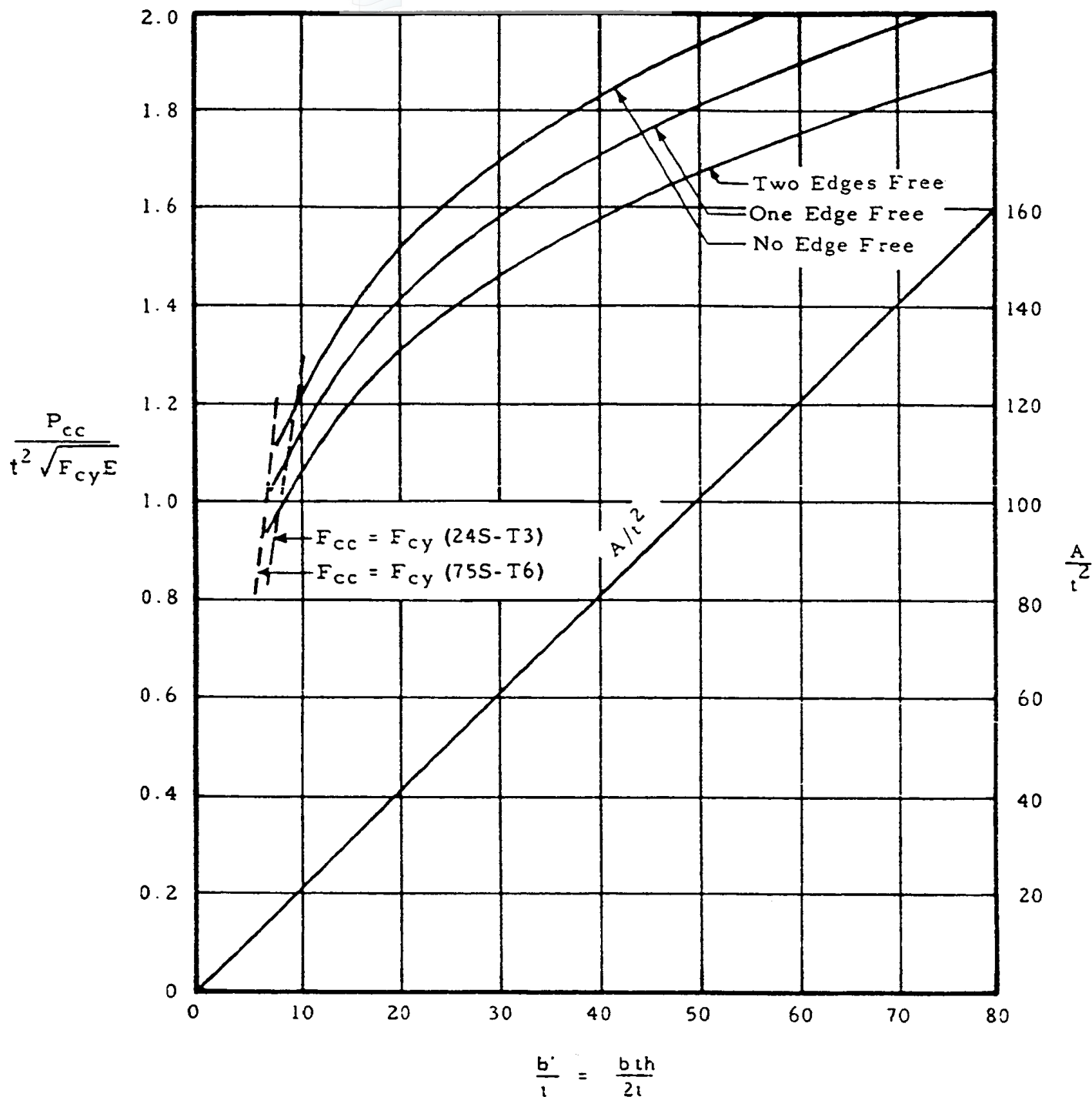
Figure 2-72. Dimensionless Crippling Load of Angle vs. b'/t

Many complex sections, such as those shown in Figure 2-73, may be treated by considering them to be composed of a number of angles. The crippling stress of these sections may be found by the following procedure: First, break the section up into a number of angles. Secondly, find the crippling load and area of each of the angles. Finally, find F_{cc} for the entire section from the following equation:

$$F_{cc} = \frac{\Sigma \text{ Crippling Load of Angles}}{\Sigma \text{ Area of Angles}} \qquad (2\text{-}29)$$
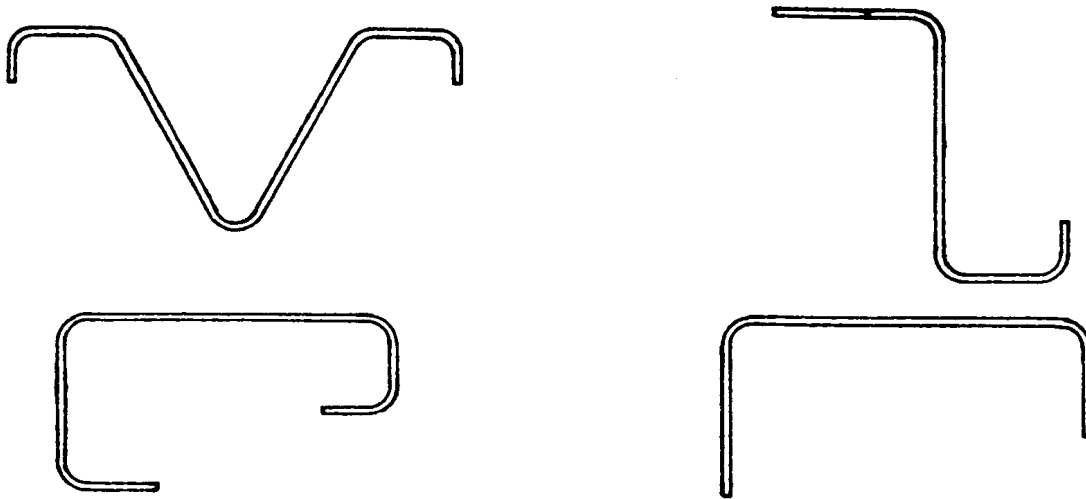
Figure 2-73. Examples of Complex Sections

This procedure is illustrated in the following example.

2.3.2.5   Sample Problem - Crippling Stress of a Complex Shape

Given: Column with the cross sectional shape shown in Figure 2-74. It is composed of an aluminum alloy for which $E = 10^7$ psi and $F_{cy} = 50$ kips.
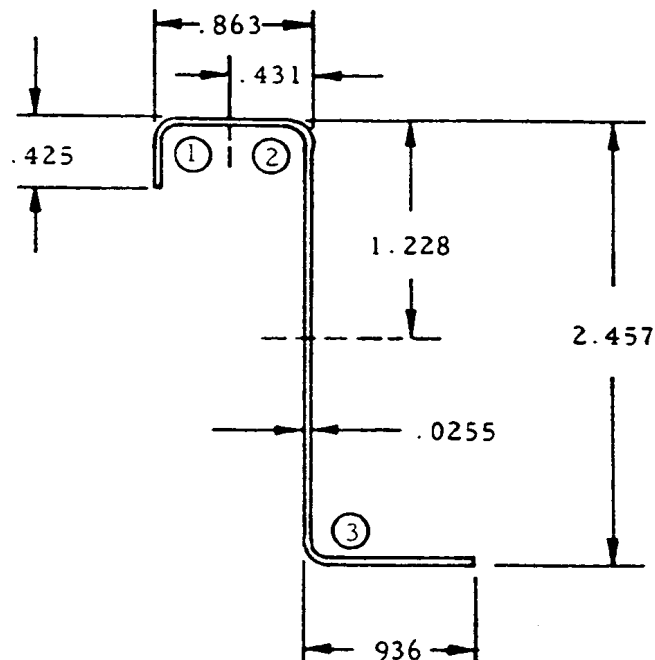
Figure 2-74.   Cross Section of Column Used for Illustration of Crippling Failure of Complex Shape

Find: The crippling stress F_{cc}.

Solution: This section may be broken into three angle sections as shown by the broken lines above. The calculation of the crippling load and area of each angle section is summarized in the table below:

Section	b	h	Edge Condition	$\frac{b+h}{2t}$	$\frac{P_{cc}}{t^2\sqrt{F_{cy}E}}$	P_{cc}	$\frac{A}{t^2}$	A
1	0.425	0.431	One Edge Free	16.8	1.33	$1.33 t^2\sqrt{F_{cy}E}$	32.5	$32.5 t^2$
2	0.431	1.228	No Edge Free	32.6	1.72	$1.72 t^2\sqrt{F_{cy}E}$	64.0	$64.0 t^2$
3	0.936	1.228	One Edge Free	42.5	1.72	$1.72 t^2\sqrt{F_{cy}E}$	83.9	$83.9 t^2$

The values of b and h in this table are as shown in Figure 2-70. The values of P_{cc} and A may either be found from Equations (2-27) and (2-28) or from Figure 2-72 which shows these equations in graphical form. The crippling stress may now be found from Equation (2-29) to be

$$F_{cc} = \frac{(1.33 + 1.72 + 1.72)t^2\sqrt{F_{cy}E}}{(32.5 + 64.0 + 83.9)t^2} = 0.0264\sqrt{F_{cy}E}$$

Substituting the material properties into the above equation gives

$$F_{cc} = 0.0265\sqrt{(5\times10^4)(30\times10^6)} = 32,400 \text{ psi}$$

2.3.2.6 Crippling Stress of I Beams

Figure 2-75 shows an I section.
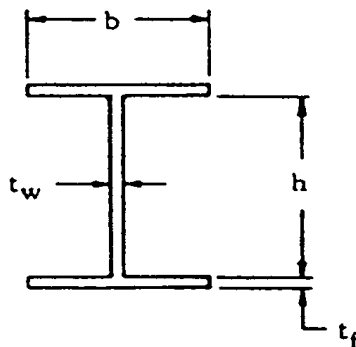
Figure 2-75. I Section

2 - 95

The crippling stress of a column of this shape is given by

$$F_{cc} = \frac{k_w \pi^2 E\, t_w^2}{12(1-u^2)h^2}$$

(2-30)

where k_w is given in Figure 2-76.
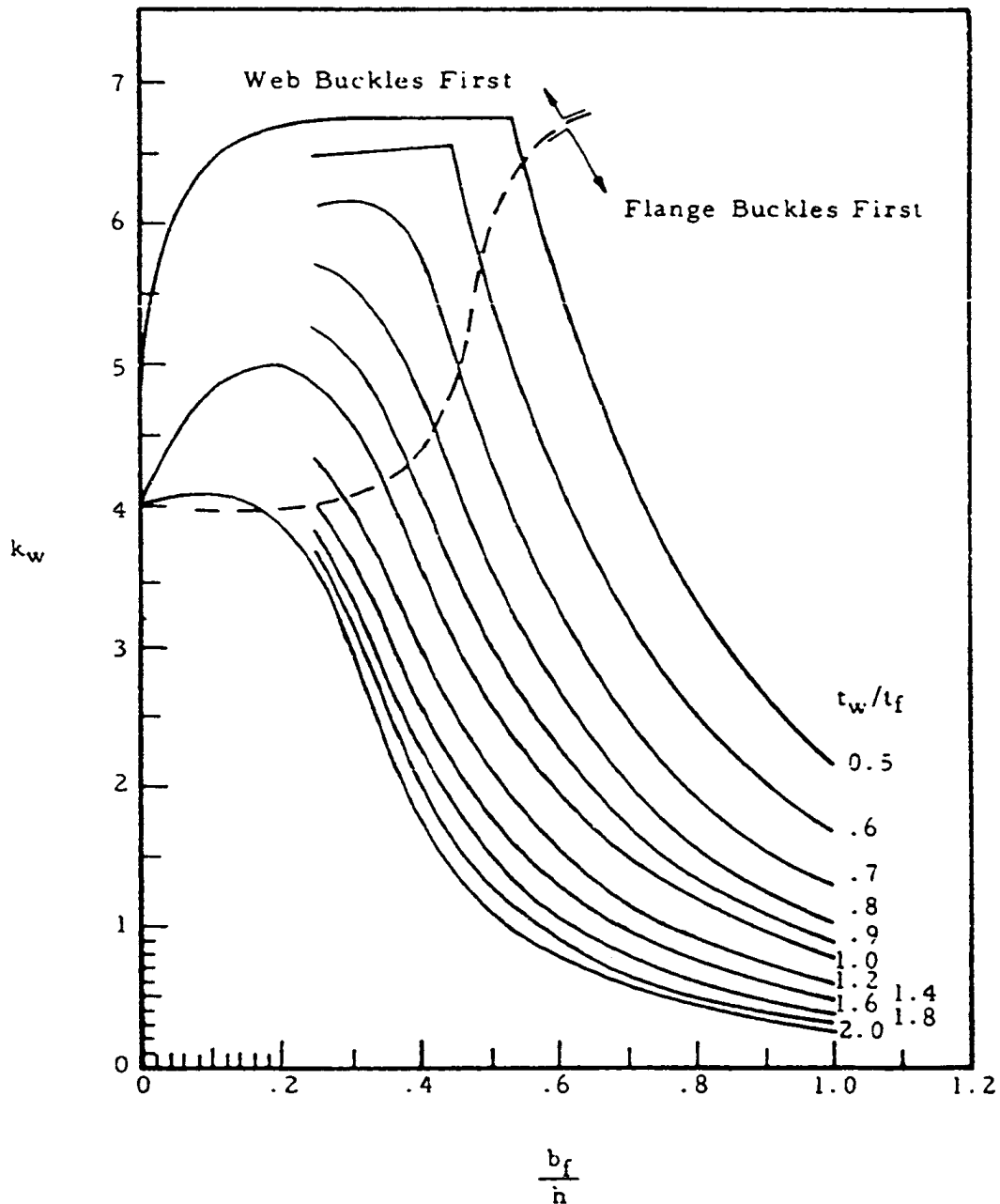
Figure 2-76. k_w for Equation (2-30)

2.4   Complex Columns

The material in previous sections treated columns that have uniform cross sections and may be considered to be one piece. This section treats of stepped and tapered columns whose cross section varies as well as of latticed columns whose action varies from that of one-piece columns.

2.4.1   Stepped and Tapered Columns

Columns of variable cross section can be solved by numerical procedures. However, charts are available that vastly simplify the solution of stepped and tapered columns.

These charts are shown in Figures 2-78 through 2-81. The use of these charts in finding a critical load is self-explanatory except for the fact that the tangent modulus of elasticity, E_t, must be used in place of E if the section is stressed beyond the proportional limit. Also, the coefficients of constraint that were discussed in Section 2.3.1.4 no longer hold for stepped or tapered columns. The columns shown in the charts have pinned ends.

2.4.2   Sample Problem - Stepped Column

Given: The concentrically loaded pin ended, stepped column shown in Figure 2-77.

$$A_1 = .4 \qquad A_2 = .5$$
$$I_1 = .25 \qquad I_2 = .5$$
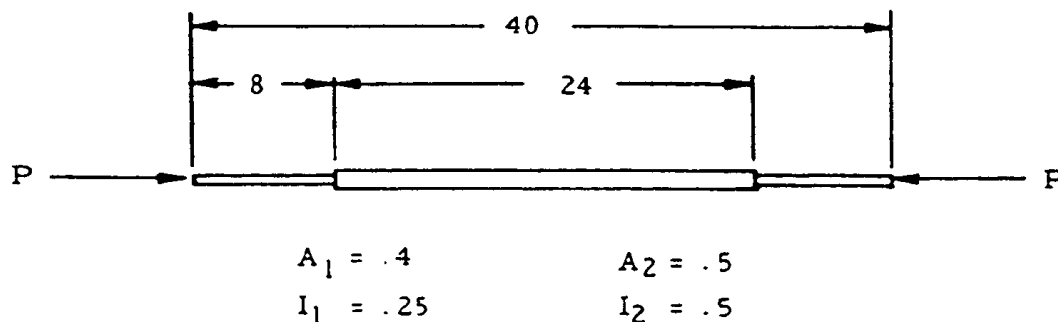
Figure 2-77.   Column Loading Used for Illustration of Effect of Stepped Columns

Find: The critical load P_{cr}.

Solution: Assume $P_{cr} = 11,600$ lb. Thus, F_{col_1} and F_{col_2} are equal to 11,600/0.4 psi and 11,600/0.5 psi, respectively. Equation (2-6) gives E_t as

$$E_t = \frac{E}{1 + 3/7 \, n\sigma^{n-1}}$$

Since $\sigma = f_c/f_1$ where f is the compressive stress which, in this case, is F_{col},

$$E_t = \frac{E}{1 + 3/7\, n\left(\dfrac{F_{col}}{f_1}\right)^{n-1}}$$

Inserting values of f_1 and n from Figure 2-46 into this equation gives

$$E_t = \frac{10.7 \times 10^6}{1 + 42.9\left(\dfrac{F_{col}}{37000}\right)^9}$$

Inserting the values of F_{col_1} and F_{col_2} into this equation gives

$$E_{t_1} = 1.86 \times 10^6 \text{ psi}$$

and

$$E_{t_2} = 6.55 \times 10^6 \text{ psi}$$

Thus

$$\frac{E_{t_1} I_1}{E_{t_2} I_2} = \frac{1.86 \times 10^6 (0.25)}{6.55 \times 10^6 (0.50)} = 0.142$$

From Figure 2-78, $P_{cr}/P_e = 0.57$ where

$$P_e = \frac{\pi^2 E_{t_2} I_2}{L^2}$$

Thus,

$$P_{cr} = P_e = \frac{0.57\,\pi^2\,(6.55 \times 10^6)(0.5)}{(40)^2}$$

or $P_{cr} = 11,600$ psi. The original guess is thus correct. If it were not, other values would have to be tried until the correct value was found.
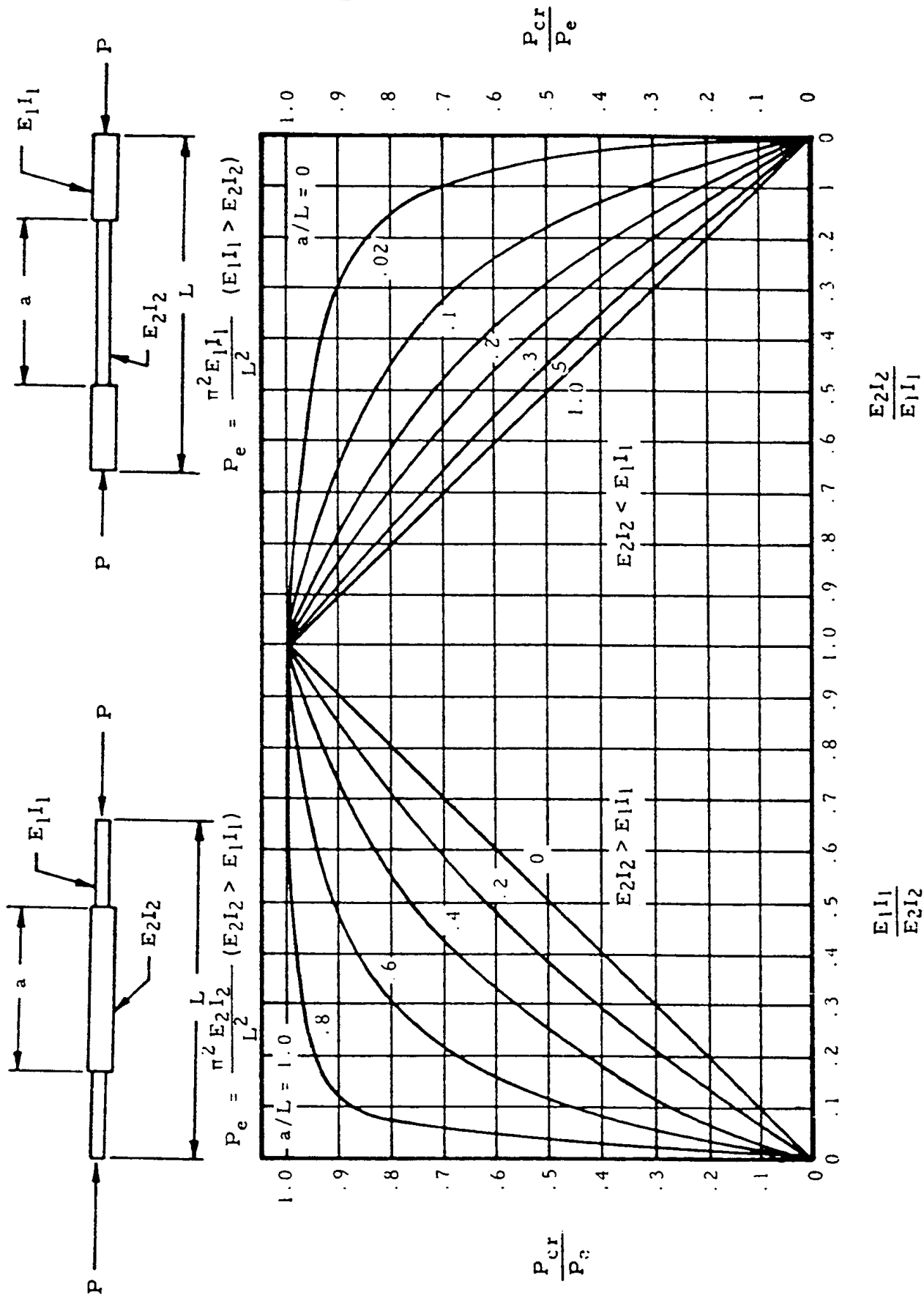
Figure 2-78. Critical Loads for Symmetrical Stepped Columns
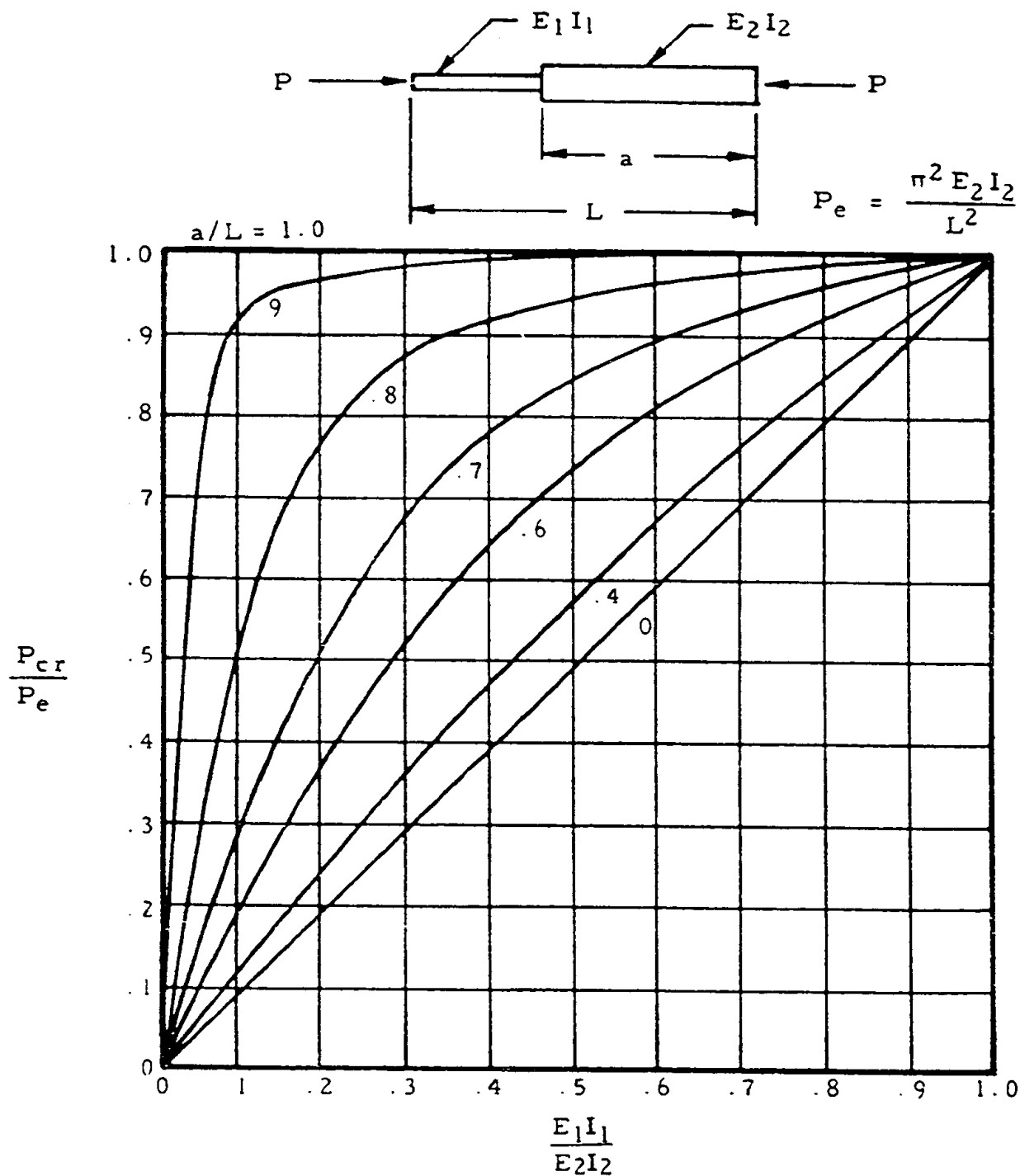
Figure 2-79. Critical Loads for Unsymmetrical Stepped Columns
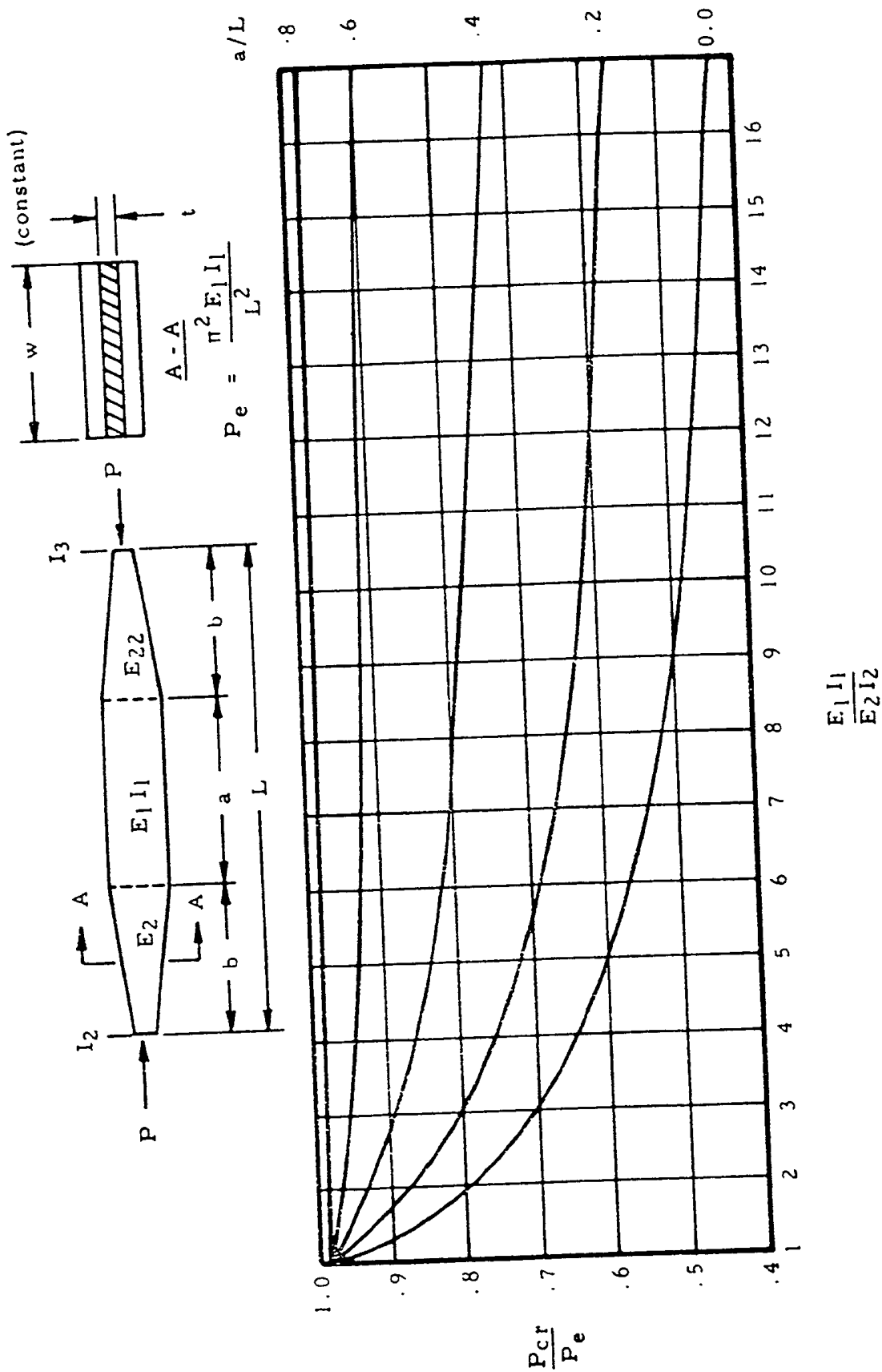
Figure 2-80. Critical Loads for Columns Tapering in Thickness
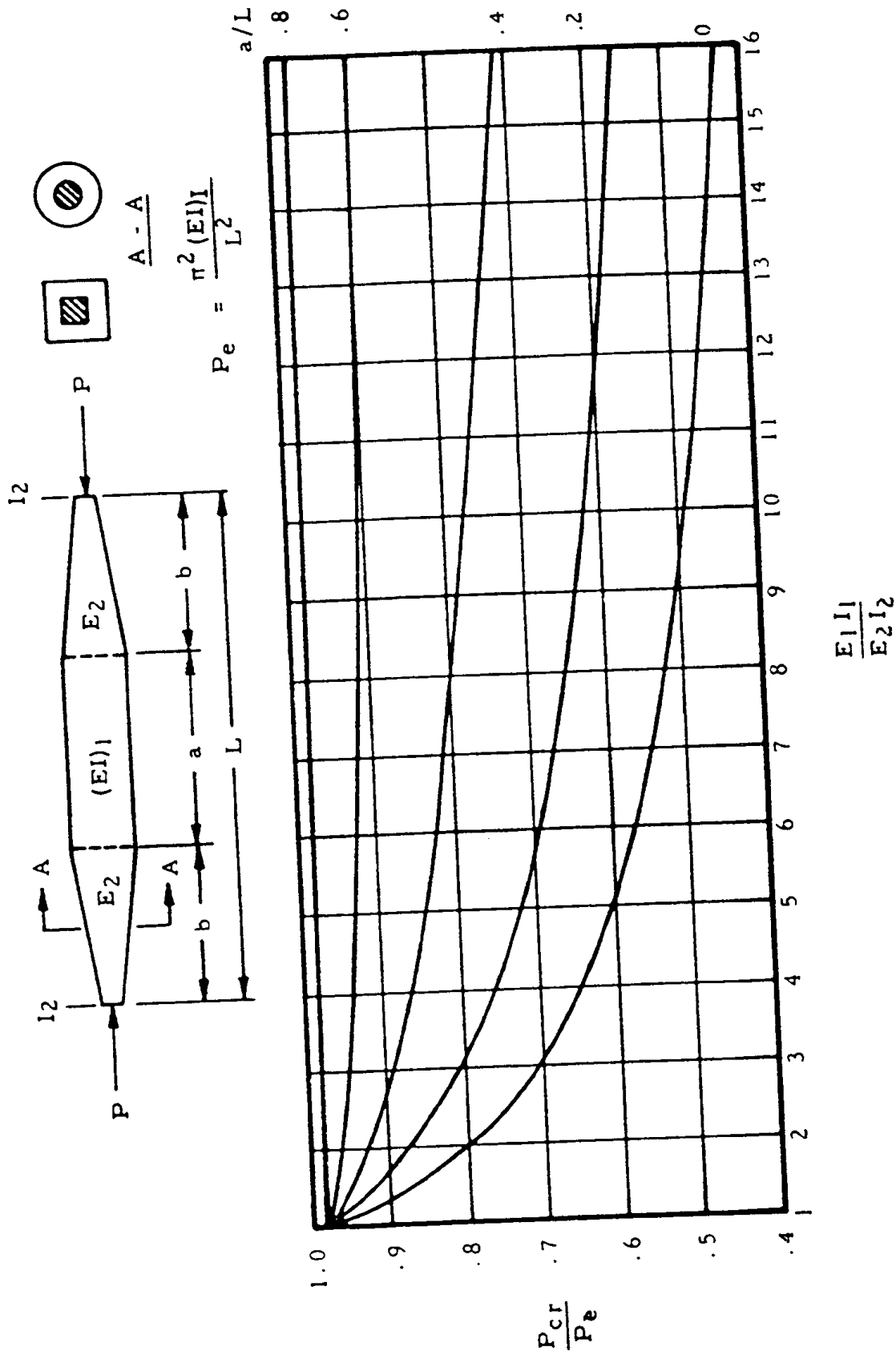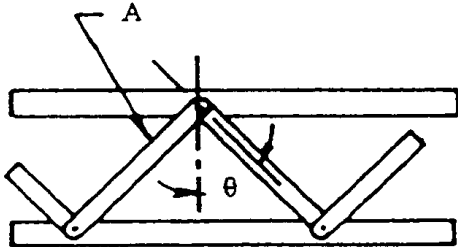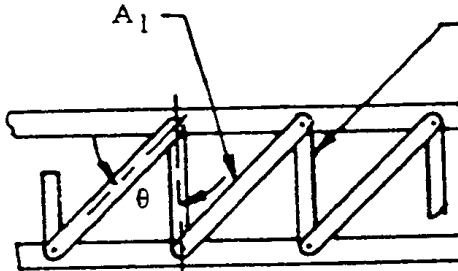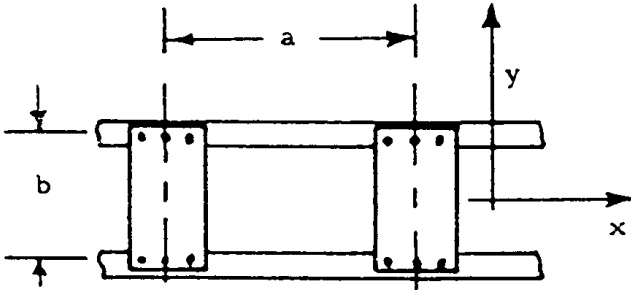
Figure 2-81. Critical Loads for Prisms Tapering in Thickness and Cylinders with Conical Taper

2.4.3   Latticed Columns

Although it is customary to assume that a latticed column acts as
a single unit and develops the full strength of the section, a column is actually
less stiff if the buckling occurs in a plane normal to that of the lacing. This
fact is unimportant if a column is designed so that buckling occurs in a plane
normal to that of the lacing, but it must be taken into account for columns
that are laced on all sides.

In order to take the effect of lacing into account, a reduced modulus
of elasticity, KE, may be used in place of E in the equations for simple columns
Equations giving K as a function of column parameters are given in Figure 2-82
for various lattice configurations.

In designing latticed columns, care must also be taken to insure
that buckling of the individual members does not occur between points of attach-
ment. In general, the slenderness ratio of a longitudinal member between
points of attachment should be less than 40 or two-thirds of the slenderness
ratio of the column as a whole, whichever is lower.

Column Configuration	K
	$$K = \cfrac{1}{1 + \cfrac{4.93\,I}{A\,L^2 \cos^2\theta \sin\theta}} \qquad \text{①}$$
	$$K = \cfrac{1}{1 + \cfrac{4.93\,I}{A_1\,L^2 \cos^2\theta \sin\theta} + \cfrac{4.93\,I}{A_2\,L^2 \tan\theta}} \qquad \text{①}$$
	$$K = \cfrac{1}{1 + \cfrac{\pi^2 I}{L^2}\left(\cfrac{ab}{12\,I_2} + \cfrac{a^2}{24\,I_1}\right)} \qquad \text{①②}$$

① I = moment of inertia of entire column with respect to axis of bending

   L = length of entire column

② I_1 = moment of inertia of a channel section about a central axis parallel to the y axis

   I_2 = moment of inertia of a vertical batten plate section about a central axis parallel to the x axis

Figure 2-82.   Values of K for Various Lattice Configurations

3. BAR ANALYSIS

3.1 Introduction to Bar Analysis

Bars are thin structural members. This chapter gives procedures for determining the resistance to yielding of bars under static loads as well as their resistance to fatigue failure under varying loads. Tensile loading of bars is considered in detail, and information applicable to the compressive, bending, and torsional loading of bars appearing in other chapters is referenced in this chapter.

3.2 Nomenclature for Bar Analysis

A = cross-sectional area, in.^{2}
f_t = tensile stress, psi
f_{ta} = alternating stress, psi
f_{tm} = mean stress, psi
F_{ty} = yield stress in tension, psi
f_{se} = endurance limit in torsion
K = stress concentration factor
K_e = effective stress concentration factor
K_t = theoretical stress concentration factor
n = factor of safety
P = load, lbs
P_a = alternating load, lbs
P_m = mean load, lbs
q = notch sensitivity factor

3.3 Static Tensile Loading of Bars

The basic formula for stress in a member of cross-sectional area A under a static tensile load P is

$$f_t = \frac{P}{A} \tag{3-1}$$

This equation, however, is somewhat limited. In order for it to be valid, the member must be centrally loaded, the section at which σ occurs must be well removed from the point of application of the load, and no stress raisers may be present near the section where σ occurs.

Bars are normally designed so that tensile loads are applied centrally. If this is not the case, they may be considered to be beams under combined tensile and bending loads and treated with the material in Chapter 1. Although the end portions of a bar are as critical as the central ones, they are not considered here since information about them more properly belongs in a treatment of connections, for example, the chapter on lug analysis in this work. According to St. Venant's principle, stress

3 - 1

patterns become regular at a distance from the point of application of a load. In this case, the stresses become uniform at a distance from the point of application of an axially applied tensile load. Stress raisers will be considered here and when they are present, Equation (3-1) no longer applies.

If a stress raiser is present in a bar loaded in tension,

$$f_t = K \left(\frac{P}{A} \right)$$

(3-2)

where K is a stress concentration factor. Equation (3-2) indicates that the stress at the discontinuity is K times the stress that would occur if no stress raiser were present. The stress concentration factor may be determined theoretically by the theory of elasticity, the photoelasticity method, etc., where it is designated as K_t. These values are not normally accurate, however, and are not in general used directly as will be discussed later. The following figures give values of the theoretical stress concentration factor for various cross-section and discontinuity shapes.

The theoretical stress concentration factor may be quite high as can be seen in the following pages; however, this value is usually in agreement with experiment. To account for this discrepancy, an effective stress concentration factor K_e is defined to be the one that holds in the actual situation encountered. The notch sensitivity factor, q, is used to relate the two and is defined by Equation (3-3):

$$q = \frac{K_e - 1}{K_t - 1}$$

(3-3)

The value of the notch sensitivity factor is a function of the material and the size and shape of the discontinuity.

For ductile materials that are statically loaded to near their limit, the yielding in the vicinity of the discontinuity may nearly eliminate stress concentration there, so that K_e is approximately equal to one and q is quite low.

Brittle homogeneous materials are not as capable of localized yielding, so that K_e is approximately equal to K_t and consequently q is approximately equal to one according to Equation (3-3). Cast iron of less than 45, with its flakes of graphite, however, is effectively saturated with stress raisers, so that the addition of another discontinuity seems to have little effect on its fatigue strength. Thus q is approximately equal to zero for cast iron.

The design equation for a bar under a static tensile load P that is not to be subjected to large-scale yielding is thus

$$F_{ty} = K_e \left(\frac{P}{A} \right)$$

(3-4)

3-2

For a ductile or cast iron bar, K_e may be assumed to be equal to unity and A is the reduced area at the section where the discontinuity occurs. For a bar of brittle homogeneous material, K_e may be assumed to be equal to K_t and A is either the cross-sectional area of the bar without the discontinuity or the reduced area at the cross section where the discontinuity occurs. Which of these areas is to be used is shown in a formula under each chart of K_t in Figures 3-1 through 3-12.
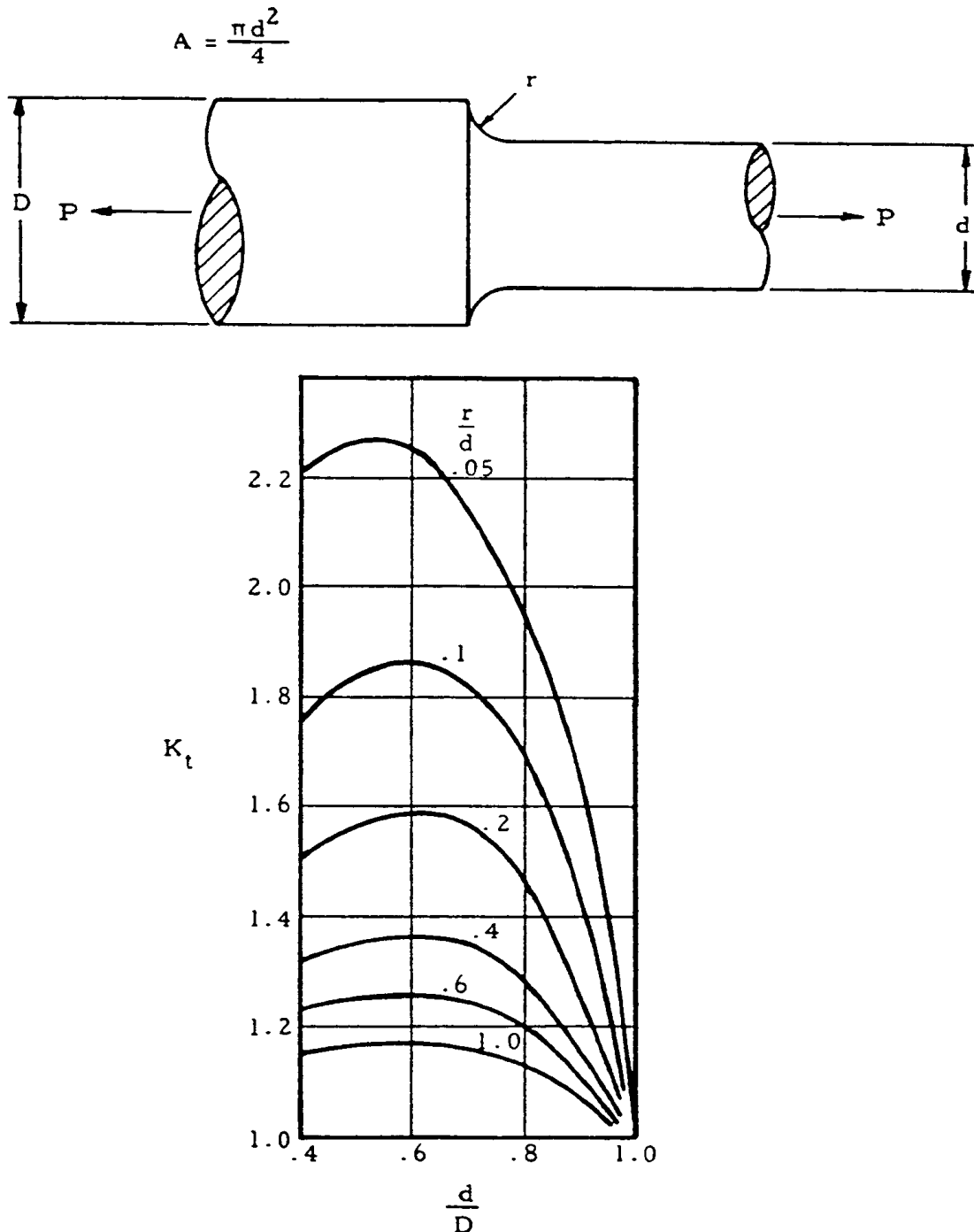
$$A = \frac{\pi d^2}{4}$$

Figure 3-1. Stepped Round Bar with Radial Fillet

$$A = \frac{\pi (D-2h)^2}{4}$$
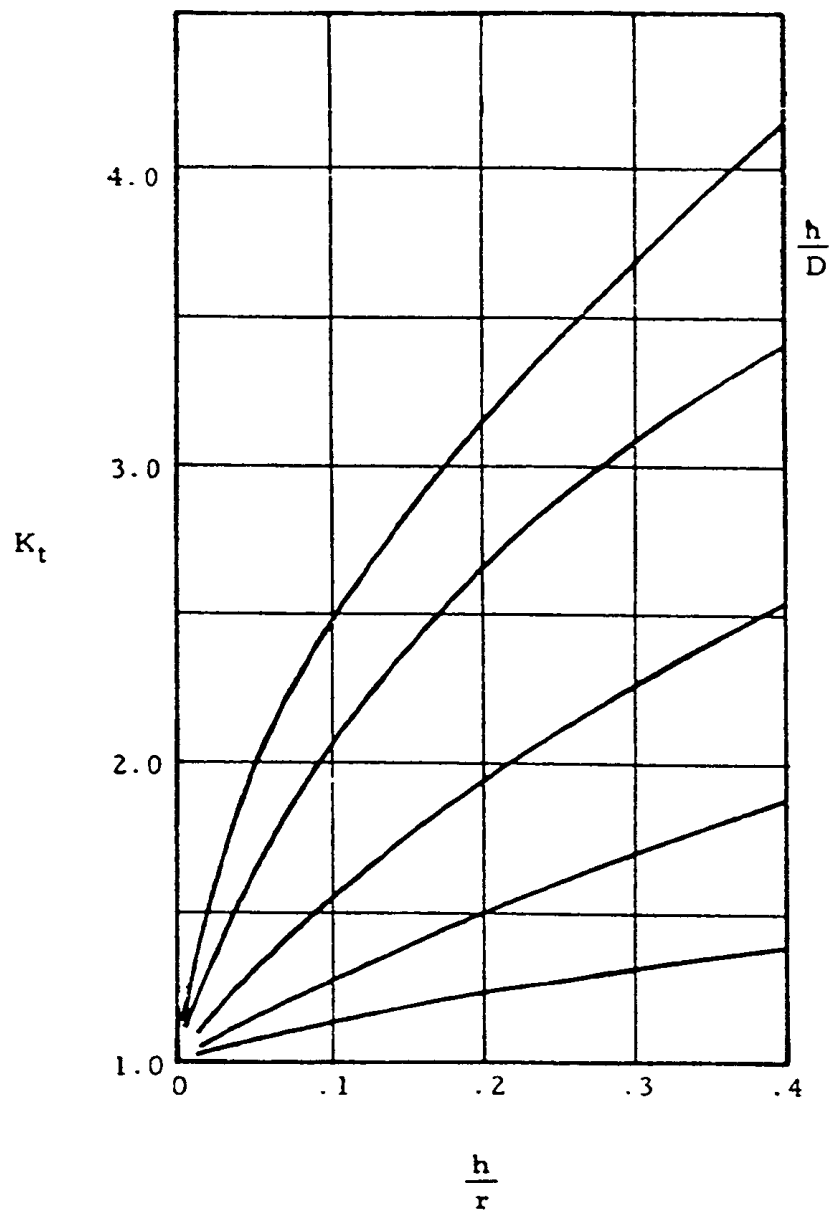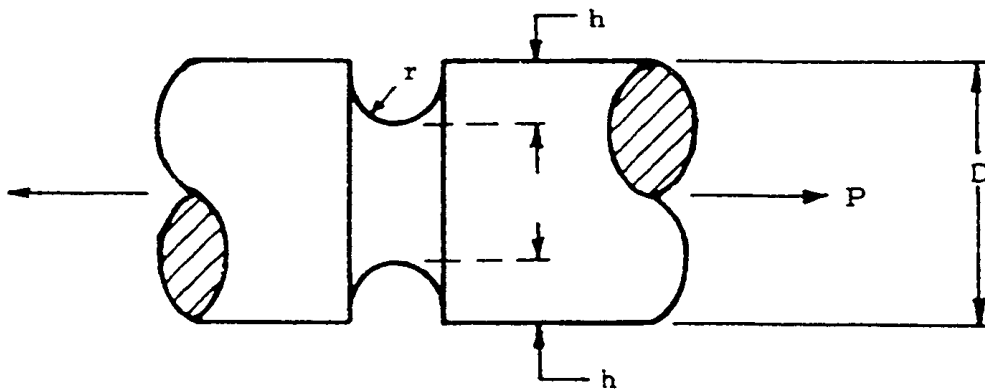
Figure 3-2. Round Bar with U Notch
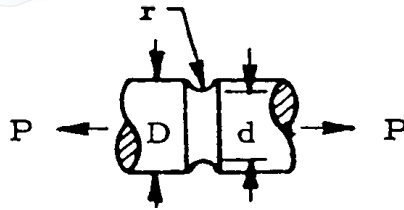
$$A = \frac{\pi d^2}{4}$$
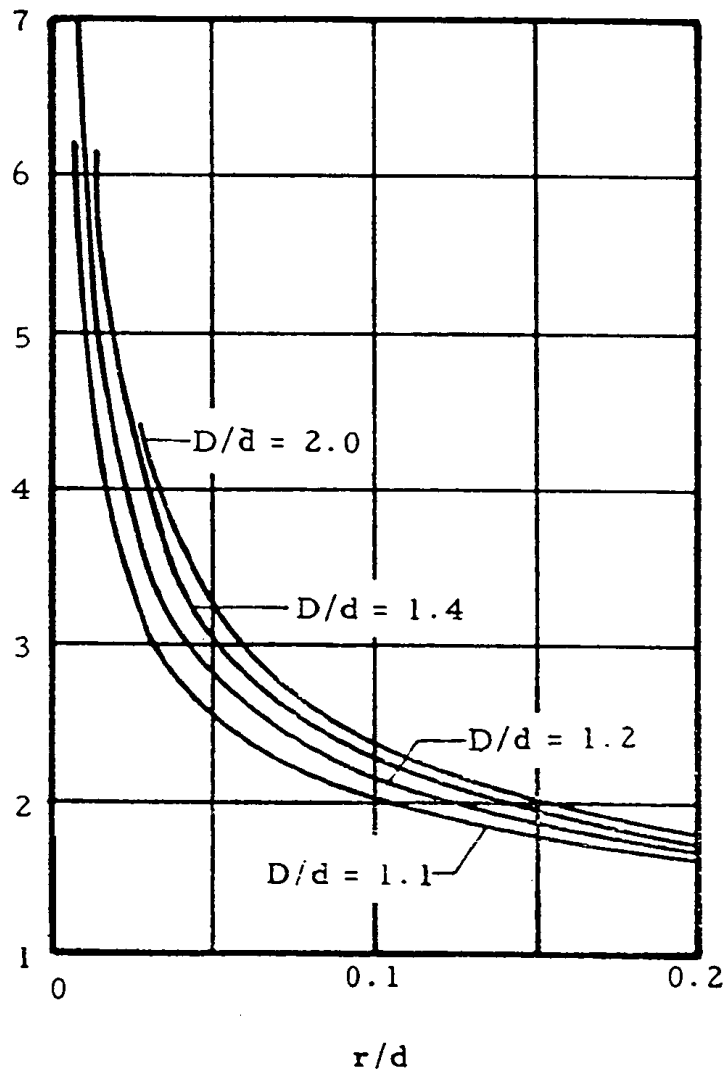
D/d = 2.0

D/d = 1.4

D/d = 1.2

D/d = 1.1

r/d

Note: The values of K_t may be used as a close approximation for any
type of V notch with a small fillet or radius r at the root of the notch

Figure 3-3. Round Bar with Hyperbolic Notch

3 - 5
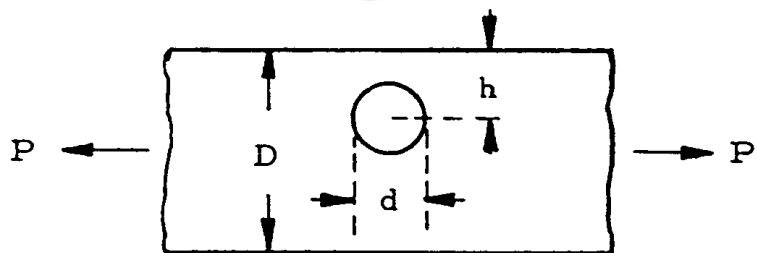
$$A = (D-d)t$$
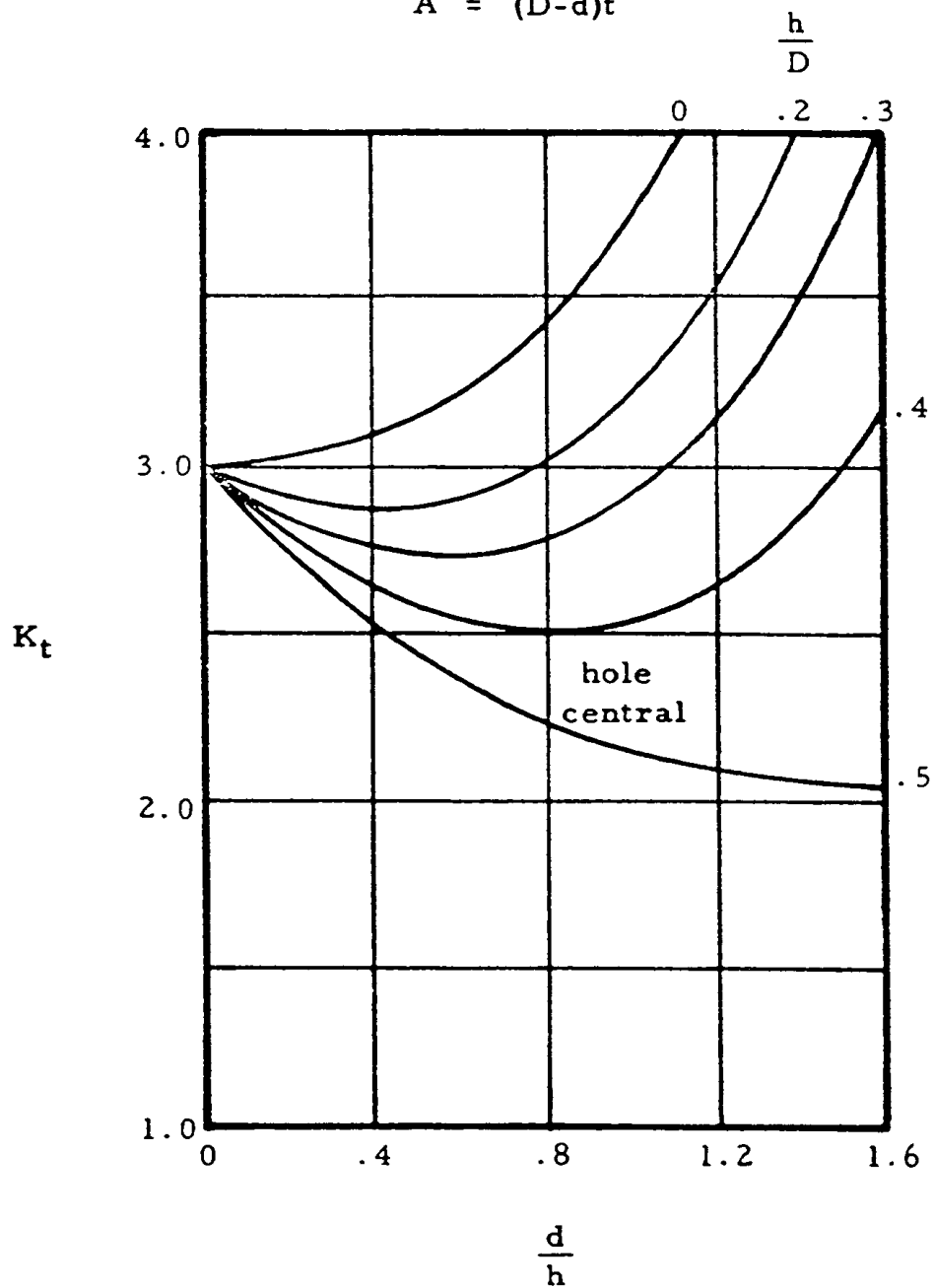
Figure 3.4 Rectangular Bar with Offset Through Hole
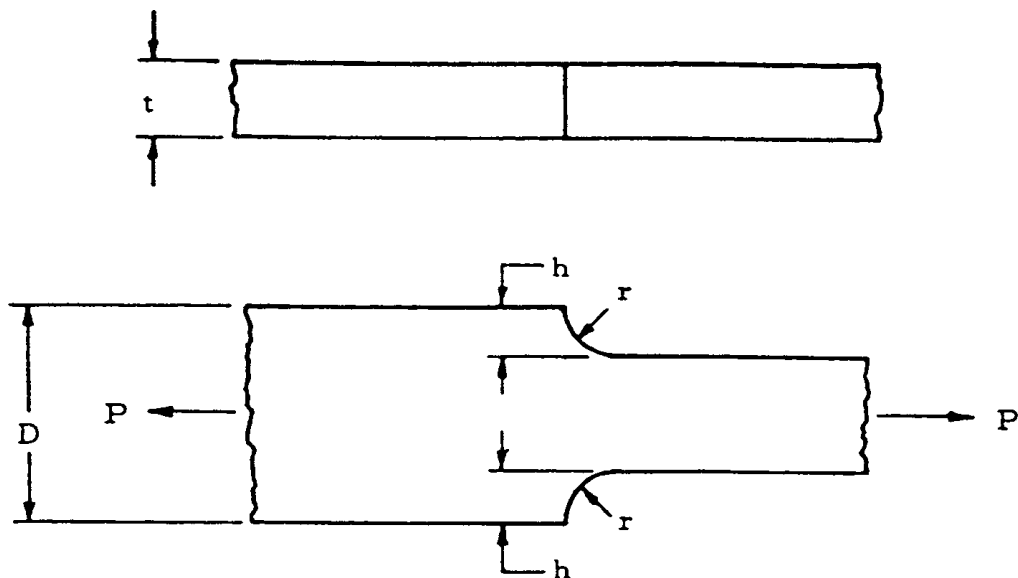
$$A = (D-2h)t$$
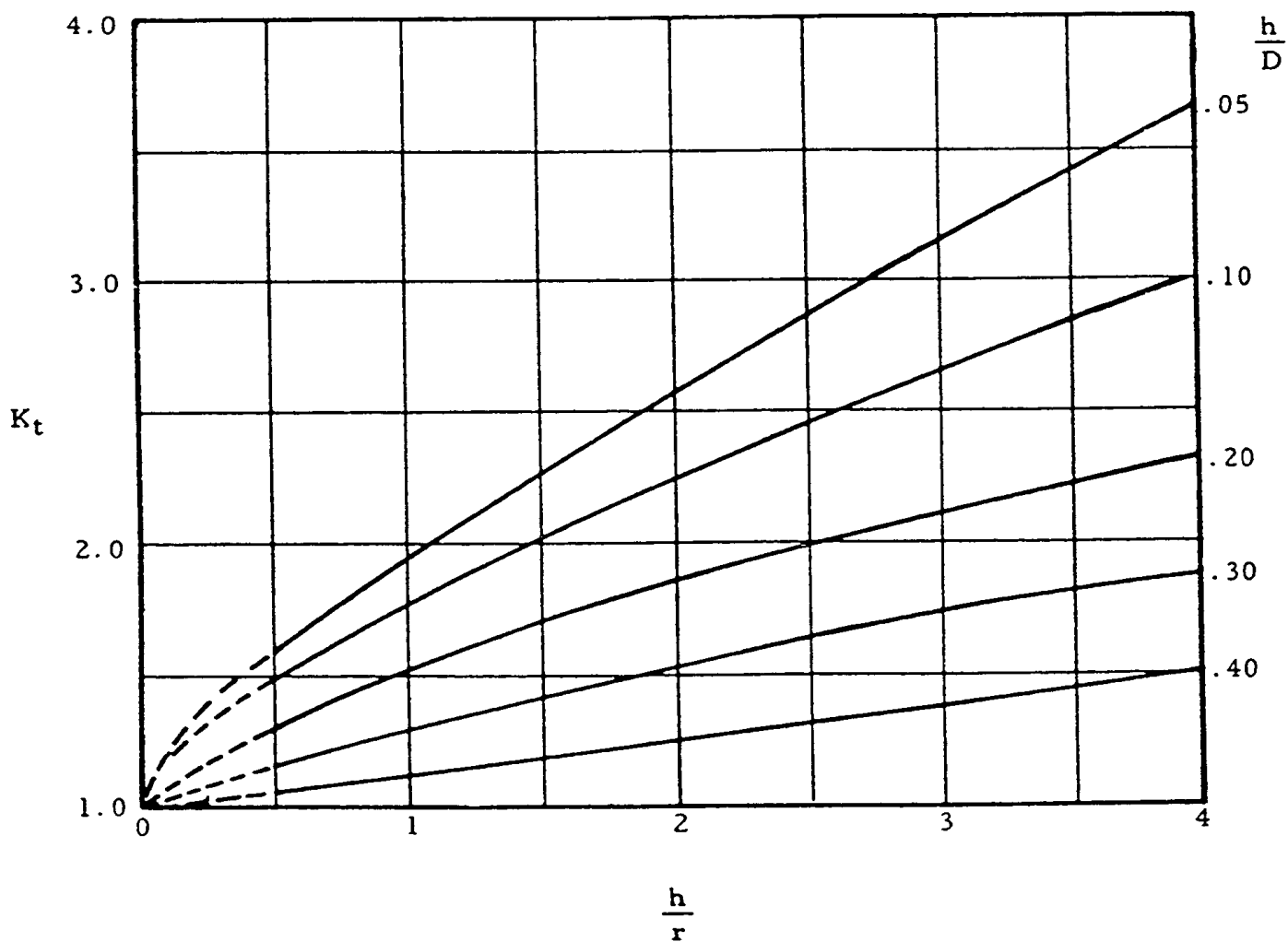
Figure 3-5. Stepped Rectangular Bar with Radial Fillet
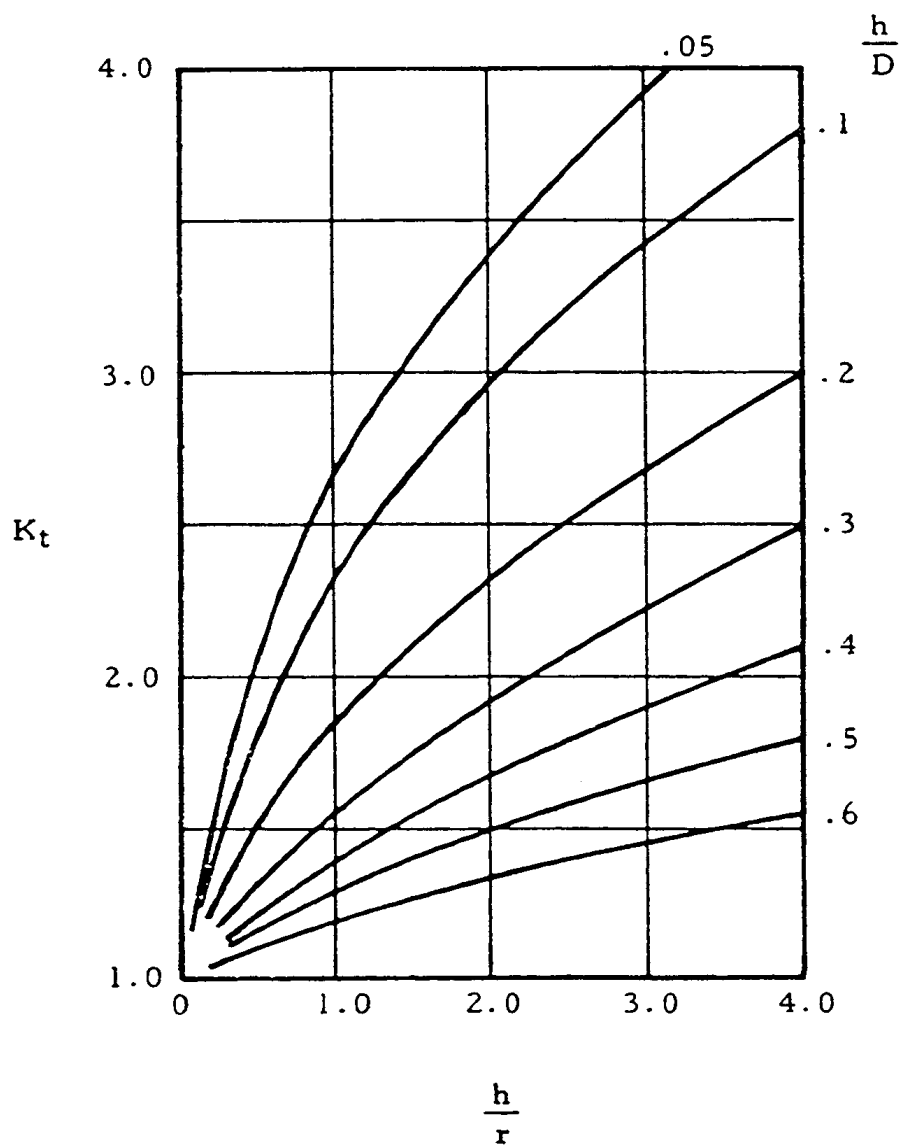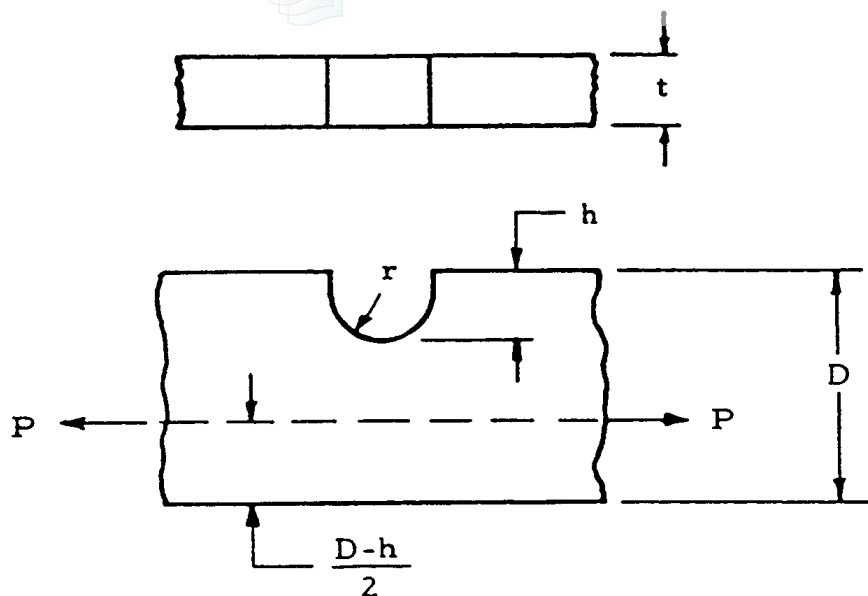
Figure 3-6.   Rectangular Bar·with U Notch (One Side

3 - 8
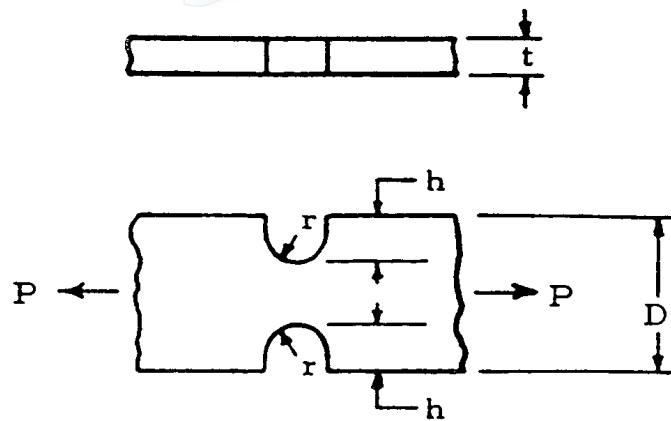
$$A = (D-2h)t$$
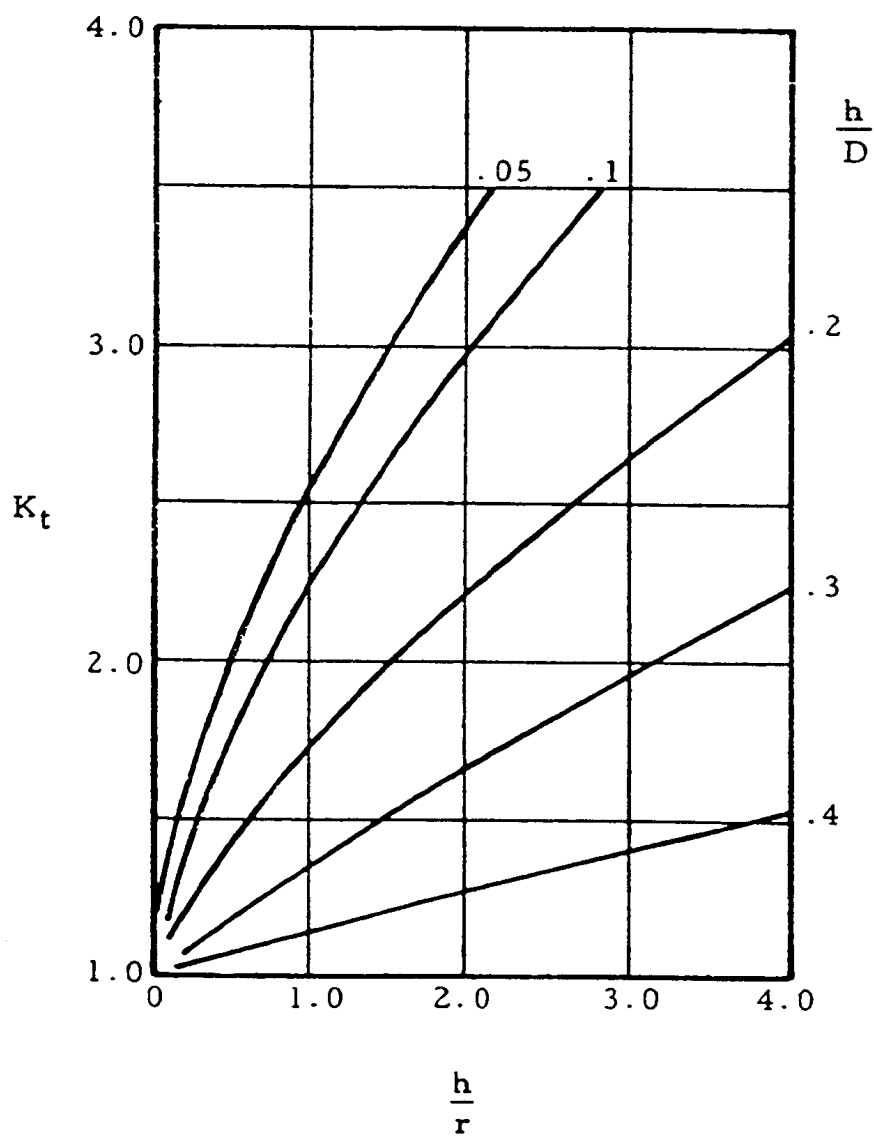
Figure 3-7.   Rectangular Bar with U Notch (Both Sid
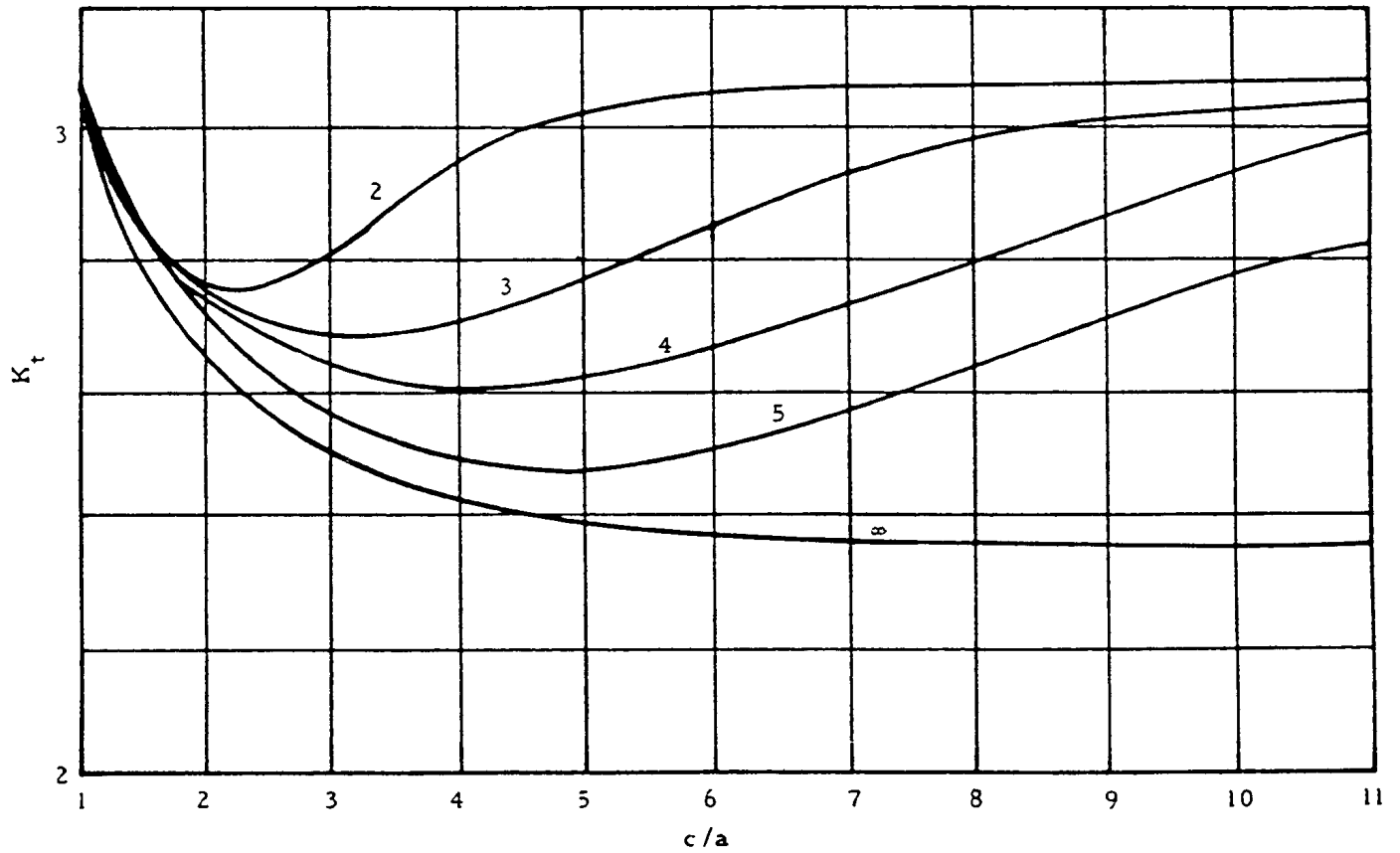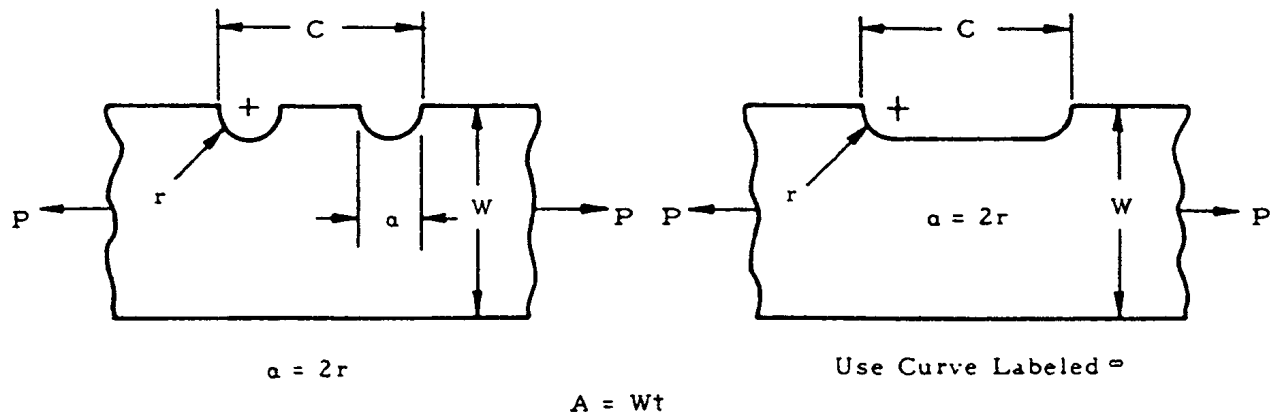
Figure 3-8.   Rectangular Bar with Multiple Semicircular Notches on One Side
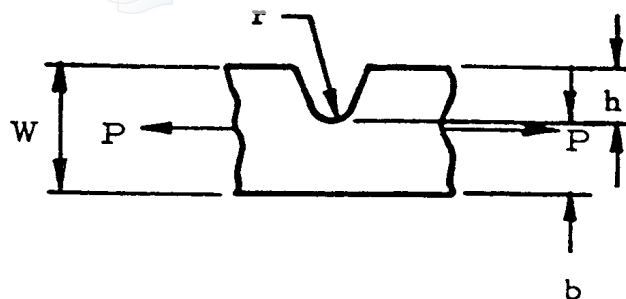
$$A = bt$$
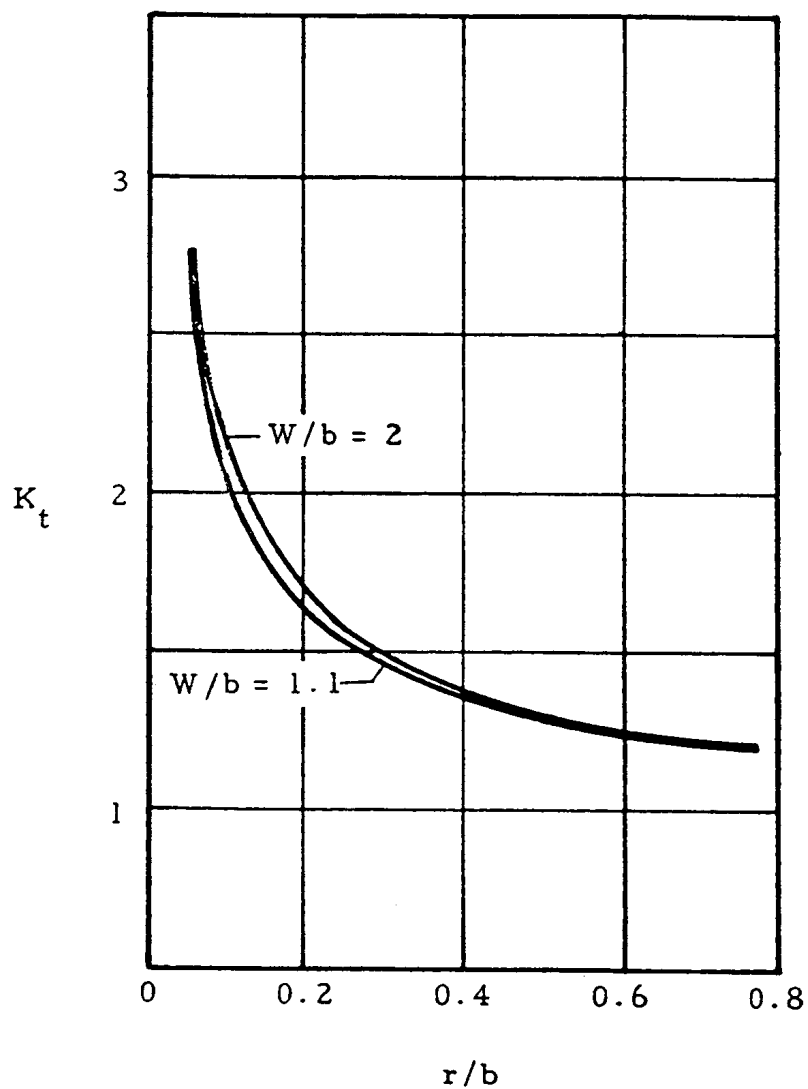
Note: The values of K_t may be used as a close approximation for any type of V notch with a small fillet or radius r at the root of the notch.

Figure 3-9. Rectangular Bar with Hyperbolic Notch (One Side)
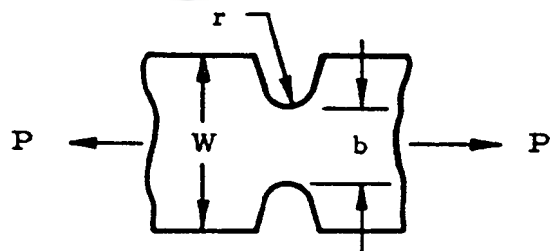
Notch Depth > 4r

$$A = bt$$
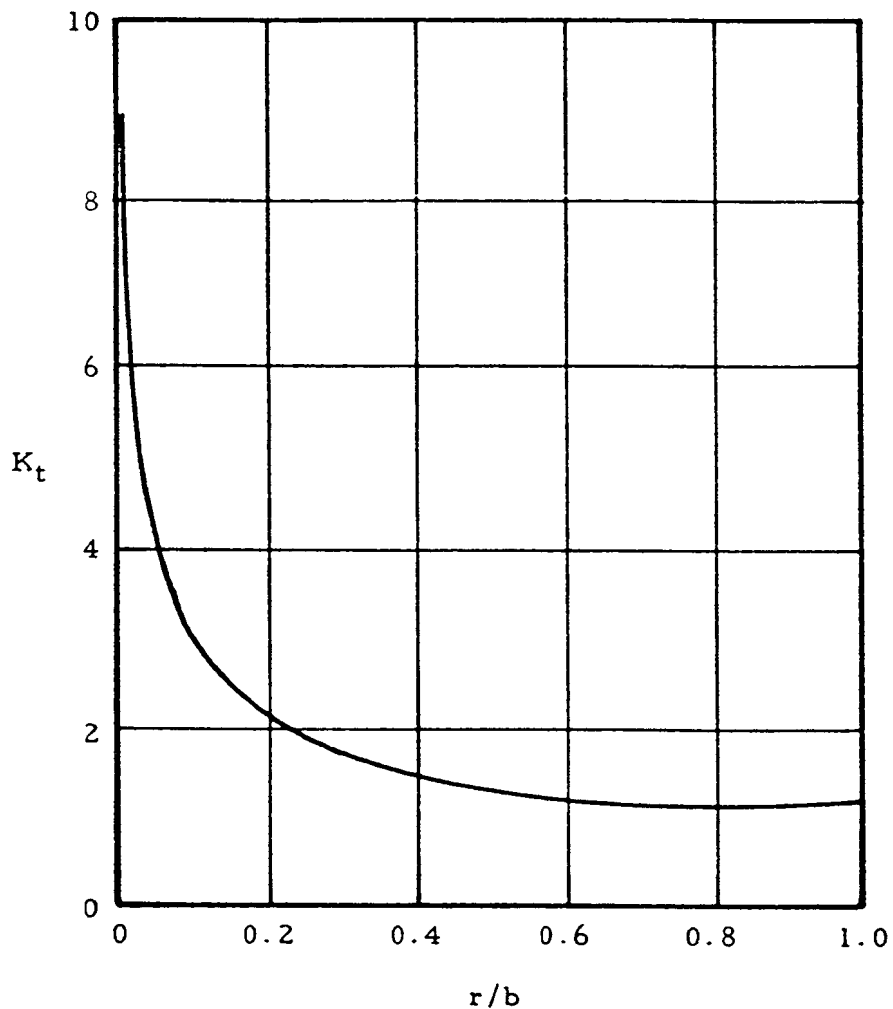
Note: The values of K_t may be used as a close approximation for any
type of V notch with a small fillet or radius r at the root of the notch.

Figure 3-10.   Rectangular Bar with Hyperbolic Notch (Each Side)

$$A = (D-h)t$$
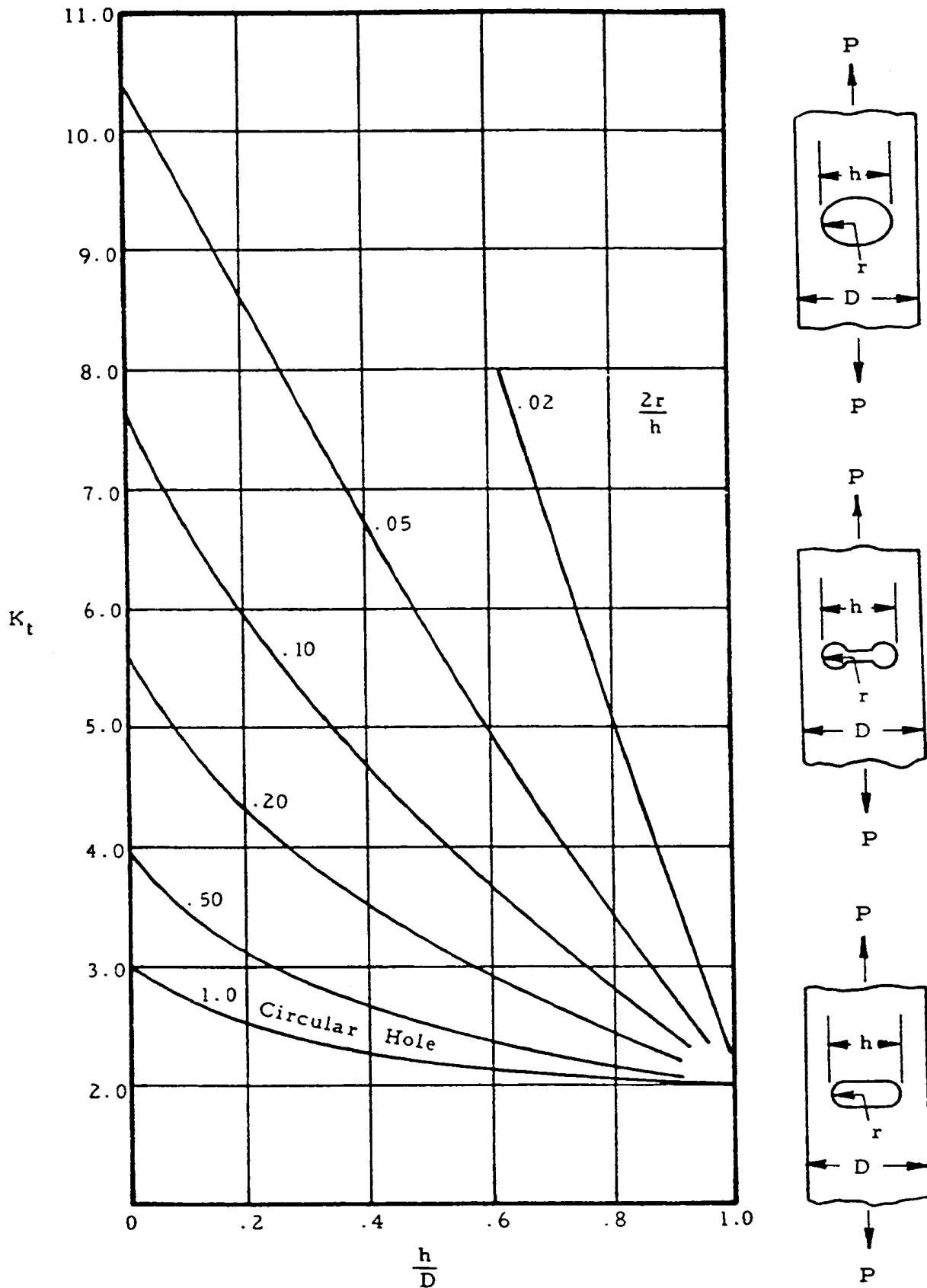
Figure 3-11.   Rectangular Plate with Various Thru Sections
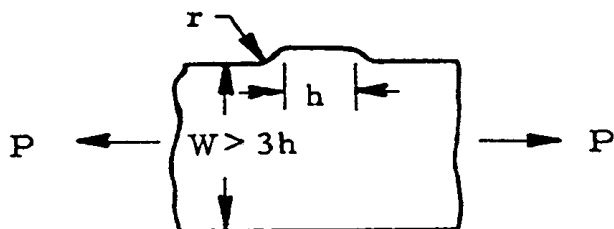
$$A = Wt$$
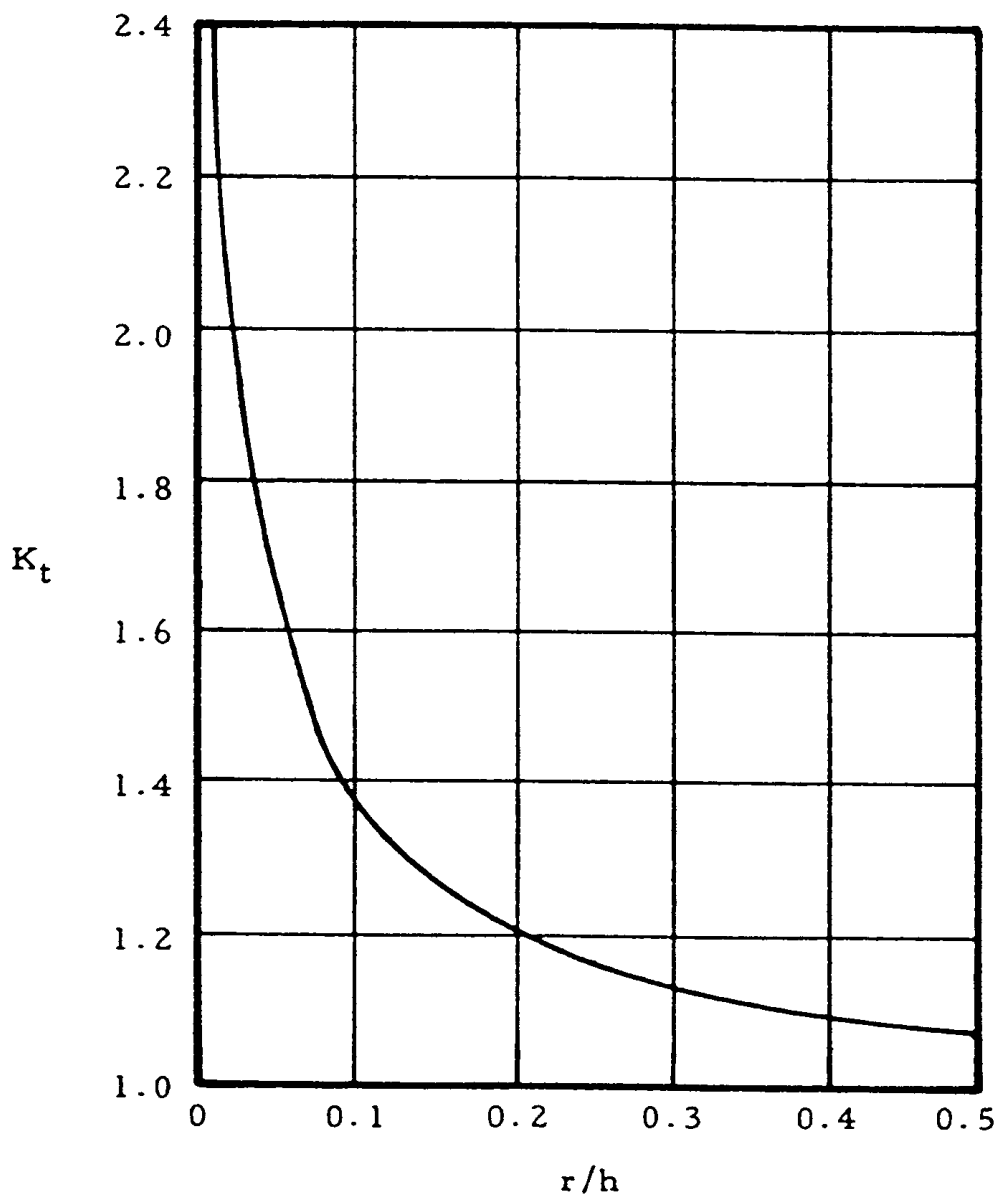
Figure 3-12.   Rectangular Bar with Protrusion on One Side

The previously described procedure yields conservative results for brittle homogeneous materials and the opposite for cast iron and ductile materials. If a low margin of safety is desired for ductile materials and cast iron, a value of q equal to 0.2 is usually sufficient to account for the effects of stress raisers.

The previously discussed material on bars in static tensile loading is summarized in Table 3-1.

<div align="center">

TABLE 3-1

Design of Bars Under Static Tensile Load

Design Equation $F_{ty} = K_e \left(\dfrac{P}{A} \right)$

</div>

Material Type	K_e	A
ductile	1.0	reduced area of cross section at the discontinuity
homogeneous brittle	K_t as found in Figures 3-1 thru 3-12	either reduced or total area of cross section as indicated by formulas in Figures 3-1 thru 3-12.
cast iron	1.0	reduced area of cross section at the discontinuity

3.4   Sample Problem—Bar Under Static Tensile Loads

Given: A circular bar is to be made of a homogeneous brittle material for which F_{ty} = 45,000 psi. It is to support a static tensile load of 50,000 lbs with a factor of safety of 1.5. It is to have a U-notch of the section shown in Figure 3-13.
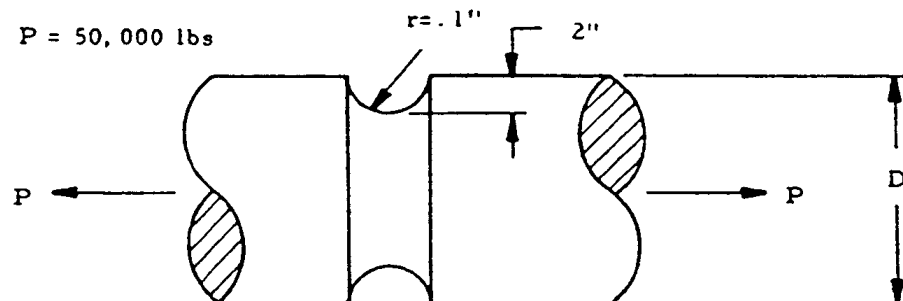
Figure 3-13.   Bar with U-Notch under Static Tensile Load

Find: The diameter

Solution: Inserting the safety factor into Equation (3-4) gives

$$\frac{F_{ty}}{1.5} = \frac{45000}{1.5} = K_e \frac{P}{A} = 30,000$$

From Section 3.3, $K_e = K_t$. Thus,

$$30,000 = K_t \frac{P}{A}.$$

Since $P = 50,000$, $.6 = \frac{K_t}{A}$.

From Figure 3-2, $h = .2$, $r = .1$ thus, $\frac{h}{r} = 2$.
and furthermore,

$$A = \frac{\pi (D-.4)^2}{4}$$

Thus,

$$0.6 = \frac{4 K_t}{\pi (D-.4)^2}$$

Assume $D = 1.05$. Thus,

$$\frac{h}{D} = \frac{.2}{1.05} = .190$$

From Figure 3-2, $K_t = 2.0$. Substituting these values gives

$$\frac{4K_t}{\pi (D-.4)^2} = \frac{4 (2.)}{\pi (1.05 - .4)^2} = 0.6$$

Thus, D is equal to 1.05 in. If the assumed value of D does not satisfy the equation, other values must be tried until a value of D satisfying this equation is found.

3.5   Cyclic Tensile Loading of Bars

The case to be considered now is that for which an alternating axial load is applied to the bar. A diagram of this loading is shown in Figure 3-14. The mean load is designated as P_m, and the alternating component is designated as P_a.

3 - 16
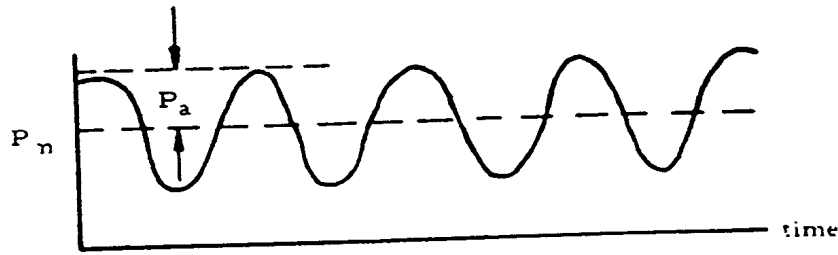
Figure 3-14. Cyclic Loading of Bar

For a brittle homogeneous material, a stress concentration factor must be applied to both the alternating and the mean stress in equations for failure under alternating loads since a static load is affected by stress concentration. Thus, the Soderberg relation becomes

$$\frac{1}{n} = \frac{K_e\, f_{tm}}{S_y} + \frac{K_e\, f_{ta}}{S_n} \qquad (3-5)$$

where S_m and S_a are equal to P_m/A and P_a/A, respectively, and n is the factor of safety. In this case, K_e may be taken to be equal to K_t, so that the basic design equation becomes

$$\frac{1}{n} = \frac{K_t\, P_m}{A F_{ty}} + \frac{K_t\, P_a}{A f_{se}} \qquad (3-6)$$

where the A is either the reduced area at the discontinuity or the full area of the bar as given in Figures 3-1 through 3-12.

For a ductile material, a stress concentration factor need only be applied to the alternating stress in equations for failure since ductile materials under static loading have an effective stress concentration factor of one. In view of this, the Soderberg relation becomes

$$\frac{1}{n} = \frac{f_{tm}}{F_{ty}} + \frac{K_e\, f_{ta}}{f_{se}} \qquad (3-7).$$

where f_{tm} and f_{ta} are equal to P_m/A_m and P_a/A_a, respectively, and n is the factor of safety. Here, A_m is the reduced area of the bar, and A_a may be either the reduced or the full area of the bar as given in Figures 3-1 through 3-12. Thus, the basic design equation for ductile rods under alternating tensile loads is

$$\frac{1}{n} = \frac{P_m}{A_m\, F_{ty}} + \frac{K_e\, P_a}{A_a\, f_{ie}} \qquad (3-8)$$

3 - 17

where K_e is equal to $q (K_t - 1) + 1$. Here, K_t is the theoretical stress concentration factor as obtained from Figures 3-1 through 3-12, and q may be obtained from Figure 3-15 for steel. For aluminum, magnesium and titanium alloys, fatigue data is scattered to the extent that a value of one is suggested for q.
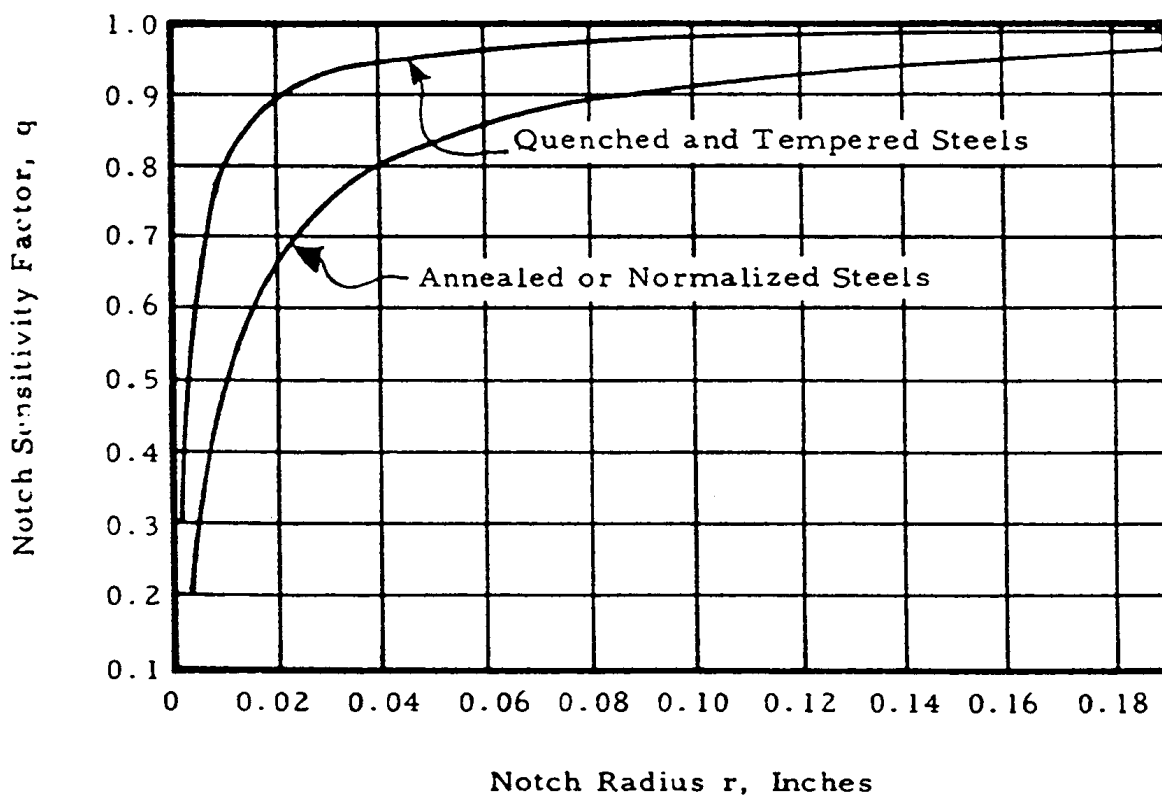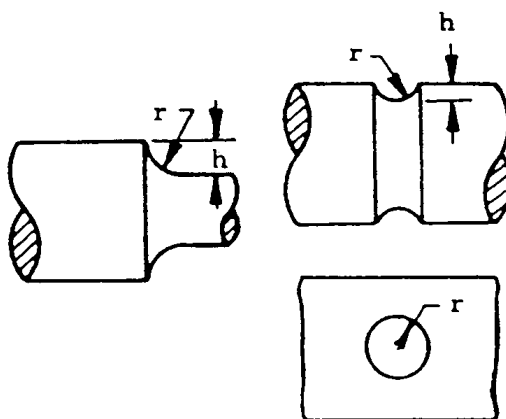
Figure 3-15.   Average Notch Sensitivity Curves.   Applicable Particularly to Normal Stresses; Used Also for Shear Stresses

Since cast iron is insensitive to stress raisers, stress concentration factors need not be applied in any formula governing alternating stresses. Thus, the Soderberg equation may be used in its basic form

$$\frac{1}{n} = \frac{f_{t_s}}{F_{ty}} + \frac{f_{t_a}}{f_{se}} \qquad (3-9)$$

where f_{t_s} and f_{t_a} are equal to P_s/A and P_a/A, respectively, and A is the reduced area of the rod. Thus, the design equation for cast iron bars under an alternating tensile load becomes

$$\frac{1}{n} = \frac{P_s}{A\,F_{ty}} + \frac{P_a}{A\,f_{se}} \qquad (3-10)$$

The previous discussion of bars under alternating tensile loads is summarized in Table 3-2.

TABLE 3-2

Design of Bars Under Cyclic Tensile Load

Material Type	Design Equation	Explanation of Terms
ductile	$\dfrac{1}{n} = \dfrac{P_s}{A_s\,F_{ty}} + \dfrac{K_e\,P_a}{A_a\,f_{sa}}$	A_s = reduced area of section. $K_e = q\,(K_t - 1) + 1$ where q is obtained from Figure 3-15 for steel or set equal to 1 for aluminum, magnesium, and titanium alloys, and where K_t is obtained from Figures 3-1 through 3-12. A_a = reduced or full area of section as given in Figures 3-1 through 3-12.
homogeneous brittle	$\dfrac{1}{n} = \dfrac{K_t\,P_s}{A\,F_{ty}} + \dfrac{K_t\,P_a}{A\,f_{so}}$	K_t = theoretical stress concentration factor as obtained from Figures 3-1 through 3-12. A = reduced or full area of section as given by Figures 3-1 through 3-12.
cast iron	$\dfrac{1}{n} = \dfrac{P_s}{A\,F_{ty}} + \dfrac{P_a}{A\,f_{so}}$	A = reduced area of section.

Sample Problem—Bar Under Cyclic Tensile Load

Given: A stepped circular bar with a fillet of .02 in. radius is to
support a cyclic tensile load that is given as P = 20,000 lbs +
10,000 sin wt. lbs. This bar, as shown in Figure 3-16, is made
of an annealed steel for which F_{ty} = 45,000 psi and f_{se} = 35,000 psi.
Use a factor of safety of 1.5.
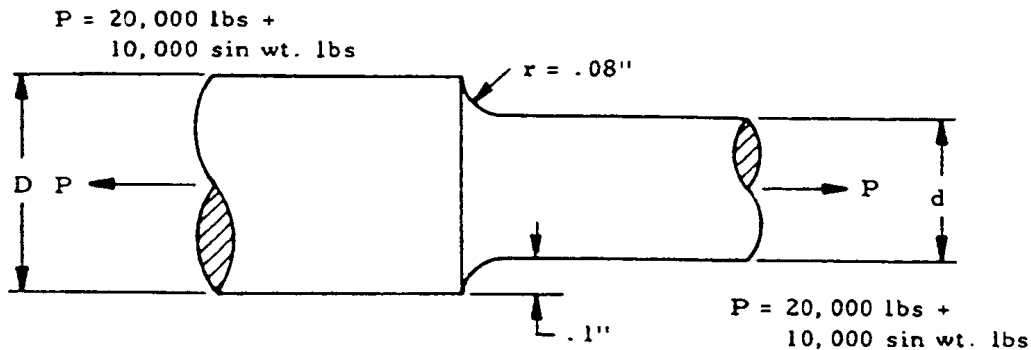
Figure 3-16. Bar Under Cyclic Tensile Load

Find: The diameter d.

Solution: From Section 3.5, the basic design equation for a ductile
material is

$$\frac{1}{n} = \frac{P_a}{A_x F_{ty}} + \frac{K_e P_a}{A_a f_{se}}$$

(3-11)

P_a, P_a, and n are equal to 20,000 lbs, 10,000 lbs. and 1.5,
respectively. By checking the explanation of terms in Section 3.5
and checking the figure referred to there, we find that both A_a
and A_a are the reduced area $\pi d^2/4$. This explanation of terms
also tells us that K_e = q (K_t - 1) + 1, where q is given by Figure
3-15. Consulting this figure, q = .89 and thus K_e = .89 (K_t - 1)+1.

The above values may now be substituted into the basic equation
to obtain

$$\frac{1}{1.5} = \frac{20000}{\frac{\pi d^2}{4}(45000)} + \frac{[.89 (K_t - 1) + 1] 10000}{\frac{\pi d^2}{4}(35000)}$$

Simplifying this equation gives

$$0.66 = \frac{.605 + .323 K_t}{d^2}$$

3 - 20

Try d = 1.33. Since d/D and r/d are equal to .870 and .0601, respectively, K_t = 1.75 according to Figure 3-1. Substituting this in the above equation gives 0.6 = 0.6. Thus the guess for diameter is correct. If it were not, other diameters would have to be chosen to see if one satisfies the equation.

3.7   Compressive Loading of Bars

Bars that are subjected to compressive loads may be considered to be columns. The behavior of columns may be obtained by referring to Chapter 2.

3.8   Bending Loads on Bars

Bars that are subjected to bending loads may be considered to be beams and treated with the material on beams in bending appearing in Chapter 1.

3.9   Torsional Loading of Bars

Bars that sustain a torsional load may be studied by using the information on beams in torsion in Chapter 1 or that on shafts in torsion in Chapter 10.

3.10   Lacing Bars in Columns

The function of lacing bars in a column composed of channels or other structural shapes connected by them is to resist transverse shear due to bending. Although these lacing bars resist shear as a group, each individual bar is loaded in either tension or compression if its ends may be considered to be pinned. For example, the type of loading on each of the lacing bars in Figure 3-17 is indicated by a "T" on that bar if it is in tension or by a "C" if it is in compression.
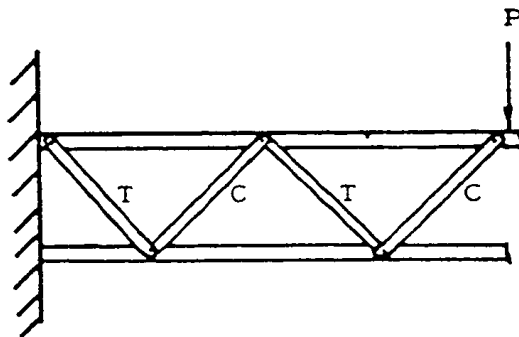
Figure 3-17.   Example of Lacing Bars

These lacing bars may be studied by the information given early in this chapter if they are in tension, or they may be considered as individual columns and studied by the information given in Chapter 2 if they are in compression. In addition to the strength of lacing bars as individual members, their effect on overall column behavior must be considered. This effect is treated in Chapter 2.

4.   TRUSSES

4.1   Introduction to Trusses

A truss is a structure composed entirely of two-force members; that is, the members that have two equal and opposite forces applied at two points. Thus, since the members do not exert any torque on each other at the joints, they are considered to be pin connected. However, welded and riveted joints may be considered to be pinned joints if the member is so long compared with its lateral dimensions that the connection can exert little restraint against rotation.

Section 4.3 discusses statically determinate trusses, and Section 4.4 treats statically indeterminate trusses.

4.2   Nomenclature for Trusses

A = cross-sectional area of truss member
E = modulus of elasticity
L = length of truss member
P = force in truss member
R = reaction force
u = force in truss member due to a unit load
X = force in redundant member of a truss
δ = deflection

4.3   Statically Determinate Trusses

4.3.1   Introduction to Statically Determinate Trusses

The forces carried by the members of a statically determinate truss may be determined by passing sections through certain members and applying the equations of statics. The method of joints (Section 4.3.2) consists of choosing these sections so that they completely surround a single joint. If the sections that are chosen do not surround a single joint, the procedure used is referred to as the method of sections (Section 4.3.4). This method is especially useful if it is desired to determine the load in only certain members. In many cases, a combination of the method of joints and the method of sections may be advantageous in the analysis of a given truss.

Before either of these methods may be applied, the reaction forces on the truss should be determined by the equations of statics.

Deflections in statically determinate trusses are treated in Section 4.3.6.

4.3.2   Application of the Method of Joints to Statically Determinate Trusses

If a truss as a whole is in equilibrium, each joint in the truss must likewise be in equilibrium. The method of joints consists of isolating a joint as a free body and applying the equilibrium equations to the resulting force system. Since the forces in the members at a truss joint intersect at a common point, only two equations of equilibrium may be written for each joint in a planar truss. Thus, only two unknowns may exist at a joint and the procedure is to start at a joint where only two unknowns exist and continue progressively throughout the truss joint by joint. This procedure is illustrated in Section 4.3.3.

4.3.3   Sample Problem - Application of the Method of Joints to Statically Determinate Trusses

Given: The truss shown in Figure 4-1.
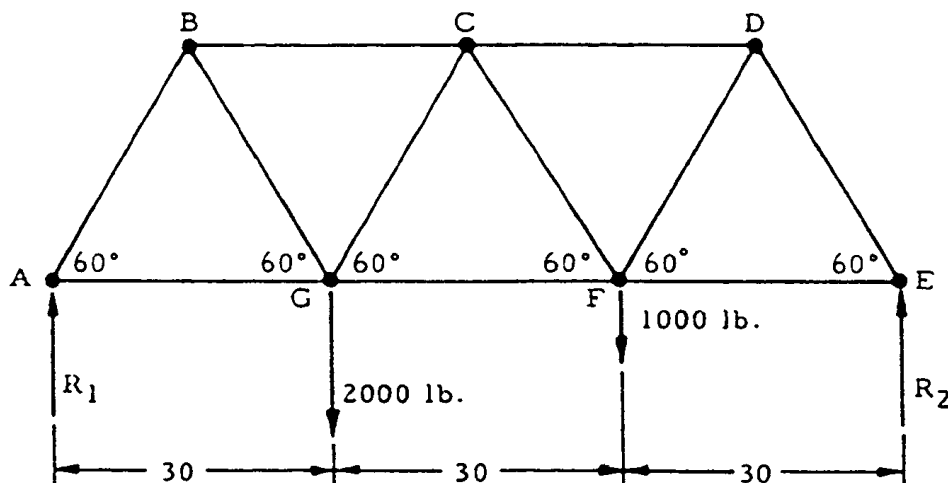
Figure 4-1.   Planar Truss

Find: The forces in all of the members.

Solution: Applying the equations of statics to the entire truss gives R_1 = 1667 lb. and R_2 = 1333 lb. Free body diagrams may be drawn for the joints in the order shown in Figure 4-2 and solved for the forces in the members. Summarizing, if tensile forces are taken as positive, the forces in the members are

$$P_{AB} = -1925 \text{ lb.} \qquad P_{CF} = -382 \text{ lb.}$$
$$P_{AG} = 962 \text{ lb.} \qquad P_{CG} = 382 \text{ lb.}$$
$$P_{BC} = -1925 \text{ lb.} \qquad P_{DE} = -1541 \text{ lb.}$$
$$P_{BG} = 1925 \text{ lb.} \qquad P_{DF} = 1541 \text{ lb.}$$
$$P_{CD} = -1541 \text{ lb.} \qquad P_{EF} = 770 \text{ lb.}$$
$$P_{FG} = 1734 \text{ lb.}$$

$R_1 = 1667$

P_{AB}

(1)

$P_{AB} = -1925$ lb.

$P_{AG} = 962$ lb.

$60°$

A P_{AG}

B $60°$ P_{BC}

60

(2)

$P_{BG} = 1925$ lb.

$P_{BC} = -1925$ lb.

$P_{AB} = -1925$ P_{BG}

$P_B = 1925$ P_{CG}

$60°$ $60°$

(3) $P_{AG} = 962$ G P_{FG}

2000

$P_{CG} = 382$ lb.

$P_{FG} = 1734$ lb.

(4)

$R_2 = 1333$

P_{DE}

$60°$

P_{EF} E

$P_{DE} = -1541$ lb.

$P_{EF} = 770$ lb.

P_{CD} D

$60°$

$60°$

(5)

$P_{DF} = 1541$ lb.

$P_{CD} = -1541$ lb.

P_{DF} $P_{DE} = -1541$

P_{CF} $P_{DF} = 1541$

$60°$ $60°$

(6)   F $P_{EF} = 770$

$P_{FG} = 1734$ 1000

$P_{CF} = -382$ lb.
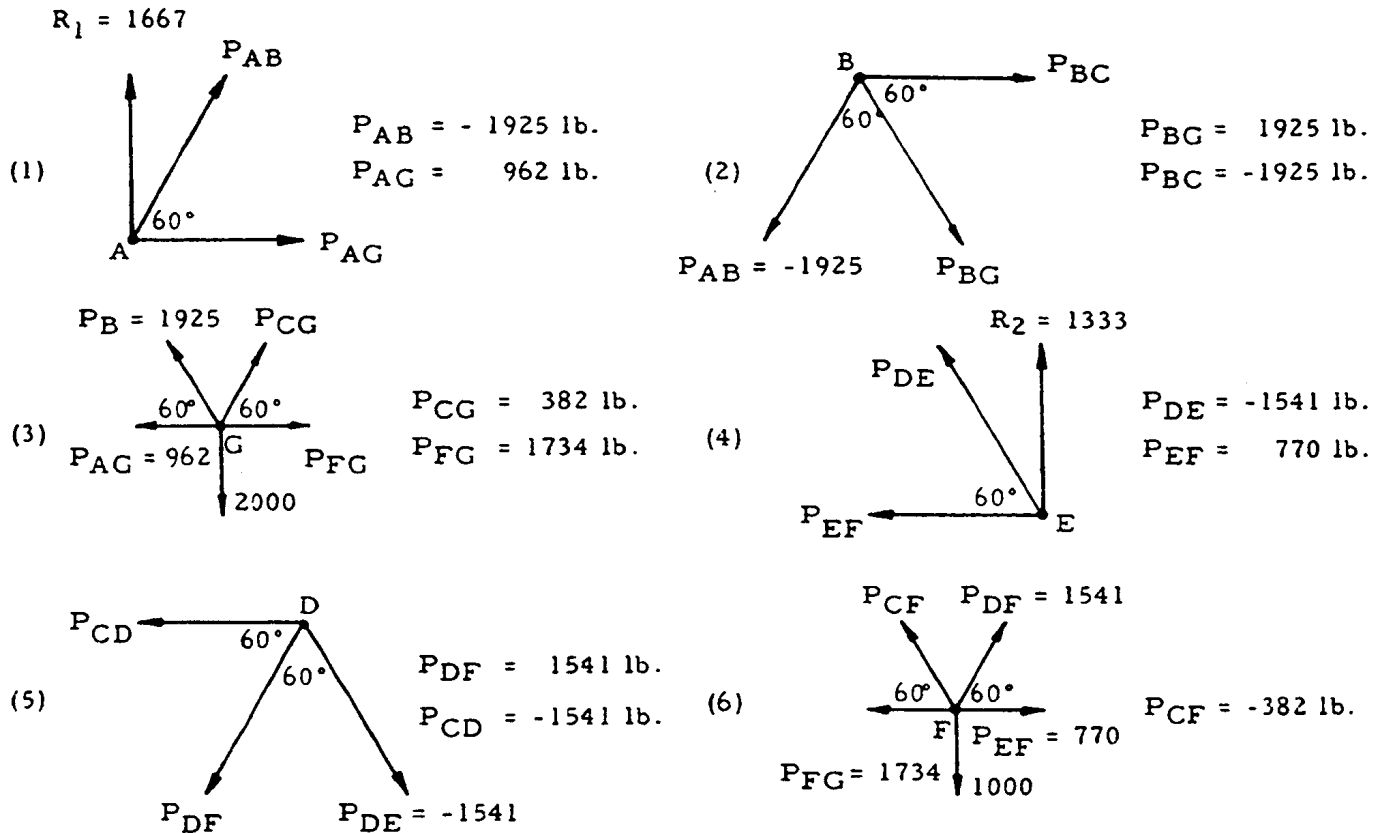
Figure 4-2. Free-Body Diagrams of the Joints in the Truss Shown in Figure 4-1

4.3.4   Application of the Method of Sections to Statically Determinate Trusses

The method of sections consists of breaking a truss up by a section and applying the equilibrium equations to the resulting portions of the truss. This method is preferable to the method of joints if the force on some interior member is desired, since the necessity of calculating the forces on other members may be eliminated. This advantage of the method of sections is illustrated in Section 4.3.5.

4.3.5   Sample Problem - Statically Determinate Trusses by the Method of Sections

Given: The truss shown in Figure 4-1.

Find: The force in member FG.

Solution: From statics, $R_1 = 1667$ lb. and $R_2 = 1333$ lb. By drawing a section through members BC, CG, and FG, the free body shown in Figure 4-3 is obtained. Summing moments about point C gives P_{FG} (30 sin 60°) -1667(45) + 2000(15). Solving gives $P_{FG} = 1734$ lb.

4 - 3
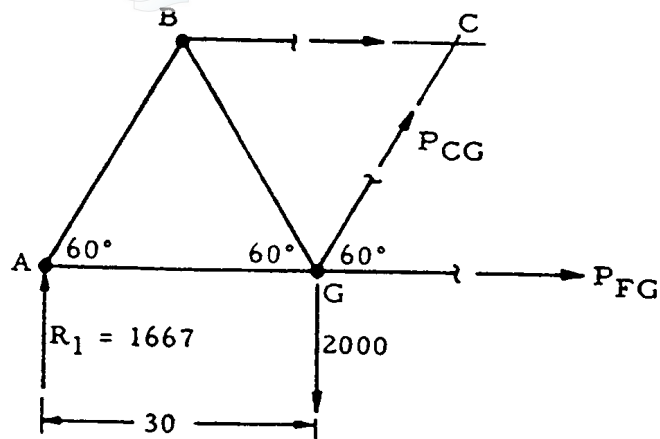
Figure 4-3. Free-Body Diagram of Part of the Truss Shown in Figure 4-1

4.3.6   Deflections in Statically Determinate Trusses

The basic equation for the deflection of statically determinate trusses is

$$\delta = \sum \frac{PuL}{AE} \qquad (4-1)$$

In this equation, L, A, and E are the length, cross-sectional area, and modulus of elasticity of each of the members of the truss. P is the force due to applied loads of a member of the truss, and u is the force in a member of the truss due to a unit load applied in the direction of the desired deflection at the point whose deflection is desired. The application of this equation is illustrated in Section 4.3.7.

4.3.7   Sample Problem - Deflections in Statically Determinate Trusses

Given: The truss shown in Figure 4-4.
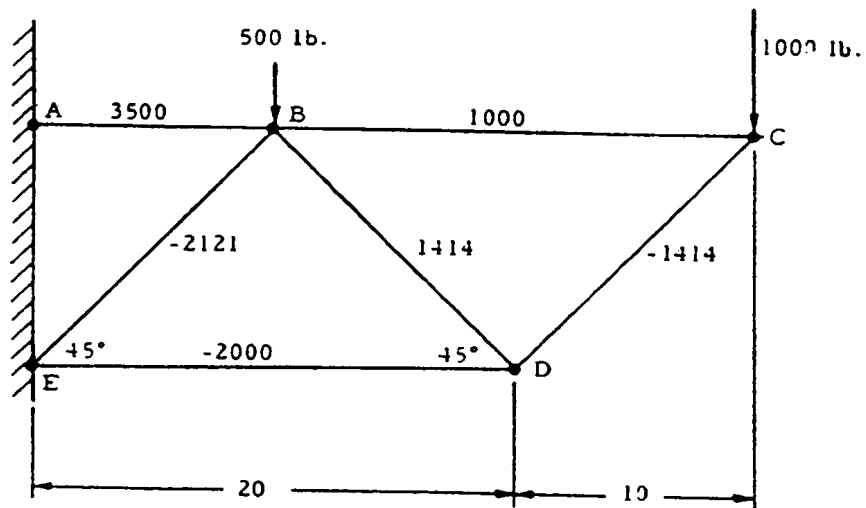
Figure 4-4. Cantilever Truss

4 - 4

<u>Find</u>: The vertical deflection of joint D.

<u>Solution</u>: The forces in the members may be found to be:
P_{AB} = 3500 lb., P_{BC} = 1000 lb., P_{BD} = 1414 lb., P_{BE} = -2121 lb.,
P_{CD} = -1414 lb., and P_{DE} = -2000 lb. The truss may be redrawn
with a unit load in the direction of the desired deflection at joint
D as shown in Figure 4-5. The forces in the members are again
calculated with the results shown in Figure 4-5. Equation (4-1)
may now be solved as shown in Table 4-1.
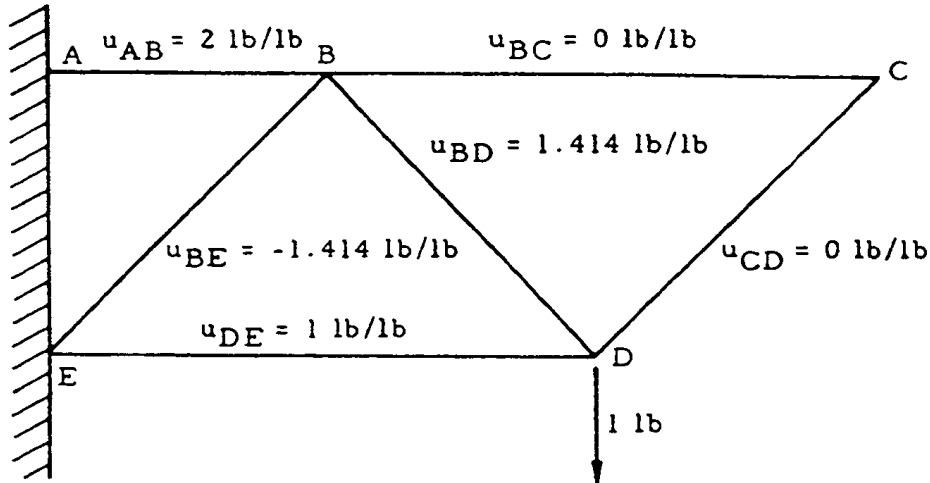
Figure 4-5. Cantilever Truss with Unit Load Applied at the
Point Whose Deflection is Desired

TABLE 4-1

Solution of Equation (4-1) for the Truss Shown in Figure 4-4

Member	P, lb.	u, lb./lb.	$\dfrac{L}{AE}$, in./lb.	$\dfrac{PuL}{AE}$, in.
AB	3500	2	$10/(2)(10 \times 10^6) = .5 \times 10^{-6}$	3.50×10^{-3}
BC	1000	0	$20/(1)(10 \times 10^6) = 2 \times 10^{-6}$	0
BD	1414	1.4.4	$14.14/(1)(10 \times 10^6) = 1.414 \times 10^{-6}$	2.82×10^{-3}
BE	-2121	-1.414	$14.14/(2)(10 \times 10^6) = .707 \times 10^{-6}$	2.12×10^{-3}
CD	-1414	0	$14.14/(1)(10 \times 10^6) = 1.414 \times 10^{-6}$	0
DE	-2000	-1	$20/(2)(10 \times 10^6) = 1 \times 10^{-6}$	2.00×10^{-3}
$\delta = \sum \dfrac{PuL}{AE} = 9.44 \times 10^{-3}$ in.				

4.4   Statically Indeterminate Trusses

4.4.1   Introduction to Statically Indeterminate Trusses

If a truss is statically indeterminate, deflection equations must be applied in addition to equilibrium equations to determine the forces in all of the members. Section 4.4.2 treats trusses with a single redundancy, and trusses with multiple redundancies are treated in Section 4.4.4.

4.4.2   Statically Indeterminate Trusses with a Single Redundancy

Trusses with a single redundancy may be treated by removing one member so that a statically determinate truss is obtained. This member is replaced by the unknown force exerted by this member, X_a. One equation may be written for the deflection of the statically determinate truss due to the applied loads including X, and another equation may be written for the deflection of the removed member due to the unknown force, X. These two equations may then be solved simultaneously to find X. Once X has been found, the forces in the other members of the truss may be obtained by the equations of statics. This procedure is illustrated in Section 4.4.3.

4.4.3   Sample Problem - Statically Indeterminate Trusses with a Single Redundancy

Given: The truss shown in Figure 4-6.
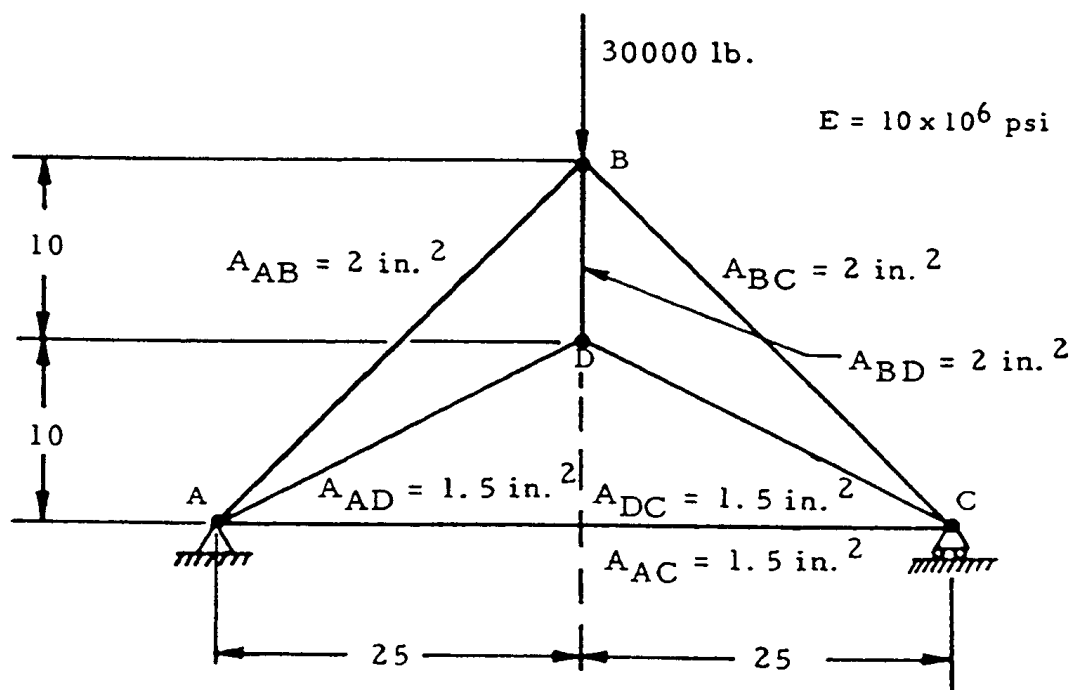
Figure 4-6.   Statically Indeterminate Truss With a Single Redundancy

<u>Find</u>: The force on member AC,

<u>Solution</u>: The truss may be redrawn with member AC replaced by the force resisted by this member, X, as shown in Figure 4-7. The force in any member of the truss, P, may be obtained by the superposition of the force due to the vertical loads alone, P_0, and that due to the horizontal loads alone. This latter force may be given as X_u where u is the force in a member of the truss due to a unit horizontal load applied at points A and C. Thus,

$$P = P_0 + X_u$$

By substituting this expression for P into Equation (4-1), the horizontal deflection between points A and C is

$$\delta = \sum \frac{P_0 uL}{AE} + X \sum \frac{u^2 L}{AE} \tag{4-2}$$

The terms $\sum \dfrac{P_0 uL}{AE}$ and $\sum \dfrac{u^2 L}{AE}$ are computed in Table 4-2. Thus,

$$\delta = -0.5645 + 47.63 \times 10^{-6} X$$

From the deflection equation for bar AC,

$$\delta = \frac{-XL_{AC}}{A_{AC} E} = \frac{-X(50)}{1.5(10 \times 10^6)} = 3.33 \times 10^{-6} X$$

Solving the last two equations simultaneously gives

$$X = 12730 \text{ lb.}$$
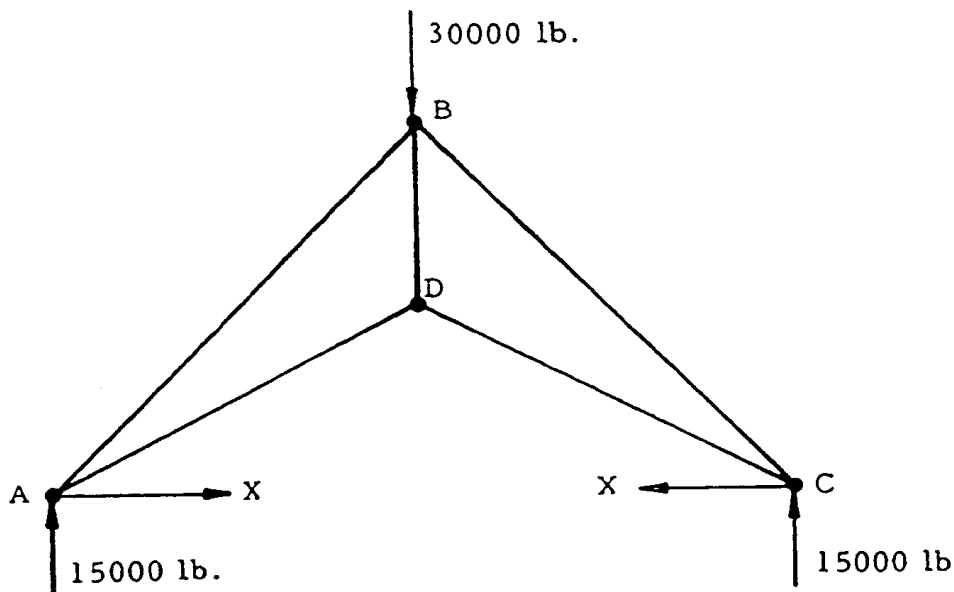
Figure 4-7. Truss From Figure 4-6 Redrawn With Member AC Removed

4 - 7

TABLE 4-2

Computation of Summations in Equation (4-2)

Man-ner	P_o, lb.	u lb/lb.	$\frac{L}{AE}$ in./lb.	$\frac{P_o uL}{AE}$ in.	$\frac{u^2 L}{AE}$ in./lb.
AB	-32000	1.785	1.600×10^{-6}	-0.0915	5.11×10^{-6}
AD	26900	-3.0	1.795×10^{-6}	-0.1450	16.15×10^{-6}
BC	-32000	1.785	1.600×10^{-6}	-0.0915	5.11×10^{-6}
BD	20000	-2.23	0.67×10^{-6}	-0.0292	3.32×10^{-6}
CD	26900	-3.0	1.795×10^{-6}	-0.1450	16.15×10^{-6}
				$\sum \frac{P_o uL}{AE} = -0.5150$	$\sum \frac{u^2 L}{AE} = 47.63 \times 10^{-6}$ in/lb

4.4.4 Statically Indeterminate Trusses with Multiple Redundancies

The analysis of trusses with more than one redundant is similar to that for a truss with one redundant. The first step is to remove redundant members or reactions in order to obtain a statically determinate base structure. The deflections of the statically determinate base structure in the directions of the redundants may then be calculated in terms of the redundant forces, and equated to the known deflections. For example, consider the truss in Figure 4-8. Members a and b may be removed to obtain a statically determinate base structure. The final force, P, in any member may be obtained by superposing the forces due to the applied loads and redundant forces. Thus,

$$P = P_o + X_a u_a + X_b u_b \tag{4-3}$$

where P_o is the force in a member of the statically determinate base structure due to the external load and u_a and u_b are the forces in a member of the statically determinate base structure due to unit loads applied in members a and b, respectively. Applying this equation to members a and b, respectively, gives

$$\delta_a = \sum \frac{P u_a L}{AE} \tag{4-4}$$

and

$$\delta_b = \sum \frac{P u_b L}{AE} \tag{4-5}$$

4 - 8

where L, A, and E are properties of the members of the statically determinate base structure and P is the force in a member of the base structure. Substituting Equation (4-3) into Equations (4-4) and (4-5) gives

$$\delta_a = \sum \frac{P_0 u_a L}{AE} + X_a \sum \frac{u_a^2 L}{AE} + X_b \sum \frac{u_a u_b L}{AE} \qquad (4-6)$$

and

$$\delta_b = \sum \frac{P_0 u_b L}{AE} + X_a \sum \frac{u_b u_a L}{AE} + X_b \sum \frac{u_b^2 L}{AE} \qquad (4-7)$$
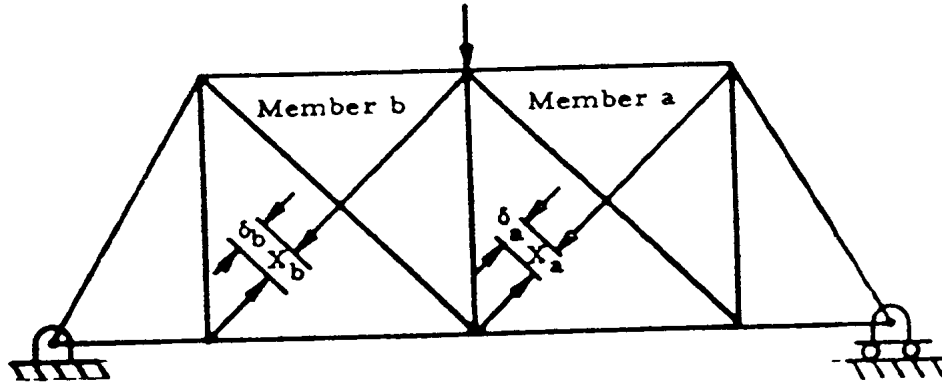
Figure 4-8. Statically Indeterminate Truss With Two Redundancies

In addition,

$$\delta_a = \frac{-X_a L_a}{A_a E} \qquad (4-8)$$

and

$$\delta_b = \frac{-X_b L_b}{A_b E} \qquad (4-9)$$

Equations (4-6) through (4-9) may be solved simultaneously to obtain the forces in the redundant members. Once this has been done, Equation (4-3) may be applied to obtain the forces in the other members.

$$\delta_a = \sum \frac{P_0 u_a L}{AE} + X_a \sum \frac{u_a^2 L}{AE} + X_b \sum \frac{u_a u_b L}{AE} + \ldots + X_n \sum \frac{u_a u_n L}{AE}$$

$$\delta_b = \sum \frac{P_0 u_b L}{AE} + X_a \sum \frac{u_a u_b L}{AE} + X_b \sum \frac{u_b^2 L}{AE} + \ldots + X_n \sum \frac{u_b u_n L}{AE} \qquad (4-10)$$

and

$$\delta_n = \sum \frac{P_0 u_n L}{AE} + X_a \sum \frac{u_n u_a L}{AE} + X_b \sum \frac{u_n u_b L}{AE} + \ldots + X_n \sum \frac{u_n^2 L}{AE}$$

Also,

$$\delta_a = \frac{-X_a L_a}{A_a E}$$

$$\delta_b = \frac{-X_b L_b}{A_b E} \qquad\qquad (4\text{-}11)$$

and

$$\delta_n = \frac{-X_n L_n}{A_n E}$$

These equations may be solved simultaneously to obtain the forces in the redundant members.

5. FRAMES AND RINGS

5.1 Introduction to Frames and Rings

Frames and rings are statically indeterminate structures. A frame is such a structure composed of prismatic elements joined rigidly at points of intersection while the element or elements of a ring are curved.

Section 5.3 treats the method of moment distribution for solving frame problems. Section 5.5 treats symmetrical rectangular frames under vertical loading. Section 5.7 gives formulas for simple rectangular, trapezoidal, and triangular frames under various simple loadings. Circular rings and arches are treated in Section 5.9.

5.2 Nomenclature for Frames and Rings

A	=	cross-sectional area
A_m	=	area under the moment diagram of a simply supported beam
a	=	linear dimension
b	=	linear dimension
c	=	linear dimension
D	=	diameter
DF	=	distribution factor
d	=	linear dimension
d	=	distance to centroid of load
E	=	modulus of elasticity
FEM	=	fixed end moment
H	=	horizontal reaction
h	=	height
I	=	moment of inertia
K	=	stiffness factor = I/L
L	=	length
M	=	moment
P	=	applied concentrated load
R	=	radius
s	=	length of upright of a trapezoidal frame
T	=	tensile force
V	=	shear force
V	=	vertical reaction
W	=	applied concentrated load
w	=	applied distributed load
x, y, z	=	rectangular coordinates
x	=	angular distance from the bottom of a circular ring
Δ	=	increment or difference
β	=	angle
θ	=	rotation of the tangent to the elastic curve of a moment at its end

ϕ = angle

ψ = rotation of the chord joining the ends of the elastic curve of a member

$(\Omega_o)_A$ = moment of the M_o portion of the moment diagram of a member (Figure 5-1) about point A.

5.3   Solution of Frames by the Method of Moment Distribution

This section treats frames composed of prismatic members whose joints do not translate.   All members of such frames are assumed to be elastic.

The five basic factors involved in the method of moment-distribution are: fixed-end moments, stiffness factors, distribution factors, distributed moments, and carry-over moments.

The fixed-end moments are obtained by the use of the following equations:

$$M_{AB} = \frac{2EI}{L} (2\theta_A + \theta_B - 3\psi_{AB}) + \frac{2}{L^2} [(\Omega_o)_A - 2(\Omega_o)_B] \qquad (5-1)$$

and

$$M_{BA} = \frac{2EI}{L} (2\theta_B + \theta_A - 3\psi_{AB}) + \frac{2}{L^2} [2(\Omega_o)_A - (\Omega_o)_B] \qquad (5-2)$$

where:

M_{AB} = the moment acting on the end of member AB labeled as A

M_{BA} = the moment acting on the end of member AB labeled as B

E = the modulus of elasticity of member AB

I = the moment of inertia of member AB

L = length of member AB

θ = rotation of the tangent to the elastic curve at the end of the member

ψ = rotation of the chord joining the ends of the elastic curve referred to the original direction of the member

$(\Omega_o)_A$ = static moment about a vertical axis through A of the area under the M_o portion of the bending moment diagram

$(\Omega_o)_B$ = static moment about an axis through B

This terminology is illustrated in Figure 5-1.

If both ends of the member are completely fixed against rotation and translation, the member is called a fixed-end beam and θ_A, θ_B, and ψ_{AB} are all equal to zero.   Thus, the last terms of Equations (5-1) and (5-2) are equal to the so-called "fixed-end moments."   Denoting the fixed-end moments as FEM,

$$FEM_{AB} = \frac{2}{L^2} [(\Omega_o)_A - 2(\Omega_o)_B] \qquad (5-3)$$

5 - 2

$$FEM_{BA} = \frac{2}{L^2} [2(\Omega_o)_A - (\Omega_o)_B] \qquad (5-4)$$

Fixed-end moments for various simple types of loading were calculated and are given in Table 5-1.

Equations (5-1) and (5-2) may be represented by one general equation by calling the near end of a member "N" and the far end "F." The stiffness factor of member NF is given by

$$K_{NF} = \frac{I_{NF}}{L_{NF}} \qquad (5-5)$$

Thus, the fundamental slope deflection equation becomes

$$M_{NF} = 2EK_{NF} (2\theta_N + \theta_F - 3\psi_{NF}) + FEM_{NF} \qquad (5-6)$$
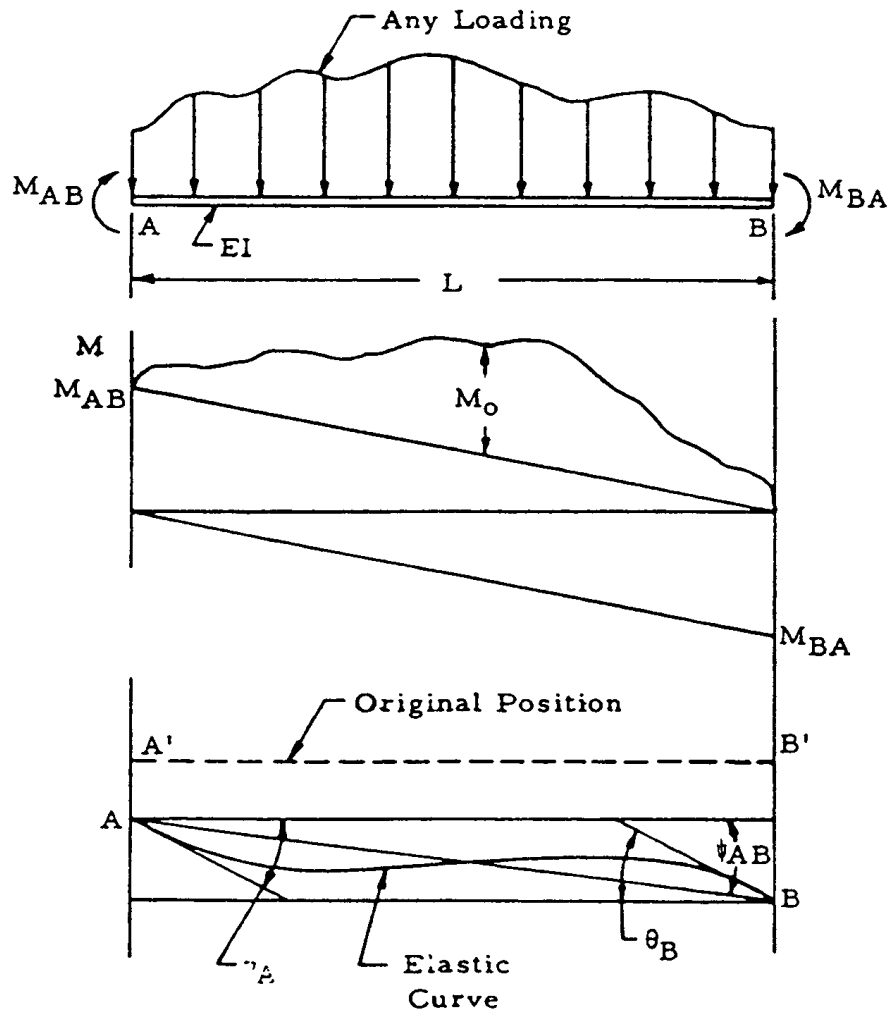
Figure 5-1. Illustration of Terminology for Method of Moment Distribution

TABLE 5-1

Fixed-End Moments for Beams
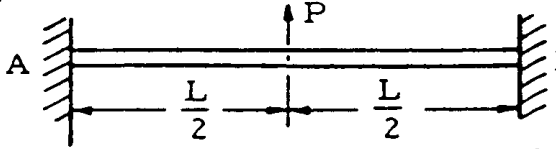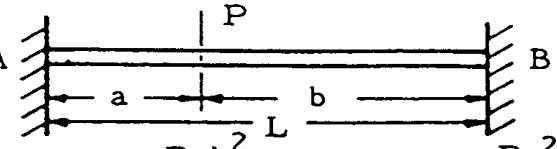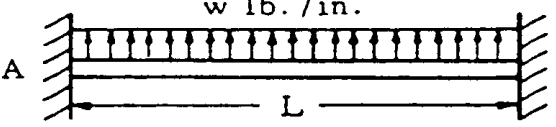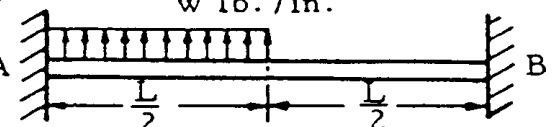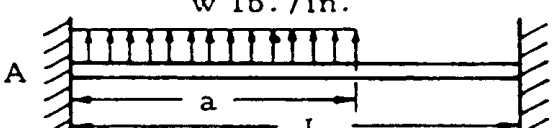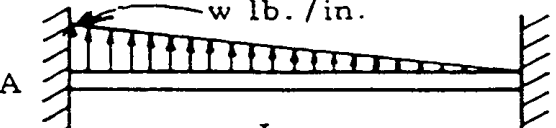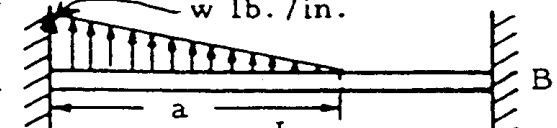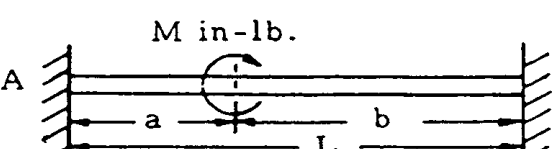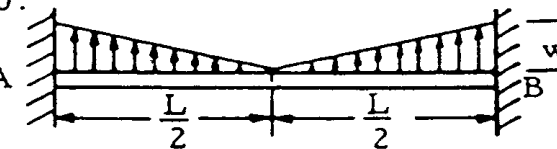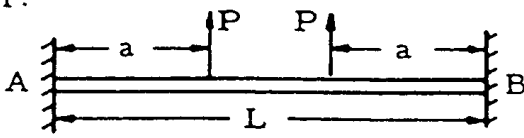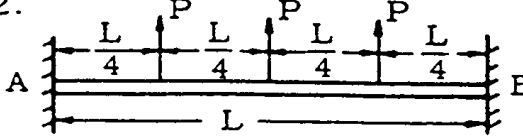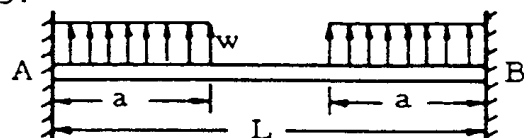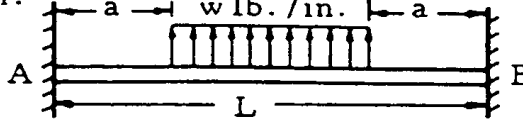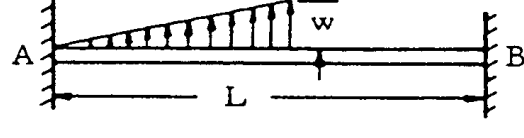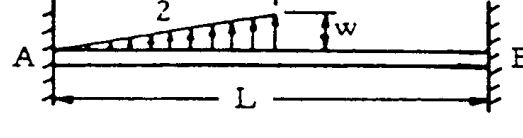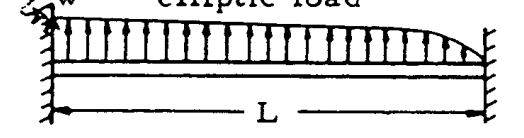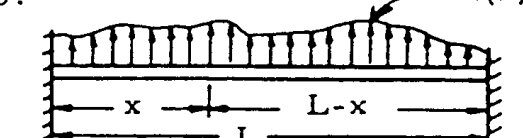
1.

$$\text{FEM}_{AB} = \frac{PL}{8} \qquad \text{FEM}_{BA} = \frac{PL}{8}$$

2.

$$\text{FEM}_{AB} = \frac{Pab^2}{L^2} \qquad \text{FEM}_{BA} = \frac{Pa^2b}{L^2}$$

3.

$$\text{FEM}_{AB} = \frac{wL^2}{12} \qquad \text{FEM}_{BA} = \frac{wL^2}{12}$$

4.

$$\text{FEM}_{AB} = \frac{11wL^2}{192} \qquad \text{FEM}_{BA} = \frac{5wL^2}{192}$$

5.

$$\text{FEM}_{AB} = \frac{wa^2}{12L^2}(6L^2 - 8aL + 3a^2)$$

$$\text{FEM}_{BA} = \frac{wa^2}{12L^2}(4aL - 3a^2)$$

6.

$$\text{FEM}_{AB} = \frac{5wL^2}{96} \qquad \text{FEM}_{BA} = -\frac{5wL^2}{96}$$

7.

$$\text{FEM}_{AB} = \frac{wL^2}{20} \qquad \text{FEM}_{BA} = \frac{wL^2}{30}$$

8.

$$\text{FEM}_{AB} = \frac{wa^2}{60L^2}(10L^2 - 10aL + 3a^2)$$

$$\text{FEM}_{BA} = \frac{wa^3}{60L^2}(5L - 3a)$$

9.

$$\text{FEM}_{AB} = \frac{Mb}{L}\left(3\frac{a}{L} - 1\right)$$

$$\text{FEM}_{BA} = \frac{Ma}{L}\left(3\frac{b}{L} - 1\right)$$

10.

$$\text{FEM}_{AB} = \frac{wL^2}{32} \qquad \text{FEM}_{BA} = -\frac{wL^2}{32}$$

TABLE 5-1

Fixed-End Moments for Beams (continued)

11.

$$FEM_{AB} = Pa(1 - \frac{a}{L})$$
$$FEM_{BA} = -FEM_{AB}$$

12.

$$FEM_{AB} = \frac{15PL}{48} \qquad FEM_{BA} = M_A$$

13.

$$FEM_{AB} = \frac{wa^2}{6L}(3L-2a) = M_B = -M_A$$

14.

$$M_A = \frac{w}{12L}(L^3 - a^2 L + 4a^3) \quad M_B = -M_A$$

15.

$$M_A = \frac{wa^2}{30}(10 - 15\frac{a}{L} + 6\frac{a^2}{L^2})$$
$$M_B = -\frac{wa^2}{20}(5 - 4\frac{a}{L})$$

16.

$$M_A = \frac{wL^2}{30} \qquad M_B = -\frac{3wL^2}{160}$$

17. elliptic load

$$M_A = \frac{wL^2}{13.52} \qquad M_B = \frac{wL^2}{15.86}$$

18. $w = f(x)$

$$M_A = \frac{1}{L^2}\int_o^L x(L-x)^2 f(x)dx$$
$$M_B = \frac{-1}{L^2}\int_o^L x^2(L-x)f(x)dx$$

The conditions to be met at a joint of a frame are: (1) the angle of rotation be the same for the ends of all members that are rigidly connected at a joint, and (2) the algebraic sum of all moments be zero. The method of moment distribution renders to zero by iteration any unbalance in moment at a joint to satisfy the second condition.

A distribution factor which represents the relative portion of the unbalanced moment which is reacted by a member is used to distribute the unbalanced moment. This distribution factor is given for any member bm by

$$DF_{bm} = \frac{K_{bm}}{\sum_b K} \tag{5-6}$$

where the summation includes all members meeting at joint b.

The distributed moment in any bar bm is then

$$M_{bm} = - DF_{bm} M \tag{5-7}$$

This equation may be interpreted as follows:

The distributed moment developed at the "b" end of member bm as joint b is unlocked and allowed to rotate under an unbalanced moment, M, is equal to the distribution factor DF_{bm} times the unbalanced moment, M, with the sign reversed.

The "carry-over" moment is obtained by applying Equation (5-6) and considering $\theta_m = \psi_{bm} = 0$ as in Figure 5-2. The "carry-over" moment is equal to half of its corresponding distributed moment and has the same sign.

$$M_{bm} = 4 EK_{bm} \theta_b \tag{5-8}$$

and

$$M_{mb} = 2 EK_{mb} \theta_b \tag{5-9}$$

Thus,

$$M_{mb} = \tfrac{1}{2} M_{bm} \tag{5-10}$$
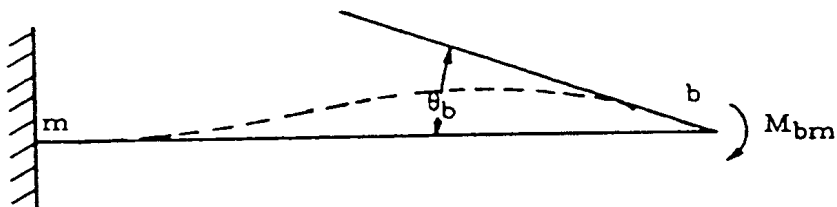
Figure 5-2. Illustration of Carry-Over Moment

The sign convention for moments in the method of moment distribution is to consider moments acting clockwise on the ends of a member as positive. This convention is illustrated in Figure 5-3.
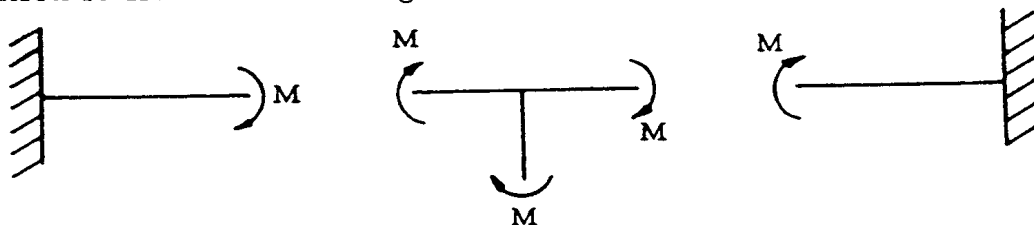
Figure 5-3. Positive Sense for Bending Moments

5 - 6

The following procedure is for the process of moment distribution analysis:

(1) Compute the stiffness factor, K, for each member and record.

(2) Compute the distribution factor, DF, of each member at each joint and record.

(3) Compute the fixed-end moments, FEM, for each loaded span and record.

(4) Balance the moments at a joint by multiplying the unbalanced moment by the distribution factor, changing sign, and recording the balancing moment below the fixed-end moment. The unbalanced moment is the sum of the fixed-end moments of a joint.

(5) Draw a horizontal line below the balancing moment. The algebraic sum of all moments at any joint above the horizontal line must be zero.

(6) Record the carry-over moment at the opposite ends of the member. Carry-over moments have the same sign as the corresponding balancing moments and are half their magnitude.

(7) Move to a new joint and repeat the process for the balance and carry-over of moments for as many cycles as desired to meet the required accuracy of the problem. The unbalanced moment for each cycle will be the algebraic sum of the moments at the joint recorded below the last horizontal line.

(8) Obtain the final moment at the end of each member as the algebraic sum of all moments tabulated at this point. The total of the final moments for all members at any joint must be zero.

(9) Reactions, vertical shear, and bending moments of the member may be found through statics by utilizing the above mentioned final moments.

The use of this procedure is illustrated in Section 5.4. It should be noted that simpler methods may be found for the solution of rectangular, trapezoidal, and triangular frames in Sections 5.5 and 5.7.

5.4 Sample Problem - Solution of Frames by the Method of Moment Distribution

Given: The frame shown in Figure 5-4.
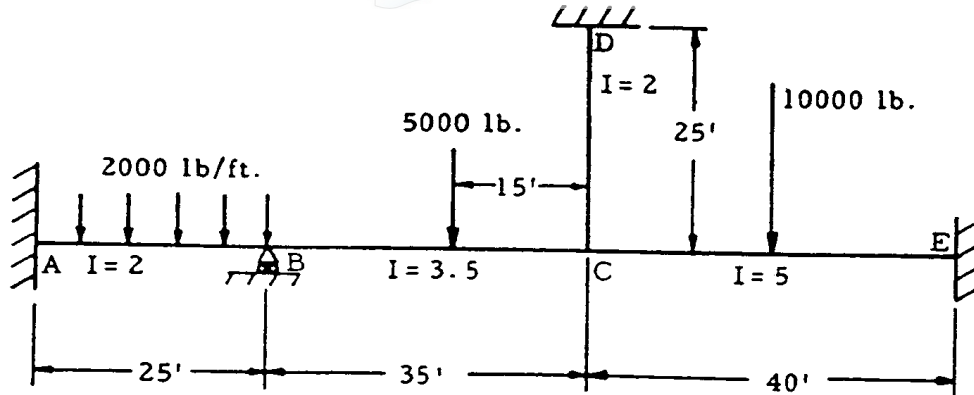
Figure 5-4.   Frame

<u>Find</u>:   The end moments and draw the moment diagrams for this frame.

<u>Solution</u>:

(1)   From Equation (5-5), the stiffness factors of the members are:

$$K_{BA} = \frac{I_{BA}}{L_{BA}} = \frac{2}{25} = 0.08$$

$$K_{BC} = \frac{I_{BC}}{L_{BC}} = \frac{3.5}{35} = 0.1$$

$$K_{CE} = \frac{I_{CE}}{L_{CE}} = \frac{5}{40} = 0.125$$

$$K_{CD} = \frac{I_{CD}}{L_{CD}} = \frac{2}{25} = 0.08$$

These are recorded in line 1 of Table 5-2.

TABLE 5-2

Solution of Frame Shown in Figure 5-4

		AB		BA	BC		DC	CB	CE	CD		EC
1	K			0.08	0.1			0.1	0.125	0.08		
2	DF			0.44	0.56			0.33	0.41	0.26		
3	FEM	-104		+104	-18		0	+25	-50	0		+50
4				-38	-48			+8	+10	+7		
5		-19			+4		+3	-24				+5
6				-2	-2			+8	+10	+6		
7		-1			+4		+3					+5
8				-2	-2							
9	Σ	-124		+62	-62		+6	+17	-30	+13		+60

5-8

(2) From Equation (5-6), the distribution factors of the members are:

$$DF_{BA} = \frac{K_{BA}}{K_{BA} + K_{BC}} = \frac{0.08}{0.08 + 0.1} = 0.44$$

$$DF_{BC} = \frac{K_{BC}}{K_{BA} + K_{BC}} = \frac{0.1}{0.08 + 0.1} = 0.56$$

$$DF_{CB} = \frac{K_{CB}}{K_{CB} + K_{CD} + K_{CE}} = \frac{0.1}{0.1 + 0.08 + 0.125} = 0.33$$

$$DF_{CE} = \frac{K_{CE}}{K_{CB} + K_{CD} + K_{CE}} = \frac{0.1}{0.1 + 0.08 + 0.125} = 0.41$$

$$DF_{CD} = \frac{K_{CD}}{K_{CB} + K_{CD} + K_{CE}} = \frac{0.1}{0.1 + 0.08 + 0.125} = 0.26$$

These distribution factors are recorded in line 2 of Table 5-2.

(3) From Table 5-1, case 3,

$$FEM_{AB} = \frac{wL^2}{12} = \frac{-2000(25)^2}{12} = -104,000 \text{ ft. lb.}$$

and

$$FEM_{BA} = \frac{-wL^2}{12} = \frac{2000(25)^2}{12} = 104,000 \text{ ft. lb.}$$

From Table 5-1, case 2,

$$FEM_{BC} = \frac{-Pab^2}{L^2} = \frac{-5000(20)(15)^2}{(35)^2} = -18,000 \text{ ft. lb.}$$

and

$$FEM_{CB} = \frac{-Pa^2b}{L^2} = \frac{5000(20)^2(15)}{(35)^2} = 25,000 \text{ ft. lb.}$$

From Table 5-1, case 1,

$$FEM_{CE} = \frac{PL}{8} = \frac{-10000(40)}{8} = 50,000 \text{ ft. lb.}$$

and

$$FEM_{EC} = \frac{-PL}{8} = \frac{10000(40)}{8} = 50,000 \text{ ft. lb.}$$

Since member CD is unloaded,

$$FEM_{CD} = FEM_{DC} = 0$$

These results are summarized in line 3 of Table 5-2.

(4)   The unbalanced moment at joint B is

$$\Sigma FEM = 104 - 18 = 86$$

The moments at joint B may be balanced by multiplying this unbalanced moment by the distribution factor and changing sign.   The result is recorded in line 4 of Table 5-2.

(5)   A horizontal line may be drawn below the balancing moments in line 4 of Table 5-2.   The algebraic sum of all the moments at this joint above this line is zero; that is,

$$-104 + 18 + 38 + 48 = 0$$

(6)   The carry-over moments at the opposite ends of the members are recorded as shown in line 5 of Table 5-2.   These carry-over moments have the same sign as the corresponding balancing moments and are half their magnitude.

(7)   Steps 4, 5, and 6 may be repeated for joint C to obtain the rest of the values shown in rows 4 and 5 of Table 5-2.   The process for the balance and carry-over of moments may be repeated for as many cycles as desired to meet the required accuracy of the problem.   The unbalanced moment for each cycle will be the algebraic sum of the moments at the joint recorded below the last horizontal line.   This process is shown on lines 6, 7, and 8 of Table 5-2.

(8)   The final moment at the end of each member may be obtained as the algebraic sum of all moments tabulated in the first seven lines of Table 5-2.   This summation is shown in line 9 of Table 5-2.

Now that the moments in each of the members at the joints are known, the moment diagrams may be drawn for the members with the aid of the equations of static equilibrium. These moment diagrams are shown in Figure 5-5.
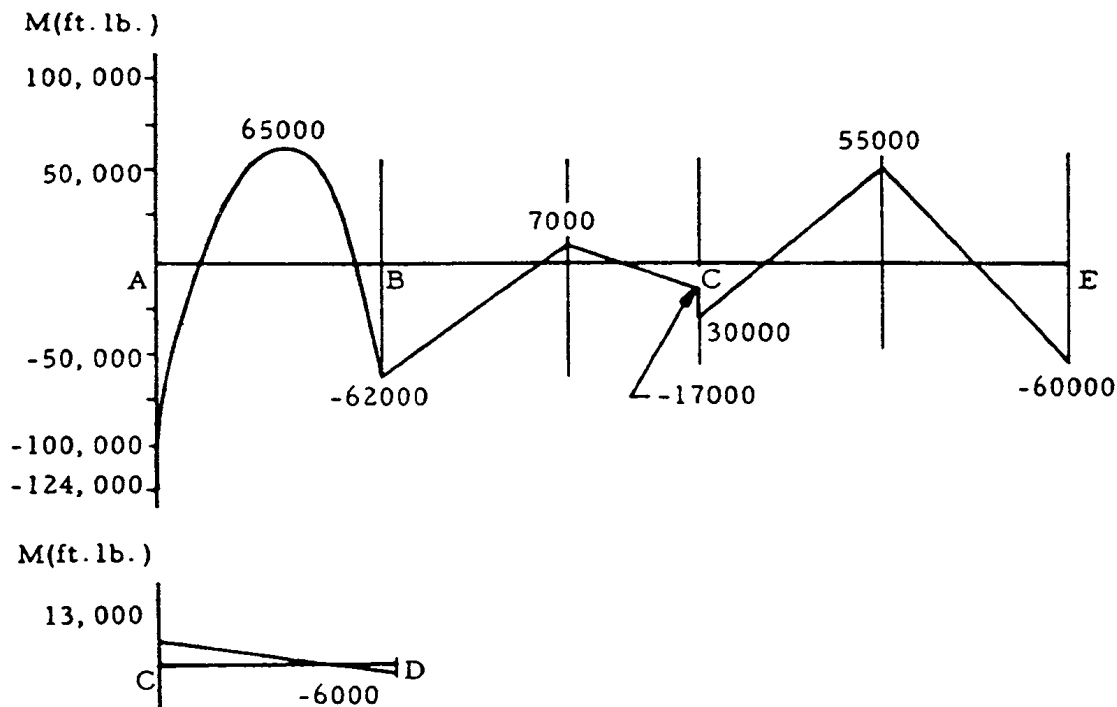
Figure 5-5. Moment Diagram for Frame Shown in Figure 5-4

5.5 Rectangular Frames

This section considers symmetrical rectangular frames that are either pinned or fixed at the ends of both of their uprights.

Figure 5-6 shows a symmetrical rectangular frame both of whose uprights are pinned under some arbitrary vertical loading. Such a frame is statically indeterminate and an equation, in addition to those of statics, must be applied to determine the moments in its members.
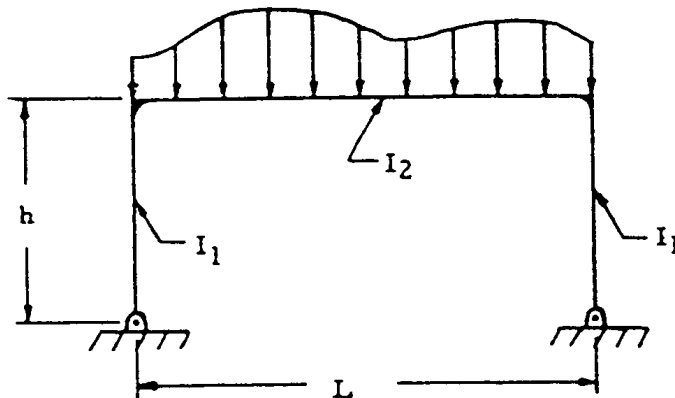
Figure 5-6. Symmetrical Rectangular Frame Under Arbitrary Vertical Loading With Both Uprights Pinned

The free-body diagram of this frame may be drawn as shown in Figure 5-7.

The horizontal reaction is given by

$$H = \frac{3 A_m}{hL(2K + 3)} \tag{5-11}$$

where

$$K = \frac{I_2 h}{I_1 L} \tag{5-12}$$

and A_m is the area under the moment diagram for a simply supported beam under the same loading as the horizontal member of the given frame. Once the horizontal reactions have been found by Equation (5-11), the moment diagrams of the frame members may be found by the equations of statics.
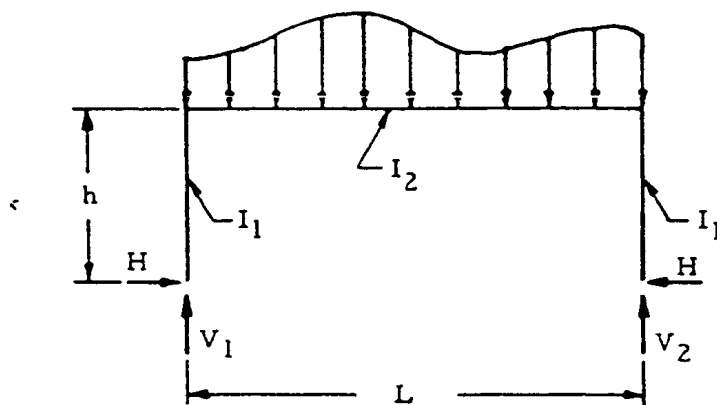
Figure 5-7.   Free-Body Diagram of the Frame in Figure 5-6

Figure 5-8 shows a symmetrical rectangular frame both of whose uprights are fixed under some arbitrary symmetrical vertical loading. Such a frame is statically indeterminate with two indeterminates, and two equations, in addition to those of statics, must be applied to determine the moments in its members.
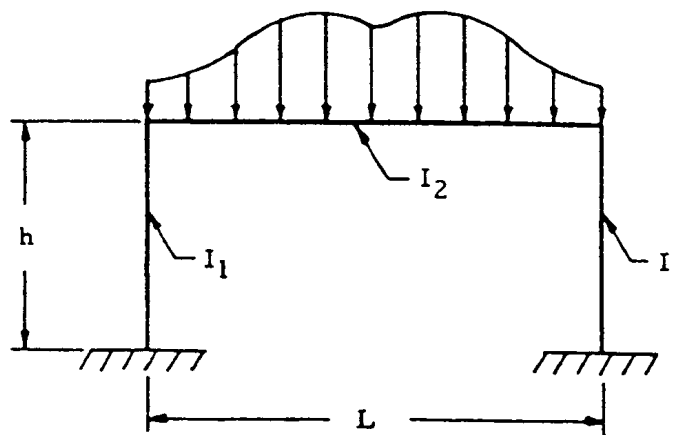
Figure 5-8.   Symmetrical Rectangular Frame Under Arbitrary Symmetrical
Vertical Loading With Both Uprights Fixed

The free-body diagram of this frame may be drawn as shown in Figure 5-9. The horizontal reaction is given by

$$H = \frac{3 A_s}{hL(K+2)} \tag{5-13}$$

where

$$K = \frac{I_2 h}{I_1 L} \tag{5-14}$$

and A_s is the area under the moment diagram for a simply supported beam under the same loading as the horizontal member of the given frame. The reaction moment on the ends of the uprights is given by

$$M = \frac{A_s}{L(K+2)} \tag{5-15}$$

where K and A_s are defined as before. Once the horizontal reactions and reaction moments have been found by Equations (5-11) and (5-13), the moment diagrams of the frame members may be found by the equations of statics. This procedure is illustrated in Section 5.6.
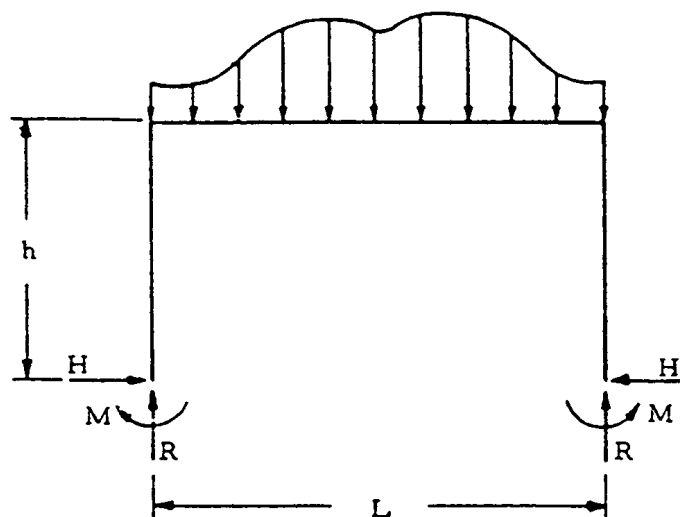
Figure 5-9. Free-Body Diagram of the Frame in Figure 5-8

It should be noted that solutions for rectangular frames under various simple loadings are given in tabular form in Section 5.7. The use of this material, when applicable, is much simpler than using the material in this section.

5.6   Sample Problem - Rectangular Frames

Given: The symmetrically loaded frame shown in Figure 5-10.
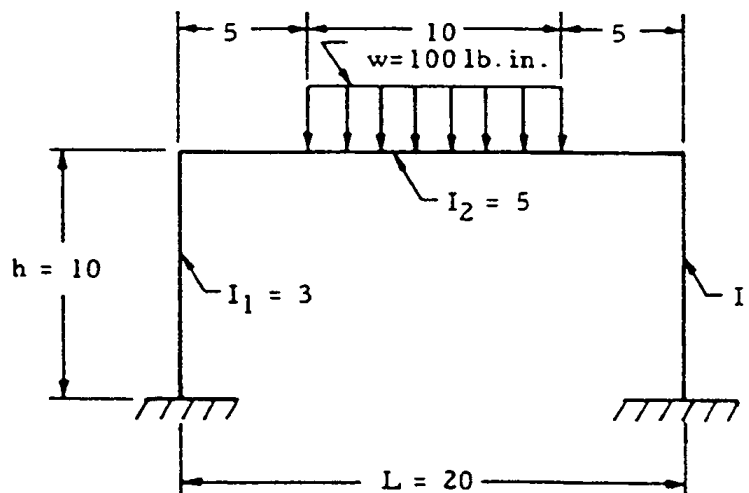
Figure 5-10.   Rectangular Frame

Find: The bending moment diagram.

Solution:

$$K = \frac{I_2 h}{I_1 L} = \frac{5(10)}{3(20)} = 0.834$$

To find A_z, consider the simply supported beam shown in Figure 5-11 and draw its moment diagram.   The area under this moment diagram may be found to be

$$A_m = 45800 \text{ in.}^2 \text{lb.}$$

Substituting this and K into Equations (5-13) and (5-15) gives

$$H = \frac{3 A_z}{hL(K+2)} = \frac{3(45800)}{10(20)(0.834+2)} = 242 \text{ lb.}$$

and

$$M = \frac{A_z}{L(K+2)} = \frac{-45800}{20(0.834+2)} = 795 \text{ in. lb.}$$

A free-body diagram may now be drawn for the frame and the vertical reactions computed as shown in Figure 5-12.   The equations of statics may now be applied to sections of this frame to obtain the moment diagram shown in Figure 5-13.

5 - 14
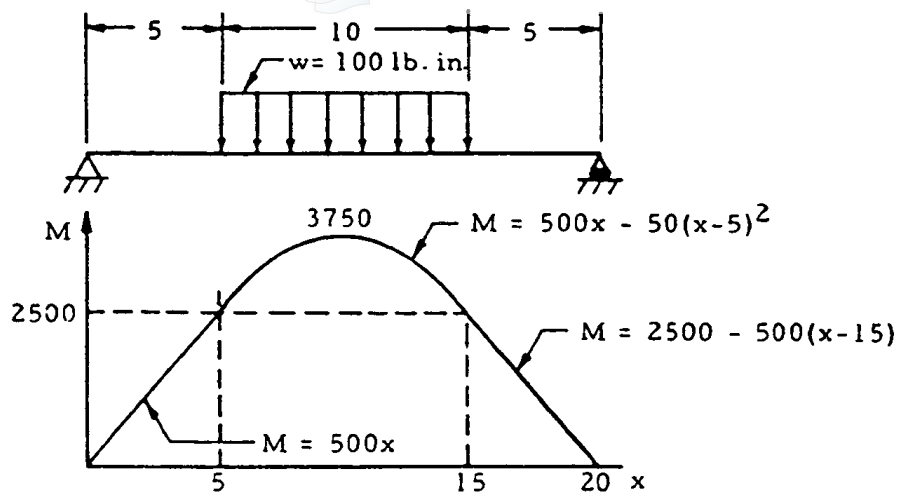
Figure 5-11.   Determination of A_s
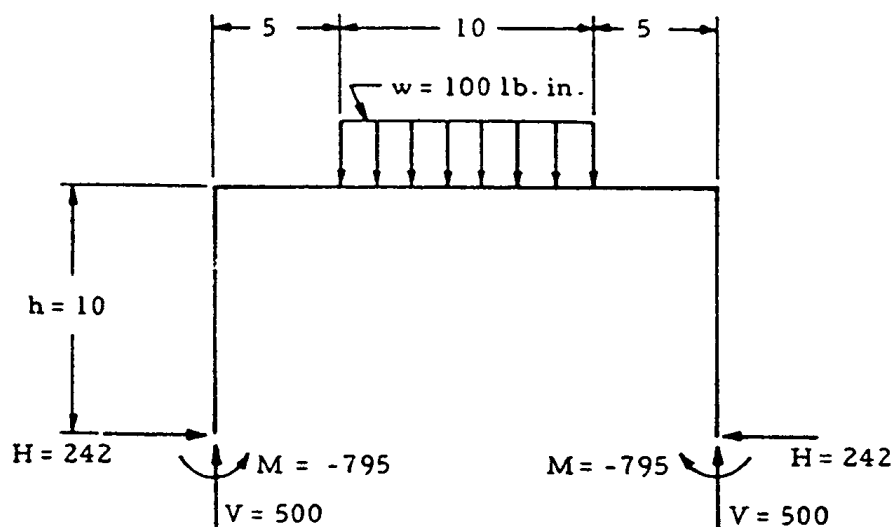
Figure 5-12.   Free-Body Diagram of Frame in Figure 5-1
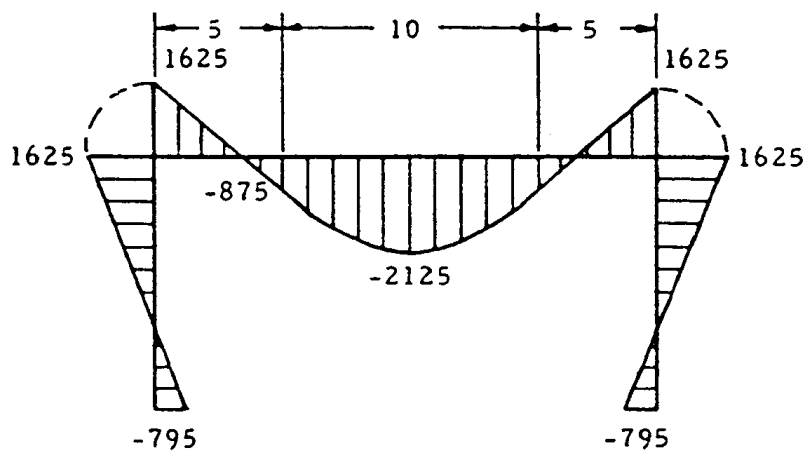
Figure 5-13.   Moment Diagram for Frame in Figure 5-1

5.7 Formulas for Simple Frames

This section presents formulas for determining the reaction forces and moments acting on simple frames under various simple loadings. The reaction forces and moments acting on frames under more complicated loadings may often be obtained by the superposition of these simple loadings.

Cases 1 through 9 of Table 5-3 give reaction forces and moments on rectangular frames, both of whose uprights are pinned; and such frames with both uprights fixed are treated by cases 9 through 18 of this table. Table 5-4 gives reaction forces and moments on trapezoidal frames. The first four cases treat such frames with both uprights pinned at the ends, and cases 5 and 6 treat trapezoidal frames with fixed-ended uprights. Table 5-5 gives reaction forces and moments on triangular frames.

5.8 Sample Problem - Formulas for Simple Frames

Given: The trapezoidal frame shown in Figure 5-14.
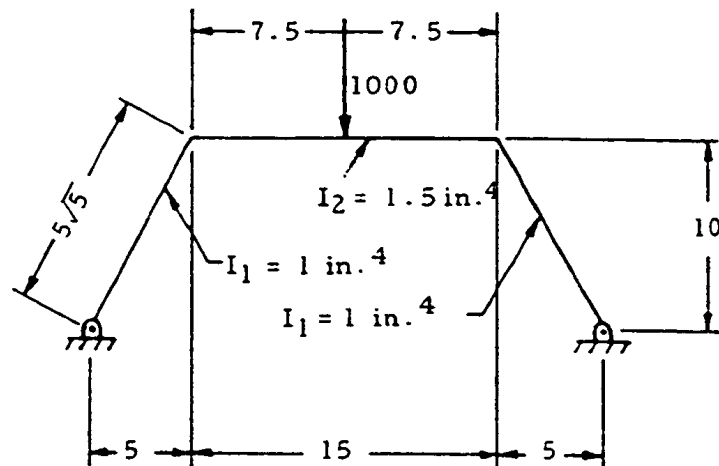
Figure 5-14.   Trapezoidal Frame

Find: The reaction forces and bending moments.

Solution: From the diagram at the top of Table 5-4,

$$F = \frac{I_2}{I_1} \left(\frac{s}{b} \right) = \frac{1.5}{1} \left(\frac{5\sqrt{5}}{15} \right) = 1.12$$

$$G = 3 + 2F = 3 + 2(1.12) = 5.24$$

$I_1 = 1 \text{ in.}^4$ $a = 5 \text{ in.}$ $h = 10 \text{ in.}$

$I_2 = 1.5 \text{ in.}^4$ $b = 15 \text{ in.}$ $s = 5\sqrt{5} \text{ in.}$

TABLE 5-3

Reaction Forces and Moments on Rectangular Frames *

$$K = \frac{I_2 h}{I_1 L}$$

d = distance to centroid of load unless otherwise used

$M_A = M_B = 0$ if uprights are pinned
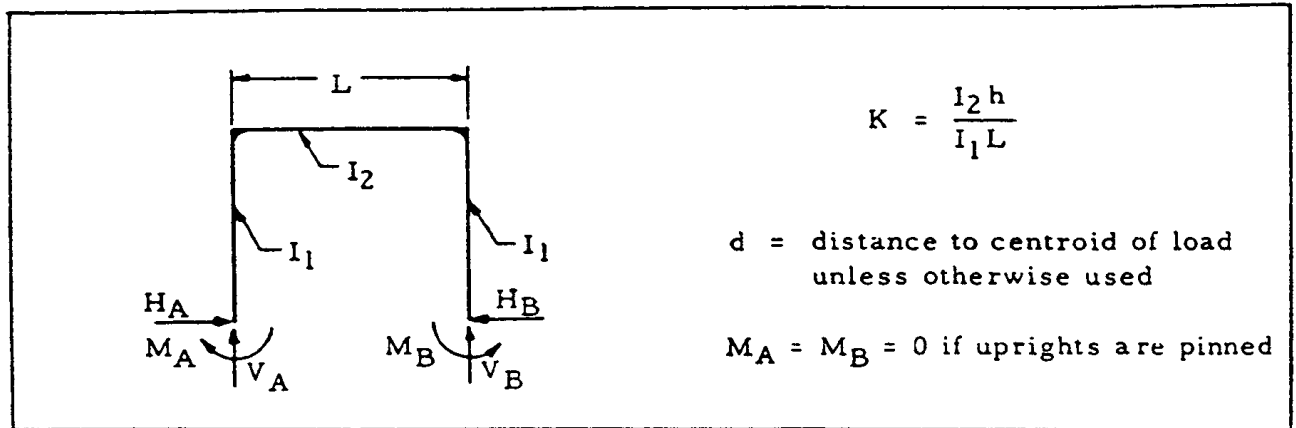
(1)
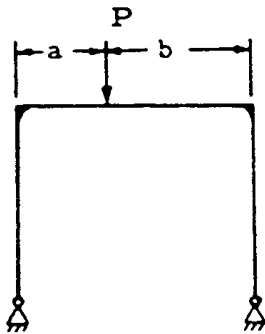
$$V_A = \frac{Pb}{L} \qquad V_B = P - V_A$$

$$H_A = H_B = \frac{3PL}{8h(2K+3)}$$

For Special Case: $a = b = L/2$

$$V_A = V_B = \frac{P}{2}$$
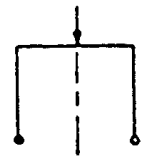
$$H_A = H_B = \frac{3PL}{8h(2K+3)}$$

(2)
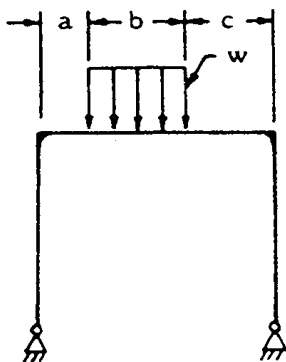
$$V_A = \frac{wb(b+2c)}{2L} \qquad V_B = wb - V_A$$

$$H_A = H_B = \frac{wb[6ac + b(3L - 2b)]}{4hL(2K+3)}$$

For Special Case: $a = c = 0$, $b = L$

$$V_A = V_B = \frac{wL}{2}$$
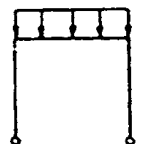
$$H_A = H_B = \frac{wL^2}{4h(2K+3)}$$

* Griffel, William, Handbook of Formulas for Stress and Strain

5 - 17

TABLE 5-3

Reaction Forces and Moments on Rectangular Frames (continued)

(3)
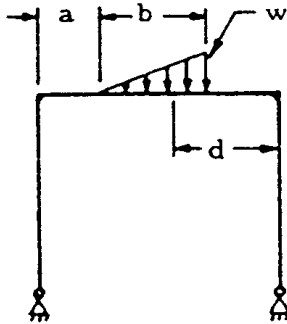
$$V_A = \frac{wbd}{2L} \qquad V_B = \frac{wb}{2} - V_A$$

$$H_A = H_B = \frac{3wb}{4Lh(2K+3)} \left(dL - \frac{b^2}{18} - d^2 \right)$$

For Special Case: $a = 0, \quad b = L, \quad d = \frac{L}{3}$

$$V_A = \frac{wL}{6} \qquad V_B = \frac{wL}{2}$$
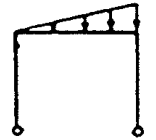
$$H_A = H_B - \frac{wL^2}{8h(2K+3)}$$

(4)
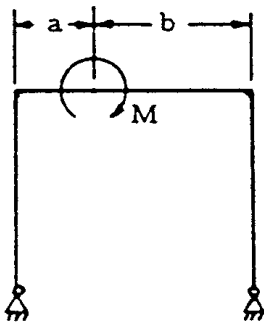
$$V_A = -V_L = \frac{-M}{L}$$

$$H_A = H_B = \frac{3(b-L/2)M}{Lh(2K+3)}$$

(5)
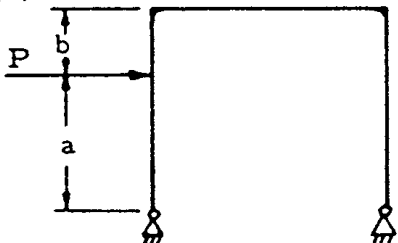
$$V_A = -V_B = \frac{-Pa}{L}$$

$$H_B = \frac{Pa}{2h} \left[\frac{bK(a+h)}{h^2(2K+3)} + 1 \right]$$

$$H_A = H_B - P$$

5 - 18

TABLE 5-3

Reaction Forces and Moments on Rectangular Frames (continued)

(6)
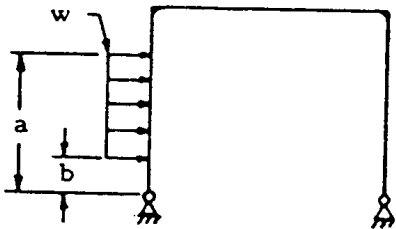
$$V_A = -V_B = \frac{w(b^2 - a^2)}{2L}$$

$$H_B = \frac{w(a^2 - b^2)}{4h} + \frac{K[w(a^2 - b^2)(2h^2 - a^2 - b^2)]}{8h^3(2K+3)}$$

$$H_A = H_F + w(b-a)$$

For Special Case: b = 0, a = h

$$V_A = -V_B = \frac{-wh^2}{2L}$$
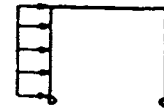
$$H_B = \frac{wh}{4}\left[1 + \frac{K}{2(2K+3)}\right]$$

$$H_A = H_B - wh$$

(7)
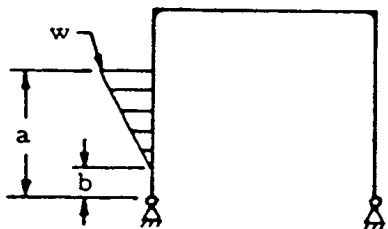
$$V_A = -V_B = \frac{w}{6L}(2a+b)(b-a)$$

$$H_B = \frac{-V_A L}{2h} + \frac{K X_{10}}{h(2K+3)}$$

Where:

$$X_{10} = \frac{w}{120h^2(a-b)}[-30h^2 b(a^2 - b^2)$$

$$+ 20h^2(a^2 - b^2) + 15b(a^4 - b^4) - 12(a^5 - b^5)]$$

$$H_A = H_B + \frac{w(b-a)}{2}$$

For Special Case: b = 0, a = L

$$V_A = -V_B = \frac{-wh^2}{3L}$$

$$H_B = \frac{wh}{10}\left(\frac{\frac{1}{4}K+5}{2K+3}\right)$$
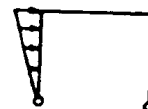
$$H_A = H_B - \frac{wh}{2}$$

TABLE 5-3

Reaction Forces and Moments on Rectangular Frames (continued)

(8)
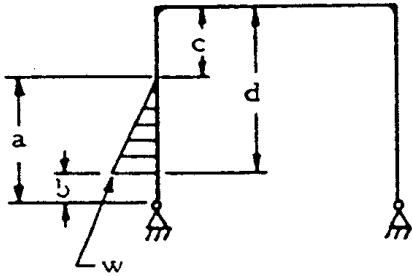
$$V_A = -V_B = \frac{-w}{6L}(a^2 + ac - 2c^2)$$

$$H_B = \frac{-V_A L}{2h} + \frac{KX_7}{(2K+3)h}$$

Where:

$$X_7 = \frac{w}{120h^2(d-c)}\left[3(4d^5 + c^5) - 15h(3d^4 + c^4)\right.$$

$$\left. + 20h^2(2d^3 + c^3) - 15cd^2(2h-d)^2\right]$$

For Special Case: $b = c = 0$, $a = d = h$

$$V_A = -V_B = \frac{-wh^2}{6L}$$

$$H_B = \frac{wh}{12}\left[1 + \frac{7K}{10(2K+3)}\right]$$

(9)
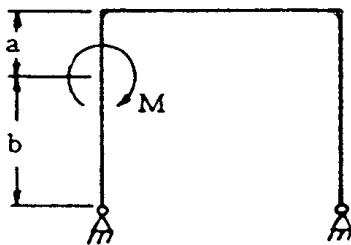
$$V_A = -V_B = \frac{-M}{L}$$

$$H_A = H_B = \frac{3\left[K(2ab+a^2) + h^2\right]M}{2h^3(2K+3)}$$

5 - 20

TABLE 5-3

Reaction Forces and Moments on Rectangular Frames (continued)

(10)
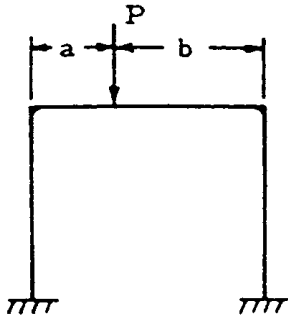
$$V_A = \frac{Pb}{L}\left[1 + \frac{a(b-a)}{L^2(6K+1)}\right] \quad V_B = P - V_A$$

$$H_A = H_B = \frac{3Pab}{2Lh(K+2)}$$

$$M_A = \frac{Pab}{L}\left[\frac{1}{2(K+2)} - \frac{(b-a)}{2L(6K+1)}\right]$$

$$M_B = \frac{Pab}{L}\left[\frac{1}{2(K+2)} + \frac{(b-a)}{2L(6K+1)}\right]$$

For Special Case: $a = b = L/2$

$$V_A = V_B = P/2$$

$$H_A = H_B = \frac{3PL}{8h(K+2)}$$

$$M_A = M_B = \frac{PL}{8(K+2)}$$
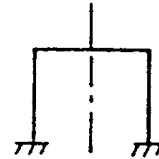
(11)
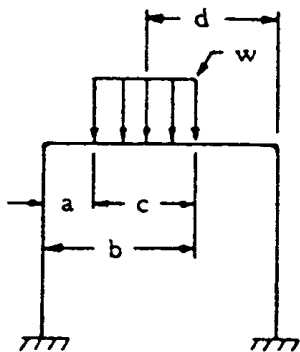
$$V_A = \frac{wcd}{L} + \frac{X_1 - X_2}{L(6K+1)} \quad V_B = wc - V_A$$

$$H_A = H_B = \frac{3(X_1 + X_2)}{2h(K+2)}$$

$$M_A = \frac{X_1 + X_2}{2(K+2)} - \frac{X_1 - X_2}{2(6K+1)}$$

$$M_B = \frac{X_1 + X_2}{2K+2} + \frac{X_1 - X_2}{2(6K+1)}$$

Where:

$$X_1 = \frac{-wc}{24L}\left[\frac{24d^3}{L} - \frac{6bc^2}{L} + \frac{3c^2}{L} + 4c^2 - 24d^2\right]$$

$$X_2 = \frac{wc}{24L}\left[\frac{24d^3}{L} - \frac{6bc^2}{L} + \frac{3c^3}{L} + 2c^2 - 48d^2 + 24dL\right]$$

5 - 21

TABLE 5-3

Reaction Forces and Moments on Rectangular Frames (continued)
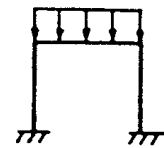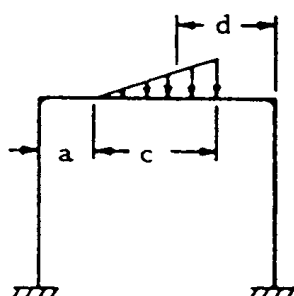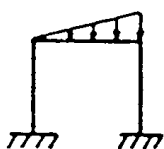
For Special Case: $a = 0, \ c = b = L, \ d = L/2$

$$V_A = V_B = \frac{wL}{2}$$

$$H_A = H_B = \frac{wL^2}{4h(K+2)}$$

$$M_A = M_B = \frac{wL^2}{12(K+2)}$$

---

(12)

$$V_A = \frac{wcd}{2L} + \frac{X_3 - X_4}{L(6K+1)} \qquad V_B = \frac{wc}{2} - V_A$$

$$H_A = H_B = \frac{3(X_3 + X_4)}{2h(K+2)}$$

$$M_A = \frac{X_3 + X_4}{2(K+2)} - \frac{X_3 - X_4}{2(6K+1)}$$

$$M_B = \frac{X_3 + X_4}{2(K+2)} + \frac{X_3 - X_4}{2(6K+1)}$$

Where:

$$X_3 = \frac{-wc}{2L}\left[\frac{d^3}{L} + \frac{c^2}{9} + \frac{51c^3}{810L} + \frac{c^2 b}{6L} - d^2\right]$$

$$X_4 = \frac{wc}{2L}\left[\frac{d^3}{L} + \frac{c^2}{18} + \frac{51c^3}{810L} - \frac{c^2 b}{6L} - 2d^2 + dL\right]$$

For Special Case: $a = 0, \ c = b = L, \ d = L/3$

$$V_A = \frac{wL}{6}\left[1 - \frac{1}{10(6K+1)}\right]$$

$$V_B = \frac{wL}{3}\left[1 + \frac{1}{20(6K+1)}\right]$$

$$H_A = H_B = \frac{wL^2}{8h(K+2)}$$

$$M_A = \frac{wL^2}{120}\left(\frac{5}{K+2} + \frac{1}{6K+1}\right)$$

$$M_B = \frac{wL^2}{120}\left(\frac{5}{K+2} - \frac{1}{6K+1}\right)$$

TABLE 5-3

Reaction Forces and Moments on Rectangular Frames (continued)

---

(13)
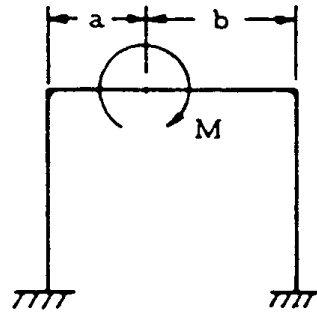
$$V_A = -V_B = \frac{-6(ab+L^2K)M}{L^3(6K+1)}$$

$$H_A = H_B = \frac{3(b-a)M}{2Lh(K+2)}$$

$$M_A = M\left\{\frac{6ab(K+2)-L[a(7K+3)-b(5K-1)]}{2L^2(K+2)(6K+1)}\right\}$$

$$M_P = M + M_A + V_A L$$

---

(14)
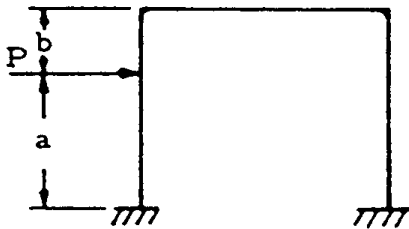
$$V_A = -V_B = \frac{-3Pa^2K}{Lh(6K+1)}$$

$$H_B = \frac{Pa}{2h}\left[\frac{h}{b} - \frac{h+b+K(b-a)}{h(K+2)}\right]$$

$$M_A = \frac{Pa}{2h}\left[\frac{-b(h+b+bK)}{b(K+2)} - h + \frac{3aK}{b(K+1)}\right]$$

$$M_B = \frac{Pa}{2h}\left[\frac{-b(h+b+bK)}{h(K+2)} + h - \frac{3aK}{6(K+1)}\right]$$

$$H_A = H_B - P$$

5 - 23

TABLE 5-3

Reaction Forces and Moments on Rectangular Frames (continued)

(15)
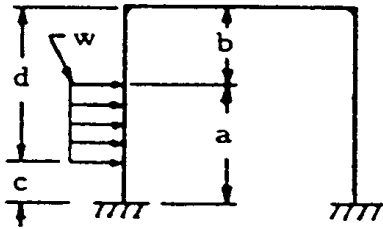
$$V_A = -V_B = \frac{M_A}{L} + \frac{M_B}{L} - \frac{w(a^2-c^2)}{2L}$$

$$H_B = \frac{w(a^2-c^2)}{2h} - \frac{X_5}{2h} + \frac{X_6(K-1)}{2h(K+2)}$$

$$H_A = H_B - w(a-c)$$

$$M_A = \frac{-\left(3K+1\right)\left[\frac{w(a^2-c^2)}{2} - X_5\right]}{2(6K+1)} - \frac{X_6}{2}\left[\frac{1}{K+2} + \frac{3K}{6K+1}\right] - X_5$$

$$M_B = \frac{\left(3K+1\right)\left[\frac{w(a^2-c^2)}{2} - X_5\right]}{2(6K+1)} - \frac{X_6}{2}\left[\frac{1}{K+2} + \frac{3K}{6K+1}\right]$$

Where:

$$X_5 = \frac{w}{12h^2}\left[d^3(4h-3d) - b^3(4h-3b)\right]$$

$$X_6 = \frac{w}{12h^2}\left[a^3(4h-3a) - c^3(4h-3c)\right]$$

For Special Case: c = 0, b = 0, a = d = h

$$V_A = -V_B = \frac{-wh^2 K}{L(6K+1)}$$
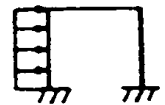
$$H_B = \frac{wh(2K+3)}{8(K+2)}$$

$$H_A = H_B - wh$$

$$M_A = \frac{-wh^2}{24}\left[\frac{30K+7}{6K+1} + \frac{1}{K+2}\right]$$

5 - 24

TABLE 5-3

Reaction Forces and Moments on Rectangular Frames (continued)

(16)
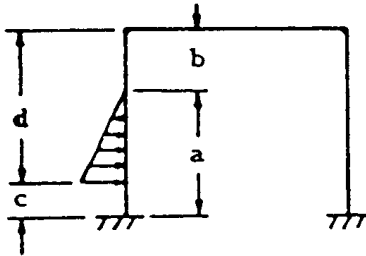
$$V_A = -V_B = \frac{M_A}{L} + \frac{M_B}{L} - \frac{w(a^2 + ac - 2c^2)}{6L}$$

$$H_B = \frac{w(a^2 + ac - 2c^2)}{12h} - \frac{X_8}{2h} + \frac{X_9(K-1)}{2h(K+2)}$$

$$H_A = H_B - \frac{w(a-c)}{2}$$

$$M_A = \frac{-\left(3K+1\right)\left[\frac{w(a^2 + ac - 2c^2)}{6} - X_8\right]}{2(6K+1)}$$

$$- \frac{X_9}{2}\left[\frac{1}{K+2} + \frac{3K}{6K+1}\right] - X_8$$

$$M_B = \frac{\left(3K+1\right)\left[\frac{w(a^2 + ac - 2c^2)}{6}\right] - X_8}{2(6K+1)}$$

$$- \frac{X_8}{2}\left[\frac{1}{K+2} - \frac{3K}{6K+1}\right]$$

Where:

$$X_8 = \frac{w}{60h^2(d-b)}\left[15(h+b)(d^4 - b^4) - 12(d^5 - b^5)\right.$$

$$\left. - 20bh(d^3 - b^3)\right]$$

$$X_9 = \frac{w}{60h^2(d-b)}\left[10d^2h^2(2d - 3b) + 10bh(4d^3 + b^2h - b^3)\right.$$

$$\left. - d^4(30h + 15b) + 12d^5 + 3b^5\right]$$

TABLE 5-3

Reaction Forces and Moments on Rectangular Frames (continued)

<u>For Special Case</u>: $b = c = 0$, $a = d = h$

$$V_A = -V_B = \frac{-wh^2 K}{4L(6K+1)}$$
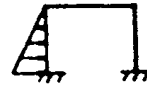
$$H_B = \frac{wh(3K+4)}{40(K+2)}$$

$$H_A = H_B - \frac{wh}{2}$$

$$M_A = \frac{wh^2}{60}\left[\frac{27K+7}{2(6K+1)} + \frac{3K+7}{K+2}\right]$$

$$M_B = \frac{wh^2}{60}\left[\frac{27K+7}{2(6K+1)} - \frac{1}{K+2}\right]$$

(17)
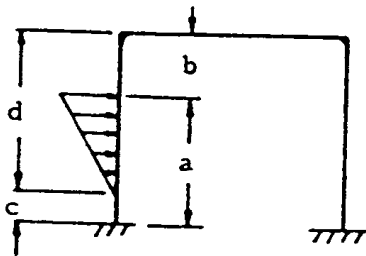
$$V_A = -V_B = \frac{M_A}{L} + \frac{M_B}{L} - \frac{w(2a+c)(a-c)}{6L}$$

$$H_B = \frac{w(2a^2 - ac - c^2)}{12h} - \frac{X_{11}}{2h} + \frac{X_{12}(K-1)}{2h(K+2)}$$

$$H_A = H_B - \frac{w(a-c)}{2}$$

$$M_A = \frac{-\left(3K+1\right)\left[\frac{w(2a^2 - ac - c^2)}{6} - X_{11}\right]}{2(6K+1)}$$

$$- \frac{X_{12}}{2}\left[\frac{1}{K+2} + \frac{3K}{6K+1}\right] - X_{11}$$

$$M_B = \frac{\left(3K+1\right)\left[\frac{w(2a^2 - ac - c^2)}{6} - X_{11}\right]}{2(6K+1)}$$

$$- \frac{X_{12}}{2}\left[\frac{1}{K+2} - \frac{3K}{6K+1}\right]$$

5 - 26

TABLE 5-3

Reaction Forces and Moments on Rectangular Frames (continued)

Where:

$$X_{11} = \frac{w}{60h^2(d-b)} \left[5hd^4 - 3d^5 - 20hdb^3 - 12b^4(d+h)\right]$$

$$X_{12} = \frac{w}{60h^2(a-c)} \left[15(h+c)(a^4-c^4) - 12(a^5-c^5)\right.$$

$$\left. - 20\,ch\,(a^3-c^3)\right]$$

For Special Case: $b = c = 0$, $a = d = h$

$$V_A = -V_B = \frac{-3Kwh^2}{4L(6K+1)}$$

$$H_B = \frac{wh(7K+11)}{40(K+2)}$$

$$H_A = H_B - \frac{wh}{2}$$

$$M_A = \frac{-wh^2}{120}\left[\frac{87K+22}{6K+1} + \frac{3}{K+2}\right]$$

$$M_B = \frac{wh^2}{40}\left[\frac{21K+6}{6K+1} - \frac{1}{K+2}\right]$$

5 - 27

TABLE 5-3

Reaction Forces and Moments on Rectangular Frames (concluded)

(18)
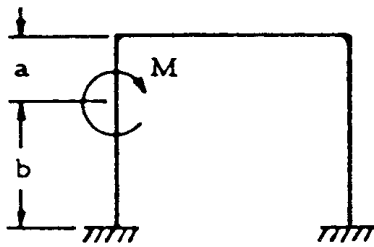
$$V_A = -V_B = \frac{-6bKM}{hL(6K+1)}$$

$$H_A = H_B = \frac{3bM[2a(K+1)+b]}{2h^3(K+2)}$$

$$M_A = \frac{-M}{2h^2(K+2)(6K+1)}[4a^2 + 2ab + b^2 + K(26a^2 - 5b^2) + 6aK^2(2a-b)]$$

$$M_B = -V_A L - M - M_A$$

TABLE 5-4

Rectangular Forces and Moments on Trapezoidal Frames *

$$F = \frac{I_2}{I_1} = \left(\frac{s}{b}\right)$$

$$G = 3 + 2f$$

$$M_A = M_B = 0 \text{ if uprights}$$
$$\text{are pinned}$$
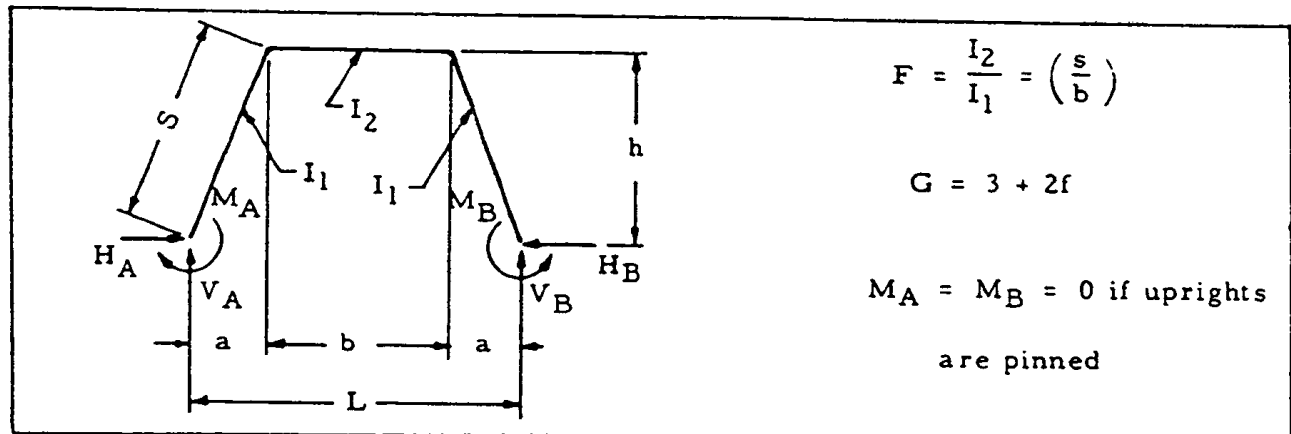
(1)
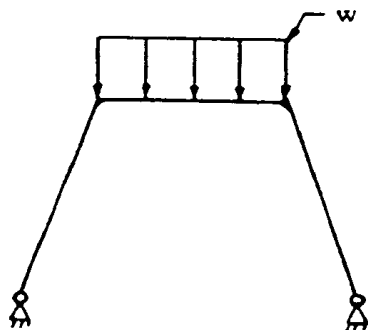
$$V_A = V_B = \frac{wb}{2}$$

$$H_A = H_B = \frac{wh}{2h}\left(a + \frac{b}{4G}\right)$$

(2)
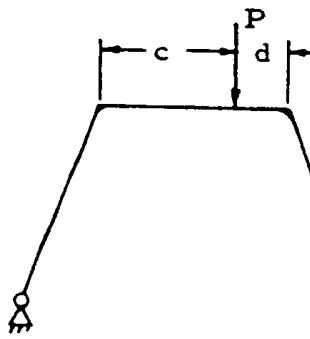
$$V_A = \frac{P(a+d)}{L} \qquad V_B = P - V_A$$

$$H_A = H_B = \frac{P}{2h}\left(a - \frac{3cd}{bG}\right)$$

(3)
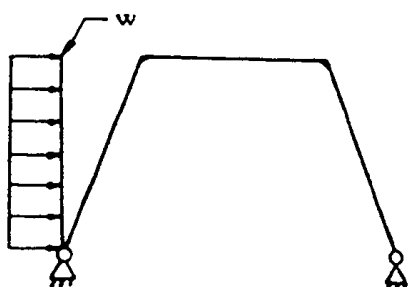
$$V_A = -V_B = \frac{-wh^2}{2L}$$

$$H_B = \frac{wh}{4}\left(1 - \frac{F}{2G}\right)$$

$$H_A = H_B - wh$$

* Griffel, William, Handbook of Formulas for Stress and Strain

TABLE 5-4

Rectangular Forces and Moments on Trapezoidal Frames (concluded)
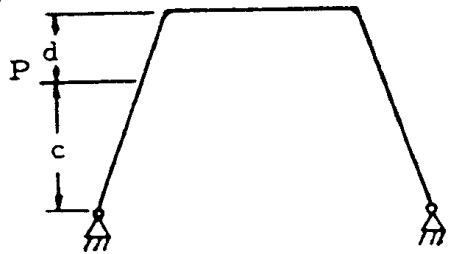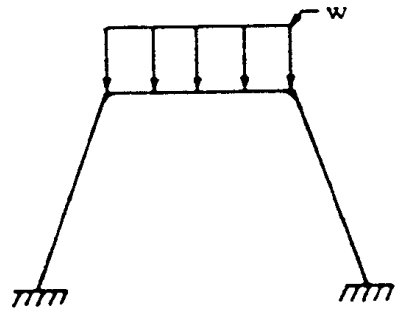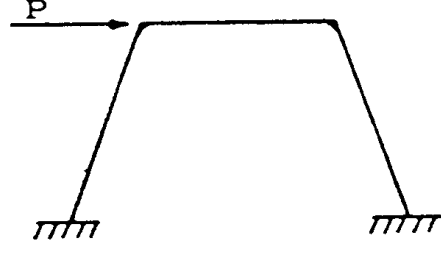
(4)

$$V_A = -V_B = \frac{-Pc}{L}$$

$$H_B = \frac{Pc}{2h}\left[1 + \frac{F}{G}\left(1 - \frac{c^2}{h^2}\right)\right]$$

$$H_A = H_B - P$$

(5)

$$V_A = V_B = \frac{wb}{2}$$

$$H_A = H_B = \frac{wb}{2h}\left[a + \frac{b}{4+2F}\right]$$

$$M_A = M_B = \frac{wb^2}{12(2+F)}$$

(6)

$$V_A = -V_B = \frac{-Ph}{L}(1-2)$$

$$H_A = -H_B = \frac{-P}{2}$$

$$M_A = -M_B = \frac{-PhZ}{2}$$

TABLE 5-5

Reaction Forces and Moments on Triangular Frames
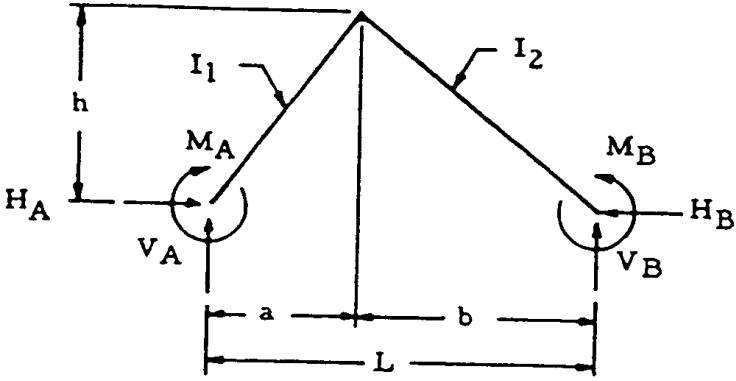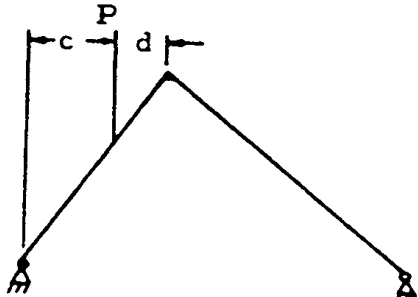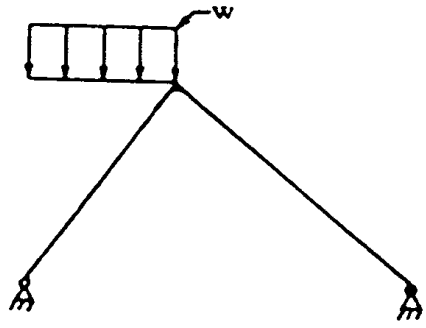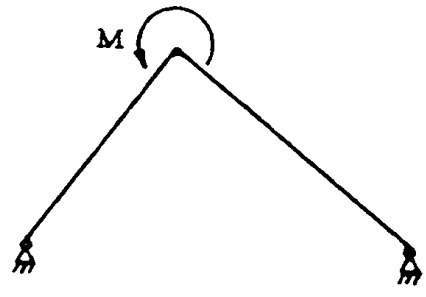
$$K = \frac{I_2 h}{I_1 L}$$

$M_A = M_B = 0$ if uprights are pinned

(1)

$$V_B = \frac{Pc}{L} \qquad V_A = P - V_B$$

$$H_A = H_B = \frac{Pc}{L}\left[\frac{b}{L} + \frac{d(a+c)}{2a^2(K+1)}\right]$$

(2)

$$V_A = wa\left(1 - \frac{a}{2L}\right) \qquad V_B = wa - V_A$$

$$H_A = H_B = \frac{wa^2}{8h}\left(\frac{4b}{L} + \frac{1}{1+K}\right)$$

(3)

$$V_A = -V_B = \frac{M}{L}$$

$$H_A = H_B = \frac{M}{hL}\left(\frac{a-bK}{K+1}\right)$$

TABLE.5-5

Reaction Forces and Moments on Triangular Frames (continued)

(4)
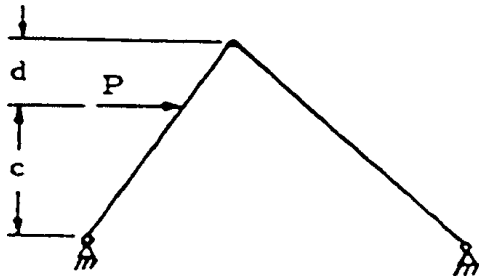
$$V_A = -V_B = \frac{-Pc}{L}$$

$$H_B = \frac{Pc}{h}\left[\frac{b}{L} + \frac{d(h+c)}{2h^2(K+1)}\right]$$

$$H_A = H_D - P$$

(5)
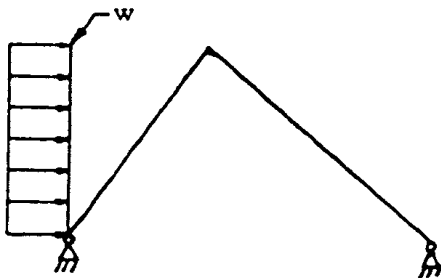
$$V_A = -V_B = \frac{wh^2}{2L}$$

$$H_B = \frac{wh}{8}\left(\frac{4b}{L} + \frac{1}{K+1}\right)$$

$$H_A = H_B - wh$$

(6)
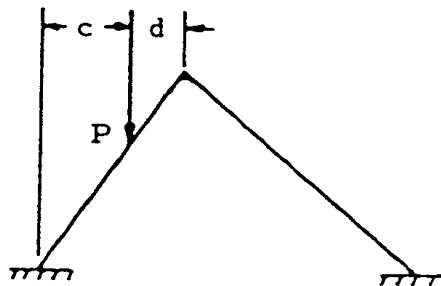
$$V_B = \frac{Pc}{L}\left[1 - \frac{d(a+d)}{2a^2}\right] \qquad V_A = P - V_B$$

$$H_A = H_B = \frac{Pcb}{Lh} + \frac{Pcd}{6La^2h(K+1)}\{[-b(3K+4)-2L]$$

$$[a+d] + 2(2L+b)(a+c)+3ac\}$$

$$M_A = \frac{-Pcd}{6a^2(K+1)}\left[(a+d)(3K+4) - 2(a+c)\right]$$

$$M_B = \frac{Pc^2d}{2a^2(K+1)}$$

TABLE 5-5

Reaction Forces and Moments on Triangular Frames (continued)

(7)
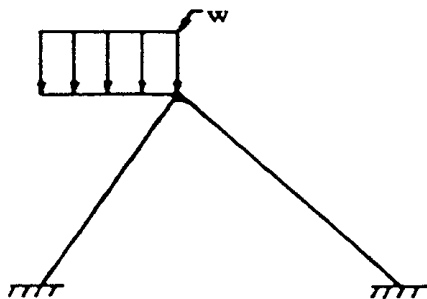
$$V_A = wa \left(1 - \frac{3a}{8L}\right) \quad V_B = \frac{3wa^2}{8L}$$

$$H_A = H_B = \frac{wa^2}{24Lh(K+1)} [b(10+9K) + 2L + a]$$

$$M_A = \frac{-wa^2(3K+2)}{24(K+1)}$$

$$M_B = \frac{wa^2}{24(K+1)}$$

(8)
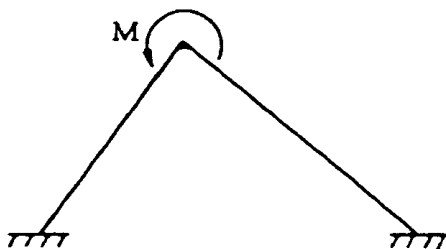
$$V_A = -V_B = \frac{3M}{2L}$$

$$H_A = H_B = \frac{3M(a-bK)}{2hL(K+1)}$$

$$M_A = \frac{-KM}{2(K+1)}$$

$$M_B = \frac{M}{2(K+1)}$$

(9)
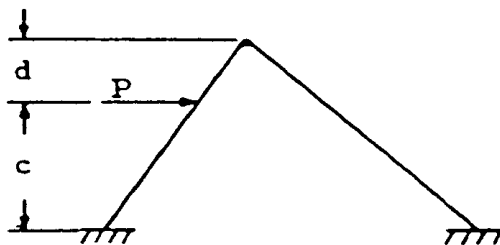
$$V_A = -V_B = \frac{-Pc}{L} \left[1 - \frac{d(h+d)}{2h^2}\right]$$

$$H_B = \frac{Pc}{Lh} \left\{b + \frac{d}{6h^2(K+1)} \left[(h+d)(-3bK-4b-2L)\right.\right.$$
$$\left.\left. + 2(2L+b)(h+c) + 3ac\right]\right\}$$

$$M_A = \frac{-Qcd}{6h^2(K+1)} [(h+d)(3K+4) - 2(h+c)]$$

$$M_B = \frac{Qcd}{6h^2(K+1)} (h + 2c + d)$$

5 - 33

TABLE 5-5

Reaction Forces and Moments on Triangular Frames (concluded)

(10)
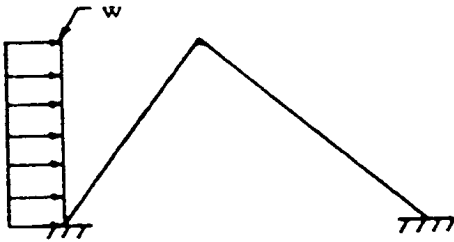
$$V_A = -V_B = \frac{-3wh^2}{8L}$$

$$H_B = \frac{wh}{8L(K+1)} \left[b(3K+4) + a \right]$$

$$H_A = H_B - wh$$

$$M_A = \frac{-wh^2(3K+2)}{24(K+1)}$$

$$M_B = \frac{wh^2}{24(K+1)}$$

From Table 5-4, case 2,

$$V_A = \frac{P(a+d)}{L} = \frac{1000(5+7.5)}{25} = 500 \text{ lb.}$$

$$V_B = P - V_A = 1000 - 500 = 500 \text{ lb.}$$

$$H_A = H_B = \frac{P}{2h} \left(a + \frac{3cd}{bG} \right) = \frac{1000}{2(10)} \left[5 + \frac{3(7.5)(7.5)}{15(5.24)} \right] = 357 \text{ lb.}$$

A free-body diagram may be constructed for a section of the frame leg, as shown in Figure 5-15. Equating the sum of the moment to zero gives

$$M = -500x_1 + 357(2x_1) = 214x_1$$
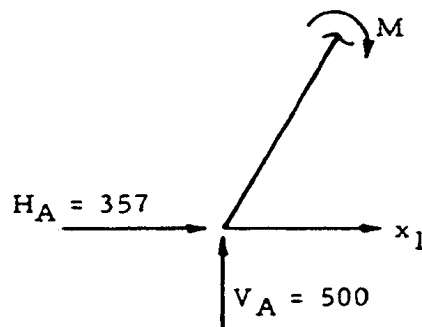
Figure 5-15. Section of Frame Leg

At the left frame joint,

$$M = 214x = 214(5) = 1070 \text{ in. lb.}$$

A free-body diagram may now be drawn for a section of the horizontal portion of the frame to the left of the load as in Figure 5-16. Equating the sum of the moments to zero gives

$$M = 1070 - 500x_2$$

By considering symmetry, the moment diagram of the given frame may be drawn as shown in Figure 5-17.
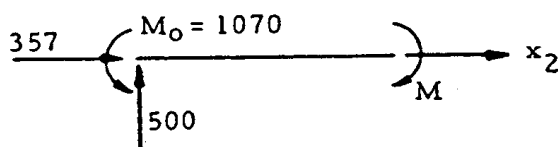
Figure 5-16. Section of Horizontal Portion of Frame
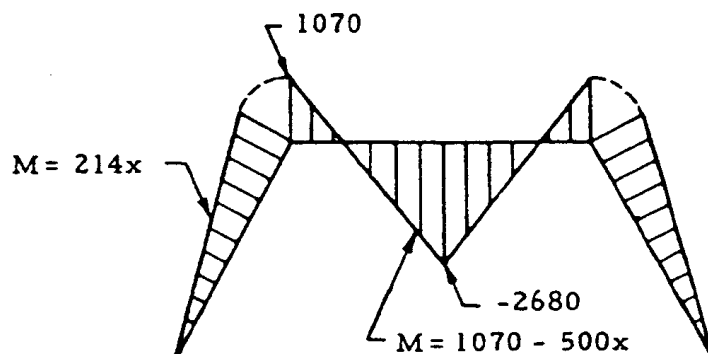
Figure 5-17. Moment Diagram for Trapezoidal Frame

5.9 Circular Rings and Arches

Table 5-6 gives formulas for the bending moments, tensions, shears, and deflections of closed circular rings and circular arches of uniform cross section loaded in various ways. Cases 1 through 21 treat closed rings, and cases 21 through 24 treat arches. By superposition, the formulas given by Table 5-6 can be combined to cover a wide variety of loading conditions.

These ring formulas are based on the following assumptions: (1) The ring is of such large radius in comparison with its radial thickness that the deflection theory for straight beams is applicable. (2) Its deflections are due solely to bending, the effect of direct axial tension or compression and that of shear being negligible. (3) It is nowhere stressed beyond the elastic limit. (4) It is not so severely deformed as to lose its essentially circular shape.

Since many of the formulas in Table 5-6 consist of a large number of terms, each of which may be large in comparison with the end result, calculations should be made with extreme care in order to ensure accurate results.

TABLE 5-6

Formulas for Closed Circular Rings of Uniform Cross Section
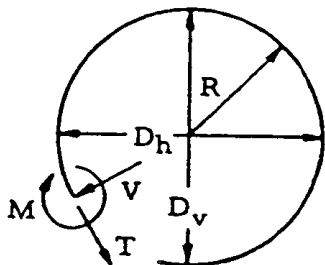
M_0 = M at $x = 0$, $y = -R$

T_0 = T at $x = 0$, $y = -R$

V_0 = V at $x = 0$, $y = -R$

I = moment of inertia of ring cross section

$a = \cos x$	$e = \cos \phi$
$b = \sin x$	$f = \sin \phi$
$c = \cos \beta$	
$d = \sin \beta$	

ΔD_h = increase in horizontal diameter

ΔD_v = increase in vertical diameter

x = angular distance from bottom of ring

(1)
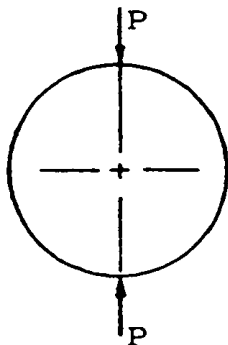
$$M = PR\left(0.3183 - \frac{b}{2}\right)$$

$$\text{Max} + M = 0.3182\, PR \text{ at } x = 0$$

$$\text{Max} - M = -0.1817\, PR \text{ at } x = \frac{\pi}{2}$$

$$T = \frac{-Pb}{2}$$

$$V = \frac{-Pa}{2}$$

$$\Delta D_h = 0.137 \frac{PR^3}{EI}$$

$$\Delta D_v = 0.149 \frac{PR^3}{EI}$$

TABLE 5-6

Formulas for Closed Circular Rings of Uniform Cross Section (continued)

---
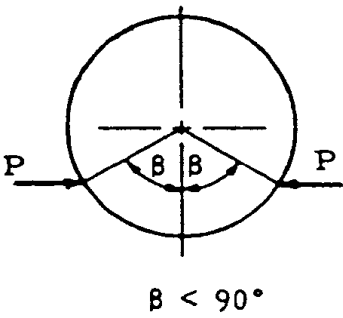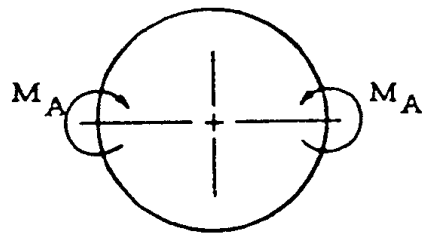
(2)

$\beta < 90°$

if $(0 < x < \beta)$

$M = PR[0.3183(d - c\beta + a - adc) - a + c]$

$T = P[0.3183\, a(\beta - dc) - a]$

$V = P[0.3183\, b(dc - \beta) + b]$

if $(\beta < x < \pi)$

$M = PR[0.3183(d - c\beta + a\beta - adc)]$

$T = P[0.3183\, u(\beta - sc)]$

$V = P[0.3183\, b(dc - \beta)]$

$\Delta D_h = \dfrac{PR^3}{EI}[0.6366(d - c\beta) + \tfrac{1}{2}(dc - \beta)]$

$\Delta D_v = \dfrac{PR^3}{EI}[0.6366(d - c\beta) + c + \dfrac{d^2}{2} - 1]$

---

(3)

$M = M_A(0.6366a - \tfrac{1}{2})$ if $(0 < x < \pi/2)$

$M = M_A(0.6366a + \tfrac{1}{2})$ if $(\pi/2 < x < \pi)$

Max + M = $M_A/2$ just above M_A

Max - M = $-M_A/2$ just below M_A

$T = 0.6366\, M_A a/R$

$V = -0.6366\, M_A a/R$

$\Delta D_h = \Delta D_v = 0$

TABLE 5-6

Formulas for Closed Circular Rings of Uniform Cross Section (continued)
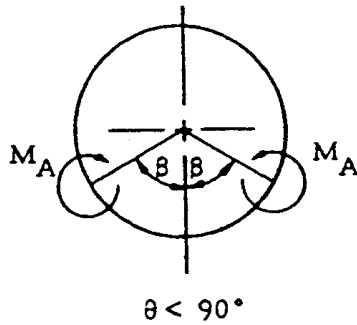
(4) $\theta < 90°$	**if** $(0 < x < \beta)$ $M = M_A[0.3183(2ad+\beta) - 1]$ $T = 0.6366\, M_o\, ad/R$ $V = 0.6366\, M_o\, bd/R$ **if** $(\theta < x < \pi)$ $M = 0.3183\, M_A(2ad+\beta)$ $T = 0.6366\, M_A\, ad/R$ $V = -0.6366\, M_A\, bd/R$ $\Delta D_h = \dfrac{M_A R^2}{EI}(0.6366\beta - d)$ $\Delta D_v = \dfrac{M_A R^2}{EI}(0.6366\beta + c - 1)$
(5) $2P$	**if** $(0 < x < \pi/2)$ $M = PR(0.3183a + b - 0.8183)$ $T = P(0.3183\,a + b)$ $V = P(a - 0.3183\,b)$ **if** $(\pi/2 < x < \pi)$ $M = PR(0.1817 + 0.3183\,a)$ $T = 0.3183\, Pa$ $V = -0.3183\, Pb$ $\Delta D_h = -0.1366\,\dfrac{PR^3}{EI}$ $\Delta D_v = 0.1488\,\dfrac{PR^3}{EI}$
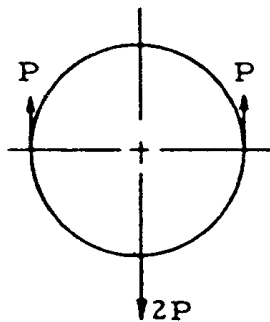
TABLE 5-6

Formulas for Closed Circular Rings of Uniform Cross Section (continued)
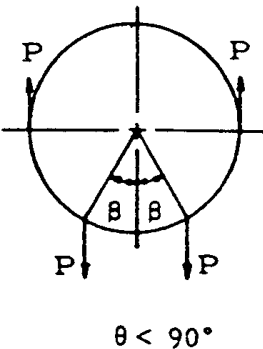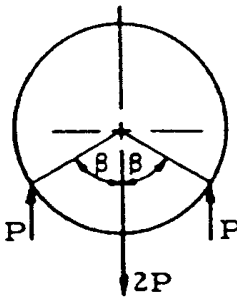
(6) $\theta < 90°$	if $(0 < x < \beta)$ $\quad M = PR[0.3183(ac^2 - d\beta - c) + d - \tfrac{1}{2}]$ $\quad T = 0.3183\ Pac^2$ $\quad V = -0.3183\ Pbc^2$ if $(\beta < x < \pi/2)$ $\quad M = PR[0.3183(ac^2 - d\beta - c) + b - \tfrac{1}{2}]$ $\quad T = P(0.3183\ ac^2 + b)$ $\quad V = P(a - 0.3183\ bc^2)$ if $(\pi/2 < x < \pi)$ $\quad M = PR[0.3183(ac^2 - d\beta - c) + \tfrac{1}{2}]$ $\quad T = P(0.3183\ ac^2)$ $\quad V = -0.3183\ Pbc^2$ $\Delta D_h = \dfrac{PR^3}{EI}[\tfrac{1}{2}(d^2 + 1) - 0.6366(d\beta + c)]$ $\Delta D_v = \dfrac{PR^3}{EI}[d - \tfrac{1}{2}(dc + \beta) - 0.6366(d\beta + c) + 0.7854]$
(7) 	if $(0 < x < \beta)$ $\quad M = PR[0.3183(d\beta + c + ad^2 - 1) - a + b]$ $\quad T = P(0.3183\ ad^2 + b)$ $\quad V = P(a - 0.3183\ bd^2)$

3 - 39

TABLE 5-6

Formulas for Closed Circular Rings of Uniform Cross Section (continued)

---
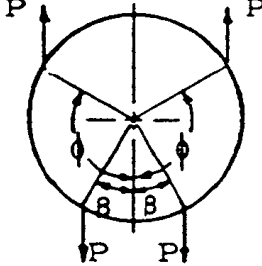
if $(\beta < x < \pi)$

$\quad M = 0.3183\ PR\,(d\beta + c + as^2 - 1)$

$\quad T = 0.3183\ Pas^2$

$\quad V = -0.3183\ Pbs^2$

$\Delta D_h = \dfrac{PR^3}{EI}\left[\dfrac{(d^2+2)}{2} + 0.6366(d\beta + c - 1) - 2d\right]\ \text{if}\ \beta > 90°$

$\Delta D_h = \dfrac{PR^3}{EI}\left[0.6366(d\beta + c - 1) - d^2/2\right]\ \text{if}\ \beta < 90°$

$\Delta D_v = \dfrac{PR^3}{EI}\left[(dc+\beta)/2 + 0.6366(d\beta + c - 1) - d\right]$

---

(8)

if $(0 < x < \beta)$

$\quad M = PR\left[0.3183(f\phi + e - d\beta - c - ad^2 + af^2) - f + d\right]$

$\quad T = 0.3183\ Pa\,(f^2 - d^2)$

$\quad V = 0.3183\ Pb\,(d^2 - f^2)$

if $(\beta < x < \phi)$

$\quad M = PR\left[0.3183\,(f\phi + e - d\beta - c - ad^2 + af^2) - f + b\right]$

$\quad T = P\left[0.3183\,a\,(f^2 - d^2) + b\right]$

$\quad V = P\left[0.3183\,b\,(d^2 - f^2) + a\right]$

if $(\phi < x < \pi)$

$\quad M = 0.3183\ PR(f\phi + e - d\beta - c - ad^2 + af^2)$

$\quad T = 0.3183\ Pa\,(f^2 - d^2)$

$\quad V = 0.3183\ Pb\,(d^2 - f^2)$

TABLE 5-6

Formulas for Closed Circular Rings of Uniform Cross Section (continued)
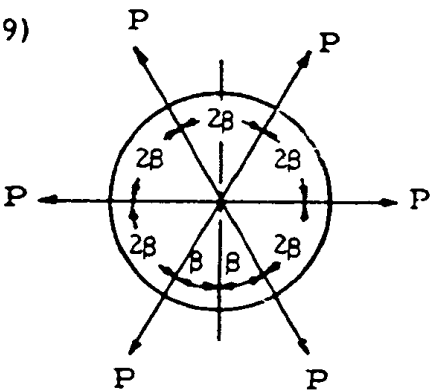
$$\Delta D_h = \frac{PR^3}{EI} [(d^2+f^2)/2 + 0.6366(f\phi+e-df-c)+1-2f]$$

$$\Delta D_v = \frac{PR^3}{EI} [(fe+\phi-dc-\beta)/2 + 0.6366(f\phi+e-d\beta-c)+d-f]$$

(9)

if $(0 < x < 0)$ $M = \frac{PR}{2}\left(\frac{a}{d} - \frac{1}{\beta}\right)$

$\text{max} + M = \frac{PR}{2}\left(\frac{1}{d} - \frac{1}{\beta}\right)$ at $x = 0,\ 2\beta,\ 4\beta \ldots$

$\text{max} - M = \frac{PR}{2}\left(\frac{1}{\beta} - \cot\beta\right)$ at each load

$\text{max } T = \frac{P}{2d}$ at $x = 0,\ 2\beta,\ 4\beta \ldots$

$T = \frac{P}{2}\cot\beta$ at loads

Radial displacement at each point load =

$$\frac{PR^3}{2EI}\left[\frac{(\beta+dc)}{2d^2} - \frac{1}{\beta}\right] \text{ outward}$$

Radial displacement at $x = 0,\ 2\beta,\ 4\beta \ldots$ =

$$\frac{PR^3}{4EI}\left(\frac{2}{\beta} - \frac{1}{d} - \frac{c\beta}{d^2}\right) \text{ inward}$$

5 – 41

TABLE 5-6

Formulas for Closed Circular Rings of Uniform Cross Section (continued)

(10)

$2wR \sin\beta$
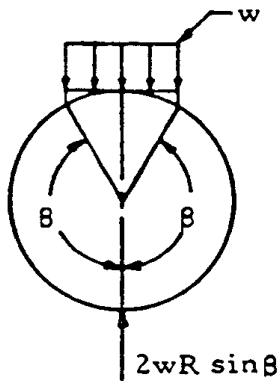
$$M_0 = wR^2 \left[\frac{1}{4} + \frac{d^2}{2} + 0.3183 \left(d - \frac{\beta d^2}{2} - \frac{d^3}{3} - \frac{3dc}{4} - \frac{\beta}{4} \right) \right]$$

$$T_0 = -0.1061\, w\, Rd^3$$

if $(0 < x < \theta)$

$$M = M_0 - wR^2 \left[db - 0.1061 d^3 (1-a) \right]$$

$$T = -wR (0.1061\, d^3 a + db)$$

$$V = wR (0.1061\, d^3 b - da)$$

if $(\theta < x < \pi)$

$$M = M_0 + wR^2 \left[0.1061 d^3 (1-a) - (d^2 + b^2)/2 \right]$$

$$T = -wR (0.1061\, d^3 a + b^2)$$

$$V = wR (0.1061\, d^3 b - ba)$$

$$\Delta D_h = \frac{2wR^4}{EI} \left[\frac{1}{4} - \frac{d}{2} + \frac{d^2}{2} - \frac{d^3}{12} - 0.3183 \left(\frac{\beta}{4} + \frac{3dc}{4} + \frac{\beta d^2}{2} - d \right) \right]$$

$$\Delta D_v = \frac{2wR^4}{EI} \left[\frac{1}{12} + \frac{d^2}{4} - \frac{d^2 c}{12} - \frac{\beta d}{4} - \frac{c}{6} - 0.3183 \right.$$

$$\left. \left(\frac{\beta}{4} + \frac{3dc}{4} + \frac{\beta d^2}{2} - d \right) \right]$$

TABLE 5-6

Formulas for Closed Circular Rings of Uniform Cross Section (continued)

(11)
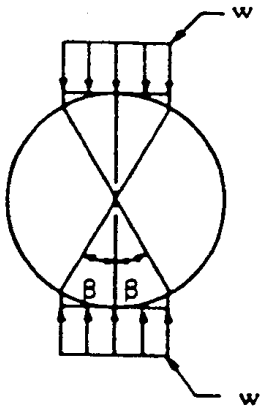
$$M_0 = wR^2 \left[0.3183 \left(\frac{\beta}{2} + \beta d^2 + \frac{3dc}{2} \right) - \frac{d^2}{2} \right]$$

$$T_0 = 0$$

if $(0 < x < \beta)$

$$M = M_0 - wR^2 b^2 / 2$$

$$T = -wRb^2$$

$$V = -wRba$$

if $(\beta < x < \pi - \beta)$

$$M = M_0 - wR^2 \left(db - \frac{d^2}{2} \right)$$

$$T = -wRdb$$

$$V = -wRda$$

$$\Delta D_h = \frac{-wR^4}{EI} \left[d + \frac{d^3}{3} - 0.3183 \beta + 3dc + 2\beta d^2 \right]$$

$$\Delta D_v = \frac{-wR^4}{EI} \left[-0.3183 \left(2\beta d^2 + 3dc + \beta \right) + d^2 - \beta d + \frac{\pi d}{2} \right.$$
$$\left. + \frac{c^3}{3} + \frac{2}{3} - c \right]$$

5 - 43

TABLE 5-6

Formulas for Closed Circular Rings of Uniform Cross Section (continued)

(12)
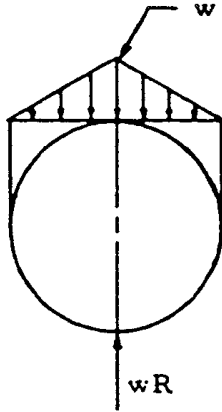
$$M_0 = 0.305 \, w \, R^2$$

$$T_0 = -wR(0.02653)$$

if $(0 < x < \pi/2)$

$$M = M_0 - T_0 R(1-a) - wR^2 b/2$$

$$T = T_0 a - wRb/2$$

$$V = -T_0 b - wRa/2$$

if $(\pi/2 < x < \pi)$

$$M = M_0 - T_0 R(1-a) - wR^2 b/2 - wR^2(1-b)^3/6$$

$$T = T_0 a - wRb/2 + wRb(1-b^2)/2$$

$$V = -T_0 b - wRa/2 + wRa(1-a^2)/2$$

$$\Delta D_h = 0.1228 \, wR^4/(EI)$$

$$\Delta D_v = -0.1220 \, wR^4/(EI)$$
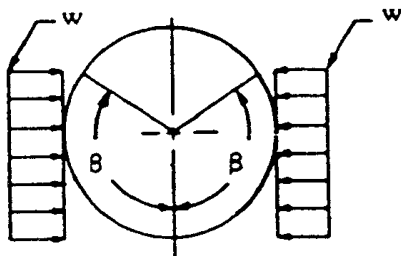
$$M_0 = wR^2 \left[0.3183 \left(\frac{2d}{3} - \beta c + \frac{dc^2}{3} + \frac{\beta c^2}{2} - \frac{3dc}{4} + \frac{\beta}{4} \right) \right.$$

$$\left. - \frac{1}{2} + c - \frac{c^2}{2} \right]$$

$$T_0 = wR \left[0.3183 \left(\frac{2d}{3} + \frac{dc^2}{3} - \beta c \right) + c - 1 \right]$$

if $(0 < x < \beta)$

$$M = M_0 - T_0 R(1-a) - wR^2(1-a^2)/2$$

$$T = T_0 a + wRa(1-a)$$

$$V = T_0 b - wRb(1-a)$$

5 - 44

TABLE 5-6

Formulas for Closed Circular Rings of Uniform Cross Section (continued)

if $(\beta < x < \pi)$

$$M = M_0 - T_0 R(1-a) - wR^2(1-c)[1+c-2a]/2$$

$$T = T_0 a + wRa(1-c)$$

$$V = -T_0 b - wRb(1-c)$$

---

(14)

$$\overline{wR(1-\cos\phi)}$$

$$M_0 = wR^3 \left[0.3183 \left(\frac{\beta}{3} + \frac{d}{9} - \frac{\beta c}{4} - \frac{13dc}{24} + \frac{11dc^2}{36} \right. \right.$$

$$\left. \left. + \frac{\beta c^2}{2} - \frac{ac^3}{12} - \frac{\beta c^3}{6} \right) - (1-c) \frac{3}{6} \right]$$

$$T_0 = wR \left[0.3183 \, (d - \beta c) + c - 1 \right]$$

if $(0 < x < \beta)$

$$M = M_0 - T_0 R (1-a) + wR^3 [(1-a)^3/6 - (1-c)(1-a)^2/2]$$

$$T = T_0 + wR^2 a(1-2c+a)(1-a)/2$$

$$V = -T_0 b - wR^2 b(1-2c+a)(1-a)/2$$

if $(\beta < x < \pi)$

$$M = M_0 - T_0 R(1-a) - wR^3(1-c)^2 \left(\frac{2}{3} + \frac{c}{3} - a \right)/2$$

$$T = T_0 a + wR^2 a(1-c)^2/2$$

$$V = -T_0 b - wR^2 b(1-c)^2/2$$

TABLE 5-6

Formulas for Closed Circular Rings of Uniform Cross Section (continued)

(15)
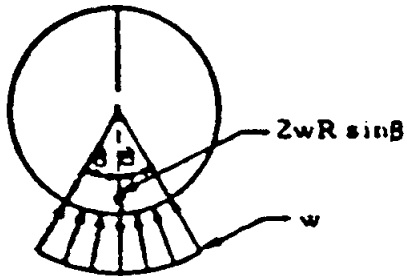
$$M_0 = wR^2 \left[c - 0.3183 (\beta c - \beta) - 1 \right]$$

$$T_0 = wR \left[0.3183 (d - c) + c - 1 \right]$$

if $(0 < x < \beta)$

$$M = M_0 - T_0 R(1-a) - wR^2 (1-a-db)$$

$$T = T_0 a + wR (db + a - 1)$$

$$V = -T_0 b + wR (db - b)$$

if $(\beta < x < \pi)$

$$M = M_0 - T_0 R(1-a) - wR^2 (ca-a)$$

$$T = T_0 a + wR (a - ca)$$

$$V = -T_0 b + wR (cb - b)$$

$$\Delta D_h = \frac{2wR^4}{EI} \left(\frac{\beta c}{4} + 0.31833 - 0.5683d \right) \text{if } \beta < \frac{\pi}{2}$$

$$\Delta D_v = \frac{2wR^4}{EI} \left(\frac{\beta c}{4} + 0.31833 + \frac{c}{2} - 0.3183d - \frac{?}{?} \right)$$

Diagram labels: $2wR \sin\beta$, w

5 - 46

TABLE 5-6

Formulas for Closed Circular Rings of Uniform Cross Section (continued)

(16)

uniform shear

P   P
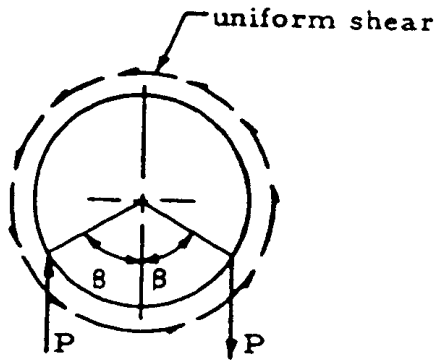
if $(0 < x < \beta)$

$$M = PR \{0.15915 [d\beta + c - f\phi - e + a(d^2 - f^2) - b(dc + \beta + fe + \phi) - x(d+f)] - (d-f)/2 + b\}$$

if $(\beta < x < 2\pi - \phi)$

$$M = PR \{0.15915 [db + c - f0 - 3 + a(d^2 - f^2) - b(dc + \beta + fe + \phi) - x(d+f)] + (d+f)/2\}$$

if $(2\pi - \phi < x < 2\pi)$

$$M = PR \{0.15915 [d\beta + c - f\phi - e + a(d^2 - f^2) - b(dc + \beta + fe + \phi) - x(d+f)] + (d + 3f/2 + b\}$$

if $(0 < x < \beta)$ or $(2\pi - \phi < x < 2\pi)$

$$T = P [0.15915 (ad^2 - af^2 - bdc - b\beta - bfe - b\phi) + b]$$

$$V = P [0.15915(-d - f - bd^2 + bf^2 - adc - a\beta - afe - a\phi) + a]$$

if $(\beta < x < 2\pi - \phi)$

$$T = 0.15915 P(ad^2 - af^2 - bdc - b\beta - bfe - b\phi)$$

$$V = 0.15915 P(-d - f - bd^2 + bf^2 - adc - a\beta - afe - a\phi)$$

5 - 47

TABLE 5-6

Formulas for Closed Circular Rings of Uniform Cross Section (continued)

---

(17)

$\dfrac{MA}{2\pi R^2} \ \dfrac{lb}{in}$
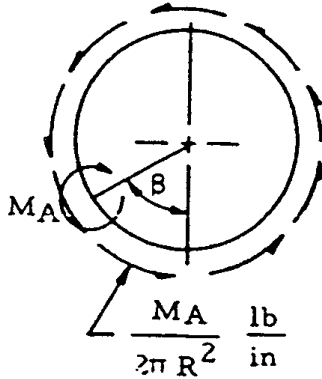
if $(0 < x < \beta)$

$M = M_A[0.3183(ad-bc+\beta/2 - x/2) - \tfrac{1}{2}]$

$T = -0.318 M_A (bc - ad)/R$

$V = -0.3183 M_A(bd + ac + \tfrac{1}{2})/R$

if $(\beta < x < 2\pi)$

$M = M_A[0.3183(bd-bc+\beta/2 - x/2) + \tfrac{1}{2}]$

$T = -0.318, M_A(bc-ad)/R$

$V = -0.3183 M_A(bd+ac+\tfrac{1}{2})/R$

---

(18)

$2\pi Rw$

w lb. per unit length of circumference
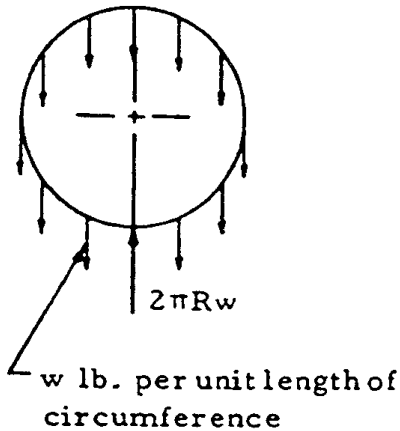
$M = wR^2(1+a/2 - \pi b + xb)$

$\text{Max} + M = M_0 = 3wR^2/2$

$\text{Max} - M = -0.642wR^2 \text{ at } x = 74.6°$

$T = wR(xb - a/2 - \pi b)$

$V = wR(xa + b/2 - \pi a)$

$\Delta D_h = 0.4292 \dfrac{wR^4}{EI}$

$\Delta D_v = -0.18765 \dfrac{wR^4}{EI}$

---

5 - 48

TABLE 5-6

Formulas for Closed Circular Rings of Uniform Cross Section (continued)

(19)

w lb. per unit length of circumference

$\pi w R \qquad \pi w R$
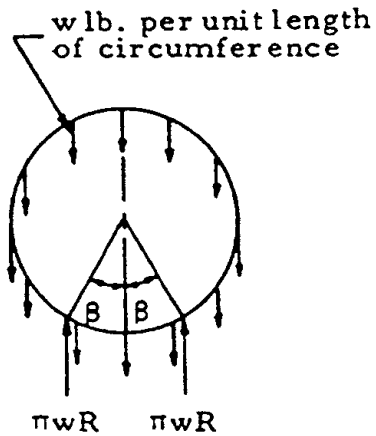
$$M_0 = wR^2(\tfrac{1}{2} + c + \beta d - \pi d + d^2)$$

$$T_0 = wR(d^2 - \tfrac{1}{2})$$

if $(0 < x < \beta)$

$$M = M_0 - T_0 R(1-a) + wR^2(xb + a - 1)$$

$$T = T_0 a + wRxb$$

$$V = -T_0 b + wRxa$$

if $(\beta < x < \pi)$

$$M = M_0 - T_0 R(1-a) + wR^2(xb + a - 1 - \pi b + \pi d)$$

$$T = T_0 a + wR(xb - \pi b)$$

$$V = -T_0 b + wR(xa - \pi a)$$

$$\Delta D_h = \frac{2wR^4}{EI} \left[c + \beta d - \frac{\pi}{4}\left(1 + d^2\right) \right]$$

$$\Delta D_v = \frac{wR^2}{EI} \left[-2.4674 + \frac{\pi}{2}\left(dc + \beta - 2d\right) + 2\left(\beta d + c\right) \right]$$

TABLE 5-6

Formulas for Closed Circular Rings of Uniform Cross Section (continued)

(20)

$\dfrac{P}{2}$ $\dfrac{P}{2}$

$\dfrac{P \sin x}{\pi R}$ lb. per unit length of circumference
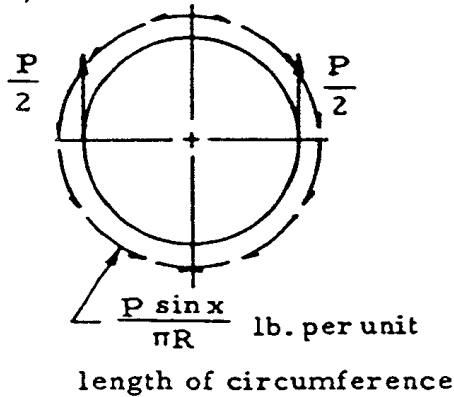
$M_0 = -0.01132\,PR$

$T_0 = -0.07958\,P$

$\max + M = 0.01456\,PR$ at $x = 66.8°$

$\max - M = -0.01456\,PR$ at $x = 113.2°$

if $(0 < x < \pi/2)$

$M = PR(0.23868a + 0.15915xb - 1/4)$

$T = P(0.15915xb - 0.07958a)$

$V = P(0.15915xa - 0.07958b)$

if $(\pi/2 < x < \pi)$

$M = PR(0.23868a + 0.15915xb - b/2 + 1/4)$

$T = P(0.15915xb - 0.07958a - b/2)$

$V = P(0.15915xa - 0.07958b - a/2)$

$\Delta D_h = \Delta D_v = 0$

---

(21)

$\dfrac{P \sin x}{\pi R}$

$\dfrac{P}{2}$ $\dfrac{P}{2}$
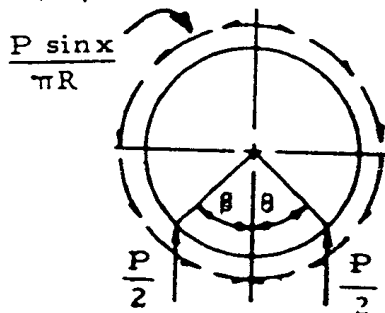
if $(0 < x < \beta)$

$M = PR[0.23868a - d/2 + 0.15915(xb + \beta d + c - ac^2)$

$T = P[0.15915(xb - ac^2) - 0.07958a]$

$V = 0.15915\,P(xa - b/2 + bc^2)$

if $(\beta < x < \pi)$

$M = PR[0.23868a - b/2 + 0.15915(xb + \beta d + c - ac^2)]$

$T = P[0.15915(xb - ac^2) - 0.07958a - b/2]$

$V = P[0.15915(xa - b/2 + bc^2) - a/2]$

$\Delta D_h = \dfrac{PR^3}{EI}\,[0.3183\,(d\beta + c) - (d^2 + 1)/4]$

$\Delta D_v = \dfrac{PR^3}{EI}\,[0.3183\,(d\beta + c) + (dc + \beta)/4 - d/2 - \pi/8]$

TABLE 5-6

Formulas for Closed Circular Rings of Uniform Cross Section (continued)

(22) Ends Pinned
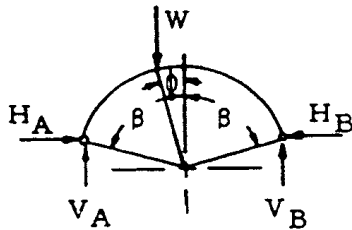
$$H_A = H_B = \frac{P}{2}\left[\frac{d^2-f^2-2c(\beta d-\phi f+c-e)-\alpha(d^2-f^2)}{\beta-3dc+2\beta c^2+\alpha(\beta+dc)}\right]$$

where $\alpha = \dfrac{1}{AR^2}$ and A = cross sectional area

$$V_A = \frac{P}{2}\left(\frac{d+f}{d}\right)$$

$$V_B = P - V_A$$

(23) Ends Pinned
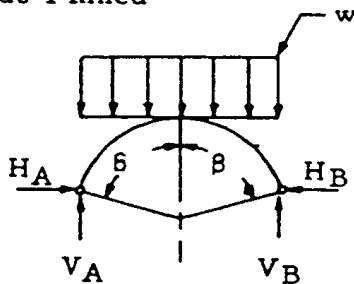
$$H_A = H_B = \frac{wR}{2}\left[\frac{\frac{4d^2}{3}+\beta c-2\beta d^2 c-dc^2+2\alpha(\beta c^2-\frac{\beta}{2}-\frac{dc}{2})}{2\beta c^2+\beta-3dc+\alpha(\beta+dc)}\right]$$

(α as for case (22))

$$V_A = wRd$$

$$V_B = 2wR - V_A$$

TABLE 5-6

Formulas for Closed Circular Rings of Uniform Cross Section (concluded)
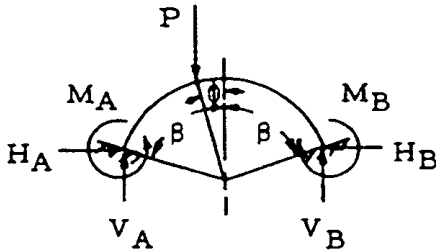
(24) Ends Fixed	$$H_A = H_B = \frac{P}{2}\left[\frac{\frac{2(de+\phi\,dn-dc)}{\beta} - d^2 - f^2 - a(d^2 - f^2)}{\beta + dc - \frac{2d^2}{\beta} + a(\beta+dc)}\right]$$ (a as for case (22)) $$V_A = \frac{P}{2}\left(\frac{\beta+\phi-cd+ef-2fc}{\beta-cd}\right)$$ $$V_B = P - V_A$$ $$M_A = V_A Rd + HR\left(\frac{\beta c - d}{\beta}\right) + \frac{PR}{2}\left(\frac{c-e-\phi f-\beta f}{\beta}\right)$$ $$M_B = M_A - 2V_A Rd + PR(d+f)$$
(25) Ends Fixed	$$H_A = H_B = \frac{\frac{1}{4}\left(\frac{d^2 c}{\beta}-d\right) + \frac{d^3}{6} + a\left(\frac{\beta}{4}-\frac{\beta c^2}{2}+\frac{dc}{4}\right)}{\frac{(\beta-d)^2}{\beta} - \frac{3\beta}{2} + 2d - \frac{dc}{2} - a\left(\frac{\beta}{2}+\frac{dc}{2}\right)}$$ (a as for case (22)) $$M_A = wR^2\left(\frac{d^2}{2}-\frac{1}{4}+\frac{dc}{4\beta}\right) - HR\left(\frac{d}{\beta}-c\right)$$ $$M_B = M_A - 2V_A Rd + 2wR^2 d^2$$ $$V_A = wRd$$ $$V_B = wRd$$
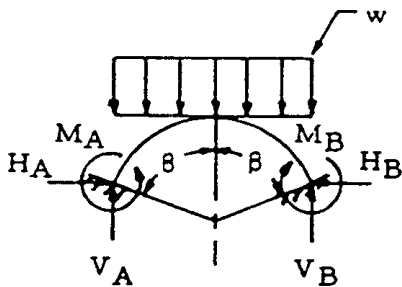
5.10 Sample Problem - Circular Rings and Arches

Given: The circular ring shown in Figure 5-18.
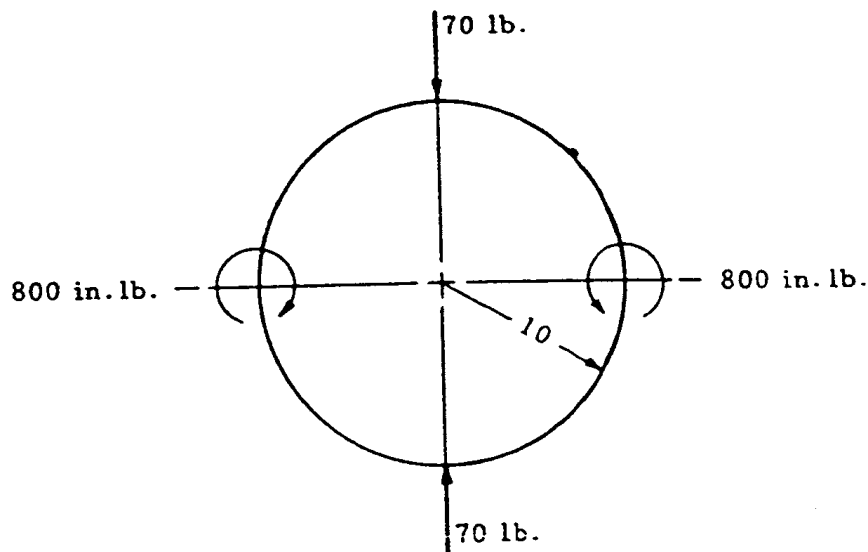
Figure 5-18. Circular Ring

Find: The bending moments in the ring.

Solution: The bending moment in the ring may be obtained by super-posing that due to the concentrated loads (M_p) and that due to the applied bending moments (M_m). From Table 5-6, case 1, the bending moment due to the concentrated loads is

$$M_p = PR(0.3183 - b/2) = 70(10)(0.3183 - \sin x/2) = 223 - 350 \sin x$$

From Table 5-6, case 3, the bending moment due to the applied moment is

$$M_m = M_A(0.6366 a - \tfrac{1}{2}) = 800(0.6366 \cos x - \tfrac{1}{2}) = 510 \cos x - 400$$

if $(0 < x < \pi/2)$

or

$$M_m = M_A(0.6366 a + \tfrac{1}{2}) = 800(0.6366 \cos x + \tfrac{1}{2}) = 510 \cos x + 400$$

if $(\pi/2 < x < \pi)$

The bending moment due to the combined loading is

$$M = M_p + M_m$$

Thus,

$$M = (223 - 350 \sin x) + (510 \cos x - 400)$$
$$= 177 - 350 \sin x + 510 \cos x$$
$$\text{if } (0 < x < \pi/2)$$

or

$$M = (223 - 350 \sin x) - (510 \cos x + 400)$$
$$= 733 - 350 \sin x + 510 \cos x$$
$$\text{if } (\pi/2 < x < \pi)$$

In the above expressions, x is the angular distance from the bottom of the ring.

6.   ANALYSIS OF PLATES

6.1   Introduction to Analysis of Plates

This chapter covers the analysis of plates as commonly used in aircraft and missile structures. In general, such plates are classified as thin; that is, deflections are small in comparison with the plate thickness. These plates are subjected to compression, bending, and shear-producing loads. Critical values of these loads produce a wrinkling or buckling of the plate. Such buckling produces unwanted aerodynamic effects on the surface of the airplane. It also may result in the redistribution of loads to other structural members, causing critical stresses to develop. Thus, it is essential that the initial buckling stress of the plate be known. In addition, if the buckling stress is above the proportional limit, the panel will experience ultimate failure very soon after buckling.

The critical buckling of a plate depends upon the type of loading, the plate dimensions, the material, the temperature, and the conditions of edge support.

This chapter considers the various loadings of both flat and curved plates, with and without stiffeners. Single loadings are considered first followed by a discussion of combined loadings. Examples are given to show the use of the analysis methods presented.

6.2   Nomenclature for Analysis of Plates

a	plate length
A_{st}	stiffener area
b	plate width
b_{ef}	effective panel width
c	core thickness, signifies clamped edge
C	compressive buckling coefficient for curved plates
e	strain
E	modulus of elasticity
E_s	secant modulus
E_t	tangent modulus
E_s, E_t	secant and tangent moduli for clad plates
f	ratio of cladding thickness to total plate thickness
F	stress
$F_{0.7}, F_{0.85}$	secant yield stress at $0.7E$ and $0.85E$
F_{cr}	critical normal stress
F_{crs}	critical shear stress
F_{pl}	stress at proportional limit
F_{cy}	compressive yield stress
F_f	crippling stress
FR	free (refers to edge fixity)

g	number of cuts plus number of flanges (Section 6.3.3)
k	buckling coefficient
k_c	compressive buckling coefficient
k_s	shear buckling coefficient
$\bar{k}_c$	equivalent compressive buckling coefficient
K	sandwich panel form factor
L'	effective column length
n	shape parameter, number of half waves in buckled plate
p	rivet pitch
P	total concentrated load
r	radius of curvature
R	stress ratio
$\bar{R}$	sandwich panel parameter
ss	simply supported
t	thickness
t_s	skin thickness
t_w	web thickness
t_1	total cladding thickness
w	unit load
W	total load, potential energy
y	deflection
Z_b	length range parameter $b^2(1-\nu_e^2)^{\frac{1}{2}}/rt$
β	ratio of cladding yield stress to core stress
β_s	crippling coefficient
ϵ	ratio of rotational rigidity of plate edge stiffeners
η	plasticity reduction factor
$\bar{\eta}$	cladding reduction factor
λ	buckle half wavelength
ν	inelastic Poisson's ratio
ν_e	elastic Poisson's ratio
ν_p	plastic Poisson's ratio
ρ	radius of gyration

6.3 Axial Compression of Flat Plates

The compressive buckling stress of a rectangular flat plate is given by Equation (6-1).

$$F_{cr} = \eta\bar{\eta}\, \frac{k\pi^2 E}{12(1-\nu_e^2)} \left(\frac{t}{b} \right)^2 \tag{6-1}$$

The relation is applicable to various types of loadings in both the elastic and the inelastic ranges and for various conditions of edge fixity.

The case of unstiffened plates is treated first and then stiffened plates are discussed.

The edge constraints which are considered vary from simply supported to fixed. A simply supported edge is constrained to remain straight at all loads up to and including the buckling load, but is free to rotate about the center line of the edge. A fixed edge is constrained to remain straight and to resist all rotation. These two conditions define the limits of torsional restraint and are represented by $\epsilon = 0$ for simply supported edges and $\epsilon = \infty$ for fixed edges.

Plates are frequently loaded so that the stresses are beyond the proportional limit of the material. If such is the case, the critical buckling stress is reduced by the factor η, which accounts for changes in k, E, and ν. This allows the values of k, E, and ν to always be the elastic values.

The second reduction factor in Equation (6-1) is the cladding factor $\overline{\eta}$. In order to obtain desirable corrosion resistance, the surface of some aluminum alloys are coated or clad with a material of lower strength, but of better corrosion resistance. The resultant panel may have lower mechanical properties than the basic core material and allowance must be made. Values for the factor $\overline{\eta}$ are given in the appropriate sections.

6.3.1   Buckling of Unstiffened Flat Plates in Axial Compression

The buckling coefficients and reduction factors of Equation (6-1) applicable to flat rectangular plates in compression are presented in this section.

Figures 6-1, 6-2, and 6-3 show the buckling coefficient k_0 as a function of the ratio a/b and the type of edge restraint; and, in the case of Figure 6-2, the buckle wave length and number of half waves. Figure 6-4 shows k_0 for infinitely long flanges and plates as a function of the edge restraint only. The edge restraint ratio ϵ is the ratio of the rotational rigidity of plate edge support to the rotational rigidity of the plate.

The condition of unequal rotational support can be treated by Equation (6-2).

$$k_c = (k_{0_1} k_{0_2})^{\frac{1}{2}}$$

(6-2)

The coefficients k_{0_1} and k_{0_2} are obtained by using each value of ϵ independently.

Figures 6-5, 6-6, and 6-7 present k_c for flanges. A flange is considered to be a long rectangular plate with one edge free.

The plasticity reduction factor η for a long plate with simply supported edges is given by Equation (6-3).

$$\eta = \left[\left(\frac{E_s}{E} \right) \left(\frac{1-\nu_s^2}{1-\nu^2} \right) \right] \left\{ 0.500 + 0.250 \left[1 + \left(\frac{3 E_t}{E_s} \right) \right] \right\}^{\frac{1}{2}}$$

(6-3)

6 - 3
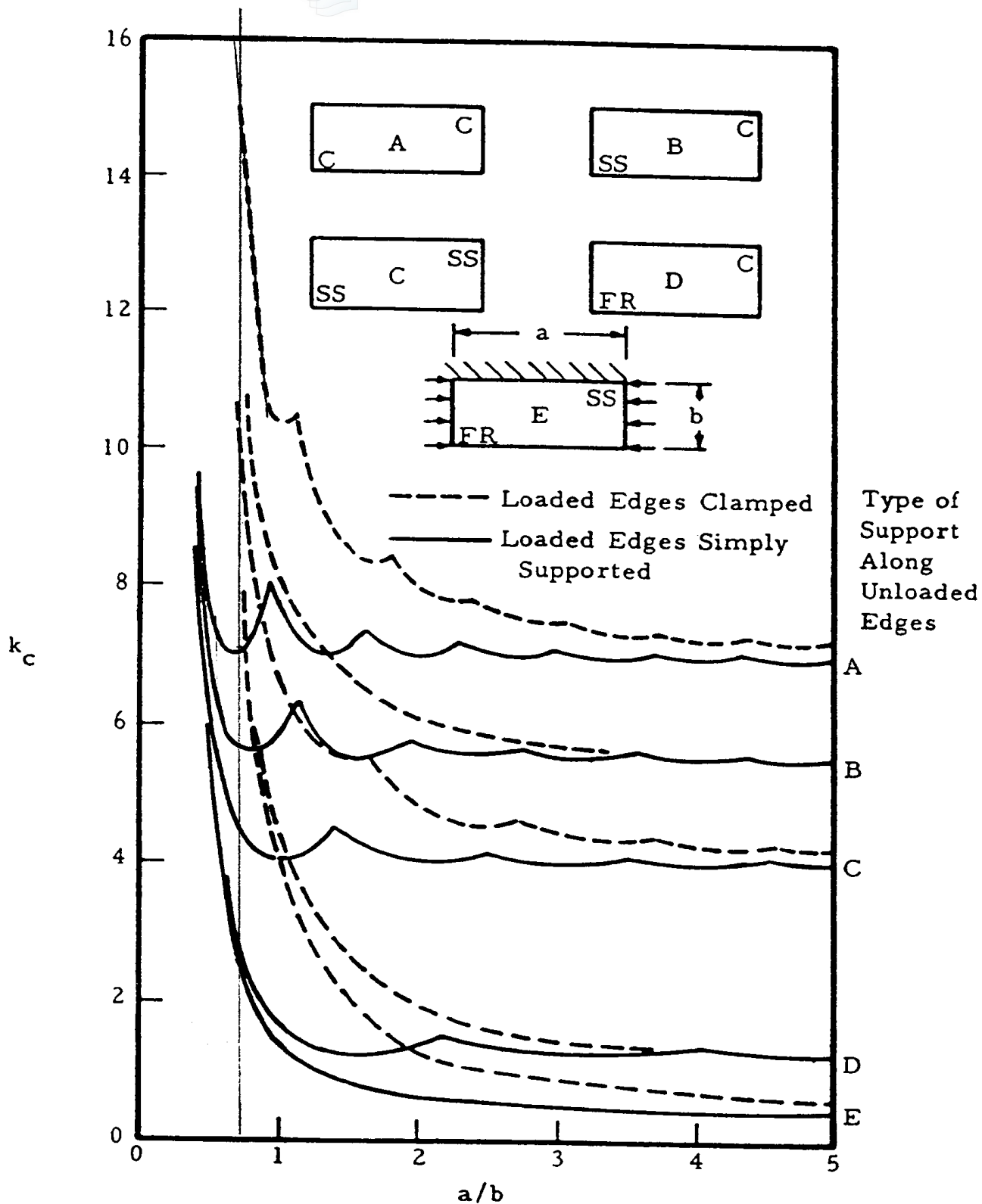
Figure 6-1, Compressive-Buckling Coefficients for Flat Rectangular Plates
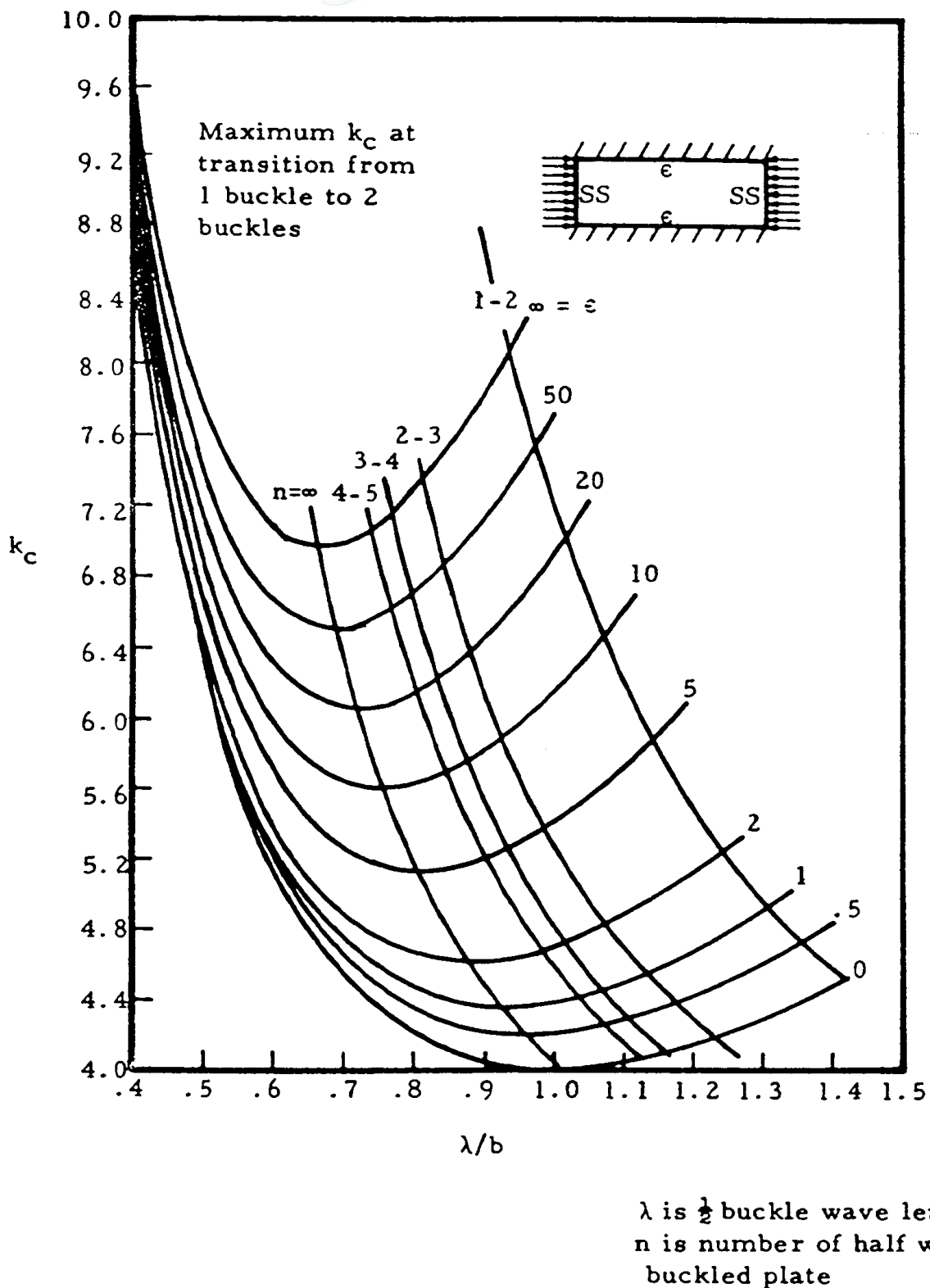
Figure 6-2. Compressive-Buckling-Stress Coefficient of Plates as a function of λ/b for Various Amounts of Edge Rotational Restraint
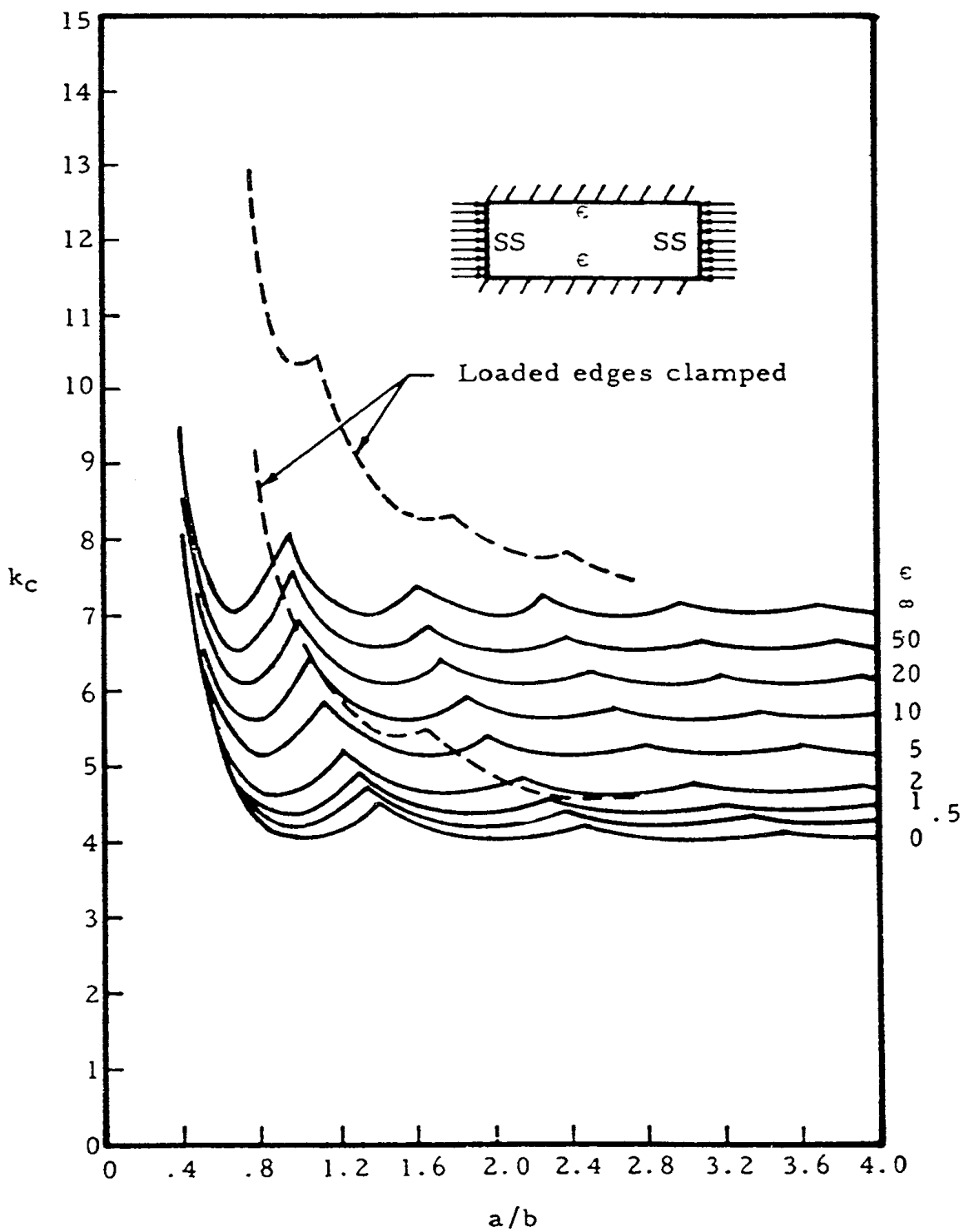
Figure 6-3. Compressive-Buckling-Stress Coefficient of Plates as a Function of a/b for Various Amounts of Edge Rotational Restraint
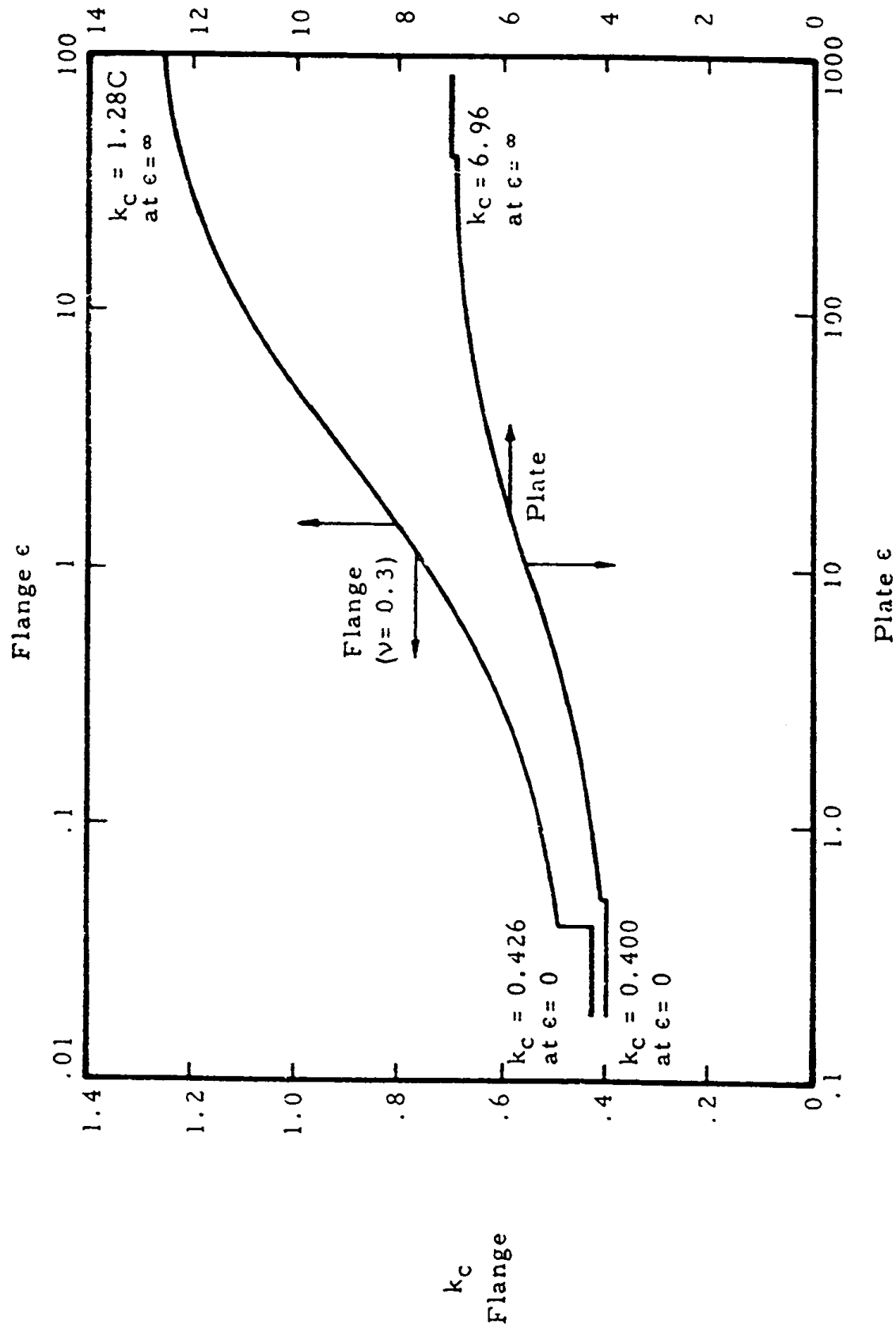
Figure 6-4. Compressive-Buckling Coefficients for Infinitely Long Flanges and Plates as Functions of Edge Rotational Restraint
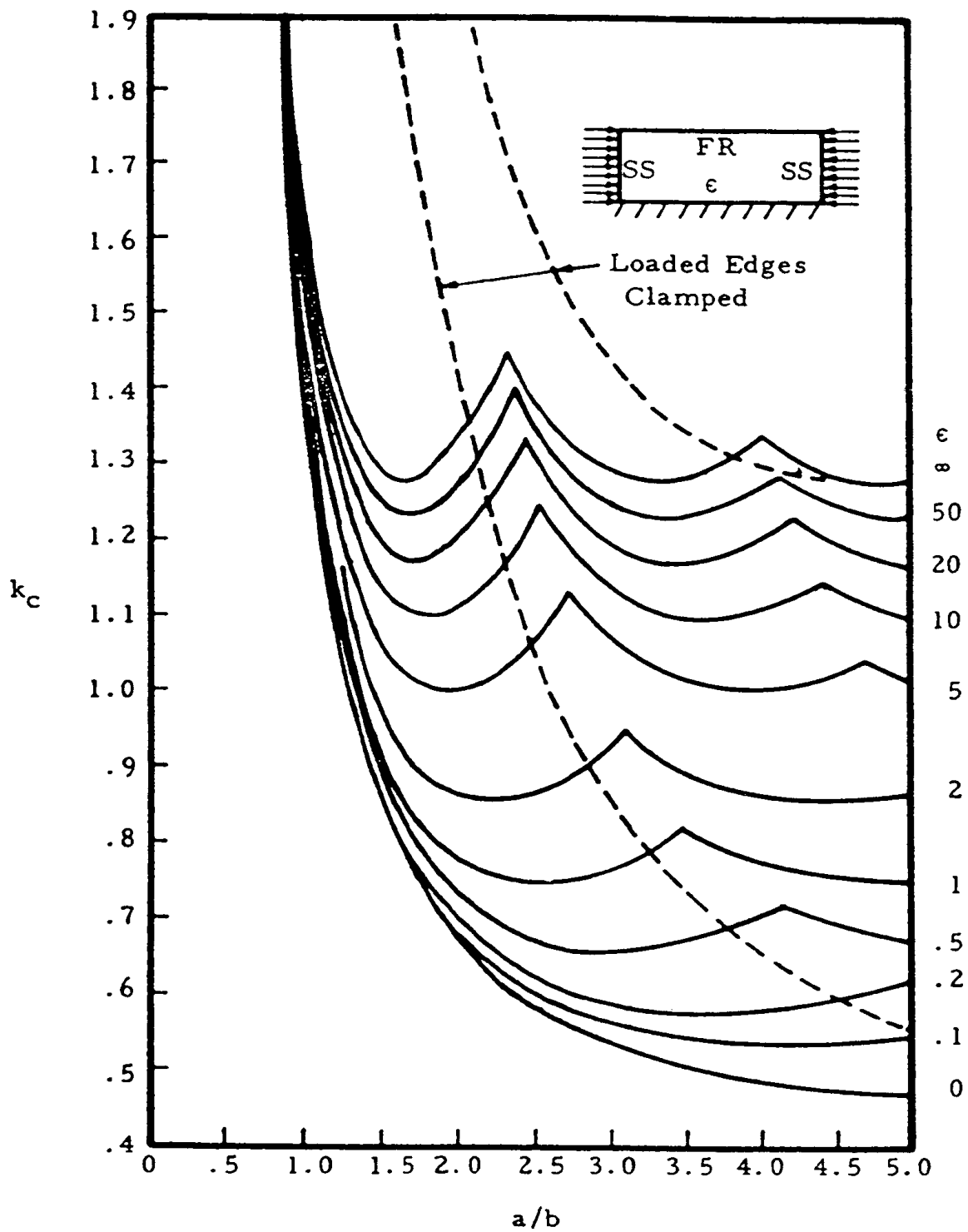
Figure 6-5. Compressive-Buckling-Stress Coefficient of Flanges as a
Function of a/b for Various Amounts of Edge Rotational Restraint
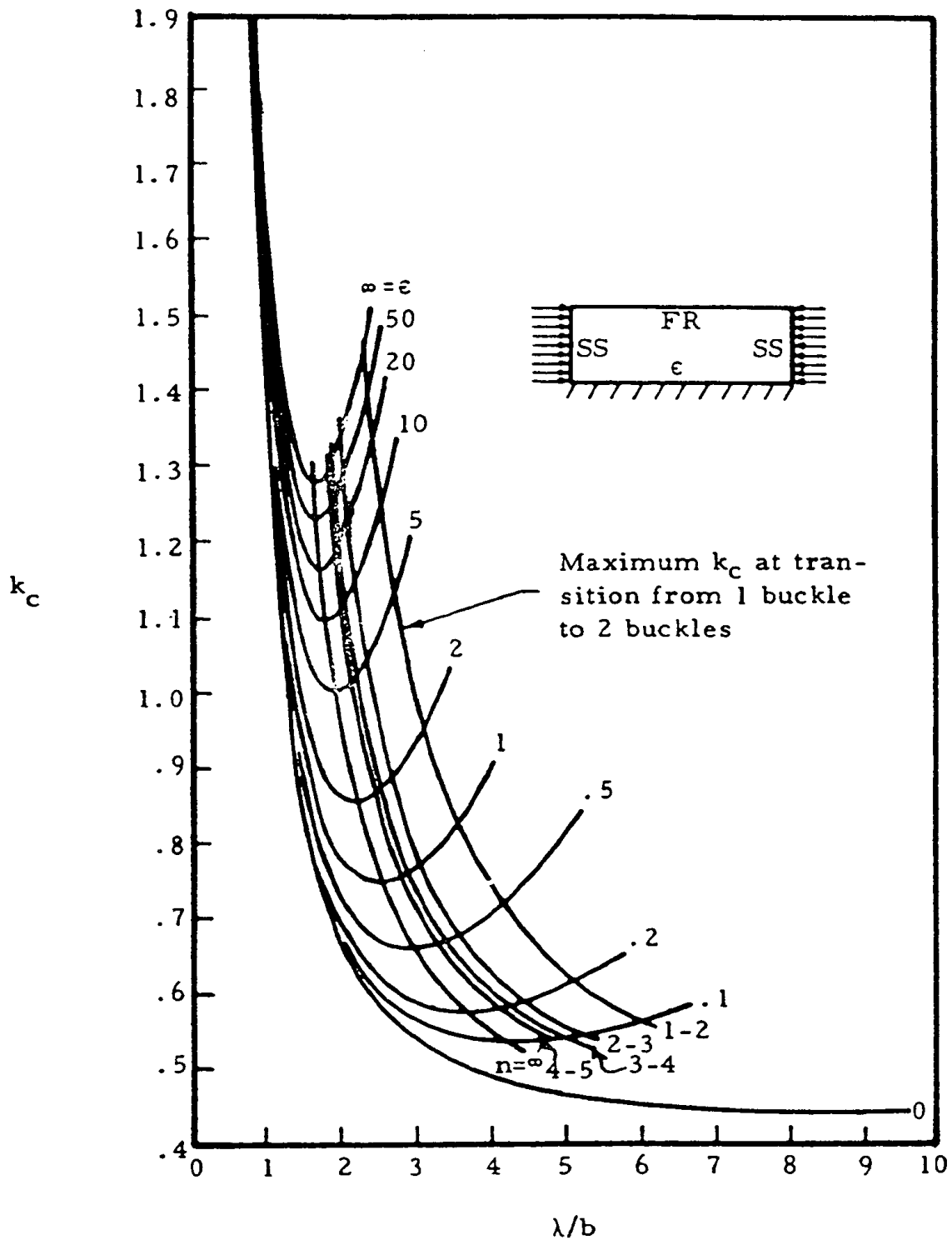
Figure 6-6. Compressive-Buckling-Stress Coefficient of Flanges as a
Function of λ/b for Various Amounts of Edge Rotational Restraint

(b) Hinged flanges
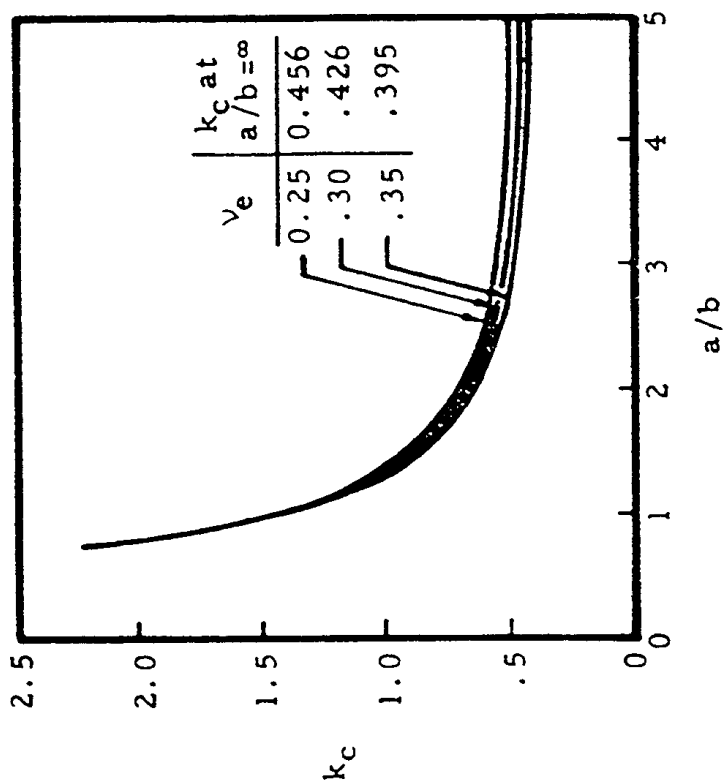
$$F_{cr} = k_c \pi^2 E/(L/t)^2$$

(a) Plate columns with hinged loaded edges
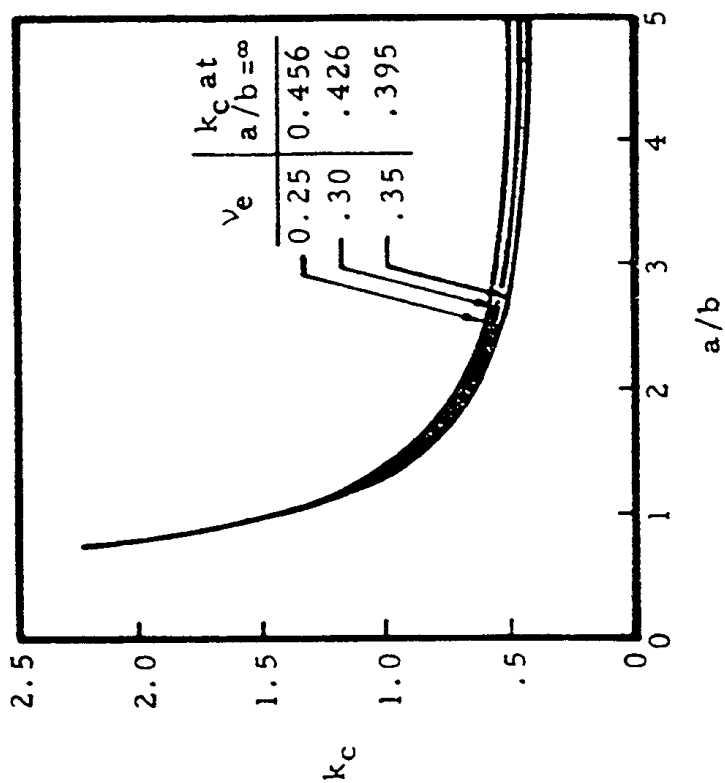
Figure 6-7.   Compressive-Buckling Coefficients of Plate Columns and
Flanges as a Function of Poission's Ratio

For a long plate with clamped edges, the factor is given by Equation (6-4).

$$\eta = \left[\left(\frac{E_s}{E}\right)\left(\frac{1-\nu_e^2}{1-\nu^2}\right)\right]\left\{0.352 + 0.324\left[1 + \left(\frac{3 E_t}{E_s}\right)\right]\right\}^{\frac{1}{2}} \qquad (6-4)$$

The value of the inelastic Poisson ratio ν is given by Equation (6-5).

$$\nu = \nu_p - (\nu_p - \nu_e)\left(\frac{E_s}{E}\right) \qquad (6-5)$$

The tangent and secant moduli can be determined from the Ramberg-Osgood relation as shown in Equations (6-6) and (6-7).

$$\left(\frac{E}{E_s}\right) = 1 + \left(\frac{3}{7}\right)\left(\frac{F}{F_{0.7}}\right)^{n-1} \qquad (6-6)$$

$$\left(\frac{E}{E_t}\right) = 1 + \left(\frac{3}{7}\right)n\left(\frac{F}{F_{0.7}}\right)^{n-1} \qquad (6-7)$$

Values of E, $F_{0.7}$, and n must be known for the material under consideration. Figure 6-8 shows the characteristics of stress-strain curves used to determine the shape factor n.

The cladding reduction factor is given by Equation (6-8).

$$\overline{\eta} = \frac{1 + 3\beta f}{1 + 3f} \qquad (6-8)$$

This relation is valid for the range $F_{cl} < F_{cr} < F_{pl}$. For the plastic range when $F_{cr} > F_{pl}$ Equation (6-9).

$$\overline{\eta} = \frac{1}{1+3f}\left[\frac{\left[1 + \left(\frac{3(f)\overline{E}_s}{E_s}\right)\right] + \left\{\left[1 + \left(\frac{3(f)\overline{E}_s}{E_s}\right)\right]\left[\left(\frac{1}{4}\right) + \left(\frac{3}{4}\right)\left(\frac{E_t}{E_s}\right) + w\right]\right\}^{\frac{1}{2}}}{1 + \left[\left(\frac{1}{4}\right) + \left(\frac{3}{4}\right)\left(\frac{E_t}{E_s}\right)\right]^{\frac{1}{2}}}\right]^{\frac{1}{2}} \qquad (6-9)$$

The potential energy factor W is given by Equation (6-10).

$$W = \left(\frac{3(f)\overline{E}_s}{E_s}\right)\left[\left(\frac{1}{4}\right) + \left(\frac{3}{4}\right)\left(\frac{\overline{E}_t}{E_s}\right)\right] \qquad (6-10)$$

6 - 11
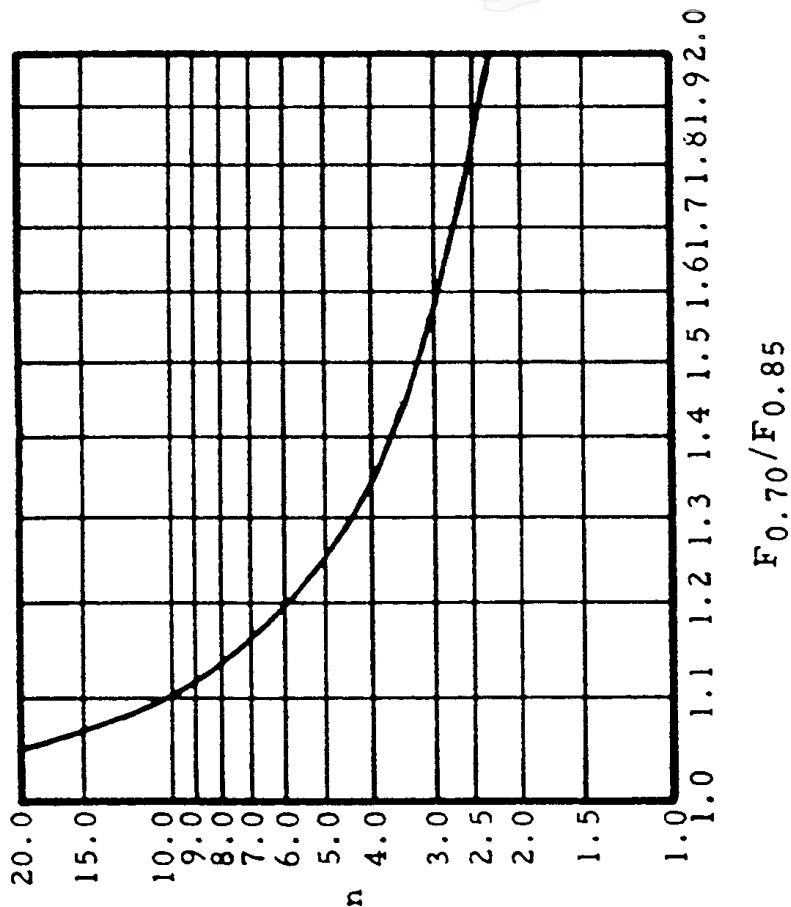
$$n = 1 + \log_e (17/7)/\log_e (F_{0.70}/F_{0.85})$$

(b) Dependence of shape factor on ratio $F_{0.70}/F_{0.85}$
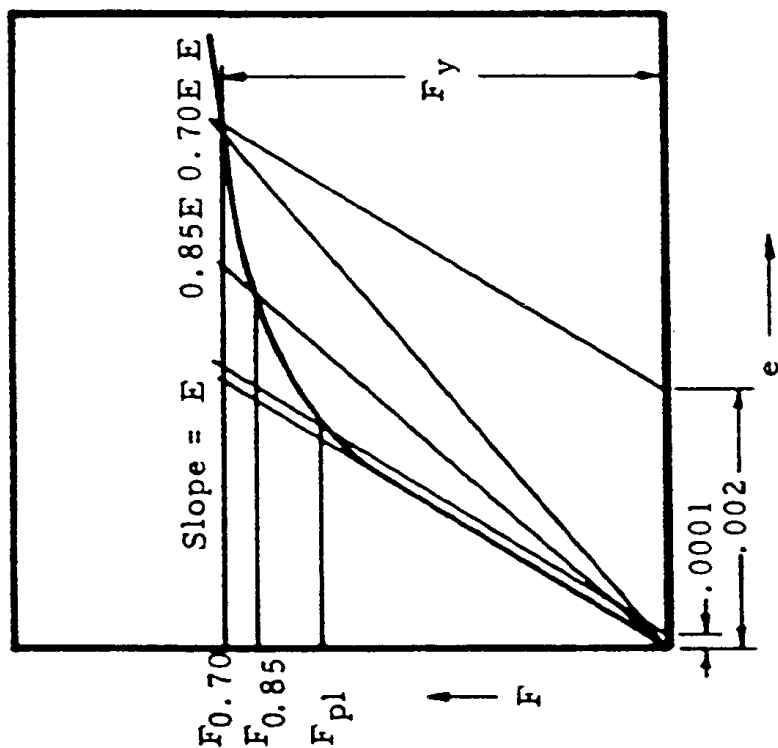
(a) Significant stress quantities on a typical stress-strain curve

Figure 6-8.   Characteristics of Stress-Strain Curves for Structural Alloys Depicting Quantities Used in Three-Parameter Method

Figures 6-9 and 6-10 present values of k_c for plates restrained by stiffeners. This data is included here instead of in the section on stiffened plates because the stiffeners are not a part of the plate. To be noted is the effect of torsional rigidity of the stiffener on the buckling coefficient of the plate.
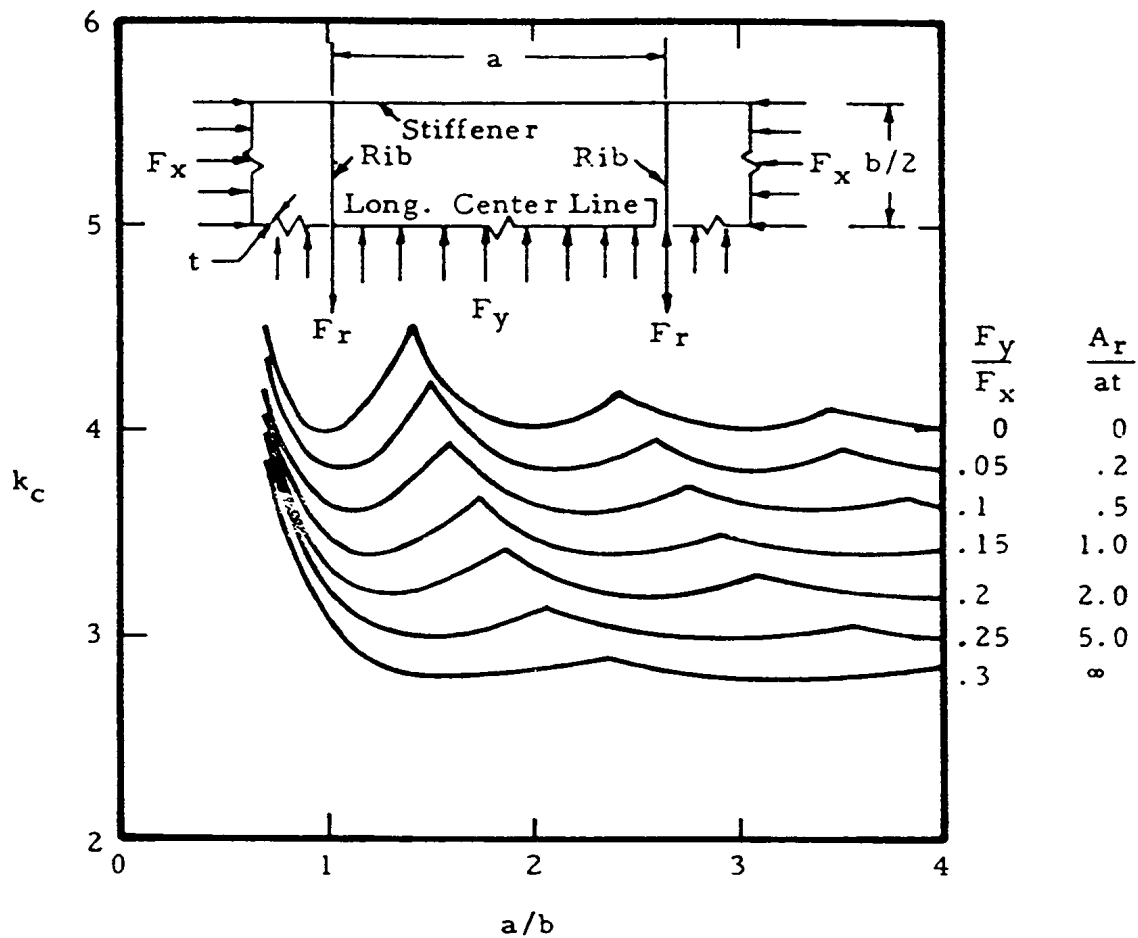
Figure 6-9. Compressive-Buckling Coefficient of Flat Plates Restrained Against Lateral Expansion. Poisson's Ratio Equals 0.3;

$$\frac{F_y}{F_x} = \frac{\left(\dfrac{\nu A_r}{at}\right)}{\left(1 + \dfrac{A_r}{at}\right)}$$
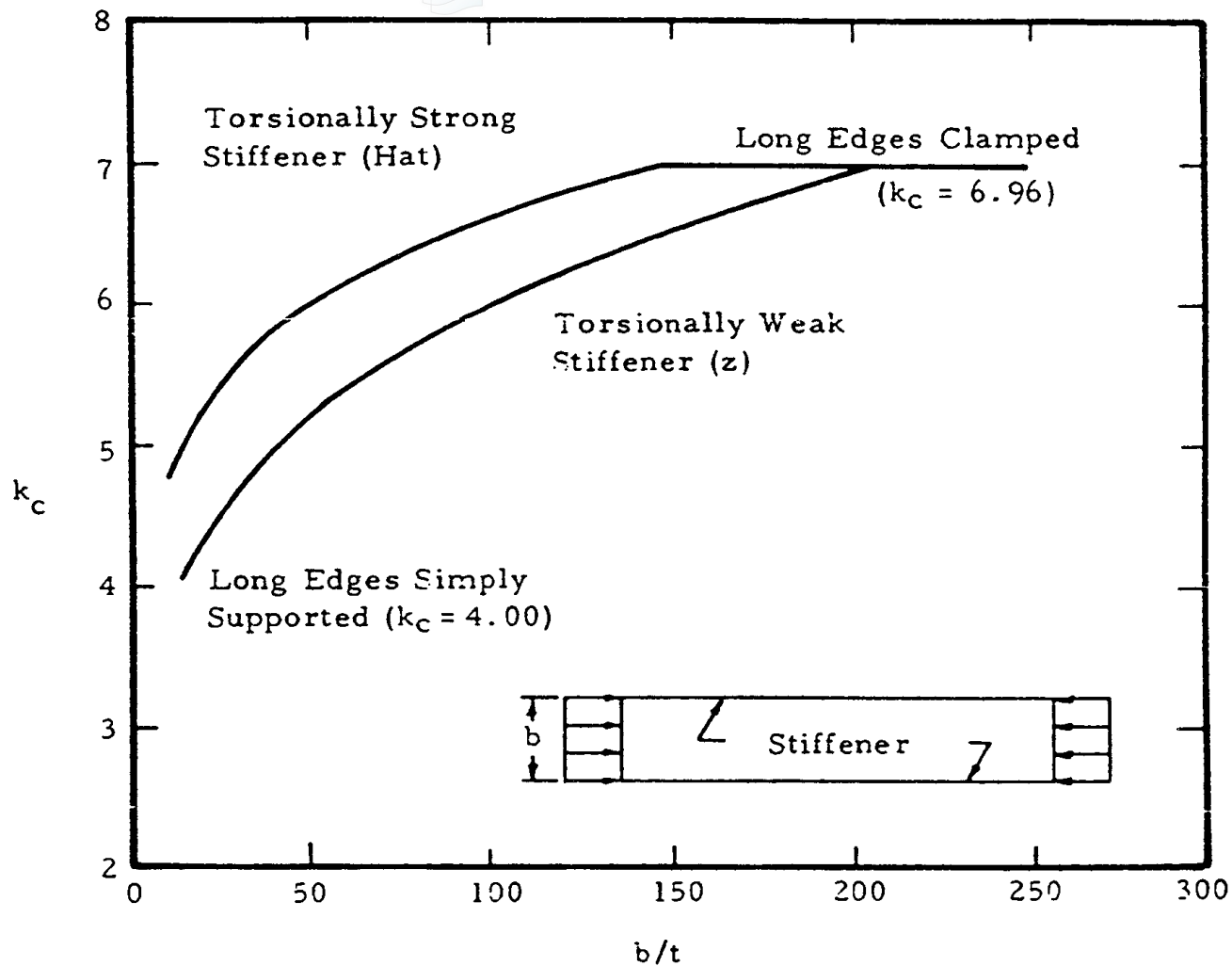
Figure 6-10. Compressive-Buckling Coefficient for Long Rectangular Stiffened Panels as a Function of b/t and Stiffener Torsional Rigidity

6.3.2   Buckling of Stiffened Flat Plates in Axial Compression

The treatment of stiffened flat plates is the same as that of unstiffened plates except that the buckling coefficient, k, is now also a function of the stiffener geometry. Equation (6-1) is the basic analysis tool for the critical buckling stress.

As the stiffener design is a part of the total design, Figures 6-11 and 6-12 present buckling coefficients for various types of stiffeners.

The applicable critical buckling equation is indicated on each figure.

A plasticity reduction factor η is applicable to channel and Z-section stiffeners as given by Equation (6-11).

$$\eta = \left(\frac{E_s}{E} \right) \left(\frac{1-\nu_e^2}{1-\nu^2} \right) \tag{6-11}$$

Figures 6-13 and 6-14 present values of the buckling coefficient for longitudinally stiffened plates. The curves of Figure 6-13 are in terms of the plate geometry and the parameter EI/bD for the plate. The curves of Figure 6-13 were based on the assumption that the stiffener section centroid was located at the midsurface of the plate. If the stiffener is located on one side of the plate, as is usually the case, an effective value of (EI/bD) must be determined. Figure 6-15 presents a plot of the function $1/Z_{nq}$ vs λ/b for one, two, or an infinite number of stiffeners to be used in Equation (6-12).

$$\frac{\left(\dfrac{EI}{bD} \right)_e}{\left(\dfrac{EI}{bD} \right)} = 1 + \frac{\left(\dfrac{A_{\bar{z}}^2}{I} \right)}{1 + \left(\dfrac{Z_{nq} A}{bt} \right)} \tag{6-12}$$

The value of (λ/b) used for Figure 6-15 must be the same as that used in Figure 6-13. This may require an iterative approach as (EI/bD)$_e$ may occur at a different value of g in Figure 6-13 than does (EI/bD) at the a/b of the n originally used to enter Figure 6-13.

Figure 6-16 presents curves for finding a value for k for plates with transverse stiffeners. It is noted that the stiffeners are allowed to have torsional stiffness in these plots, whereas in Figure 6-13 for axial stiffeners, GJ = 0 for the stiffeners. See Figure 6-10 in Section 6.3.1 for an indication of the effect of stiffener rigidity on the plate buckling coefficient.
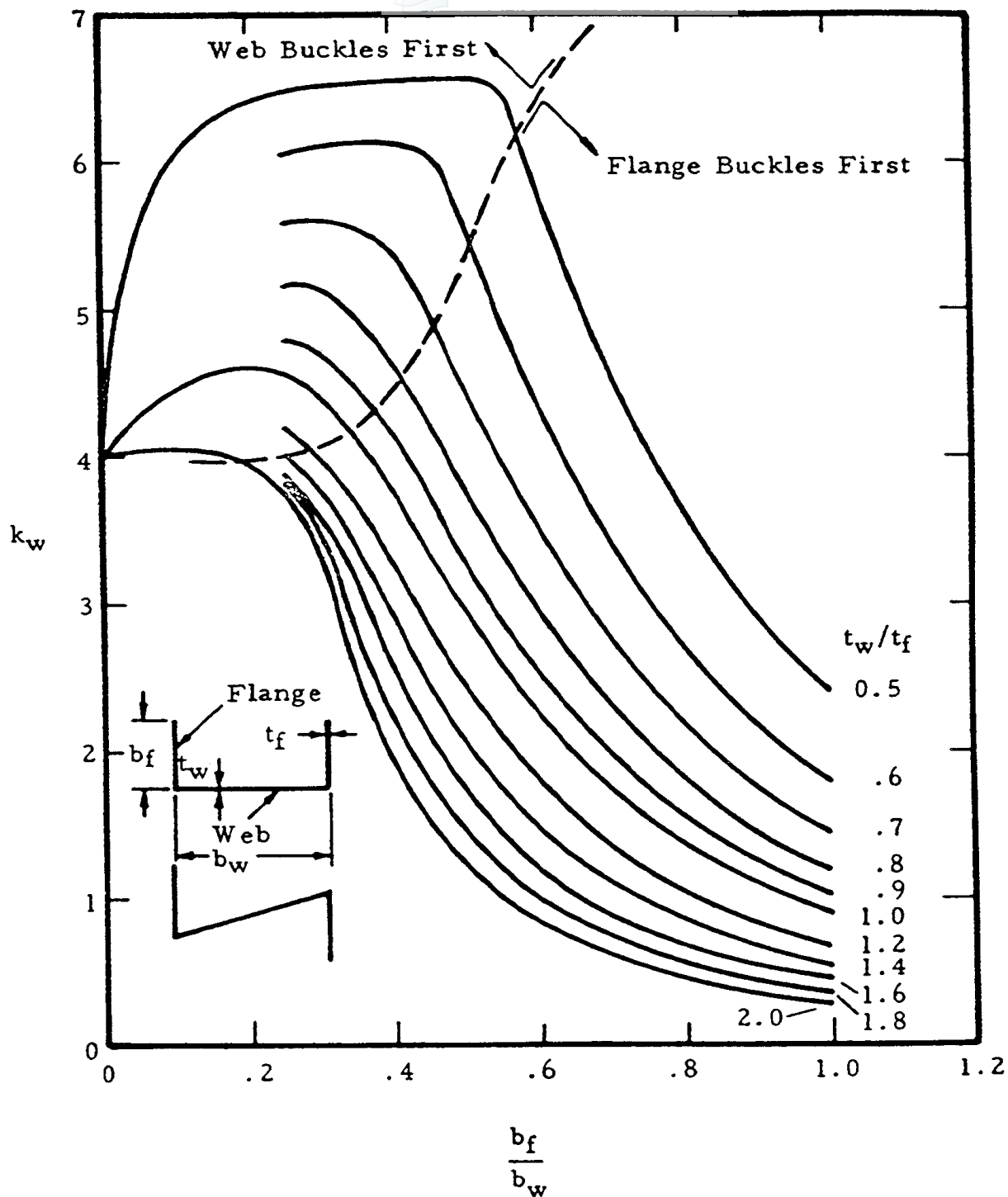
(a) Channel- and Z-section stiffeners

$$F_{cr} = \frac{k_w \pi^2 E}{12(1-\nu_e^2)} \frac{t_w^2}{b_w^2}$$

Figure 6-11. Buckling Coefficients for Stiffeners
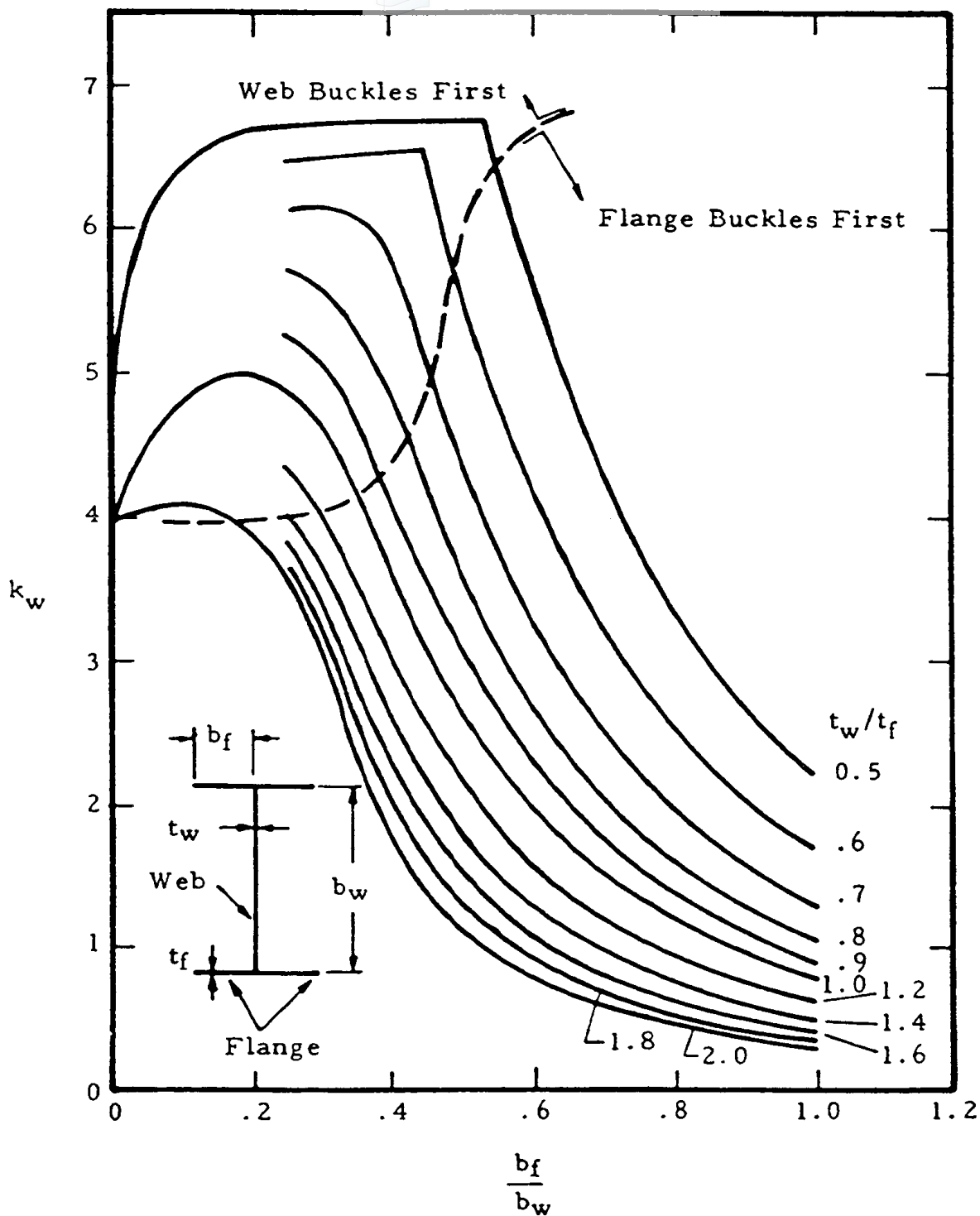
(b) H-section stiffeners

$$F_{cr} = \frac{k_w \pi^2 E}{12(1-\nu_e^2)} \frac{t_w^2}{b_w^2}$$

Figure 6-11. Buckling Coefficients for Stiffeners (continued)

6 - 17
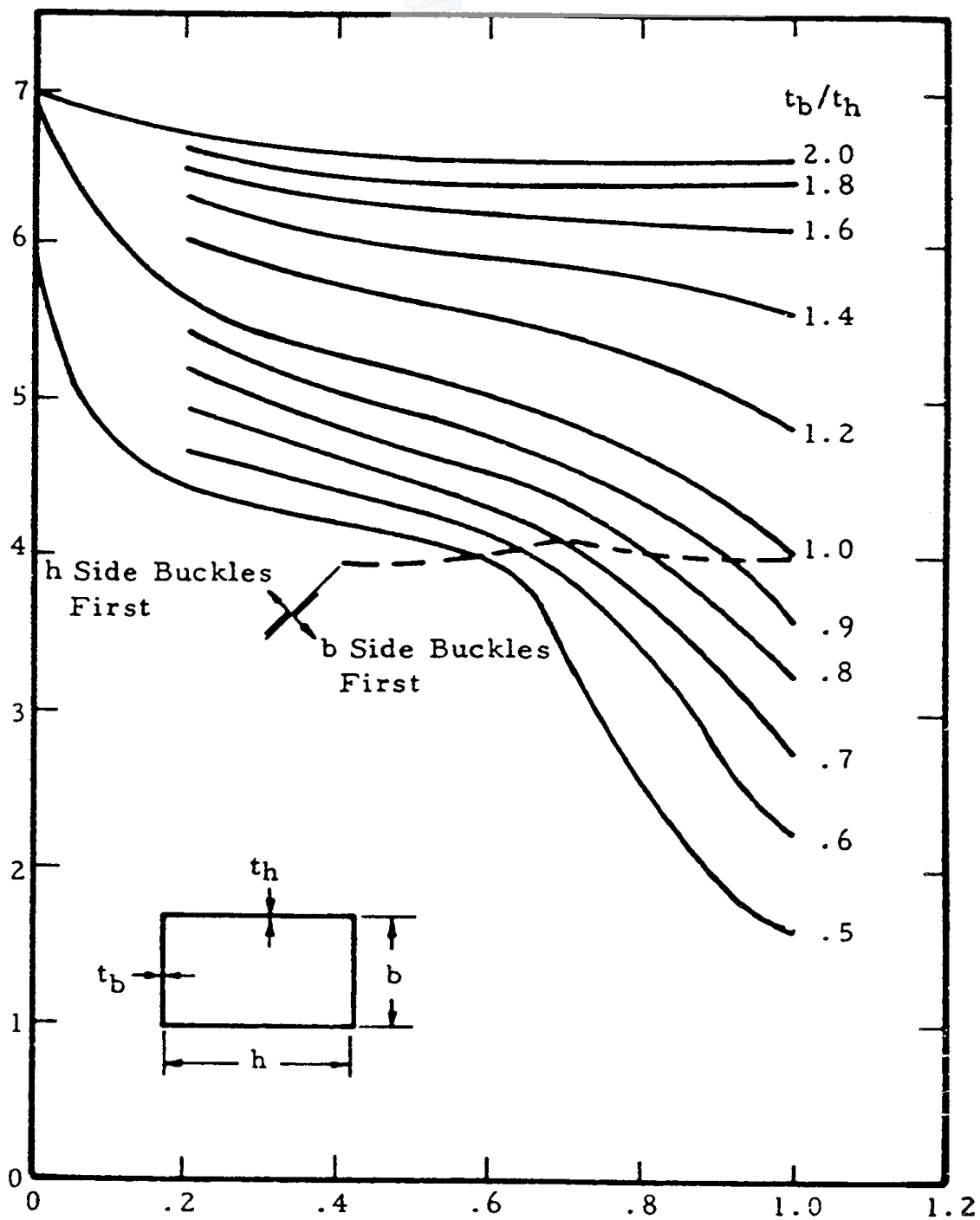
(c) Rectangular-tube-section stiffeners

$$F_{cr} = \frac{k_h \pi^2 E}{12(1-\nu_e^2)} \left(\frac{t_h}{h}\right)^2$$

Figure 6-11. Buckling Coefficients for Stiffeners (concluded)
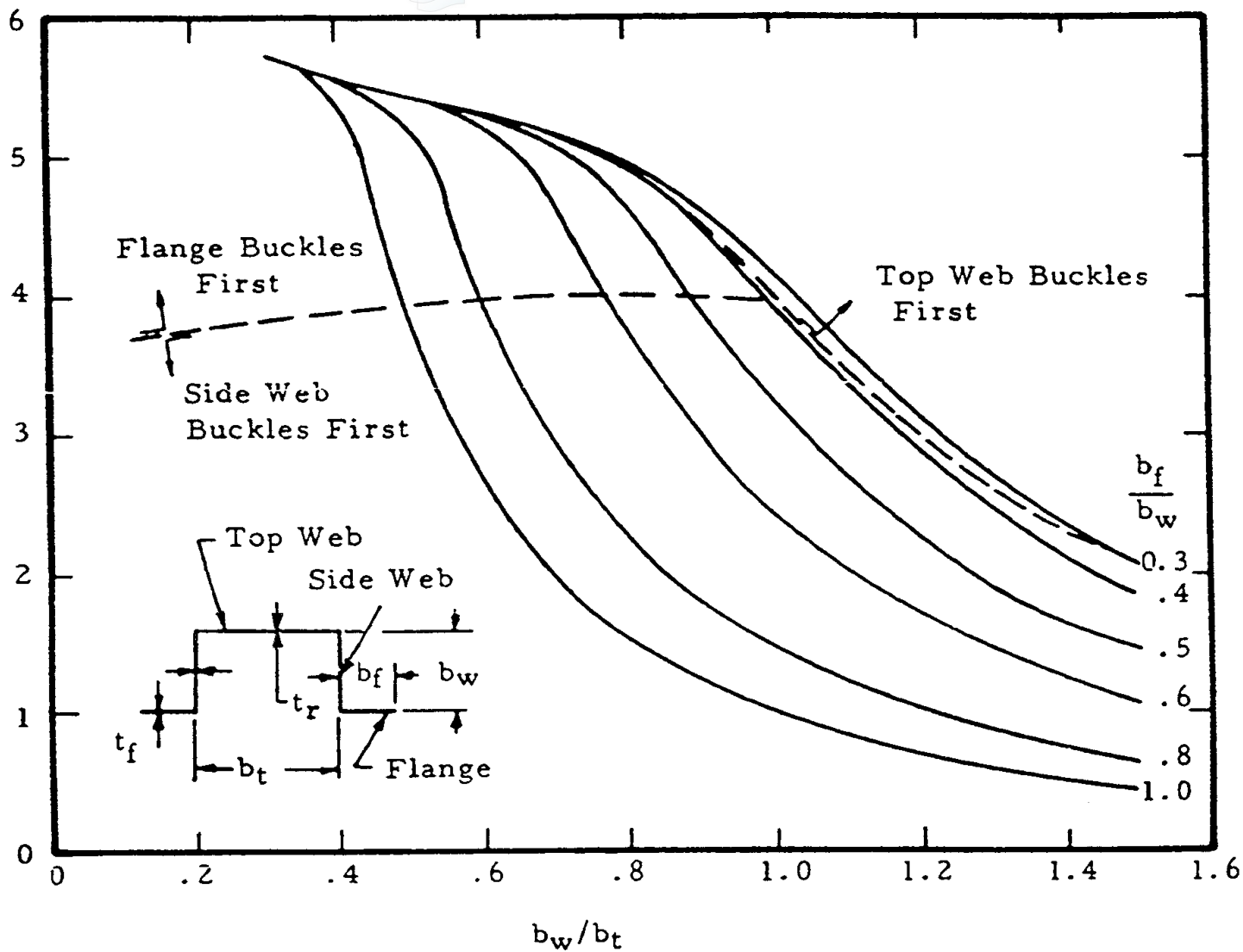
Figure 6-12. Buckling Stress for Hat-Section Stiffeners. $t = t_f = t_w = t_T$;
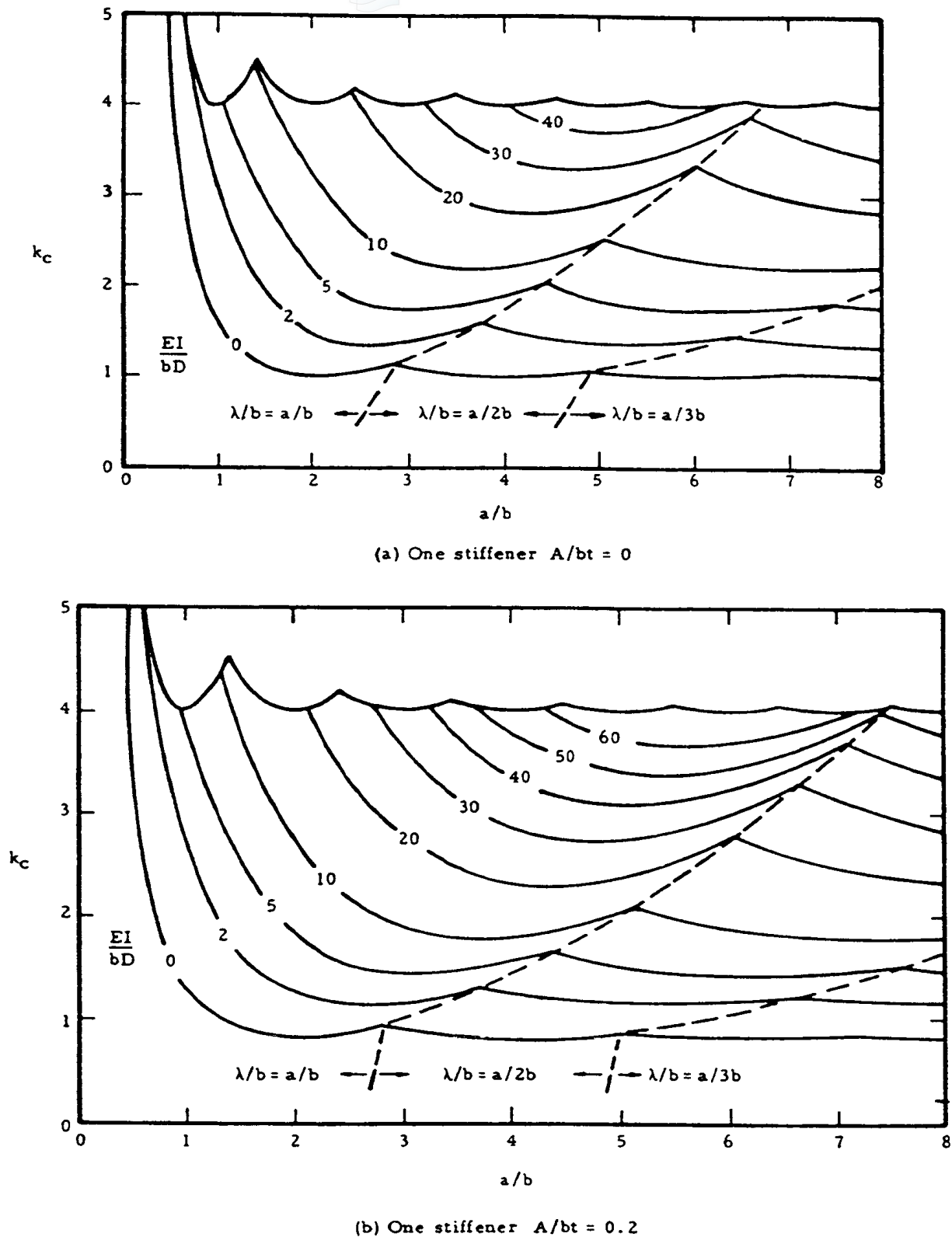
$$F_{cr} = \frac{k_T \pi^2 E}{12(1 - \nu_e{}^2)} \quad \frac{t^2}{b_T{}^2}$$

(a) One stiffener A/bt = 0

(b) One stiffener A/bt = 0.2

Figure 6-13. Compressive-Buckling Coefficients for Simply Supported Flat Plates with Longitudinal Stiffeners

$$\sigma_{cr} = \frac{k_c \pi^2 E}{12(1-\nu_e{}^2)} \left(\frac{t}{b}\right)^2$$

6 - 20
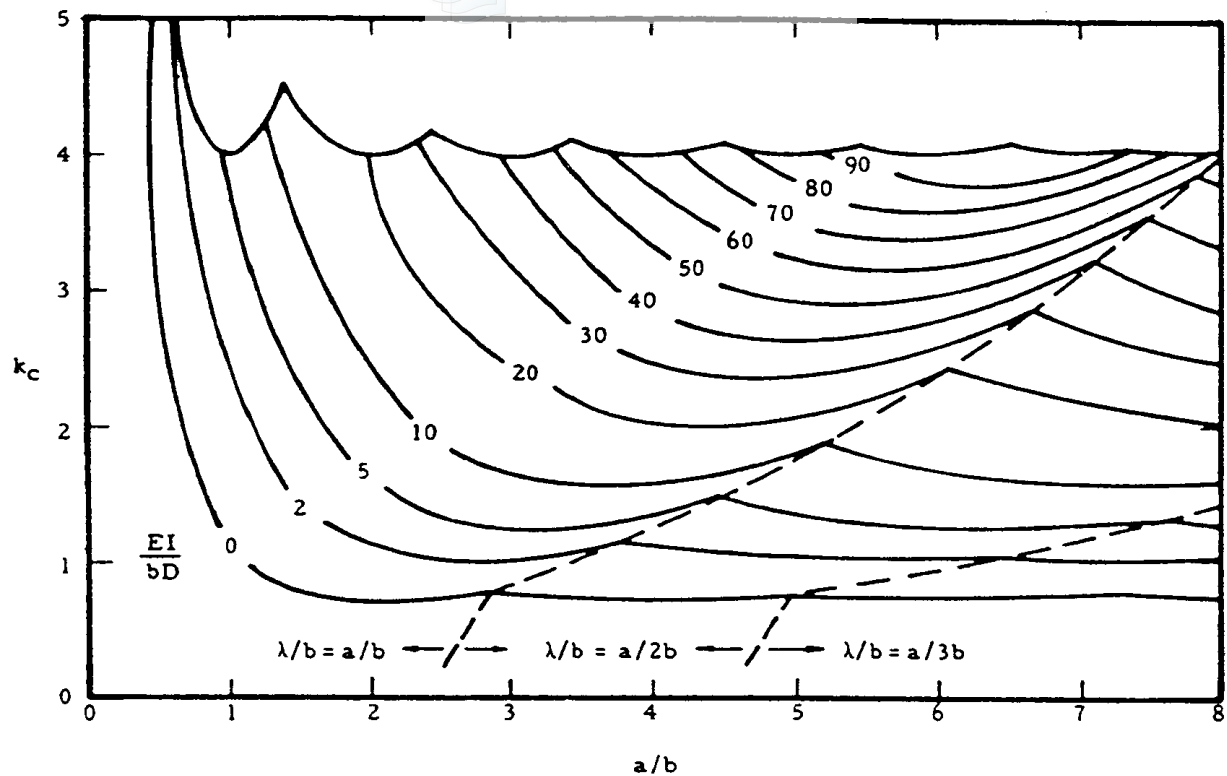
(c) One stiffener A/bt = 0.4
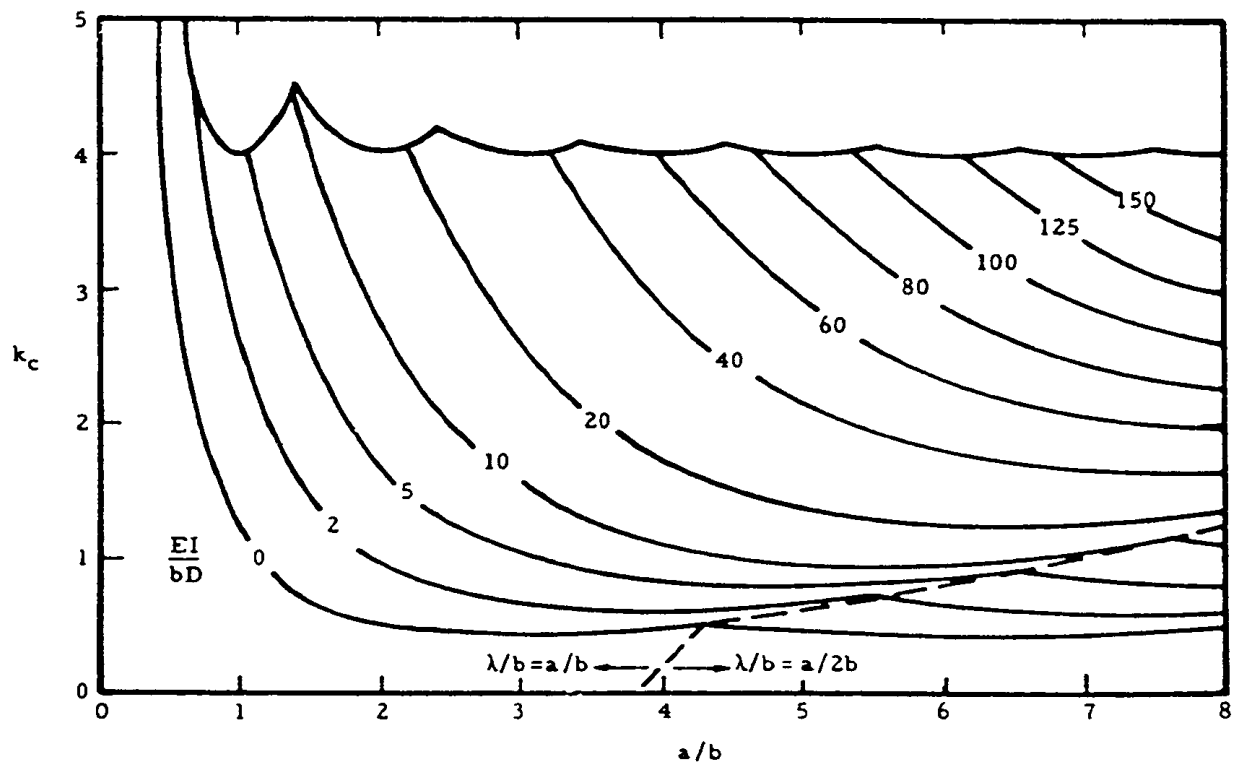
(d) Two stiffeners A/bt = 0

Figure 6-13.   Compressive-Buckling Coefficients for Simply Supported Flat
Plates with Longitudinal Stiffeners (continued)

6-21
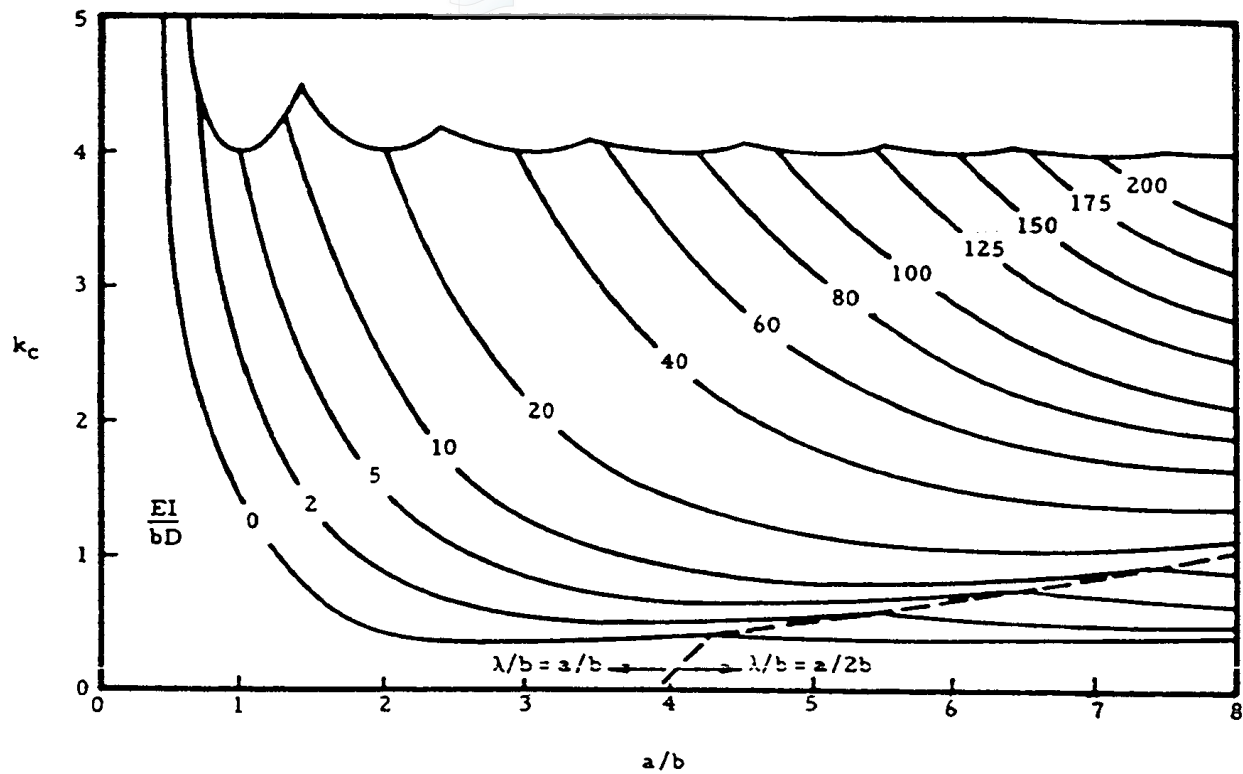
(e) Two stiffeners A/bt = 0.2
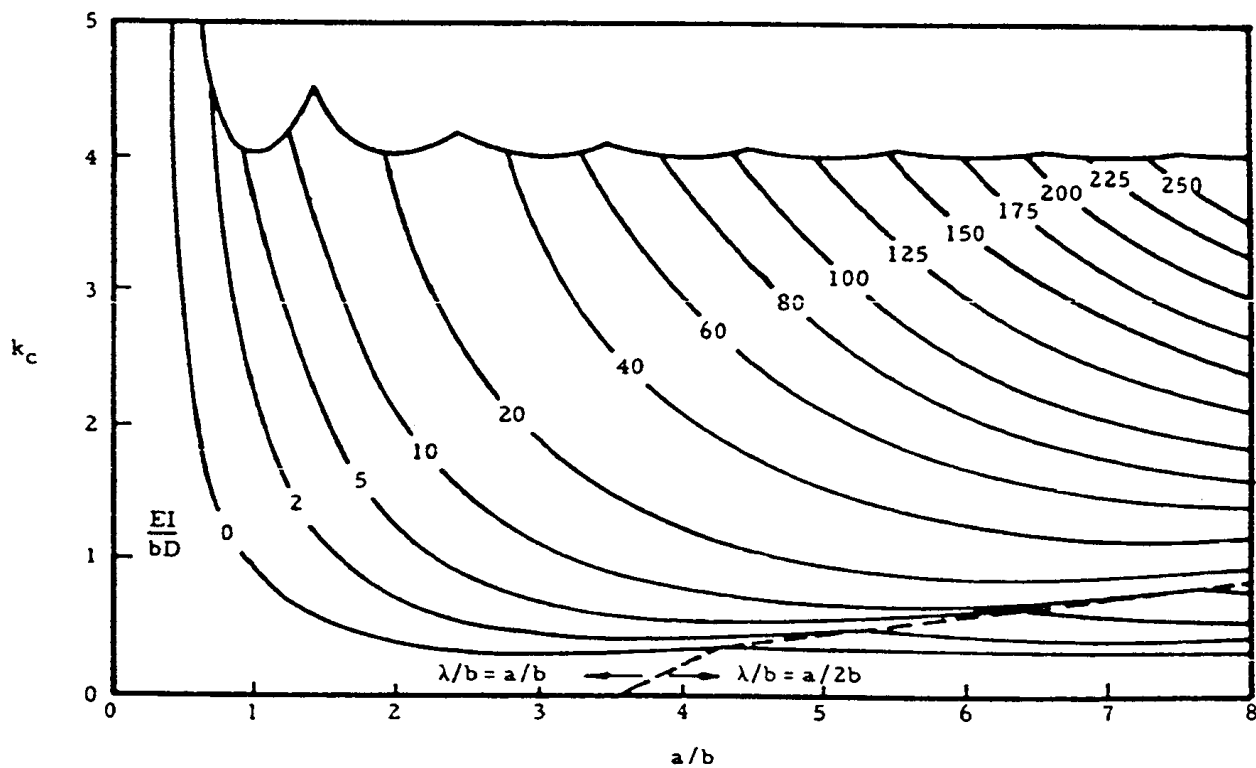
(f) Two stiffeners A/bt = 0.4

Figure 6-13. Compressive-Buckling Coefficients for Simply Supported Flat
Plates with Longitudinal Stiffeners (continued)
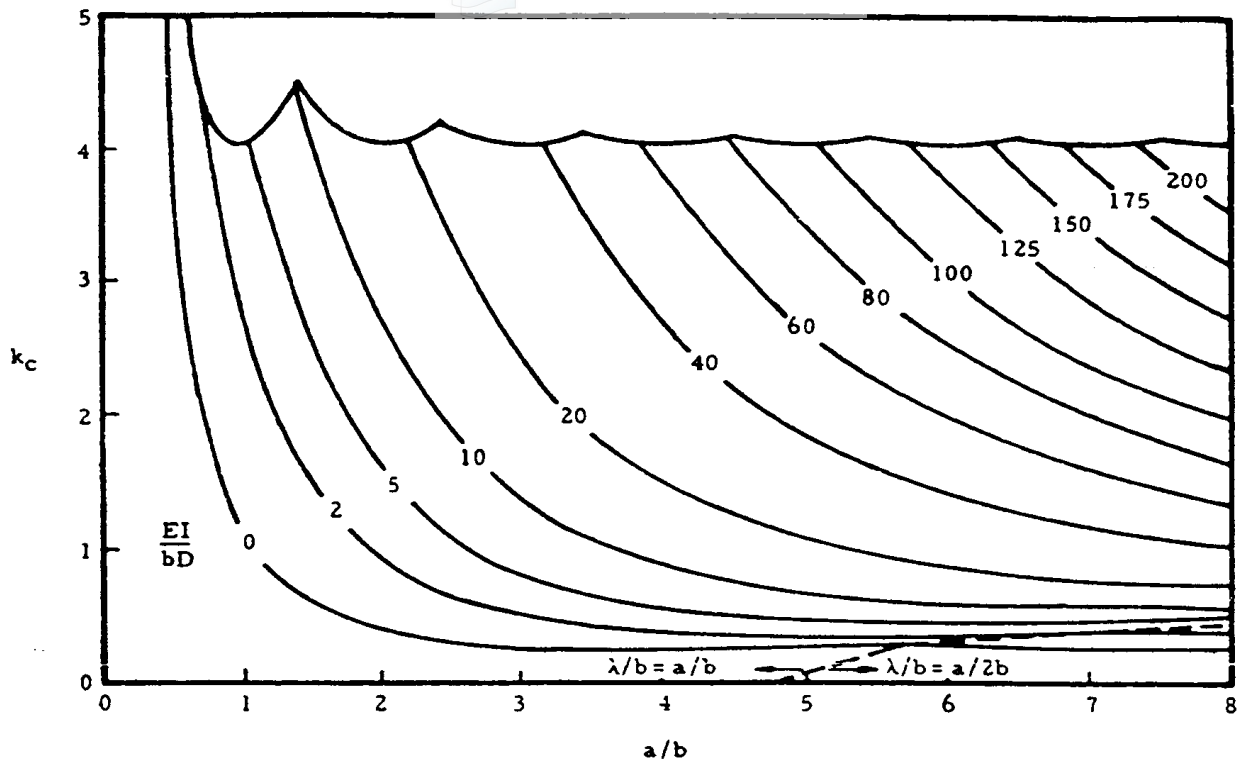
(g) Three stiffeners A/bt = 0
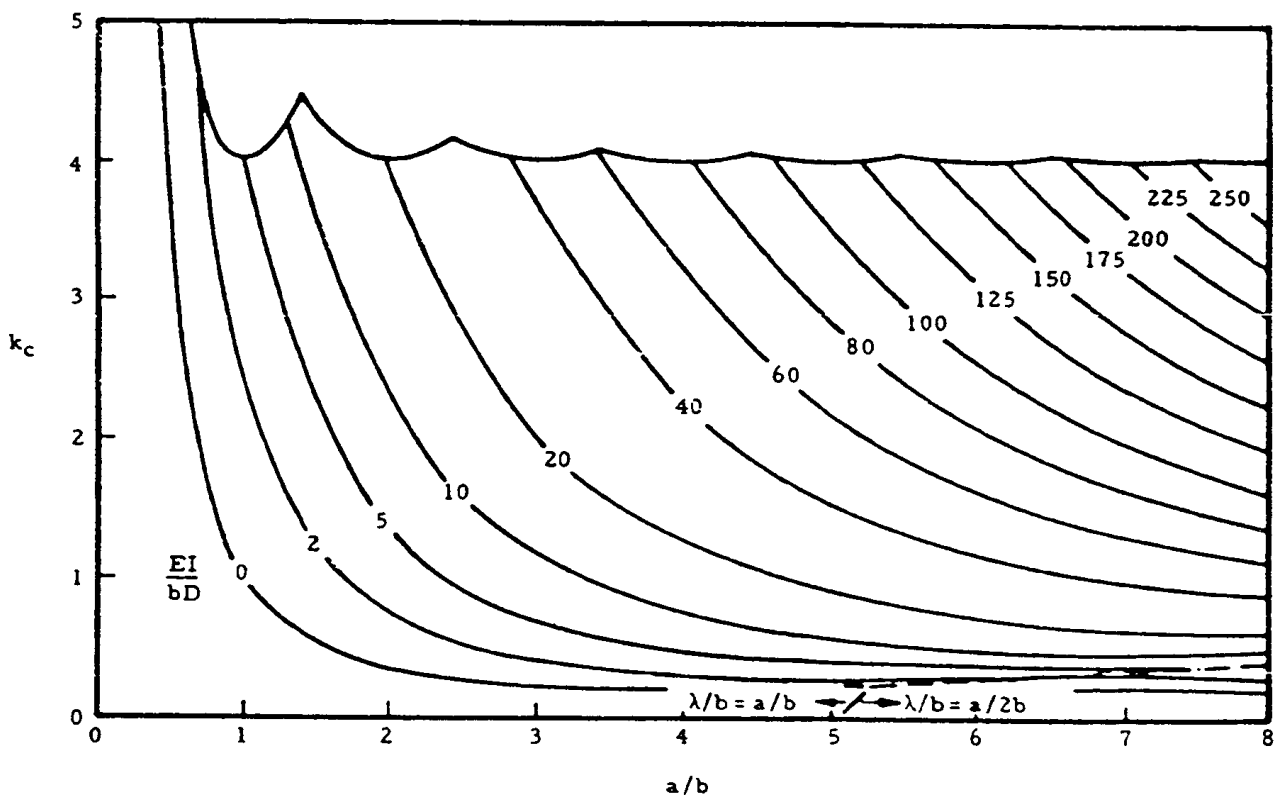
(h) Three stiffeners A/bt = 0.2

Figure 6-13.   Compressive-Buckling Coefficients for Simply Supported Flat
Plates with Longitudinal Stiffeners (continued)

6 - 23
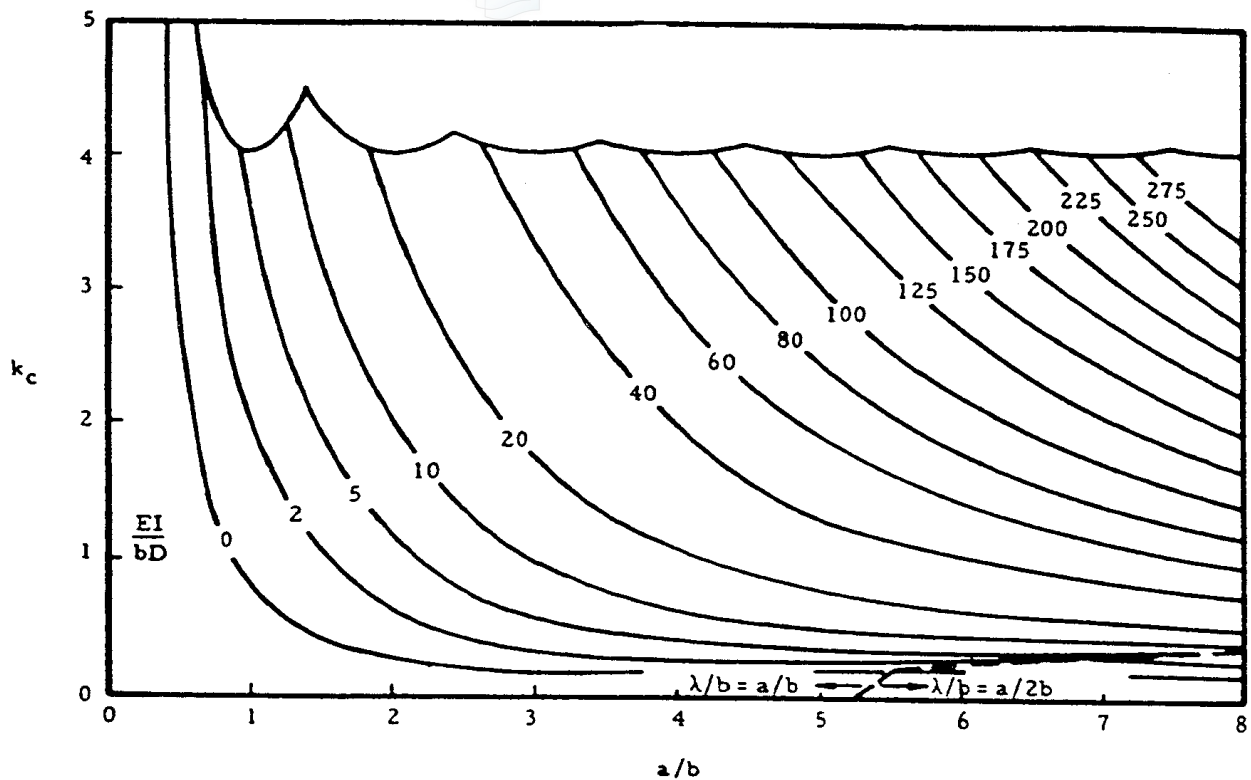
(i) Three Stiffeners A/bt = 0.4
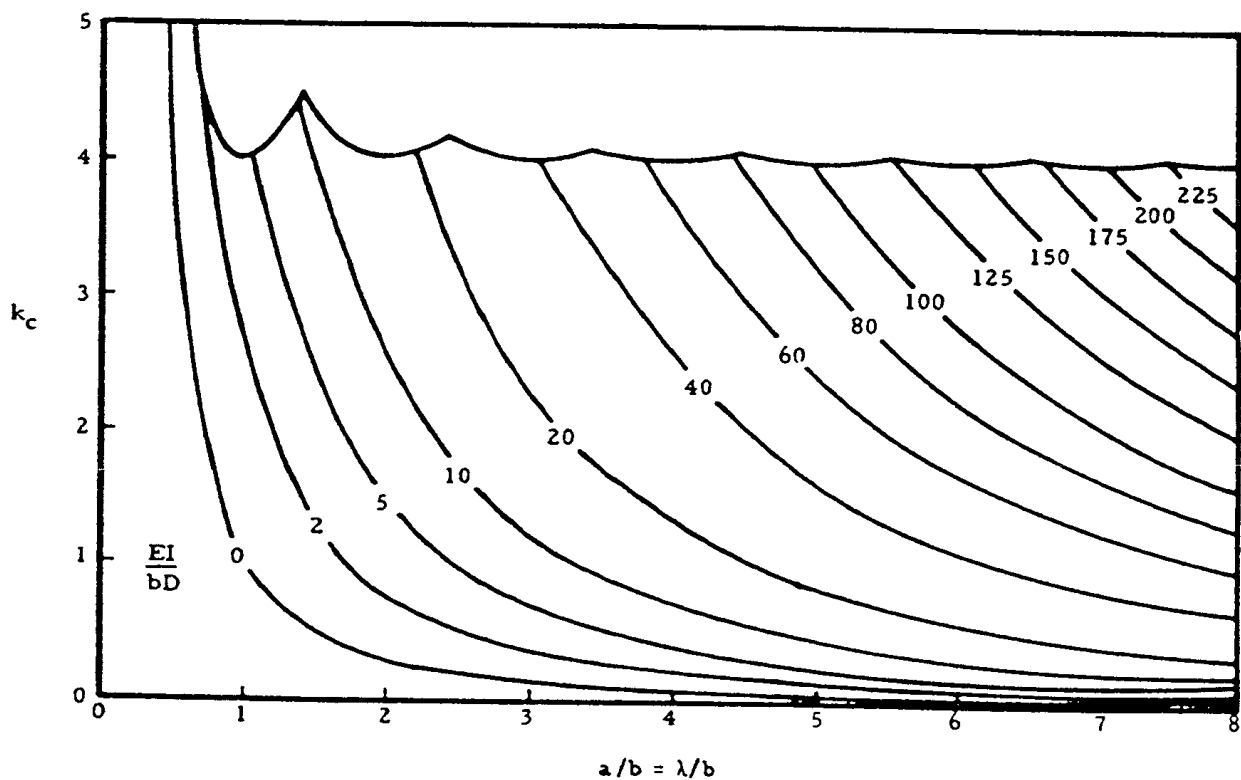
(j) Infinite number of stiffeners A/bt = 0

Figure 6-13.   Compressive-Buckling Coefficients for Simply Supported Flat
Plates with Longitudinal Stiffeners (continued)

6 - 24

$$a/b = \lambda/b$$
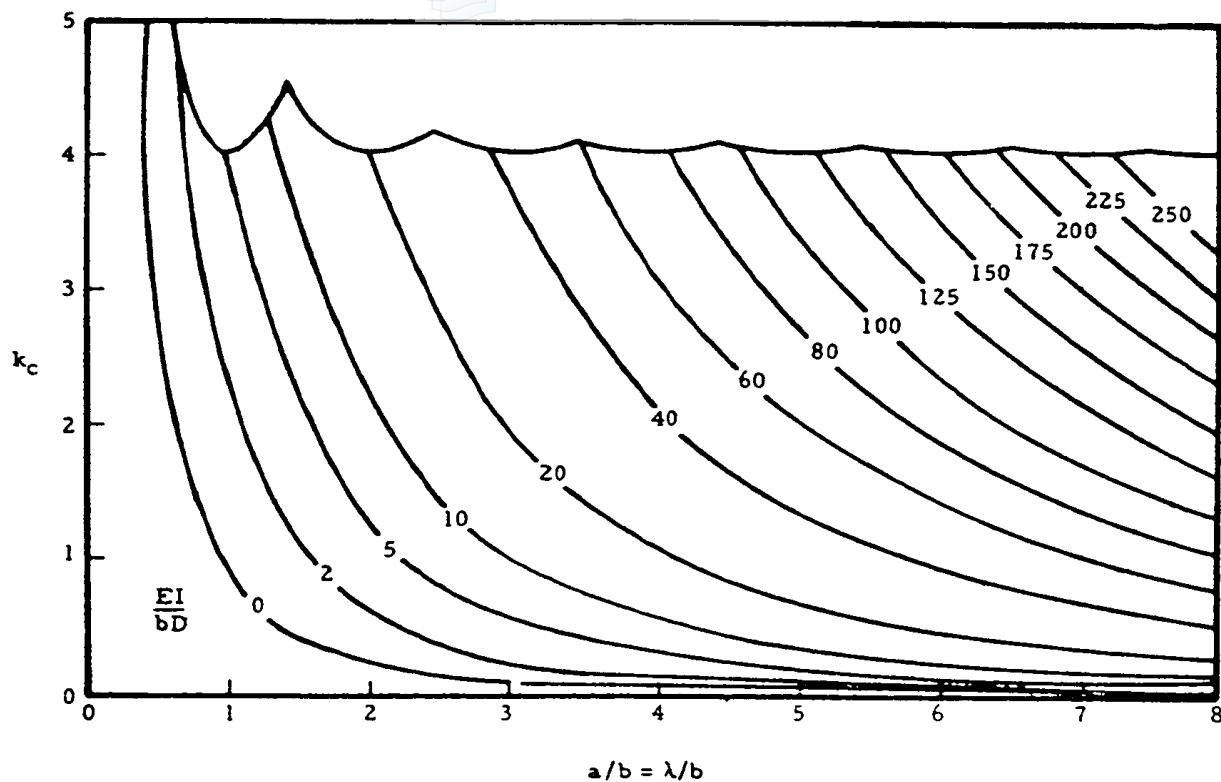
(k) Infinite number of stiffeners   A/bt = 0.2

$$a/b = \lambda/b$$
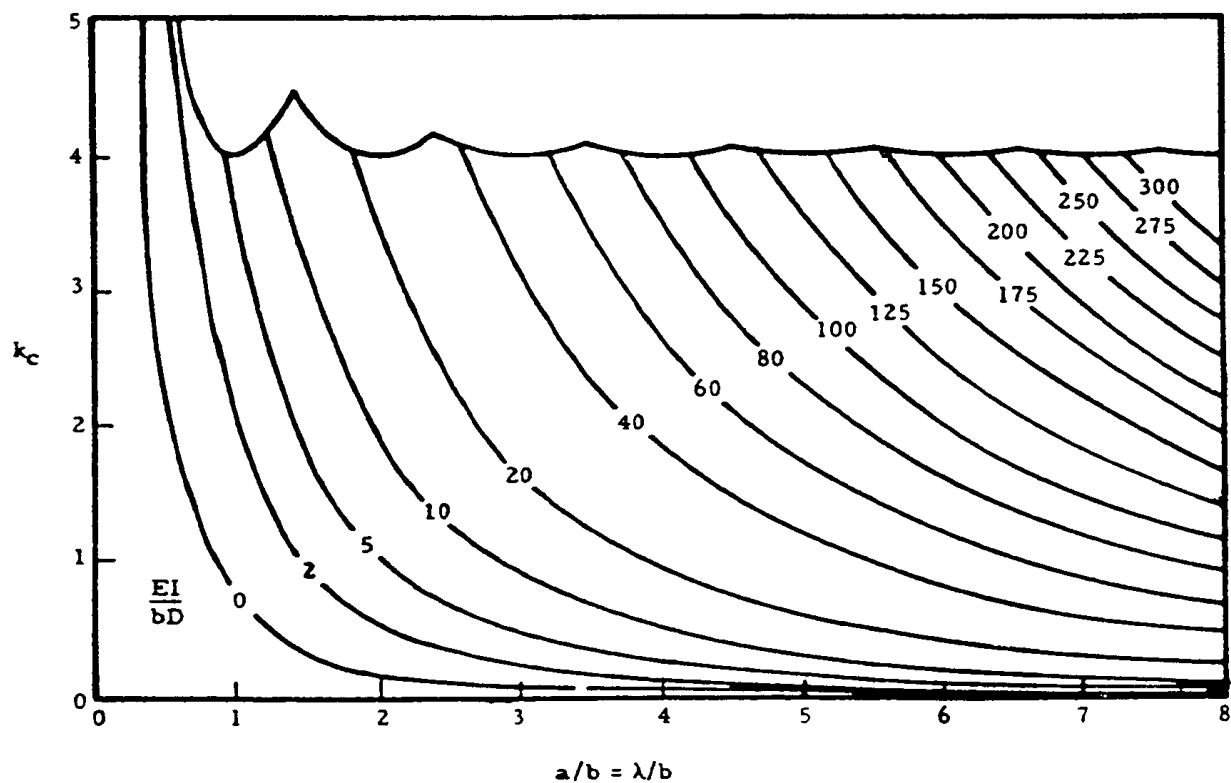
(l) Infinite number of stiffeners   A/bt = 0.4

Figure 6-13.   Compressive-Buckling Coefficients for Simply Supported Flat
Plates with Longitudinal Stiffeners (concluded)

6 - 25
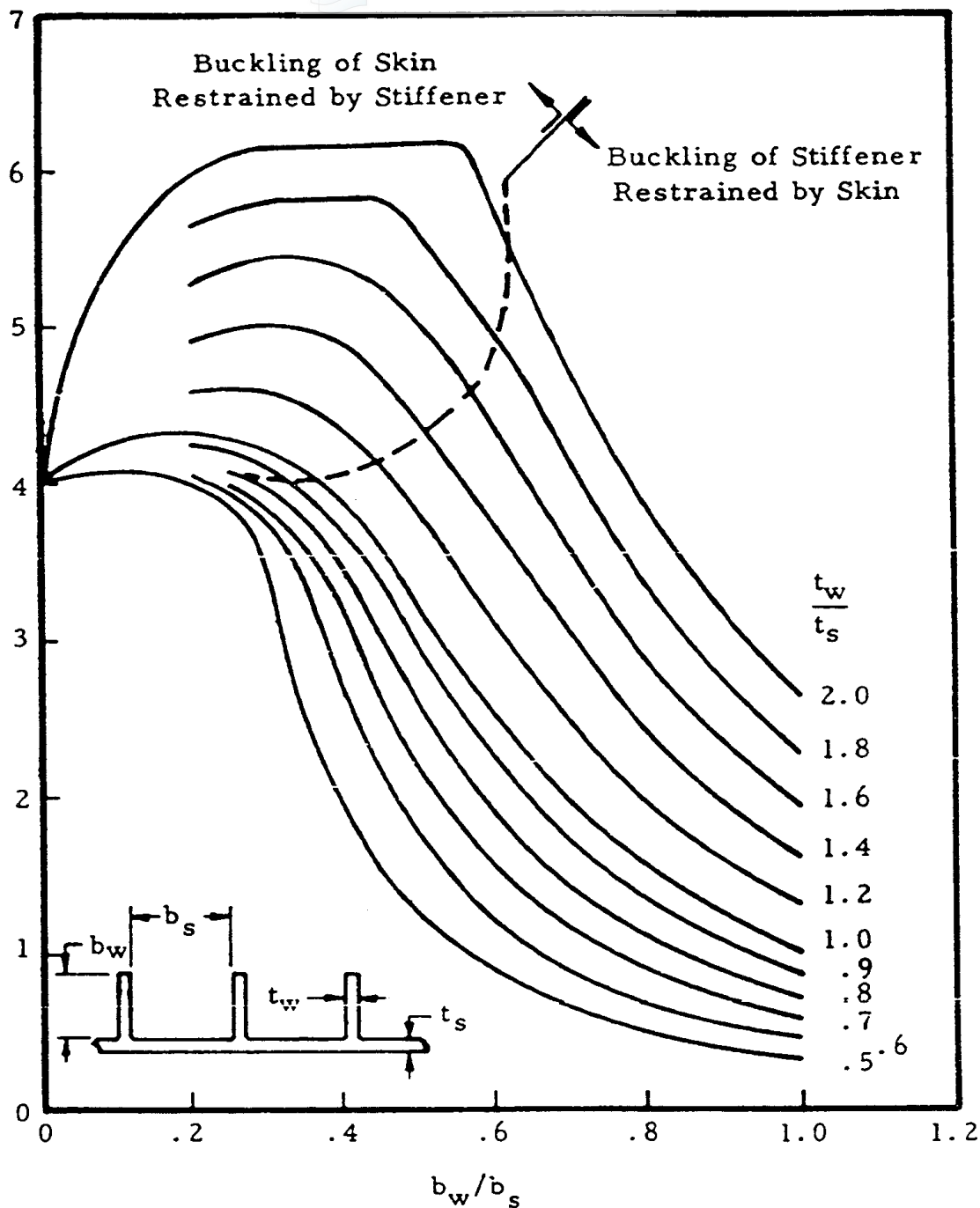
(a) Web Stiffeners $0.5 < t_w/t_s < 2.0$

Figure 6-14.   Compressive-Local-Buckling Coefficients for Infinitely Wide
Idealized Stiffened Flat Plates

$$\sigma_{cr} = \frac{k_s \, \pi^2 \, E}{12(1-\nu_s^2)} \left(\frac{t_s}{b_s}\right)^2$$
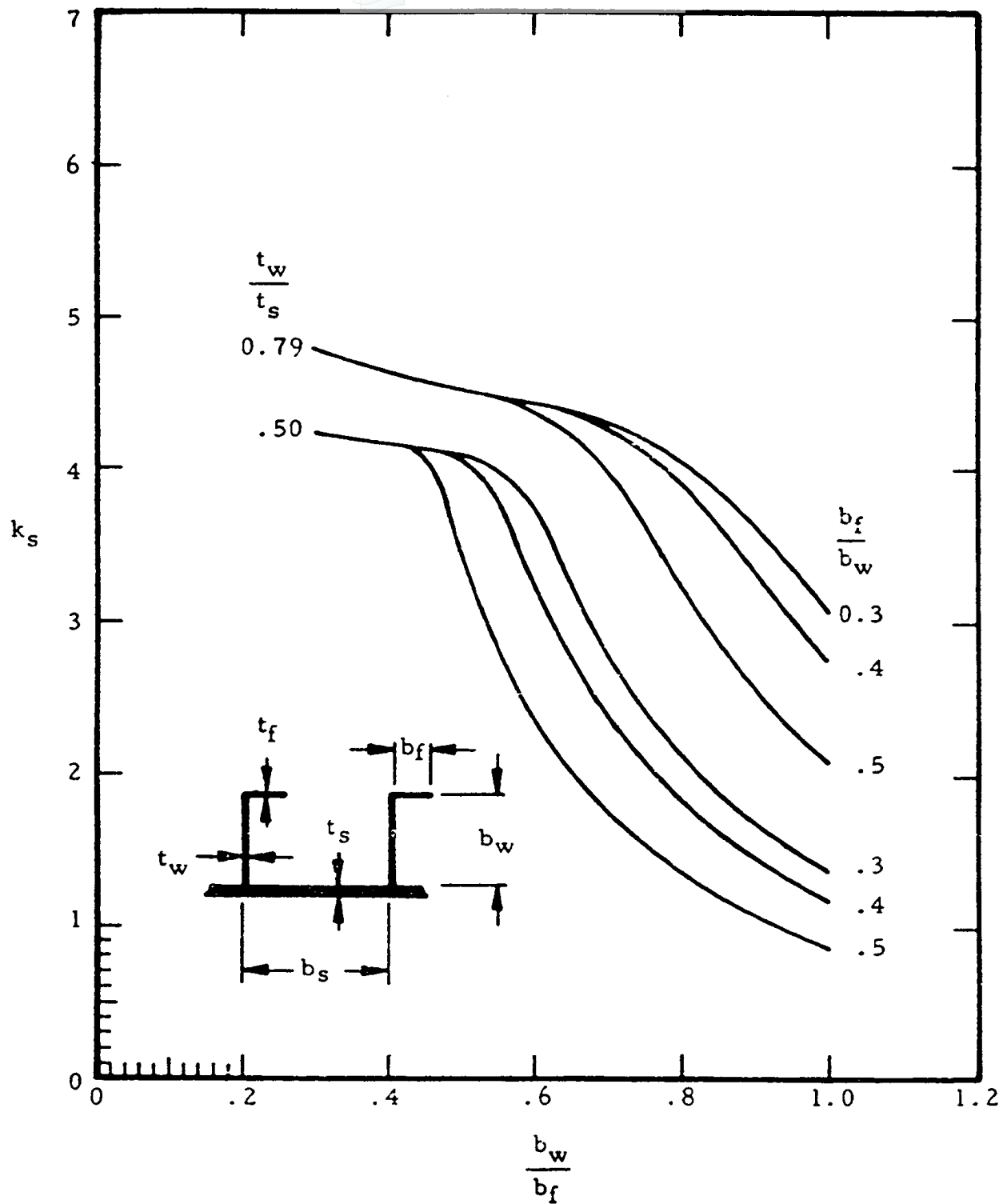
(b) Z-section stiffeners $t_w/t_s = 0.50$ and 0.79

Figure 6-14. Compressive-Local-Buckling Coefficients for Infinitely Wide
Idealized Stiffened Flat Plates (continued)
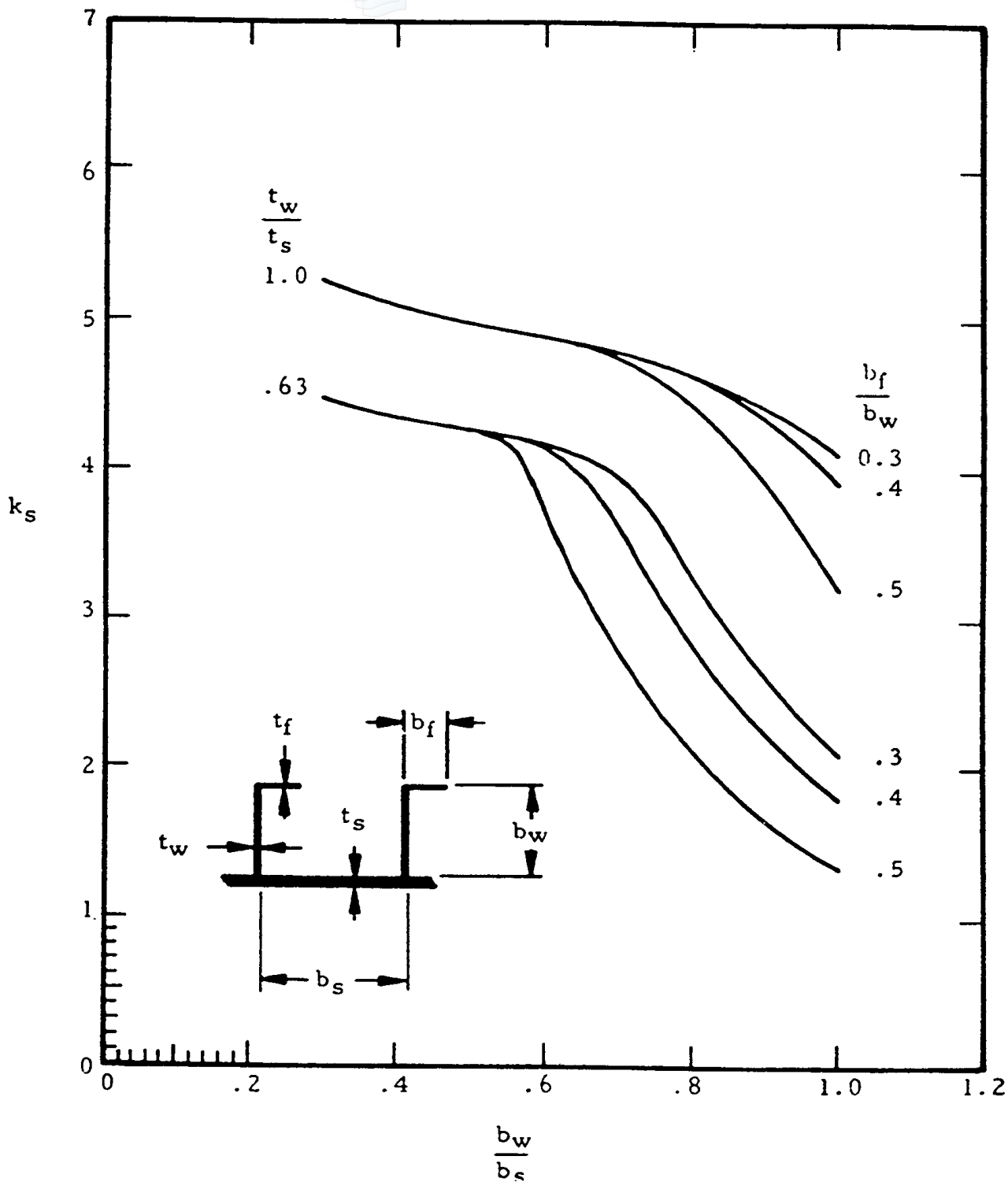
(c) Z-section stiffeners t_w/t_s = 0.63 and 1.0

Figure 6-14. Compressive-Local-Buckling Coefficients for Infinitely Wide
Idealized Stiffened Flat Plates (continued)
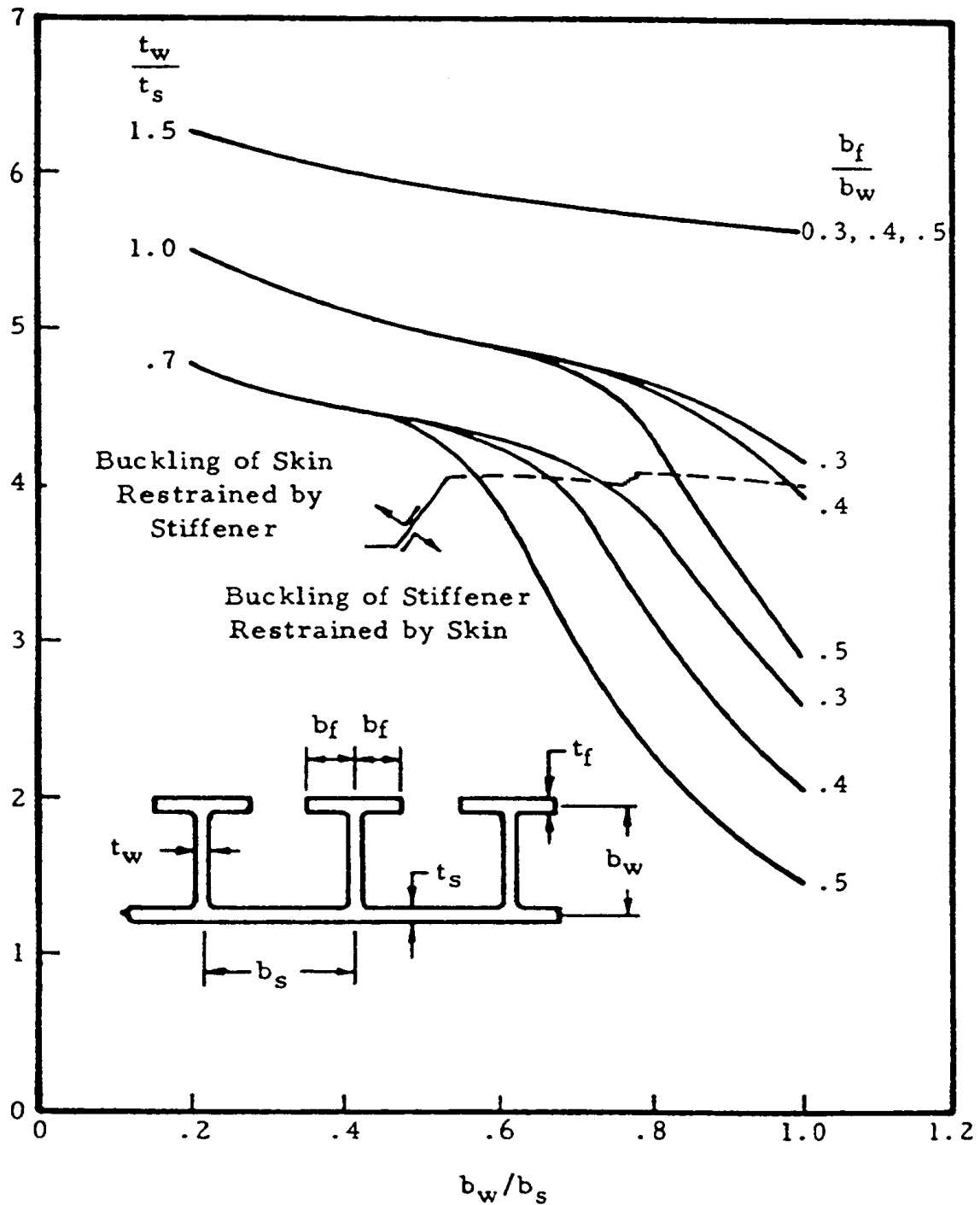
(d) T-section stiffeners. $t_w/t_f = 1.0$; $\dfrac{b_f}{t_f} > 10$; $\dfrac{b_w}{b_s} > 0.25$

Figure 6-14. Compressive-Local-Buckling Coefficients for Infinitely Wide
Idealized Stiffened Flat Plates (concluded)
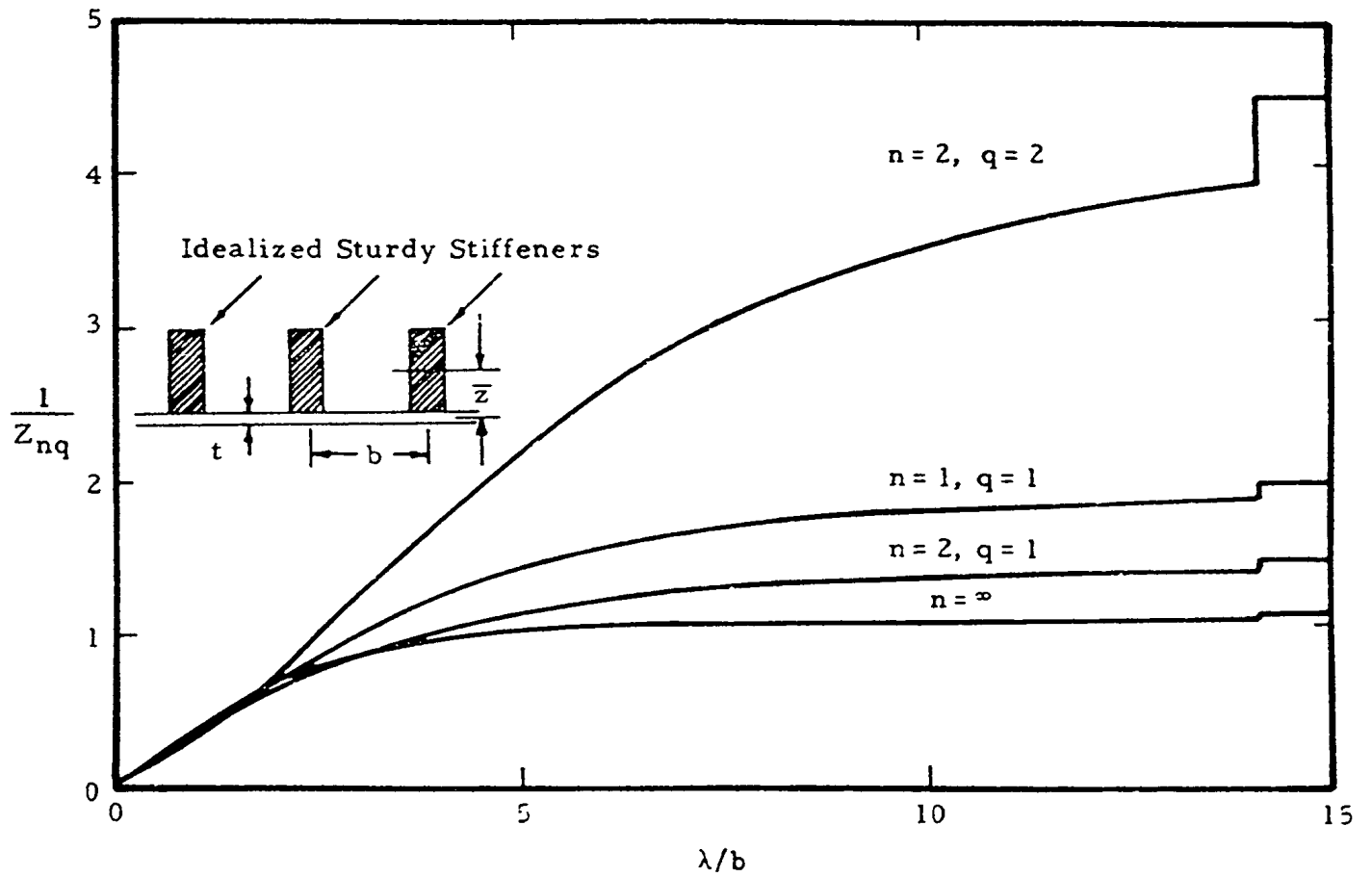
Figure 6-15. $1/Z_{nq}$ as a Function of Stiffened Plate Proportions and Buckle Pattern
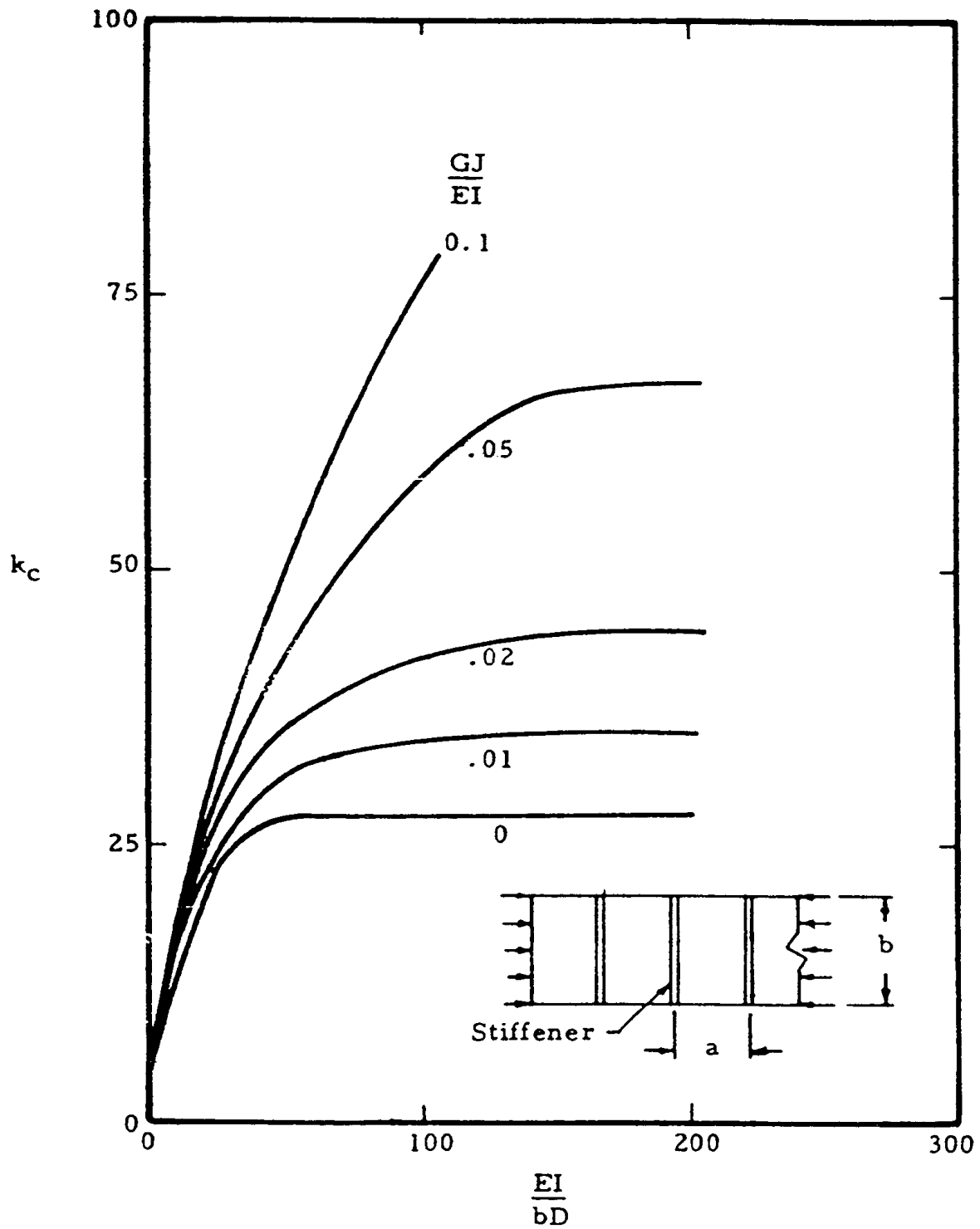
(a) a/b = 0.20

Figure 6-16.   Longitudinal-Compressive-Buckling Coefficients for Simply
Supported Plates with Transverse Stiffeners
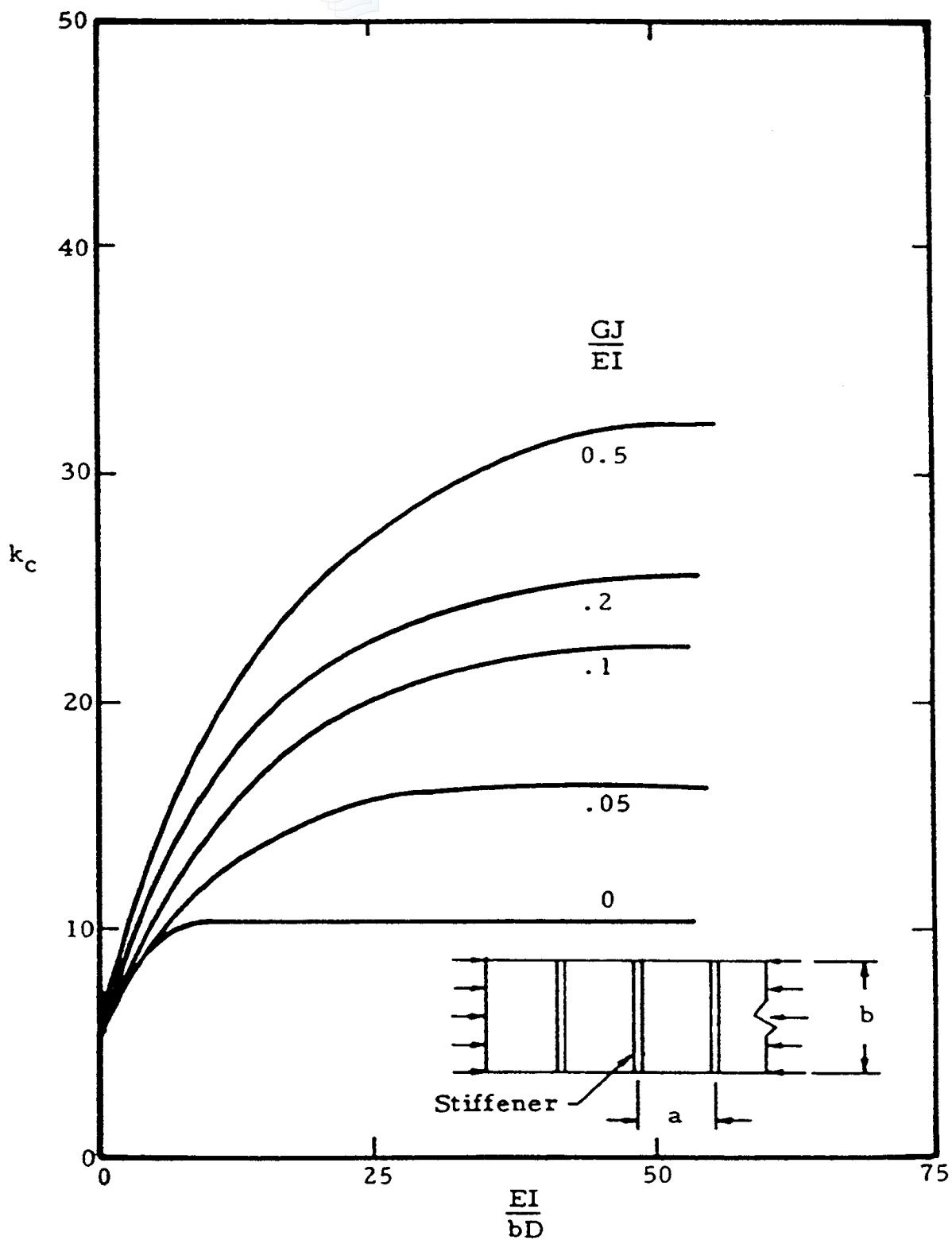
(b) a/b = 0.35

Figure 6-16.   Longitudinal-Compressive-Buckling Coefficients for Simply
Supported Plates with Transverse Stiffeners (continued)
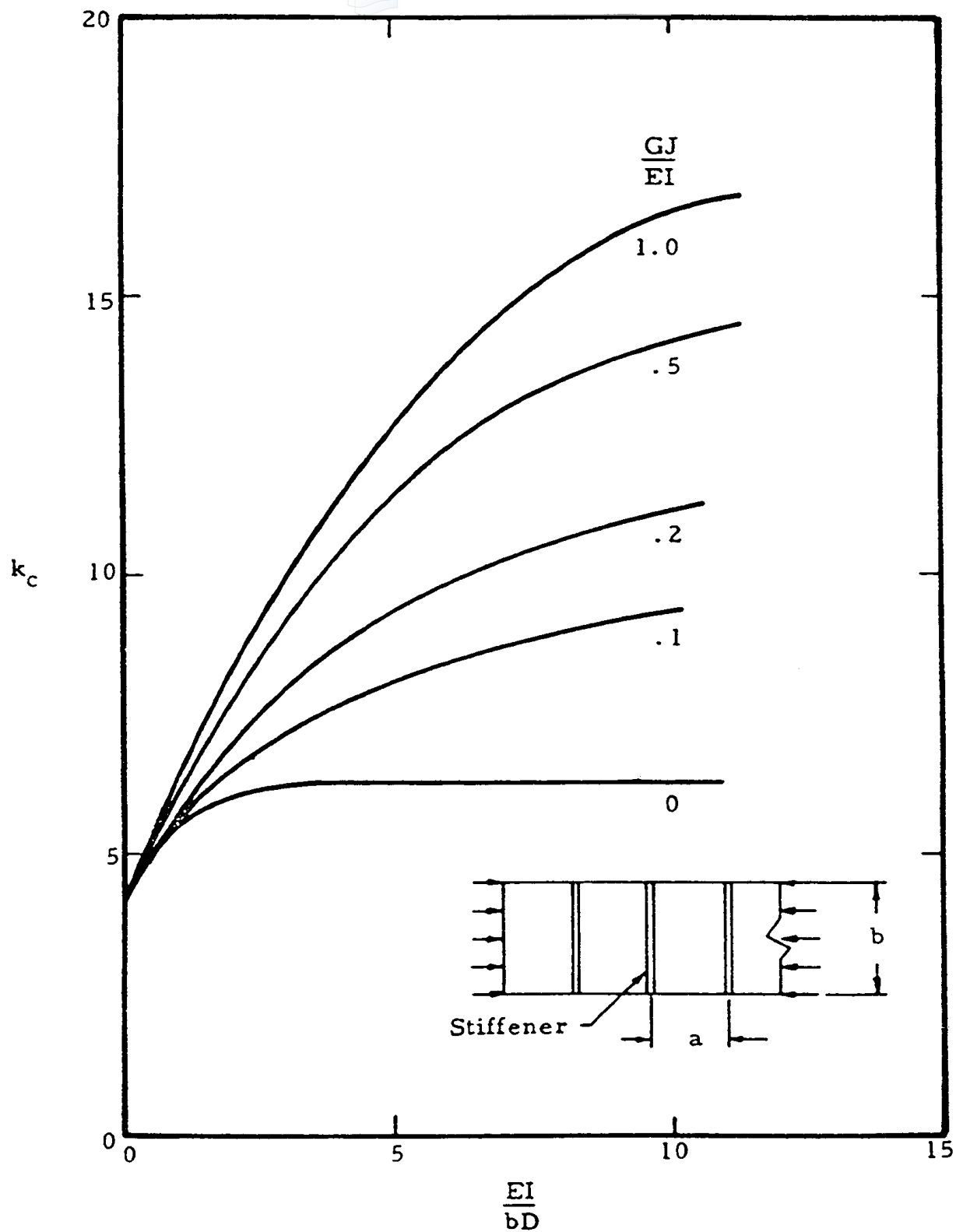
(c) a/b = 0.50

Figure 6-16. Longitudinal-Compressive-Buckling Coefficients for Simply
Supported Plates with Transverse Stiffeners (concluded)

6.3.3   Crippling Failure of Flat Stiffened Plates in Compression

For stiffened plates having slenderness ratios $L'/\rho \leqq 20$, considered to be short plates, the failure mode is crippling rather than buckling when loaded in compression. The crippling strength of individual stiffening elements is considered in Chapter 2, Column Analysis. The crippling strength of panels stiffened by angle-type elements is given by Equation (6-13).

$$\frac{\overline{F}_f}{F_{cy}} = \beta_t \left[\frac{g\, t_w\, t_s}{A} \left(\frac{\overline{\eta}\, E}{F_{cy}} \right)^{\frac{1}{2}} \right]^{0.85} \tag{6-13}$$

For more complex stiffeners such as Y sections, the relation of Equation (6-14) is used to find a weighted value of t_w.

$$\overline{t}_w = \frac{\Sigma\, a_i\, t_i}{\Sigma\, a_i} \tag{6-14}$$

where a_i and t_i are the length and thickness of the cross-sectional elements of the stiffener. Figure 6-17 shows the method of determining the value of g used in Equation (6-13) based on the number of cuts and flanges of the stiffened panels. Figure 6-18 gives the coefficient β_t for various stiffening elements.

If the skin material is different from the stiffener material, a weighted value of F_{cy} given by Equation (6-15) should be used.

$$\overline{F}_{cy} = \frac{F_{cy_s} + F_{cy_w}\left[(\overline{t}/t_s) - 1 \right]}{(\overline{t}/t_s)} \tag{6-15}$$

Here, $\overline{t}$ is the effective thickness of the stiffened panel.

The above relations assume the stiffener-skin unit to be formed monolithically; that is, the stiffener is an integral part of the skin. For riveted construction, the failure between the rivets must be considered. The interrivet buckling stress is determined as to plate buckling stress, and is given by Equation (6-16).

$$F_i = \frac{\epsilon\, \pi^2\, \eta\, \overline{\eta}\, E}{12\,(1-\nu^2)} \left(\frac{t_s}{p} \right)^2 \tag{6-16}$$

Values of ϵ, the edge fixity, are given in Table 6-1.

g=19   g=19   g=19   g=19   g=18
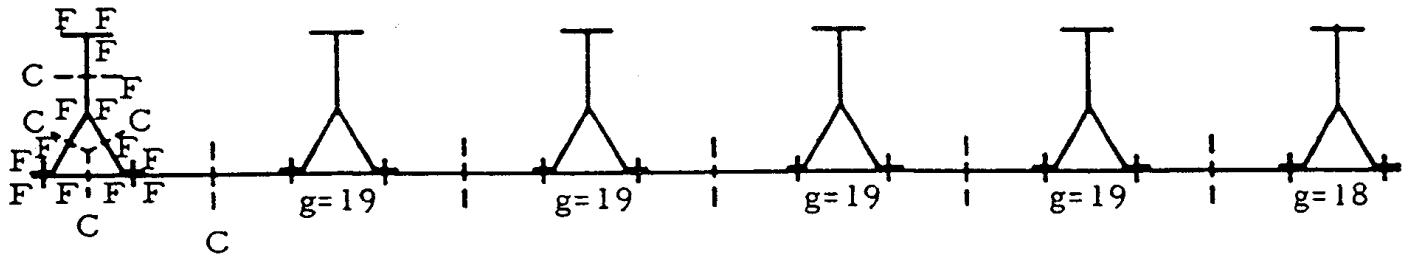
5 cuts
14 flanges
19 = g

Average g = 18.85

(a) Y-stiffened panel

g=8   g=8   g=8   g=8   g=7
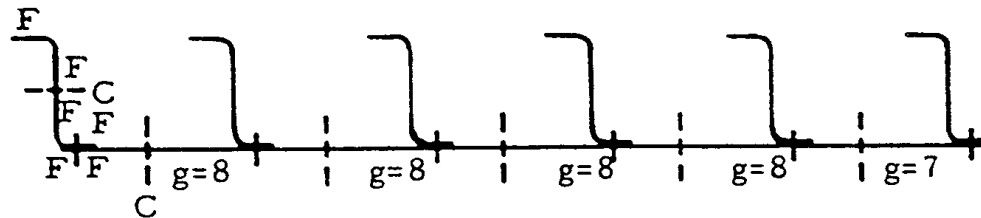
2 cuts
6 flanges
8 = g

Average g = 7.83

(b) Z-stiffened panel

g=17   g=17   g=17   g=17   g=16
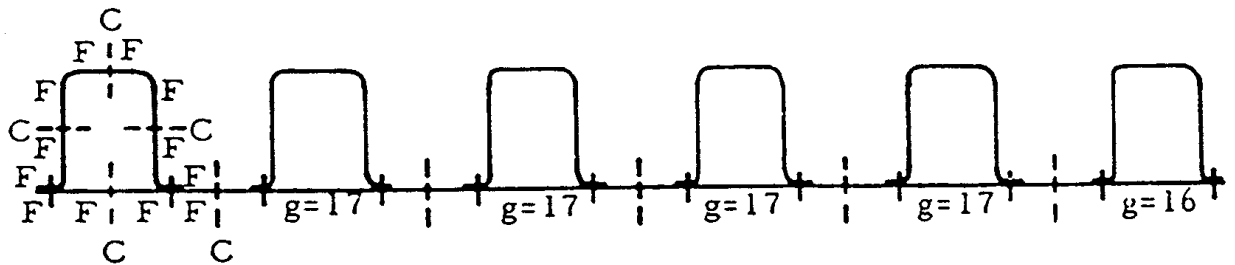
5 cuts
12 flanges
17 = g

Average g = 16.83

(c) Hat-stiffened panel

Figure 6-17.   Method of Cutting Stiffened Panels to Determine g
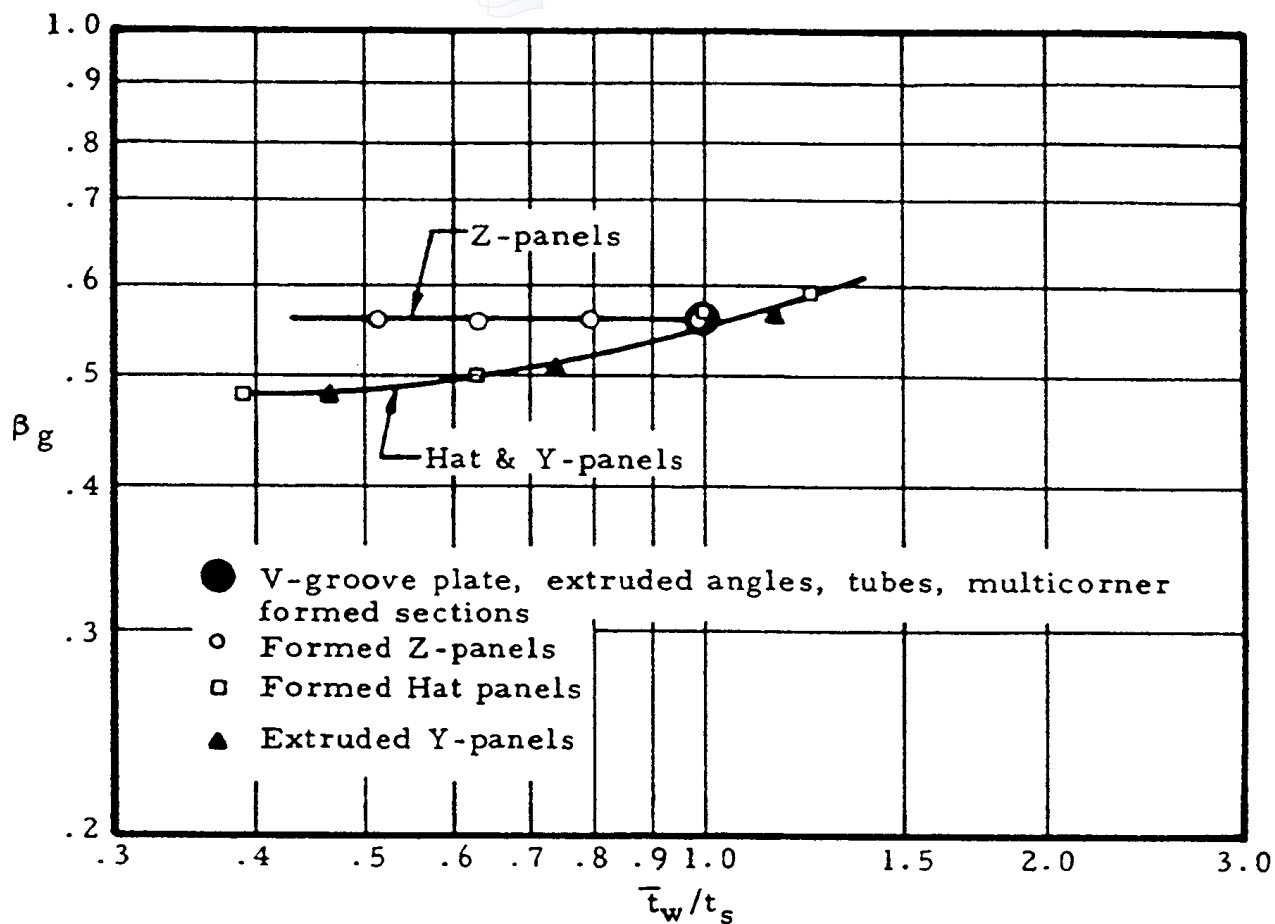
Figure 6-18. Crippling Coefficients for Angle-Type Elements

TABLE 6-1

End-Fixity Coefficients for Interrivet Buckling

Fastener Type	(Fixity-Coefficient) ϵ
Flathead rivet	4
Spotwelds	3.5
Brazier-head rivet	3
Countersunk rivet	1

After the interrivet buckling occurs, the resultant failure stress of the panel is given by Equation (6-17).

$$\overline{F}_{f_r} = \frac{F_i \, (2\,b_{ei} \, t_s) + \overline{F}_{f_{st}} \, A_{st}}{(2\,b_{ei} \, t_s) + A_{st}} \tag{6-17}$$

Here the value b_{ei} is the effective width of skin corresponding to the interrivet buckling stress F_i. The failure stress of short riveted panels by wrinkling can be determined. The following quantities are used:

$\overline{F}_{f_{st}}$ crippling strength of stringer alone (see Chapter 2, Column Analysis)

$\overline{F}_w$ wrinkling strength of the skin

$\overline{F}_f$ crippling strength of a similar monolithic panel

$\overline{F}_{f_r}$ strength of the riveted panel

The wrinkling strength of the skin can be determined from Equation (6-18) and Figure 6-19. Here, f is the effective rivet offset distance given in Figure 6-20. This was obtained for aluminum rivets having a diameter greater than 90% of the skin thickness.

$$F_w = \frac{k_w \, \pi^2 \, \eta \, \overline{\eta} \, E}{12(1-\nu^2)} \left(\frac{t_s}{b_s}\right)^2 \tag{6-18}$$

Now, based on the stringer stability, the strength of the panel can be calculated. Table 6-2 shows the various possibilities and solutions.

TABLE 6-2

Riveted Panel Strength Determination

Stringer Stability	Panel Strength
$\overline{F}_{f_{st}} \geq \overline{F}_w$ — stable	$\overline{F}_{fr} = \overline{F}_w$
$\overline{F}_{f_{st}} < \overline{F}_w$ — unstable	$\overline{F}_{fr} = \dfrac{\overline{F}_w \, b_s t_s + \overline{F}_{f_{st}} \, A_{st}}{b_s t_s + A_{st}}$
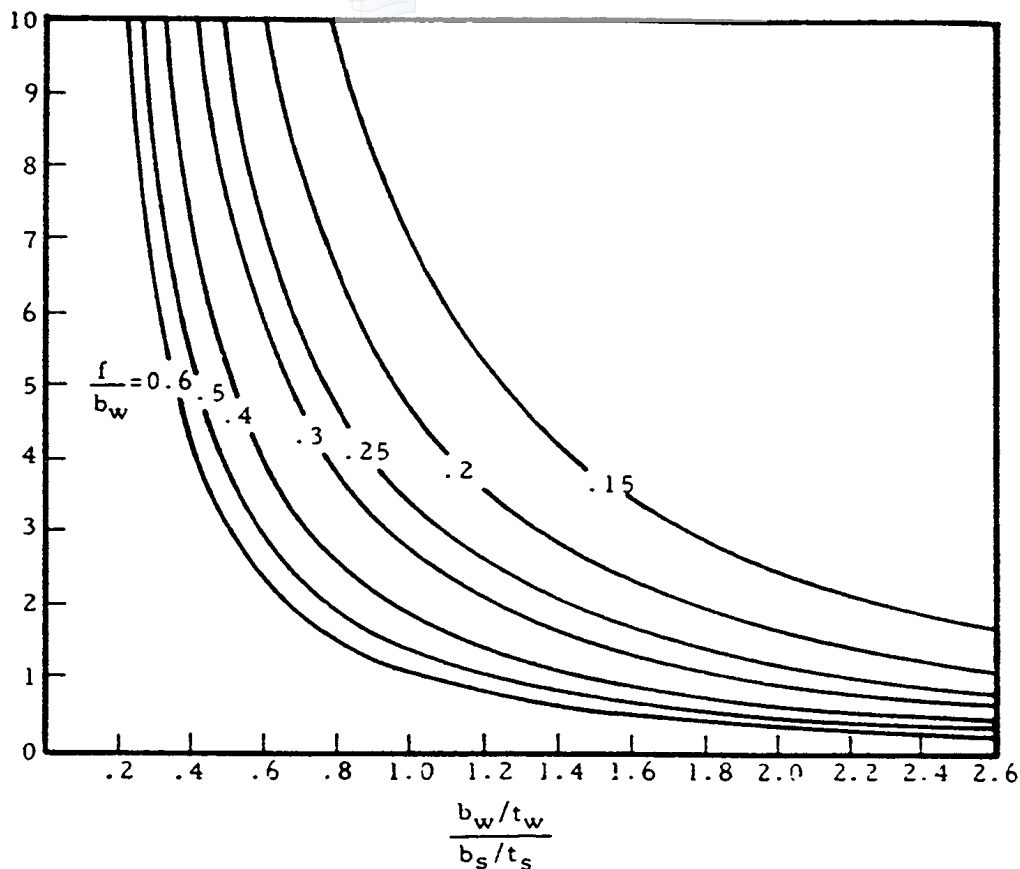
Figure 6-19.   Experimentally Determined Coefficients for Failure in
Wrinkling Mode
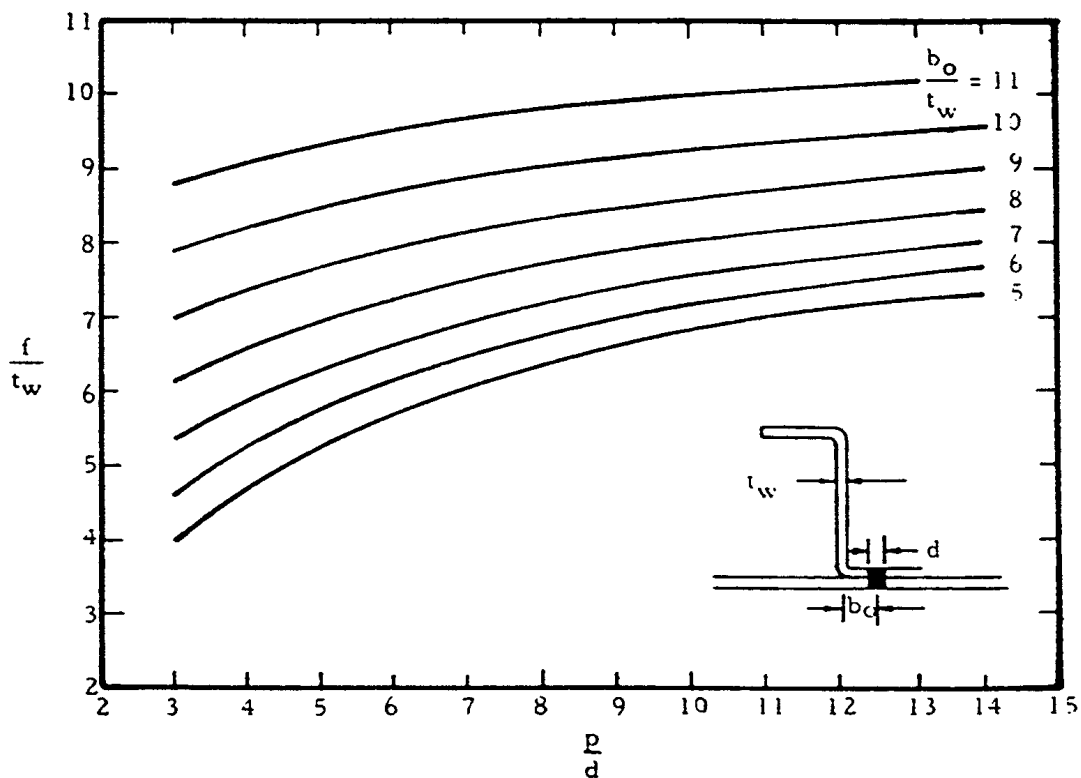
Figure 6-20.   Experimentally Determined Values of Effective Rivet Offset

It is noted that in no case should $\overline{F}_{sr} > \overline{F}_f$. Thus, the lower of these two values should be used.

The use of the coefficient k_w is based upon aluminum alloy data for other materials. The procedure is to use Equation (6-19) for the panel crippling strength.

$$\frac{F_{fr}}{F_{cy}} = 17.9 \left(\frac{t_w}{f}\right)^{4/3} \left(\frac{t_w}{b_w}\right)^{1/6} \left[\frac{t_s}{b_s}\left(\frac{\eta E}{F_{cy}}\right)\right]^{1/2} \tag{6-19}$$

6.4   Bending of Flat Plates

The bending of flat plates in aircraft structures can be caused by both in-plane forces or by normal forces. The quantities of interest in the analysis and design of such plates are the magnitude and location of the maximum stress and the maximum deflection.

The following sections present plots and tables allowing the calculation of these quantities.

6.4.1   Unstiffened Flat Plates in Bending

The general buckling relation for plates subjected to in-plane bending is given by Equation (6-20).

$$F_b = \eta \overline{\eta} \frac{k_b \pi^2 E}{12(1-\nu_e^2)} \left(\frac{t}{b}\right)^2 \tag{6-20}$$

Values of bending coefficient, k_b, are given in Figure 6-21 for various edge restraints and the number of buckles versus λ/b, the buckle wave length ratio, and in Figure 6-22 for various edge restraints versus the ratio a/b.

For plates loaded with uniformly distributed normal force, the maximum stress and maximum deflection can be represented by simple relations by the use of a series of constants which depend upon the plate geometry and loading. Tables 6-3 through 6-8 present loading coefficients for use with Equations (6-21) through (6-25).
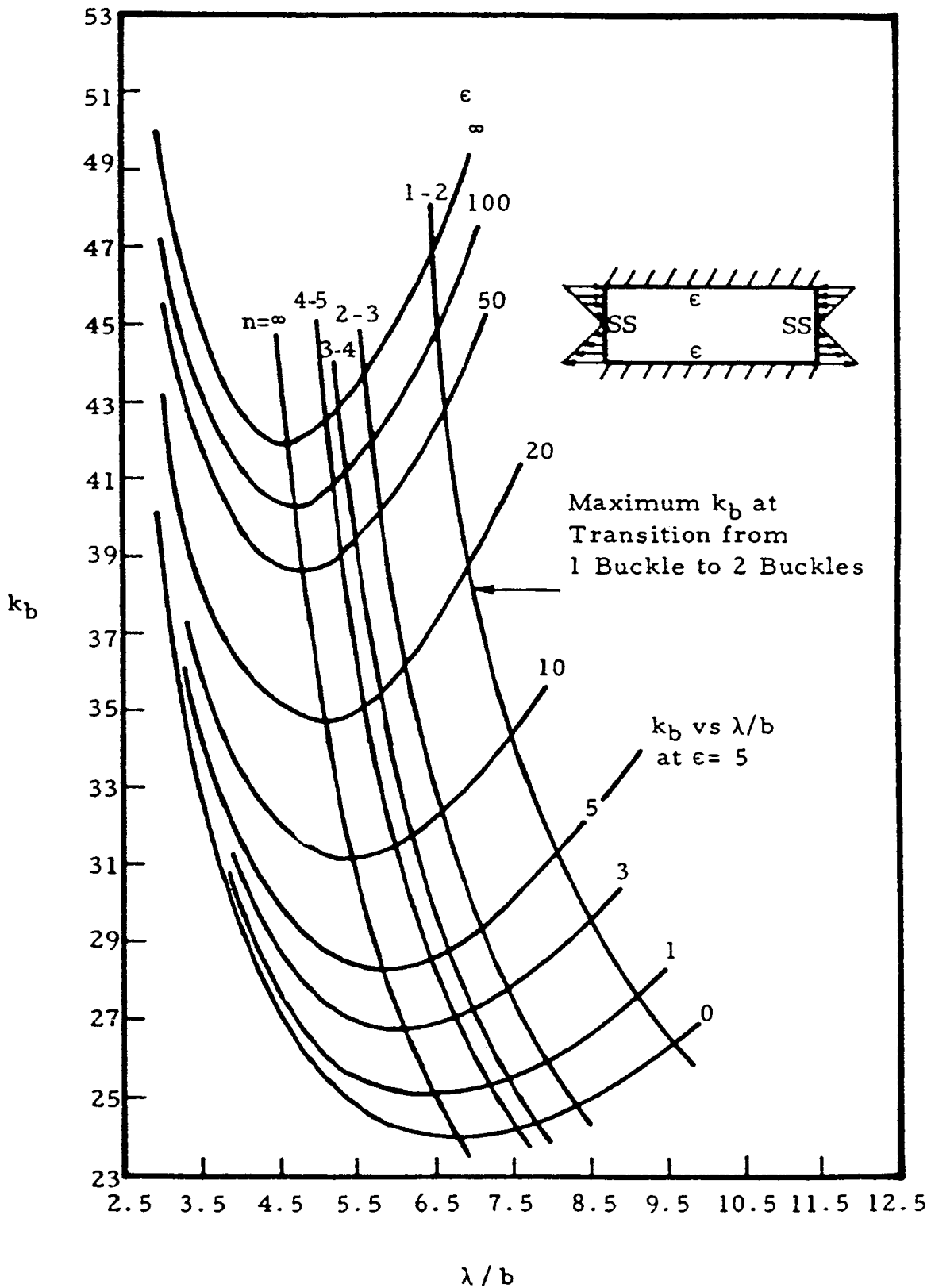
Figure 6-21. Bending-Buckling Coefficient of Plates as a Function of λ/b for Various Amounts of Edge Rotational Restraint
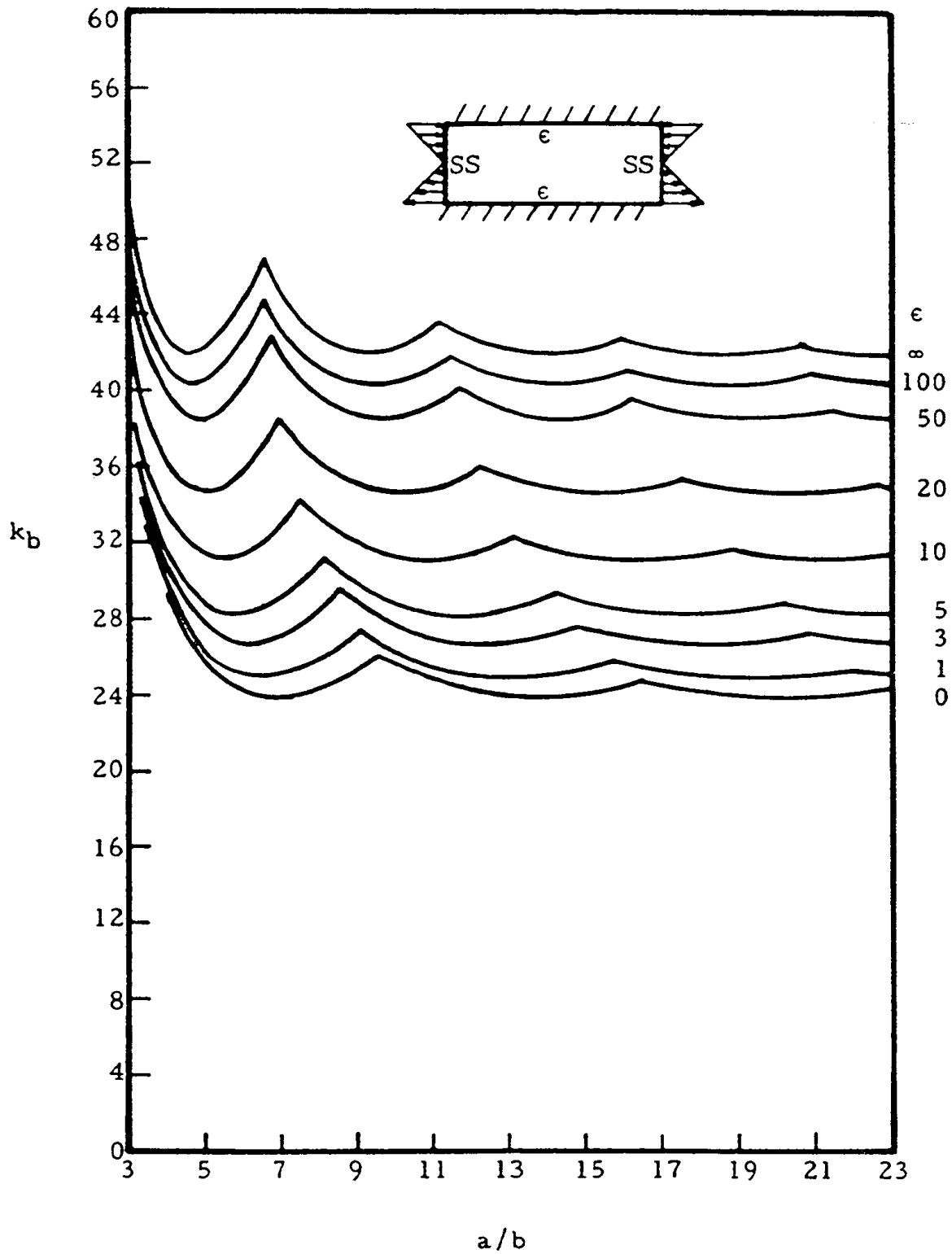
Figure 6-22.   Bending-Buckling Coefficient of Plates as a Function of a/b
for Various Amounts of Edge Rotational Restraint

TABLE 6-3

Loading Coefficients for Flat Rectangular Plates Under Various Loadings *

MANNER OF LOADING:	a/b 1.0 K	K₁	1.2 K	K₁	1.4 K	K₁	1.6 K	K₁	1.8 K	K₁	2.0 K	K₁	2.5 K	K₁	3.0 K	K₁	4.0 K	K₁	∞ K	K₁	L	Locations of stress and deflection
All edges supported, Uniform load over entire surface	0.044	0.29	0.062	0.38	0.077	0.45	0.091	0.52	0.10	0.57	0.11	0.61	0.12	0.64	0.13	0.61	0.14	0.61			b	F max. at center; Y max. at center
All edges supported, Distributed load varying linearly along length	0.022	0.16	0.019	0.21	0.040	0.25	0.048	0.24	0.053	0.31	0.060	0.34	0.070		0.078	0.41	0.091	0.49			b	
All edges supported, Distributed load varying linearly along breadth	0.022	0.16	0.031	0.21	0.038	0.25	0.045	0.24	0.051	0.31	0.056	0.12	0.063	0.15	0.067	0.37	0.070	0.38			b	
All edges fixed, Uniform load over entire surface	0.014	0.31	0.019	0.38	0.023	0.44	0.025	0.47	0.027	0.49	0.028	0.50	0.028	0.50	0.028	0.50	0.028	0.50			b	F max. at center of long edge; Y max. at center
Long edges fixed, short edges supported, Uniform load over entire surface	0.021	0.420	0.24	0.46	0.026	0.49	0.027	0.50	0.028	0.50	0.028	0.50	0.028	0.50	0.028	0.50	0.028	0.50			b	F max. at center of fixed edges; Y max. at center
Short edges fixed, long edges supported, Uniform load over entire surface	0.021	0.42	0.034	0.52	0.050	0.60	0.066	0.65	0.080	0.69	0.099	0.71	0.13	0.71	0.11	0.71	0.13	0.71			b	F max. at center of fixed edge; Y max. at center
One long edge clamped, other three edges supported, Uniform load over entire surface	0.010	0.50	0.016	0.58	0.012	0.61	0.017	0.68	0.030	0.71	0.054	0.740	0.054	0.74	0.051	0.75	0.054	0.75			b	F max. at center of fixed edge; Y max. at center
One short edge clamped, other three edges supported. Uniform load over entire surface	0.019	0.500	0.050	0.58	0.064	0.64	0.088	0.71	0.090	0.71	0.10	0.74	0.122	0.74	0.132	0.75	0.139	0.75			b	F max. at center of fixed edge; Y max. at center
One short edge free, other three edges supported, Uniform load over entire surface	0.160	0.67	0.15	0.74	0.16	0.76	0.16	0.77	0.16	0.78	0.16	0.79	0.17	0.80	0.17	0.80	0.17	0.80			b	F max. at center of free edge; Y max. at center
One short edge free, other three edges supported, Uniform load over entire surface	0.040	0.20	0.045	0.24	0.048	0.27	0.051	0.29	0.053	0.31	0.058	0.32	0.054	0.15	0.067	0.16	0.070	0.37			b	F max. at center of free edge; Y max. at center
One long edge free, other three edges supported. Distributed load varying linearly along length	0.14	0.67	0.12	0.57	0.11	0.48	0.10	0.42	0.090	0.38	0.080	0.36	0.080	0.36	0.080	0.16	0.080	0.16			b	F max. at center of free edge; Y max. at center
One long edge free, other three edges supported. Distributed load varying linearly along length	0.040	0.20	0.036	0.18	0.033	0.17	0.030	0.15	0.024	0.13	0.023	0.11									b	F max. at center of free edge; Y max. at center
All edges supported. Distributed load in form of a triangular prism	0.029	0.041	0.040	0.063	0.050	0.090	0.058	0.118	0.065	0.358	0.071	0.441	0.082	0.450	0.085	0.476	0.091	0.500	a/b 0.091	0.500	b	F max. at center; Y max. at center

Manner of loading	b/a 0.6 K	K₁	0.8 K	K₁	1 K	K₁	1.2 K	K₁	1.4 K	K₁	1.6 K	K₁	1.8 K	K₁	2.0 K	K₁	Locations of stress and deflection
All edges fixed, distributed load varying linearly along length	0.0016	0.11	0.0047	0.14	0.0074	0.17	0.009	0.18	0.011	0.18	0.013	0.18	0.013	0.19	0.014	0.19	Max. F_b is at x = .55b; y = 0.55a
	0.0016	0.064	0.0047	0.069	0.0074	0.076	0.009	0.071	0.061	0.013	0.041	0.011	0.011	0.014	0.014	0.014	Max. F_b at x = 0; L = 0.4a; Max. V_a is at x = 0; y = 0
	0.0016	0.083	0.0047	0.18	0.0074	0.24	0.009	0.24	0.011	0.21	0.013	0.31	0.013	0.16	0.014	0.30	For F_a at x = 0; y = 0
	0.0016	0.021	0.0047	0.050	0.0074	0.090	0.009	0.12	0.011	0.15	0.013	0.16	0.013	0.17	0.014	0.17	For V_a at x = 0; y = 0
	0.0016	0.041	0.0047	0.063	0.0074	0.090	0.009	0.10	0.011	0.11	0.013	0.12	0.013	0.11	0.014	0.11	y = .60

*Griffel, William, *Handbook of Formulas for Stress and Strain*

6 - 42

TABLE 6-4

Loading Coefficients for Corner and Edge Forces for Flat Simply Supported Rectangular Plates Under Various Loadings *

(a) Uniform Loading

	K		K_1
b/a	V_x(max.)	V_y(max.)	R
1	0.420	0.420	0.065
1.1	0.440	0.440	0.070
1.2	0.455	0.453	0.074
1.3	0.468	0.464	0.079
1.4	0.478	0.471	0.083
1.5	0.486	0.480	0.085
1.6	0.491	0.485	0.086
1.7	0.496	0.488	0.088
1.8	0.499	0.491	0.090
1.9	0.502	0.494	0.091
2.0	0.503	0.496	0.092
3.0	0.505	0.498	0.093
4.0	0.502	0.500	0.094
5.0	0.501	0.500	0.095
∞	0.500	0.500	0.095

Remarks

L = a for V_x and V_y
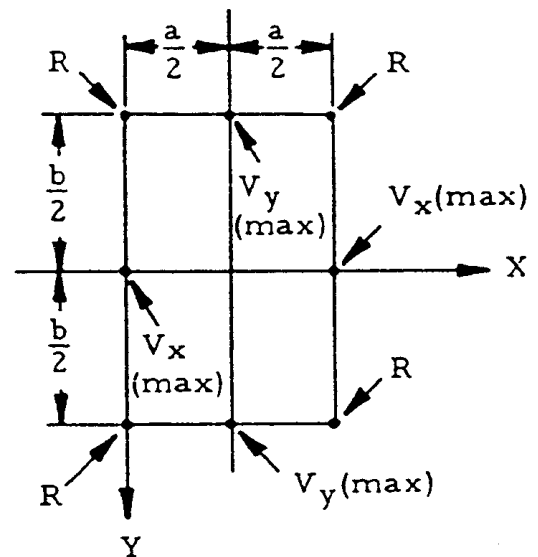
*Griffel, William, Handbook of Formulas for Stress and Strain

TABLE 6-4

Loading Coefficients for Corner and Edge Forces for Flat Simply Supported Rectangular Plates Under Various Loadings (continued) *

(b) Distributed Loadings

b/a	K V_{x1}	V_{x2}	V_y	K_1 R_1	R_2	Remarks
1.0	0.126	0.294	0.210	0.026	0.039	Use L = a for V_{x1}, V_{x2}
1.1	0.136	0.304	0.199	0.026	0.038	
1.2	0.144	0.312	0.189	0.026	0.037	Use L = b for V_y
1.3	0.150	0.318	0.178	0.026	0.036	Because the load is not symmetrical, the reactions R_1 are different from the reactions R_2, also V_{x1} is different than V_{x2}. The same applies to case V-3.
1.4	0.155	0.323	0.169	0.025	0.035	
1.5	0.159	0.327	0.160	0.024	0.033	
1.6	0.162	0.330	0.151	0.023	0.032	
1.7	0.164	0.332	0.144	0.022	0.030	
1.8	0.166	0.333	0.136	0.021	0.029	
1.9	0.167	0.334	0.130	0.021	0.028	
2.0	0.168	0.335	0.124	0.020	0.026	
3.0	0.169	0.336	0.083	0.014	0.018	
4.0	0.168	0.334	0.063	0.010	0.014	
5.0	0.167	0.334	0.050	0.008	0.011	
∞	0.167	0.333	--	--	--	

$\boxed{a < b}$
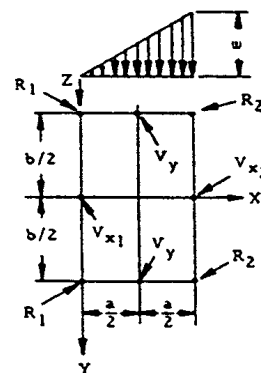
Notes:

1. In this case only, the formula (V) for the corner force R can be used when substituting a for b
2. V_x(max.) and V_y(max.) are at the middle of sides b and a respectively as shown in the figure for this table

(b) Distributed Loadings (Cont'd.)

a/b	K V_{x1}	V_{x2}	V_y	K_1 R_1	R_2	Remarks
∞	--	--	0.250	--	--	Use L = a for V_{x1}, V_{x2}
5.0	0.008	0.092	0.250	0.002	0.017	
4.0	0.013	0.112	0.251	0.004	0.020	Use L = b for V_y
3.0	0.023	0.143	0.252	0.006	0.025	
2.0	0.050	0.197	0.251	0.013	0.033	
1.9	0.055	0.205	0.251	0.014	0.034	
1.8	0.060	0.213	0.249	0.016	0.035	
1.7	0.066	0.221	0.248	0.017	0.036	
1.6	0.073	0.230	0.245	0.018	0.037	
1.5	0.080	0.240	0.243	0.020	0.037	
1.4	0.088	0.250	0.239	0.021	0.038	
1.3	0.097	0.260	0.234	0.023	0.039	
1.2	0.106	0.271	0.227	0.024	0.039	
1.1	0.116	0.282	0.220	0.025	0.039	
1.0	0.126	0.294	0.210	0.026	0.039	

$\boxed{a > b}$

*Griffel, William, Handbook of Formulas for Stress and Strain

6 - 44

TABLE 6-4

Loading Coefficients for Corner and Edge Forces for Flat Simply Supported Rectangular Plates Under Various Loadings (concluded) *

(b) Distributed Loadings (Cont'd.)

b/a	K V_x(max.)	V_y(max.)	K_1 R	Remarks
1.0	0.147	0.250	0.038	Use L = a for V_x
1.1	0.161	0.232	0.038	
1.2	0.173	0.216	0.037	Use L = b for V_y
1.3	0.184	0.202	0.036	
1.4	0.193	0.189	0.035	
1.5	0.202	0.178	0.034	
1.6	0.208	0.108	0.033	
1.7	0.214	0.158	0.031	
1.8	0.220	0.150	0.030	
1.9	0.224	0.142	0.029	
2.0	0.228	0.135	0.028	
3.0	0.245	0.090	0.019	
∞	0.250	--	--	

$a < b$

(b) Distributed Loadings (Cont'd.)

a/b	K V_x(max.)	V_y(max.)	K_1 R	Remarks
∞	--	0.50	--	Use L = a for V_x
3.0	0.027	0.410	0.010	
2.0	0.057	0.365	0.023	Use L = b for V_y
1.9	0.062	0.358	0.024	
1.8	0.098	0.350	0.026	
1.7	0.074	0.342	0.028	
1.6	0.081	0.332	0.029	
1.5	0.090	0.322	0.031	
1.4	0.099	0.311	0.033	
1.3	0.109	0.298	0.035	
1.2	0.120	0.284	0.036	
1.1	0.133	0.268	0.037	
1.0	0.147	0.250	0.038	

$a > b$
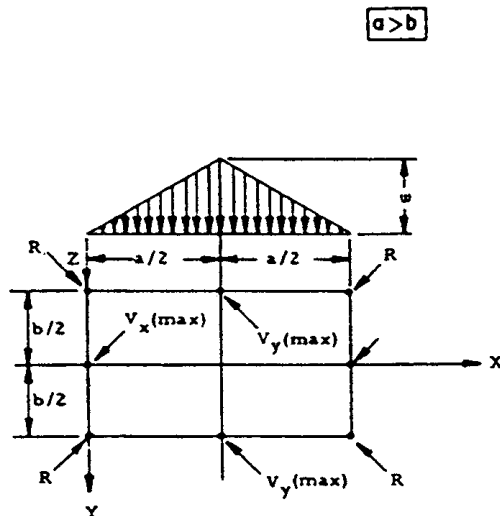
*Griffel, William, Handbook of Formulas for Stress and Strain

TABLE 6-5

Loading Coefficients for Partially Loaded Rectangular Flat Plates *

All edges supported. Uniform load over central rectangular area shown shaded
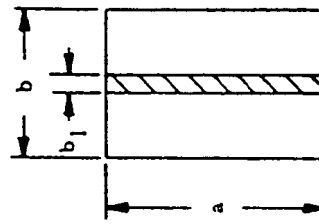
All edges supported. Uniform load along the axis of symmetry parallel to the dimension a (b, very small)

K_1 factor for maximum stress at center ($F = F_b$)

a/b = 1

a_1/b →	0	0.2	0.4	0.6	0.8	1.0
b_1/b ↓						
0	--	1.82	1.38	1.12	0.93	0.76
0.2	1.82	1.28	1.08	0.90	0.76	0.63
0.4	1.39	1.07	0.84	0.72	0.62	0.52
0.6	1.12	0.90	0.72	0.60	0.52	0.43
0.8	0.92	0.76	0.62	0.51	0.42	0.36
1.0	0.76	0.63	0.52	0.42	0.35	0.30

a/b = 1.4

a_1/b →	0	0.2	0.4	0.8	1.2	1.4
b_1/b ↓						
0	--	2.0	1.55	1.12	0.84	0.75
0.2	1.78	1.43	1.23	0.95	0.74	0.64
0.4	1.39	1.13	1.00	0.80	0.62	0.55
0.6	1.10	0.91	0.82	0.68	0.53	0.47
0.8	0.90	0.76	0.68	0.57	0.45	0.40
1.0	0.75	0.62	0.57	0.47	0.38	0.33

a/b = 2

a_1/b →	0	0.4	0.8	1.2	1.6	2.0
b_1/b ↓						
0	--	1.64	1.20	0.97	0.78	0.64
0.2	1.73	1.31	1.03	0.84	0.68	0.57
0.4	1.32	1.08	0.88	0.74	0.60	0.50
0.6	1.04	0.90	0.76	0.64	0.54	0.44
0.8	0.87	0.76	0.63	0.54	0.44	0.38
1.0	0.71	0.61	0.53	0.45	0.38	0.30

Note: Total load $W = w a_1 b_1$

K factor for maximum deflection

b > a L a							
b/a	2	1.5	1.4	1.3	1.2	1.1	1.0
K	0.108	0.099	0.096	0.092	0.087	0.081	0.074

b < a L b							
a > b	1.1	1.2	1.3	1.4	1.5	2.0	∞
K	0.088	0.101	0.114	0.126	0.137	0.178	0.227

Note: Use unit applied load w in this case (lb./in.)

*Griffel, William, Handbook of Formulas for Stress and Strain

TABLE 6-6

Loading Coefficients for Flat Elliptical Plates Under Uniform Load *

Manner of Loading	Edge Supported Uniform Load Over Entire Surface		Edge Fixed Uniform Load Over Entire Surface	
	K	K_1	K	K_1
a/b	1.0	0.70	1.24	0.171	0.75
1.0	0.70	1.24	0.171	0.75
1.1	0.84	1.42	0.20	0.90
1.2	0.95	1.57	0.25	1.04
1.3	1.06	1.69	0.28	1.14
1.4	1.17	1.82	0.30	1.25
1.5	1.26	1.92	0.30	1.34
1.6	1.34	2.04	0.33	1.41
1.7	1.41	2.09	0.35	1.49
1.8	1.47	2.16	0.36	1.54
1.9	1.53	2.22	0.370	1.59
2.0	1.58	2.26	0.379	1.63
2.5	1.75	2.45	0.40	1.75
3.0	1.88	2.60	0.42	1.84
3.5	1.96	2.70	0.43	1.89
4.0	2.02	2.78	0.43	1.9
L	b		b	
Locations of stress and deflection	F max. at center Y max. at center		F max. at end of shorter principal axis. Y max. at center	
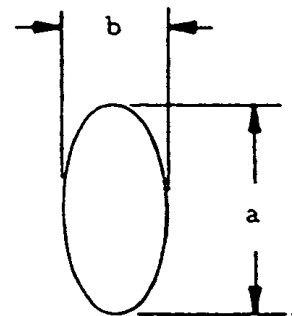
*Griffel, William, Handbook of Formulas for Stress and Strain

TABLE 6-7

Loading Coefficients for Various Shaped Flat Plates Under Distributed Uniform Load*

CIRCULAR SECTOR, SOLID

Manner of loading	45°		60°		90°		180°		L	Locations of stress and deflection
	K	K₁	K	K₁	K	K₁	K	K₁		
Edges supported	0.0054	0.11	0.01	0.15	0.025	0.22	0.087	0.31	a	F_L max. (tangential) at midpoint of circular edge; Y max. at midpoint of circular edge
Distributed load over entire surface	0.0054	0.10	0.01	0.15	0.025	0.24	0.087	0.52	a	F max. (radial) on line to midpoint of circular edge; Y max. at midpoint of circular edge

PARALLELOPIPED (SKEW SLAB)

Manner of loading	0°		30°		45°		60°		75°		L	Locations of stress and deflection
	K	K₁	K	K₁	K	K₁	K	K₁	K	K₁		
All edges supported Distributed load over entire surface	--	0.50	--	0.50	--	0.45	--	0.40	--	0.16	b	F_b maximum at center; No data available for deflection
Edges b supported, Edges a free Distributed load over entire surface	--	0.76	--	0.61	--	0.44	--	0.25	--	--	a	F maximum at center; No data available for deflection
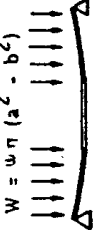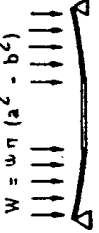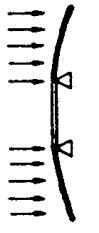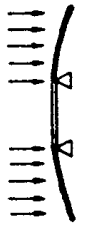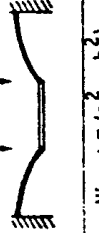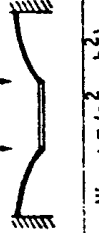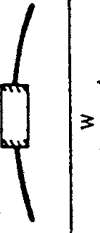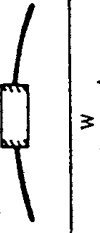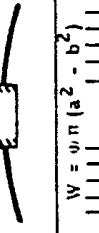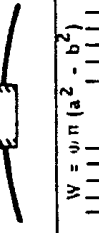
RIGHT ANGLE ISOSCELES TRIANGLE, SOLID

Manner of loading	K	K₁	L	Location of stress and deflection
Edges supported Distributed load over entire surface	0.0095	0.13	a	F maximum at center; Y maximum at center

EQUILATERAL TRIANGLE, SOLID

Manner of loading	K	K₁	L	Location of stress and deflection
Edges supported	0.01	0.149	a	F_x max at y = 0, x = -0.062a; Y maximum at center
Distributed load over entire surface	0.01	0.155	a	F_y maximum at y = 0, x = 0.129a; Y maximum at center

*Griffel, William, Handbook of Formulas for Stress and Strain

TABLE 6-8

Loading Coefficients for Circular Flat Plates Under Various Loadings *

Factors:
K for deflection
K_1 for stress
K_2 for slope

Loading	Factors	a/b or a/r_o = 1	1.25	1.5	2	3	4	5
Outer edge supported Uniform load over entire actual surface $W = w \pi (a^2 - b^2)$	K	--	0.163	0.237	0.290	0.295	0.297	0.269
	K_1 (F_t at inner edge)	--	0.524	0.559	0.612	0.673	0.744	0.725
	K_2 at outer edge	--	0.786	0.679	0.640	0.441	0.401	0.179
	K_2 at inner edge	--	0.919	0.741	0.612	0.447	0.355	0.292
Outer edge supported Uniform load along inner edge	K	--	0.341	0.519	0.642	0.734	0.724	0.704
	K_1 (F_t at inner edge)	--	1.10	1.26	1.48	1.88	2.17	2.34
	K_2 at outer edge	--	1.646	1.470	1.237	1.006	0.895	0.832
	K_2 at inner edge	--	1.758	1.650	1.475	1.238	1.082	0.932
Inner edge supported Uniform load over entire actual surface $W = w \pi (a^2 - b^2)$	K (at outer edge)	--	0.179	0.281	0.383	0.437	0.444	0.434
	K_1 (F_t at inner edge)	--	0.584	0.682	0.867	1.196	1.458	1.688
	K_2 at outer edge	--	0.884	0.794	0.606	0.565	0.492	0.448
	K_2 at inner edge	--	1.012	0.910	0.862	0.791	0.726	0.642
Outer edge fixed and supported Uniform load over entire actual surface $W = w \pi (a^2 - b^2)$	K	--	0.0018	0.0035	0.024	0.046	0.055	0.0576
	K_1 (F_t at inner edge)	--	0.0072	0.025	0.069	0.145	0.192	0.222
	K_2 at inner edge	--	0.013	0.035	0.069	0.096	0.096	0.089
	K_1 (F_r at outer edge)	--	0.093	0.148	0.204	0.235	0.240	0.242
Outer edge fixed and supported Uniform load along inner edge	K	--	0.005	0.024	0.081	0.171	0.215	0.237
	K_1 (F_t at inner edge)	--	0.025	0.087	0.269	0.670	1.018	1.300
	K_1 (F_r at outer edge)	--	0.195	0.320	0.455	0.539	0.538	0.532
	K_2 at inner edge	--	0.045	0.115	0.269	0.448	0.510	0.522
Inner edge fixed and supported Uniform load over entire actual surface $W = w \pi (a^2 - b^2)$	K (at outer edge)	--	0.002	0.010	0.040	0.105	0.152	0.187
	K_1 (F_r at inner edge)	--	0.119	0.235	0.442	0.770	1.014	1.22
	K_2 at outer edge	--	0.012	0.040	0.097	0.177	0.223	0.252
Inner edge fixed and supported Uniform load along outer edge	K (at outer edge)	--	0.0051	0.025	0.088	0.209	0.293	0.350
	K_1 (at inner edge)	--	0.227	0.428	0.753	1.205	1.514	1.745
	K_2 at outer edge	--	0.046	0.105	0.239	0.403	0.499	0.544
Outer edge supported, inner edge fixed Uniform load over entire actual surface $W = w \pi (a^2 - b^2)$	K	--	0.003	0.018	0.053	0.104	0.141	0.163
	K_1 (F_r at inner edge)	--	0.108	0.192	0.314	0.433	0.491	0.526
	K_2 at outer edge	--	0.091	0.123	0.197	0.260	0.297	0.306

Circular Solid Plate

Circular Plate with Concentric Hole or Circular Flange

*Griffel, William, Handbook of Formulas for Stress and Strain

TABLE 6-8

Loading Coefficients for Circular Flat Plates Under Various Loadings (continued) *

Circular Solid Plate   Circular Plate with Concentric Hole or Circular Flange

Loading	Factors: K_1 for stress, K_2 for slope, K for deflection	1	1.25	1.5	2	3	4	5
Outer edge fixed Uniform moment along inner edge	K max. at inner edge	--	0.20	0.48	0.85	0.94	0.80	0.66
	K_1 max. at inner edge	--	0.37	0.86	2.44	4.10	4.84	5.11
	K_2 at inner edge	--	2.20	3.16	3.88	3.31	3.12	2.72
Inner edge fixed Uniform moment along outer edge	K max. at outer edge	--	0.23	0.66	1.49	2.55	3.10	3.41
	K_1 max. at inner edge	--	6.87	7.50	8.14	8.71	8.94	9.04
	K_2 at outer edge	--	2.30	3.84	5.67	6.94	7.82	8.17
Inner edge supported Uniform moment along outer edge	K max. at outer edge	--	10.37	9.23	7.80	6.11	5.62	5.23
	K_1 max. (F_t at inner edge)	--	33.3	21.6	16.0	13.5	12.8	12.5
	K_2 at outer edge	--	51.00	28.00	16.40	11.60	10.23	9.61
	K_2 at inner edge	--	53.30	27.80	15.60	8.78	6.24	4.86
Outer edge supported Uniform moment along inner edge	K_1 max. at inner edge	--	8.87	6.92	4.65	2.58	1.69	1.21
	K_1 max. F_t at inner	--	27.36	15.60	10.0	7.50	6.80	6.50
	K_2 at outer edge	--	42.70	18.75	7.81	2.93	1.56	0.94
	K_2 at inner edge	--	44.90	22.35	11.27	5.52	4.08	3.17
Outer edge fixed and supported, inner edge fixed Uniform load over entire actual surface	K	--	0.0004	0.003	0.010	0.023	0.031	0.037
	K_1 (F_r at inner edge)	--	0.036	0.065	0.104	0.151	0.176	0.192
	K_1 (F at outer edge)	--	0.062	0.105	0.153	0.195	0.212	0.221
Outer edge fixed and supported, inner edge fixed Uniform load along inner edge	K	--	0.0013	0.0064	0.024	0.062	0.092	0.114
	K_1 (F_r at inner edge)	--	0.115	0.220	0.405	0.703	0.933	1.130
	K_1 (F_r at inner edge)	--	0.098	0.168	0.257	0.347	0.390	0.415
Both edges fixed Balance loading (piston)	K	--	0.0007	0.003	0.014	0.039	0.061	0.077
	K_1 (F_r at inner edge)	--	0.080	0.156	0.302	0.551	0.756	0.927
No support Uniform edge moment	K max. at center	4	..	..	..	..	..	..
	K_1 ($F_1 = F_1$ at any point)	6	..	..	..	..	..	..
	At edge	8	..	..	..	..	..	..

where $W = \pi \eta (a^2 - b^2)$

Griffel, William, Handbook of Formulas for Stress and Strain

TABLE 6-8

Loading Coefficients for Circular Flat Plates Under Various Loadings (concluded) *

Loading		a/b or a/r_o							Factors:
		1	1.25	1.5	2	3	4	5	K for deflection = K
Edges supported Uniform load over concentric circular area of radius r_o $W = w \pi r_o^2$	K	0.212	0.295	0.350	0.413	0.469	0.492	0.503	K_1 (F_r at center)
	K_1	0.398	0.568	0.700	0.900	1.167	1.353	1.500	K_2
	K_2	0.636							K_1 for stress, K_2 for slope

Manner of loading		r_o/a																K_2 slope K_1 stress
		0.1	0.15	0.20	0.25	0.30	0.35	0.40	0.45	0.50	0.55	0.60	0.65	0.70	0.75	0.80	
Edges supported Central couple, trunnion loading	K_2 max. at center	0.71	0.97	1.22	1.60	2.0	2.50	3.53	5.60	8.54	12.00	16.30	24.10	41.4	82.0	162.0	K_2 max. at center
	K_1 max. F at center	4.36	3.80	3.27	2.80	2.37	2.10	1.84	1.58	1.41	1.16	1.07	0.90	0.78	0.70	0.57	K_1 max. F at center
Edges fixed Central couple, trunnion loading	K_2 max. at center	0.87	1.23	1.68	2.31	3.10	4.00	5.45	8.20	12.40	18.0	28.5	44.0	77.9	156.0	314.0	K_2 max. at center
	K_1 max. F at center	6.06	5.40	4.52	3.40	2.65	2.15	1.75	1.45	1.14	0.89	0.68	0.57	0.47	0.35	0.26	K_1 max. F at center

*Griffel, William, Handbook of Formulas for Stress and Strain

Equation (6-21)(a), (b) pertains to rectangular, square, triangular, and elliptical plates.

$$y = \frac{K w L^4}{E t^3} \qquad \text{(a)}$$

$$F = \frac{K_1 w L^2}{t^2} \qquad \text{(b)}$$

(6-21)

Equation (6-22)(a), (b) pertains to corner and edge forces for simply supported rectangular plates.

$$R = K_1 w ab \qquad \text{(a)}$$

$$V = K w L \qquad \text{(b)}$$

(6-22)

Equation (6-23)(a), (b) pertains to partially loaded rectangular plates with supported edges.

$$y = \frac{K w L^3}{E t^3} \qquad \text{(a)}$$

$$F = \frac{K_1 W}{t^2} \qquad \text{(b)}$$

(6-23)

Equation (6-24)(a), (b), (c) pertains to circular plates.

$$y = \frac{K W a^2}{E t^3} \qquad \text{(a)}$$

$$F = \frac{K_1 W}{t^2} \qquad \text{(b)}$$

$$\theta = \frac{K_2 W a}{E t^3} \qquad \text{(c)}$$

(6-24)

Equation (6-25)(a), (b), (c), (d), (e) pertains to circular plates with end moments.

$$y = \frac{K M a^2}{E t^3} \qquad \text{(a)}$$

$$F = \frac{K_1 M}{t^2} \qquad \text{(b)}$$

$$\theta = \frac{K_2 M a}{E t^3} \qquad \text{(c)} \qquad\qquad (6\text{-}25)$$

$$F = \frac{K_1 M}{a t^2} \qquad \text{(d)}$$

$$\theta = \frac{M}{K_2 E t^3} \qquad \text{(e)}$$

Equation (6-25) (d) and (e) applies to trunnion-loaded plates only. (See Table 6-8).

These equations have been developed with a value of 0.3 for Poisson's ratio; however, they may be applied to materials with other values without significant error.

6.4.2   Beam-Supported Flat Plates in Bending *

The treatment of unstiffened flat plates in Section 6.4.1 included considerations of the edge restraints. These were considered to be rigid in most instances. This section presents methods of analysis which consider the bending of the support beams. Figure 6-23 shows an idealized view of a beam-supported plate. The loading may be either concentrated at the center of the plate or distributed uniformly.
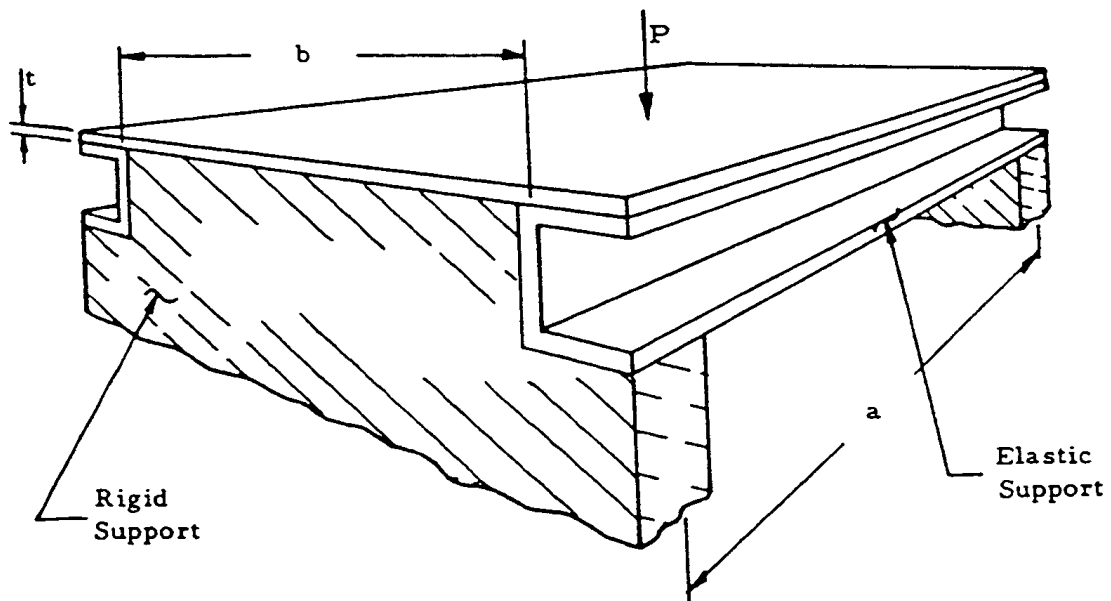
Figure 6-23.   Beam-Supported Plate

*Griffel, William, Handbook of Formulas for Stress and Strain

Table 6-9 is used in conjunction with Figure 6-24 to find the maximum of either the plate or supporting beam. The rigidity ratio, H, is given by Equation (6-26).

$$H = \frac{(1-\nu^2) E_b I_b}{E_p I_p} \quad , \text{ where } I_p = \frac{at^3}{12} \tag{6-26}$$

Table 6-10 is used with Figures 6-25 and 6-26 to find the maximum stress in the plate and the beam.

6.5 Shear Buckling of Flat Plates

The critical shear-buckling stress of flat plates may be found from Equation (6-27).

$$F_{crs} = \eta \bar{\eta} \frac{k_s \pi^2 E}{12(1-\nu_e)^2} \left(\frac{t}{b}\right)^2 \tag{6-27}$$

Figure 6-27 presents the shear coefficient k_s as a function of the size ratio a/b for clamped and hinged edges. For infinitely long plates, Figure 6-28 presents k_s as a function of λ/b. Figure 6-29(a) presents $k_{s\infty}$ for long plates as a function of edge restraint, and Figure 6-29(b) gives $k_s/k_{s\infty}$ as a function of b/a, thus allowing the determination of k_s.

The nondimensional chart in Figure 6-30 allows the calculation of inelastic shear buckling stresses if the secant yield stress, $F_{0.7}$, and n the shape parameter is known (Table 6-11).

The plasticity-reduction factor η and the clodding factor $\bar{\eta}$ can be obtained from Equations (6-28), (6-29), and (6-30).

$$\eta = \frac{E_s}{E} \left(\frac{1-\nu_e^2}{1-\nu^2}\right) \tag{6-28}$$

$$\eta = \frac{1 + 3f\beta}{1 + 3f} \text{ for } F_{el} < F_{crs} < F_{pl} \tag{6-29}$$

$$\eta = \frac{1}{1+3f} \frac{\left[1+3f\left(\frac{E_s}{E_s}\right)\right]+\left\{\left[1+3f\left(\frac{E_s}{E_s}\right)\right]\left[\frac{1}{4} + \frac{3}{4}\left(\frac{E_t}{E_s}\right)+ w\right]\right\}^{\frac{1}{2}}}{1 + \left[\frac{1}{4} + \frac{3}{4}\left(\frac{E_t}{E_s}\right)\right]^{\frac{1}{2}}} \tag{6-30}$$

for $F_{crs} > F_{pl}$

TABLE 6-9

Factors for Determining Maximum Plate and Beam Deflection *

b/a	H = 0				H = 0.1				H = 0.2				H = 0.5			
	K_1	K_2	K_3	K_4	K_1	K_2	K_3	K_4	K_1	K_2	K_3	K_4	K_1	K_2	K_3	K_4
0.33	0.1591	0.146	0.7593	0.7641	0.0983	0.1013	0.4718	0.4681	0.0714	0.0724	0.3449	0.3375	0.0398	0.0390	0.1957	0.1837
0.5	0.1579	0.170	0.5076	0.5008	0.1122	0.1162	0.3677	0.3477	0.0879	0.0882	0.2932	0.2664	0.0549	0.0512	0.1925	0.1565
0.6	0.1573	0.172	0.4264	0.4110	0.1180	0.1220	0.3280	0.2979	0.0956	0.0947	0.2720	0.2336	0.0636	0.0567	0.1910	0.1412
0.8	0.1563	0.174	0.3305	0.2937	0.1264	0.1296	0.2774	0.2240	0.1080	0.1037	0.2446	0.1810	0.0796	0.0648	0.1942	0.1150
1.0	0.1557	0.175	0.2789	0.2189	0.1327	0.1341	0.2485	0.1715	0.1179	0.1090	0.2290	0.1409	0.0940	0.0698	0.1975	0.0919
1.2	0.1554	0.175	0.2491	0.1665	0.1317	0.1366	0.2312	0.1324	0.1258	0.1121	0.2195	0.1098	0.1064	0.0728	0.2000	0.0727
1.4	0.1553	0.176	0.2312	0.1278	0.1415	0.1382	0.2206	0.1024	0.1322	0.1140	0.2135	0.0855	0.1167	0.0747	0.2016	0.0571
1.6	0.1554	0.176	0.2202	0.0985	0.1446	0.1391	0.2139	0.0793	0.1374	0.1150	0.2095	0.0664	0.1253	0.0757	0.2024	0.0446
1.8	0.1556	0.176	0.2135	0.0760	0.1473	0.3196	0.2097	0.0614	0.1416	0.1156	0.2071	0.0515	0.1321	0.0763	0.2028	0.0347
2.0	0.1557	0.176	0.2093	0.0596	0.1493	0.1399	0.2071	0.0484	0.1449	0.1160	0.2055	0.0408	0.1375	0.0767	0.2029	0.0279
3.0	0.1565	0.189	0.2031	0.0156	0.1551	0.1403	0.2030	0.0126	0.1543	0.1165	0.2029	0.0106	0.1528	0.0772	0.2028	0.0072

INSTRUCTIONS - TABLE 6.9

1. For a uniformly distributed load, w, use K_1 for plate and K_2 for beam calculations.
2. For concentrated load, P, at center of plate, use K_3 for plate and K_4 for beam calculations.
3. Nomogram of Figure 6.24 is to be used with these K values to determine maximum deflection (at center) of plate and beam.

*Griffel, William, Handbook of Formulas for Stress and Strain

TABLE 6-9

Factors for Determining Maximum Plate and Beam Deflection (concluded) *

b/a	H=1.0				H=2.0				H=4.0				H=∞			
	K_1	K_2	K_3	K_4	K_1	K_2	K_3	K_4	K_1	K_2	K_3	K_4	K_1	K_2	K_3	K_4
0.33	0.0234	0.0221	0.1187	0.1044	0.0135	0.0118	0.0718	0.0588	0.0079	0.0061	0.0456	0.0291	0.0019	0.0049	0.0174	0
0.5	0.0358	0.0301	0.1340	0.0928	0.0233	0.0165	0.0958	0.0511	0.0160	0.0087	0.0736	0.0269	0.0079	0.0070	0.0489	0
0.6	0.0439	0.0340	0.1429	0.0857	0.0307	0.0189	0.1098	0.0479	0.0228	0.0100	0.0902	0.0254	0.0140	0.0081	0.0689	0
0.8	0.0609	0.0398	0.1610	0.0715	0.0476	0.0225	0.1374	0.0407	0.0395	0.0120	0.1230	0.0219	0.0301	0.0098	0.1063	0
1.0	0.0776	0.0436	0.1758	0.0582	0.0656	0.0249	0.1600	0.0335	0.0581	0.0134	0.1501	0.0182	0.0492	0.0109	0.1385	0
1.2	0.0927	0.0460	0.1863	0.0465	0.0825	0.0265	0.1761	0.0271	0.0761	0.0143	0.1696	0.0150	0.0684	0.0117	0.1619	0
1.4	0.1057	0.0474	0.1930	0.0368	0.0974	0.0274	0.1866	0.0215	0.0921	0.0149	0.1826	0.0117	0.0856	0.0121	0.1776	0
1.6	0.1165	0.0482	0.1972	0.0288	0.1098	0.0280	0.1932	0.0169	0.1056	0.0152	0.1907	0.0092	0.1004	0.0124	0.1877	0
1.8	0.1252	0.0487	0.1996	0.0235	0.1200	0.0283	0.1972	0.0142	0.1165	0.0154	0.1957	0.0082	0.1125	0.0125	0.1938	0
2.0	0.1321	0.0490	0.2010	0.0194	0.1280	0.0285	0.1996	0.0112	0.1253	0.0155	0.1887	0.0066	0.1222	0.0126	0.1975	0
3.0	0.1517	0.0494	0.2027	0.0047	0.1509	0.0287	0.2027	0.0027	0.1503	0.0156	0.2026	0.0015	0.1496	0.0127	0.2026	0

*Griffel, William, Handbook of Formulas for Stress and Strain
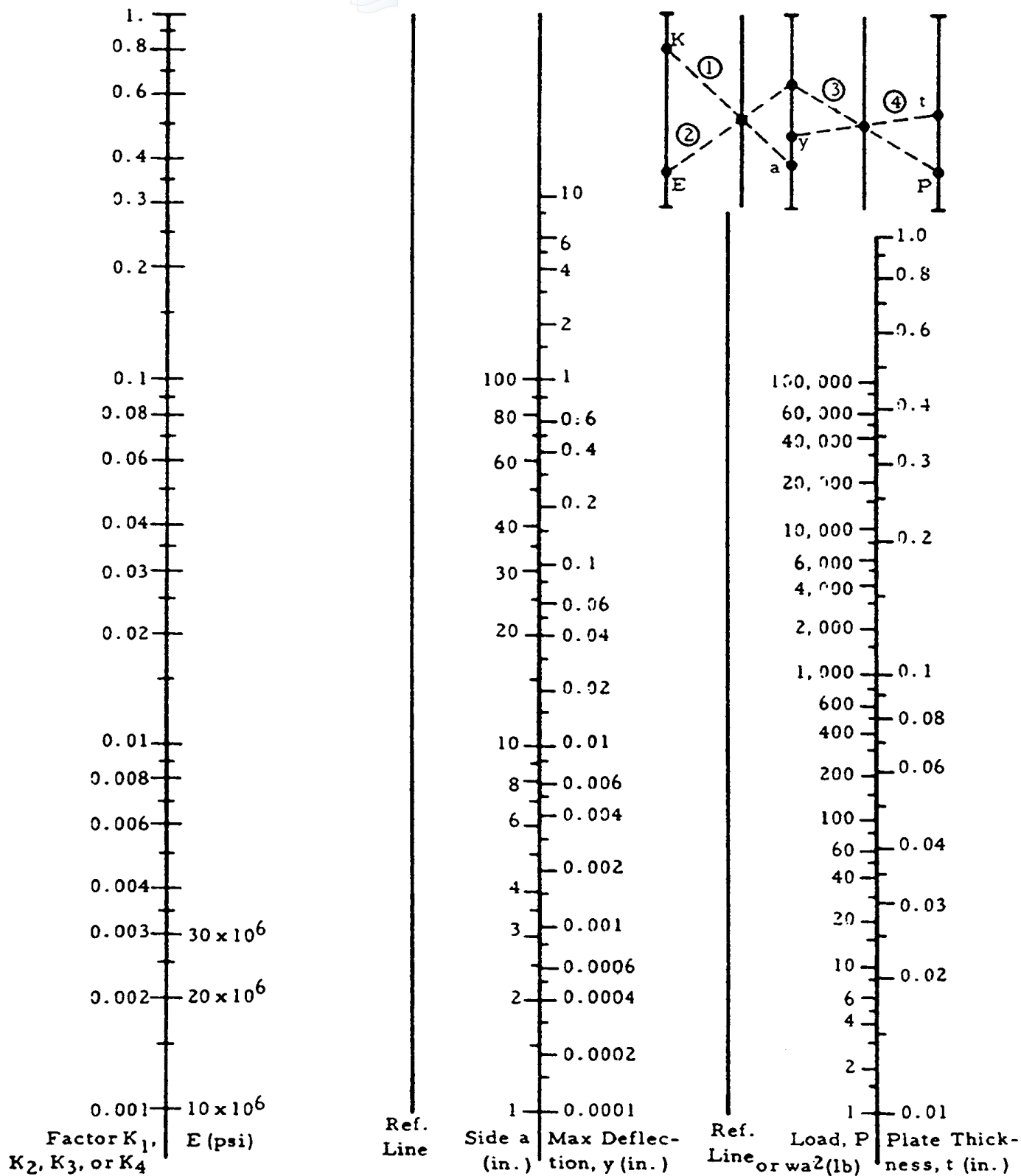
Figure 6-24.   Nomogram for Determining Plate Deflections y_a and y_b.
(Actual deflections are about 91 per cent of those indicated
by nomogram.) *

*Griffel, William, Handbook of Formulas for Stress and Strain

TABLE 6-10

Factors for Determining Maximum Plate and Beam Bending Stress *

b/a	H=0				H=0.05				H=0.1				H=0.2				H=0.5			
	K_5	K_6	K_7	K_8	K_5	K_6	K_7	K_8	K_5	K_6	K_7	K_8	K_5	K_6	K_7	K_8	K_5	K_6	K_7	K_8
0.33	0.732	0	4.09	0	0.551	0.0033	3.17	0.026	0.468	0.0052	2.62	0.042	0.339	0.0076	1.99	0.060	0.196	0.0103	1.25	0.082
0.5	0.733	0	2.86	0	0.615	0.0040	2.47	0.018	0.532	0.0067	2.21	0.030	0.424	0.0103	1.86	0.046	0.279	0.0152	1.40	0.068
0.6	0.732	0	2.48	0	0.634	0.0055	2.23	0.015	0.562	0.0095	2.03	0.026	0.464	0.0150	1.79	0.040	0.324	0.0228	1.43	0.060
0.8	0.735	0	2.06	0	0.662	0.0057	1.93	0.011	0.607	0.0101	1.83	0.019	0.528	0.0164	1.69	0.030	0.406	0.0261	1.46	0.048
1.0	0.735	0	1.83	0	0.667	0.0058	1.76	0.008	0.640	0.0104	1.70	0.014	0.577	0.0172	1.61	0.023	0.475	0.0282	1.48	0.038
1.2	0.738	0	1.69	0	0.697	0.0059	1.66	0.006	0.664	0.0106	1.63	0.011	0.615	0.0177	1.58	0.018	0.534	0.0294	1.49	0.030
1.4	0.739	0	1.63	0	0.708	0.0059	1.60	0.005	0.682	0.0107	1.57	0.008	0.645	0.0179	1.55	0.014	0.583	0.0301	1.50	0.023
1.6	0.742	0	1.57	0	0.717	0.0060	1.57	0.004	0.697	0.0108	1.55	0.006	0.624	0.0181	1.54	0.011	0.619	0.0305	1.51	0.018
1.8	0.748	0	1.55	0	0.724	0.0060	1.54	0.003	0.709	0.0108	1.54	0.005	0.687	0.0182	1.52	0.008	0.648	0.0308	1.51	0.014
2.0	---	0	1.54	--	---	0.0060	1.53	---	---	0.0108	1.52	---	---	0.0182	1.52	---	---	0.0309	1.51	---
3.0	---	0	1.51	--	---	0.0060	1.51	---	---	0.0108	1.51	---	---	0.0182	1.51	---	---	0.0310	1.51	---
∞	---	0	--	--	---	0.0060	--	---	---	0.0109	--	---	---	0.0183	--	---	---	0.0311	--	---

INSTRUCTIONS - TABLE 6.10

1. For a uniformly distributed load, w, use K_5 for plate and K_6 for beam calculations.
2. For a concentrated load, P, at center of plate, use K_7 for plate and K_8 for beam calculations.
3. Use K_5 and K_7 with nomogram of Figure 6.25 to determine maximum stress in plates.
4. Use K_6 and K_8 with nomogram of Figure 6.26 to determine maximum stress in beams.

*Criffel, William, Handbook of Formulas for Stress and Strain

6 - 58

TABLE 6.? 2

Factors for Determining Maximum Plate and Beam Bending Stress (concluded)*

b/a	H = 1.0				H = 2.0				H = 4.0				H = ∞			
	K_5	K_6	K_7	K_8	K_5	K_6	K_7	K_8	K_5	K_6	K_7	K_8	K_5	K_6	K_7	K_8
0.33	0.131	0.0177	0.864	0.093	0.079	0.0126	0.636	0.100	0.054	0.0131	0.510	0.103	0.027	0.0134	0.360	0.106
0.5	0.167	0.0180	1.120	0.080	0.139	0.0199	0.966	0.088	0.106	0.0210	0.858	0.093	0.070	0.0217	0.750	0.096
0.6	0.238	0.0276	1.210	0.073	0.179	0.0198	1.060	0.081	0.145	0.0328	0.996	0.086	0.106	0.0349	0.876	0.092
0.8	0.325	0.0325	1.310	0.060	0.268	0.0370	1.220	0.068	0.233	0.0398	1.150	0.073	0.193	0.0430	1.090	0.079
1.0	0.407	0.0357	1.390	0.048	0.356	0.0412	1.330	0.056	0.325	0.0446	1.280	0.060	0.287	0.0487	1.240	0.066
1.2	0.478	0.0376	1.440	0.038	0.435	0.0438	1.400	0.045	0.408	0.0477	1.370	0.049	0.375	0.0524	1.330	0.053
1.4	0.536	0.0388	1.470	0.030	0.502	0.0454	1.440	0.035	0.480	0.0496	1.430	0.039	0.454	0.0546	1.450	0.042
1.6	0.583	0.0395	1.480	0.024	0.556	0.0463	1.470	0.028	0.538	0.0507	1.460	0.030	0.517	0.0560	1.450	0.033
1.8	0.620	0.0399	1.490	0.018	0.599	0.0469	1.480	0.022	0.586	0.0514	1.470	0.024	0.568	0.0568	1.470	0.028
2.0	---	0.0402	1.500	---	---	0.0472	1.490	---	---	0.0518	1.490	---	---	0.0573	1.480	---
3.0	---	0.0404	1.510	---	---	0.0475	1.510	---	---	0.0520	1.510	---	---	0.0575	1.510	---
∞	---	0.0405	---	---	---	0.0477	---	---	---	0.0523	---	---	---	0.0579	---	---

*Griffel, William, Handbook of Formulas for Stress and Strain

6 - 59
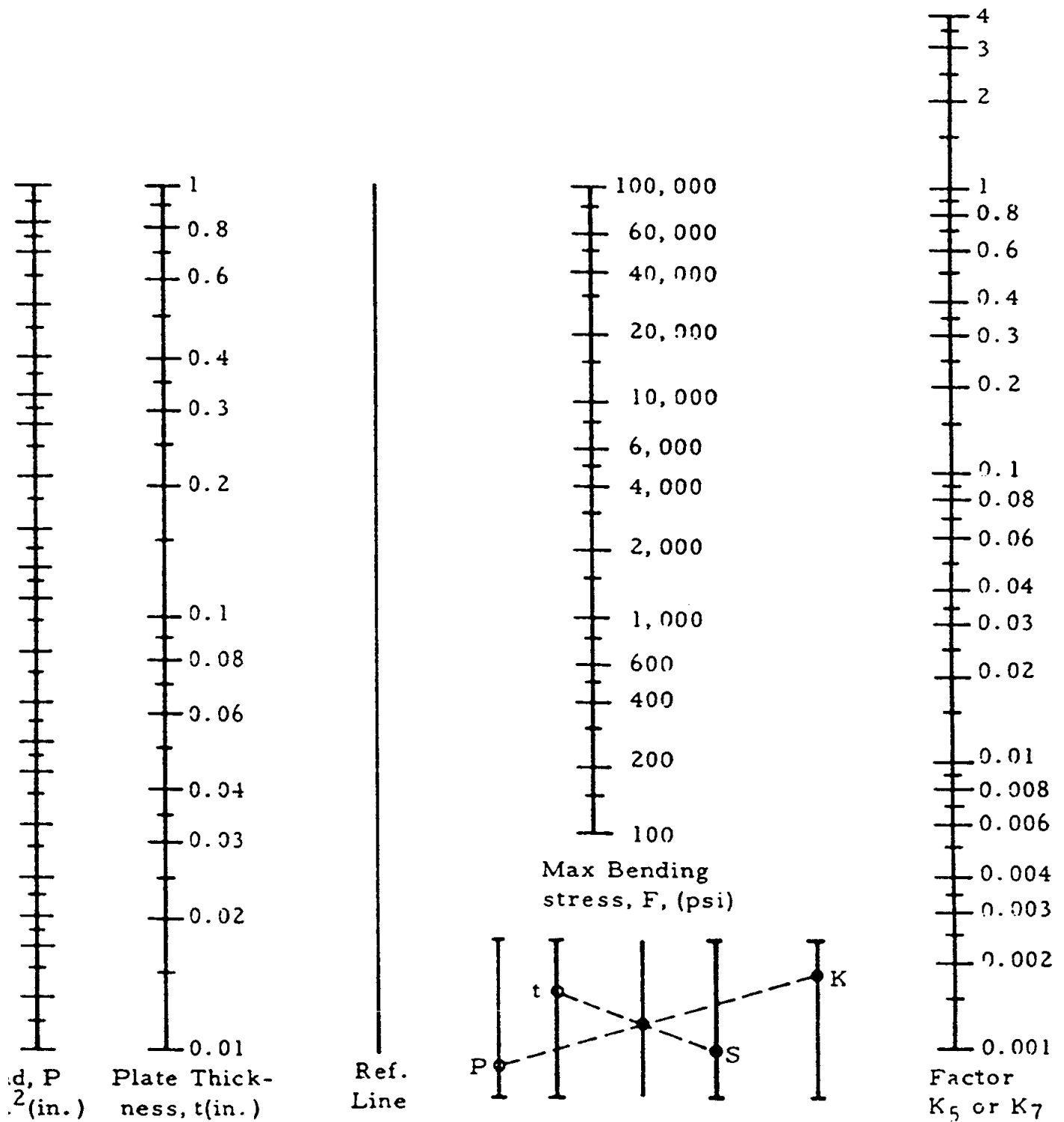
Figure 6-25.   Nomogram for Determining Plate Stress F_s *

*Griffel, William, Handbook of Formulas for Stress and Strain

Figure 6-26. Nomogram for Determining Beam Stress F_b *

*Griffel, William, Handbook of Formulas for Stress and Strain
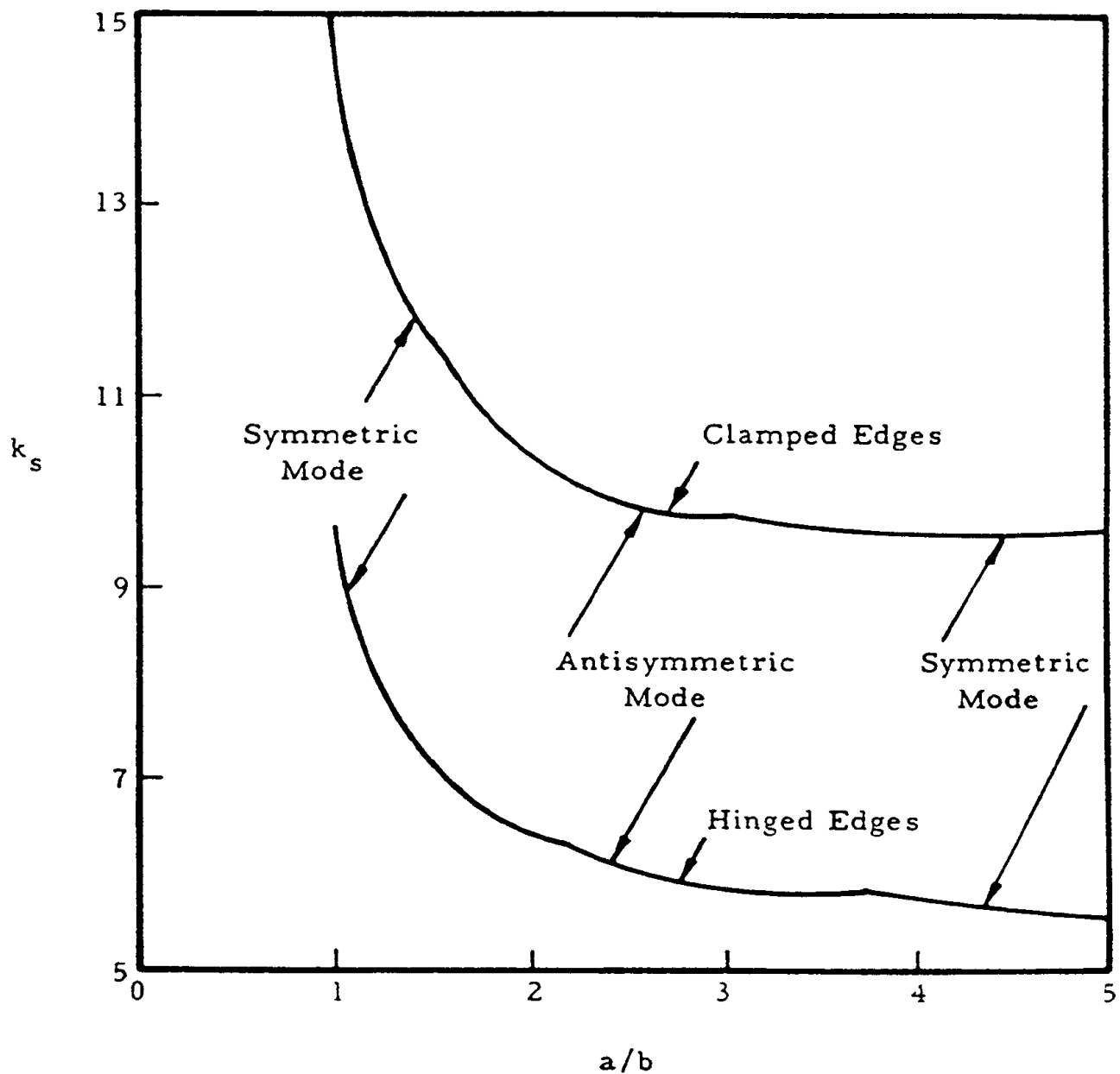
Figure 6-27. Shear-Buckling-Stress Coefficient of Plates as a Function of a/b for Clamped and Hinged Edges
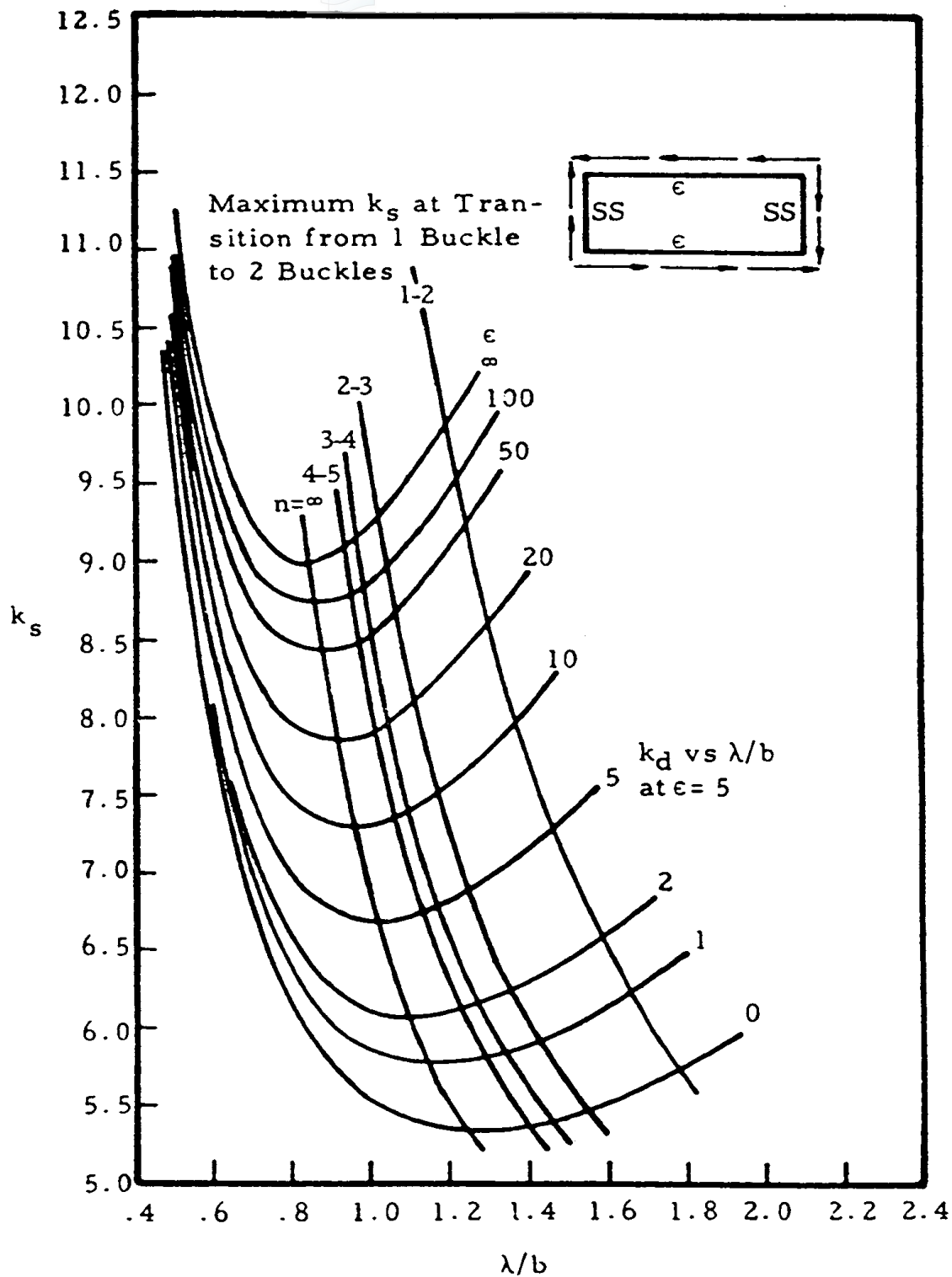
Figure 6-28.   Shear-Buckling-Stress Coefficient for Plates Obtained From Analysis of Infinitely Long Plates as a Function of λ/b for Various Amounts of Edge Rotational Restraint
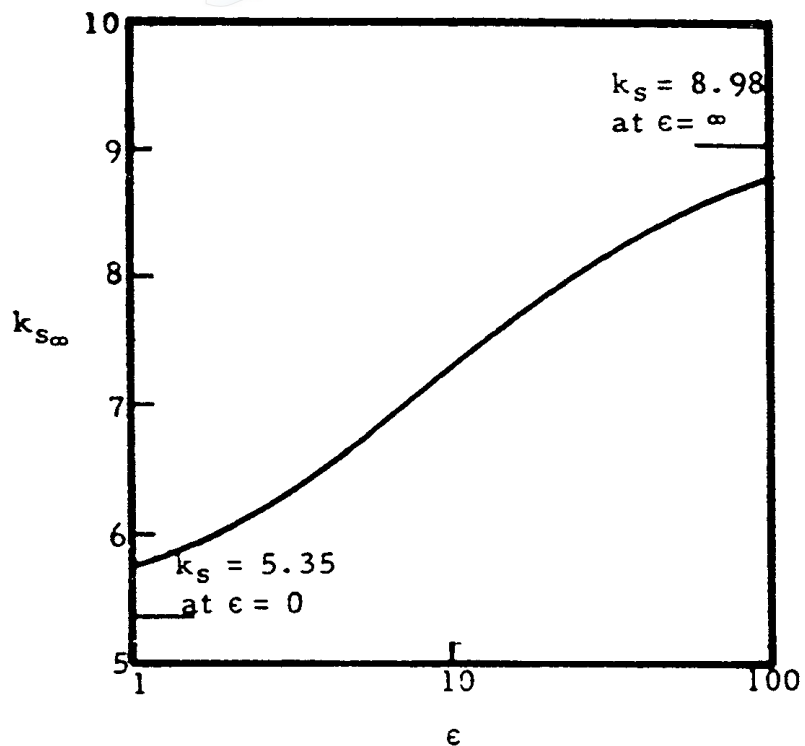
(a) k_{s_∞} as a function of ϵ
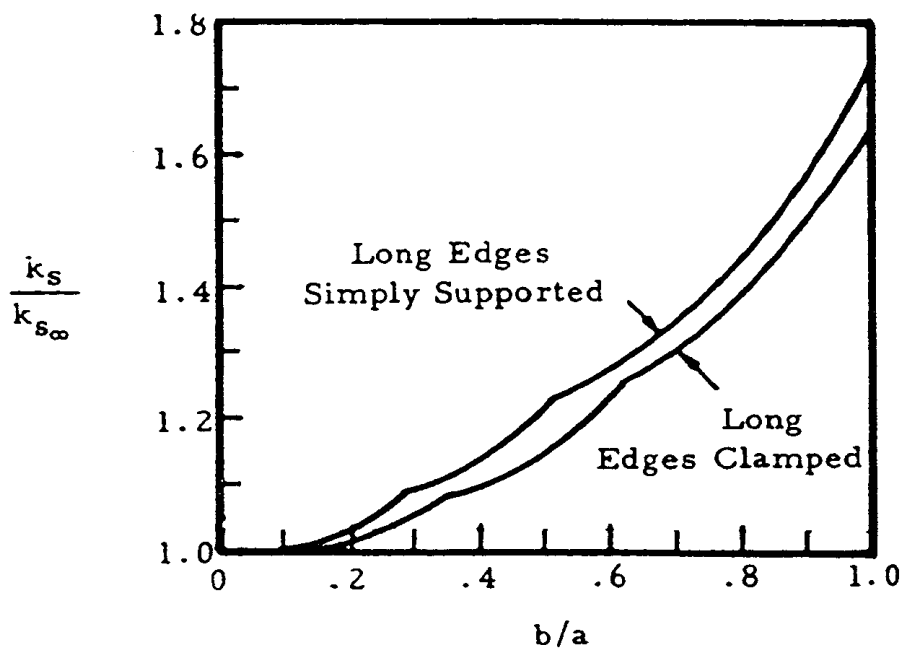
(b) k_s/k_{s_∞} as a function of b/a

Figure 6-29. Curves for Estimation of Shear-Buckling Coefficient of Plates
with Various Amounts of Edge Rotational Restraint
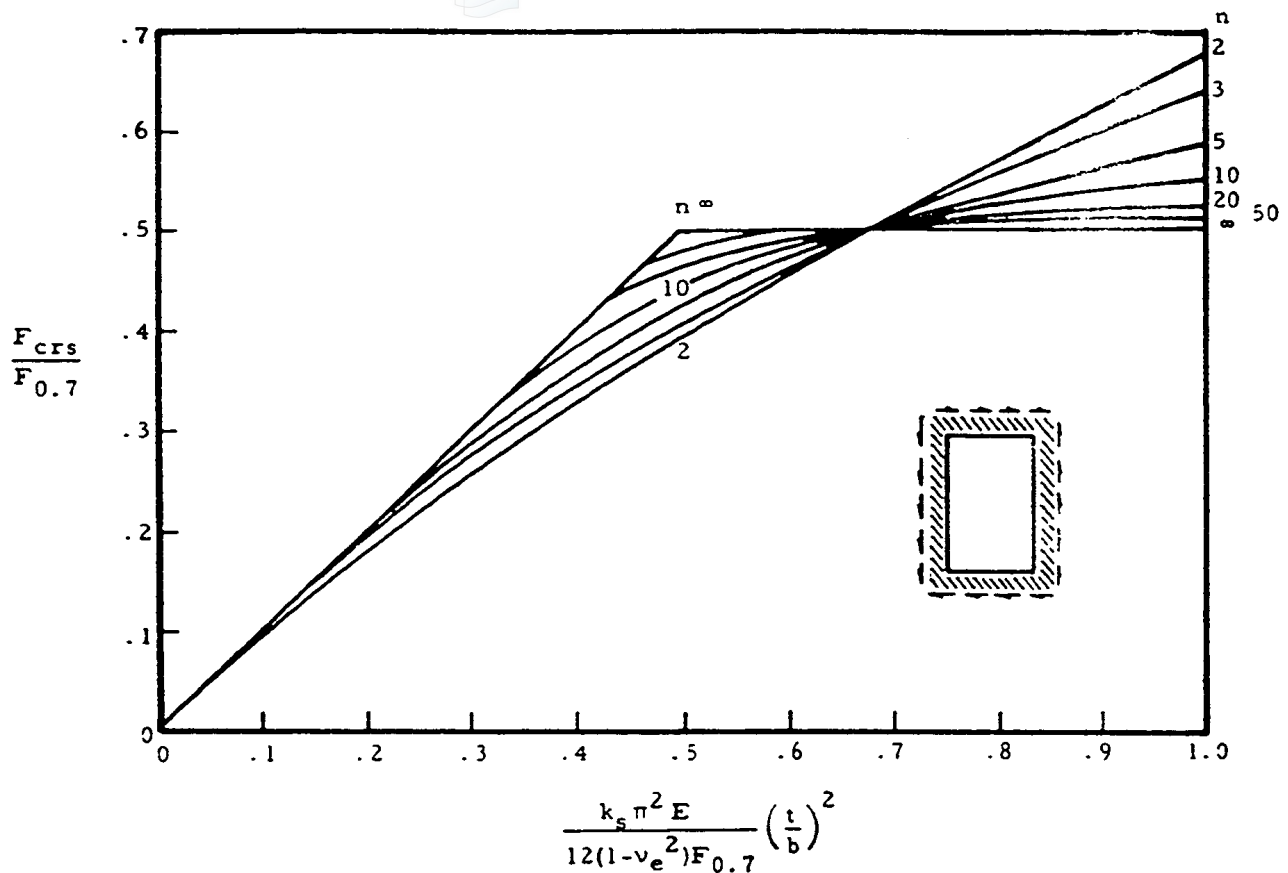
Figure 6-30. Chart of Nondimensional Shear Buckling Stress for Panels with Edge Rotational Restraint

The chart plots $\dfrac{F_{crs}}{F_{0.7}}$ versus $\dfrac{k_s \pi^2 E}{12(1-\nu_e^2)F_{0.7}}\left(\dfrac{t}{b}\right)^2$

TABLE 6-11

Values of Shape Parameter n for Several Engineering Materials

n	Material
3	One-fourth hard to full hard 18-8 stainless steel, with grain One-fourth hard 18-8 stainless steel, cross grain
5	One-half hard and three-fourths hard 18-8 stainless steel, cross grain
10	Full hard 18-8 stainless steel, cross grain 2024-T and 7075-T aluminum-alloy sheet and extrusion 2024R-T aluminum-alloy sheet
20 to 25	2024-T80, 2024-T81, and 2024-T86 aluminum-alloy sheet 2024-T aluminum-alloy extrusion SAE 4130 steel heat-treated up to 100,000 psi ultimate stress
35 to 50	2014-T aluminum-alloy extrusions SAE 4130 steel heat-treated above 125,000 psi ultimate stress
∞	SAE 1025 (mild) steel

6.6   Axial Compression of Curved Plates

The radius of curvature of curved plates determines the method to be used to analyze their buckling stress.   For large curvature ($b^2/rt < 1$), they may be analyzed as flat plates by using the relations in Section 6.3.   For elastic stresses in the transition length and width ranges, Figure 6-31 may be used to find the buckling coefficient for use in Equation (6-31).

$$F_{cr} = \frac{k_c \pi^2 E}{12(1-\nu_2^2)} \left(\frac{t}{b}\right)^2 \tag{6-31}$$
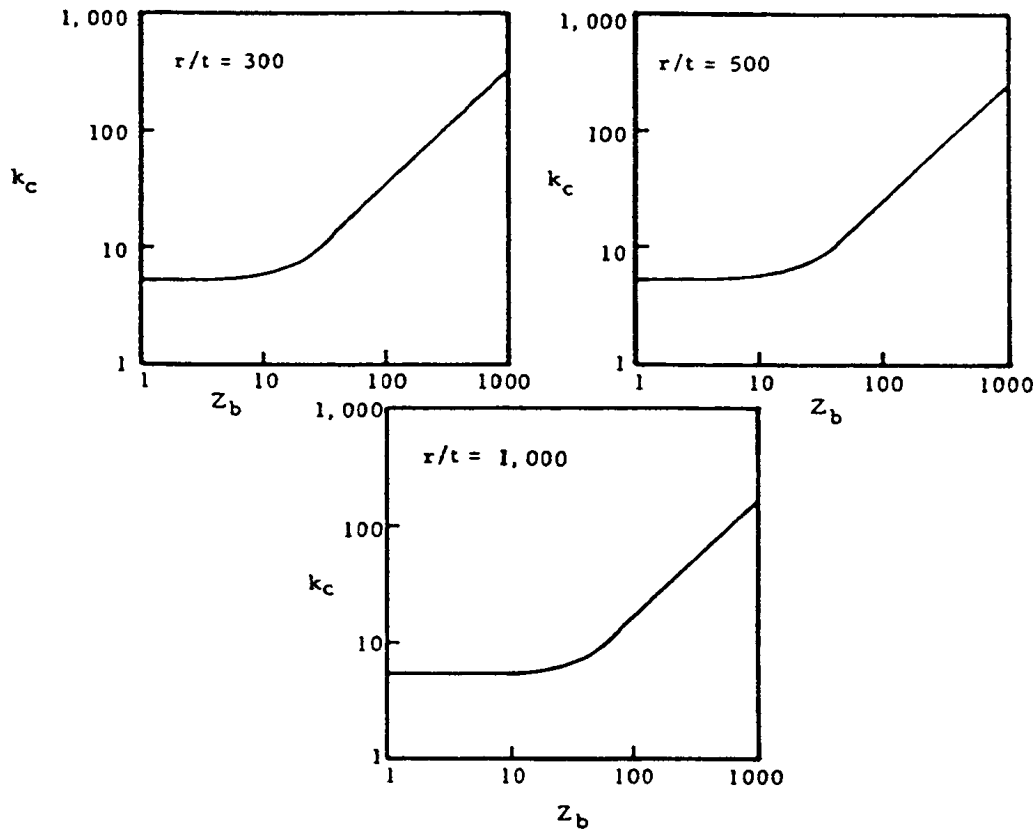
Figure 6-31.   Buckling Coefficient Grouped According to r/t Values for Curved Plates

For sharply curved plates, ($b^2/rt > 100$), Equations (6-32) and (6-33) can be used.

$$F_{cr} = \eta C E \left(\frac{t}{r}\right) \tag{6-32}$$

$$\eta = \frac{E_s}{E} \frac{E_t}{E_s} \frac{(1-\nu_e^2)}{(1-\nu^2)} \tag{6-33}$$

Figure 6-32 gives values of C in terms of r/t.   Figure 6-33 gives η in a nondimensional form.   Here the quantity $\epsilon_{cr} = Ct/r$.
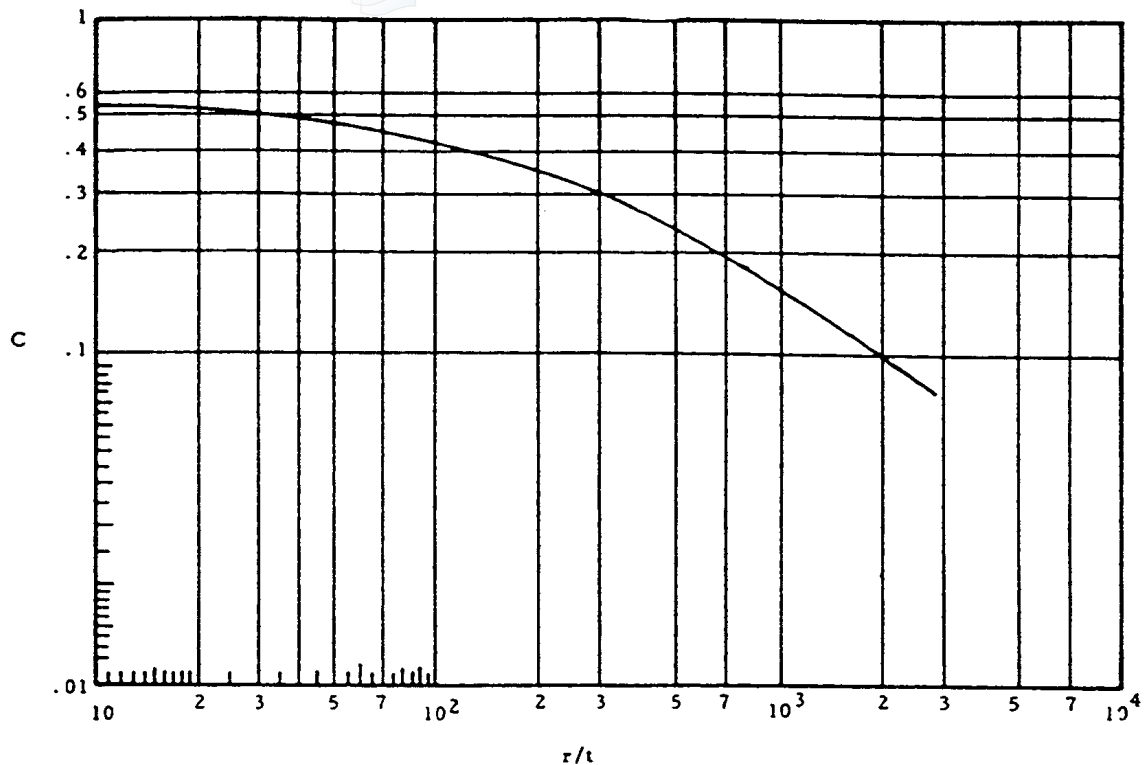
Figure 6-32.   Modified Classical Buckling Coefficient as a Function
of r/t for Axially Compressed Cylindrical Plates
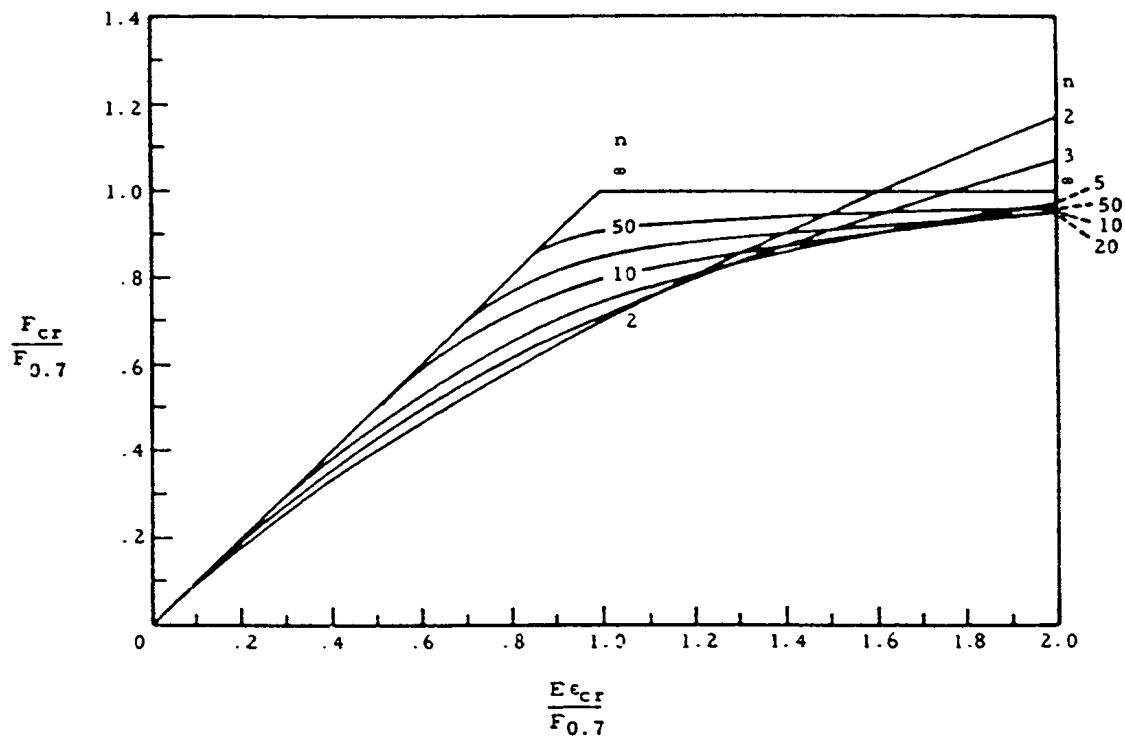
Figure 6-33.   Nondimensional Buckling Chart for Axially Compressed Curved Plate

$$\eta = (E_s/E)\left[(E_t/E)(1-\nu_e^2)/(1-\nu^2)\right]^{\frac{1}{2}}$$

6.7   Shear Loading of Curved Plates

Large radius curved plates ($b^2/rt < 1$) loaded in shear may be analyzed as flat plates by the methods of Section 6.5. For transition length plates ($1 < b^2/rt < 30$), Figure 6-34 can be used to find k_s for use in Equation (6-34).

$$F_{crs} = \frac{k_s \pi^2 E}{12(1-\nu_e^2)} \left(\frac{t}{b}\right)^2 \tag{6-34}$$

For ($b^2/rt > 30$), Equation (6-35) may be used.

$$F_{crs} = 0.37 (Z_b)^{\frac{1}{2}} (F_{crs})_{flat\ plate} \tag{6-35}$$

Curved plates under shear loading with stiffeners can be analyzed by using Figure 6-35 for the value of the buckling coefficient k_s. Both axial stiffeners and circumferential stiffeners are treated.

6.8   Plates Under Combined Loadings

In general, the loadings on aircraft elements are a combination of two or more simple loadings. Design of such elements must consider the inter-action of such loadings and a possible reduction of the allowable values of the simple stresses when combined loads are present. The method using stress ratios, R, has been used extensively in aircraft structural design. The ratio R is the ratio of the stress in the panel at buckling under combined loading to the buckling stress under the simple loading. In general, failure occurs when Equation (6-36) is satisfied. The exponents x and y must be determined experimentally and depend upon the structural element and

$$R_1^x + R_2^y = 1 \tag{6-36}$$

the loading condition.

6.8.1   Flat Plates Under Combined Loadings

Table 6-12 gives the combined loading condition for flat plates. Figures 6-36 and 6-37 give interaction curves for several loading and support conditions. It is noted that the curves present conditions of triple combinations.

6 - 68
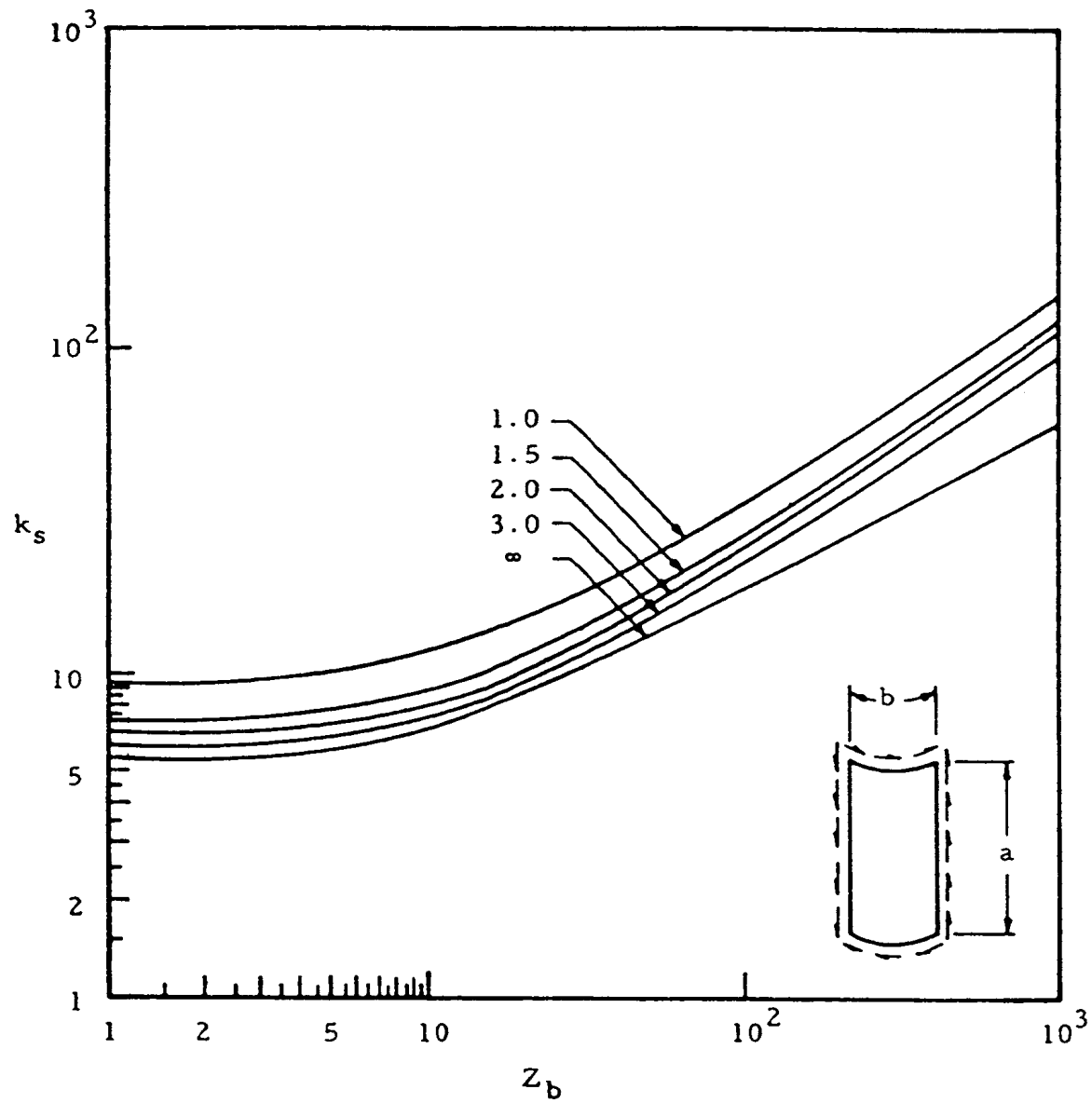
(a) Long simply supported plates

Figure 6-34. Shear Buckling Coefficients for Various Curved Plates

$$F_{or} = \frac{k_s \pi^2 E}{12(-\nu_e^2)} \left(\frac{t}{b}\right)^2 ; \quad Z_b = \frac{b^2}{rt} (1-\nu_e^2)^{\frac{1}{2}}$$
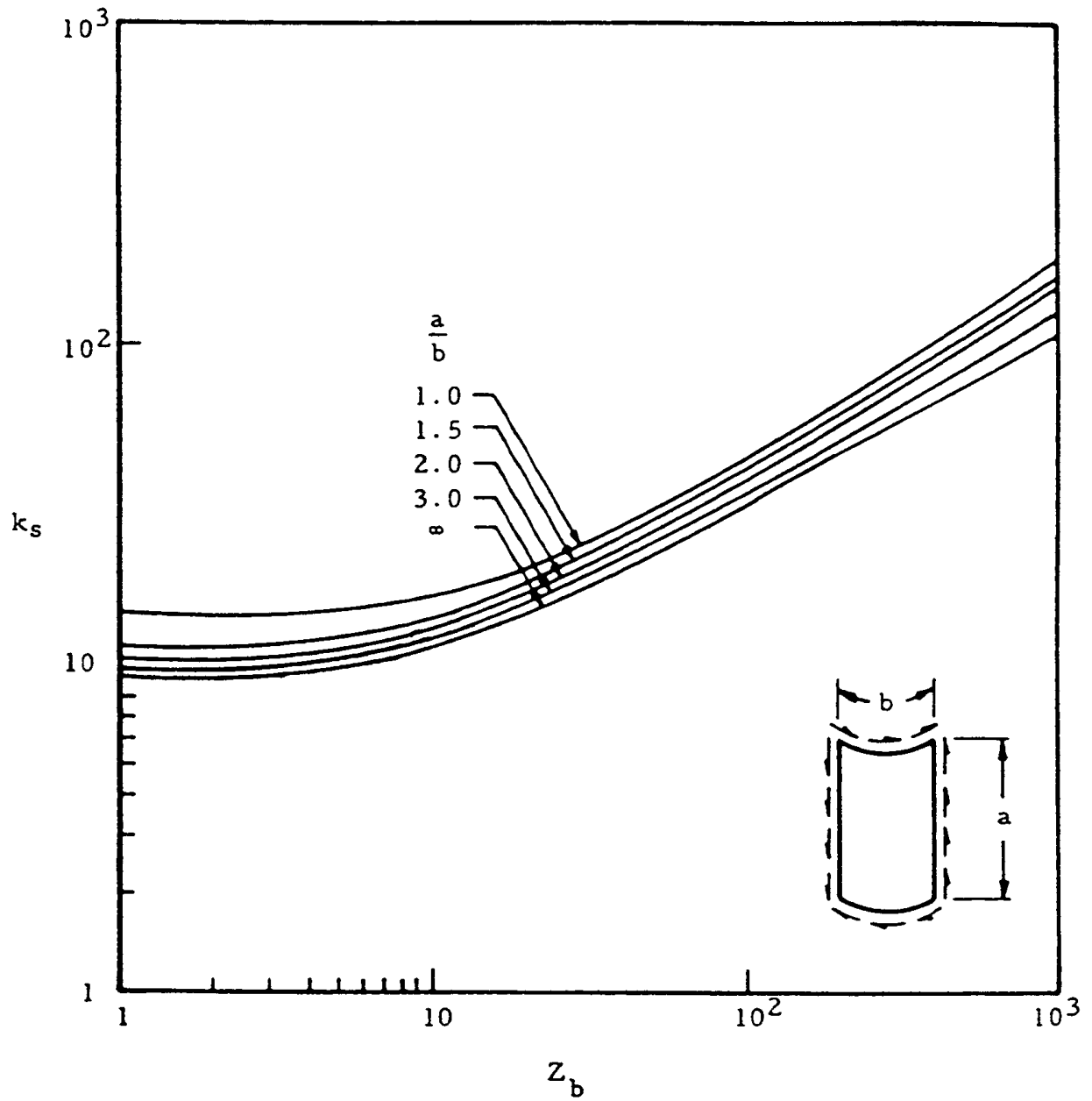
(b)   Long clamped plates

Figure 6-34.   Shear Buckling Coefficients for Various Curved Plates (continued)
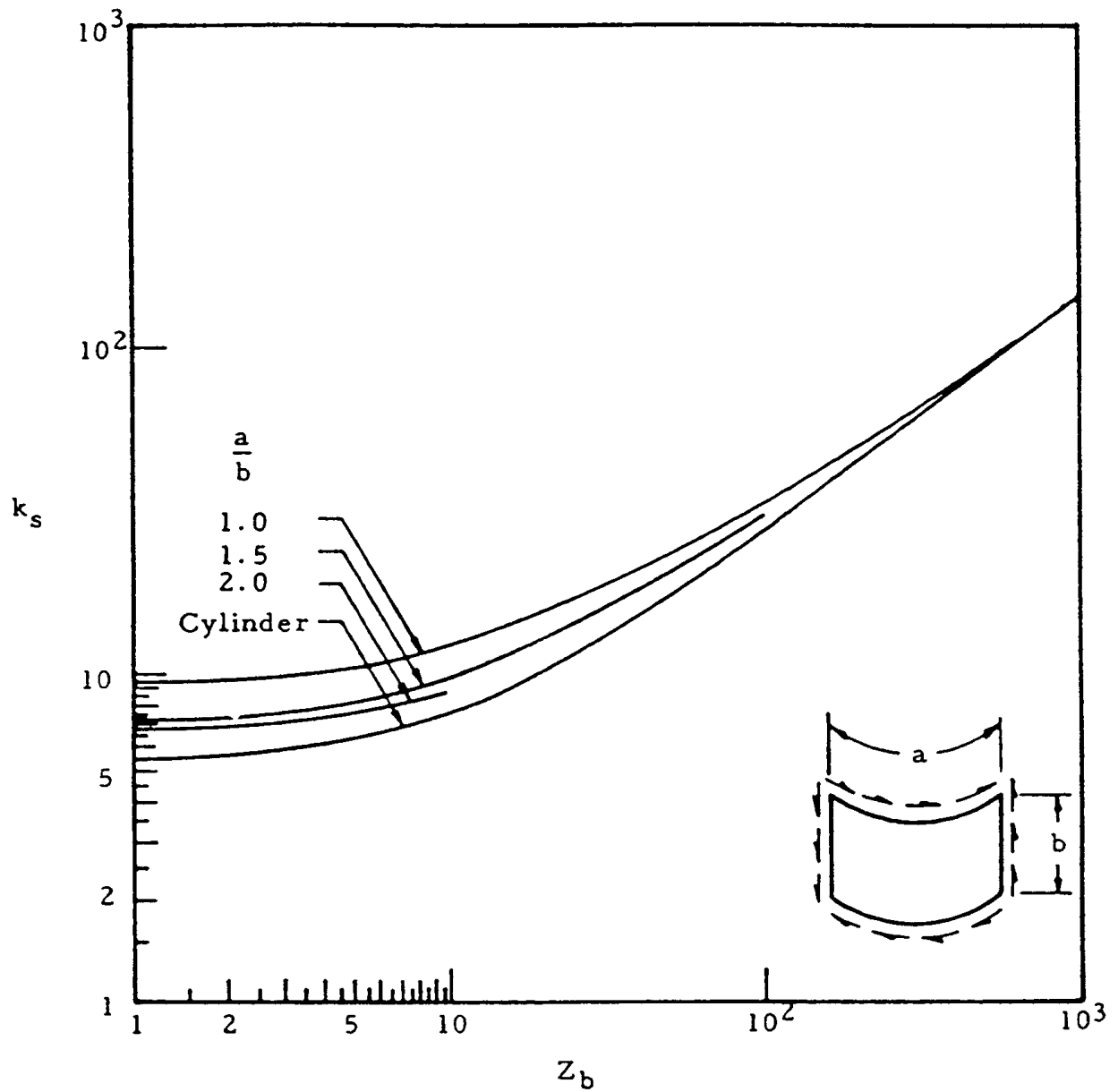
(c) Wide, simply supported plates

Figure 6-34. Shear Buckling Coefficients for Various Curved Plates (continued)
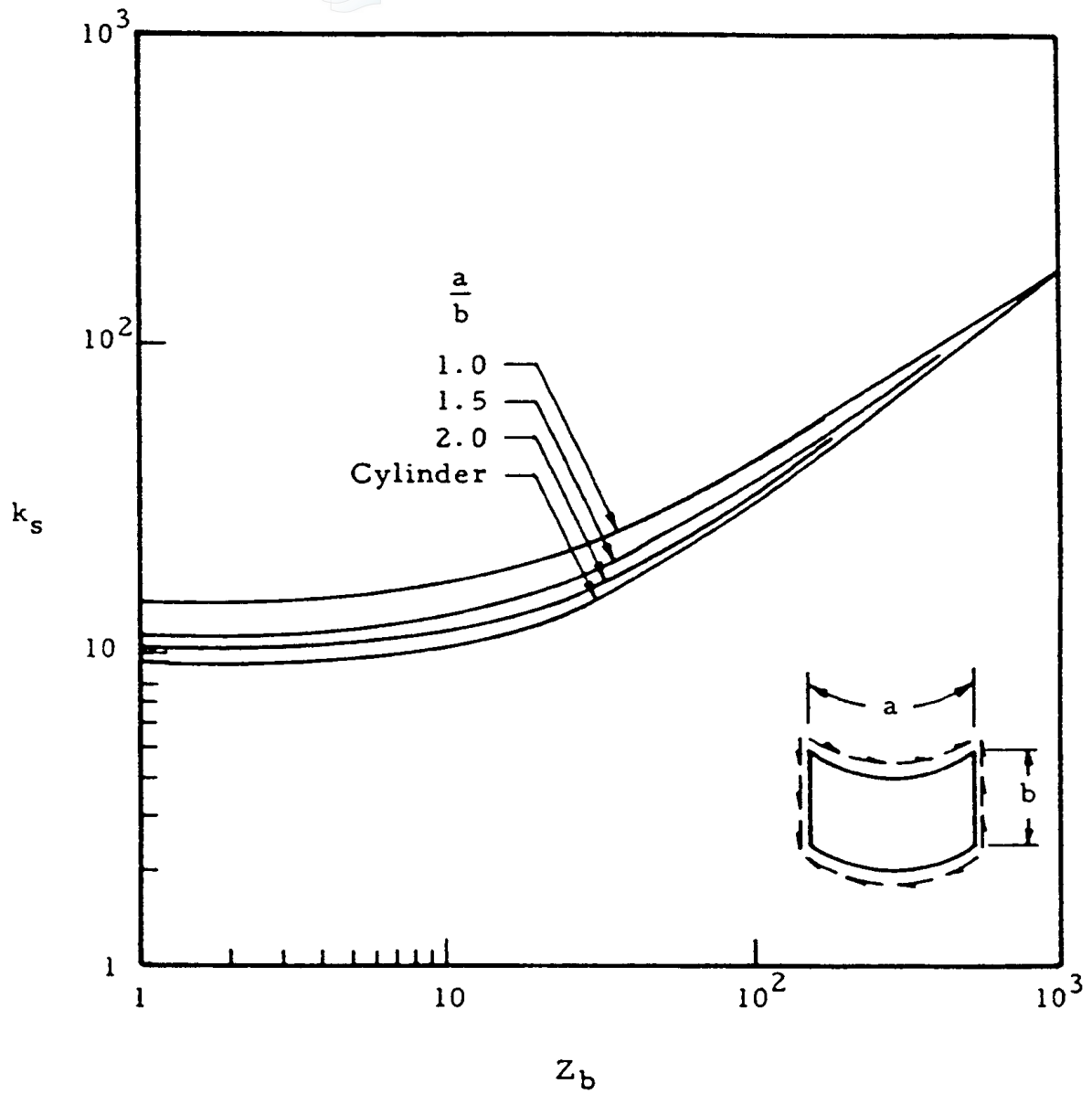
(d) Wide clamped plates

Figure 6-34. Shear Buckling Coefficients for Various Curved Plates (concluded)
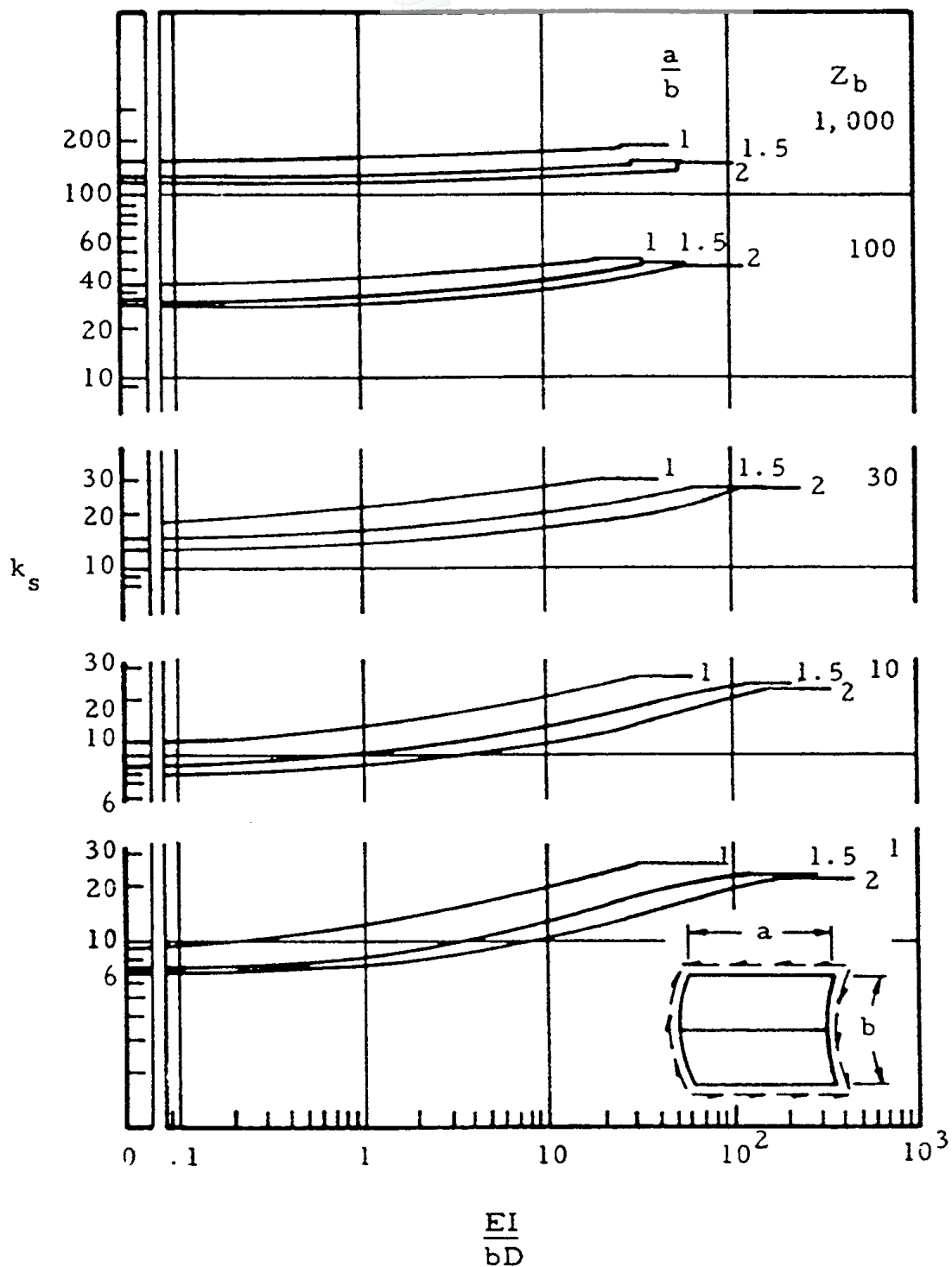
(a) Center axial stiffener; axial length greater than circumferential width

Figure 6-35.   Shear-Buckling Coefficients for Simply Supported Curved Plates with Center Stiffener
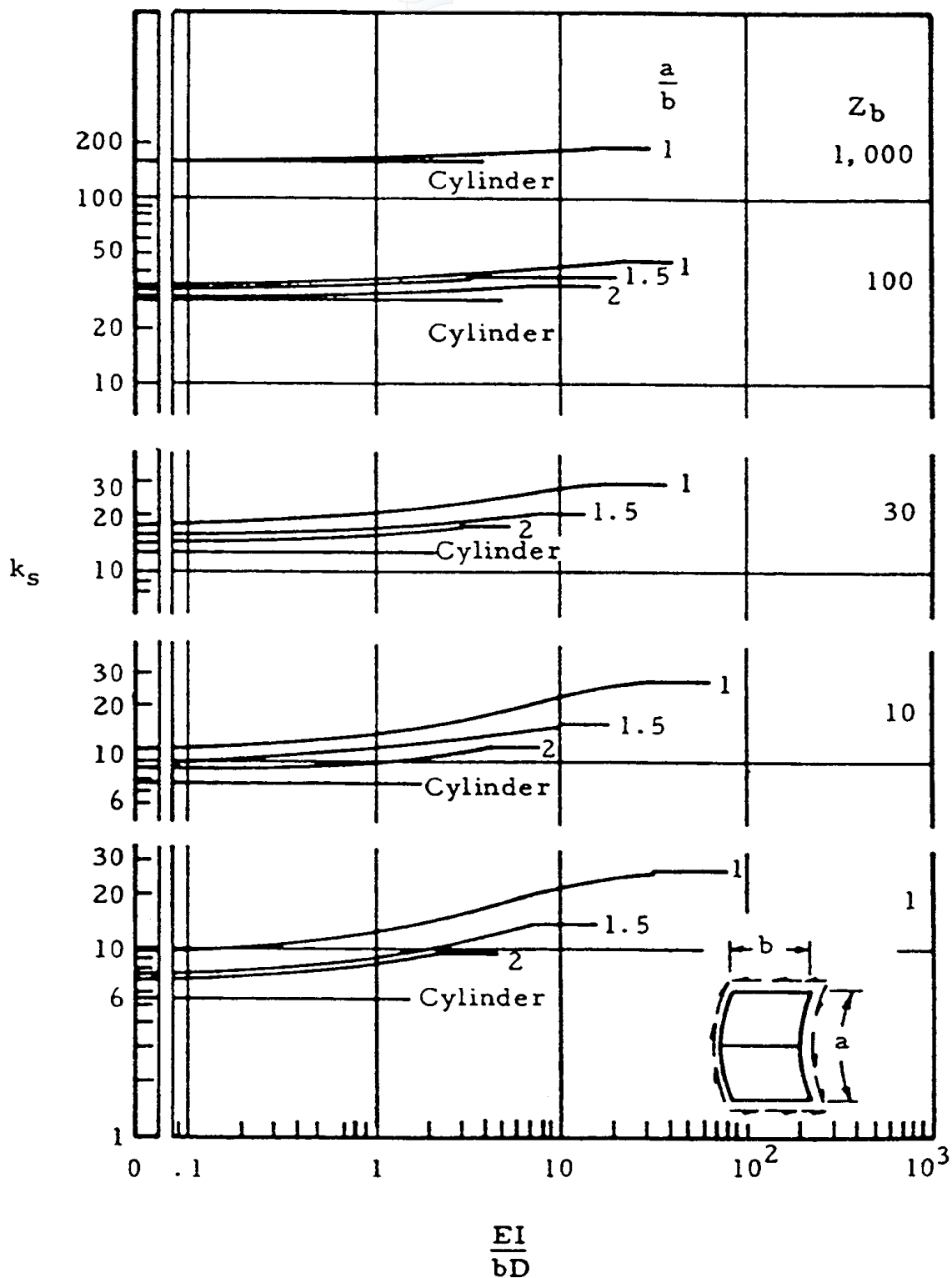
(b) Center axial stiffener; circumferential width greater than
   axial length.

Figure 6-35.   Shear-Buckling Coefficients for Simply Supported
   Curved Plates with Center Stiffener (continued)
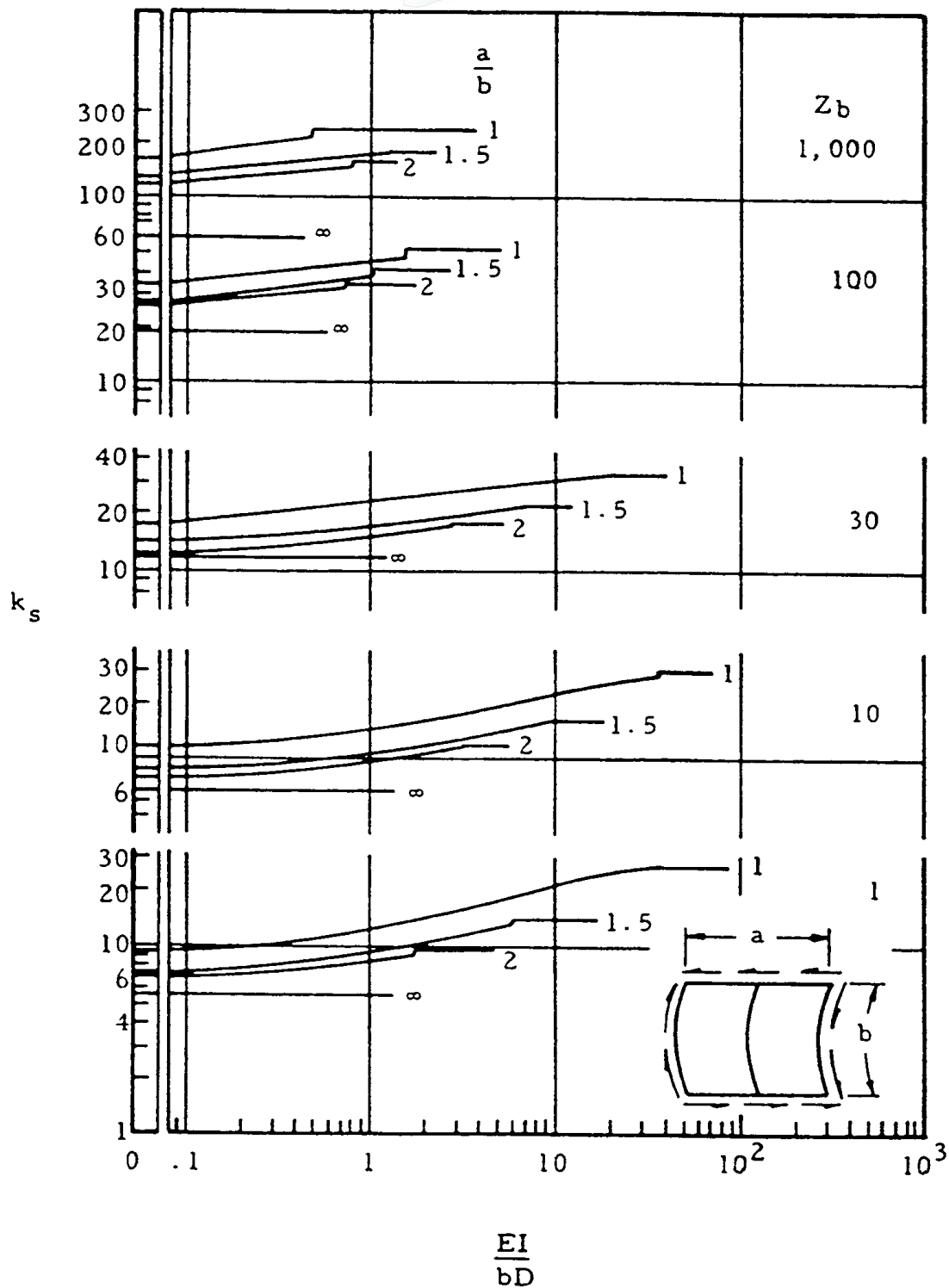
(c) Center circumferential stiffener; axial length greater than circum-
ferential width.

Figure 6-35.   Shear-Buckling Coefficients for Simply Supported
Curved Plates with Center Stiffener (continued)
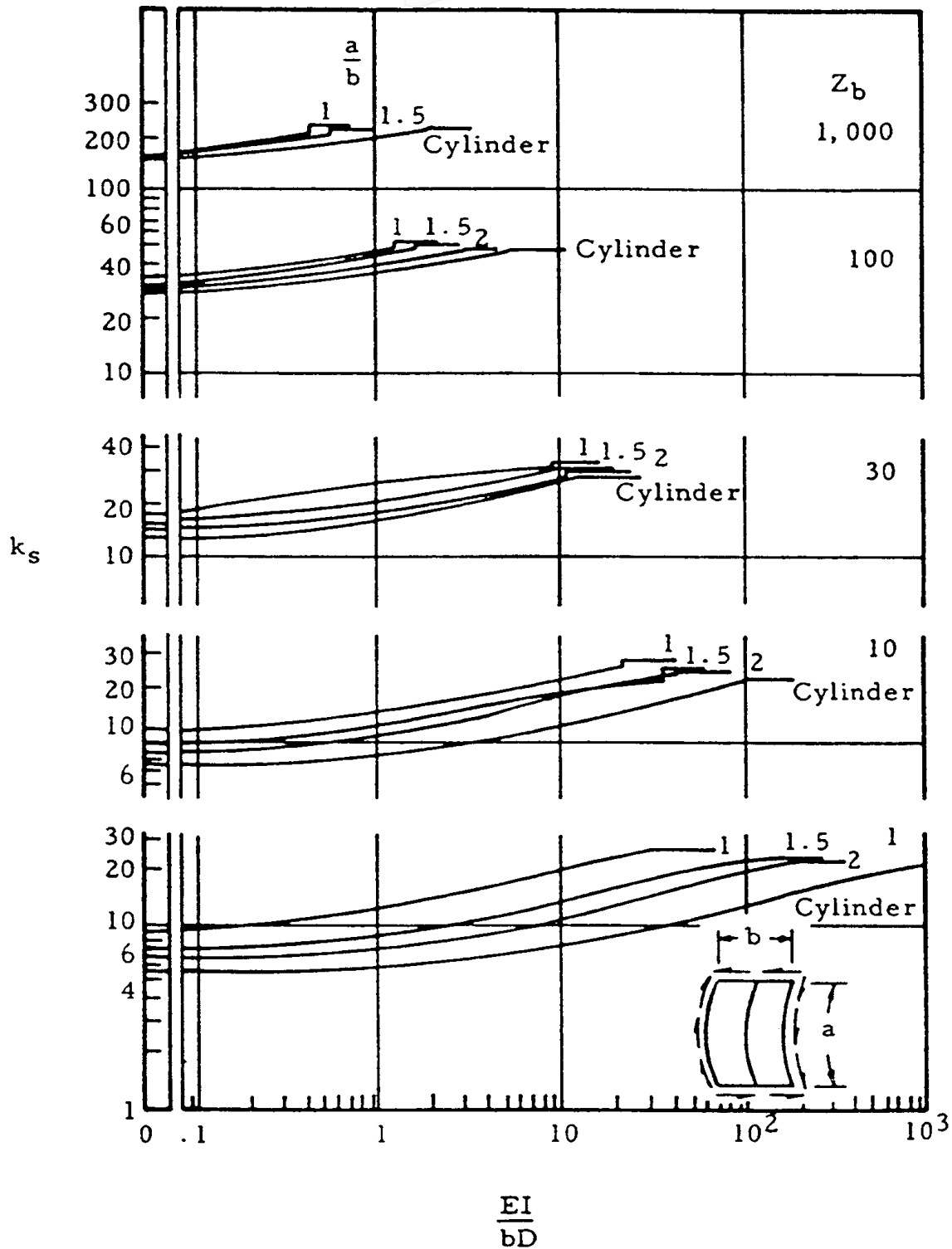
(d) Center circumferential stiffener; circumferential width greater than axial length

Figure 6-35.   Shear-Buckling Coefficients for Simply Supported
Curved Plates with Center Stiffener (concluded)
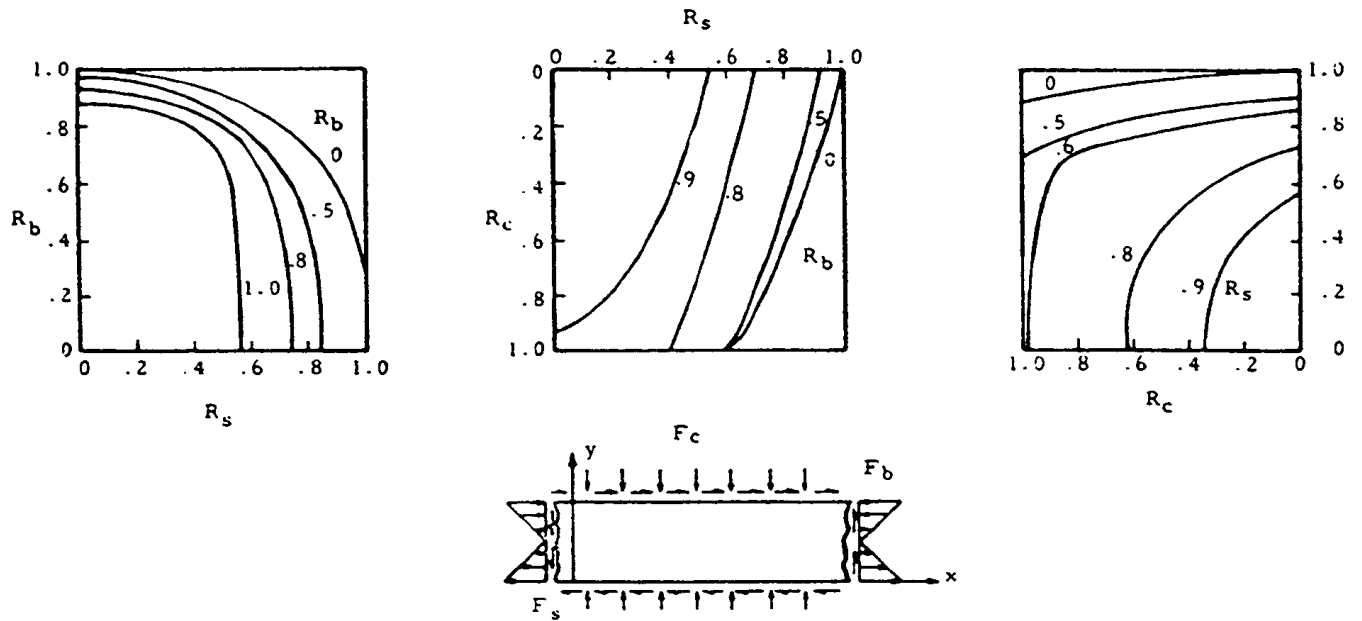
(a) Upper and lower edges simply supported
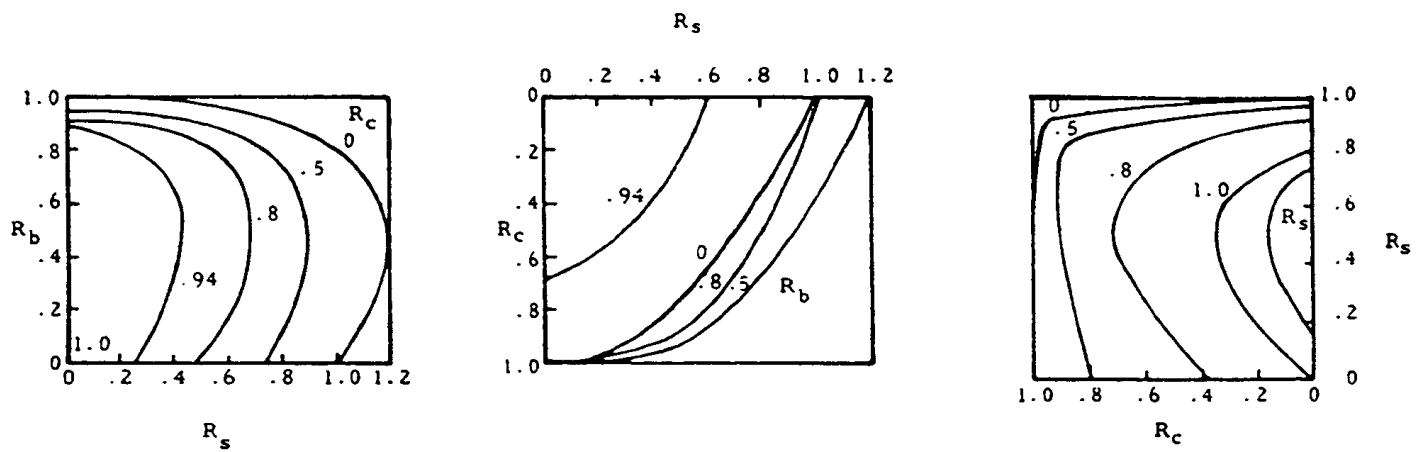
(b) Upper edges simply supported, lower edges clamped

Figure 6-36. Interaction Curves for Long Flat Plates Under Various
Combinations of Compression, Bending, and Shear

(a) a/b = 0.8

(b) a/b = 1.0

(c) a/b = 1.20

(d) a/b = 1.60

(e) a/b = 2.0

(f) a/b = 3.0

(g) a/b = ∞
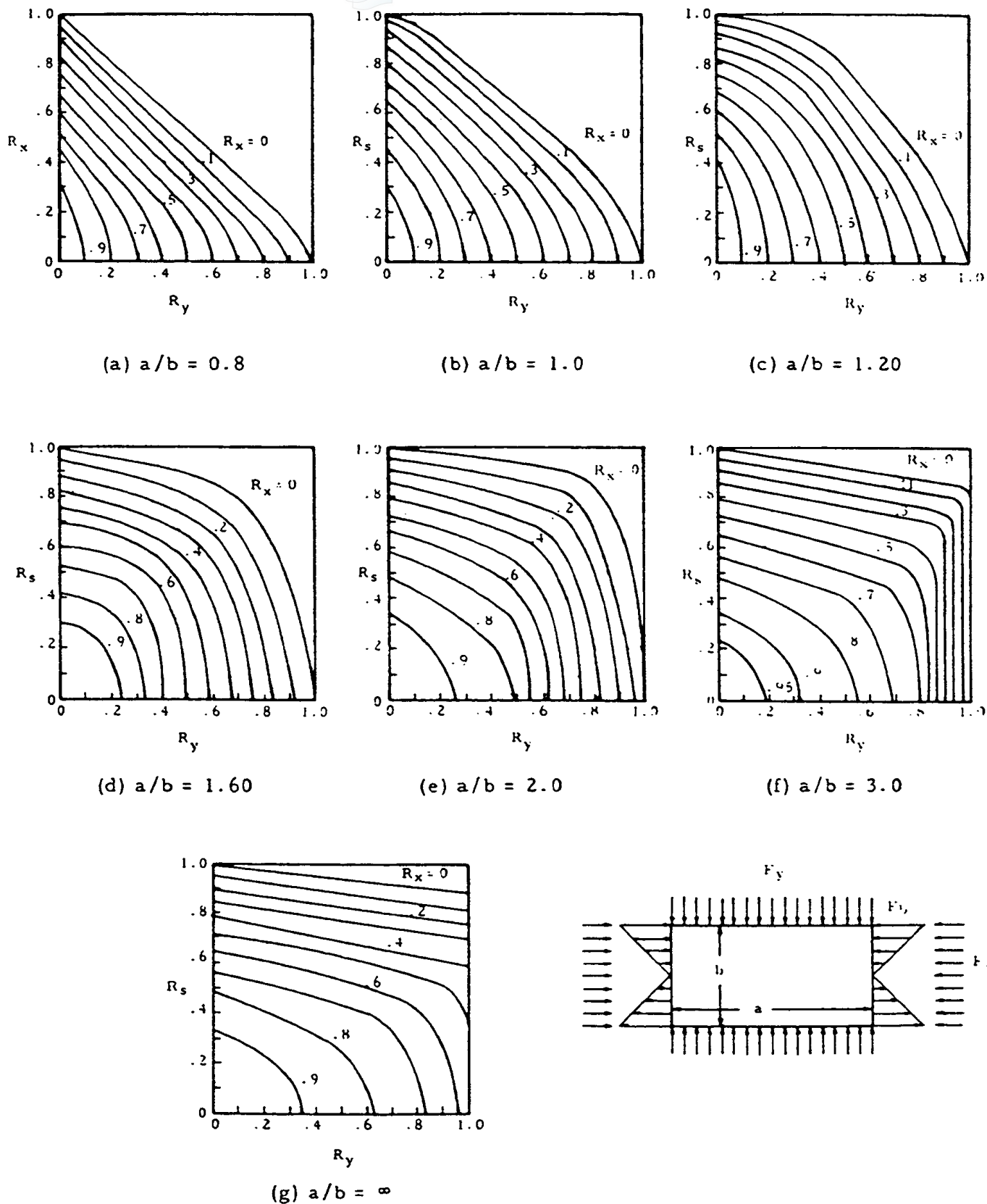
Figure 6-37.   Interaction Curves for Flat Rectangular Plates Under Combined
Biaxial-Compression and Longitudinal-Bending Loadings

TABLE 6-12

Combined Loading Conditions for Which Interaction Curves Exist

Theory	Loading Combination	Interaction Equation	Figure
Elastic	Biaxial compression	For plates that buckle in square waves, $R_x + R_y = 1$	6.37
	Longitudinal compression and shear	For long plates, $R_c + R_s^2 = 1$	6.36
	Longitudinal compression and bending	None	6.37
	Bending and shear	$R_b^2 + R_s^2 = 1$	6.36
	Bending, shear, and transverse compression	None	6.36
	Longitudinal compression and bending and transverse compression	None	6.37
Inelastic	Longitudinal compression and shear	$R_c^2 + R_s^2 = 1$	

Figure 6-38 presents buckling coefficients for right angle isosceles triangular plates loaded under shear and compression. Equation (6-37) is the interaction equation for shear and normal stress on this type of plate.

$$\left(\frac{2F_s}{F_{crs+} + F_{crs-}} + u \right)^2 + \frac{F}{F_{cr}} (1-u^2) = 1 \qquad (6-37)$$

The + and - subscripts refer to either tension or compression along the altitude upon the hypotenuse of the triangle caused by pure shear loading. Table 6-13 contains values of k_c, k_{s+} and k_{s-} for various edge supports.

TABLE 6-13

Buckling Coefficients for Right-Angle Isosceles Triangular Plates Loaded Independently in Uniform Compression, Positive Shear, and Negative Shear

Edge Supports (a)	k_c	k_{s+}	k_{s-}
All edges simply supported	10.0	62.0	23.2
Sides simply supported, hypotenuse clamped	15.6	70.8	34.0
Sides clamped, hypotenuse simply supported	18.8	80.0	44.0

[a]Hypotenuse = b in Figure 6.38
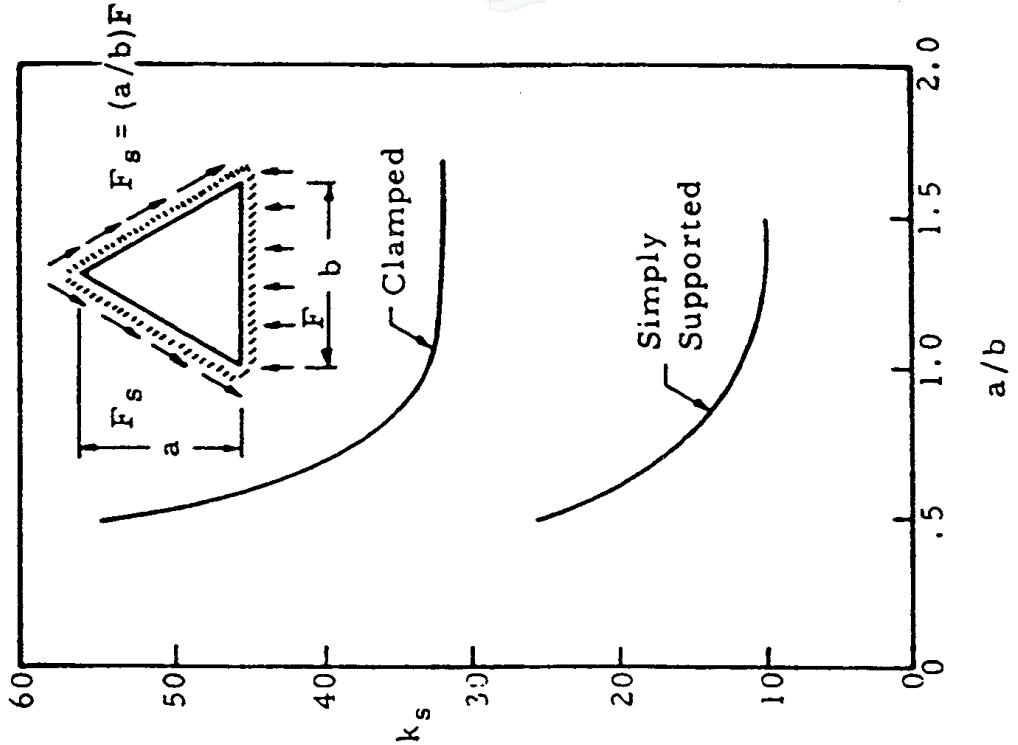
(b) Shear

(a) Uniform Compression
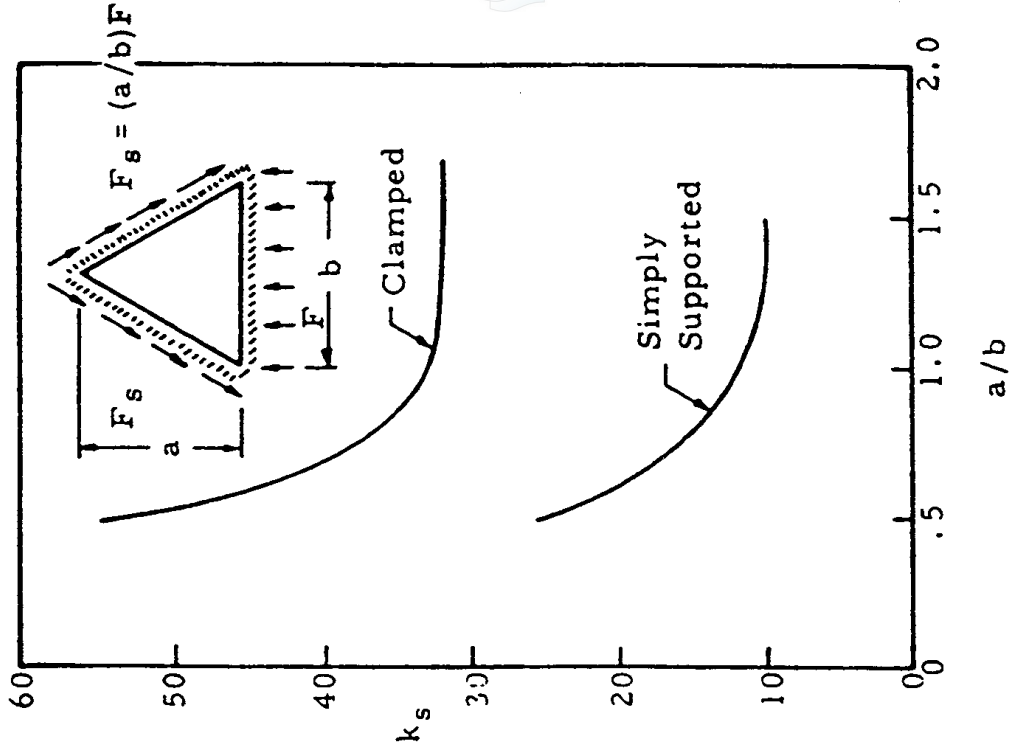
Figure 6-38. Buckling Coefficients for Isosceles Triangular Plates

6.8.2   Curved Plates Under Combined Loadings

For curved plates under combined axial loading and shear with $10 < Z_b < 100$ and $1 < a/b < 3$, the interaction relation of Equation (6-39) may be used.

$$R_s{}^2 + R_x = 1 \qquad\qquad (6-39)$$

This may be used for either compression or tension with tension being denoted by a negative sign.

6.9   Buckling of Oblique Plates

In many instances, the use of rectangular panels is not possible. Figures 6-39 and 6-40 give buckling coefficients for panels which are oriented oblique to the loading. Figure 6-39 covers flat plates divided into oblique parallelogram panels by nondeflecting supports. Figure 6-40 covers single oblique panels.

6.10   Sample Problem - Plate Analysis

Find: The buckling stress of a flat plate under uniform longitudinal compression, simply supported on all four sides.

Given: a = 12 in.,   b = 4 in,   t = 0.100 in.

Material: Bare 2024-T3 Sheet   Material Properties: $E = 10.7 \times 10^6$ psi
$$\nu = 0.33$$
$$F_{cy} = 34,000 \text{ psi}$$

Solution: $$F_{cr} = \bar{\eta}\,\eta \, \frac{k_c \pi^2 E}{12(1-\nu^2)} \left(\frac{t}{b}\right)^2$$

From Figure 6-1 for a/b = 3, $k_c = 4.00$.

$$\bar{\eta} = 1.0 \text{ for no cladding}$$

$$\eta = 1.0 \text{ for elastic buckling}$$

$$F_{cr} = \frac{(4.0)(\pi^2)(10.7)10^6}{12[1 - (.33)^2]} \left(\frac{100}{2}\right)^2$$

$$F_{cr} = 24,600 \text{ psi}$$

As this is below the compression yield strength, no allowance for elasticity need be made.

6 - 81
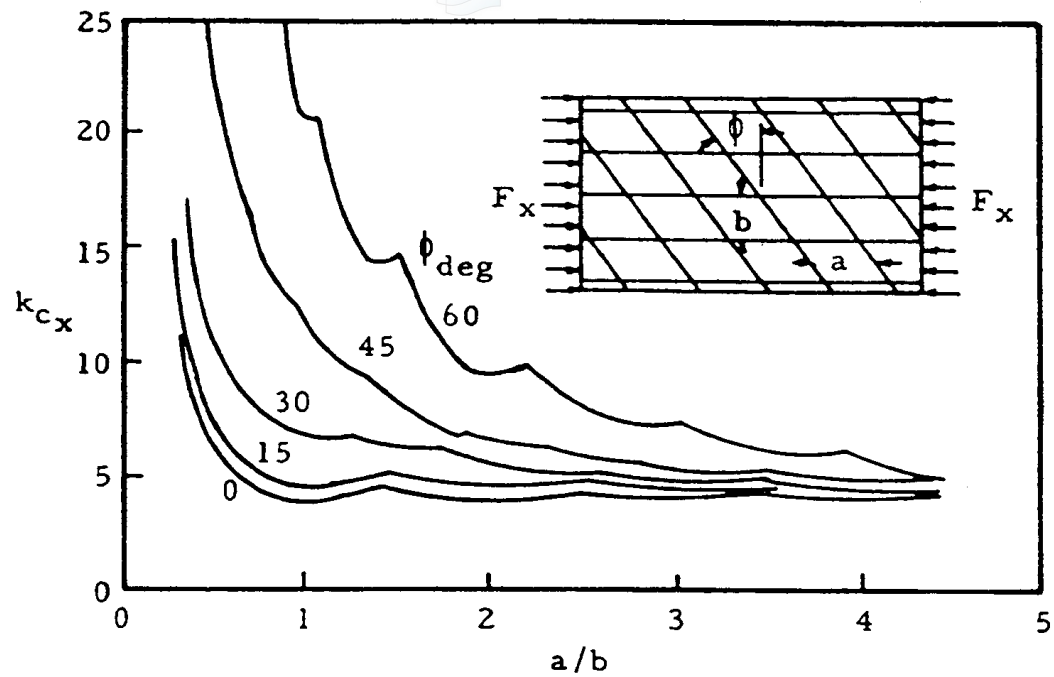
(a) Loading in x-direction
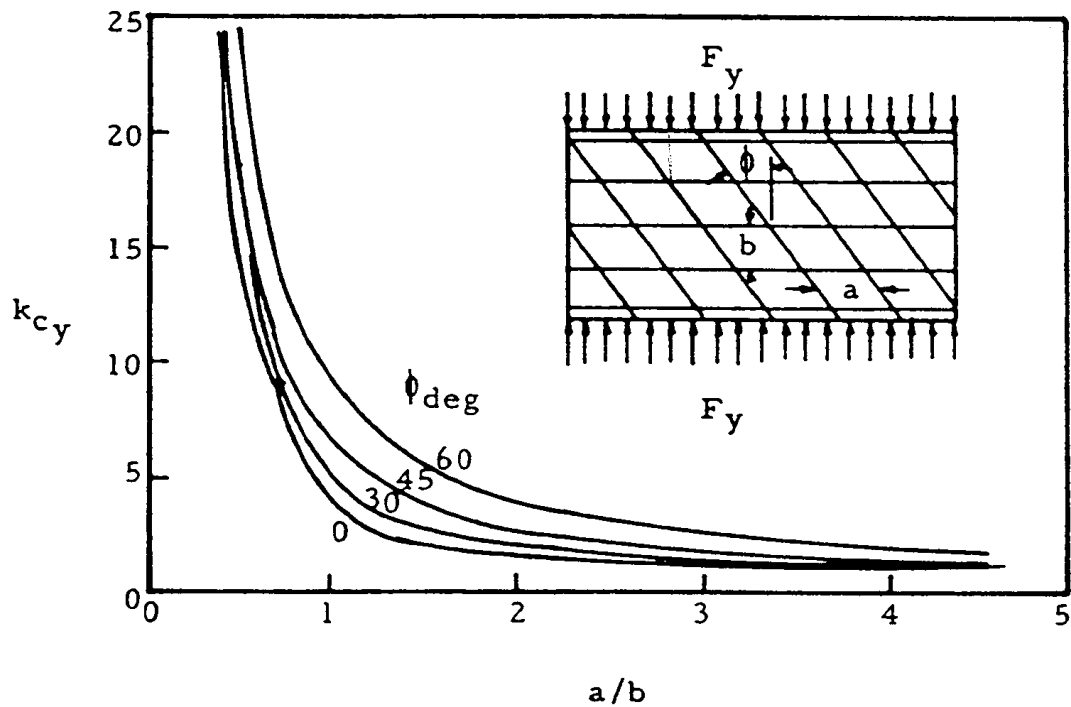
(b) Loading in y-direction

Figure 6-39.   Compressive-Buckling Coefficients for Flat Sheet on
Nondeflecting Supports Divided into Parallelogram-
Shaped Panels.   All panel sides are equal.

(a) Compressive loading

(b) Shear loading
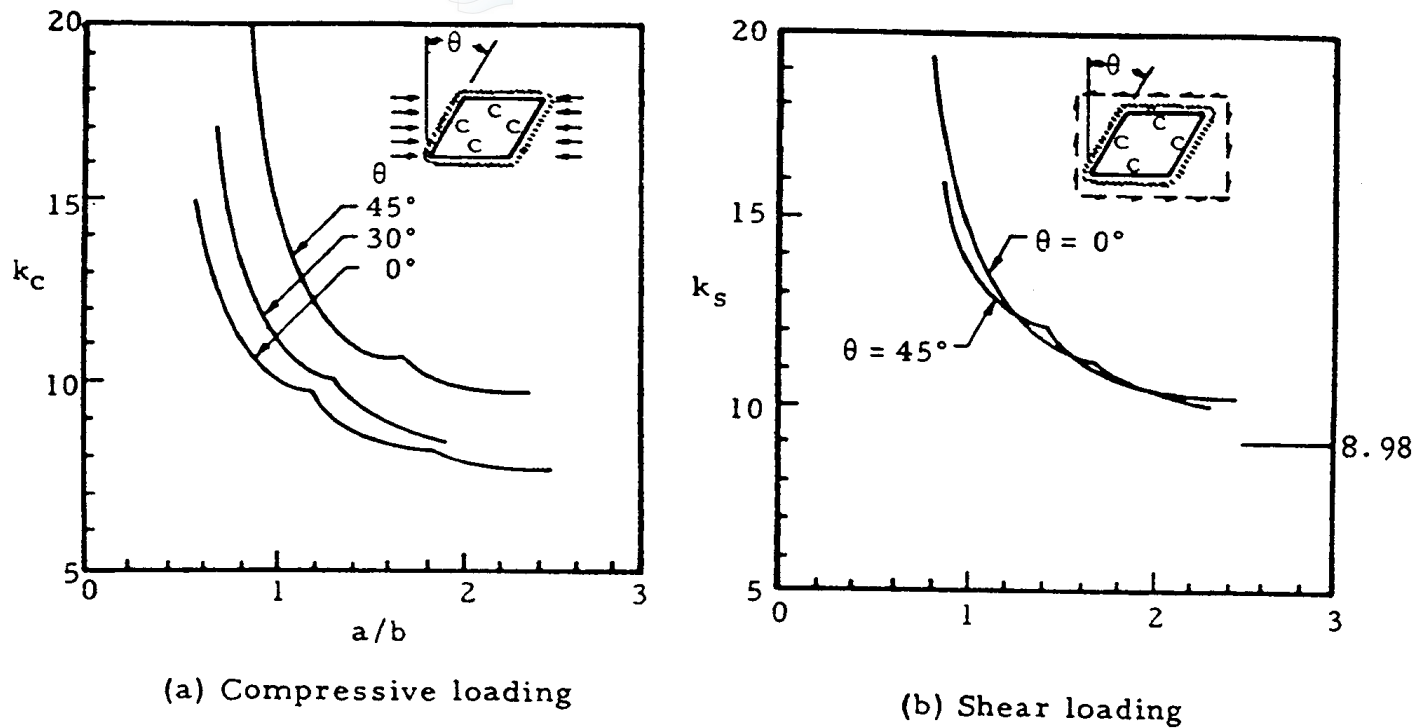
Figure 6-40.   Buckling Coefficient of Clamped Oblique Flat Plates

6.11   Buckling of Sandwich Panels

The use of sandwich construction for skin panels of aircraft has become commonplace.   Panel construction consists of primary and secondary skins separated by a core which is usually some form of honeycomb or expanded foam material.   The critical buckling stress of such a composite can be calculated from Equation (6-40).

$$F_{cr} = C K F_{crf} \tag{6-40}$$

The quantity F_{crf} is the buckling stress of the two faces if they were not connected by the core.   Use the total thickness of the faces.   The coefficient C is obtained from Figure 6-41 and K is a form factor given in Equation (6-41).

$$K = 1 + 3 \left(1 + \frac{c}{t} \right) \tag{6-41}$$

The data in Figure 6-41 is given as a family of curves of parameter R which is given in Equation (6-42).

$$R = \frac{G_{core}}{K \, F_{crf}} \tag{6-42}$$
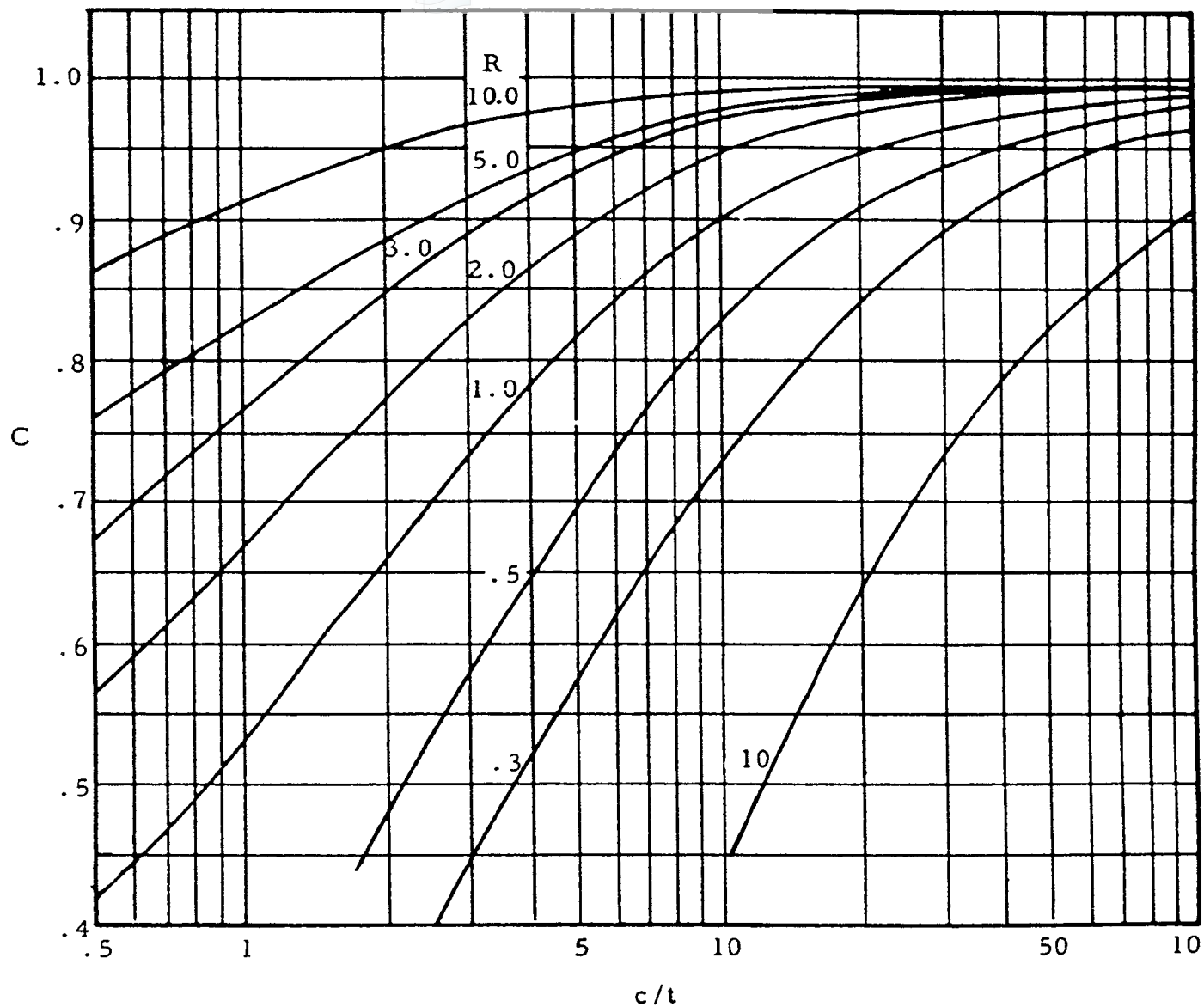
Figure 6-41.   Logarithmic Buckling-Stress Diagram for Simply Supported
Rectangular Sandwich Panels

7. MEMBRANES

7.1 Introduction to Membranes

A membrane may be defined to be a plate that is so thin that it may be considered to have no bending rigidity. The only stresses present are in the plane of the surface and are uniform throughout the thickness of the membrane.

Section 7.3 of this chapter treats of circular membranes, and Section 7.5 deals with square and rectangular membranes.

7.2 Nomenclature for Membranes

a	=	longitudinal dimension of membrane
D	=	diameter
E	=	modulus of elasticity
f	=	calculated stress
f_{max}	=	calculated maximum stress
n_1-n_7	=	coefficients given in Figure 7-9
p	=	pressure
R	=	outside radius of circular membrane
r	=	cylindrical coordinate
t	=	thickness of membrane
x, y	=	rectangular coordinates
δ	=	deflection
δ_c	=	center deflection of circular membrane
μ	=	Poisson's ratio

7.3 Circular Membranes

Figure 7-1 shows two views of a circular membrane with the clamped edge under a uniform pressure, p.

The maximum deflection of this membrane is at the center and is given by

$$\delta_c = 0.662 \, R \sqrt[3]{\frac{pR}{Et}} \qquad (7-1)$$

The deflection of the membrane at a distance, r, from the center is

$$\delta = \delta_c \left[1 - .09 \left(\frac{r}{R} \right)^2 - 0.1 \left(\frac{r}{R} \right)^5 \right] \qquad (7-2)$$
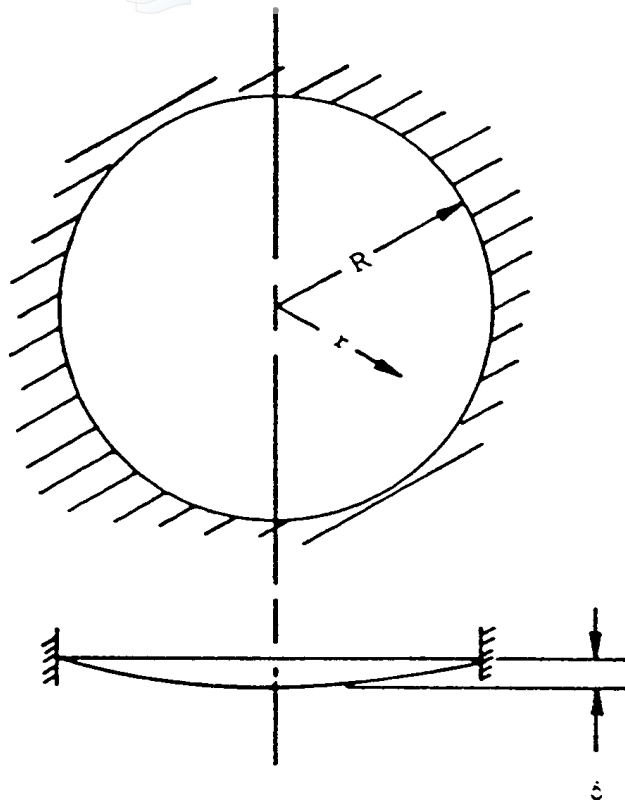
Figure 7-1. Circular Membrane with Clamped Edge

The stress at the center of this membrane is

$$f = 0.423 \sqrt[3]{\frac{E p^2 R^2}{t^2}} \tag{7-3}$$

while that at the edge is

$$f = 0.328 \sqrt[3]{\frac{E p^2 R^2}{t^2}} \tag{7-4}$$

7.4 Sample Problem - Circular Membranes

Given: The circular membrane shown in Figure 7-2

Find: The center deflection and the stresses at the center and at the edge of the membrane.

Solution:

$$\frac{p}{E} \left(\frac{D}{t} \right)^4 = \frac{10}{10 \times 10^6} \left(\frac{15}{0.1} \right)^4 = 506$$
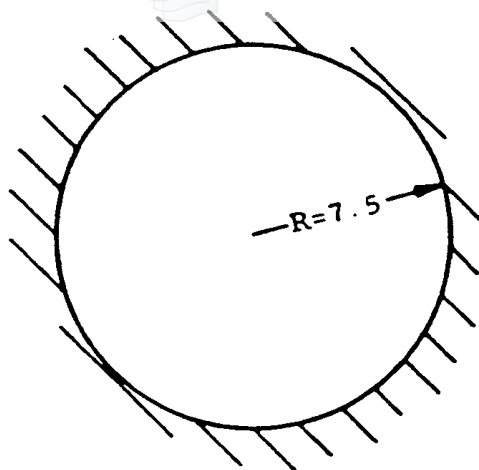
$t = 0.1$ inch

$p = 10$ psi

$E = 10 \times 10^6$

Figure 7-2.   Circular Membrane with Clamped Edge

From Section 7.5.3.2, a square plate, for which $p/E\,(b/t)^4$ is greater than 250, may be considered to be a membrane. Assuming this to be approximately true for a circular plate with D used in the relation instead of b, the given plate may be treated as a membrane.

From Equation (7-1), the center deflection of the given membrane is

$$\delta_c = 0.662\,R\sqrt[3]{\frac{pR}{Et}} = 0.662\,(7.5)\sqrt[3]{\frac{10\,(7.5)}{10^7\,(0.1)}} = 0.21 \text{ in.}$$

From Equation (7-3), the stress at the center of the membrane is

$$f = 0.423\sqrt[3]{\frac{E\,p^2\,R^2}{t^2}} = 0.423\sqrt[3]{\frac{10^7\,(10^2)\,(7.5^2)}{(0.1)^2}} = 7,500 \text{ psi}$$

From Equation (7-4), the stress at the edge of the membrane is

$$f = 0.328\sqrt[3]{\frac{E\,p^2\,R^2}{t^2}} = 0.328\sqrt[3]{\frac{10^7\,(10^2)(7.5^2)}{(0.1)^2}} = 5,870 \text{ psi}$$

7.5   Rectangular Membranes

For purposes of analysis, rectangular membranes may be divided into two classes: long rectangular membranes where the ratio of length to width (a/b) is greater than five, and short rectangular membranes where this ratio is less than five.

7.5.1   Long Rectangular Membranes

Figure 7-3 shows a long rectangular membrane (a/b > 5) clamped along all four sides.
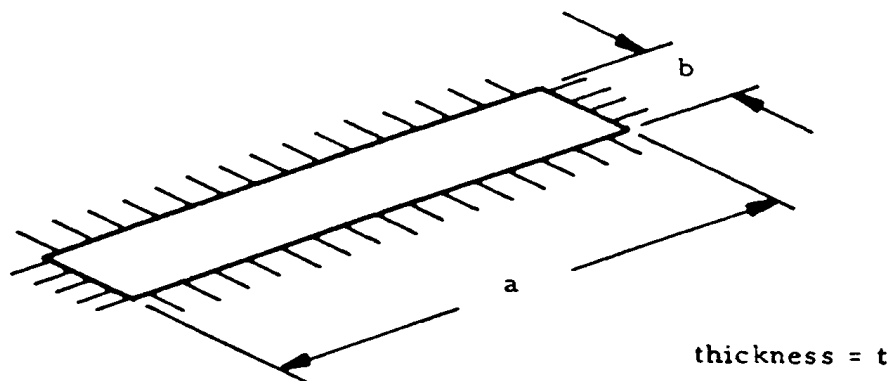
Figure 7-3.   Long Rectangular Membrane Clamped on Four Sides

The deflection and stress at the center of such a plate are approximately the same as those in a long membrane clamped along the two long sides. Such a membrane is shown in its deflected position in Figure 7-4.
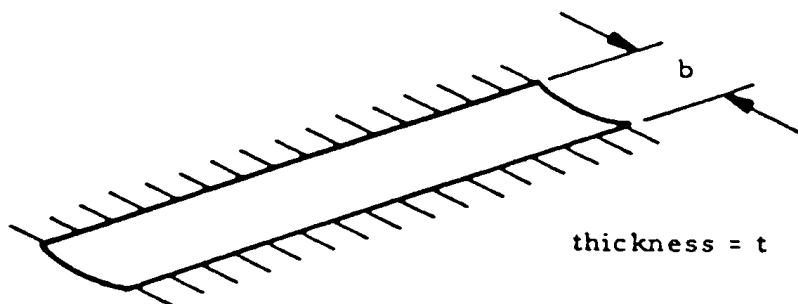
Figure 7-4.   Long Rectangular Membrane Clamped on Two Sides

The maximum stress and center deflection of the membrane in Figure 7-4 under uniform pressure p are given by Equations (7-5) and (7-6).

$$f_{max} = \left[\frac{p^2 E b^2}{24(1-\mu^2)t^2} \right]^{1/3} \qquad (7-5)$$

$$\frac{\delta}{b} = \frac{1}{8} \left[\frac{24(1-\mu^2)pb}{Et} \right]^{1/3} \qquad (7-6)$$

These equations are presented graphically in Figures 7-5 and 7-6 for μ = 0.3.

7 - 4
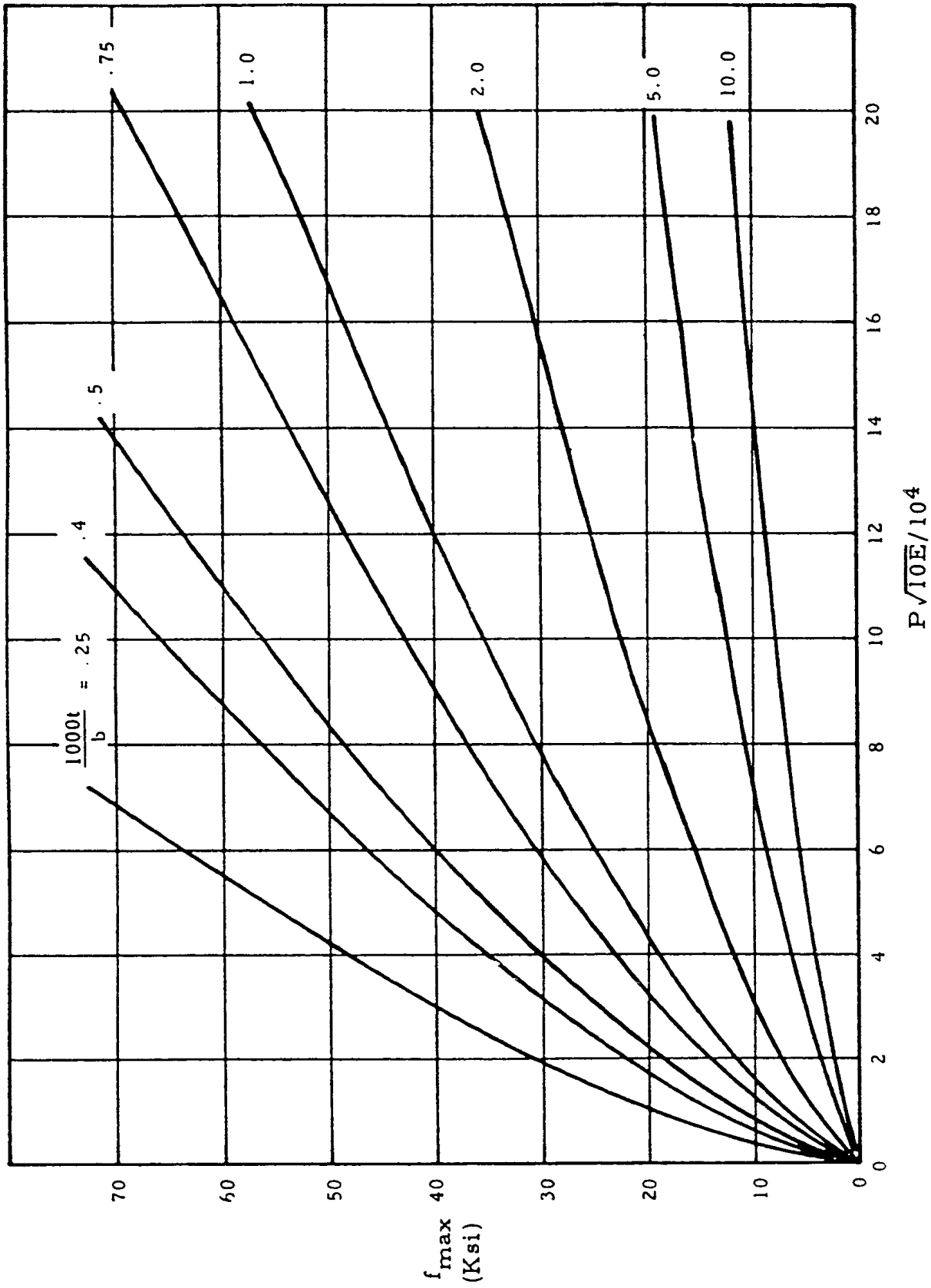
Figure 7-5. Maximum Stress in Long Rectangular Membranes (a/b > 5) Held Along Long Sides ($\mu = 0.3$)
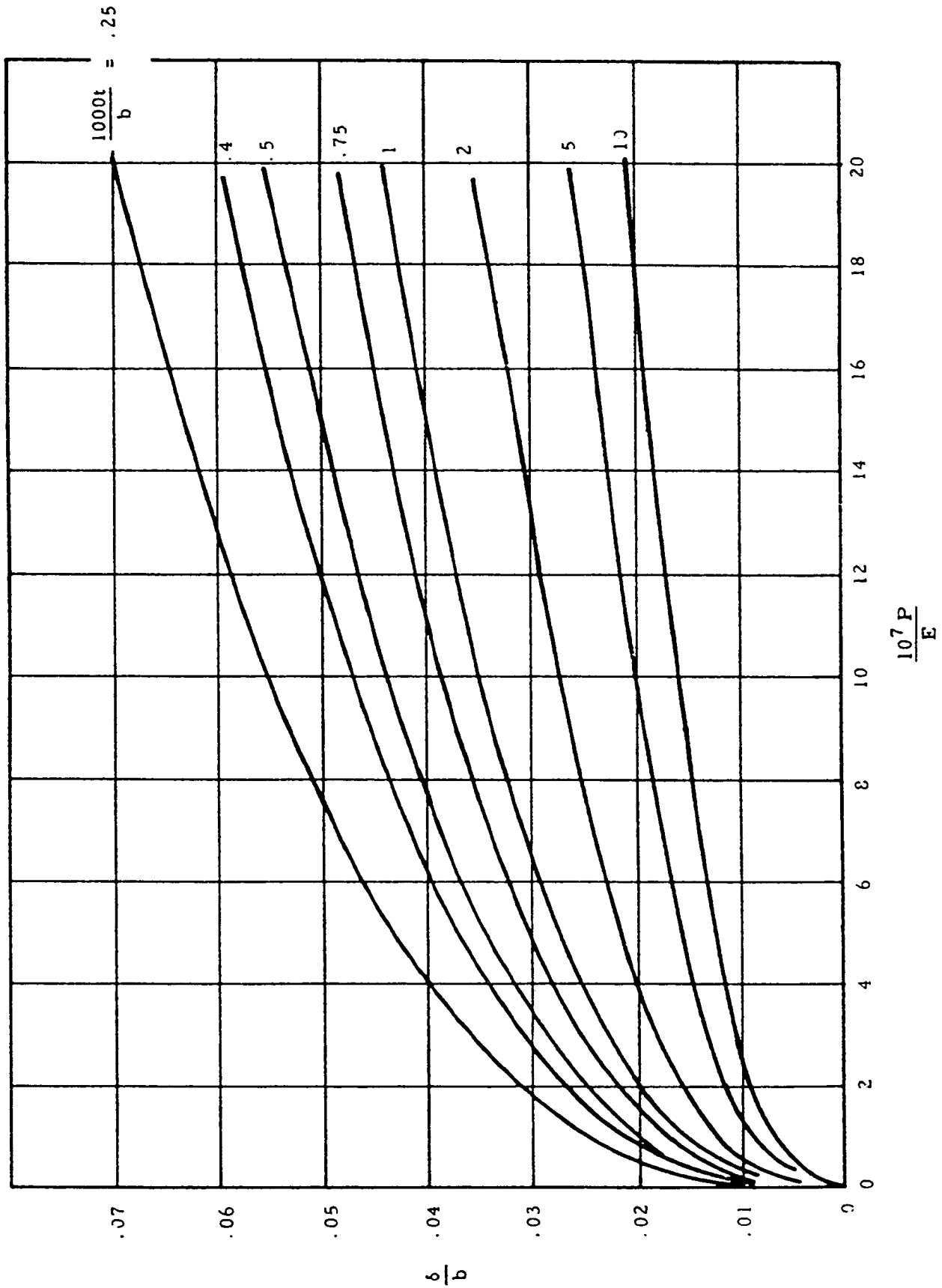
Figure 7-6. Center Deflection of Long Rectangular Membranes (a/b > 5) Held Along Long Sides (μ = 0.3)

7-6

A long rectangular plate may be considered to be a membrane if $p/E \, (b/t)^4$ is greater than 100.

7.5.2   Sample Problem - Long Rectangular Membrane

Given: The membrane shown in Figure 7-7.

$$t = 0.1 \text{ inch}$$
$$p = 15 \text{ psi}$$
$$E = 10 \times 10^6 \text{ psi}$$
$$\mu = 0.316$$
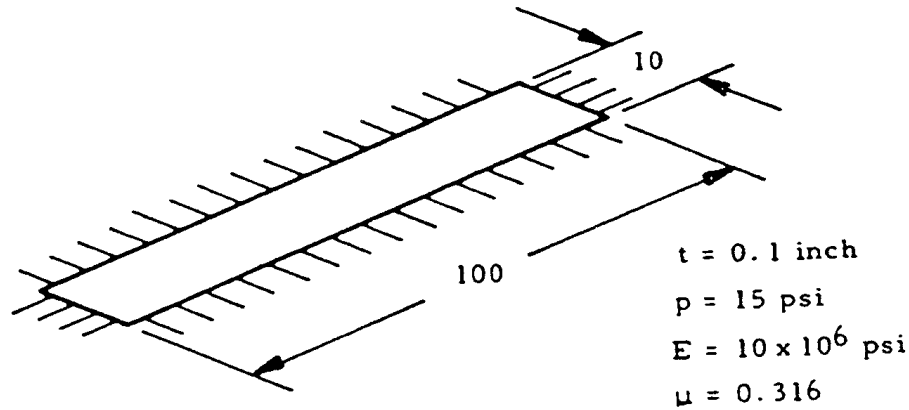
Figure 7-7. Long Rectangular Membrane

Find: The maximum stress and center deflection

Solution:

$$\frac{p}{E} \left(\frac{b}{t} \right)^4 = \frac{15}{10 \times 10^6} \left(\frac{10}{0.1} \right)^4 = 150$$

Since this quantity is greater than 100, the given plate may indeed be considered to be a membrane.

From Equation (7-5),

$$f_{max} = \left[\frac{p^2 E b^2}{24 (1-\mu^2) t^2} \right]^{1/3} = \left[\frac{15^2 (10^7)(10^2)}{24 (1-0.316^2)(0.1^2)} \right]^{1/3}$$

$$= 10130$$

From Equation (7-6),

$$\frac{\delta}{b} = \frac{1}{8} \left[\frac{24(1-\mu^2) pb}{Et} \right]^{1/3} = \frac{1}{8} \left[\frac{24(1-0.316^2)(15)(10)}{10^7 (0.1)} \right]^{1/3}$$

$$= 0.0185$$

Thus,

$$\delta = 0.0185\, b = 0.0185\, (10) = 0.185 \text{ in.}$$

For quick calculations, the graphs in Figures 7-5 and 7-6 could have been used. However, this procedure would give answers that are not theoretically exact since these graphs are based on a Poisson's ratio of 0.3 rather than 0.316.

7.5.3   Short Rectangular Membranes

7.5.3.1   Theoretical Results for Short Rectangular Membranes

Figure 7-8 shows a short rectangular membrane (a/b < 5) clamped on four sides under a uniform pressure p.
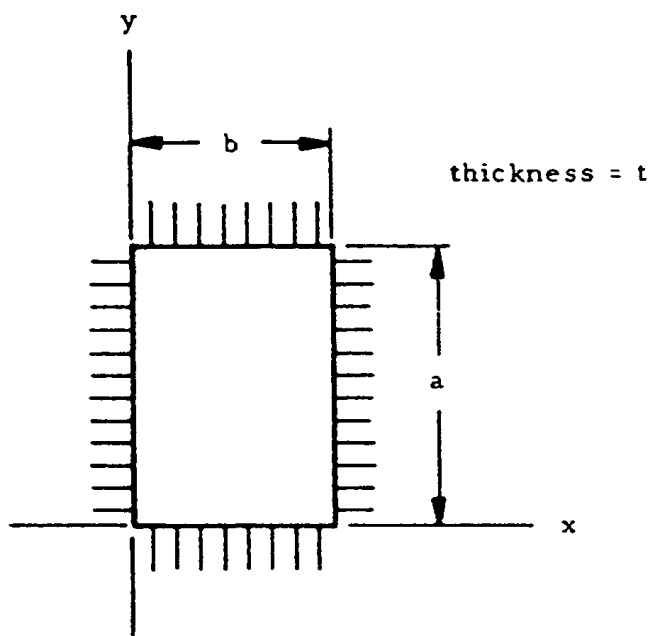
Figure 7-8.   Short Rectangular Membrane Clamped on Four sides

The deflection at the center of such a membrane is

$$\delta = n_1 a \sqrt[3]{\frac{p\,a}{E t}} \tag{7-7}$$

where n_1 is given in Figure 7-9.

The stresses at various locations on short rectangular membranes are given by the following equations for which the values of the coefficients n_2 through n_7 are given in Figure 7-9.

7 - 8
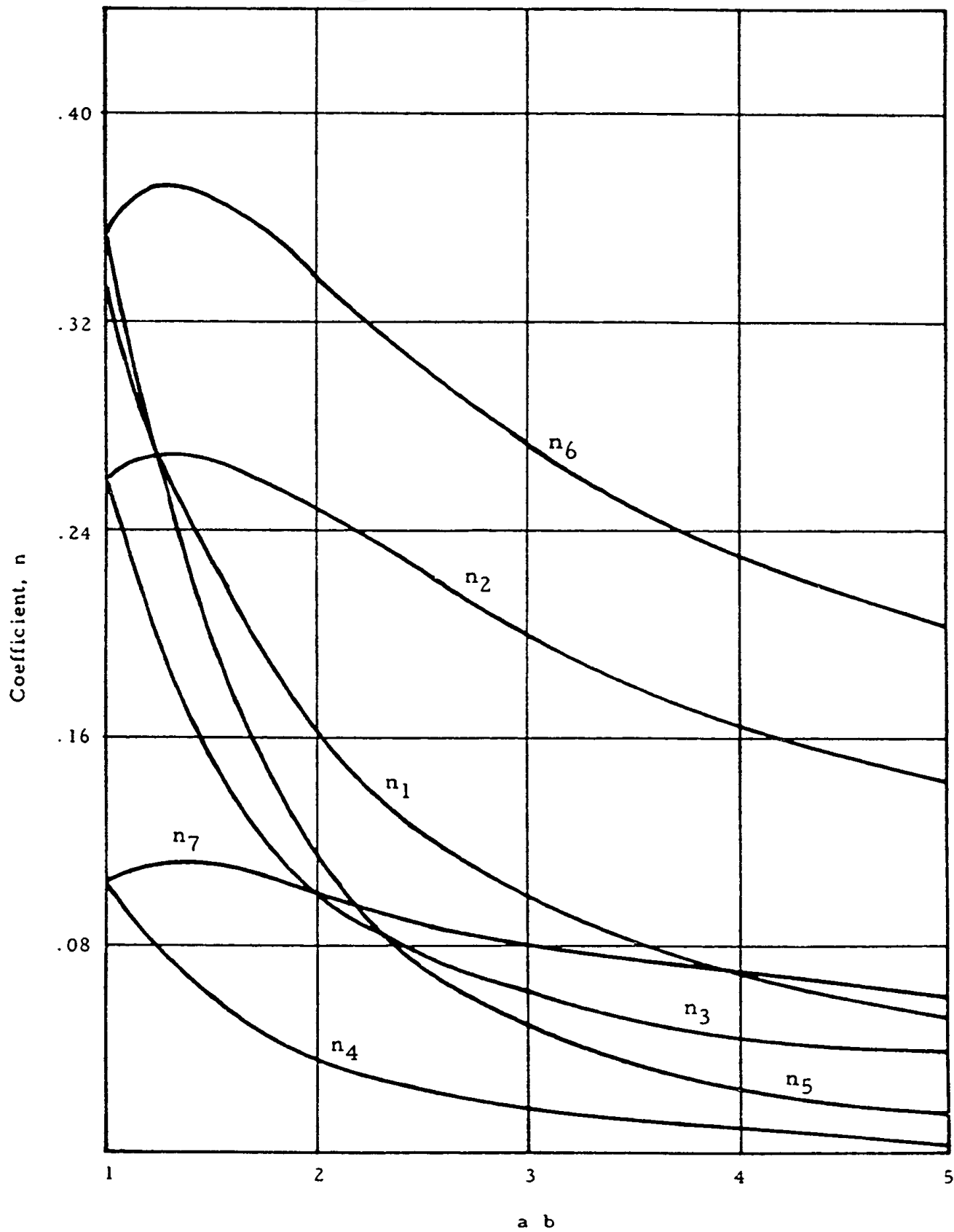
Figure 7-9. Coefficients for Equations (7-7) Through (7-13)

Center of plate (x = b/2, y = a/2)

$$f_x = n_2 \sqrt[3]{p^2 E \left(\frac{a}{t}\right)^2} \qquad (7-8)$$

$$f_y = n_3 \sqrt[3]{p^2 E \left(\frac{a}{t}\right)^2} \qquad (7-9)$$

Center of short side (x = b/2, y = 0)

$$f_x = n_4 \sqrt[3]{p^2 E \left(\frac{a}{t}\right)^2} \qquad (7-10)$$

$$f_y = n_5 \sqrt[3]{p^2 E \left(\frac{a}{t}\right)^2} \qquad (7-11)$$

Center of long side (x = 0, y = a/2)

$$f_x = n_6 \sqrt[3]{p^2 E \left(\frac{a}{t}\right)^2} \qquad (7-12)$$

$$f_y = n_7 \sqrt[3]{p^2 E \left(\frac{a}{t}\right)^2} \qquad (7-13)$$

It should be noted that the maximum membranes stress occurs at the center of the long side of the plate.

7.5.3.2   Applicability of Theoretical Results for Short Rectangular Membranes

Figures 7-10 and 7-11 give the deflections of plates with various length-to-width ratios obtained from the equations in Section 7.5.3.1 and compare these deflections with experimental values for 10-inch-wide aluminum plates.

For square plates (a/b = 1.0), the thick plate theory should be used for values of $(p/E)(b/t)^4$ from 0 to 100. If $100 < (p/E)(b/t)^4 < 250$, no theoretical method compares closely with test although the membrane theory should be used for conservative results. If $(p/E)(b/t)^4$ is greater than 250, the membrane theory produces results that compare closely with experiments for square plates.
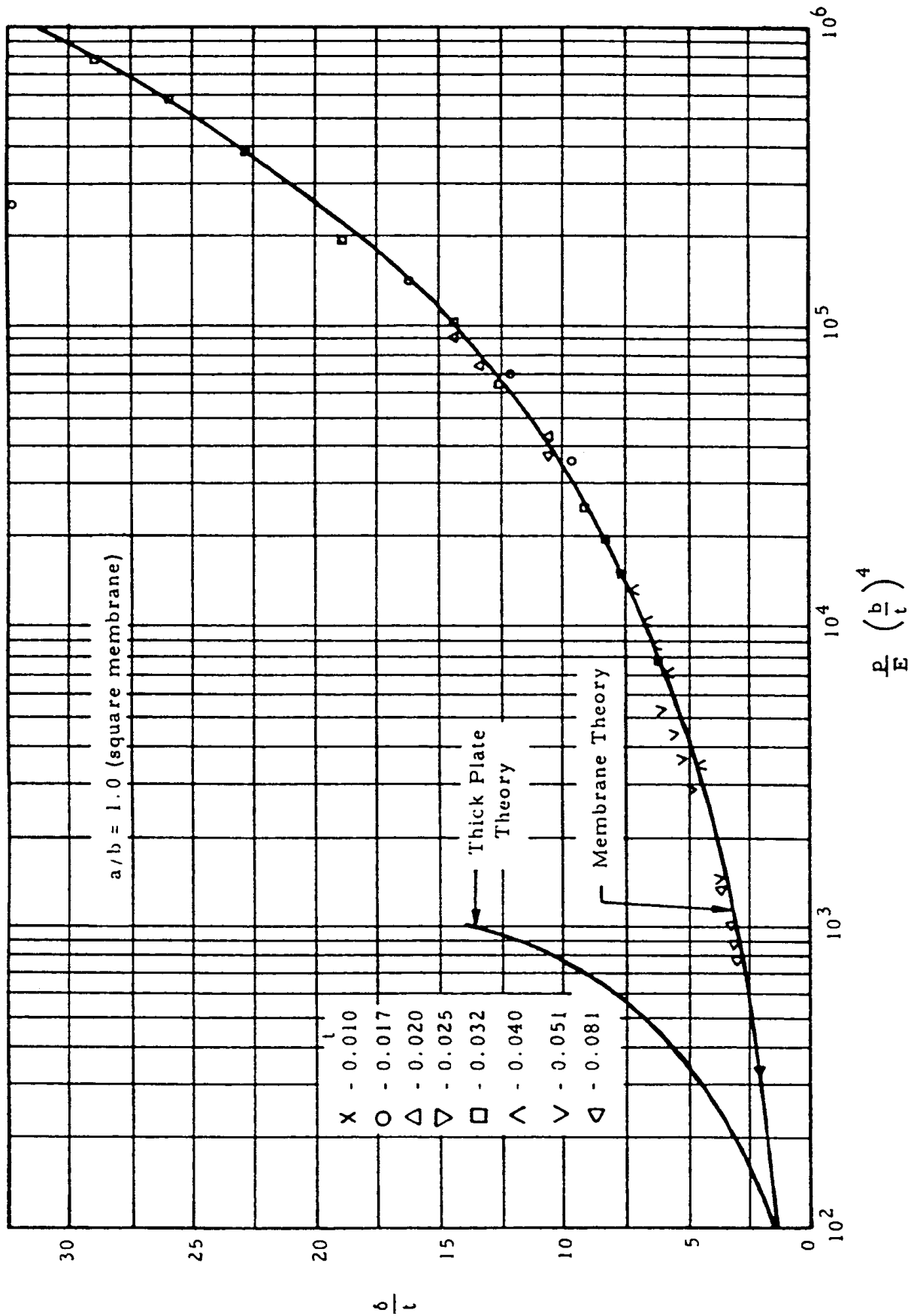
Figure 7-10.   Comparison of Theoretical and Experimental Results for Short Rectangular Membranes

7-10. Comparison of Theoretical and Experimental Results for Short Rectangular Membranes (Cont'd)

7-11. Comparison of Theoretical and Experimental Results for Short Rectangular Membranes
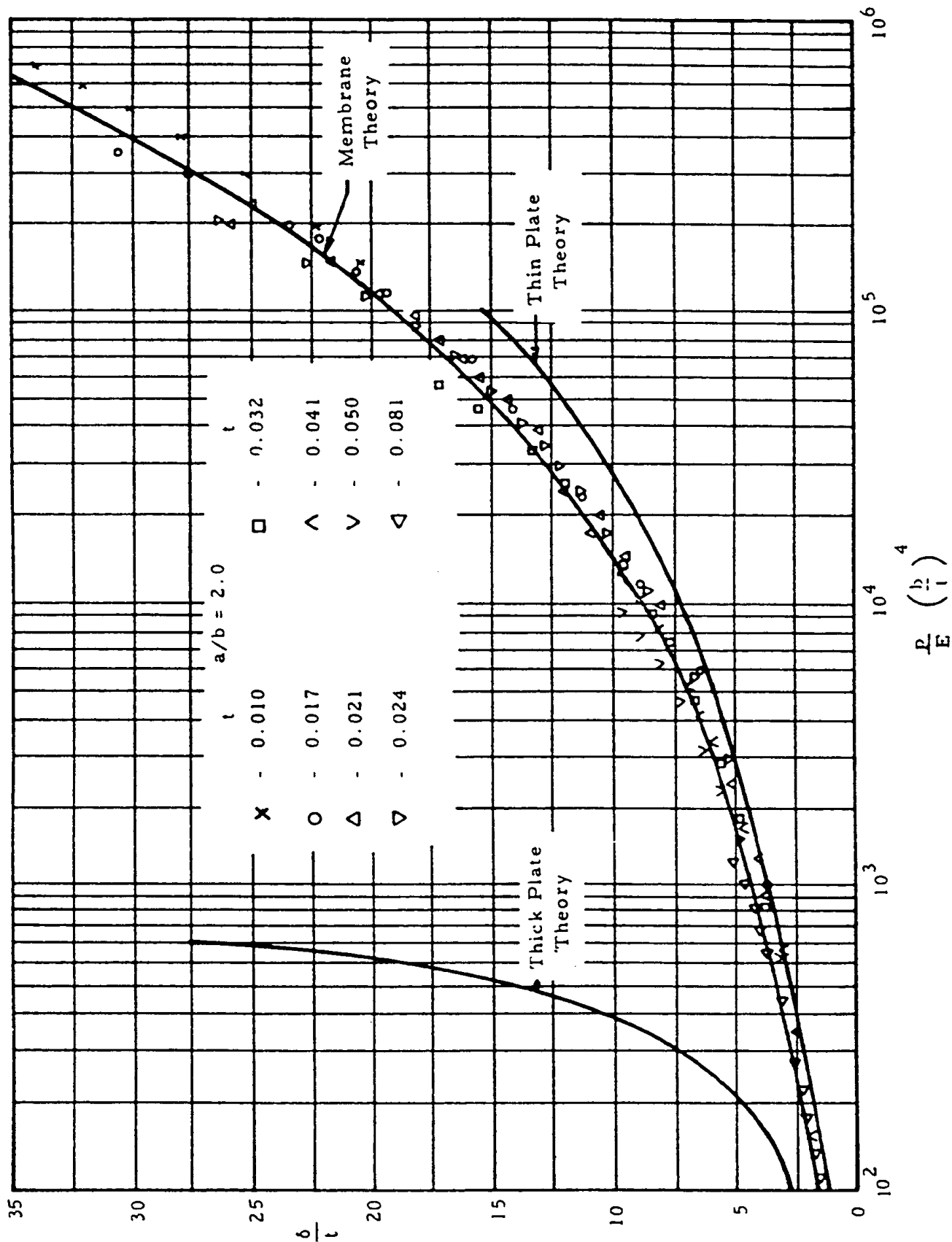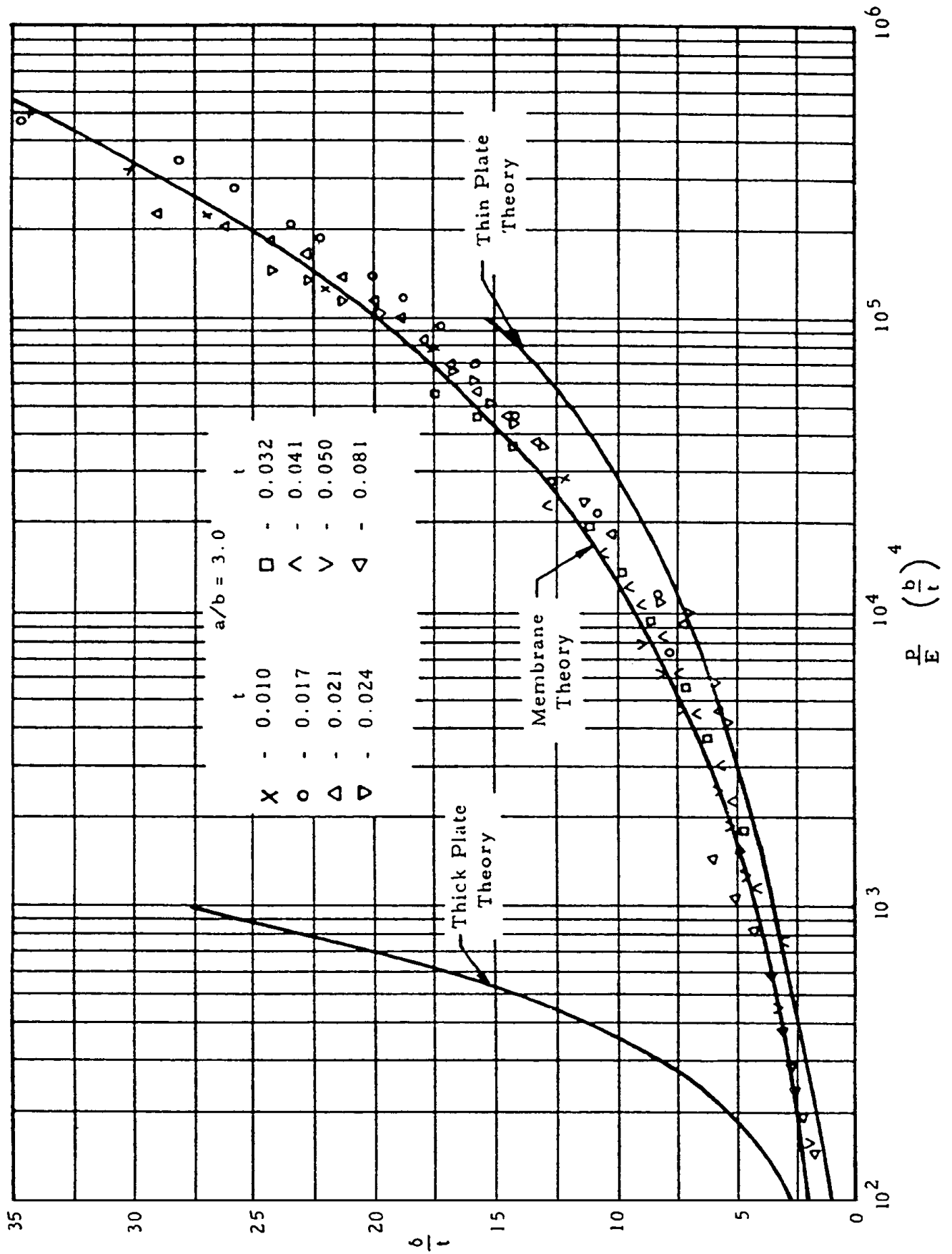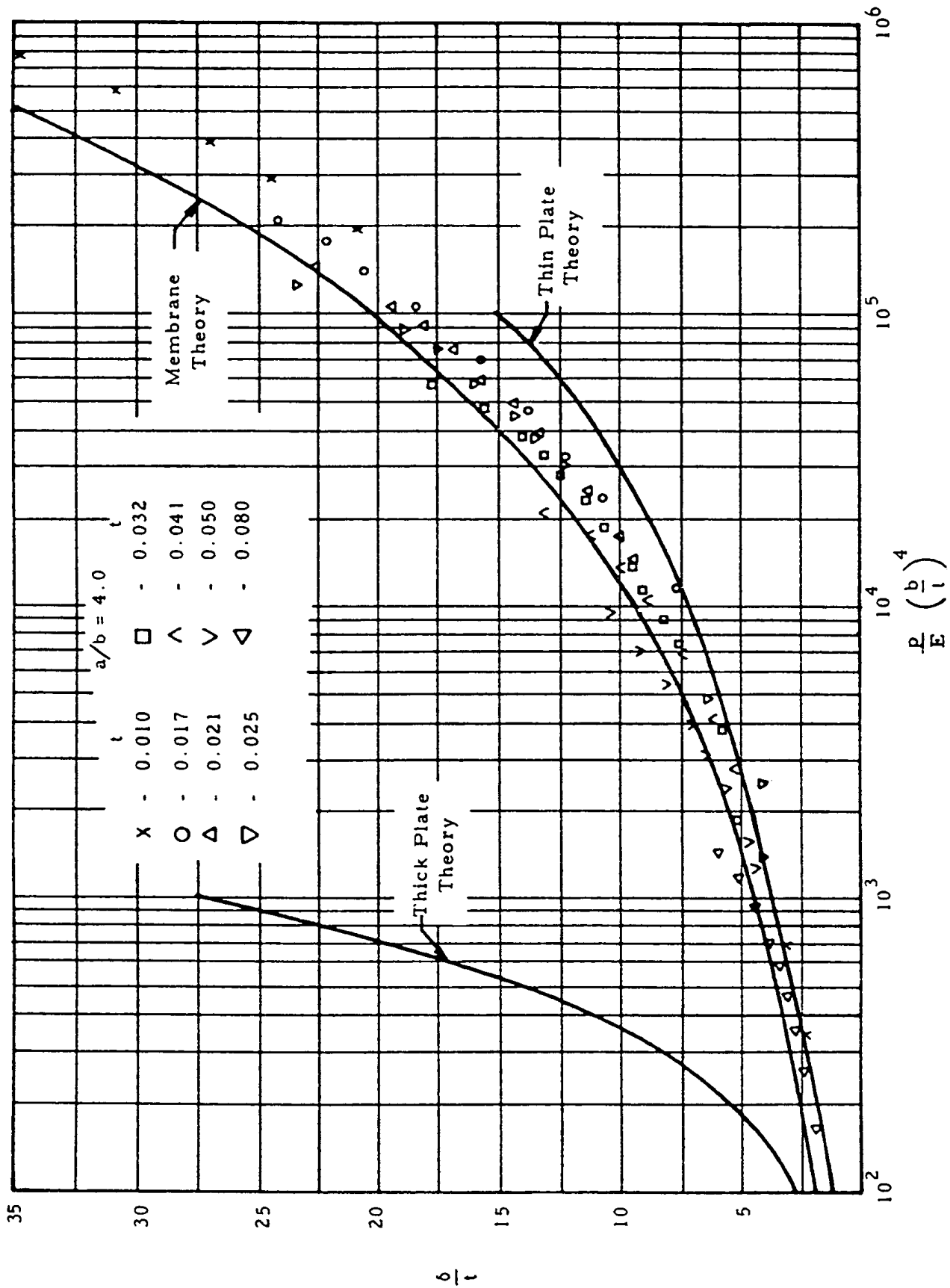
Figure 7-11. Comparison of Theoretical and Experimental Results for Short Rectangular Membranes (Cont'd)

A rectangular plate (a/b > 1.0) may be considered as a membrane if $(p/E)(b/t)^4 > 100$, with results becoming more conservative as a/b decreases.

7.5.3.3   Sample Problem - Short Rectangular Membranes

Given: The membrane shown in Figure 7-12

$p = 15$ psi

$t = 0.1$ in.

$E = 10 \times 10^6$ psi
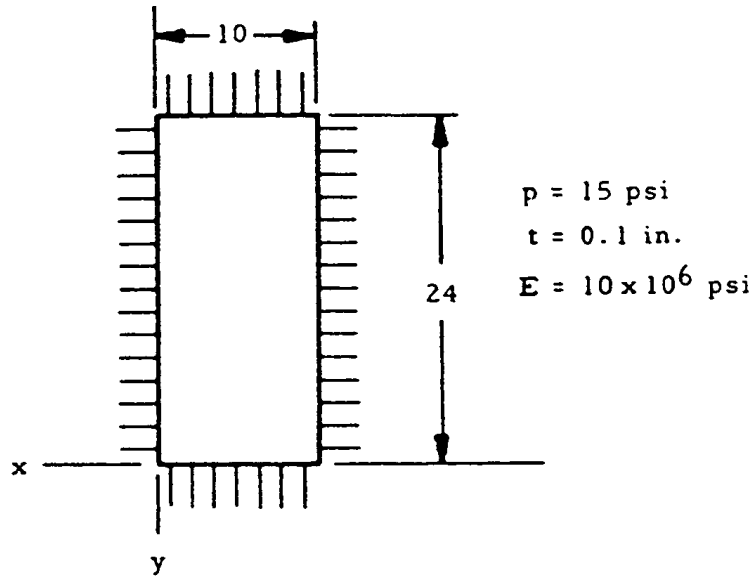
Figure 7-12.   Short Rectangular Membranes

Find: The center deflection and stresses

Solution:

$$\left(\frac{p}{E}\right)\left(\frac{b}{t}\right)^4 = \frac{15}{10^7}\left(\frac{10}{0.1}\right)^4 = 150$$

Since this value is greater than 100, the given plate may be treated by membrane equations, according to Section 7.5.3.2.

$$\frac{a}{b} = \frac{24}{10} = 2.4$$

From Figure 7-9:

$n_1 = 0.130$ $n_5 = 0.077$

$n_2 = 0.230$ $n_6 = 0.311$

$n_3 = 0.080$ $n_7 = 0.090$

$n_4 = 0.026$

From Equation (7-7), the deflection of the center of the membrane is

$$\delta = n_1 a \sqrt[3]{\frac{p a}{E t}} = 0.130(24) \sqrt[3]{\frac{15(24)}{10^7(0.1)}} = 0.222 \text{ in.}$$

From Equation (7-8) through (7-13), the stresses in the membrane are as follows:

Center of plate (x = 5, y = 12)

$$f_x = n_2 \sqrt[3]{p^2 E \left(\frac{a}{t}\right)^2} = 0.230 \sqrt[3]{(15)^2(10^7)\left(\frac{24}{0.1}\right)^2} = 11,650 \text{ psi}$$

$$f_y = n_3 \sqrt[3]{p^2 E \left(\frac{a}{t}\right)^2} = 0.080 \sqrt[3]{(15)^2(10^7)\left(\frac{24}{0.1}\right)^2} = 4,050 \text{ psi}$$

Center of short side (x = 5, y = 0)

$$f_x = n_4 \sqrt[3]{p^2 E \left(\frac{a}{t}\right)^2} = 0.026 \sqrt[3]{(15)^2(10^7)\left(\frac{24}{0.1}\right)^2} = 1,315 \text{ psi}$$

$$f_y = n_5 \sqrt[3]{p^2 E \left(\frac{a}{t}\right)^2} = 0.077 \sqrt[3]{(15)^2(10^7)\left(\frac{24}{0.1}\right)^2} = 3,900 \text{ psi}$$

Center of long side (x = 0, y = 12)

$$f_x = n_6 \sqrt[3]{p^2 E \left(\frac{a}{t}\right)^2} = 0.311 \sqrt[3]{(15)^2(10^7)\left(\frac{24}{0.1}\right)^2} = 15,750 \text{ psi}$$

$$f_y = n_7 \sqrt[3]{p^2 E \left(\frac{a}{t}\right)^2} = 0.090 \sqrt[3]{(15)^2(10^7)\left(\frac{24}{0.1}\right)^2} = 4,550 \text{ psi}$$

The greatest stress is 15,750 psi at the center of the long side.

8.   PRESSURE VESSELS

8.1   Introduction to Pressure Vessels

For purposes of analysis, pressure vessels may be divided into two
classes, thick and thin.   Thin pressure vessels are those for which the ratio
of the least radius of curvature of the wall to its thickness is greater than ten.
These thin pressure vessels are further subdivided into simple ones which
are discussed in Section 8.3.1 and stiffened ones which are discussed in Sec-
tion 8.3.2.   Thick pressure vessels are discussed in Section 8.4.   Section 8.5
gives a brief discussion of anisotropic pressure vessels and in particular
glass filament vessels.

8.2   Nomenclature for Pressure Vessels

A	=	cross-sectional area
A	=	$\alpha a/2$ for stiffened cylinder
A_r	=	$\dfrac{r^2}{\dfrac{b}{b'}\left(\dfrac{e}{t_r}\right)^3 (1+\mu^2) + \dfrac{r^2}{A_r'}}$
A_r'	=	minimum cross-sectional area of ring
A_{st}	=	cross section of stringer
a	=	one-half the major diameter of semi-elliptical head
a	=	distance between rings
a	=	inside radius of thick sphere or cylinder
B	=	$\beta a/2$ for stiffened cylinder
b	=	one-half the minor diameter of semi-elliptical head
b	=	stringer spacing
b	=	outside radius of thick sphere or cylinder
b	=	subscript, bending
b'	=	distance between adjacent edge of stringers
C_n	=	constant
c	=	subscript, compressive
c_s	=	distance from neutral axis of skin-stringer combination to outer fiber of skin
c_{st}	=	distance from neutral axis of skin-stringer combination to outer fiber of stringer
co	=	subscript, crippling
cr	=	subscript, critical
D	=	$EI_{,st}$ for stiffened cylinder
d	=	mean diameter
d	=	A_{st}/bt for stiffened cylinder
d_i	=	inside diameter
d_o	=	outside diameter

E	=	modulus of elasticity
E_{ring}	=	modulus of elasticity of ring
E_s	=	secant modulus of elasticity
E_t	=	tangent modulus of elasticity
e	=	eccentricity of ring attachment to skin
F_{bmer}	=	meridional bending stress
F_{bs}	=	bending stress in skin
F_{bst}	=	bending stress in stringer
F_{bt}	=	circumferential bending stress
F_{cc}	=	crippling stress of unpressurized cylinder
F_{ccP}	=	crippling stress of pressurized cylinder
F_{cp}	=	proportional limit in compression
F_{cr}	=	critical stress
F_{cy}	=	compressive yield stress
F_{max}	=	maximum stress
F_{mer}	=	meridional or axial stress
F_{mermax}	=	maximum meridional stress
F_{msor}	=	meridional membrane stress
F_{mt}	=	circumferential membrane stress
F_r	=	radial stress
F_{rmax}	=	maximum radial stress
F_{scc}	=	crippling shear stress of unpressurized cylinder
F_{sccp}	=	crippling shear stress of pressurized cylinder
F_{smax}	=	maximum shear stress
F_{smer}	=	meridional shear stress
F_{stmer}	=	meridional stress in stringer
F_t	=	tangential or circumferential stress
F_{tmax}	=	maximum circumferential stress
f_s	=	calculated shear stress
I	=	moment of inertia

$$I_{mer} = \text{stress ratio} = \frac{F_{mermax}}{pd/2t}$$

$$I_p = \text{polar moment of inertia}$$

$$I_s = \text{stress ratio} = \frac{F_{smax}}{pd/2t}$$

$$I_{sst} = \text{moment of inertia of sheet-stringer combination per inch of circumference}$$

$$I_t = \text{stress ratio} = \frac{F_{tmax}}{pd/2t}$$

$$i = \text{subscript, inside}$$

$$K = \frac{\sqrt{t'E/D}}{2r} \quad \text{for stiffened cylinder}$$

k_p	=	buckling coefficient for sphere
k_y	=	buckling coefficient for cylinder
L	=	cylinder length
M	=	bending moment
M_{cr}	=	critical bending moment
M_o	=	discontinuity moment
M_{sst}	=	bending moment of skin-stringer combination per inch of circumference
M_{ssts}	=	bending moment of skin-stringer combination per inch of circumference at midspan between rings
M_{sstr}	=	bending moment of skin-stringer combination per inch of circumference at ring
$_m$	=	subscript, membrane
$_s$	=	subscript, midspan
$_{mer}$	=	subscript, meridional
N_{mmer}	=	meridional membrane stress times wall thickness ($F_{mmer}t$)
N_{mt}	=	tangential membrane stress times wall thickness ($F_{mt}t$)
n	=	$\dfrac{\text{distance from midplane of flat head to joint}}{\text{head thickness}}$
$_o$	=	subscript, outside
P	=	axial load
P	=	reaction force
P	=	$\dfrac{pr^2}{t'E}\left[1 - \dfrac{\mu t'}{2(t+t_s)}\right]$ for stiffened cylinders
P	=	pressure difference ($p_i - p_o$)
$_p$	=	subscript, polar
$_p$	=	subscript, pressurized
P_i	=	internal pressure
P_o	=	external pressure
Q	=	$\dfrac{A_r E_{ring} a^3}{32\,Dr^2}$ for stiffened cylinder
Q_o	=	discontinuity force
R	=	radius curvature
R	=	radius to centroid of minimum area of ring
R_b	=	applied bending moment/critical bending moment
R_c	=	applied compressive load/critical compressive load
R_{mer}	=	meridional radius of curvature
R_s	=	$\dfrac{\text{applied transverse shear load}}{\text{critical transverse shear load}}$
R_{st}	=	$\dfrac{\text{applied torsional moment}}{\text{critical torsional moment}}$

R_t = tangential or circumferential radius of curvature

r = mean radius

r = radius to the inside of the skin of stiffened cylinder

r = cylindrical or polar coordinate

r = subscript, radial

r = subscript, ring

r_i = inside radius of dished head

r_k = knuckle radius in dished head

s = subscript, shear

s = subscript, skin

st = subscript, stringer

T = head thickness

T = torque

T = $pr/2$ for stiffened cylinder

t = wall thickness

t = subscript, tangential or circumferential

t' = $\dfrac{t + ts}{1 + (1-\mu^2)ts/t}$ for stiffened cylinder

t_r = thickness of flange attachment to skin

t_s = A_{st}/b for stiffened cylinder

w_1 = radial deflection of head due to Q_0 and M_0

w_2 = radial deflection of cylinder due to Q_0 and M_0

w_{s_1} = radial deflection of head due to internal pressure

w_{s_2} = radial deflection of cylinder due to internal pressure

y = subscript, yield

x, y, z = rectangular coordinates

α = half the apex angle of a cone

α = $\sqrt{K + \dfrac{T}{4D}}$ for stiffened cylinder

β = angle of contact of saddle support

β = $\sqrt{\left| K - \dfrac{T}{4D} \right|}$ for stiffened cylinder

Δ = increment or difference

Δ_n = parameter in Figures 8-45 through 8-49

δ = radial deflection of shell

δ_s = radial deflection of shell midway between rings

δ_r = radial deflection of shell at ring

η = plasticity reduction factor

θ_1 = angular rotation of head due to Q_0 and M_0

θ_2 = angular rotation of cylinder due to Q_0 and M_0

λ_1 = $\sqrt[4]{3(1-\mu^2)/r^2T^2}$

8 - 4

$$\lambda_2 \quad = \quad \sqrt[4]{3(1-\mu^2)/r^2 t^2}$$

$\mu \quad = \quad$ Poisson's ratio

$\mu_{\bullet} \quad = \quad$ elastic Poisson's ratio $\left[\mu_p \left(\dfrac{E_{\bullet}}{E} - 1 \right) + \mu \right] \dfrac{E}{E_{\bullet}}$

$\mu_p \quad = \quad$ plastic Poisson's ratio (generally 0.5)

$\Omega_n \quad = \quad$ parameter in Figures 8-41 through 8-44

$\varphi_0 \quad = \quad$ angle between cylinder axis and normal to head at head-cylinder junction

8.3   Thin Pressure Vessels

This section deals with pressure vessels for which the ratio of minimum radius of curvature of the wall to its thickness is greater than ten. These thin pressure vessels are further subdivided for purposes of discussion into simple and stiffened pressure vessels. A simple pressure vessel is defined here as one that does not have stiffeners while a stiffened one may have rings and/or stringers stiffening its walls.

8.3.1   Simple Thin Pressure Vessels

This class of pressure vessel includes unstiffened vessels for which the ratio of the minimum radius of curvature of the wall to its thickness is greater than ten.

Membrane stresses in simple thin pressure vessels are considered first here and then the problem of discontinuity stresses at the junction of a cylinder and its head is considered. The material in these first sections is based on the assumption that failure by buckling under external pressures does not occur. The possibility of buckling is treated in Section 8.3.1.3. The previously mentioned sections cover stresses due to pressure loads alone. Section 8.3.1.4 deals with stresses due to external loads from support, and Section 8.3.1.5 treats of the effect of internal pressure upon the crippling stress of thin cylinders under various loads.

8.3.1.1   Membrane Stresses in Simple Thin Shells of Revolution

In a thin pressure vessel, no stresses other than those tangential to the surface are present at points sufficiently removed from discontinuities in the curvature, slope, or thickness of the wall. These tangential or membrane stresses are constant throughout the thickness of the shell. At points near discontinuities, such as the junction of a cylinder and its head discontinuity, stresses must be superposed upon the membrane stresses in order to obtain the total stress. These discontinuity stresses are discussed in Section 8.3.1.2.2.

In the following discussion, the difference between internal and external pressure $(p_i - p_o)$ is assumed to be uniform over the surface.

Figure 8-1 shows a general thin shell of revolution. The meridian lines of this shell are defined by the intersection of the shell and a plane passing through the axis of rotation of the surface. The circles of rotation are the intersection of the shell with planes perpendicular to the axis of rotation.
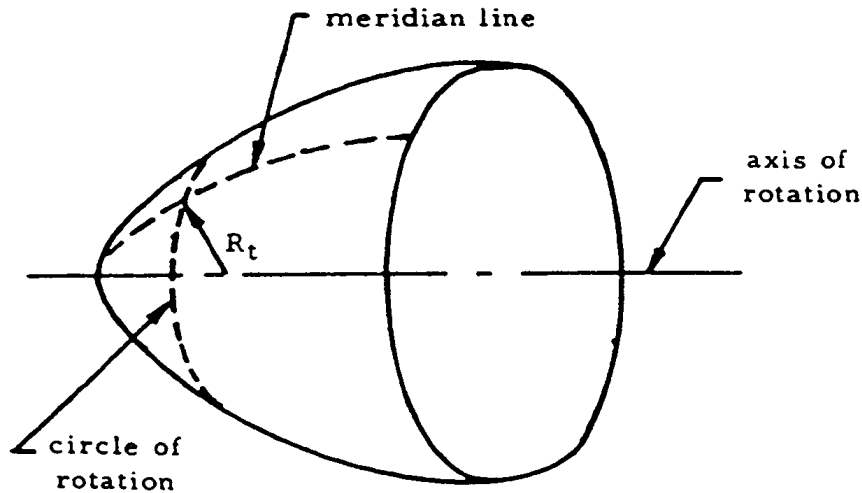
Figure 8-1. General Shell of Revolution

The two basic equations for a thin shell of revolution are

$$\frac{N_{mer}}{R_{mer}} + \frac{N_{mt}}{R_t} = (p_i - p_o) \qquad (8-1)$$

and

$$N_{mer} = (p_i - p_o) \frac{R_t}{2} \qquad (8-2)$$

In these equations, R_{mer} is the radius of curvature of a meridian line and R is the distance from the shell to its axis of rotation along a normal to the shell. Both of these radii are taken to a surface located midway between the inside and outside surfaces of the shell. N_{mer} is the stress in the direction of the meridian line times the shell thickness and N_{mt} is the stress in the direction of a circle of rotation times the shell thickness.

8.3.1.1.1   Membrane Stresses in Thin Cylinders

Figure 8-2 shows a thin cylindrical shell (R/t > 10).

$$R_{mer} = \infty$$

$$R_t = r$$
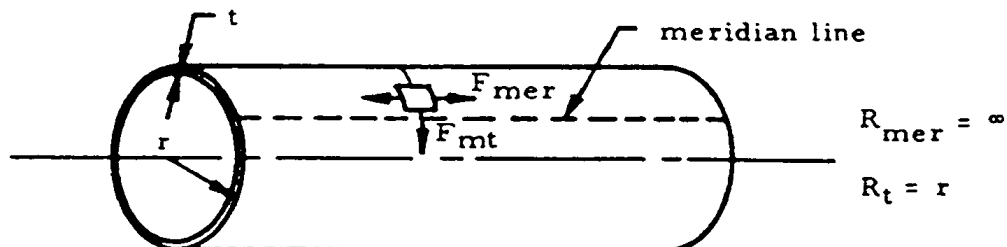
Figure 8-2. Thin Cylindrical Shell

Since the meridian lines are straight, R_t, which is their radius of curvature, is equal to infinity. Similarly, R_{mer} may be found to be equal to r by applying its definition. Inserting these values into Equations (8-1) and (8-2) and solving gives

$$N_{st} = (p_i - p_o) r \qquad (8-3)$$

and

$$N_{mmer} = (p_i - p_o) \, r/2 \qquad (8-4)$$

Since $N_{st} = F_{st} t$ and $N_{mmer} = F_{mmer} t$,

$$F_{st} = \frac{N_{st}}{t} = \frac{p_i - p_o)r}{t} \qquad (8-5)$$

and

$$F_{mmer} = \frac{N_{mm}}{t} = \frac{(p_i - p_o)r}{2t} \qquad (8-6)$$

From these equations, it can be seen that the ratio of the longitudinal to the circumferential stress, F_{mmer}/F_{st}, is equal to 0.5. Thus, the strength of a girth joint may be as low as one-half that of a longitudinal joint as is illustrated in Figure 8-3.
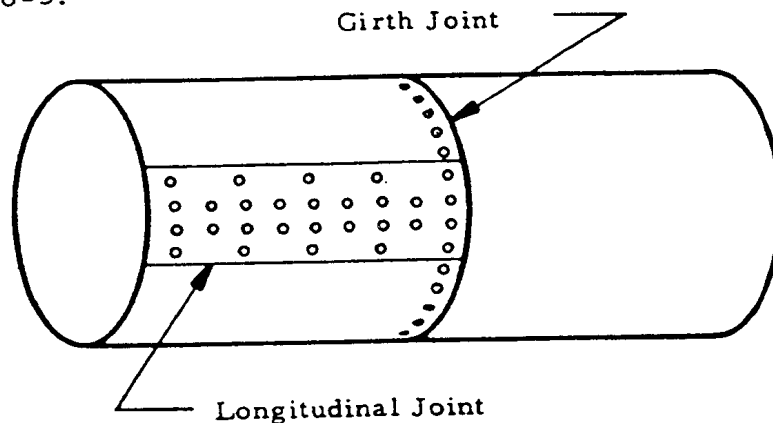
Figure 8-3. Joints on a Cylindrical Pressure Vessel

8.3.1.1.2   Membrane Stresses in Thin Spheres

Figure 8-4 shows a thin spherical shell ($r/t > 10$). Applying Equations (8-1) and (8-2) to the shape in Figure 8-4 gives

$$N_{st} = N_{mmer} = \frac{(p_i - p_o)r}{2} \qquad (8-7)$$

Thus,

$$F_{st} = F_{mmer} = \frac{(p_i - p_o)r}{2t} \qquad (8-8)$$

$$R_{mer} = R_t = r$$
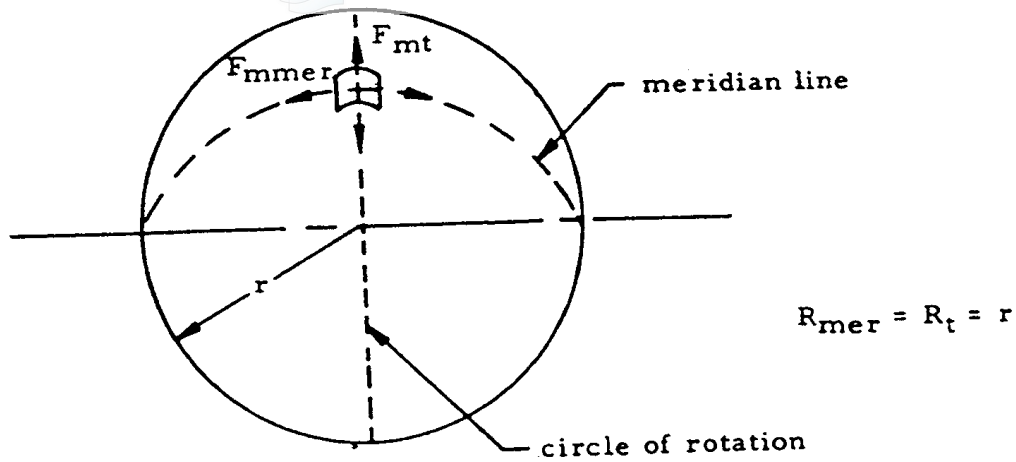
Figure 8-4.   Thin Spherical Shell

8.3.1.1.3   Sample Problem - Membrane Stresses in Thin Cylinders and Spheres

Given: The cylindrical pressure vessel shown in Figure 8-5.
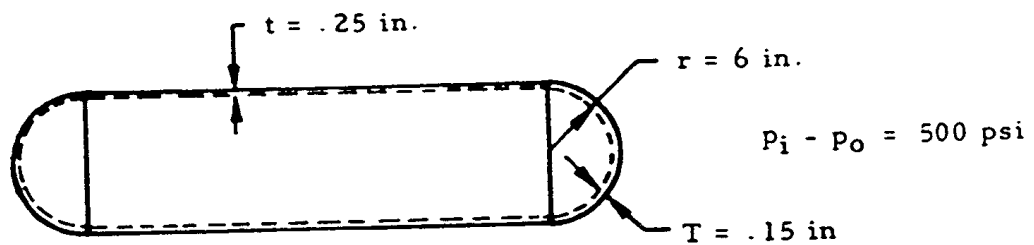
Figure 8-5.   Thin Cylindrical Pressure Vessel with Hemispherical Heads

Find: The membrane stresses in the cylinder and the heads.

Solution: Applying Equations (8-5) and (8-6) to the cylindrical portion gives

$$F_{st} = \frac{500\,(6)}{.25} = 12,000 \text{ psi}$$

and

$$F_{smer} = \frac{500\,(6)}{2\,(.25)} = 6,000 \text{ psi}$$

Applying Equation (8-8) to the hemispherical heads gives

$$F_{st} = F_{smer} = \frac{500\,(6)}{2\,(.25)} = 10,000 \text{ psi}$$

8 - 8

It should be noted that the discontinuity stresses at the head-cylinder junction may be much greater than these membrane stresses.

8.3.1.2   Heads of Thin Cylindrical Pressure Vessels

In the previous discussion, membrane stresses in thin pressure vessels, the slope, curvature, and direction of the meridian lines as well as wall thickness were assumed to be continuous. However, one or more of these assumptions do not hold true at the connection between a cylindrical pressure vessel and any of the types of heads used in practice.

The tendency of the head of a cylindrical pressure vessel to deform radially and angularly at a different rate than the cylindrical portion, combined with the requirement of geometric compatibility, necessitates certain discontinuity stresses near the head joint. Thus, unconservative designs will be obtained if the membrane stresses are the only ones considered. These discontinuity stresses are discussed more fully in Section 8.3.1.2.2.

By proper design of a pressure vessel, the discontinuity stresses may be greatly reduced so that localized yielding will level out any stress peaks and these stresses need not be considered for static strength analysis. In the A.S.M.E. code for unfired pressure vessels, formulas for the thickness of shells and heads (except in the case of flat heads) consider membrane stresses only. But the proper design to prevent excessive discontinuity stresses is specified. For example, proper design of a dished head requires that the inequalities shown in Figure 8-6 be satisfied.

$$r_i < d_o$$

$$r_k > .06\, d_i$$

Note:

Knuckle must be so curved along the meridian to avoid sudden changes of slope
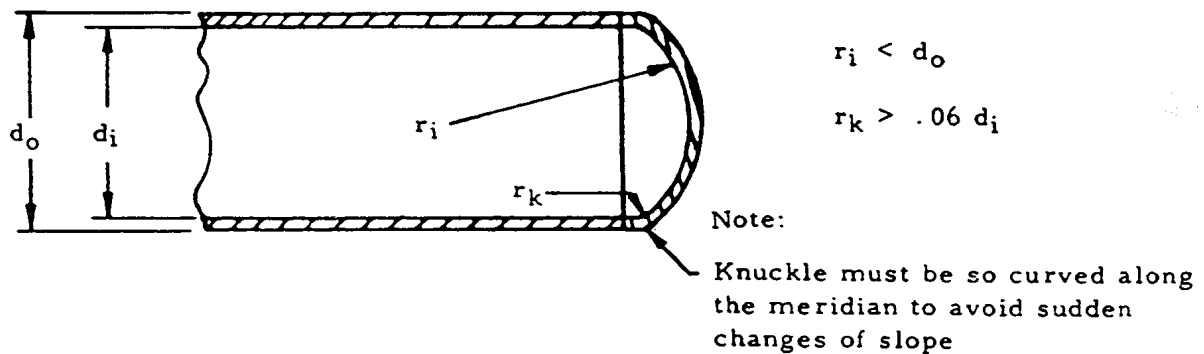
Figure 8-6.   Proper Design of Dished Head

Formulas for membrane stresses in several types of thin heads are given in Section 8.3.1.2.1.
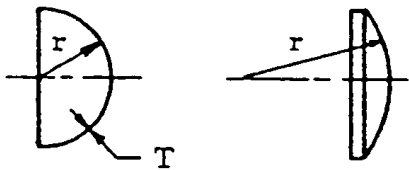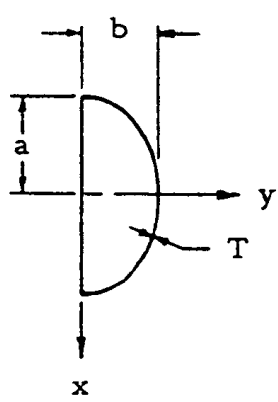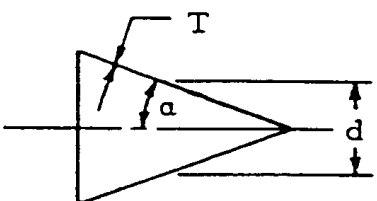
If a pressure vessel is subjected to repeated loadings where fatigue is considered likely, stress peaks due to discontinuity stresses are of great importance since localized yielding is no longer beneficial.

8 - 9

8.3.1.2.1   Membrane Stresses in Heads of Thin Cylindrical Pressure
Vessels

Formulas may be found for membrane stresses in several common types of heads by the use of Equations(8-1) and (8-2). These are listed in Table 8-1.

TABLE 8-1

Equations for Membrane Stresses in Thin Heads

Type of Head		Membrane Stresses
hemispherical or dished		$F_{mmer} = F_{mt} = \dfrac{(p_i - p_o)r}{2T}$
semielliptical		$F_{mmer} = \dfrac{(p_i - p_o)(a^4 y^2 + b^4 x^2)^{1/2}}{2Tb^2}$ $F_{mt} = \left[\dfrac{(p_i - p_o)(a^4 y^2 + b^4 x^2)^{1/2}}{b^2 T}\right] \times \left[1 - \dfrac{a^4 b^2}{2(a^4 y^2 + b^4 x^2)}\right]$ at cylinder-head joint, $y = 0$ and $x = a$. Thus, $F_{mmer} = \dfrac{(p_i - p_o)a}{2T}$ $F_{mt} = \dfrac{pa}{T}\left(1 - \dfrac{a^2}{2b^2}\right)$
conical		$F_{mmer} = \dfrac{(p_i - p_o)d}{4T\cos\alpha}$ $F_{mt} = \dfrac{(p_i - p_o)d}{2T\cos\alpha}$

It can be seen from the equation for F_{mt} at $x = a$ for an elliptical head that this hoop stress is compressive if a is greater than $\sqrt{2}b$. Thus, the displacement of the edge would actually be inward in this case. This is an undesirable situation because of a possibility of high discontinuity stresses.

Wherever discontinuity stresses cannot be ignored, they may be superposed upon the membrane stresses. Discontinuity stresses are discussed in the following section.

8.3.1.2.2   Discontinuity Stresses at the Junction of a Thin Cylindrical Pressure Vessel and Its Head

8.3.1.2.2.1   Introduction to Discontinuity Stresses

If there is an abrupt change in the thickness or in the meridional slope or curvature at any circumference of a thin vessel, bending stresses occur in addition to the membrane stresses. These "discontinuity stresses" are of four types: *

(1)   a meridional bending stress, $F_{b_{mer}}$, which varies linearly throughout the thickness of the wall,

(2)   a circumferential or hoop bending stress, F_{bt}, which varies linearly throughout the thickness of the wall,

(3)   an additional hoop stress, F_t, uniform throughout the thickness of the wall, and

(4)   a meridional shear stress, $F_{s_{mer}}$, assumed uniform throughout the thickness of the wall.

In order to determine the state of stress of a pressure vessel, it is necessary to find membrane stresses and discontinuity stresses. The total stresses may be obtained from the superposition of these two states of stress.

8.3.1.2.2.2   Discontinuity Stresses at Junction of Thin Cylindrical Pressure Vessel and Head

If a cylindrical pressure vessel is subjected to pressure, the cylindrical part and its head will tend to expand at different rates as shown in Figure 8-7. The head alone would displace radially a distance w_{m1} because of internal pressure, and the cylindrical portion would displace w_{m2} if it were not attached to the head. However, geometric compatibility requires the head and cylinder to displace equal amounts. Thus, the force Q_0 and the moment M_0 must exist between the head and the cylinder to hold them together. These, in turn, cause discontinuity stresses near the junction between the cylinder and its head.

The following procedure may be used to solve for discontinuity stresses. First, the difference in radial displacements due to Q_0 and M_0 must cancel the difference in radial displacements due to internal pressure. That is,

* Griffel, William, Handbook of Formulas for Stress and Strain

8 - 11

$$w_1 - w_2 = w_{\bullet 2} - w_{\bullet 1} \tag{8-9}$$
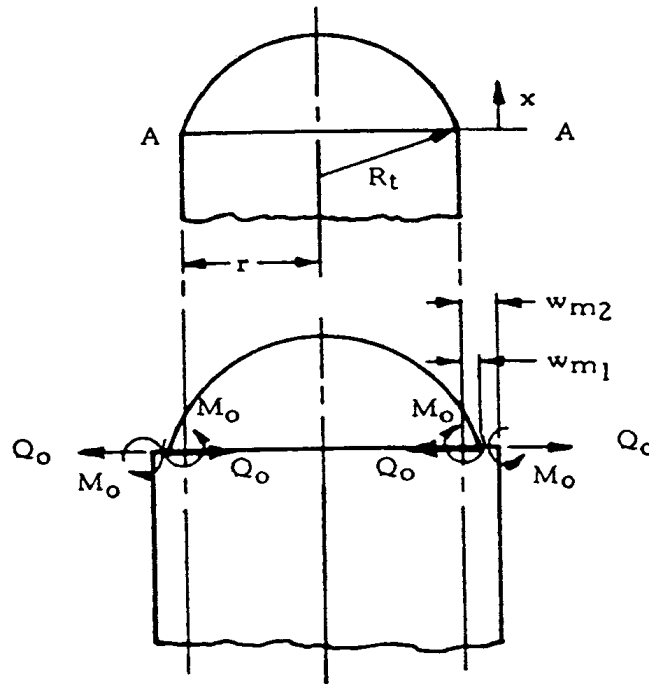
Figure 8-7. Illustration of the Necessity of Discontinuity
Stresses *

The values of $w_{\bullet 1}$ and $w_{\bullet 2}$ as functions of pressure may be obtained in Table 8-2
for various head shapes, and values for w_1 and w_2 as functions of Q_o and M_o may
be obtained from Table 8-3. The angles of rotation of the cylinder and head
edges due to Q_o and M_o must be equal. That is,

$$\theta_1 = \theta_2 \tag{8-10}$$

Values of these angles are given as functions of Q_o and M_o in Table 8-3.
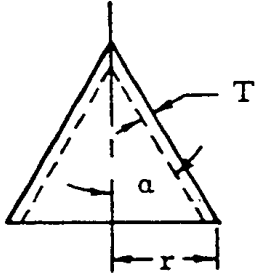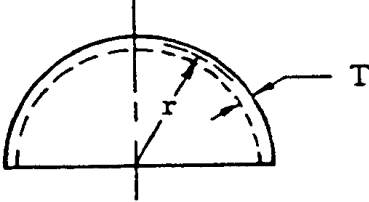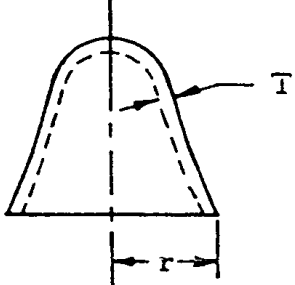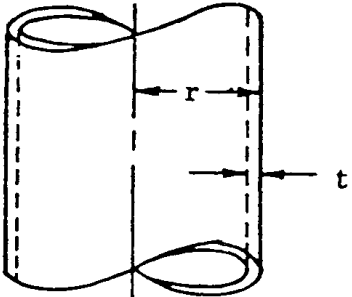
By substituting the values of displacements and angles obtained
from Tables 8-2 and 8-3 into Equations (8-9) and (8-10) and solving these Q_o.
and M_o may be obtained as functions of pressure and the geometry and material
of the pressure vessel. The discontinuity stresses are given as functions of Q_o,
M_o, and position in Figure 8-4. The curves given in Figure 8-8 are useful in
the evaluation of the stresses given by the equations in Table 8-4.

The previously described method of obtaining discontinuity
stresses is time-consuming, although it provides insight into the nature of
these stresses. More rapid solutions for the discontinuity stresses in thin
cylindrical pressure vessels with flat or conical heads may be obtained
through the curves given in Sections 8.3.1.2.2.3 and 8.3.1.2.2.4.

* Griffel, William, Handbook of Formulas for Stress and Strain

TABLE 8-2
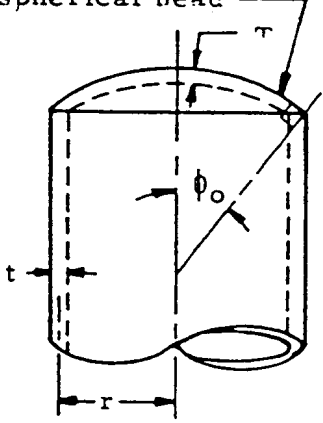
Displacement of Heads and Cylinders Due to Internal Pressure *

Form of Vessel	Radial Displacement, w_m
Conical Head	$w_{m_1} = \dfrac{pr^2}{ET \cos a}\left(1 - \dfrac{\mu}{2}\right)$
Hemispherical Head	$w_{m_1} = \dfrac{pr^2}{2\,ET}\,(1-\mu)$
Any Figure of Revolution	$w_{m_1} = \dfrac{pr^2}{2\,ET}\left(2-\mu-\dfrac{r}{R_{mer}}\right)$
Cylinder	$w_{m_2} = \dfrac{pr^2}{Et}\left(1 - \dfrac{\mu}{2}\right)$

* Griffel, William, <u>Handbook of Formulas for Stress and Strain</u>

TABLE 8-3

Radial and Angular Displacements Due to Edge Loading *

Form of Vessel	Radial Displacement	Angle of Rotation
semielliptical, conical, dished or hemispherical head — (diagram with T, ϕ_0, t, r)	$w_1 = \frac{12(1-\mu^2)}{ET^3}\left(-\frac{Q_o}{2\lambda_1^3}\sin^2\phi_o - \frac{M_o}{2\lambda_1^2}\sin\phi_o\right)$ $w_2 = \frac{12(1-\mu^2)}{Et^3}\left(\frac{Q_o}{2\lambda_2^3}\sin^2\phi_o - \frac{M_o}{2\lambda_2^2}\sin\phi_o\right)$	$\theta_1 = \frac{12(1-\mu^2)}{ET^3}\left(\frac{Q_o}{2\lambda_1^2}\sin\phi_o - \frac{M_o}{\lambda_1}\right)$ $\theta_2 = \frac{12(1-\mu^2)}{Et^3}\left(\frac{Q_o}{2\lambda_2^2}\sin\phi_o + \frac{M_o}{\lambda_2}\right)$
	Note: $\quad \lambda_1 = \sqrt[4]{3(1-\mu^2)/r^2T^2}$ $\lambda_2 = \sqrt[4]{3(1-\mu^2)/r^2t^2}$	
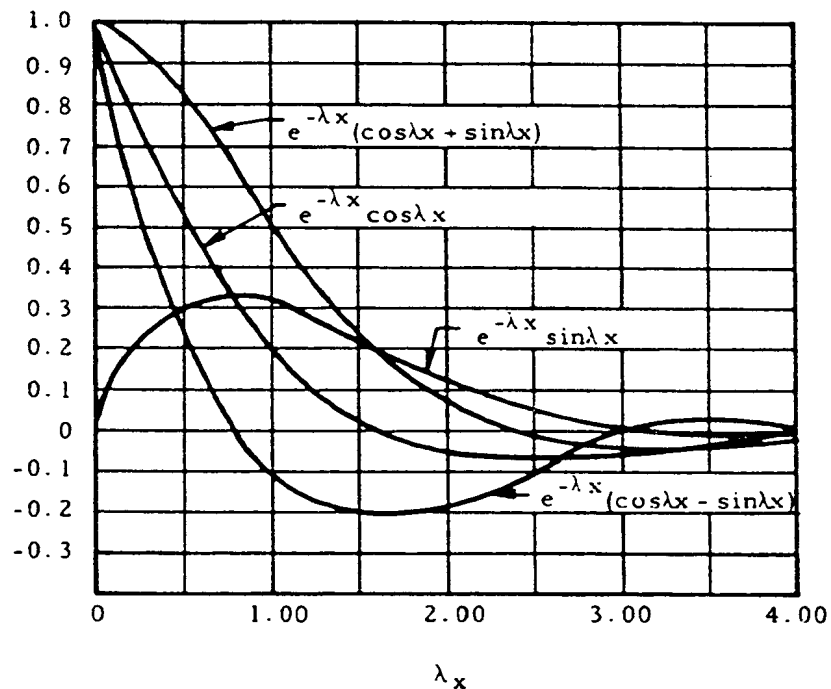
Figure 8-8. Curves for the Evaluation of the Equations in Table 8-4 *

* Griffel, William, <u>Handbook of Formulas for Stress and Strain</u>

TABLE 8-4

Equations for Discontinuity Stresses *

Expressions for Discontinuity Stresses of Distance x Measured
Along Meridian from Discontinuity Circle AA (see Figure 8-7)

---

(1)   Hoop Normal Stress:

$$F_t = \frac{2\lambda r}{t} \left(\frac{r}{R_t}\right) e^{-\lambda x} \left[Q_o \cos \lambda x - \lambda M_o (\cos \lambda x - \sin \lambda x)\right]$$

---

(2)   Meridional Shear Stress:

$$F_{saer} = \frac{r}{tR_t} \sqrt{\frac{r}{R_t}} \; e^{-\lambda x} \left[Q_o (\cos \lambda x - \sin \lambda x) + 2\lambda M_o \sin \lambda x\right]$$

---

(3)   Maximum Meridional Bending Stress:

$$F_{baer} = \frac{6r}{t^2 R_t} \left(\frac{1}{\lambda}\right) e^{-\lambda x} \left[-Q_o \sin \lambda x + \lambda M_o (\cos \lambda x + \sin \lambda x)\right]$$

---

(4)   Maximum Hoop Bending Stress:

$$F_{bt} = \mu F_{baer} + \frac{Et}{2} \left(\frac{\cot \varphi_o}{R_t}\right) \left[\frac{6(1-\mu^2)}{Et^3 \lambda^2}\right] e^{-\lambda x} \left[Q_o (\cos \lambda x + \sin \lambda x)\right.$$

$$\left. - 2\lambda M_o \cos \lambda x\right]$$

Note: For stress in cylinder, $\lambda = \lambda_2$. For stress in head, let $\lambda = \lambda_1$ and $t = T$

* Griffel, William, Handbook of Formulas for Stress and Strain.

8 - 15

8.3.1.2.2.2.1   Sample Problem - Discontinuity Forces in Cylindrical Pressure Vessel with Dished Head

Given: The pressure vessel shown in Figure 8-9.
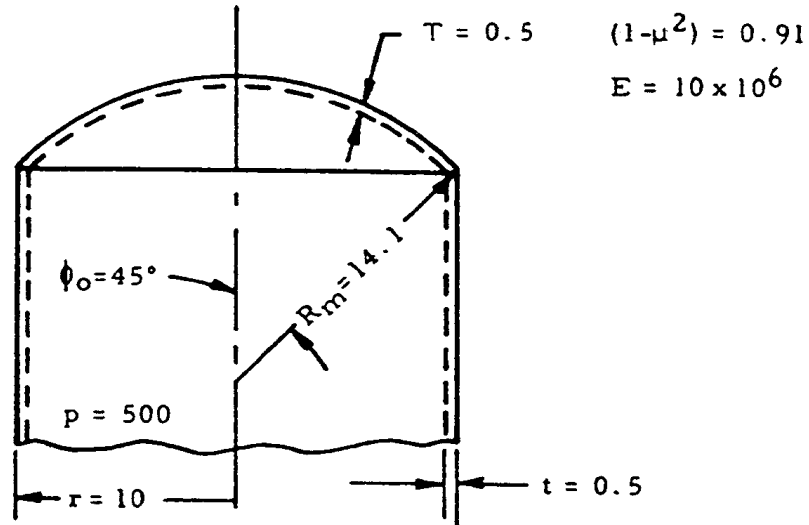
Figure 8-9. Cylindrical Pressure Vessel with Dished Head

Find: The discontinuity force and moment at the junction of the cylinder and its head.

Solution: From Tables 8-3 and 8-4,

$$w_{s_1} = \frac{pr^2}{2ET}\left(2 - \mu - \frac{r}{R_s}\right)$$

$$w_{s_2} = \frac{pr^2}{Et}\left(1 - \frac{\mu}{2}\right)$$

and

$$w_1 = \frac{12(1-\mu^2)}{ET^3}\left(\frac{-Q_o}{2\lambda_1^3}\sin^2\varphi_o \; \frac{-M_o}{2\lambda_1^2}\sin\varphi_o\right)$$

$$w_2 = \frac{12(1-\mu^2)}{Et^3}\left(\frac{Q_o}{2\lambda_2^3}\sin^2\varphi_o - \frac{M_o}{2\lambda_2^2}\sin\varphi_o\right)$$

From Table 8-3,

$$\lambda_1 = \sqrt[4]{3(1-\mu^2)/r^2T^2}$$

and

$$\lambda_2 = \sqrt[4]{3(1-\mu^2)/r^2T^2}$$

8-16

In this case,

$$\lambda_1 = \lambda_2 = \sqrt[4]{3(.91)/(10^2)(.5^2)} = .575$$

Substituting this and other parameters into the above equations gives

$$w_{s_1} = 4.97 \times 10^{-3}$$

$$w_{s_2} = 2.12 \times 10^{-3}$$

$$w_1 = -15.2 \times 10^{-6} Q_o - 9.36 \times 10^{-6} M_o$$

$$w_2 = 15.2 \times 10^{-6} Q_o - 9.36 \times 10^{-6} M_o$$

Substituting these into Equation (8-9) and solving for Q_o gives

$$Q_o = 93.6$$

Substituting the pressure vessel parameters into the equations for θ_1 and θ_2 in Table 8-3 gives

$$\theta_1 = 9.38 \times 10^{-6} Q_o - 15.2 \times 10^{-6} M_o$$

$$\theta_2 = 9.38 \times 10^{-6} Q_o + 15.2 \times 10^{-6} M_o$$

Applying Equation (8-10) gives

$$\theta_1 = \theta_2$$

Thus,

$$M_o = 0.$$

The values obtained for Q_o and M_o may be substituted into the equations in Table 8-4 to obtain the discontinuity stresses. Superposing these discontinuity stresses on the membrane stresses then gives the total stresses at the head-cylinder junction.

8.3.1.2.2.3 Discontinuity Stresses in Thin Cylindrical Pressure Vessels with Flat Heads

For flat-headed pressure vessels, the only significant discontinuity stresses are in the meridional direction. Thus, such a vessel will have as its maximum stress either the membrane stress in the tangential direction (pd/2t), or the stress in the axial direction if the discontinuity stress is great enough.

In treating axial discontinuity stresses, a stress ratio, I_{mer}, may be defined to be the ratio of the maximum stress in the meridional direction to the tangential membrane stress ($F_{mermax}/pd/2t$). The advantage of this stress ratio is that it tells immediately whether the tangential membrane stress or the total axial stress is the maximum stress.

The following equation was derived for the stress ratio I_{mer} in a flat headed cylinder as a function of head thickness T and cylinder thickness t: *

$$I_{mer} = \frac{1}{2} + \frac{C_1 (T/t)^3 - 2C_2 n(T/t) + C_3(d/t)^{3/2} + 2C_4 n(T/t)(d/t) + C_5 (d/t)(T/t)}{C_6 (T/t)^3 + 2C_7 n(T/t) + \dfrac{C_8}{(T/t)} + C_9(d/t)^{1/2} + \dfrac{4C_{10}n^2(T/t)^2}{(d/t)^{1/2}} + \dfrac{C_{11}(T/t)^2}{(d/t)^{1/2}}} \qquad (8-11)$$

Here, nT is the distance from the midplane of the head thickness to the joint as shown in Figure 8-10. The coefficients C_1 through C_{11} are given below:

$C_1 = 2.94317$ $C_6 = 1.90702$

$C_2 = 3.74071$ $C_7 = 4.84761$

$C_3 = 1.00000$ $C_8 = 1.02862$

$C_4 = 0.908912$ $C_9 = 2.66667$

$C_5 = 0.385077$ $C_{10} = 4.40610$

$C_{11} = 1.46869$
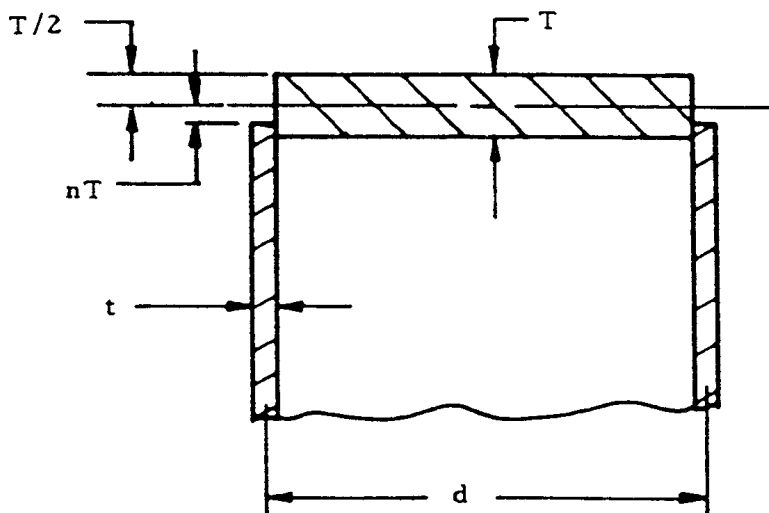
Figure 8-10. Junction of Cylinder and Flat Head

* Griffel, William, Handbook of Formulas for Stress and Strain

8-18

The first term in Equation (8-11) represents the axial membrane stress in the cylinder, and the second term accounts for discontinuity stresses.

Equation (8-11) is presented graphically in Figure 8-11 for n = 0.5 (junction at inner surface of head) and in Figure 8-12 for n = 0 (head fitted inside the shell).
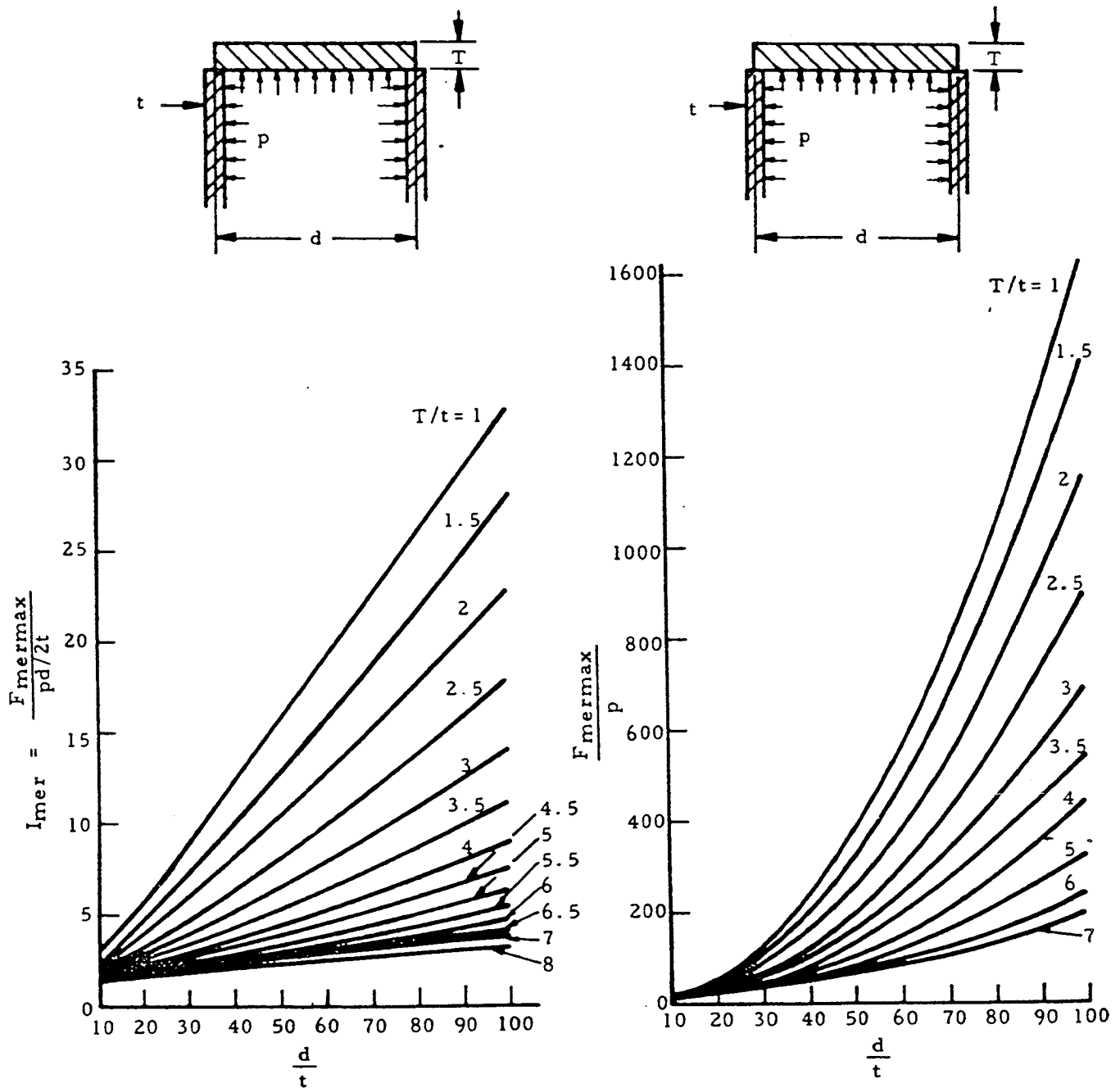
Figure 8-11. Graphical Presentation of Equation (8-11) for n = .5 *

* Griffel, William, Handbook of Formulas for Stress and Strain
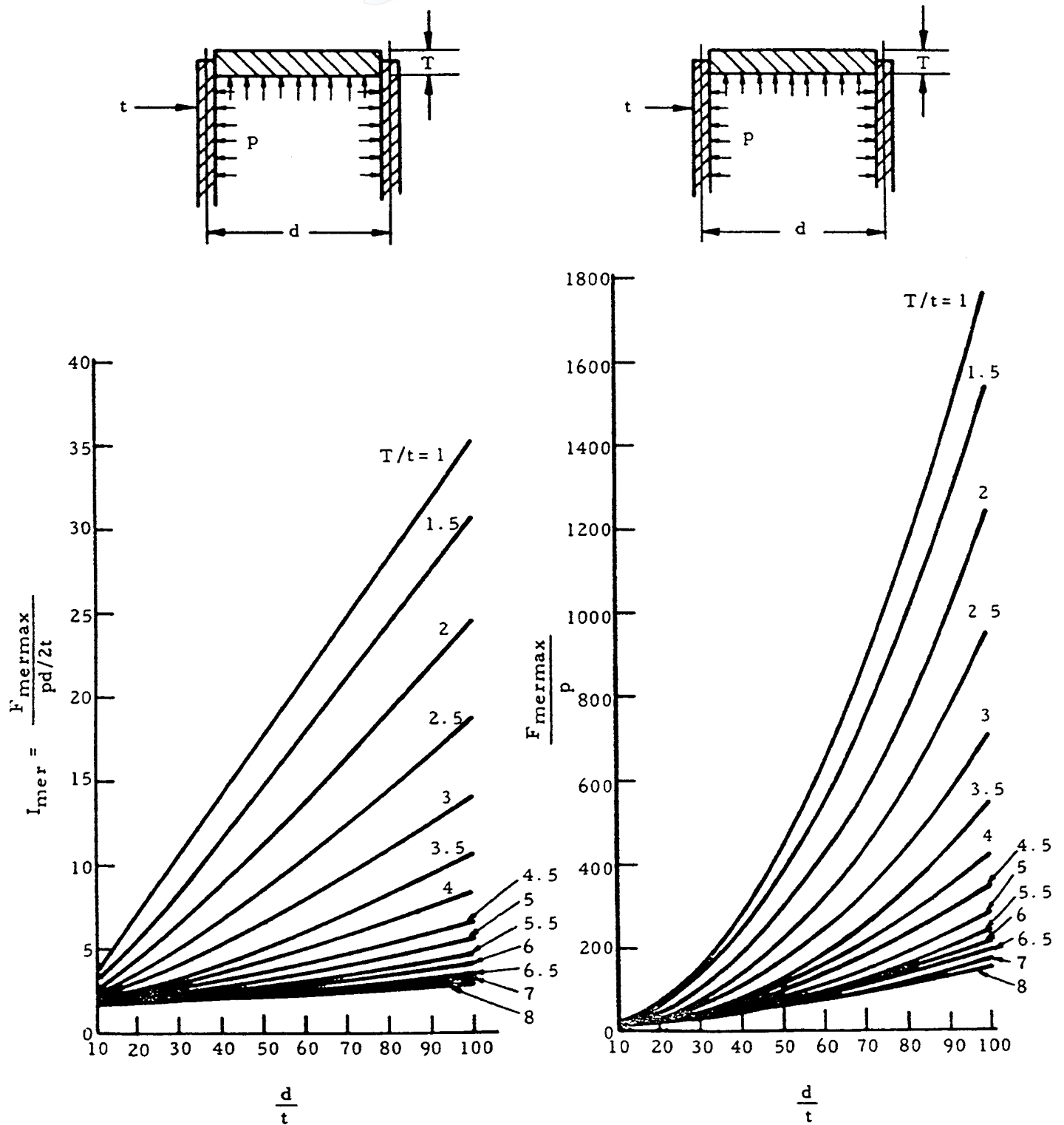
Figure 8-12. Graphical Presentation of Equation (8-11) for n = 0 *

* Griffel, William, Handbook of Formulas for Stress and Strain

8 - 20

8.3.1.2.2.3.1   Sample Problem - Discontinuity Stresses in
Pressure Vessels with Flat Heads

Given: The pressure vessel shown in Figure 8-13.
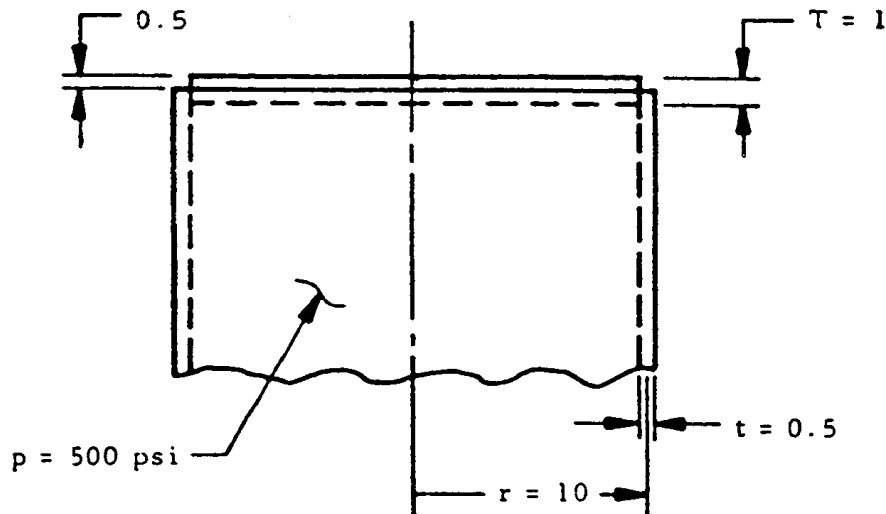
Figure 8-13.   Thin Cylindrical Pressure Vessel with
Flat Head

Find: The maximum circumferential and meridional
stresses in the cylinder.

Solution: Since the only significant discontinuity stresses
in a flat-headed cylinder are in the axial direction, the
maximum circumferential stress may be taken to be the
membrane stress in that direction. Thus, using Equation
(8-5) gives

$$F_{tmax} = F_{st} = \frac{pr}{t} = \frac{500 \ (10)}{0.5} = 10,000 \text{ psi}$$

The distance from the center of the head to the joint (nT)
is equal to zero. Thus, n = 0 and the graphs in Figure 8-12
may be used. Here, d/t = 40 and T/t = 2. From Figure
8-12,

$$I_{mer} = \frac{F_{sermax}}{pd/2t} = 8.6$$

Since this stress ratio is greater than one, $F_{sermax} > F_{st}$.
Rearranging and substituting the correct values into the
above relation gives

$$F_{sermax} = 8.6 \frac{pd}{2t} = 8.6 \frac{500 \ (20)}{2(.5)} = 86,000 \text{ psi}$$

8 - 21

8.3.1.2.2.4   Discontinuity Stresses in Thin Cylindrical Pressure Vessels with Conical Heads

For conical headed pressure vessels, there may exist appreciable discontinuity stresses in the circumferential and axial directions as well as an axial shear stress. Stress ratios are defined here in the same way as for flat-headed vessels. I_{aer} is the ratio of the maximum axial stress to the tangential stress ($F_{aoraax}/pd/2t$) as before, and $I_t = F_{taax}/pd/2t$ and $I_s = F_{saax}/pd/2t$ where F_{taax} and F_{saax} are the maximum circumferential and shear stresses, respectively.

Pertinent geometric parameters for a cylindrical pressure vessel with a conical head are shown in Figure 8-14.
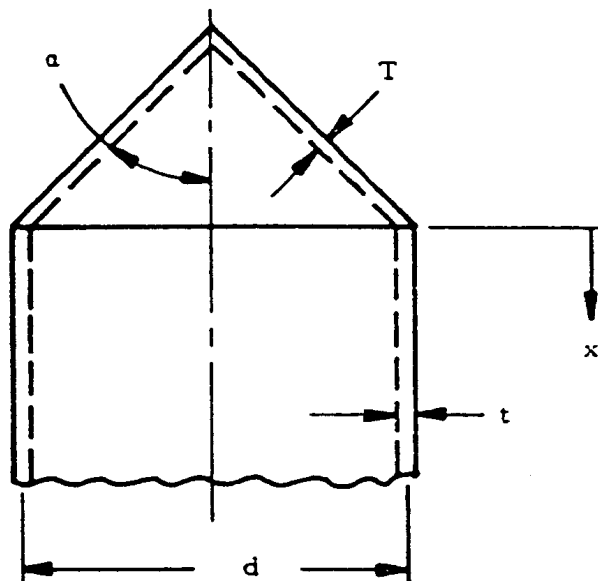
Figure 8-14.   Cylindrical Pressure Vessel with Conical Head

Figures 8-15 through 8-18 give the stress ratios, I_{aer} and I_s, for various cone apex angles. The maximum axial and shear stresses at the junction may in turn be calculated from these. Figures 8-19 through 8-22 show the stress ratio I_t from which the maximum circumferential stresses in a cylinder may be calculated. For the maximum axial stress, a solid line is used if the stress is located in the cylinder, and a dashed line is used in Figures 8-15 through 8-19 if it is located in the conical head.

It is important to note that when an internal pressure is applied to a conical headed vessel, the cylinder always deflects outward and the conical head inward. Thus, it is impossible to design a conical head to eliminate moment and shear at the junction. It may be seen from Figures 8-15 through 8-18 that the greatest stress is the axial stress at the junction and that it is desirable to make the cone and cylinder equally thick if α is less than 45 degree in order to minimize this axial stress. If this is not possible, the cone should have a greater thickness than the cylinder. Vertex angles of greater than 45 degrees require a thicker head.
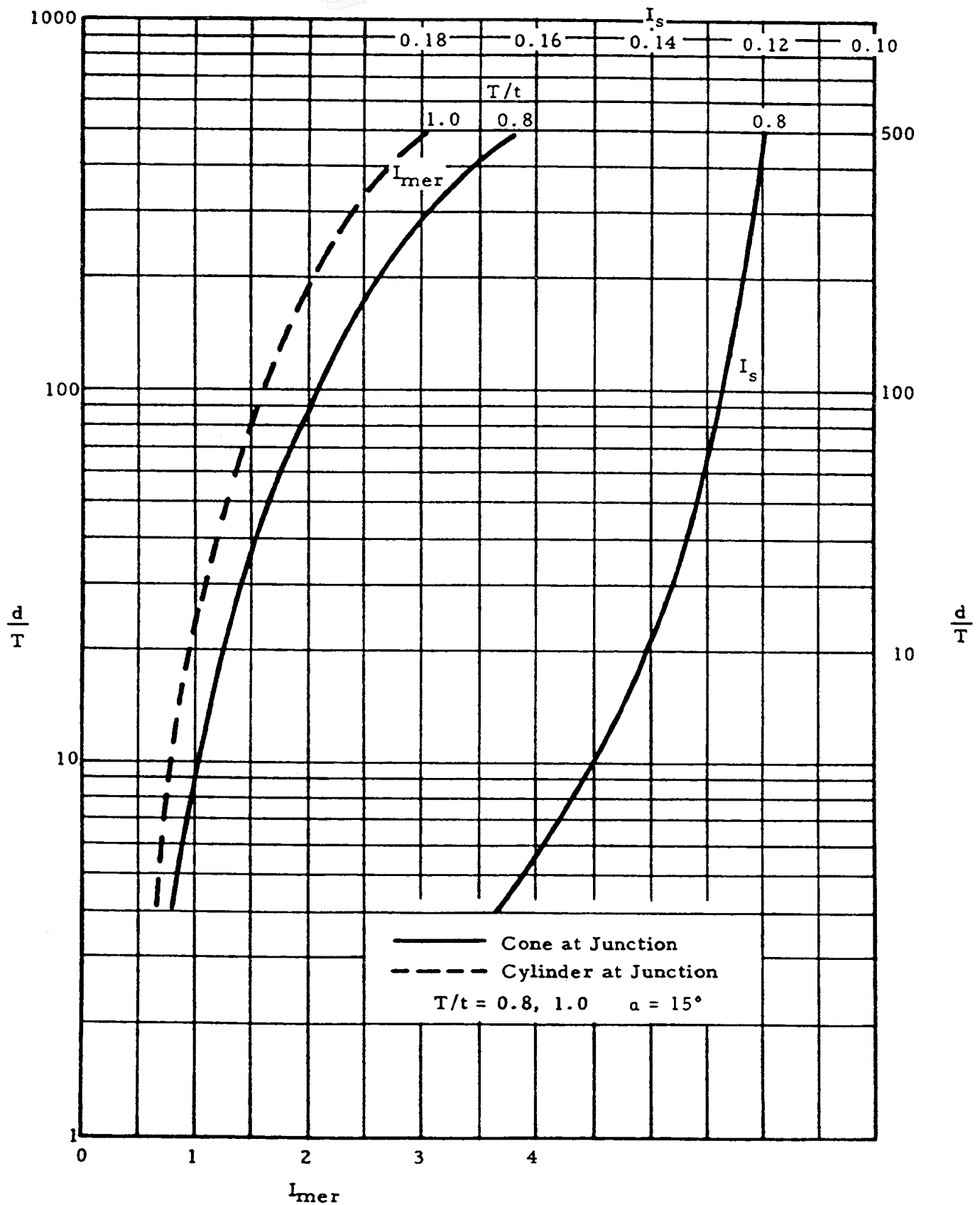
Figure 8-15. Stress Ratios for Pressure Vessels with Conical Head Closures *

* Griffel, William, Handbook of Formulas for Stress and Strain

8 – 23
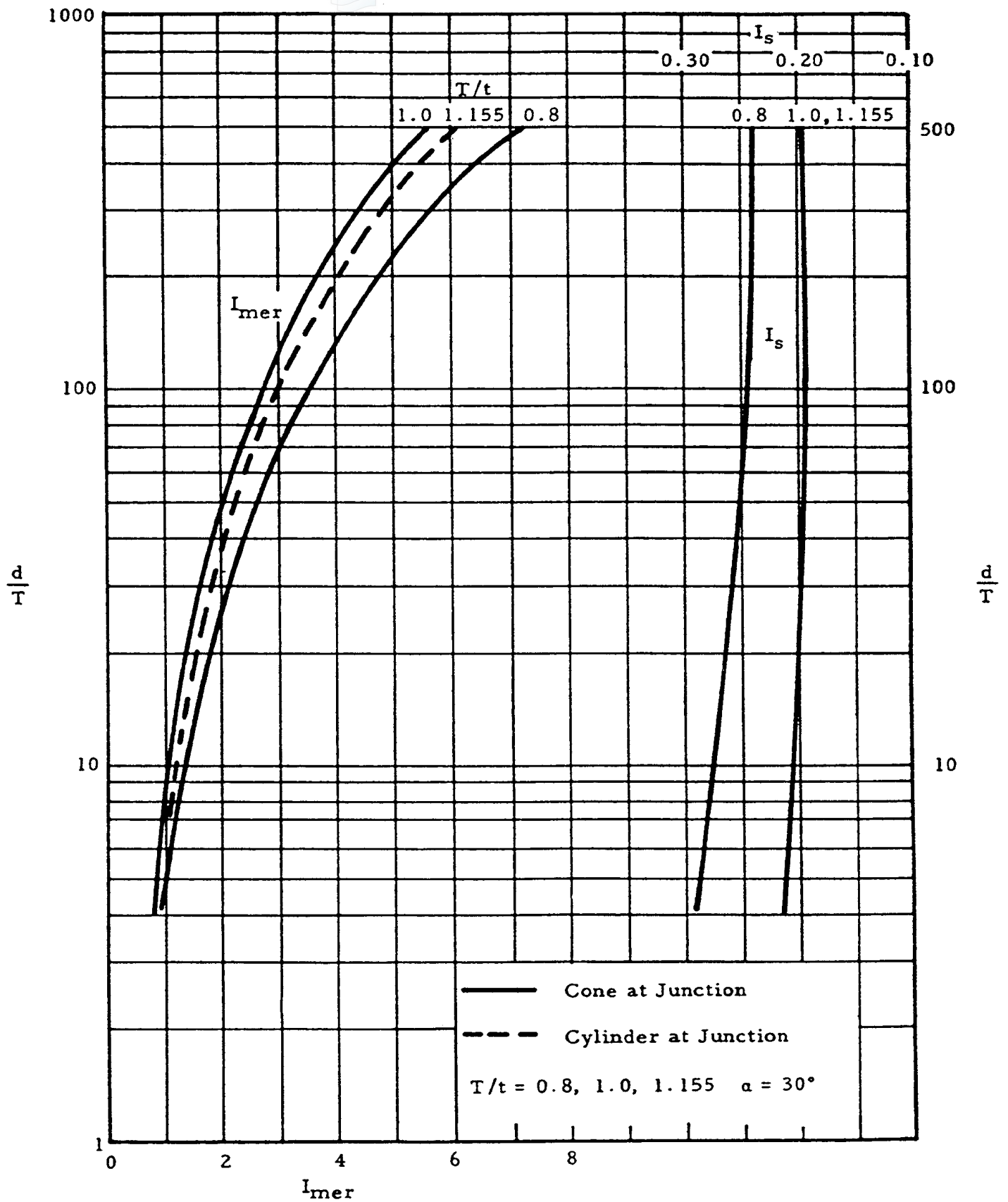
Figure 8-16.   Stress Ratios for Pressure Vessels with Conical Head Closures *

* Griffel, William, <u>Handbook of Formulas for Stress and Strain</u>
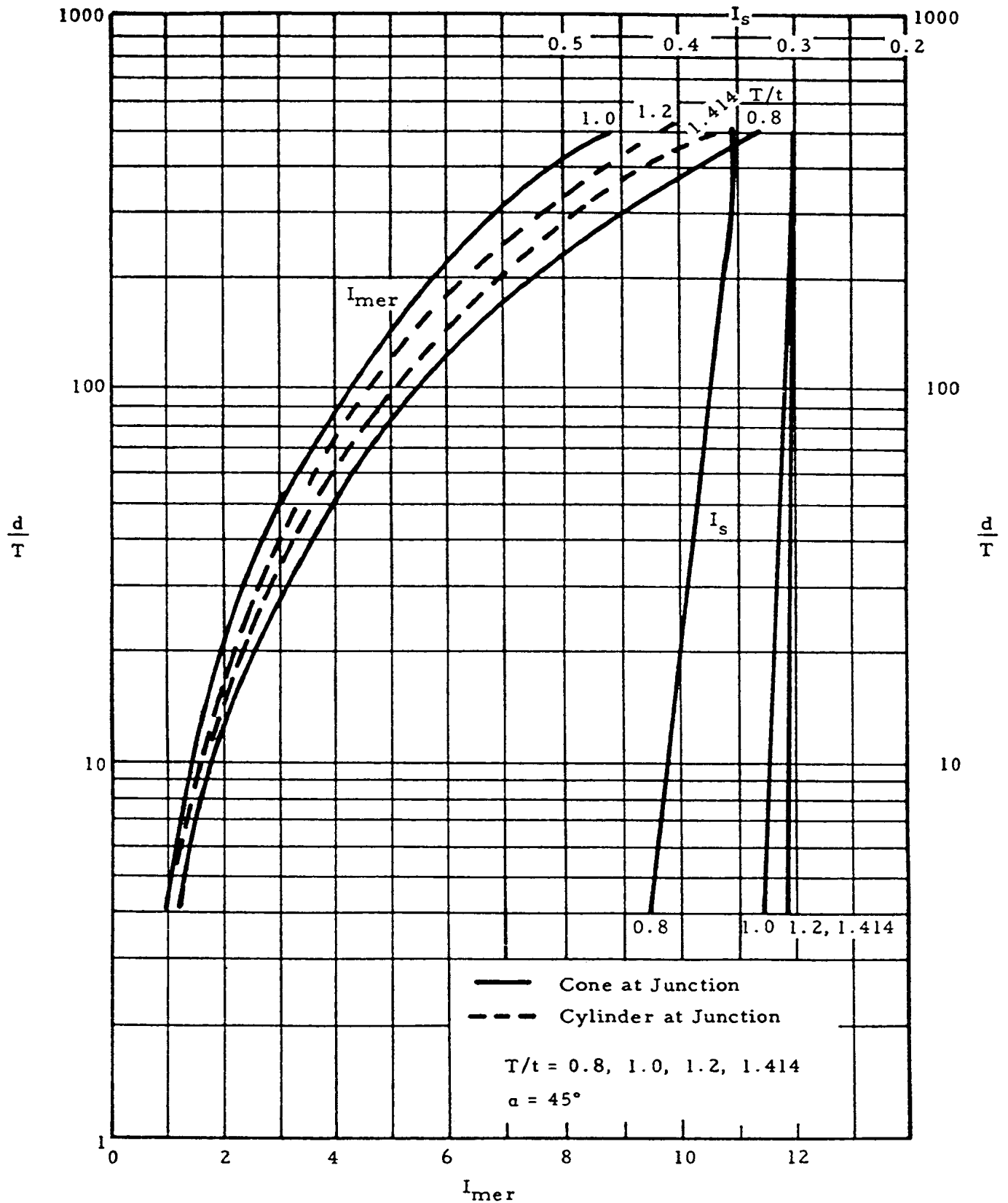
Figure 8-17. Stress Ratios for Pressure Vessels with Conical Head Closures *

* Griffel, William, Handbook of Formulas for Stress and Strain
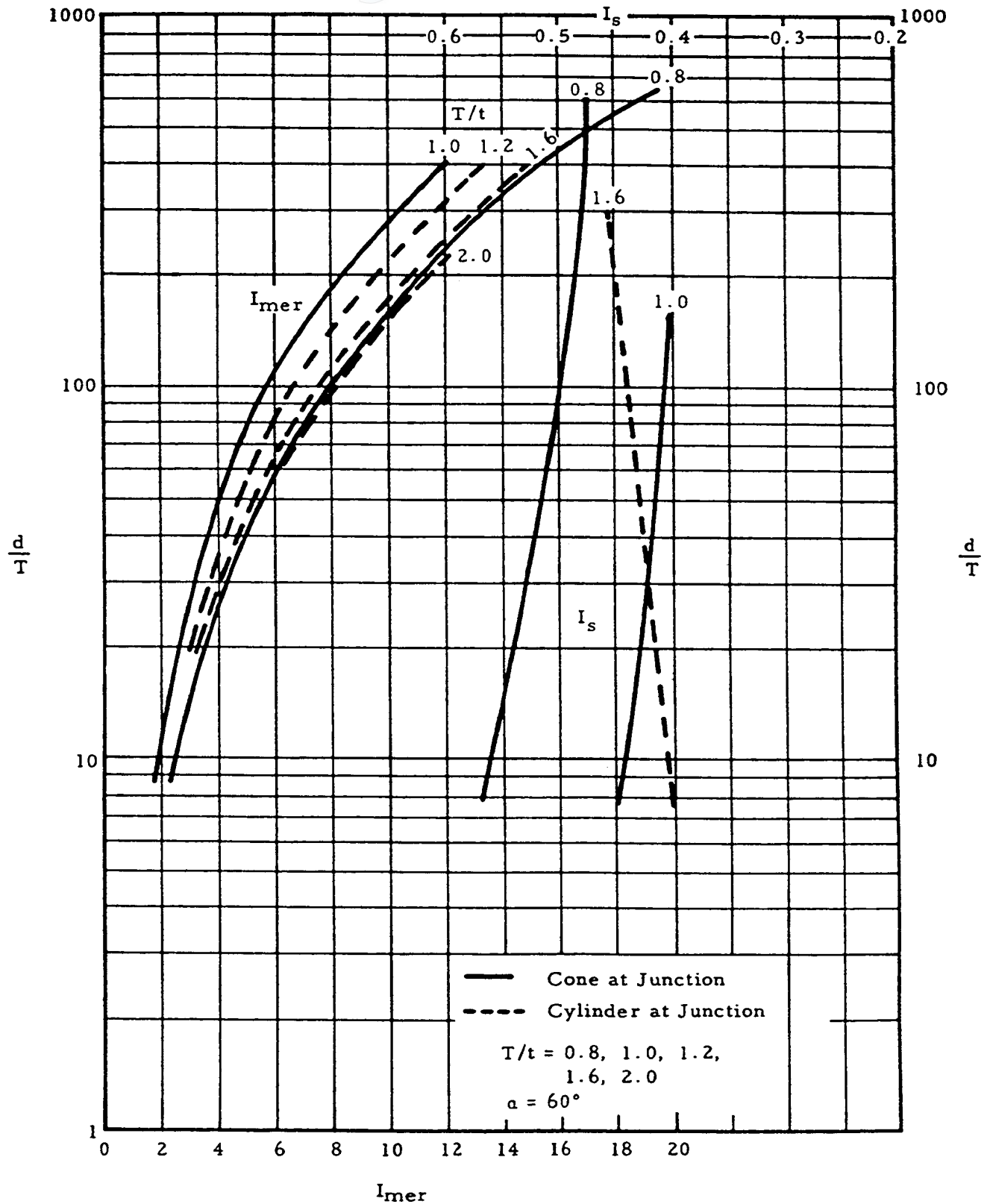
Figure 8-18. Stress Ratios for Pressure Vessels with Conical Head Closures *

* Griffel, William, Handbook of Formulas for Stress and Strain
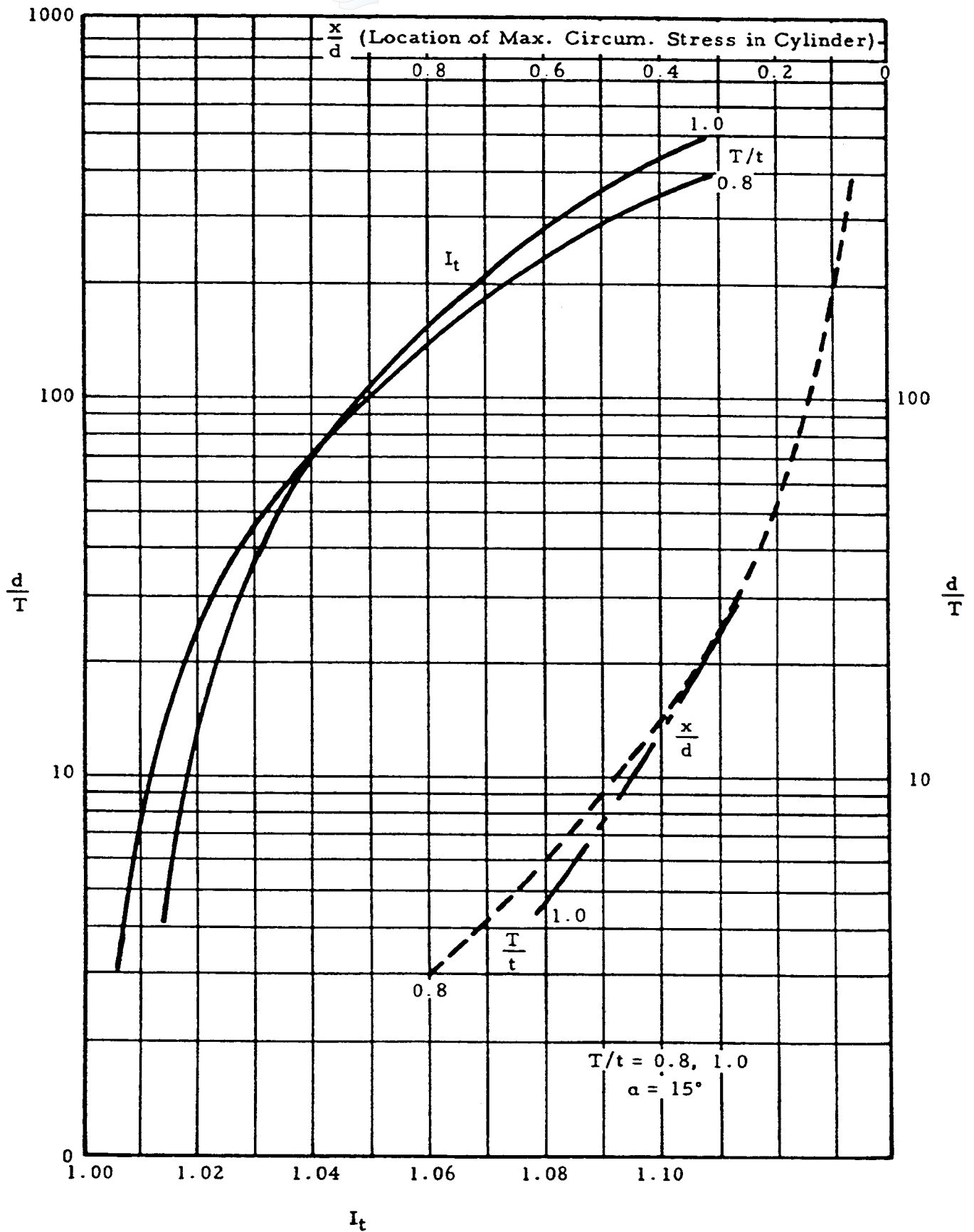
Figure 8-19. Stress Ratios for Pressure Vessels with Conical Head Closures *

* Griffel, William, Handbook of Formulas for Stress and Strain

8 - 27
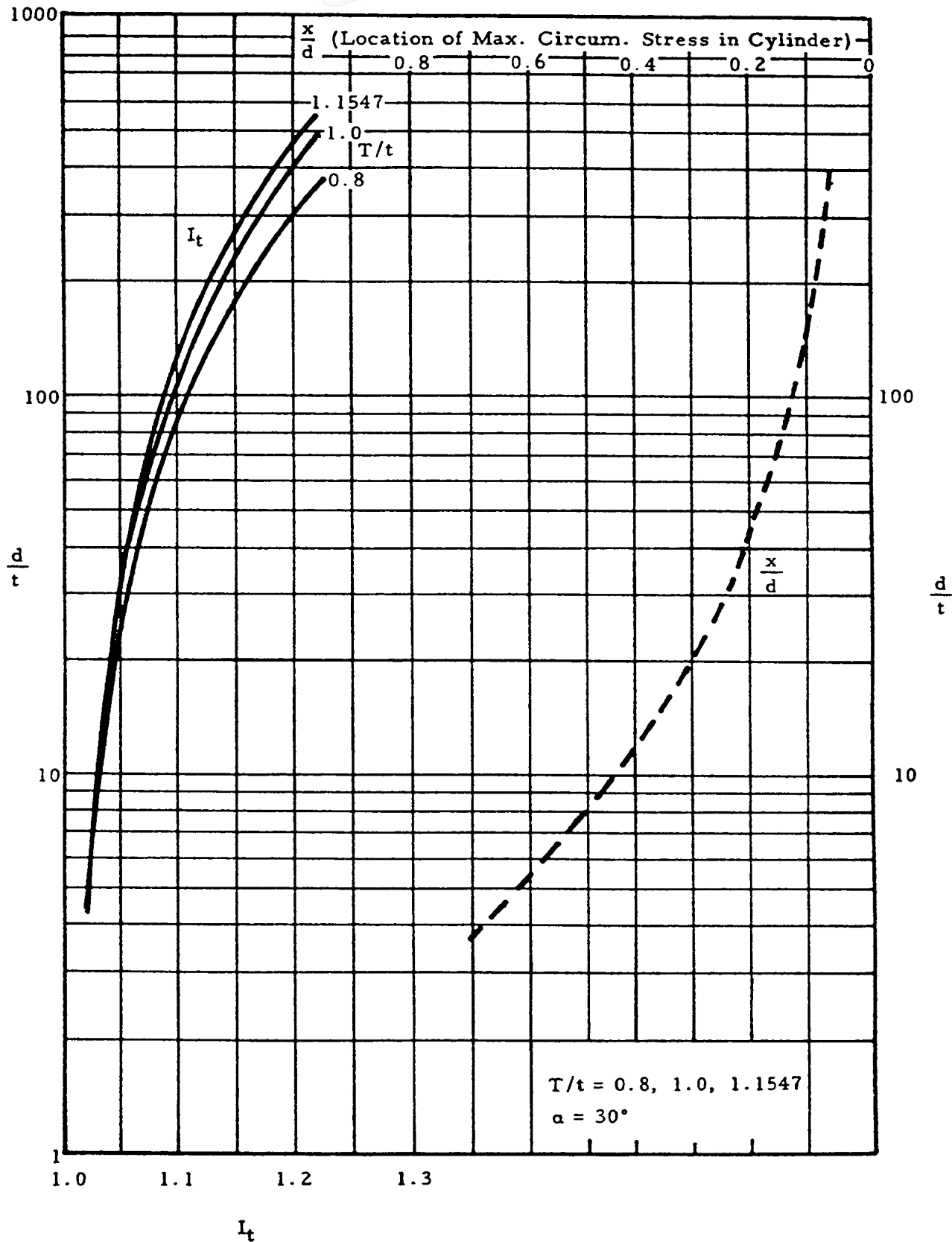
Figure 8-20. Stress Ratios for Pressure Vessels with Conical Head Closures *

* Griffel, William, Handbook of Formulas for Stress and Strain
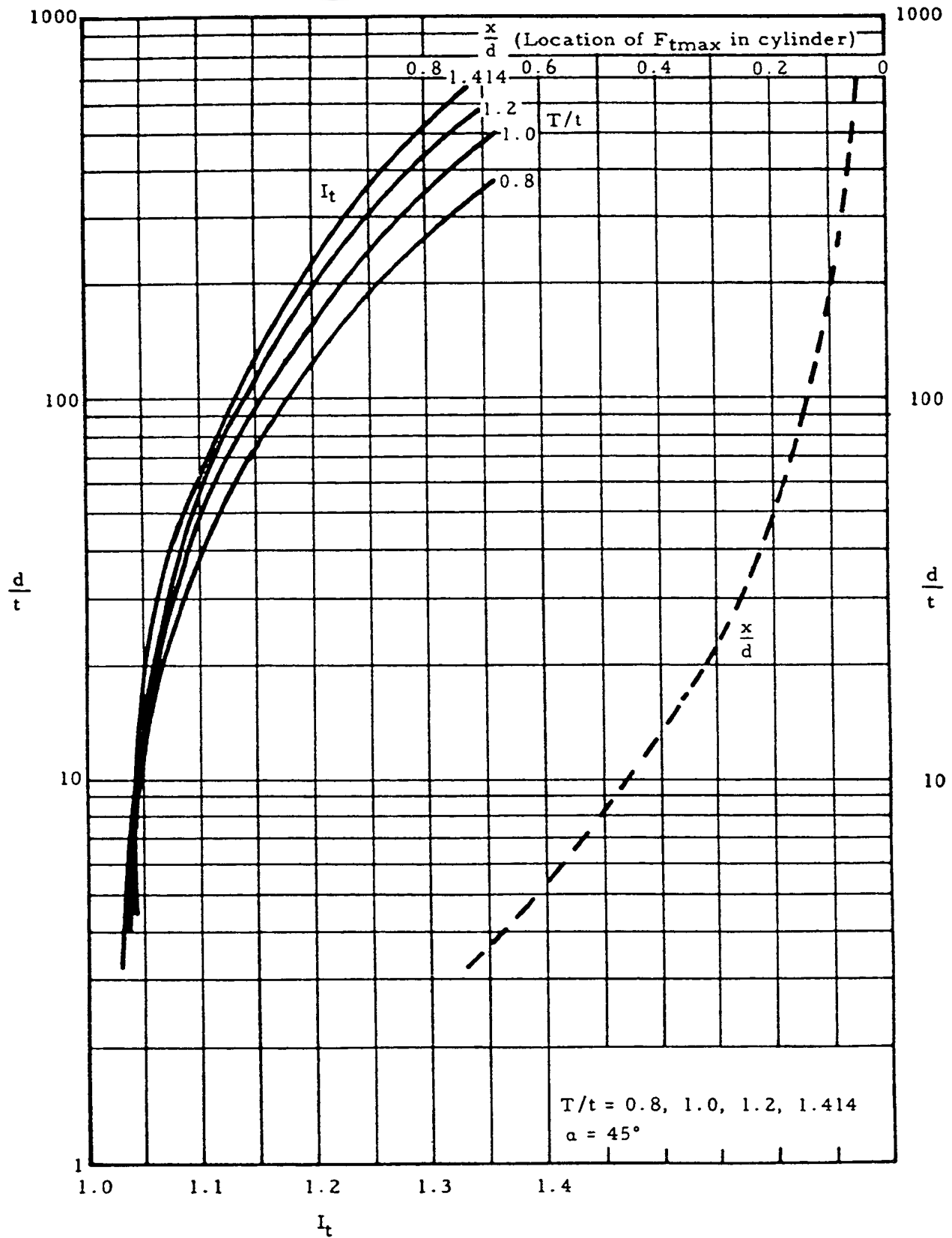
Figure 8-21. Stress Ratios for Pressure Vessels with Conical Head Closures *
* Griffel, William, Handbook of Formulas for Stress and Strain
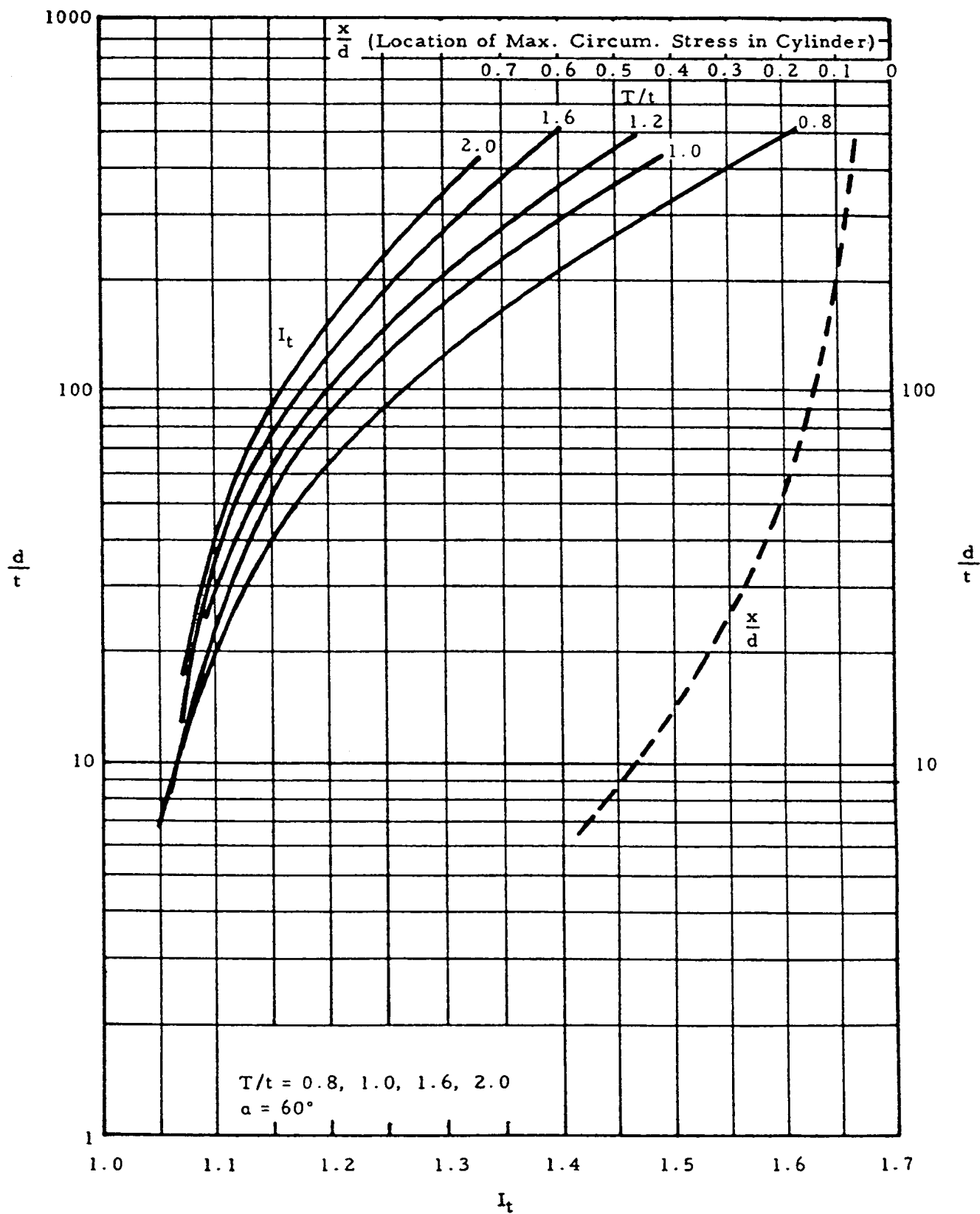
Figure 8-22.   Stress Ratios for Pressure Vessels with Conical Head Closures *

* Griffel, William, Handbook of Formulas for Stress and Strain

8.3.1.2.2.4.1   Sample Problem - Discontinuity Stresses in Pressure Vessels with Conical Heads

Given: The pressure vessel shown in Figure 8-23.
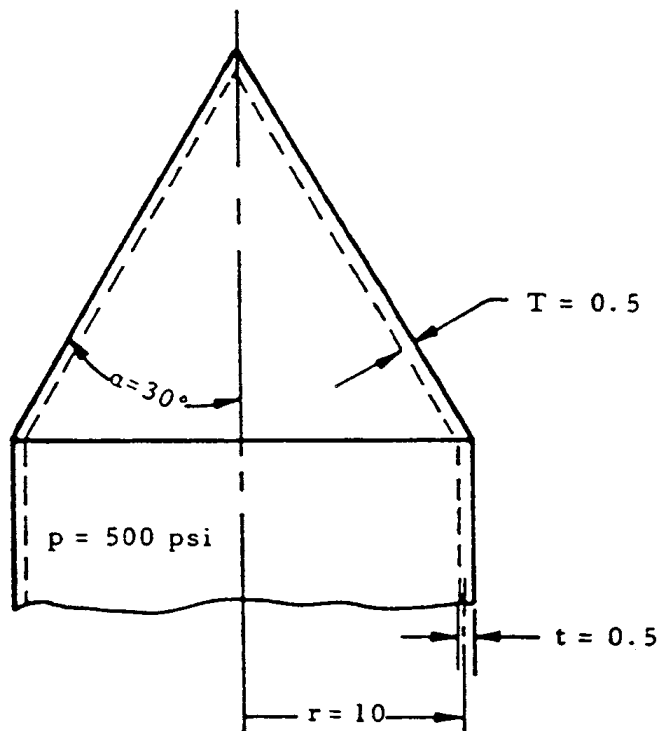
Figure 8-23.   Thin Cylindrical Pressure Vessel with Conical Head

Find: The maximum meridional, tangential, and shear stresses at the head-cylinder junction.

Solution: For this pressure vessel, $d/T = 40$ and $T/t = 1$. Figures 8-16 and 8-20 give stress ratios for conical heads with an angle of 30°. From these figures,

$$I_{mer} = 1.8$$
$$I_t = 1.055$$
$$I_s = 0.205$$

The circumferential membrane stress is

$$\frac{pd}{2t} = \frac{500(20)}{2(.5)} = 10,000 \text{ psi}$$

Applying the definitions of the stress ratio gives

$$F_{mermax} = I_{mer}\left(\frac{pd}{2t}\right) = 1.8(10,000) = 18,000 \text{ psi}$$

8 - 31

$$F_{t_{max}} = I_t \left(\frac{pd}{2t} \right) = 1.055(10,000) = 10,500 \text{ psi}$$

$$F_{s_{max}} = I_s \left(\frac{pd}{2t} \right) = 0.205(10,000) = 2,050 \text{ psi}$$

Since the appropriate graphs in Figure 8-16 are solid lines, $F_{sc_{max}}$ and $F_{s_{max}}$ occur in the cone at the junction. From the dashed line in Figure 8-20, the location of $F_{t_{max}}$, x/d is 0.22. Thus, $F_{t_{max}}$ occurs at $x = 0.22$ $d = 4.4$ inches from the junction of the cylinder and its head in the cylinder.

8.3.1.3 Buckling of Thin Simple Pressure Vessels Under External Pressure

In previous sections, it was assumed that the pressure is either internal or external, but of small enough magnitude not to cause buckling. However, thin pressure vessels must be checked for buckling if they are externally loaded.

8.3.1.3.1 Buckling of Thin Simple Cylinders Under External Pressure

The formula for the critical stress in short cylinders ($L^2/rt < 100$) which buckle elastically under radial pressure is

$$F_{cr} = \frac{k_y \pi^2 E}{12 (1-\mu_e^2)} \left(\frac{t}{L} \right)^2 \tag{8-12}$$

where k_y is obtained from Figure 8-24. If the membrane stress in the cylinder is greater than this, the cylinder will buckle.

The critical stress for long cylinders, $[100 \, t/r < (L/r)^2 < 5 \, r/t]$, under external radial pressure is

$$F_{cr} = 0.93 \, E \left(\frac{t}{r} \right)^{3/2} \left(\frac{r}{L} \right) \tag{8-13}$$

For very long cylinders, $[(L/r)^2 > 5 \, r/t]$, the buckling stress is given by

$$F_{cr} = \eta \, \frac{0.25 \, E}{(1-\mu_e^2)} \left(\frac{t}{r} \right)^2 \tag{8-14}$$

where η is the plasticity-reduction factor given in this case by

$$\eta = \frac{E_s}{E} \, \frac{(1-\mu_e^2)}{(1-\mu^2)} \left(\frac{1}{4} + \frac{3}{4} \, \frac{E_t}{E_s} \right) \tag{8-15}$$
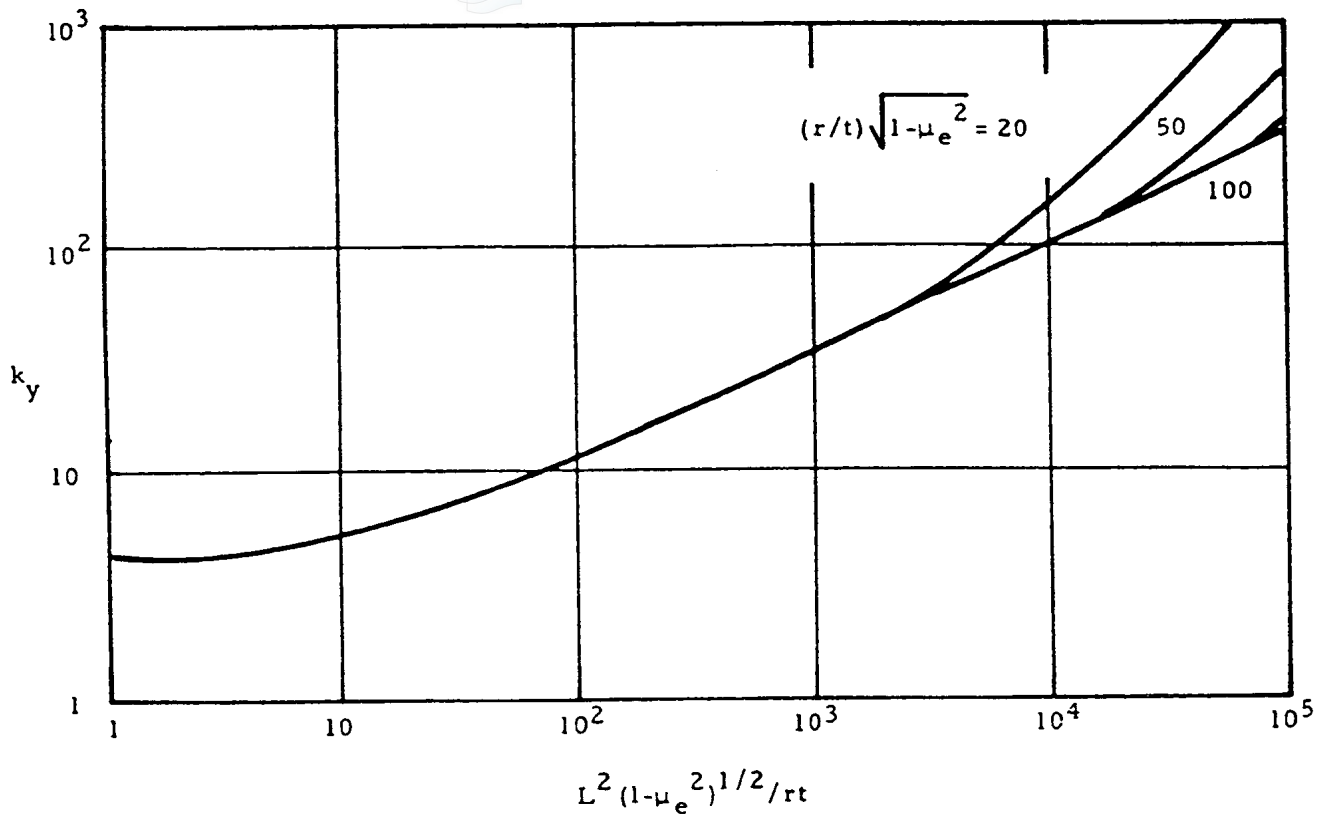
$$F_{cr} = \frac{k_y \pi^2 E}{12(1-\mu_e^2)} \left(\frac{t}{L}\right)^2$$

Figure 8-24.   Buckling of Short Cylinders Under External Radial Pressure

8.3.1.3.1.1   Sample Problem - Buckling of Thin Simple Cylinders Under
External Pressure

Given: The cylinder shown in Figure 8-25.
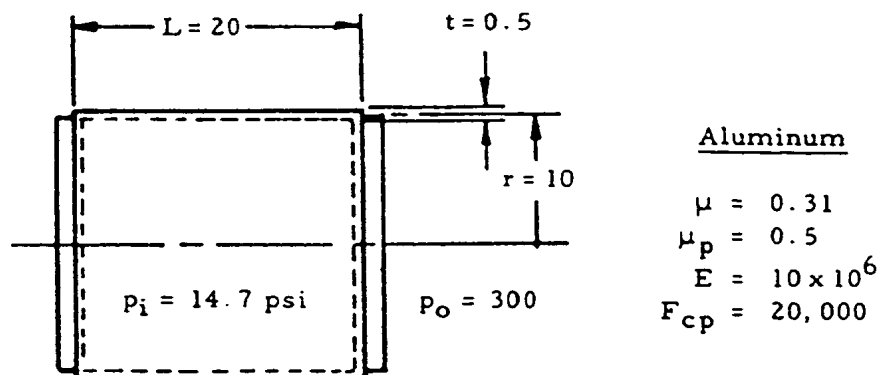
Figure 8-25.   Cylinder Under External Pressure

<u>Find</u>: The critical buckling stress, F_{cr}, and determine whether the cylinder will buckle.

<u>Solution</u>:

$$\frac{L^2}{rt} = \frac{20^2}{10\,(.5)} = 80$$

Since this ratio is less than 100, Equation (8-12) for short cylinders may be used. Before proceeding further, the elastic Poisson's ratio must be found. From the nomenclature section,

$$\mu_e = \left[\mu_p\left(\frac{E_s}{E} - 1\right) + \mu\right]\frac{E}{E_s}$$

Assume the critical stress is less than the proportional limit of the material. If this is true, $E = E_s$ and thus, $\mu_e = \mu$. Compute

$$L^2\,(1-\mu_e{}^2)^{1/2}/rt = \frac{20^2[1-(.31)^2]^{1/2}}{10\,(.25)} = 152$$

From Figure 8-24, $k_y = 12.2$. Substituting this into Equation (8-12) gives

$$F_{cr} = \frac{12.2(\pi^2)(10)(10^6)}{12[1-(.31)^2]}\left(\frac{.25}{20}\right)^2 = 17,300 \text{ psi}$$

Since this is less than the proportional limit of the material, the original assumption is correct. If it were not correct, a value of F_{cr} would have to be assumed and a value of E_s corresponding to this value found. This value would, in turn, be used to calculate μ_e which would be used in the Equation (8-12) to calculate F_{cr}. This trial and error process would have to be repeated until the assumed and calculated values of F_{cr} were in agreement.

From Equation (8-5), the stress in the cylinder is

$$F_{st} = \frac{(p_i - p_o)r}{t} = \frac{(14.7-300)(10)}{.25} = 11,400 \text{ psi}$$

Since this is less than F_{cr}, the cylinder does not fail.

8 - 34

8.3.1.3.2   Buckling of Thin Simple Spheres Under External Pressure

For computation of elastic-buckling stresses of thin spherical plates under external pressure, Equation (8-16) applies for all diameter ranges.

$$F_{cr} = \frac{k_p \, \pi^2 \, E}{12 \, (1 - \mu_e^2)} \left(\frac{t}{d} \right)^2$$

where k_p is given in Figure 8-26.
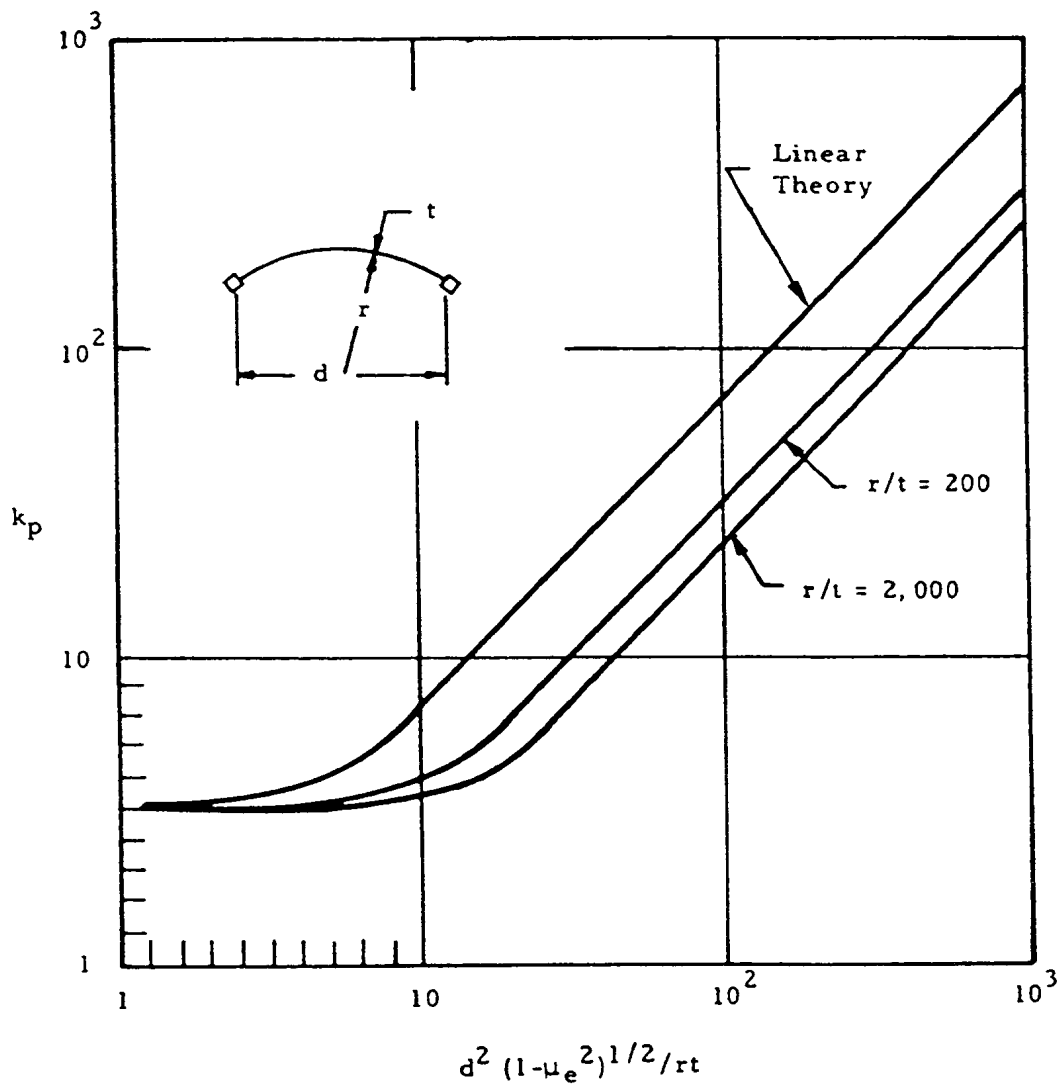
$$F_{cr} = \frac{k_p \, \pi^2 \, E}{12 \, (1 - \mu_e^2)} \left(\frac{t}{d} \right)^2$$

Figure 8-26.   Buckling Coefficient for Spherical Plates
Under External Pressure

8.3.1.4 Stresses in Simple Cylindrical Pressure Vessels Due to Supports

Figure 8-27 shows a cylindrical pressure vessel resting on saddle supports.
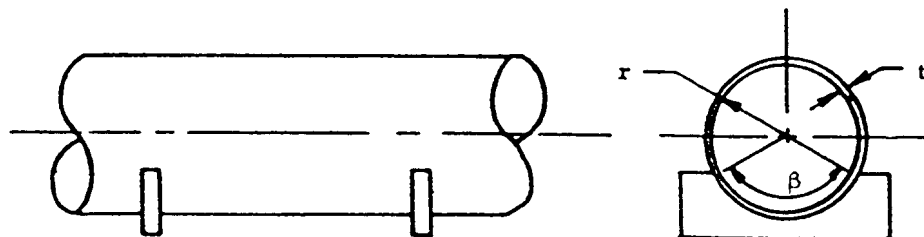
Figure 8-27. Cylindrical Pressure Vessel on Saddle Supports

There are high local longitudinal and circumferential stresses adjacent to the tips of the saddles. Although these stresses are difficult to predict exactly, their maximum value will probably not exceed that given by Equation (8-17) if the cylinder fits the saddle well.

$$F_{max} = [0.02 - 0.00012 (\beta - 90)] \frac{P}{t^2} \log_e \left(\frac{r}{t} \right)$$ (8-17)

In this equation, P is the reaction at each saddle and R, t, and β are as shown in Figure 8-27 where β is in degrees. Equation (8-17) contains no term for the thickness of the saddle since stresses are practically independent of this for the ordinary range of dimensions.

The maximum reaction, P, that the vessel can sustain is about twice the value that will produce a maximum stress equal to the yield point of the material according to Equation (8-17).

If a pipe is supported in flexible slings instead of in rigid saddles, the maximum stresses occur at the points of tangency between the sling and pipe section. These stresses are usually less than the corresponding stresses in a saddle supported pipe, but are of the same order of magnitude.

8.3.1.5 Crippling Stress of Pressurized and Unpressurized Thin Simple Cylinders

The crippling stress of thin simple cylinders is increased if internal pressure is applied. The following sections present curves to determine the crippling stress in pressurized and unpressurized cylinders subjected to compression, bending, torsion, or any combination of these. The parameters for such a cylinder are shown in Figure 8-28. Only buckling in the elastic range is considered in this section.
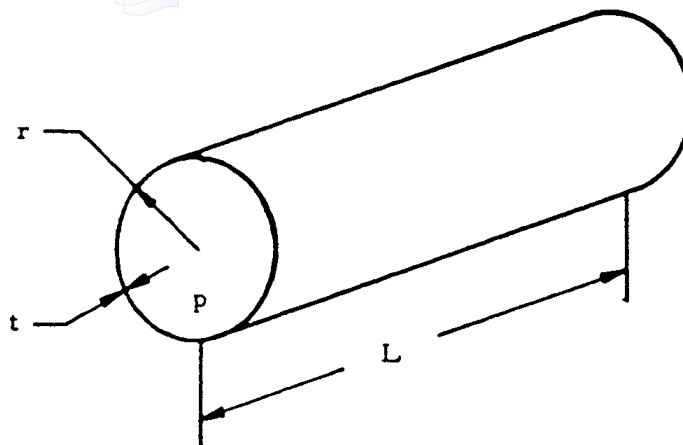
Figure 8-28.   Pressurized Cylinder

8. 3. 1. 5. 1   Crippling Stress of Simple Thin Cylinders in Compression

8. 3. 1. 5. 1. 1   Crippling Stress of Unpressurized Simple Thin Cylinders in Compression

Equation (8-18) is an empirical relationship for the crippling stress of short cylinders ($L/r \leqq 1$).

$$F_{cc} = E \left[11.28 \left(\frac{t}{r} \right)^{1.6} + 0.109 \left(\frac{t}{L} \right)^{1.3} \right] \tag{8-18}$$

For long cylinders ($L/r > 1$), the best fitting relationship for the crippling stress is

$$F_{cc} \quad E \left[11.28 \left(\frac{t}{r} \right)^{1.6} + .109 \left(\frac{t}{L} \right)^{1.3} - 1.418 \left(\frac{t}{L} \right)^{1.6} \text{Log} \left(\frac{L}{r} \right) \right] \tag{8-19}$$

For 99% probability values of F_{cc}, Figure 8-29 should be used.

Crippling occurs when the average compressive stress in the cylinder exceeds F_{cc}.

8. 3. 1. 5. 1. 2   Crippling Stress of Pressurized Simple Thin Cylinders in Compression

Figure 8-30 gives in graphical form the incremental increase in the crippling stress (ΔF_{cc}) of a cylinder due to internal pressure. These curves are for 99% probability values. Because of limited testing of pressurized cylinders, the value obtained for ΔF_{cc} can be considered reliable only in the ranges $1 < L/r < 6$, $600 < r/t < 2800$ and $pr/t < .625 \, F_{cy}$.
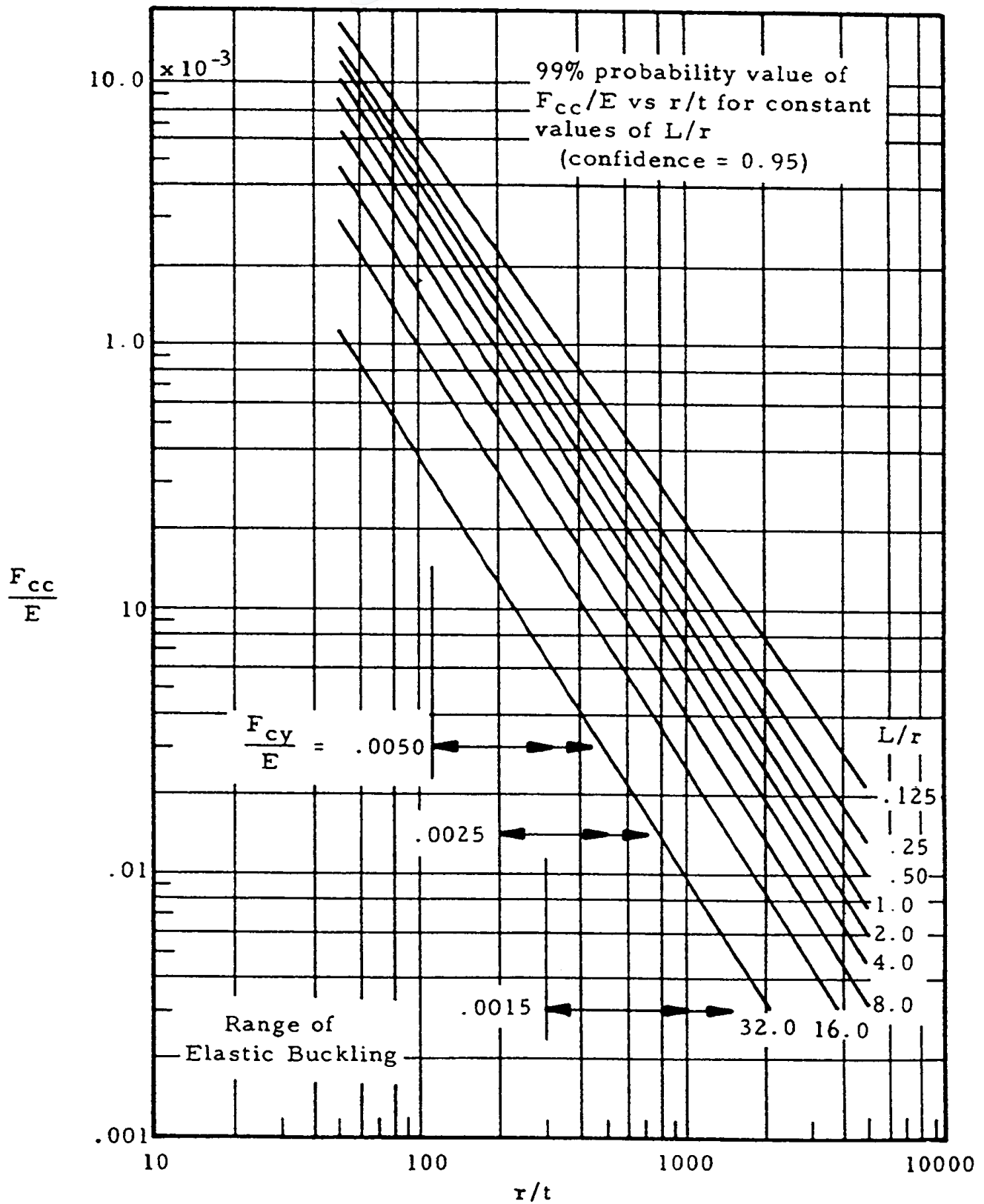
Figure 8-29. Unpressurized, Simple Circular Cylinders
in Compression with Clamped Ends

$$\frac{\Delta F_{cc} r}{Et} = 0.221 \text{ (constant)}$$

Notes:

1. For use only in conjunction with the 99% probability values for unpressurized cylinders (Figure 8.29)

2. Applies only if $pr/t \leq 625 F_{cy}$

$$\Delta F_{cc} = F_{ccp} - F_{cc}$$

1.0   2.0

$$\frac{p}{E} \left(\frac{r}{t}\right)^2$$
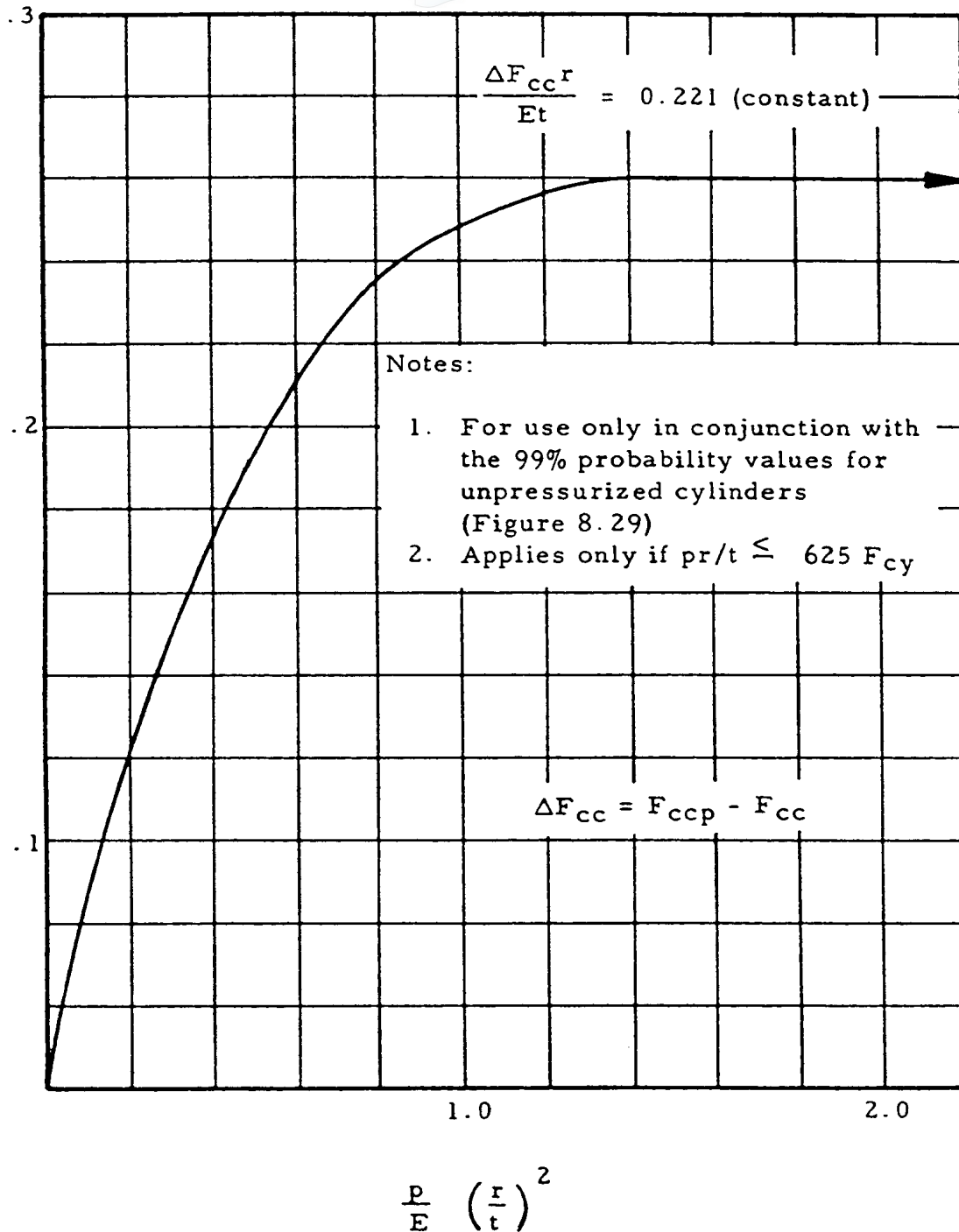
Figure 8-30. 99% Probability Value of ΔF_{cc} for Pressurized Circular Cylinder in Compression

8 - 39

8.3.1.5.2   Crippling Stress of Simple Thin Cylinders in Bending

8.3.1.5.2.1   Crippling Stress of Unpressurized Simple Thin Cylinders
in Bending

Figure 8-31 gives 99% probability curves for the crippling
of unpressurized cylinders in bending.   These curves parallel those for ur
pressurized cylinders in compression but yield crippling stresses about 1
greater.

99% probability value of
F_{cc}/E vs r/t for constant
values of L/r
(confidence = 0.95)

Range of
Elastic Buckling

$\dfrac{F_{cy}}{E}$ = 0050

.0025

0015

L/r

.125

.25

.5

1

2

4

8

16

Dashed lines are extrapolated
into untested regions.

r/t
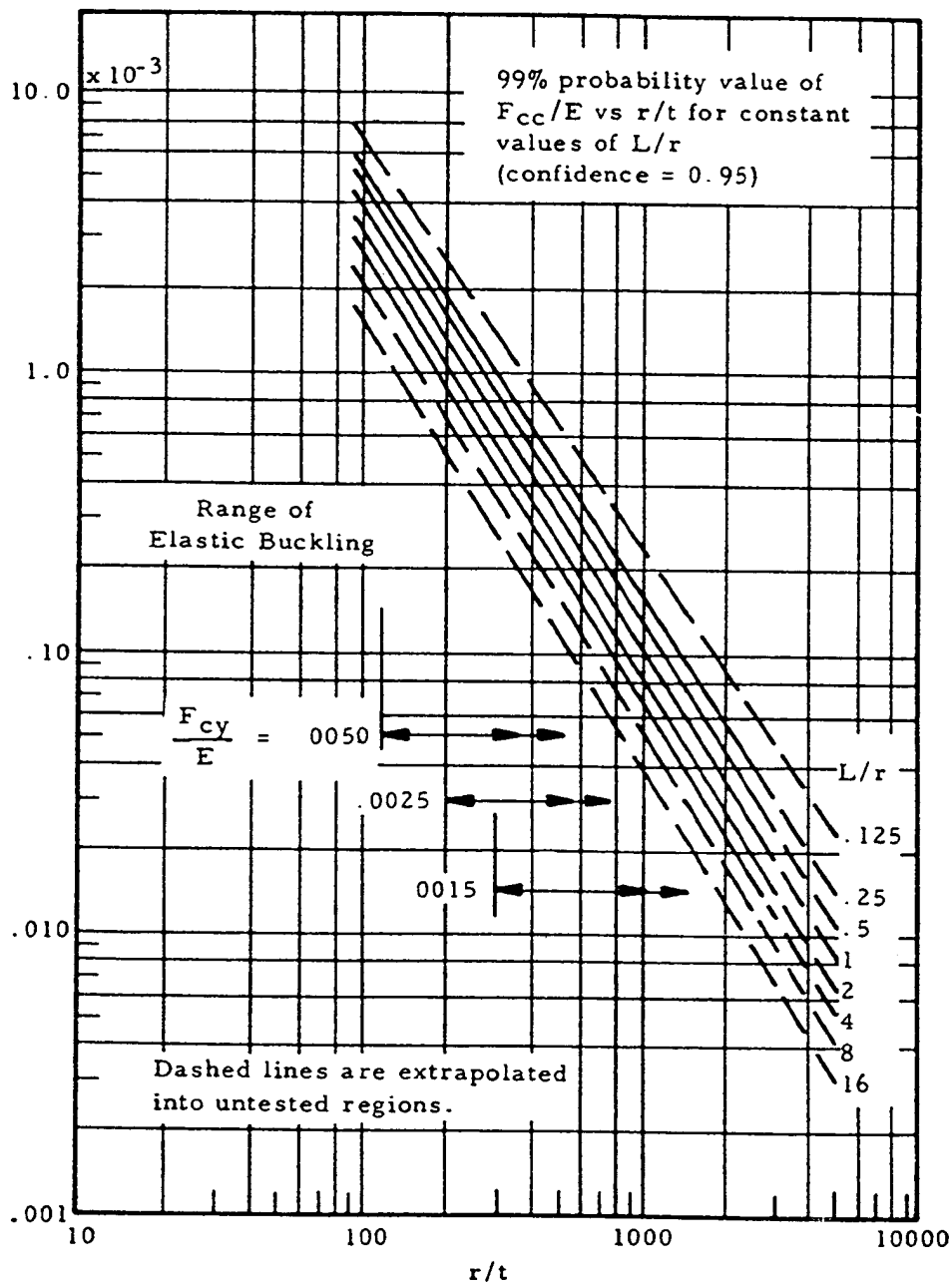
Figure 8-31.   Unpressurized, Simple Circular Cylinders
in Pure Bending with Clamped Ends

8 - 40

Crippling failure occurs when the maximum bending stress in the cylinder (Mr/I) exceeds F_{cc}.

8.3.1.5.2.2 Crippling Stress of Pressurized Simple Thin Cylinders in Bending

Figure 8-32 gives the incremental increase in the crippling stress (ΔF_{cc}) of a cylinder in bending due to internal pressure. This curve is based on experiments on pressurized cylinders that were preloaded axially to balance the longitudinal stress, $pr/2t$, due to internal pressure. It should be noted that this curve is based on very limited data.
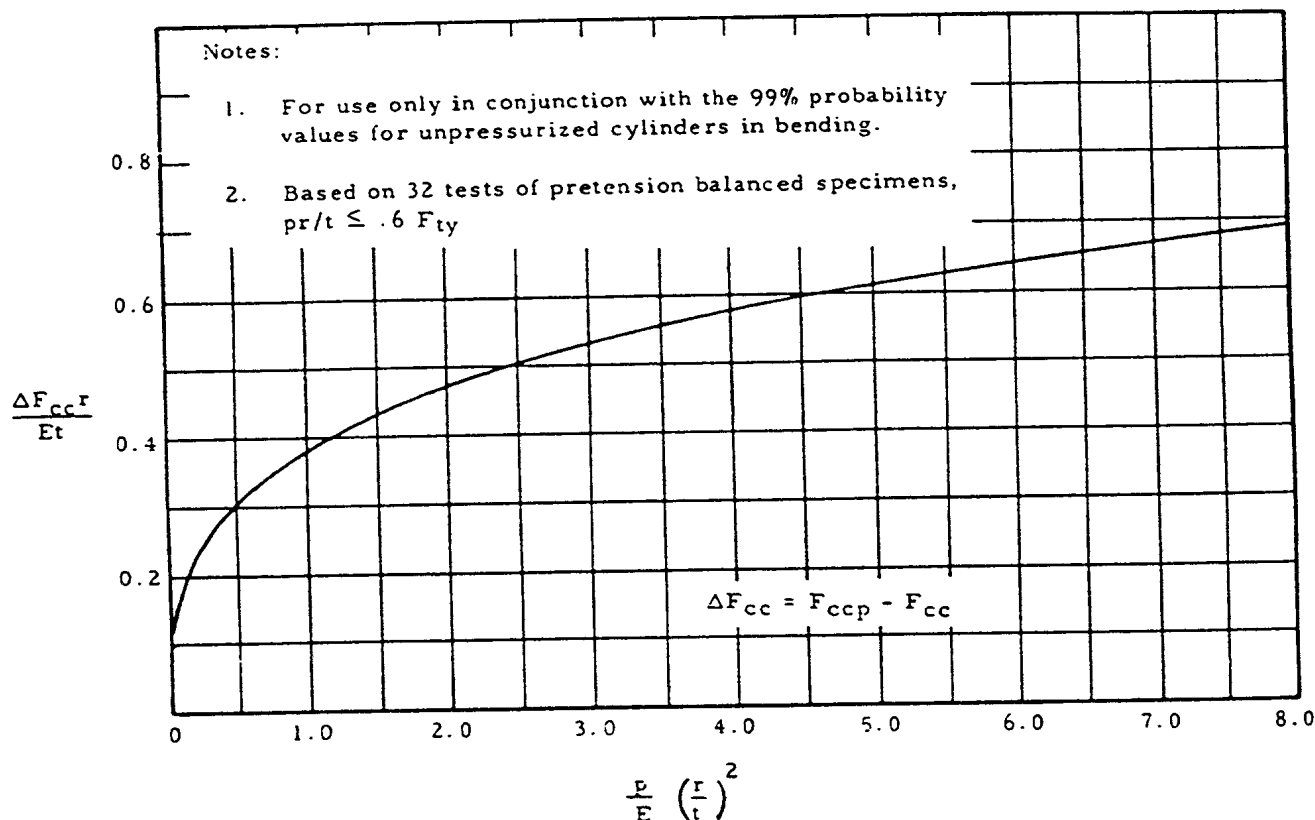
Figure 8-32. 99% Probability Value of ΔF_{cc} for Pressurized Circular Cylinders in Bending

8.3.1.5.3 Crippling Stress of Simple Thin Cylinders in Torsion

8.3.1.5.3.1 Crippling Stress of Unpressurized Simple Thin Cylinders in Torsion

Torsional buckling of thin, unpressurized cylinders does not exhibit the sudden snap-through behavior observed in the case of compression and bending. Instead, the buckling process under torsion is more gradual and

8-41

a slight difference is observed between initial and ultimate buckling. However, this difference is too small to be of any value so that the critical buckling stress is taken to be the failure stress.

Figure 8-33 gives the 99% probability values for the crippling shear stress of cylinders in torsion. These curves are applicable if

$$6 < \sqrt{1-\mu^2} \left(\frac{L^2}{2\,tr} \right) < 5 \left(\frac{r}{t} \right)^2 \qquad (8\text{-}20)$$
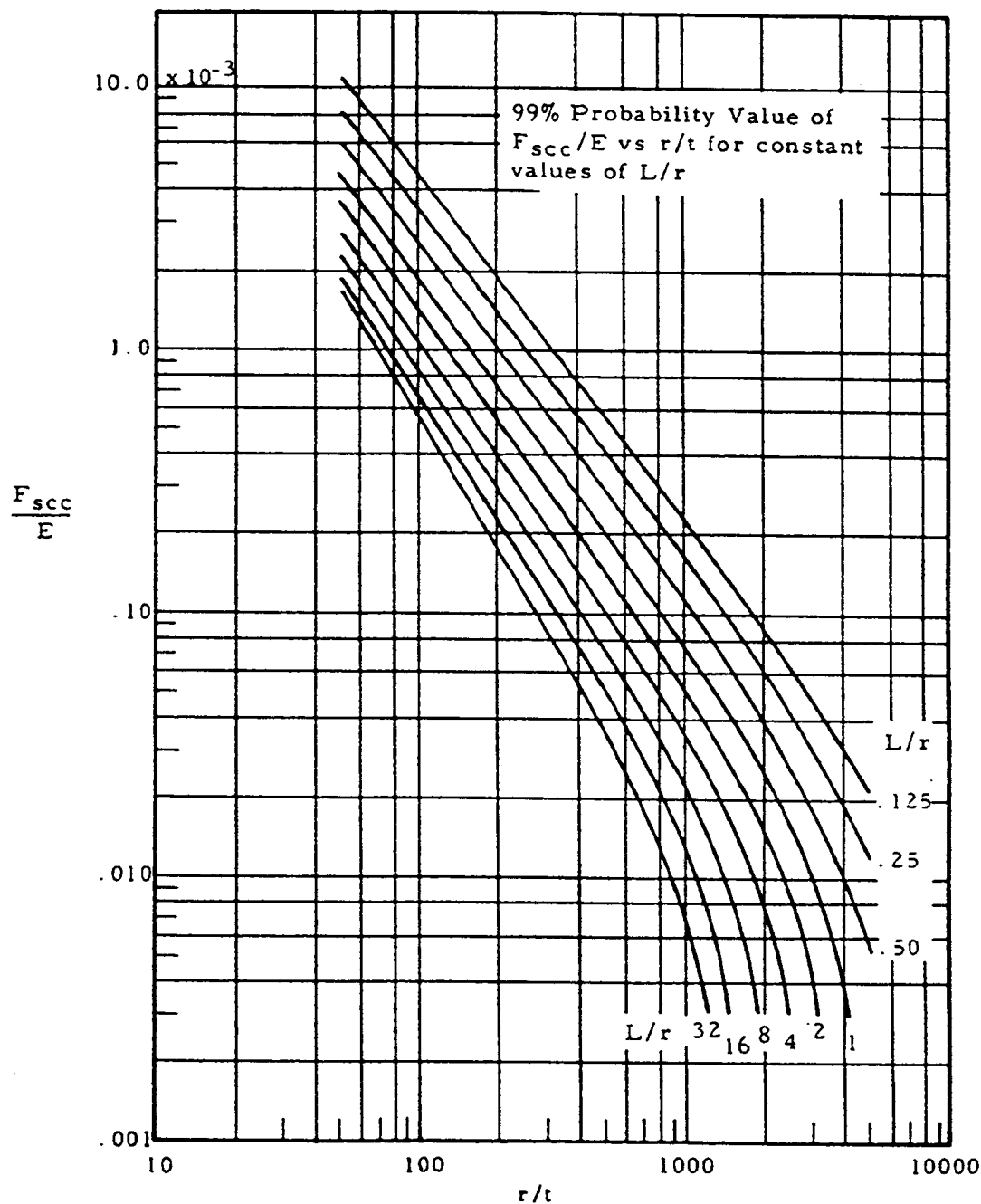
Figure 8-33. Torsional Buckling of Unpressurized Circular Cylinders

However, analysis indicates that the range of use of these curves may be amended to

$$6 < \sqrt{1-\mu^2} \left(\frac{L^2}{2tr}\right) < 10 \left(\frac{r}{t}\right)^2 \qquad (8\text{-}21)$$

Failure occurs if the shear stress in a cylinder under torsion Tr/I_p is greater than the crippling shear stress, F_{scc}.

8.3.1.5.3.2 Crippling Stress of Pressurized Simple Thin Cylinders in Torsion

Figure 8-34 gives the incremental increase in the crippling shear stress of a cylinder in torsion (ΔF_{scc}) due to internal pressure. Since few tests are available on buckling of circular cylinders under torsion and these tests are for very low pressure ranges, design curves may not be established on a statistical basis.

Note:

For use in conjunction with Figure 8.33

$$\Delta F_{scc} = F_{sccp} - F_{scc}$$
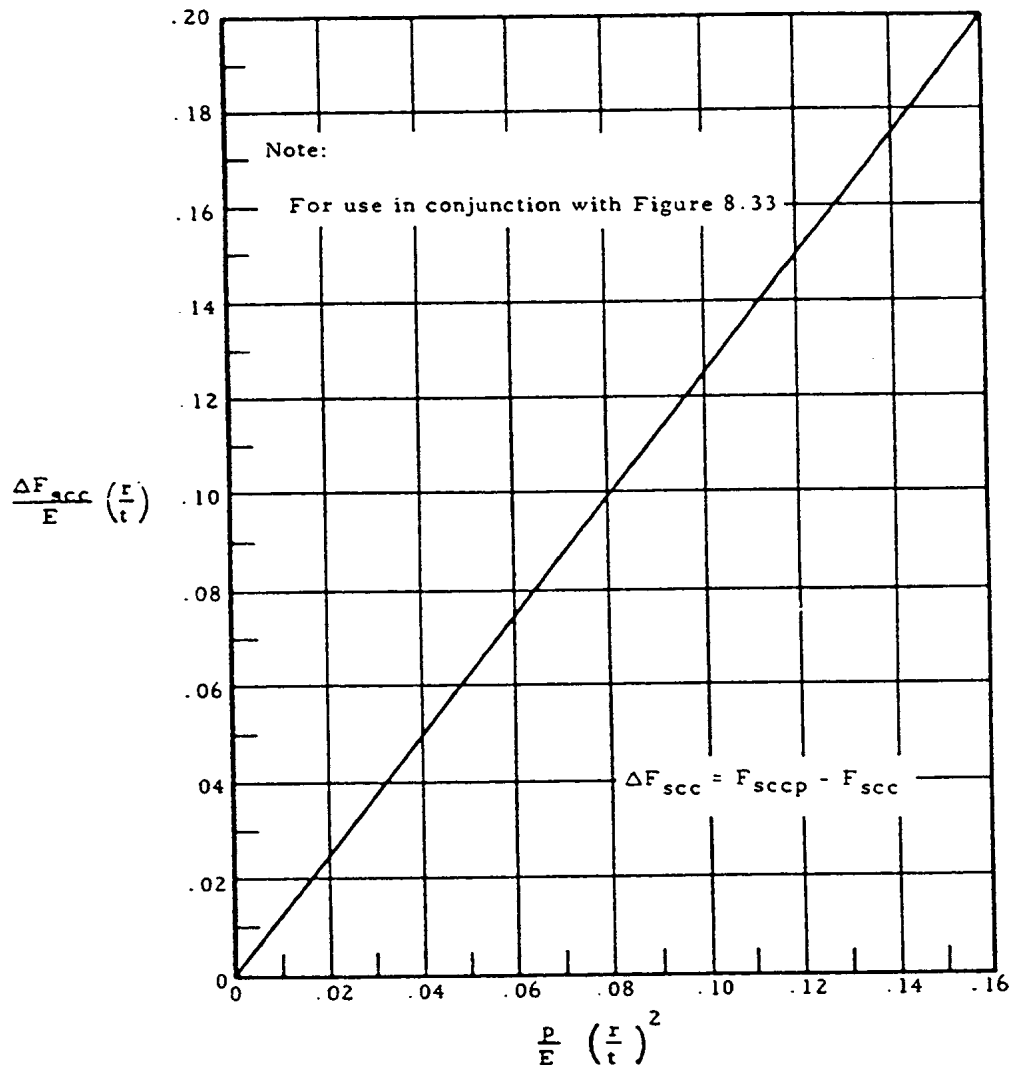
Figure 8-34. ΔF_{scc} for Pressurized Circular Cylinders in Torsion

8.3.1.5.3.2.1   Sample Problem - Cripppling Stress of Pressurized Simple Thin Cylinders in Torsion

Given: The pressurized cylinder shown in Figure 8-35.
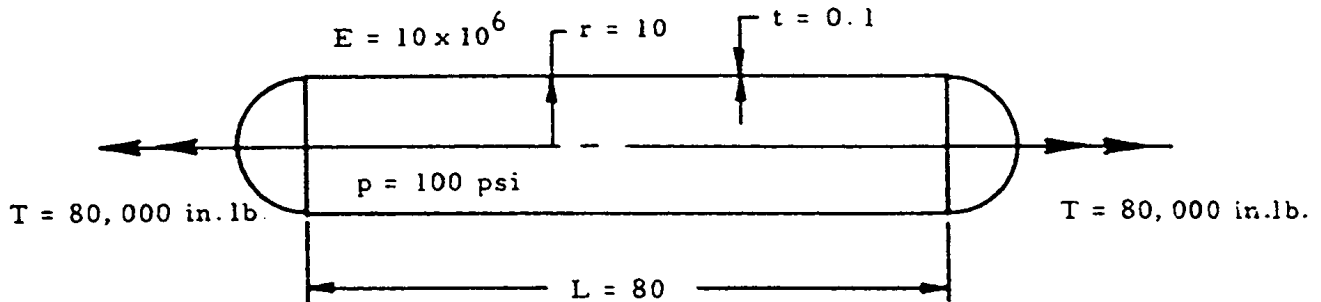
Figure 8-35. Pressurized Cylinder in Torsion

Find: The crippling shear stress, F_{sccp}, and examine for failure by crippling.

Solution: $L/r = 8$ and $r/t = 100$. From Figure 8-33,

$$\frac{F_{scc}}{E} = 8 \times 10^{-4}$$

for unpressurized cylinders. Thus, $F_{scc} = 8,000$ psi.

From Figure 8-34,

$$\frac{\Delta F_{scc}}{E} \left(\frac{r}{t} \right) = 0.125$$

Thus,

$$\Delta F_{scc} = .125 \ \frac{Et}{r} = .125 \ \frac{(10 \times 10^6)(.1)}{10} = 10,000 \text{ psi}$$

The crippling stress in a cylinder under pressure (F_{sccp}) is equal to that of an unpressurized cylinder plus ΔF_{scc}.

$$F_{sccp} = F_{scc} + \Delta F_{scc} = 8,000 + 10,000 = 18,000 \text{ psi}$$

It can be seen that internal pressure more than doubles the resistance of the cylinder to crippling. The shear stress in the cylinder is

$$f_s = \frac{Tr}{I_p} = \frac{(80,000)(10)}{\frac{\pi (10.05^4 - 9.95^4)}{32}} = 20,300 \text{ psi}$$

8 - 44

Since this stress is greater than F_{scep}, the cylinder will fail by crippling.

8.3.1.5.4   Interaction Formulas for the Crippling of Pressurized and and Unpressurized Cylinders

Table 8-5 gives interaction relationships for various combinations of loads. The combined load interactions apply to the initial buckling of both pressurized and unpressurized thin-walled circular cylinders. The terms used for pressurized cylinders are defined as follows:

$$R_b = \frac{\text{applied bending moment}}{\text{critical bending moment}}$$

$$R_c = \frac{\text{applied compressive load}}{\text{critical compressive load}}$$

$$R_s = \frac{\text{applied transverse shear load}}{\text{critical transverse shear load}}$$

$$R_{st} = \frac{\text{applied torsional moment}}{\text{critical torsional moment}}$$

The terms for unpressurized cylinders are defined in the same way except that stress ratios are used rather than load ratios.

8.3.1.5.4.1   Sample Problem - Crippling Interaction of Simple Thin Cylinders in Compression and Bending

Given: The cylinder shown in Figure 8-36.
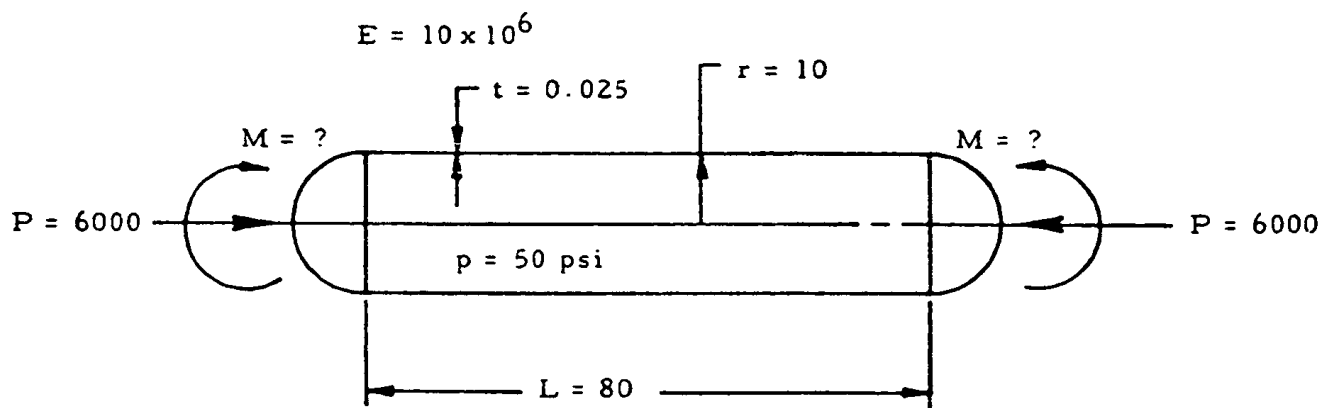
Figure 8-36.   Pressurized Cylinder in Compression and Bending

Find: The maximum bending moment, M.

Solution: From Figure 8-29, $F_{cc}/E = 1.6 \times 10^{-4}$ for compressive loading. Thus,

$$F_{cc} = (1.6 \times 10^{-4})(10 \times 10^6) = 1,6000 \text{ psi}$$

From Figure 8-30, $\Delta F_{cc} r/Et = .235$. Thus,

$$\Delta F_{cc} = .235 \frac{Et}{r} = .235 \frac{(10 \times 10^6)(.025)}{10} = 5,870 \text{ psi}$$

TABLE 8-5

Combined Load Interactions for the Buckling of Pressurized and Unpressurized Circular Cylinders

Combined Loading Condition	Interaction Equation (99% Probability Values)
Axial Comp. + Pure Bending	$R_c + R_b = 1.0$
Axial Comp. + Pure Bending + Transverse Shear	$R_c \sqrt[3]{R_s^3 \quad R_b^3} = 1.0$
Pure Bending + Transverse Shear	$(R_s)^3 + (R_b)^3 = 1.0$
Axial Comp. + Torsion	$R_c + R_{st}^2 = 1.0$
Axial Tens. + Torsion	$R_{st}^3 - R_t = 1.0 \qquad R_t < 0.8$
Pure Bending + Torsion	$R_b^{1.5} + R_{st}^2 = 1.0$
Pure Bending + Torsion + Transverse Shear	$R_b^p + (R_s + R_{st})^q = 1.0$ where: $1.5 \le p \le 3.0$ $2.0 \le q \le 3.0$
Axial Comp. + Pure Bending + Transverse Shear + Torsion	$R_c + R_{st}^2 + \sqrt[3]{R_s^3 + R_b^3} = 1.0$
Axial Load (Ten. or Comp.) + Pure Bending + Torsion	$R_s + R_b + R_{st}^2 = 1.0$

For compressive loading,

$$F_{ccp} = F_{cc} + \Delta F_{cc} = 1,600 + 5,870 = 7,470 \text{ psi}$$

The critical compressive load is thus,

$$7470A = 7470 \left[\pi (20)(.025) \right] = 11,700 \text{ psi}$$

Since the applied compressive load is 6,000 lb.,

$$R_c = \frac{\text{applied compressive load}}{\text{critical compressive load}} = \frac{6,000}{11,700} = .513$$

From Table 8-5,

$$R_c + R_b = 1.0$$

Thus,

$$R_b = 1.0 - R_c = 1.0 - .513 = 0.487$$

Now, the allowable bending load may be found once the critical bending load is found. From Figure 8-31 and 8-32, $F_{cc} = 2,200$ and $\Delta F_{cc} = 9,000$. Thus,

$$F_{ccp} = F_{cc} + \Delta F_{cc} = 2,200 + 9,000 = 11,200 \text{ psi}$$

The formula for the critical bending moment is

$$M_{cr} = \frac{IF_{ccp}}{r} = \frac{\frac{\pi}{64}(10.0125^4 - 9.9875^4)(11,200)}{10} = 5,500 \text{ in-lb.}$$

Since,

$$R_b = \frac{\text{applied bending moment}}{\text{critical bending moment}} = 0,487,$$

$$M = R_b M_{cr} = 0.487(5,500) = 2,430 \text{ in-lb.}$$

8.3.2   Stiffened Thin Pressure Vessels

This section treats of thin pressure vessels that are reinforced with stringers and/or rings.

8.3.2.1 Thin Cylindrical Pressure Vessels with Stringers Under Internal Pressure

Figure 8-37 shows a cross section of a thin cylindrical pressure vessel reinforced with stringers.
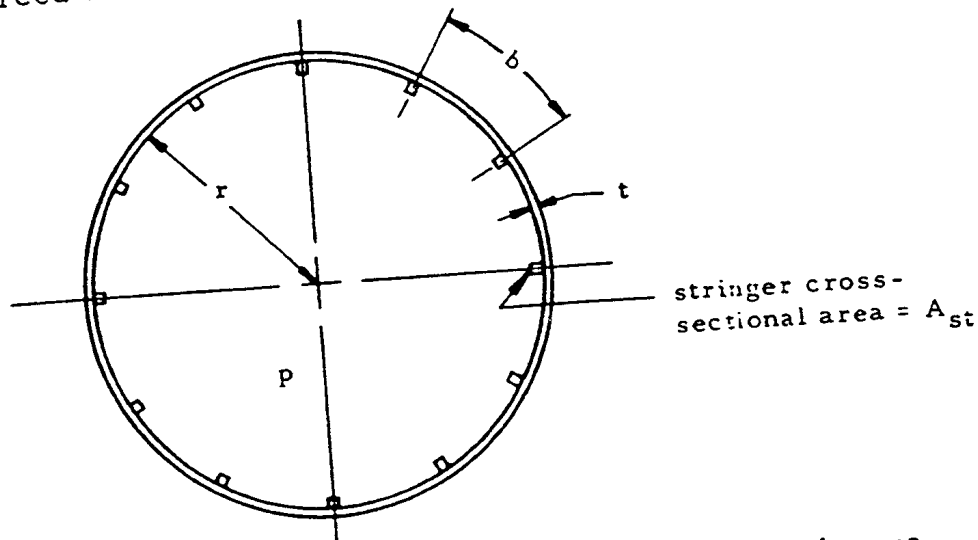
Figure 8-37.   Cross Section of Shell with Stringers

The axial stress in the shell is

$$F_{shfor} = \frac{pr}{2l}\left(\frac{bt + 2\mu A_{st}}{bt + A_{st}}\right)$$

(8-22)

and that in the stringer is

$$F_{stmer} = \frac{pr}{2t}\left[\frac{bt\,(1-2\mu)}{bt + A_{st}}\right]$$

(8-23)

The circumferential stress is the same as that in a simple thin cylinder

$$F_{st} = \frac{pr}{t}$$

(8-24)

8.3.2.1.1 Sample Problem - Thin Cylindrical Pressure Vessels with Stringers Under Internal Pressure

Given: The cylindrical pressure vessel shown in Figure 3-38.

Find: The stresses in the shell and stringers.

$\mu = 0.31$

$p = 100$ psi

$r = 20$

8 stringers
($A_{st} = 0.5$)

$t = 0.1$
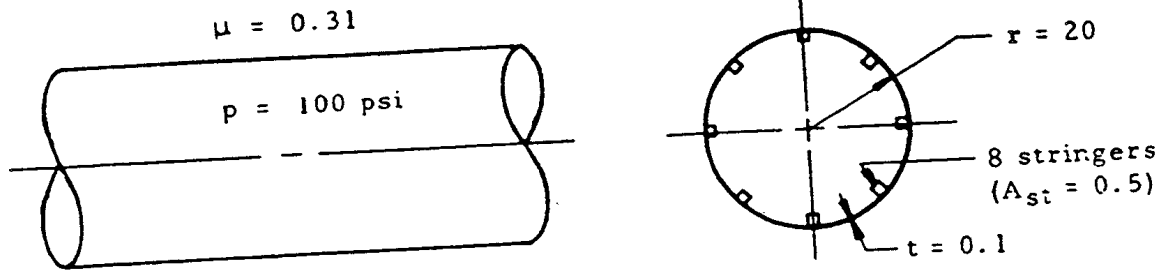
Figure 8-38. Thin Cylindrical Pressure Vessel with Stringers

Solution: The distance between stringers is one-eighth the circumference of the cylinder.

$$b = 2\pi r/8 = \frac{2\pi(20)}{8} = 15.72 \text{ in.}$$

From Equation (8-22), the meridional stress in the shell is

$$F_{smer} = \frac{pr}{2t}\left(\frac{bt + 2\mu A_{st}}{bt + A_{st}}\right) = \frac{100(20)}{2(0.1)}\left[\frac{15.72(0.1)+2(0.31)(.5)}{15.72(0.1)+0.5}\right]$$

$$= 9,100 \text{ psi}$$

From Equation (8-24), the tangential stress in the shell is

$$F_{st} = \frac{pr}{t} = \frac{100(20)}{0.1} = 20,000 \text{ psi}$$

The only stress in the stringer is a meridional stress given by Equation (8-23).

$$F_{stmer} = \frac{pr}{2t}\left[\frac{bt(1-2\mu)}{bt + A_{st}}\right] = \frac{100(20)}{2(0.1)}\left[\frac{15.72(0.1)(1-0.62)}{15.72(0.1)+0.5}\right]$$

$$= 2,890 \text{ psi}$$

8.3.2.2 Thin Cylindrical Pressure Vessels with Rings Under Internal Pressure (Stringers Optional)

Figure 8-39 shows two views of a thin shell with rings and stringers and appropriate geometric parameters. An enlarged view of the section of the ring is shown in Figure 8-40.

8 - 49

I_{sst} = moment of inertia of skin stringer combination per inch of circumference

ring spacing

a

ring with modulus of elasticity E_{ring}

E = modulus of elasticity of skin and stringers

t = shell thickness

stringers of area A_{st}

r

shell length

L

inside radius of shell

stringer spacing

b
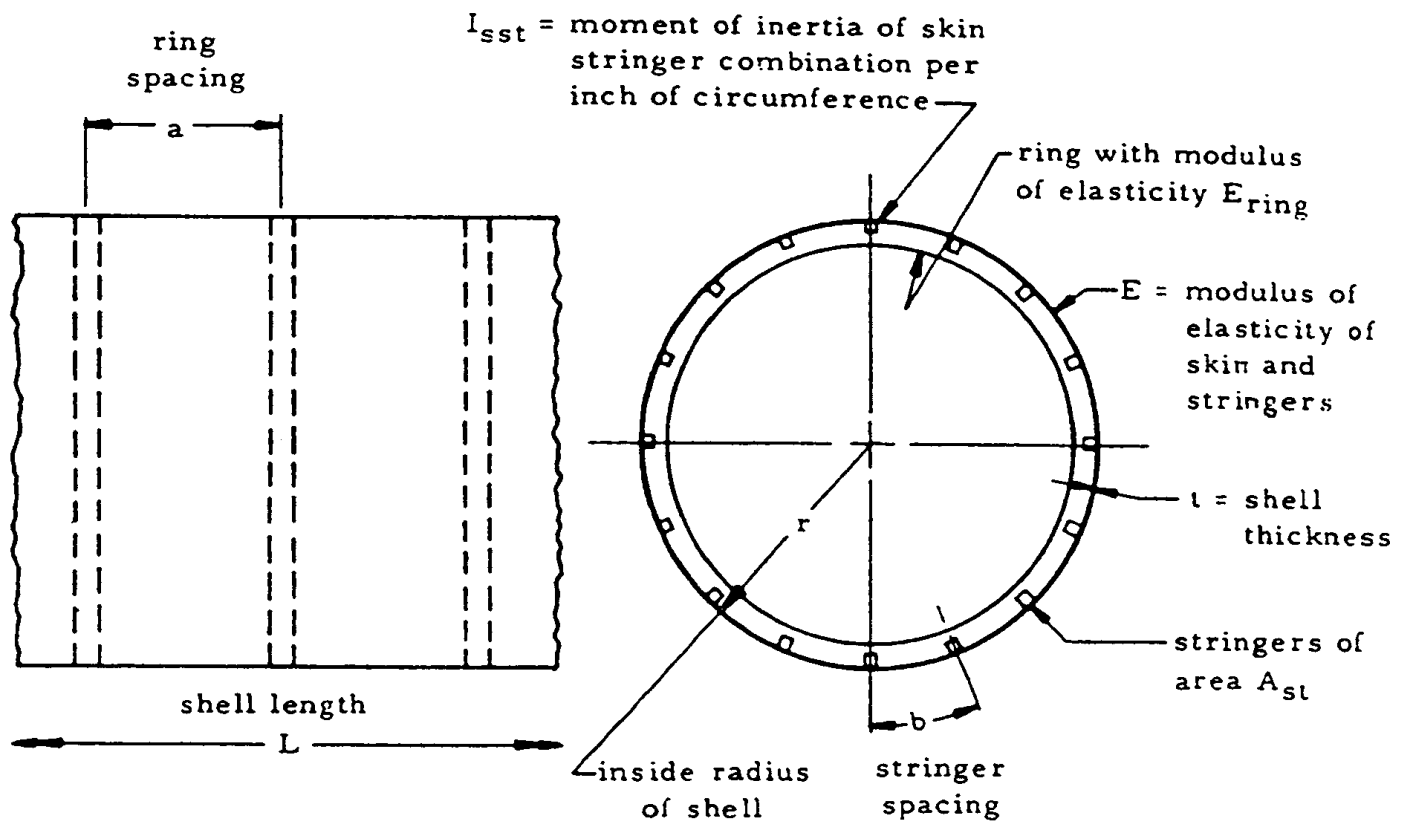
Figure 8-39.   Shell with Rings and Stringers

A

b

b'

A

r

₵ of attachment

e

t_r

r

centroid of A_r'

R

Cross Hatched Area is A_r'
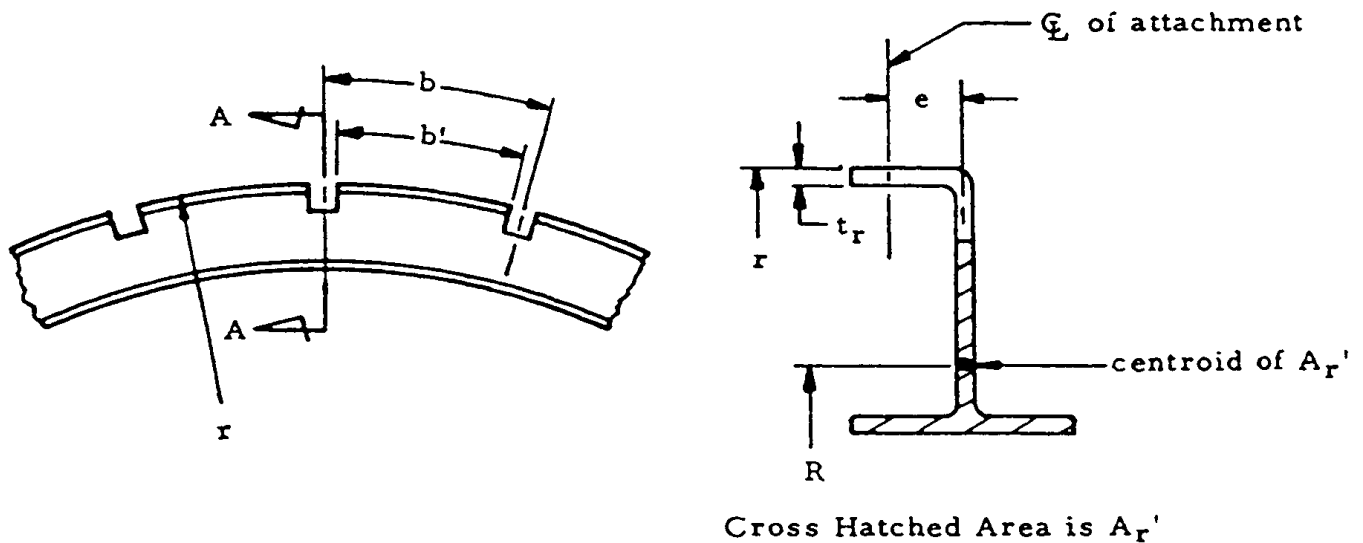
Figure 8-40.   Section of Stiffening Ring

8 - 50

The definition of the following parameters facilitates the
of pressure vessel behavior.

$$d \equiv \frac{A_{st}}{bt}$$

$$T \equiv \frac{pr}{2}$$

$$t_s \equiv \frac{A_{st}}{b}$$

$$t' \equiv \frac{t + t_s}{1 + (1-\mu^2)\dfrac{t_s}{t}}$$

$D \equiv EI_{sst}$ of sheet stringer combination
per inch of circumference

$$K \equiv \frac{\sqrt{t'\,E/D}}{2r}$$

$$\alpha \equiv \sqrt{K + \frac{T}{4D}}$$

$$\beta \equiv \sqrt{\left|K - \frac{T}{4D}\right|}$$

$$A \equiv \frac{\alpha a}{2}$$

$$B \equiv \frac{\beta a}{2}$$

$$P \equiv \frac{pr^2}{t'E}\left[1 - \frac{\mu t'}{2(t + t_s)}\right]$$

$$A_r \equiv \frac{r^2}{\dfrac{b}{b'}\left(\dfrac{e}{t_r}\right)^3(1-\mu^2) + \dfrac{r^2}{A_r'}}$$

$$Q \equiv \frac{A_r \, E_r \, a^3}{32 \, D \, r^2}$$

The deflections and moments on the shell at the ring and at midspan between rings are dependent on the relationship between K and T/4D. Two conditions are possible — $K \geqq T/4D$ and $K < T/4D$.

If $K \geqq T/4D$, the radial deflections of the shell at the ring (δ_r) and midway between the rings (δ_a) are given by Equations (8-25) and (8-26). In this case, the bending moments of the skin stringer combination per inch of circumference at the ring (M_{sstr}) and midway between rings M_{ssts} are given by Equations (8-27) and (8-28).

$$\delta = \frac{-P}{1 + \dfrac{Q}{\Omega_1}} \tag{8-25}$$

$$\delta_a = -P \left(1 - \frac{\Omega_2}{1 + \dfrac{\Omega_1}{Q}} \right) \tag{8-26}$$

$$M_{sstr} = \frac{4 \, PD \, \Omega_4}{a^2 \left(1 + \dfrac{\Omega_1}{Q} \right)} \quad \text{in lb/in} \tag{8-27}$$

$$M_{ssts} = \frac{-M_{ssr} \, \Omega_3}{\Omega_4} \quad \text{in lb/in} \tag{8-28}$$

In the above equations, Ω_a values may be obtained from Figures 8-41 through 8-44.

If $K < T/4D$, the equations for deflections and moments on the shell are the same as Equations (8-25) through (8-28) except that the Ω_a terms are replaced by Δ_a terms. These Δ_a terms are given as functions of A and B in Figures 8-45 through 8-49.
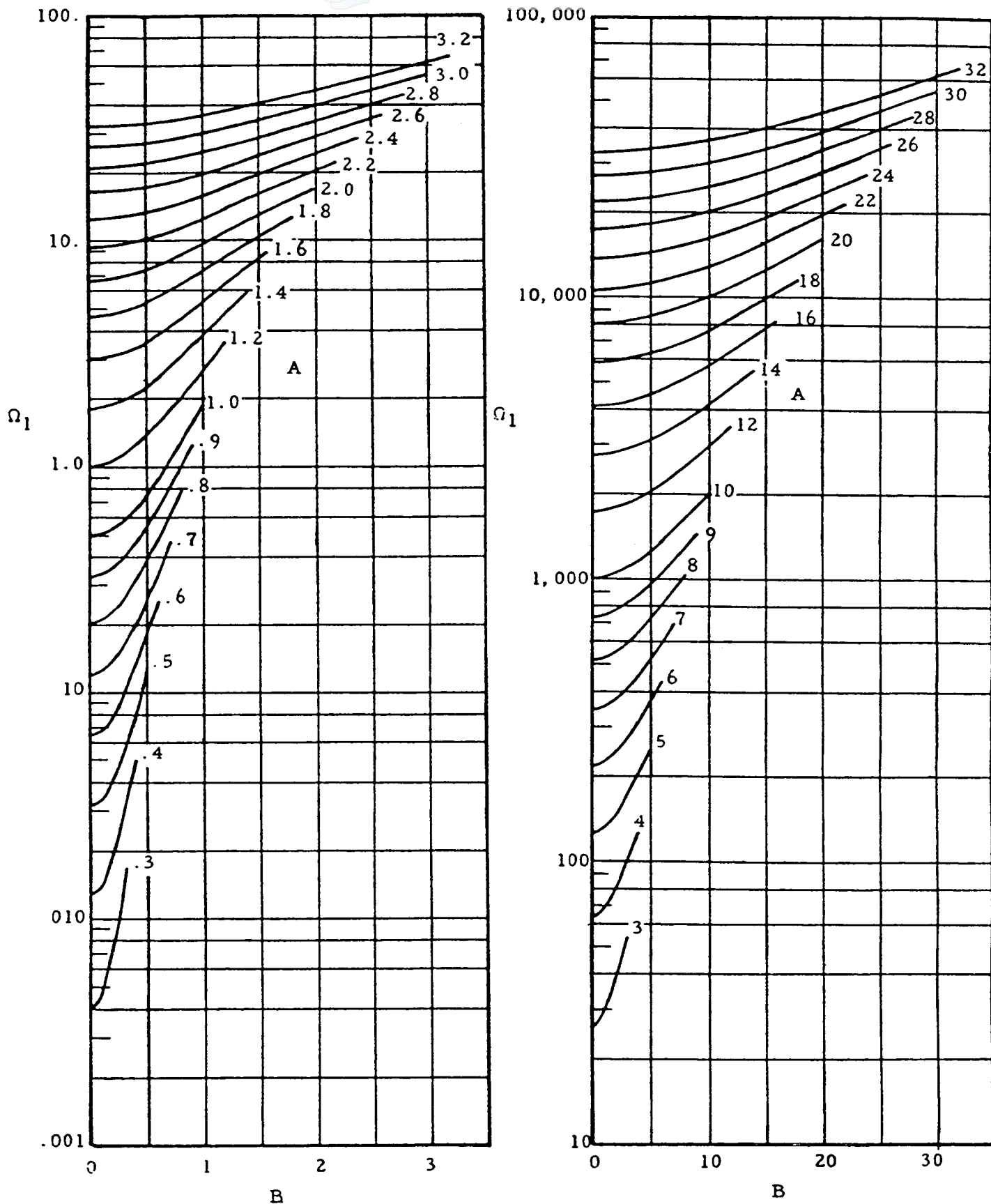
Figure 8-41. Ω_1 as a Function of A and B
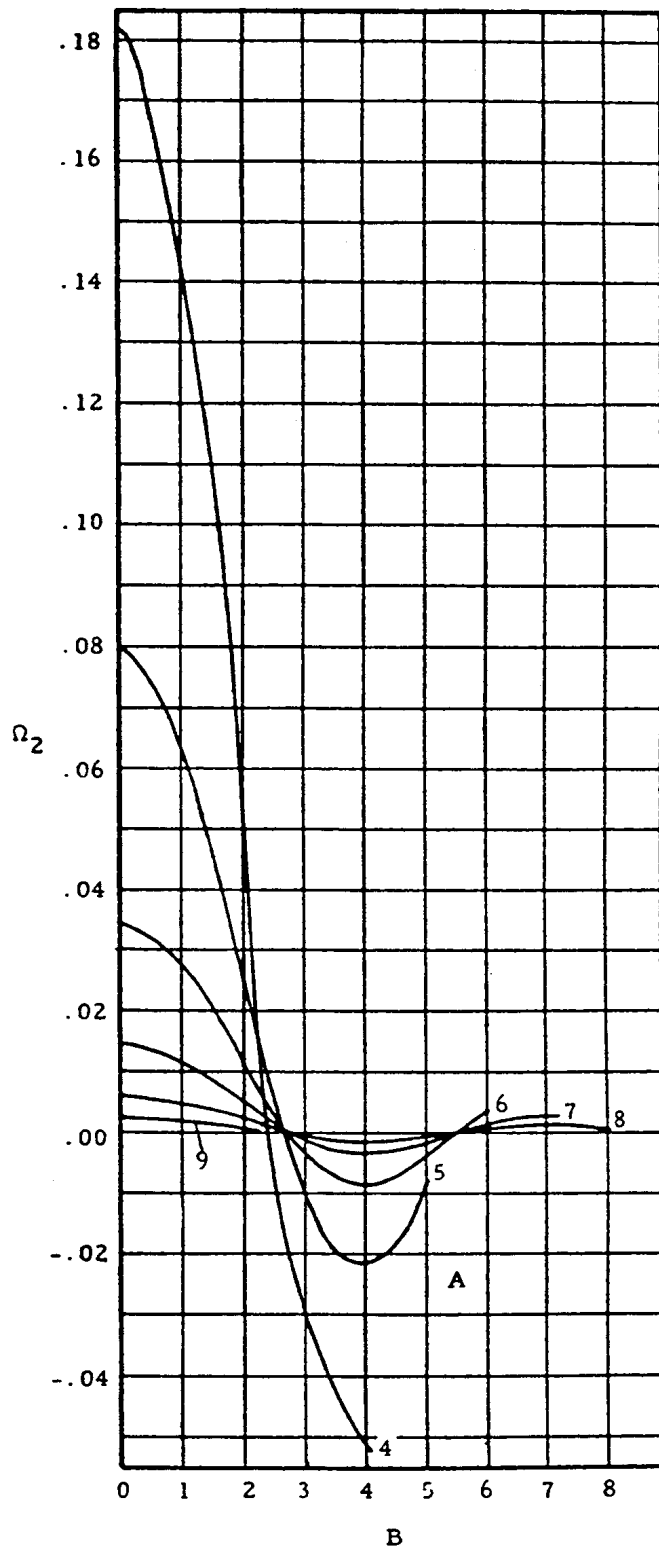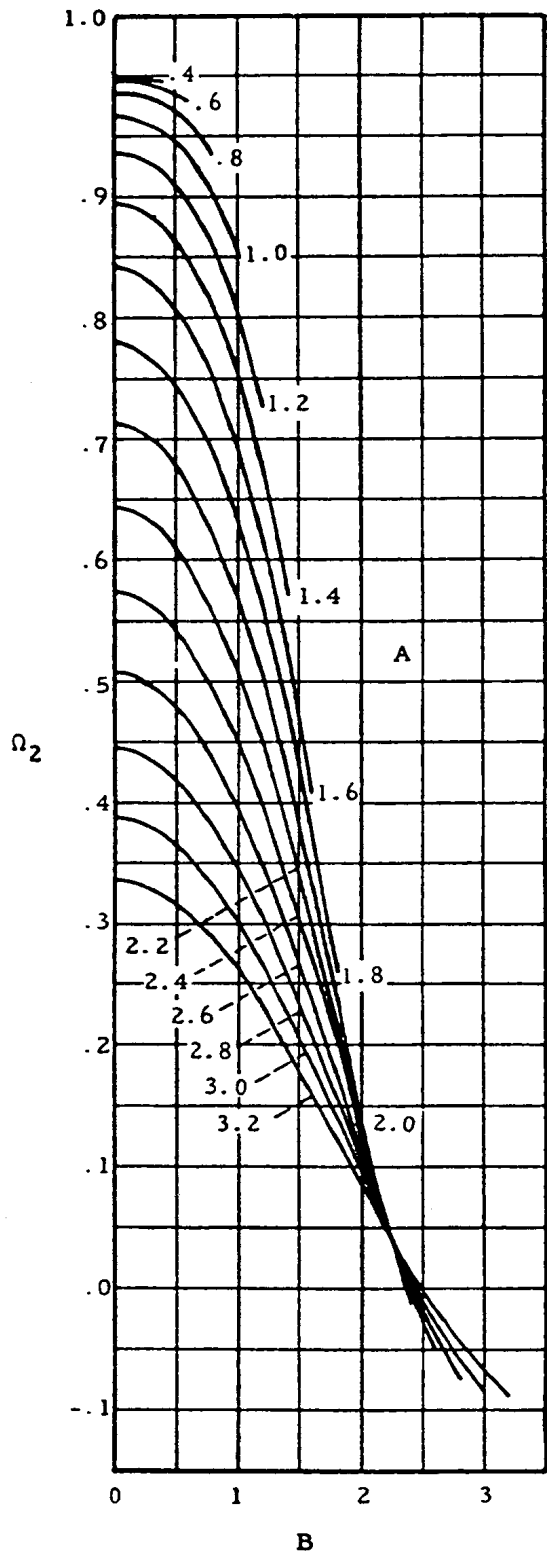
Figure 8-42. Ω_2 as a Function of A and B
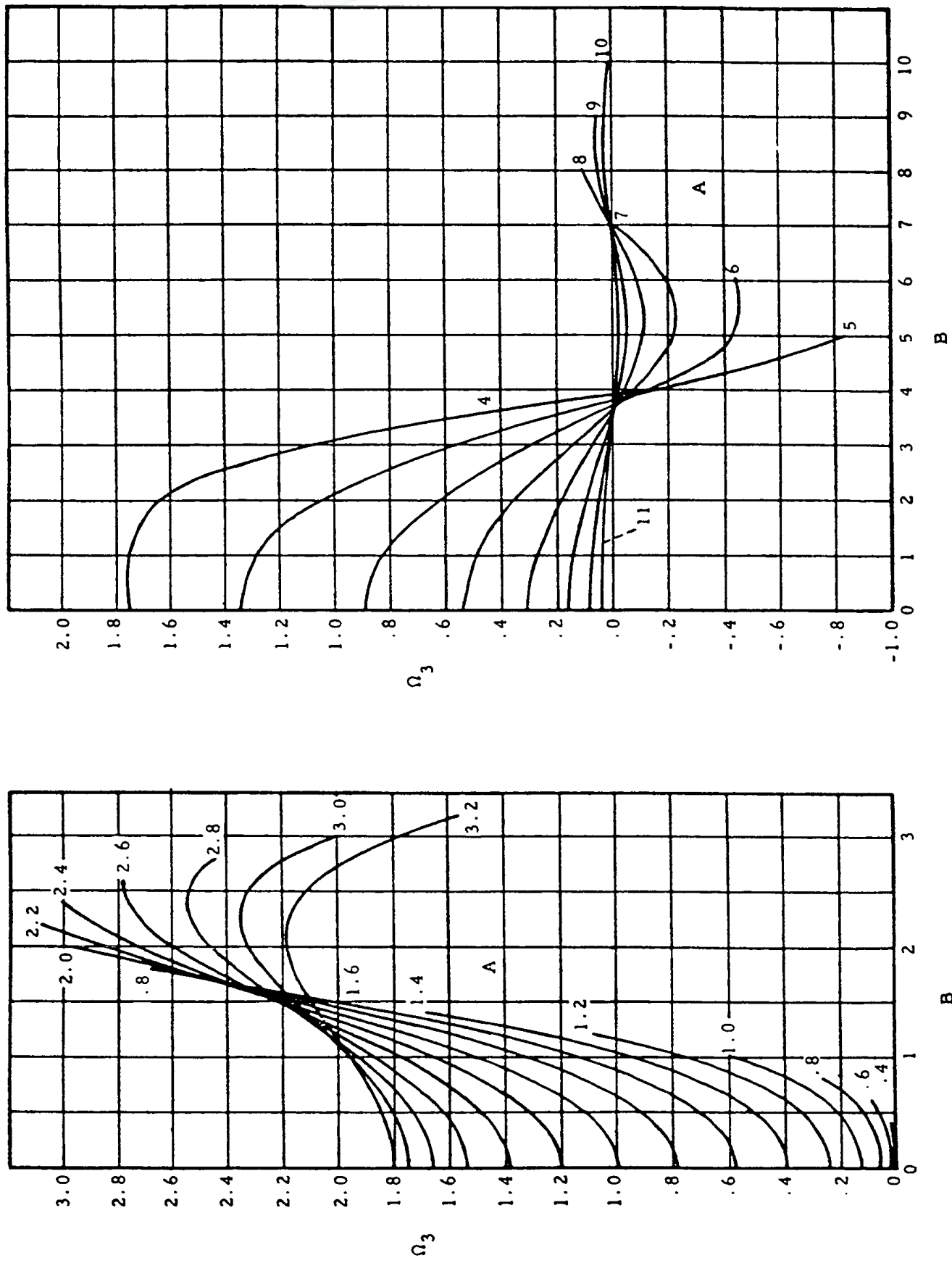
Figure 8-43. Ω_3 as a Function of A and B
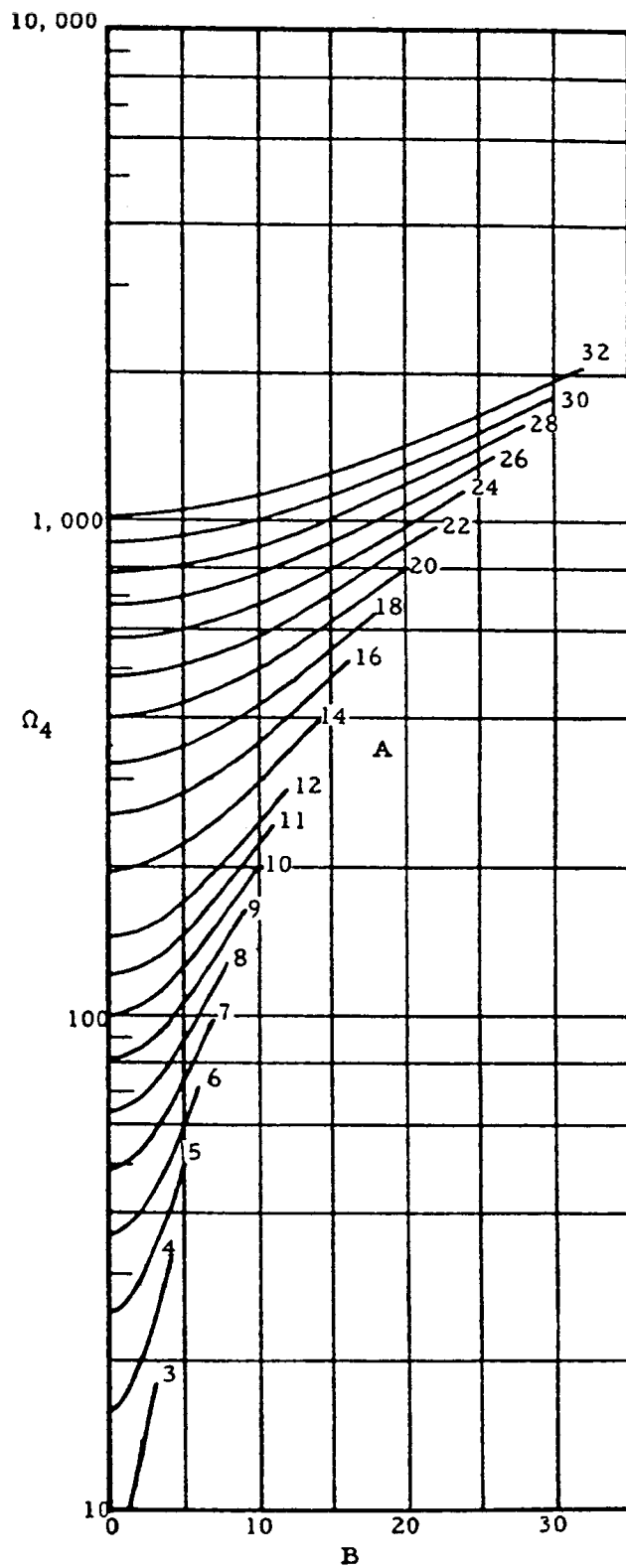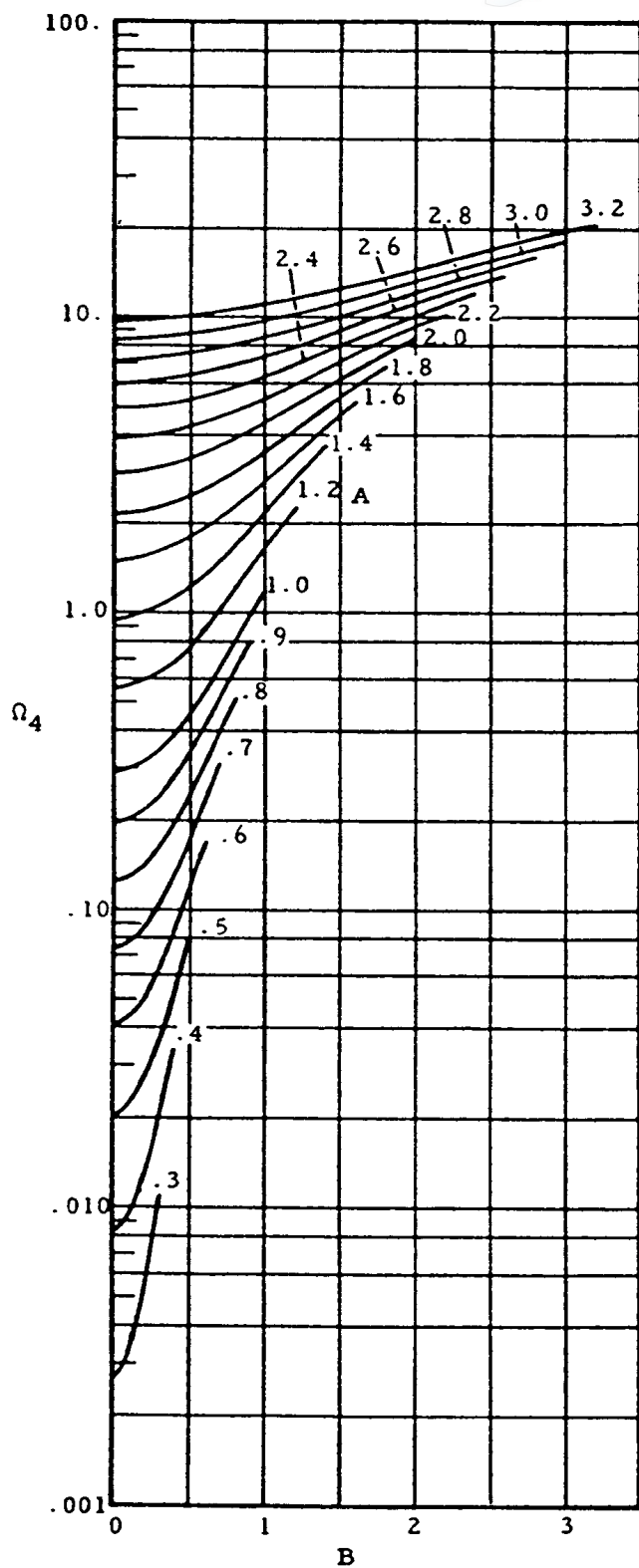
Figure 8-44. Ω_4 as a Function of A and B
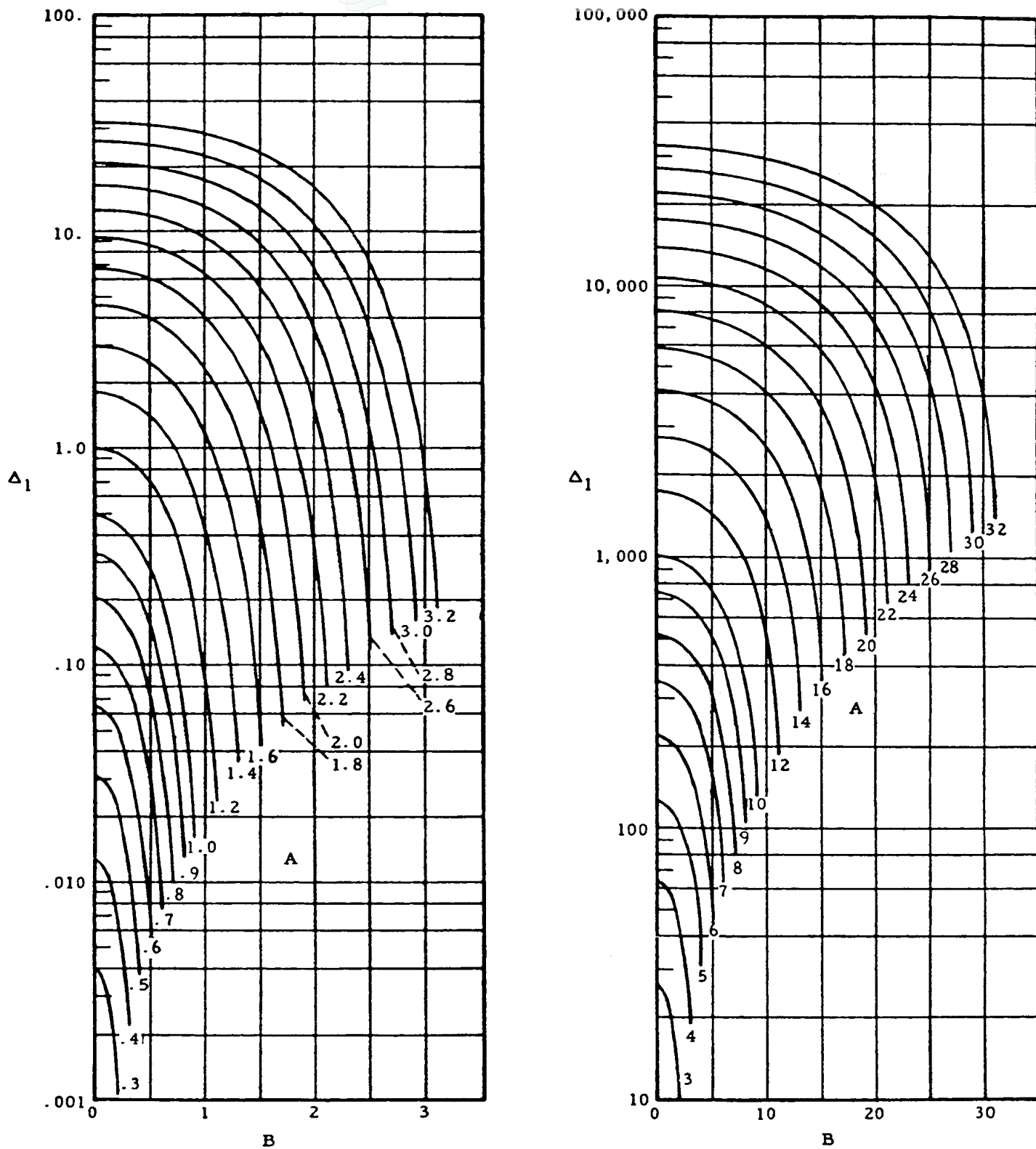
Figure 8-45. Δ_1 as a Function of A and B
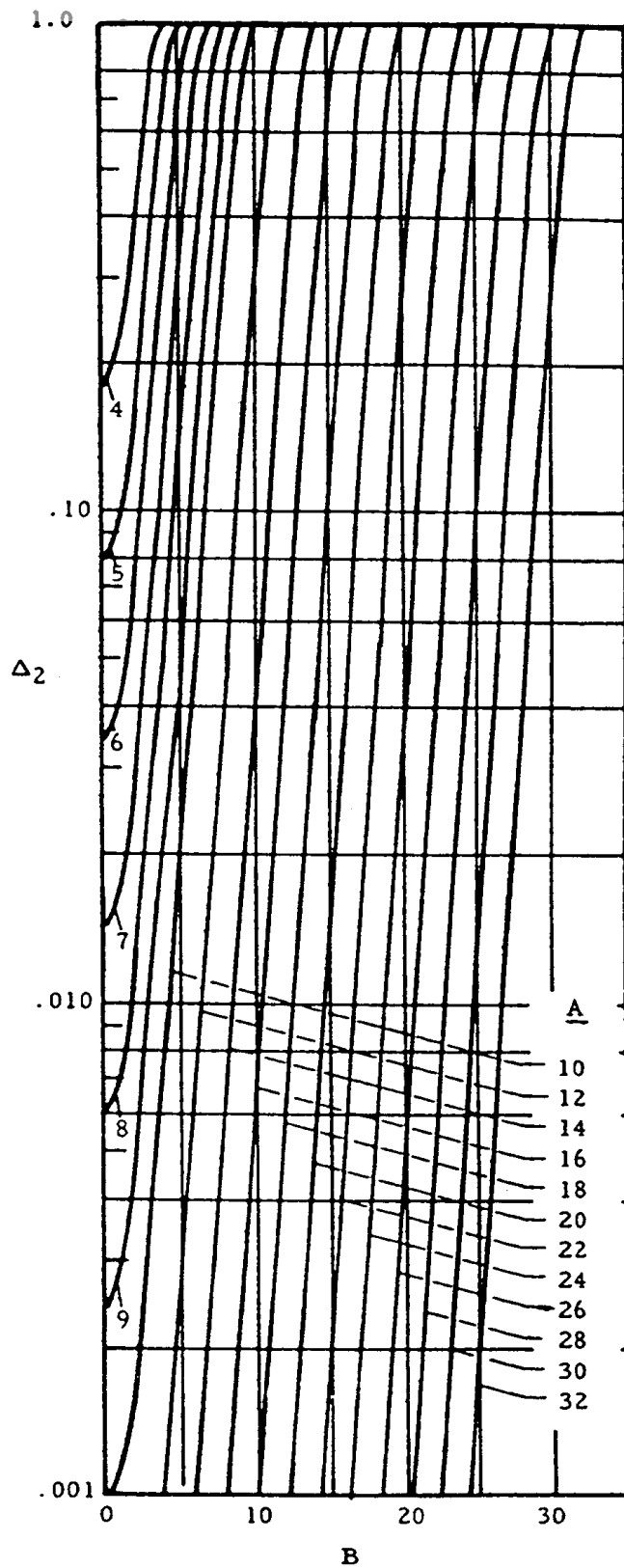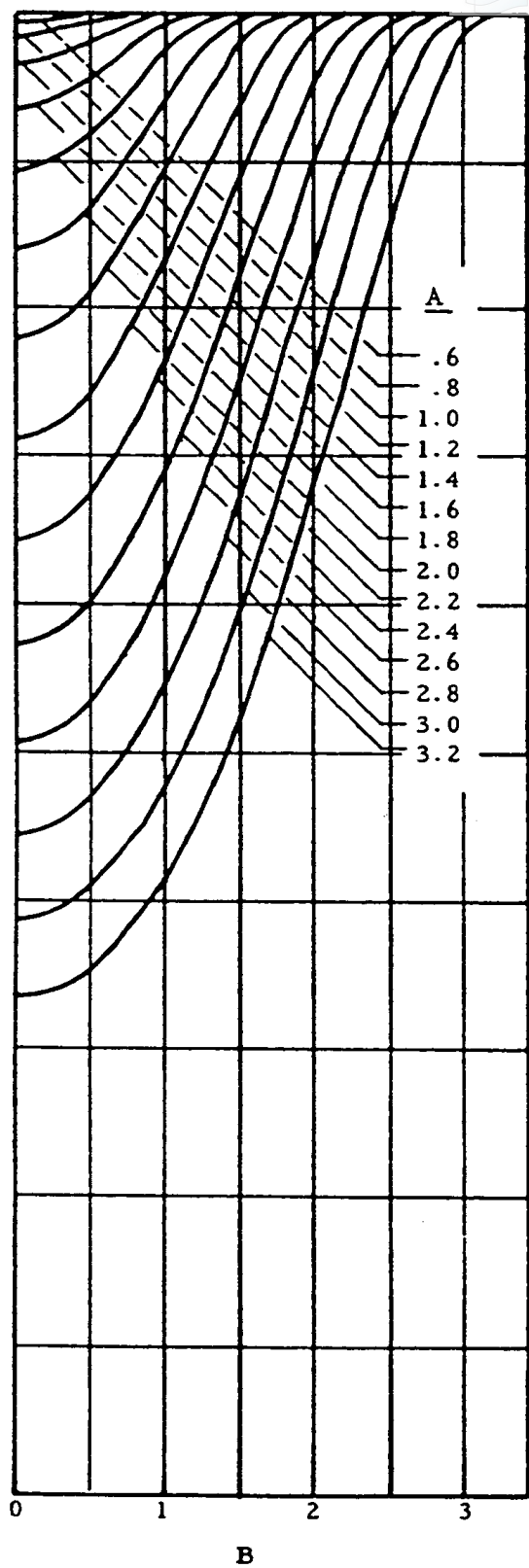
Figure 8-46. Δ_2 as a Function of A and B
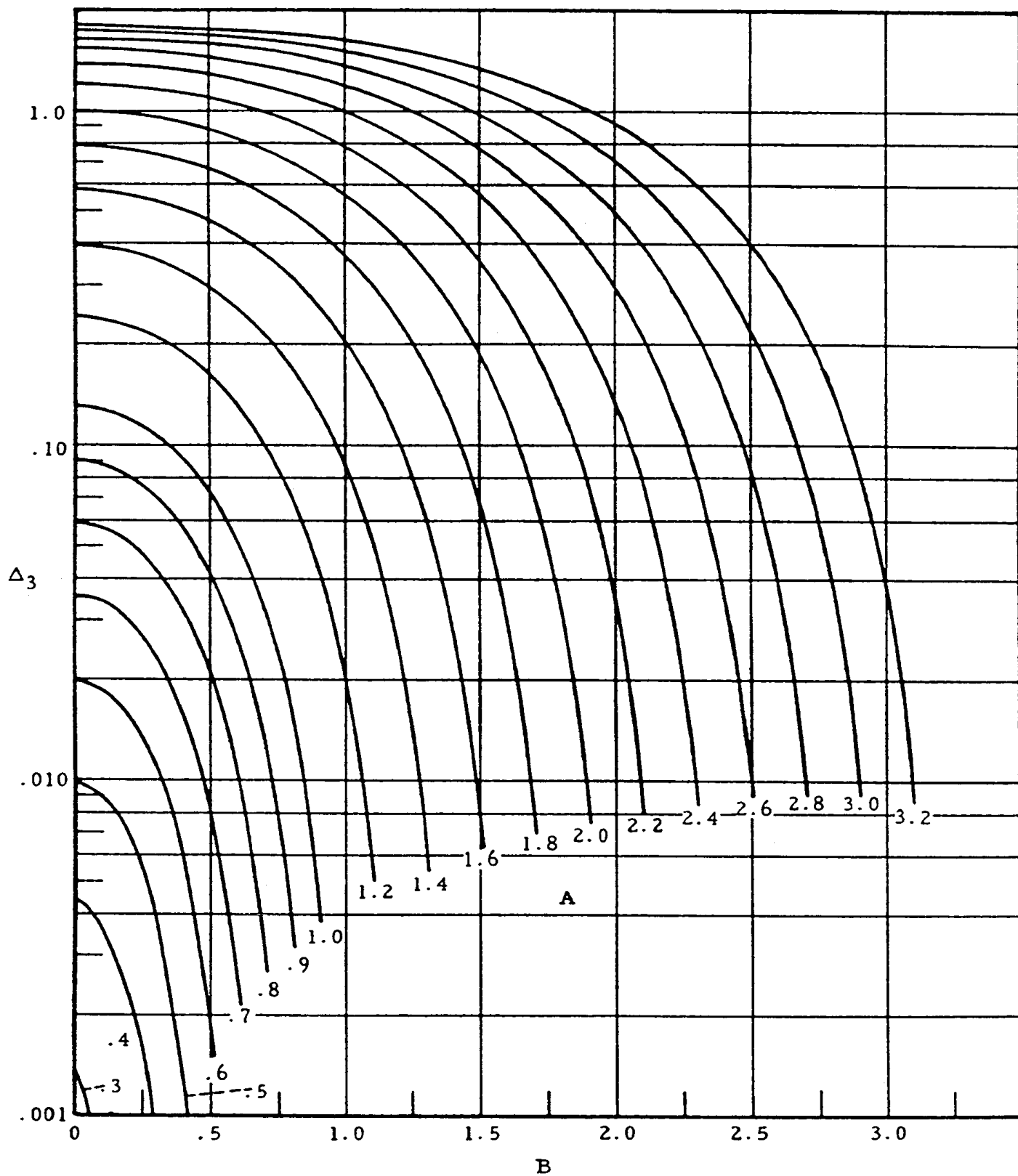
Figure 8-47. Δ_3 as a Function of A and B
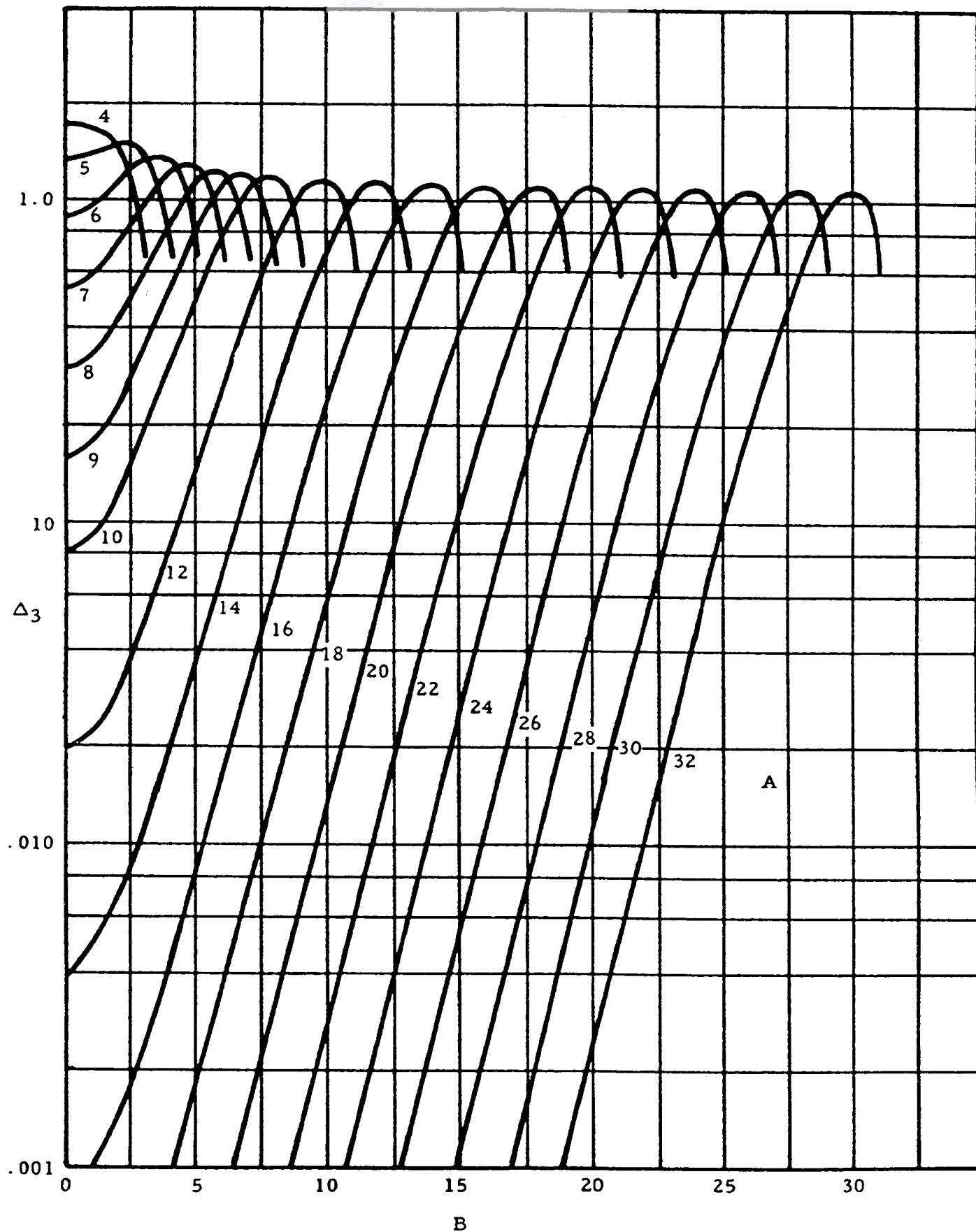
Figure 8-48. Δ_3 as a Function of A and B
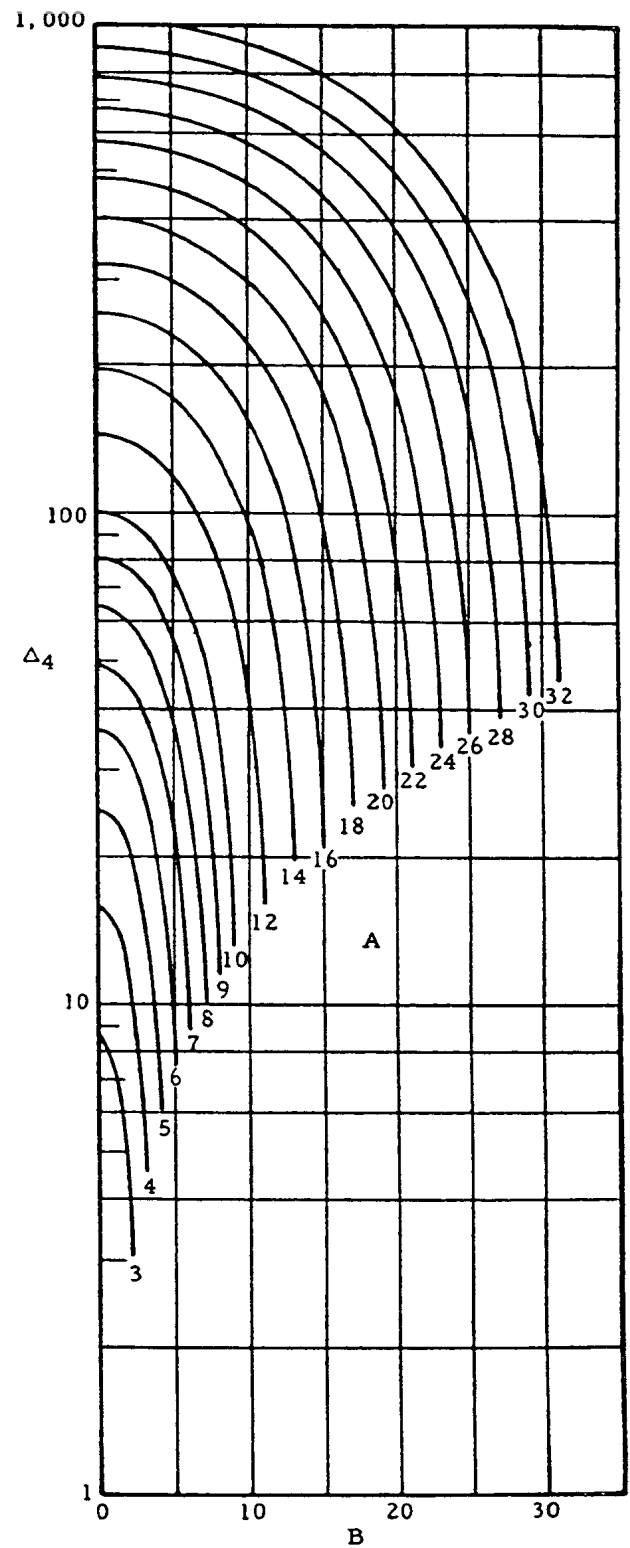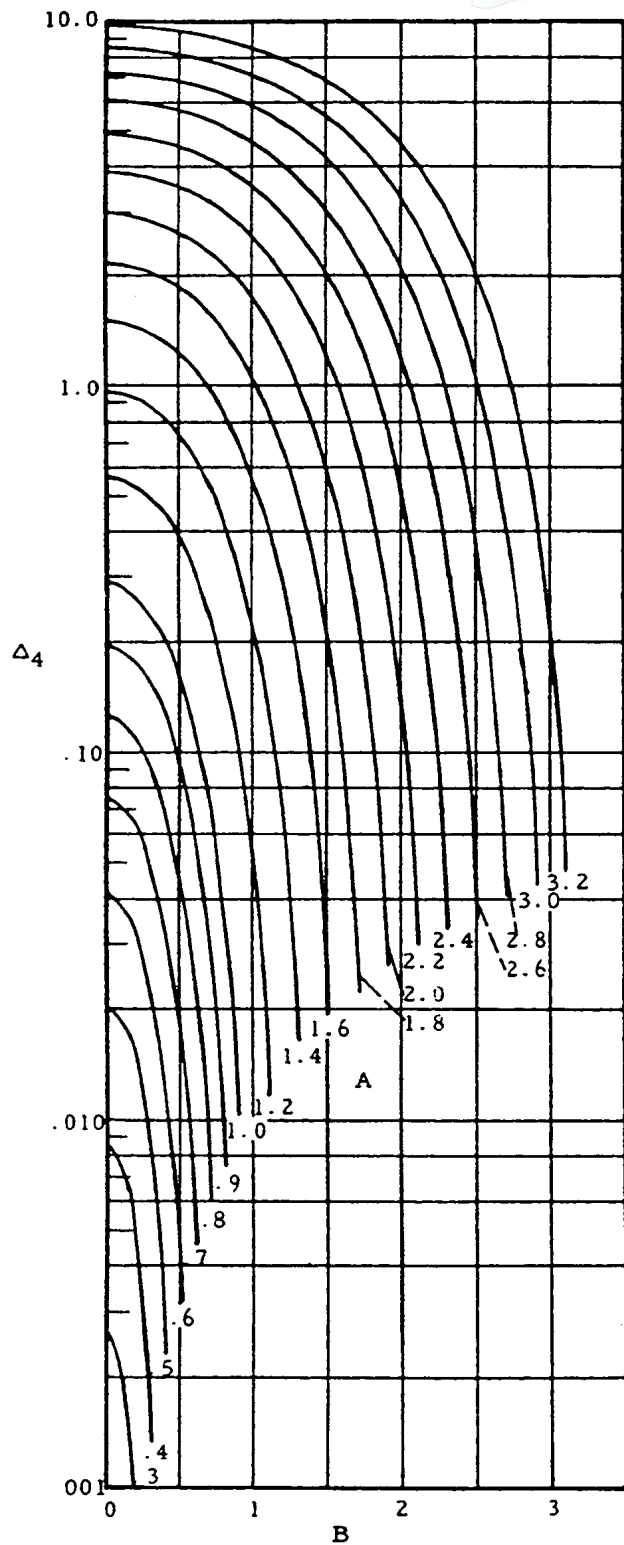
Figure 8-49. Δ_4 as a Function of A and B

The skin of a thin cylindrical pressure vessel with rings and stringers has stresses that are uniform throughout their thickness and that are given by

$$F_{sor} = \frac{T - \mu E t_s \left(\frac{\delta}{r}\right)}{t + (1-\mu^2) t_s} \qquad (8\text{-}29)$$

and

$$F_{st} = \frac{\mu T - E(t + t_s)\left(\frac{\delta}{r}\right)}{t + (1-\mu^2) t_s} \qquad (8\text{-}30)$$

In addition, the skin has a maximum axial bending stress of

$$F_{bs} = \frac{M c_s}{I_{sst}} \qquad (8\text{-}31)$$

where c_s is the distance from the neutral axis of the skin-stringer combination to the outer fiber of the skin.

The stringers have a uniform axial stress given by

$$F_{stsor} = \frac{T(1-\mu^2) + \mu E t \left(\frac{\delta}{r}\right)}{t + (1-\mu^2) t_s} \qquad (8\text{-}32)$$

in addition to a maximum bending stress of

$$F_{bst} = \frac{M c_{st}}{I_{ss}} \qquad (8\text{-}33)$$

where c_{st} is the distance from the neutral axis of the skin-stringer combination to the outer fiber of the stringer.

The rings have a circumferential stress given by

$$F_t = \frac{E_{ring} \delta_r}{R} \qquad (8\text{-}34)$$

8.3.2.2.1   Sample Problem - Stiffened Thin Cylindrical Pressure
Vessel with Internal Pressure

Given: A shell reinforced with rings and stringers under
an internal pressure of 15 psi. The vessel parameters
as shown in Figures 8-39 and 8-40 are as follows:

$r = 66$ in., $a = 11.34$ in., $t = 0.030$ in., $b = 2.7$ in.,

$A_{st} = 0.1048$ in.^{2}, $I_{sst} = 0.00493$ in.^{2}, $R = 63.2$ in.,

$t_r = 0.040$ in., $e = 0.35$ in., $b' = 2.2$ in., $A_r' = 0.276$ in.,

$c_s = 0.208$ in. to skin, $c_{st} = 0.572$ in., $E = E_{ring} = 17 \times 10^6$ psi,

$\mu = 0.316$, therefore $1 - \mu^2 = 0.9$.

Find: The stresses in the skin, stringers, and rings.

Solution: From the definitions of parameters in
Section 8.2.2.2,

$$d \equiv \frac{A_{st}}{bt} = \frac{0.1048}{2.7(.030)} = 1.29$$

$$T \equiv \frac{pr}{2} = \frac{15(66)}{2} = 495$$

$$t_s \equiv \frac{A_{st}}{b} = \frac{0.1048}{2.7} = 0.0388$$

$$t' \equiv \frac{t + t_s}{1 + (1 - \mu^2)\, ts/t} = \frac{0.030 + 0.0388}{1 + 0.9\,(0.0388/0.030)} = 0.0318$$

$$D \equiv EI_{sst} = 17 \times 10^6 (0.00493) = 8.38 \times 10^4$$

$$K \equiv \frac{\sqrt{t'\, E/D}}{2r} = \frac{\sqrt{0.0318\,(17 \times 10^6)(8.38 \times 10^4)}}{2(66)} = 0.01925$$

$$\frac{T}{4D} \equiv \frac{495}{4(8.38 \times 10^4)} = 0.001477$$

$$\alpha \equiv \sqrt{K + \frac{T}{4D}} = \sqrt{0.01925 + 0.001477} = 0.144$$

$$\beta \equiv \sqrt{\left| K - \frac{T}{4D} \right|} = \sqrt{\left| 0.01925 - 0.001477 \right|} = 0.1333$$

$$A \equiv \frac{\alpha a}{2} = \frac{0.144(11.34)}{2} = 0.817$$

$$B \equiv \frac{\beta a}{2} = \frac{0.1333(11.34)}{2} = 0.756$$

$$P \equiv \frac{pr^2}{t'E} \left[1 - \frac{\mu t'}{2(t + t_s)} \right] = \frac{15(66)^2}{0.0318(17 \times 10^6)}$$

$$\left[1 - \frac{0.316(0.318)}{2(0.030 + 0.038)} \right] = 0.1122$$

$$A_r \equiv \frac{r^2}{\frac{b}{b'}\left(\frac{e}{t_r}\right)^3 (1 + \mu^2) + \frac{r^2}{A_r'}} = \frac{(66)^2}{\frac{2.7}{2.2}\left(\frac{0.35}{0.40}\right)^3 (0.9)\frac{(63.2)^2}{0.276}}$$

$$= 0.286$$

$$Q \equiv \frac{A_r E_{ring} a^3}{32 D_r^2} = \frac{0.286(17 \times 10^6)(11.34)^3}{32(8.38 \times 10^4)(66)^2} = 0.607$$

Since $K > T/4D$, Equations (8-25) through (8-28)
may be used to obtain deflections and moments.
From Figures 8-41 through 8-44 with A = 0.817
and B = 0.756,

$$\Omega_1 = 0.76, \quad \Omega_2 = 0.94, \quad \Omega_3 = 0.24, \quad \text{and} \quad \Omega_4 = 0.49$$

These values may now be substituted into Equations
(8-25) through (8-28) to obtain the following:

Deflection at ring = $\delta_r = \dfrac{-P}{1 + \dfrac{Q}{\Omega_1}} = \dfrac{-.1122}{1 + \dfrac{0.607}{0.76}}$

$$= 0.0624 \text{ in. (outward)}$$

Deflection at midspan $= \delta_s = -P \left(1 - \dfrac{\Omega_2}{1 + \dfrac{\Omega 1}{Q}} \right)$

$= -0.1122 \left(1 + \dfrac{0.94}{1 + \dfrac{0.76}{0.607}} \right) = -0.0654$ in. (outward)

Moment at ring $= M_{sstr} = \dfrac{4 \, PD\Omega_4}{a^2 \left(1 + \dfrac{\Omega 1}{Q} \right)}$

$= \dfrac{4 \times 0.1122(8.38 \times 10^4)(0.49)}{(11.34)^2 \left(1 + \dfrac{0.76}{0.607} \right)} = 63.7$ in. -lb/in.

Moment at midspan $= M_{ssts} = \dfrac{M_{ssr}\Omega_3}{\Omega_4}$

$= \dfrac{-63.7(0.24)}{(0.49)} = -31.2$ in-lb./in.

Stresses in Skin

The stresses in the skin consist of

(1) a meridional membrane stress, F_{smer}

(2) an axial bending stress F_{bs}, and

(3) a tangential membrane stress F_{mt}.

These must be computed at both the midspan and
the ring. From Equation (8-29),

$$F_{smer} = \dfrac{T - \mu \, Et_s(\delta/r)}{t + (1-\mu^2) \, t_s} = \dfrac{495 - 0.316(17 \times 10^6)(.0388)\delta/66}{0.030 + 0.9(0.0388)}$$

$= 7,630 - 48,660 \, \delta$

At the midspan,

$F_{smer} = 7,630 - 48,660 \, \delta_s = 7,630 + 48,660 \, (0.0654)$

$= 10,810$ psi

At the ring,

$$F_{smr} = 7,630 - 48,660 \delta_r = 7,630 + 48,660 (0.0624)$$

$$= 10,670 \text{ psi}$$

From Equation (8-31),

$$F_{bs} = \frac{M c_s}{I_{sst}} = \frac{M(0.208)}{0.00493} = 42.1M$$

At the midspan,

$$F_{bs} = 42.1 M_{ssts} = 42.1 (31.2) = 1,320 \text{ psi}$$

At the ring,

$$F_{bs} = 42.1 M_{sstr} = 42.1 (-63.7) = -2,680 \text{ psi}$$

From Equation (8-30),

$$F_{st} = \frac{\mu T - E(t+t_s)\delta/r}{t + (1-\mu^2) t_s} = \frac{(0.316)(495)}{.030 + (0.9)(0.0388)}$$

$$\frac{(17 \times 10^6)(0.030 + 0.0388)\delta/66}{.030 + (0.9)(0.0388)} = 2,410 - 273,000 \delta$$

At the midspan,

$$F_{st} = 2,410 - 273,000 (0.0654) = 20,260 \text{ psi}$$

At the ring,

$$F_{st} = 2,410 - 273,000 (0.0624) = 19,440 \text{ psi}$$

The maximum meridional stress in the skin at the midspan is given by

$$F_{msrmax} = F_{smr} + F_{bs} = 10,810 + 1,320 = 12,130 \text{ psi}$$

and that at the ring is

$$F_{msrmax} = F_{smr} + F_{bs} = 10,670 - 2,680 = 7,990 \text{ psi}$$

The critical stress occurs in the skin at the midspan where both the meridional and circumferential stresses are greatest.

Stresses in Stringer

The stresses in the stringers consist of

(1) a uniform axial stress, F_{stor}, and

(2) an axial bending stress, F_{bst}.

From Equation (8-32),

$$F_{stor} = \frac{T(1-\mu^2) + \mu\, Et(\delta/r)}{t + (1-\mu^2)\, t_s} = \frac{495\,(0.9)}{(0.3) + (0.9)(0.388)}$$

$$+ \frac{(0.316)(17 \times 10^6)(0.3)(\delta/66)}{(0.3) + (0.9)(0.388)} = 6,860 + 37,620\,\delta$$

At the midspan

$$F_{stor} = 6,860 + 37,620\,\delta = 6,860 - 37,620(0.0654) = 4,400 \text{ psi}$$

At the ring,

$$F_{stor} = 6,860 + 37,620\,\delta = 6,860 - 37,620(0.0624)$$
$$= 4,510 \text{ psi}$$

From Equation (8-33),

$$F_{bst} = \frac{M\, c_{st}}{I_{ss}} = \frac{M(0.572)}{0.00493} = 116M$$

At the midspan,

$$F_{bst} = 116\, M_{ssts} = 116(-31.2) = -3,730 \text{ psi}$$

At the ring,

$$F_{bst} = 116\, M_{sstr} = 116(63.7) = 7,410 \text{ psi}$$

The maximum stress in the stringers is given by

$$F_{ssmax} = F_{stor} + F_{bst}$$

This occurs at the ring where

$$F_{s \, r \, max} = 4,510 + 7,410 = 11,910 \text{ psi}$$

Stresses in Ring

The rings have a circumferential stress F_t. From Equation (8-34),

$$F_t = \frac{E_{ring} \, \delta_r}{R} = \frac{(17 \times 10^6)(0.0624)}{63.2} = 16,770 \text{ psi}$$

8.4   Thick Pressure Vessels

If the ratio of the minimum radius of curvature of a wall to its thickness is less than ten, stresses may no longer be considered constant throughout the wall thickness and radial stresses may not be ignored. Thus, the equations for thin-walled pressure vessels that were developed with these assumptions are no longer valid. This section presents solutions for the stresses in thick-walled cylinders and spheres.

Thick vessels, other than cylindrical and spherical ones, have bending stresses even if there are no discontinuities present. The analysis of these stresses is difficult and is not established on a satisfactory basis as yet. Thus, it is best to determine the intensity of the maximum stresses that exist in unconventional designs by strain gauge measurements or other experimental means.

8.4.1   Thick Cylindrical Pressure Vessels

Figure 8-50 shows a cross section of a thick cylindrical pressure vessel of internal radius a and external radius b.
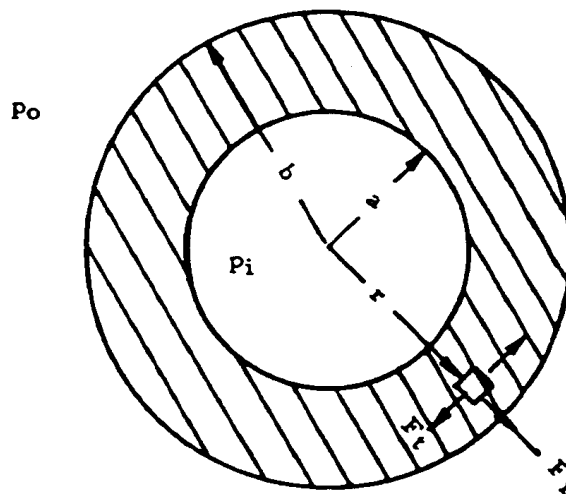
Figure 8-50. Thick Cylindrical Pressure Vessel

The radial, tangential, and axial stresses, F_r, F_t, and F_{xr}, in such a cylinder are given by Equations (8-35), (8-36), and (8-37), respectively.

$$F_r = \frac{a^2 p_i - b^2 p_o}{b^2 - a^2} - \frac{a^2 b^2 (p_i - p_o)}{(b^2 - a^2) r^2} \qquad (8\text{-}35)$$

$$F_t = \frac{a^2 p_i}{b^2 - a^2} \left(1 - \frac{b^2}{r^2} \right) \qquad (8\text{-}36)$$

$$F_{xr} = \frac{p_i a^2 - p_o b^2}{b^2 - a^2} \qquad (8\text{-}37)$$

In order for Equation (8-37) to apply, the point considered must be far enough removed from the ends for St. Venant's principle to apply.

8.4.1.1   Thick Cylindrical Pressure Vessels Under Internal Pressure Only

If $p_o = 0$, Equations (8-35) and (8-36) reduce to

$$F_r = \frac{a^2 p_i}{b^2 - a^2} \left(1 - \frac{b^2}{r^2} \right) \qquad (8\text{-}38)$$

and

$$F_t = \frac{a^2 p_i}{b^2 - a^2} \left(1 + \frac{b^2}{r^2} \right) \qquad (8\text{-}39)$$

Both of these stresses have maximum magnitudes at $r = a$. If the maximum shear stress theory of failure is to be used, the design equation becomes

$$F_{smax} = \frac{F_{tmax} - F_{rmax}}{2} = \frac{b^2}{b^2 - a^2} p_i \qquad (8\text{-}40)$$

8.4.1.2   Thick Cylindrical Pressure Vessels Under External Pressure Only

If $p_i = 0$, Equations (8-35) and (8-36) reduce to

$$F_r = \frac{-p_o b^2}{b^2 - a^2} \left(1 - \frac{a^2}{r^2} \right) \qquad (8\text{-}41)$$

and

$$F_t = \frac{-P_o b^2}{b^2 - a^2} \left(1 + \frac{a^2}{r^2}\right)$$ (8-42)

In this case, both the tangential and radial stresses are always compressive, with the former always the larger of the two. The maximum compressive stress occurs at the inner surface of the cylinder where the radial stress is equal to zero. This maximum compressive stress is given by

$$F_{tmax} = \frac{-2b^2 P_o}{b^2 - a^2}$$ (8-43)

8.4.1.3 Sample Problems - Thick Cylindrical Pressure Vessel

Given: The pressure vessel shown in Figure 8-51.

$P_o = 15$ psi

$b = 15$ $a = 10$

$p_i = 10000$ psi
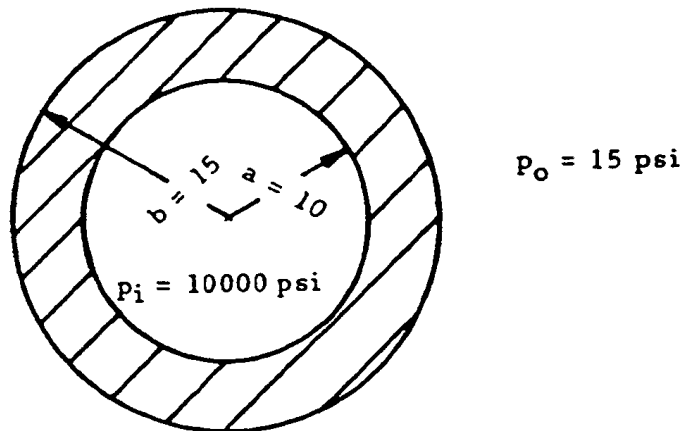
Figure 8-51. Thick Cylindrical Pressure Vessel

Find: The maximum shear stress in the vessel.

Solution: Assume the external pressure is negligible and apply Equation (8-40). Thus,

$$F_{smax} = \left(\frac{b^2}{b^2 - a^2}\right) p_i = \frac{(15)^2 (10,000)}{[(15)^2 - (10)^2]} = 22,500 \text{ psi}$$

8.4.2 Thick Spherical Pressure Vessels

The radial and tangential stresses at a distance r from the center of a spherical pressure vessel of inner radius a and outer radius b are given by Equations (8-44) and (8-45).

$$F_r = \frac{P_o b^3 (r^3 - a^3)}{r^3 (a^3 - b^3)} + \frac{P_i (b^3 - r^3)}{r^3 (a^3 - b^3)}$$ (8-44)

$$F_t = \frac{p_o b^3 (2r^3 + a^3)}{2r^3 (a^3 - b^3)} - \frac{p_i a^3 (2r^3 + b^3)}{2r^3 (a^3 - b^3)} \tag{8-45}$$

The terminology here is the same as that shown in Figure 8-50 for cylindrical pressure vessels.

If $p_o = 0$,

$$F_t = \frac{p_i a^3}{2r^2} \frac{(2r^3 + b^3)}{b^3 - a^3} \tag{8-46}$$

and the greatest tangential tension is at the inner surface at which

$$F_{t_{max}} = \frac{p_i}{2} \frac{2a^3 + b^3}{b^3 - a^3} \tag{8-47}$$

8.5 Anisotropic Pressure Vessels

The use of glass filaments in the construction of pressure vessels offers several advantages. Glass has an ultimate strength of approximately 300,000 lb/in.^{2} in the direction of the fiber when it is drawn into fine filaments. In order to fully utilize this high unidirectional strength, however, it is necessary to run the fiber in the direction of the maximum principal stress. This is done by winding the fibers on a mandrel. During the winding process, the filaments are impregnated with resin which, after curing, will develop sufficient shear strength to realize the high tensile strength of the fibers. In analyzing these structures, it is assumed that the fibers sustain the primary loads with only the secondary loads being resisted by the resin binder.

Since the principal stresses will vary in an actual vessel, the fibers may actually be wrapped at more than a single wrap angle as may be seen in Figure 8-52.
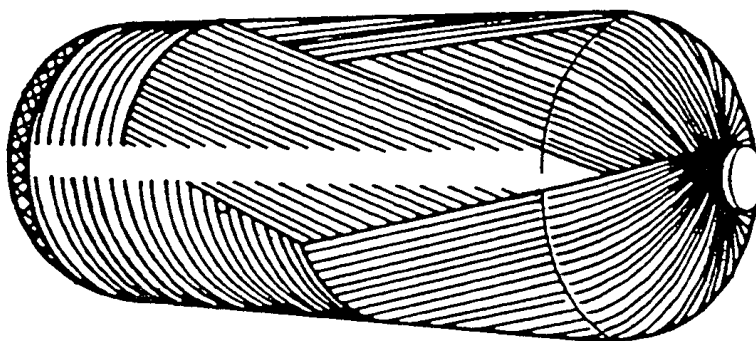
Figure 8-52. Filament-Wound Pressure Vessel

For a thin cylindrical pressure vessel, all stresses other than membrane stresses are negligible. The optimum wrap angle is 55 degrees as shown in Figure 8-53.
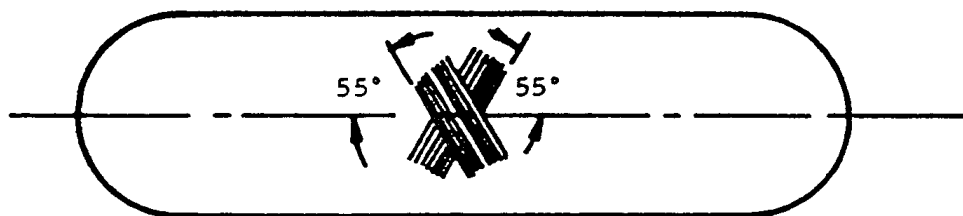
Figure 8-53. Optimum Wrap Angle for Thin Cylindrical Pressure Vessel

In addition to providing a structure of high strength-to-weight ratio, the glass pressure vessels offer other advantages. Connections can be eliminated and end closures, skirts, etc., fabricated as a single unit. In addition, pressure vessels may be made in any proportions and sizes over wide ranges.

9. LUG ANALYSIS

9.1 Introduction to Lug Analysis

Lugs are connector-type elements widely used as structural supports for pin connections. In the past, the lug strength was overdesigned since weight and size requirements were for the most part unrestricted. However, the refinement of these requirements have necessitated conservative methods of design.

This section presents static strength analysis procedures for uniformly loaded lugs and bushings, for double shear joints, and for single shear joints, subjected to axial, transverse, or oblique loading. Also listed is a section which applies to lugs made from materials having ultimate elongations of at least 5% in any direction in the plane of the lug. Modifications for lugs with less than 5% elongation are also presented. In addition, a short section on the stresses due to press fit bushings is presented.

9.2 Lug Analysis Nomenclature

F_{bru_L} = Lug ultimate bearing stress
F_{bry_L} = Lug yield bearing stress
F_{tux} = Cross grain tensile ultimate stress of lug material
F_{tyx} = Cross grain tensile yield stress of lug material
F_{bru} = Allowable ultimate bearing stress, MHB5
F_{bry} = Allowable yield bearing stress, MHB5
F_{tu} = Ultimate tensile stress
F_{nu_L} = Allowable lug net-section tensile ultimate stress
F_{ny_L} = Allowable lug net-section tensile yield stress
F_{bry_B} = Allowable bearing yield stress for bushings
F_{cy_B} = Bushing compressive yield stress
F_{bru_B} = Allowable bearing ultimate stress for bushings
F_{su_p} = Ultimate shear stress of the pin material
F_{tu_p} = Pin ultimate tensile stress
F_{tu_T} = Allowable ultimate tang stress
$F_{br_{max_L}}$ = Maximum lug bearing stress
$F_{br_{max_B}}$ = Maximum bushing bearing stress
$F_{s_{max_p}}$ = Maximum pin shear stress
$F_{b_{max_p}}$ = Maximum pin bending stress
P_{bru_L} = Allowable lug ultimate bearing load
P_{nu_L} = Allowable lug net-section ultimate load
P_{u_B} = Allowable bushing ultimate load
P_{u_L} = Allowable design ultimate load
$P_{u_{L_B}}$ = Allowable lug-bushing ultimate load
P_{us_p} = Pin ultimate shear load
P_{ub_p} = Pin ultimate bending load

P_{ub_p}	=	"Balanced design" pin ultimate bending load
P_{all}^{max}	=	Allowable joint ultimate load
P_T	=	Lug tang strength
P_{tru_L}	=	Allowable lug transverse ultimate load
P_{tru_B}	=	Allowable bushing transverse ultimate load
K_n	=	Net-tension stress coefficient
K_{b_p}	=	Plastic bending coefficient for pin
K_{b_T}	=	Plastic bending coefficient for tang
K_{br_L}	=	Plastic bearing coefficient for lug
K_{b_L}	=	Plastic bending coefficient for lug
K_{tru}	=	Transverse ultimate load coefficient
K_{try}	=	Transverse yield load coefficient
M_{max_p}	=	Maximum pin bending moment
M_{u_p}	=	Ultimate pin failing moment
A	=	Area, in.^{2}
a	=	Distance from edge of hole to edge of lug, inches
B	=	Ductility factor for lugs with less than 5% elongation
b	=	Effective bearing width, inches
D	=	Hole diameter of pin diameter, inches
E	=	Modulus of elasticity, psi
e	=	Edge distance, inches
f	=	Stress, psi
f_a	=	Cyclic stress amplitude on net section of given lug, lbs/in.^{2}
f_m	=	Mean cyclic stress on net section of given lug, lbs/in.^{2}
f_{max}	=	Maximum cyclic stress on net section of given lug, lbs/in.^{2}
f_{min}	=	Minimum cyclic stress on net section of given lug, lbs/in.^{2}
g	=	Gap between lugs, inches
$h_1..h_4$	=	Edge distances in transversely loaded lug, inches
h_{av}	=	Effective edge distance in transversely loaded lug
K	=	Allowable stress (or load) coefficient
k_1, k_2, k_3	=	Fatigue parameters
M	=	Bending moment, in.-lbs.
N	=	Fatigue life, number of cycles
P	=	Load, lbs.
R	=	Stress ratio, f_{min}/f_{max}
t_B	=	Bushing wall thickness, inches
t	=	Lug thickness, inches
w	=	Lug width, inches
α	=	Angle of load to axial direction, degrees
ϵ	=	Strain, inches/inch
ρ	=	Density, lbs/in.^{3}

Subscripts

all	= Allowable	opt	= Optimum
ax	= Axial	p	= Pin
B	= Bushing	s	= Shear
b	= Bending	T	= Tang
br	= Bearing	t	= Tensile
c	= Compression	tr	= Transverse
L	= Lug	u	= Ultimate
max	= Maximum	x	= Cross grain
n	= Net tensile	y	= Yield
o	= Oblique	1, 2	= Female and male lugs

9.3 Lug and Bushing Strength Under Uniform Axial Load

Axially loaded lugs in tension must be checked for bearing strength and
for net-section strength. The bearing strength of a lug loaded in tension, as
shown in Figure 9-1, depends largely on the interaction between bearing,
shear-out, and hoop-tension stresses in the part of the lug ahead of the pin.
The net-section of the lug through the pin must be checked against net-tension
failure. In addition, the lug and bushing must be checked to ensure that the
deformations at design yield load are not excessive.
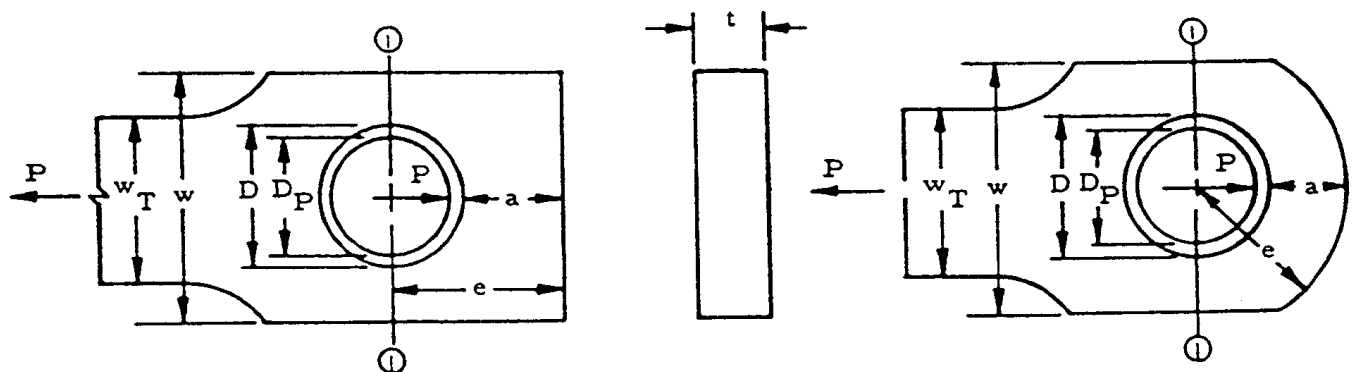
Figure 9-1. Schematics of Lugs Loaded in Tension

9.3.1 Lug Bearing Strength Under Uniform Axial Load

The bearing stresses and loads for lug failure involving bearing,
shear-tearout, or hoop tension in the region forward of the net-section
in Figure 9-1 are determined from the equations below, with an allowable
load coefficient (K) determined from Figures 9-2 and 9-3. For values of
e/D less than 1.5, lug failures are likely to involve shear-out or hoop-
tension; and for values of e/D greater than 1.5, the bearing is likely to be
critical. Actual lug failures may involve more than one failure mode, but

such interaction effects are accounted for in the values of K. The lug ultimate bearing stress (F_{bru_L}) is

$$F_{bru_L} = K \frac{a}{D} F_{tux} , \quad (e/D < 1.5) \qquad (9\text{-}1a)$$

$$F_{bru_L} = K F_{tux} , \quad (e/D \geqq 1.5) \qquad (9\text{-}1b)$$

The graph in Figure 9-2 applies only to cases where D/t is 5 or less, which covers most of the cases. If D/t is greater than 5, there is a reduction in strength which can be approximated by the curves in Figure 9-3. The lug yield bearing stress (F_{bry_L}) is

$$F_{bry_L} = K \frac{a}{D} F_{tyx}, \quad (e/D < 1.5) \qquad (9\text{-}2a)$$

$$F_{bry_L} = K F_{tyx}, \quad (e/D \geqq 1.5) \qquad (9\text{-}2b)$$
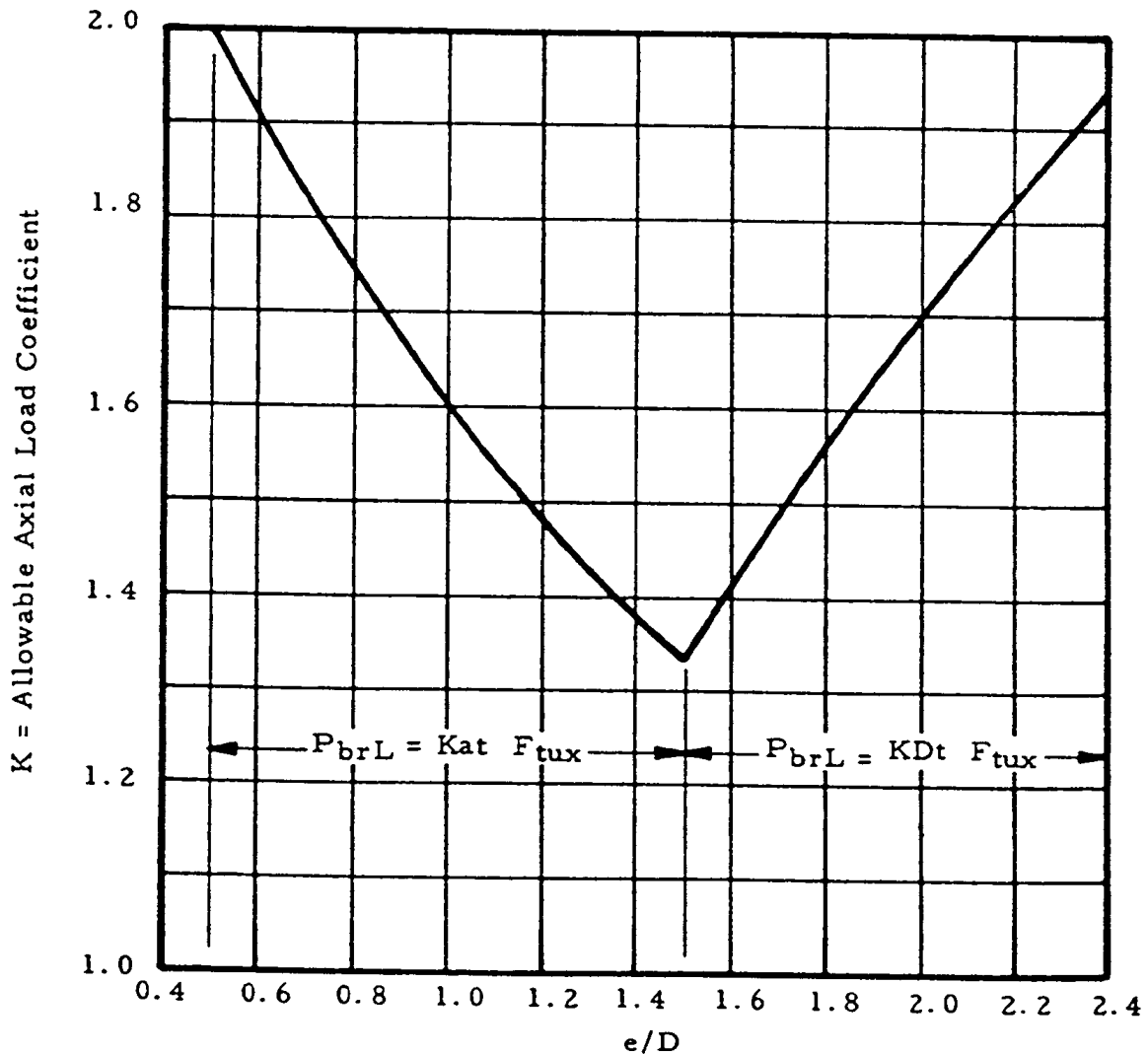
Figure 9-2. Allowable Uniform Axial Load Coefficient
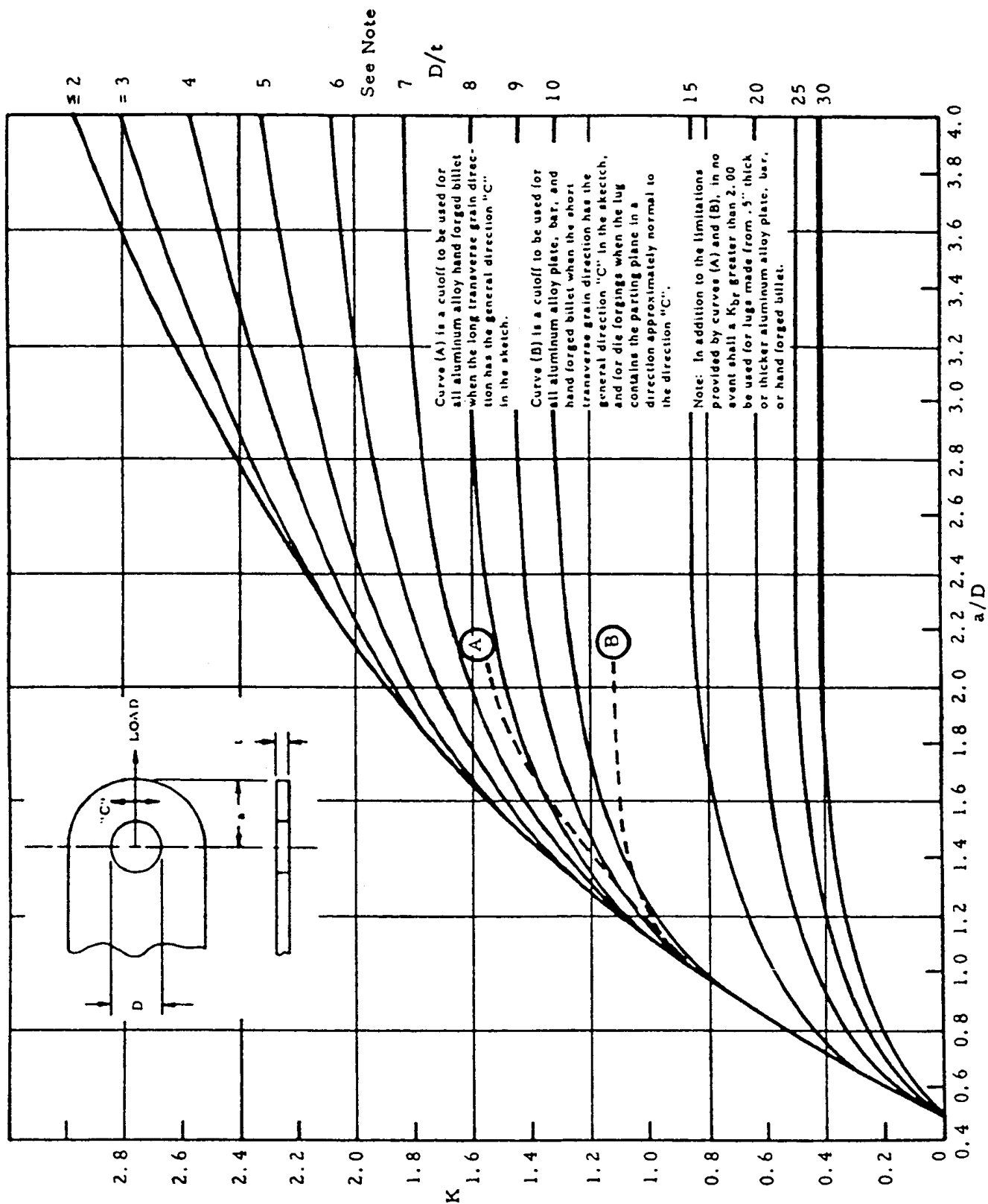
Figure 9-3. Bearing Efficiency Factors of Lugs, Aluminum Alloys, and Alloy Steel with F_{tu} <160 KSI

The allowable lug ultimate bearing load (P_{bru_L}) for lug failure in bearing, shear-out, or hoop tension is

$$P_{bru_L} = F_{bru_L} Dt, \quad (\text{if } F_{tux} \leq 1.304 F_{tyx}) \qquad (9\text{-}3a)$$

$$P_{bru_L} = 1.304 F_{bry_L} Dt, \quad (\text{if } F_{tux} > 1.304 F_{tyx}) \qquad (9\text{-}3b)$$

P_{bru_L}/Dt should not exceed either F_{bru} or $1.304 F_{bry}$, where F_{bru} and F_{bry} are the allowable ultimate and yield bearing stresses for the lug material for $e/D = 2.0$, as given in MIL-HDBK-5 or other applicable specification.

Equations (9-3a) and (9-3b) apply only if the load is uniformly distributed across the lug thickness. If the pin is too flexible and bends excessively, the load on the lug will tend to peak up near the shear faces and possibly cause premature failure of the lug.

A procedure to check the pin bending strength in order to prevent premature lug failure is given in Section 9.4 entitled "Double Shear Joint Strength Under Uniform Axial Load."

9.3.2   Lug Net-Section Strength Under Uniform Axial Load

The allowable lug net-section tensile ultimate stress (F_{nu_L}) on Section 1-1 in Figure 9-4a is affected by the ability of the lug material to yield and thereby relieve the stress concentration at the edge of the hole.

$$F_{nu_L} = K_n F_{tu} \qquad (9\text{-}4)$$

K_n, the net-tension stress coefficient, is obtained from the graphs shown in Figure 9-4 as a function of the ultimate and yield stress and strains of the lug material in the direction of the applied load. The ultimate strain (ϵ_u) can be obtained from MIL-HDBK-5.

(a)
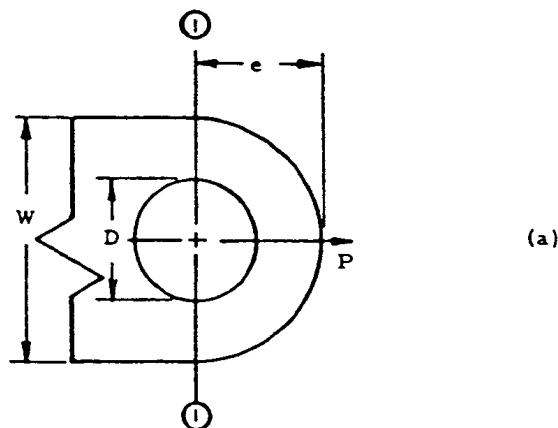
Figure 9-4.   Net Tension Stress Coefficient
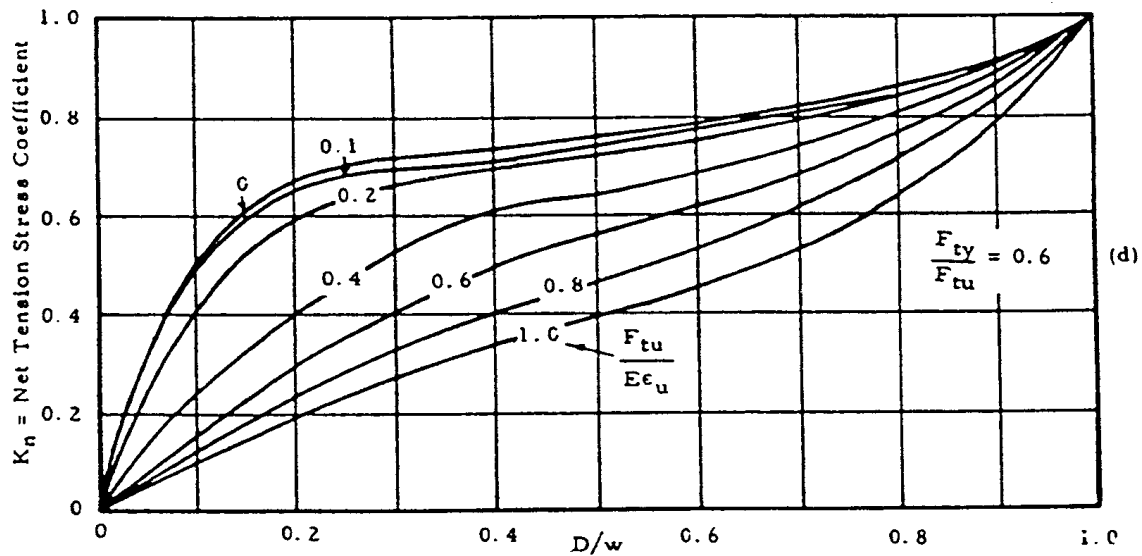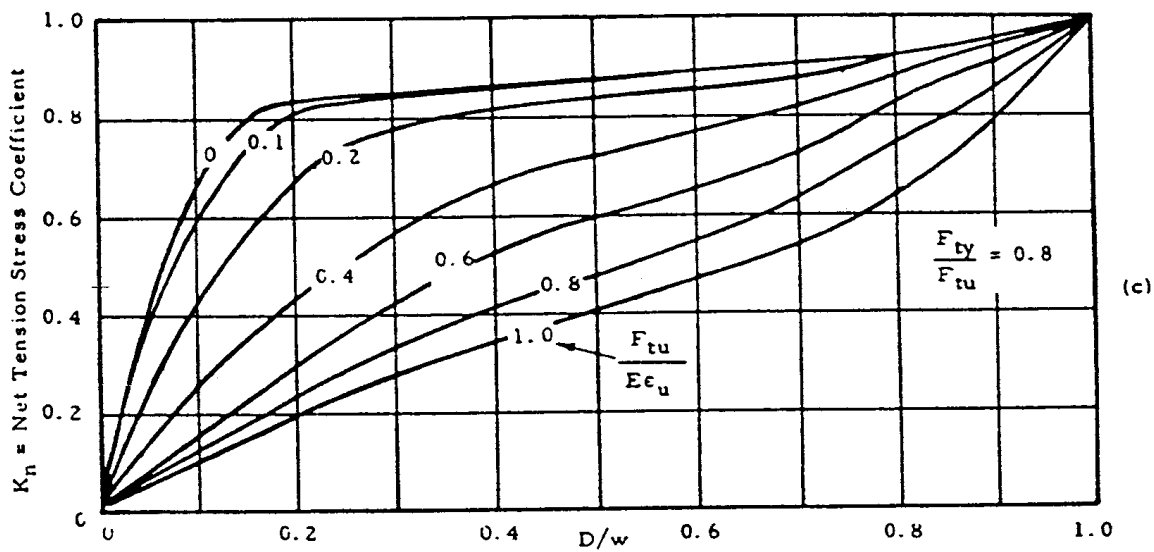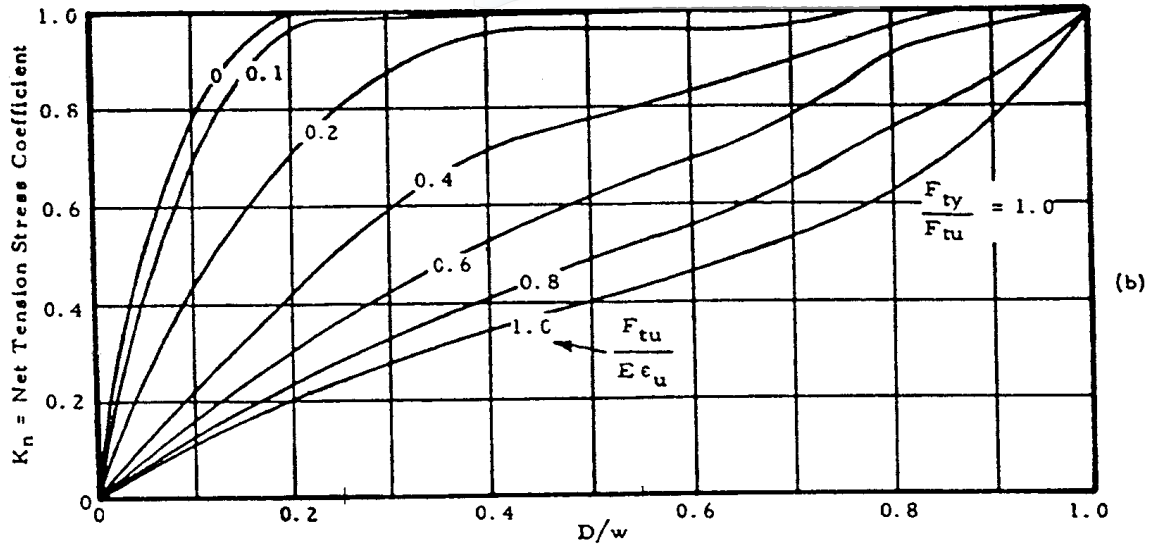
Figure 9-4. Net Tension Stress Coefficient (concluded)

The allowable lug net-section tensile yield stress (F_{ny_L}) is

$$F_{ny_L} = K_n F_{ty} \qquad \qquad (9\text{-}5)$$

The allowable lug net-section ultimate load (P_{nu_L}) is

$$P_{nu_L} = F_{nu_L} (w-D)t, \ (\text{if } F_{tu} \leqq 1.304 \, F_{ty}) \qquad (9\text{-}6a)$$

$$P_{nu_L} = 1.304 \, F_{ny_L} (w-D)t, \ (\text{if } F_{tu} > 1.304 \, F_{ty}) \qquad (9\text{-}6b)$$

9.3.3 Lug Design Strength Under Uniform Axial Load

The allowable design ultimate load for the lug (P_{u_L}) is the lower of the values obtained from Equations (9-3) and (9-6).

$$P_{u_L} \leqq P_{bru_L} \ (\text{Equations (9-3a) and (9-3b)}, \ \text{or}$$
$$P_{nu_L} \ (\text{Equations (9-6a) and (9-6b)}) \qquad (9\text{-}7)$$

9.3.4 Bushing Bearing Strength Under Uniform Axial Load

The allowable bearing yield stress for bushings (F_{bry_B}) is restricted to the compressive yield stress (F_{cy_B}) of the bushing material, unless higher values are substantiated by tests.

The allowable bearing ultimate stress for bushings (F_{bru_B}) is

$$F_{bru_B} = 1.304 \, F_{cy_B} \qquad \qquad (9\text{-}8)$$

The allowable bushing ultimate load (P_{u_B}) is

$$P_{u_B} = 1.304 \, F_{cy_B} D_p t \qquad \qquad (9\text{-}9)$$

This assumes that the bushing extends through the full thickness of the lug.

9.3.5 Combined Lug-Bushing Design Strength Under Uniform Axial Load

The allowable lug-bushing ultimate load ($P_{u_{L_B}}$) is the lower of the loads obtained from Equations (9-7) and (9-9).

$$P_{u_{L_B}} \leqq P_{u_L} \ (\text{Equation (9-7)}, \ \text{or} \ P_{u_B} \ (\text{Equation (9-9)}) \qquad (9\text{-}10)$$

9.4 Double Shear Joint Strength Under Uniform Axial Load

The strength of a joint such as the one shown in Figure 9-5 depends on the lug-bushing ultimate strength ($P_{u_{L_B}}$) and on the pin shear and pin bending strengths.
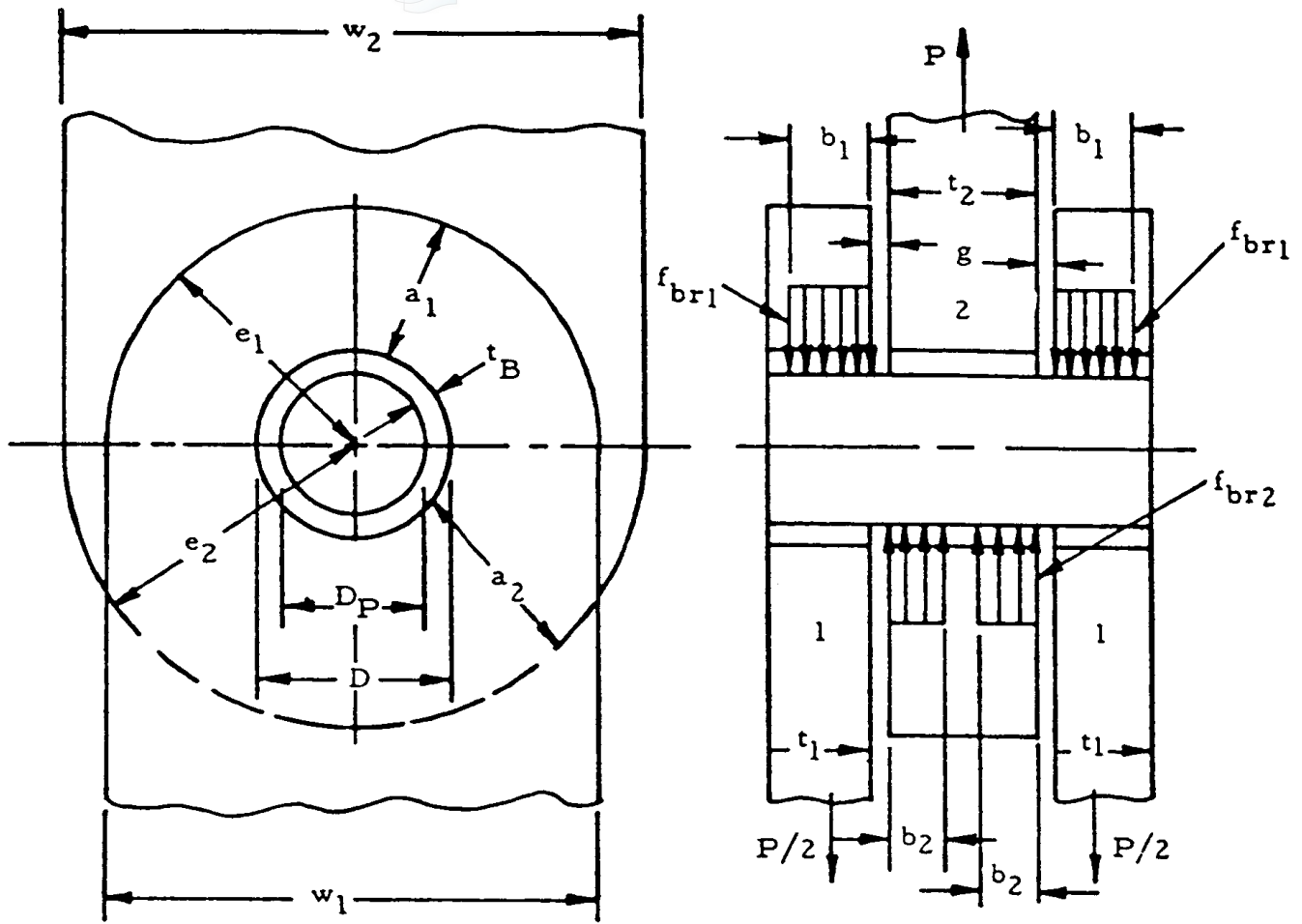
Figure 9-5. Double Shear Lug Joint

9.4.1   <u>Lug-Bushing Design Strength for Double Shear Joints Under Uniform Axial Load</u>

The allowable lug-bushing ultimate load $(P_{u_{LB}})$ for the joint is computed, using Equation (9-10). For the symmetrical joint shown in the figure, Equation (9-10) is used to calculate the ultimate load for the outer lugs and bushings $(2P_{u_{LB_1}})$ and the ultimate load for the inner lug and bushing $(P_{u_{LB_2}})$. The allowable value of $P_{u_{LB}}$ for the joint is the lower of these two values.

$$P_{u_{LB}} \leqq 2P_{u_{LB_1}} \text{ (Equation (9-10)), or } P_{u_{LB_2}} \text{ (Equation (9-10))} \qquad (9-11)$$

9.4.2 Pin Shear Strength for Double Shear Joints Under Uniform Axial Load

The pin ultimate shear load (P_{us_p}) for the symmetrical joint shown in Figure 9-5 is the double shear strength of the pin:

$$P_{us_p} = 1.571 \, D_p^2 \, F_{su_p} \qquad (9\text{-}12)$$

where F_{su_p} is the ultimate shear stress of the pin material.

9.4.3 Pin Bending Strength for Double Shear Joints Under Uniform Axial Load

Although actual pin bending failures are infrequent, excessive pin deflections can cause the load in the lugs to peak up near the shear planes instead of being uniformly distributed across the lug thickness, thereby leading to premature lug or bushing failures at loads less than those predicted by Equation (9-11). At the same time, however, the concentration of load near the lug shear planes reduces the bending arm and, therefore, the bending moment in the pin, making the pin less critical in bending. The following procedure is used in determining the pin ultimate bending load.

Assume that the load in each lug is uniformly distributed across the lug thickness ($b_1 = t_1$, and $2b_2 = t_2$). For the symmetrical joint shown in Figure 9-5, the resulting maximum pin bending moment is

$$M_{max_P} = \frac{P}{2} \left(\frac{t_1}{2} + \frac{t_2}{4} + g \right) \qquad (9\text{-}13)$$

The ultimate failing moment for the pin is

$$M_{u_p} = 0.0982 \, k_{b_p} \, D_p^3 \, F_{tu_p} \qquad (9\text{-}14)$$

where k_{b_p} is the plastic bending coefficient for the pin. The value of k_{b_p} varies from 1.0 for a perfectly elastic pin to 1.7 for a perfectly plastic pin, with a value of 1.56 for pins made from reasonably ductile materials (more than 5% elongation).

The pin ultimate bending load (P_{ub_p}) is, therefore,

$$P_{ub_p} = \frac{0.1963 \, k_{b_p} \, D_p^3 \, F_{tu_p}}{\left(\frac{t_1}{2} + \frac{t_2}{4} + g \right)} \qquad (9\text{-}15)$$

If P_{ub_p} is equal to or greater than either $P_{u_{L_B}}$ (Equation (9-11)) or P_{us_p} (Equation (9-12)), then the pin is a relatively strong pin that is not critical in bending, and no further pin bending calculations are required. **The** allowable load for the joint (P_{all}) can be determined by going directly to Equation (9-19a).

If P_{ub_p} (Equation (9-15)) is less than both $P_{u_{L_B}}$ (Equation (9-11)) and P_{us_p} (Equation (9-12)), the pin is considered a relatively weak pin, critical in bending. However, such a pin may deflect sufficiently under load to shift the c.g. of the bearing loads toward the shear faces of the lugs, resulting in a decreased pin bending moment and an increased value of P_{ub_p}. These shifted loads are assumed to be uniformly distributed over widths b_1 and $2b_2$, which are less than t_1 and t_2, respectively, as shown in Figure 9-5. The portions of the lugs and bushings not included in b_1 and $2b_2$ are considered ineffective. The new increased value of pin ultimate bending load is

$$P_{ub_p} = \frac{0.1963\ k_{b_p}\ D_p^{\ 3}\ F_{tu_p}}{\left(\dfrac{b_1}{2} + \dfrac{b_2}{2} + g\right)} \tag{9-15a}$$

The maximum allowable value of P_{ub_p} is reached when b_1 and b_2 are sufficiently reduced so that P_{ub_p} (Equation (9-15a)) is equal to $P_{u_{L_B}}$ (Equation (9-11)), provided that b_1 and $2b_2$ are substituted for t_1 and t_2, respectively, At this point we have a balanced design where the joint is equally critical in pin-bending failure or lug-bushing failure.

The following equations give the "balanced design" pin ultimate bending load ($P_{ub_{p\ max}}$) and effective bearing widths ($b_{1\ min}$ and $2b_{2\ min}$):

$$P_{ub_{p\ max}} = 2C\ \sqrt{\frac{P_{ub_p}}{C}\left(\frac{t_1}{2} + \frac{t_2}{4} + g\right) + g^2} - 2Cg \tag{9-16}$$

where

$$C = \frac{P_{u_{L_{B1}}}\ P_{u_{L_{B2}}}}{P_{u_{L_{B1}}}\ t_2 + P_{u_{L_{B2}}}\ t_1}$$

The value of P_{ub_p} on the right hand side of Equation (9-16) and the values of $P_{u_{L_{B1}}}$ and $P_{u_{L_{B2}}}$ in the expression for C are based on the assumption that the full thicknesses of the lugs are effective and have already been calculated. (Equations (9-10) and (9-15)).

If the inner lug strength is equal to the total strength of the two outer lugs ($P_{u_{L_{B2}}} = 2P_{u_{L_{B1}}}$), and if $g = 0$, then

$$P_{ub_{P\ max}} = \sqrt{P_{ub_P} \ P_{u_{L_{B2}}}} \qquad (9-17)$$

The "balanced design" effective bearing widths are

$$b_{1_{min}} = \frac{P_{ub_{P\ max}} \ t_1}{2P_{u_{L_{B1}}}} \qquad (9-18a)$$

$$2b_{2_{min}} = \frac{P_{ub_{P\ max}} \ t_2}{P_{u_{L_{B2}}}} \qquad (9-18b)$$

where $P_{ub_{P\ max}}$ is obtained from Equation (9-16) and $P_{u_{L_{B1}}}$ and $P_{u_{L_{B2}}}$ are the previously calculated values based on the full thicknesses of the lugs. Since any lug thicknesses greater than $b_{1_{min}}$ or $b_{2_{min}}$ are not considered effective, an efficient static strength design would have $t_1 = b_{1_{min}}$ and $t_2 = 2b_{2_{min}}$.

The allowable joint ultimate load (P_{all}) for the double-shear joint is obtained as follows:

If P_{ub_P} (Equation (9-15) is greater than either $P_{u_{L_B}}$ (Equation (9-11) or P_{us_P} (Equation (9-12)), then P_{all} is the lower of the values of $P_{u_{L_B}}$ or P_{us_P}.

$$P_{all} \leqq P_{u_{L_B}} \text{ (Equation (9-11) or } P_{us_P} \text{ (Equation (9-12))} \qquad (9-19a)$$

If P_{ub_P} (Equation (9-15)) is less than both $P_{u_{L_B}}$ and P_{us_P}, then P_{all} is the lower of the values of P_{us_P} and $P_{ub_{P\ max}}$

$$P_{all} \leqq P_{us_P} \text{ (Equation (9-12) or } P_{ub_{P\ max}} \text{ (Equation (9-16))} \qquad (9-19b)$$

9.4.4   <u>Lug Tang Strength for Double Shear Joints Under Uniform Axial Load</u>

If Equation (9-19a) has been used to determine the joint allowable load, then we have a condition where the load in the lugs and tangs is assumed uniformly distributed. The allowable stress in the tangs is F_{tu_T}. The lug tang

strength (P_T) is the lower of the following values.

$$P_T = 2F_{tu_T} \, w_{T1} \, t_1 \tag{9-20a}$$

$$P_T = F_{tu_{T2}} \, w_{T2} \, t_2 \tag{9-20b}$$

If Equation (9-19b) was used to determine the joint allowable load, the tangs of the outer lugs should be checked for the combined axial and bending stresses resulting from the eccentric application of the bearing loads. Assuming that the lug thickness remains constant beyond the pin, a load $(P/2)$ applied over the width b_1 in each outer lug will produce the following bending moment in the tangs:

$$M_1 = \frac{P}{2} \left(\frac{t_1 - b_1}{2} \right)$$

A simple, but generally conservative, approximation to the maximum combined stress in the outer lug tangs is

$$F_{t_{T1}} = \frac{P}{2w_{T1} \, t_1} + \frac{6M_1}{k_{b_T} \, w_{T1} \, t_1^2} \tag{9-21}$$

where k_{b_T}, the plastic bending coefficient for a lug tang of rectangular cross-section, varies from 1.0 for a perfectly elastic tang to 1.5 for a perfectly plastic tang, with a value of 1.4 representative of rectangular cross sections with materials of reasonable ductility (more than 5% elongation). The allowable value of $F_{t_{T1}}$ is $F_{tu_{T1}}$. The lug tang strength is the lower of the following values:

$$P_T = \frac{2F_{tu_{T1}} \, w_{T1} \, t_1}{1 + \dfrac{3}{k_{b_T}} \left(1 - \dfrac{b_{1\min}}{t_1} \right)} \tag{9-22a}$$

$$P_T = F_{tu_{T2}} \, w_{T2} \, t_2 \tag{9-22b}$$

where $b_{1\min}$ is given by Equation (9-18a)

9.5 Single-Shear Joint Strength Under Uniform Axial Load

In single-shear joints, lug and pin bending are more critical than in double-shear joints. The amount of bending can be significantly affected by bolt clamping. In the cases considered in Figure 9-6, no bolt clamping is assumed, and the bending moment in the pin is resisted by socket action in the lugs.
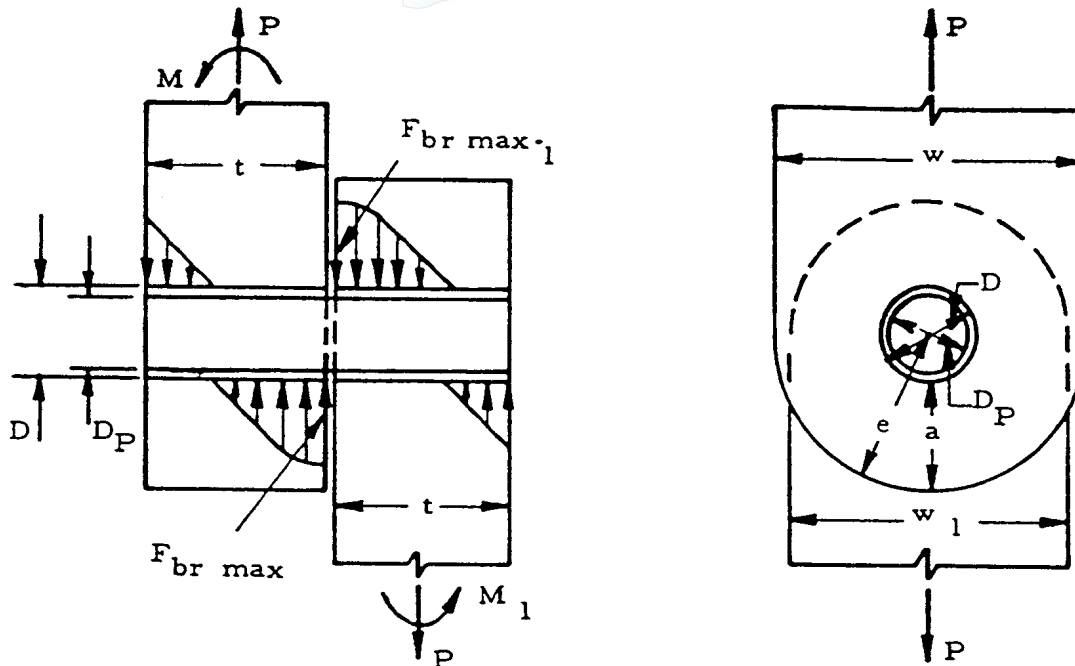
Figure 9-6.   Single Shear Lug Joint

In Figure 9-6 a representative single-shear joint is shown, with centrally applied loads (P) in each lug, and bending moments (M and M_1) that keep the system in equilibrium.   (Assuming that there is no gap between the lugs, $M + M_1 = P(t + t_1)/2$).   The individual values of M and M_1 are determined from the loading of the lugs as modified by the deflection, if any, of the lugs, according to the principles of mechanics.

The strength analysis procedure outlined below applies to either lug. The joint strength is determined by the lowest of the margins of safety calculated for the different failure modes defined by Equations (9-23) through (9-27).

9.5.1   Lug Bearing Strength for Single Shear Joints Under Uniform Axial Loads

The bearing stress distribution between lug and bushing is assumed to be similar to the stress distribution that would be obtained in a rectangular cross section of width (D) and depth (t), subjected to a load (P) and moment (M). At ultimate load the maximum lug bearing stress ($F_{br \; max \; L}$) is approximated by

$$F_{br \; max \; L} = \frac{P}{Dt} + \frac{6M}{k_{br_L} Dt^2} \qquad (9-23)$$

where k_{br_L} is a plastic bearing coefficient for the lug material, and is assumed to be the same as the plastic bending coefficient (k_{b_L}) for a rectangular section.

9 - 14

The allowable ultimate value of $F_{br\ max_L}$ is either F_{bru_L} (Equations (9-1a) (9-1b)) or $1.304\ F_{bry_L}$ (Equations (9-2a) (9-2b)), whichever is lower.

9.5.2 Lug Net-Section Strength for Single Shear Joints Under Uniform Axial Load

At ultimate load the nominal value of the outer fiber tensile stress in the lug net-section is approximated by

$$F_{t\ max} = \frac{P}{(w-D)t} + \frac{6M}{k_{b_L}\ (w-D)t^2} \tag{9-24}$$

where k_{b_L} is the plastic bending coefficient for the lug net-section.

The allowable ultimate value of $F_{t\ max}$ is F_{nu_L} (Equation (9-4)) or $1.304\ F_{ny_L}$ (Equation (9-5)), whichever is lower.

9.5.3 Bushing Strength for Single Shear Joints Under Uniform Axial Load

The bearing stress distribution between bushing and pin is assumed to be similar to that between the lug and bushing. At ultimate bushing load the maximum bushing bearing stress is approximated by

$$F_{br\ max\ B} = \frac{P}{D_p t} + \frac{6M}{k_{br_L}\ D_p t^2} \tag{9-25}$$

where k_{br_L}, the plastic bearing coefficient, is assumed the same as the plastic bending coefficient (k_{b_L}) for a rectangular section.

The allowable ultimate value of $F_{br\ max\ B}$ is $1.304\ F_{cy_B}$, where F_{cy_B} is the bushing material compressive yield strength.

9.5.4 Pin Shear Strength for Single Shear Joints Under Uniform Axial Load

The maximum value of pin shear can occur either within the lug or at the common shear face of the two lugs, depending upon the value of M/Pt At the lug ultimate load the maximum pin shear stress $(F_{s\ max\ P})$ is approximated by

$$F_{s\ max\ P} = \frac{1.273\ P}{D_p^2}, \quad \left(\text{if } \frac{M}{Pt} \leq 2/3\right) \tag{9-26a}$$

$$F_{s\ max\ P} = \frac{1.273\ P}{D_p^2} \frac{\left(\sqrt{\left(\frac{2M}{Pt}\right)^2 + 1} - 1\right)}{\left(\frac{2M}{Pt} + 1 - \sqrt{\left(\frac{2M}{Pt}\right)^2 + 1}\right)}, \quad \left(\text{if } \frac{M}{Pt} > 2/3\right) \tag{9-26b}$$

Equation (9-26a) defines the case where the maximum pin shear is obtained at the common shear face of the lugs, and Equation (9-26b) defines the case where the maximum pin shear occurs away from the shear face.

The allowable ultimate value of $F_{b\ max\ p}$ is F_{su_p}, the ultimate shear stress of the pin material.

9.5.5   Pin Bending Strength for Single Shear Joints Under Uniform Axial Load

The maximum pin bending moment can occur within the lug or at the common shear faces of the two lugs, depending on the value of M/Pt. At the lug ultimate load the maximum pin bending stress ($F_{b\ max\ p}$) is approximated by

$$F_{b\ max\ p} = \frac{10.19M}{k_{bp}\ D_p^{\ 3}} \left(\frac{Pt}{2M} - 1 \right), \quad \left(\text{if } \frac{M}{Pt} \leqq 3/8\right) \tag{9-27a}$$

$$F_{b\ max\ p} = \frac{10.19M}{k_{bp}\ D_p^{\ 3}} \ \frac{\left(\sqrt{\left(\frac{2M}{Pt}\right)^2 + 1} - 1 \right)}{\frac{2M}{Pt}}, \tag{9-27b}$$

$$\left(\text{if } \frac{M}{Pt} > 3/8\right)$$

where k_{bp} is the plastic bending coefficient for the pin.

Equation (9-27a) defines the case where the maximum pin bending moment is obtained at the common shear face of the lugs, and Equation (9-27b) defines the case where the maximum pin bending moment occurs away from the shear face, where the pin shear is zero.

The allowable ultimate value of $F_{b\ max\ p}$ is F_{tu_p}, the ultimate tensile stress of the pin material.

9.6   Example of Uniform Axially Loaded Lug Analysis

Determine the static strength of an axially loaded, double shear joint, such as shown in Section 9.4, with dimensions and material properties given in Table 9-1.

Table 9-1. Dimensions and Properties

	Female Lugs, 1	Male Lug, 2	Bushings, 1 and 2	Pin
Material	2024-T351 Plate	7075-T651 Plate	Al. Bronze	4130 Steel
F_{tu}	64000 psi (X-grain)	77000 psi (X-grain)	110,000 psi	125,000 psi
F_{ty}	40000 psi (X-grain)	66000 psi (X-grain)	60,000 psi	103,000 psi
F_{cy}			60,000 psi	
F_{su}				82,000 psi
E	10.5×10^6 psi	10.3×10^6		29×10^6 psi
ε_u	0.12	0.06		
D or D_p	$D = 1.00$ in.	$D = 1.00$ in.	$D_p = 0.75$ in., $D = 1.00$ in.	$D_p = 0.75$ in.
e	1.25 in.	1.50 in.		
a	0.75 in.	1.00 in.		
$w = W_T$	2.50 in.	3.00 in.		
t	0.50 in.	0.75 in.	0.50 and 0.75 in.	
g	0.10 in.			

(1) Female Lugs and Bushings

$F_{tux} = 64,000$ psi; $1.304\ F_{tyy} = 1.304 \times 40000 = 52160$ psi.

a) Lug Bearing Strength (Equations (9-2a) and (9-3b))

$$\frac{e_1}{D} = \frac{1.25}{1.00} = 1.25; \text{ therefore } K_1 = 1.46 \text{ (from Figure 9-2)}$$

$$P_{bru_{L_1}} = 1.304 \times 1.46 \times 0.75 \times 40000 \times 1.00 \times 0.50 = 28600 \text{ lbs.}$$

b) Lug Net-Section Tension Strength (Equations (9-5) and (9-6b))

$$\frac{D}{w_1} = \frac{1.00}{2.50} = 0.40; \quad \frac{F_{ty}}{F_{tu}} = \frac{40000}{64000} = 0.625;$$

$$\frac{F_{tu}}{E\varepsilon_u} = \frac{64000}{10.5 \times 10^6 \times 0.12} = 0.051; \text{ therefore, } k_{n_1} = 0.74$$

(by interpolation from Figure 9-4)

$$P_{nu_L} = 2 \times 1.304 \times .74 \times 4000 \times (2.5 - 1.0) \times .5 = 57,898 \text{ lbs.}$$

c) <u>Lug Design Strength (Equation (9-7))</u>

$$P_{u_{t_1}} = P_{bru_{t_1}} = 28600 \text{ lbs.}$$

d) <u>Bushing Bearing Strength (Equation (9-9))</u>

$$P_{u_{B_1}} = 1.304 \times 60000 \times 0.75 \times 0.50 = 29300 \text{ lbs.}$$

e) <u>Combined Lug-Bushing Design Strength (Equation (9-10))</u>

$$P_{u_{t_{B_1}}} = P_{u_{t_1}} = 28600 \text{ lbs.}$$

(2) <u>Male Lug and Bushing</u>

$$F_{tux} = 77000 \text{ psi; } 1.304 \, F_{tyx} = 1.304 \times 66000 = 86100 \text{ psi.}$$

a) <u>Lug Bearing Strength (Equations (9-1b) and (9-3a))</u>

$$\frac{e_2}{D} = \frac{1.50}{1.00} = 1.50; \text{ therefore, } K_2 = 1.33 \text{ (from Figure 9-7)}$$

$$P_{bru_{t_2}} = 1.33 \times 77000 \times 1.00 \times 0.75 = 77000 \text{ lbs.}$$

b) <u>Lug Net-Section Tension Strength (Equations (9-4) and (9-6a))</u>

$$\frac{D}{w_2} = \frac{1.00}{3.00} = 0.333; \quad \frac{F_{ty}}{F_{tu}} = \frac{66000}{77000} = 0.857;$$

$$\frac{F_{tu}}{E\epsilon_u} = \frac{77000}{10.3 \times 10^6 \times 0.06} = 0.125; \text{ therefore } K_{n_2} = 0.87$$

(by interpolation from Figure 9-4)

$$P_{nu_t} = 1.304 \times 87 \times 66000 \times (3.0 - 1.0) \times .75 = 112,313 \text{ lbs.}$$

c) <u>Lug Design Strength (Equation (9-7))</u>

$$P_{u_{t_2}} = P_{bru_{t_2}} = 77000 \text{ lbs.}$$

d) <u>Bushing Bearing Strength (Equation (9-9))</u>

$$P_{u_{B_2}} = 1.304 \times 60000 \times 0.75 \times 0.75 = 44000 \text{ lbs.}$$

e) <u>Combined Lug-Bushing Design Strength (Equation (9-10))</u>

$$P_{u_{t_{B_2}}} = P_{u_{B_2}} = 44000 \text{ lbs.}$$

(3) **Joint Analysis**

a) <u>Lug-Bushing Strength (Equation (9-11))</u>

$$P_{u_{L_B}} = P_{u_{L_{B2}}} = 44000 \text{ lbs.}$$

b) <u>Pin Shear Strength (Equation (9-12))</u>

$$P_{u_{s_p}} = 1.571 \times (0.75)^2 \times 82000 = 72400 \text{ lbs.}$$

c) <u>Pin Bending Strength (Equation (9-15))</u>

The pin ultimate bending load, assuming uniform bearing across the lugs, is

$$P_{u_{b_p}} = \frac{0.1963 \times 1.56 \times (0.75)^3 \times 125000}{0.25 + 0.1875 + 0.10} = 30100 \text{ lbs.}$$

Since $P_{u_{b_p}}$ is less than both $P_{u_{L_B}}$ and $P_{u_{s_p}}$, the pin is a relatively weak pin which deflects sufficiently under load to shift the bearing loads toward the shear faces of the lugs. The new value of pin bending strength is, then,

$$P_{u_{b \; max}} = 2C \times \left(\sqrt{\frac{30100}{C} \times (0.25 + 0.1875 + 0.10) + (0.10)^2} - 0.10 \right),$$

(from Equation (9-16)) where $C = \dfrac{28600 \times 44000}{286 \times 0.75 + 44000 \times 0.050}$

$$= 29000 \text{ lbs/in.}$$

Therefore, $P_{u_{b_p \; max}} = 2 \times 29000 \times (0.754 - 0.10) = 37900 \text{ lbs.}$

The "balanced design" effective bearing widths are

$$b_{1_{min}} = \frac{37900 \times 0.50}{2 \times 28600} = 0.331 \text{ in. (from Equation (9-18a))}$$

$$2_{b_{2 \; min}} = \frac{37900 \times 0.75}{44000} = 0.646 \text{ in. (from Equation (9-18b))}$$

Therefore, the same value of $P_{u_{b_p \; max}}$ would be obtained if the thickness of each female lug was reduced to 0.331 inches and the thickness of the male lug reduced to 0.646 inches.

d) <u>Joint Strength (Equation (9-19b))</u>

The final allowable load for the joint, exclusive of the lug tangs, is

9-19

$$P_{all} = P_{ub, \, max} = 37900 \text{ lbs.}$$

(4) Lug Tang Analysis

$$P_T = \frac{2 \times 64000 \times 2.50 \times 0.50}{1 + \dfrac{3}{1.4} \times \left(.1 - \dfrac{0.331}{0.500}\right)} = 92700 \text{ lbs. (from Equation (9-22a))}$$

or

$$P_T = 77000 \times 3.00 \times 0.75 = 173300 \text{ lbs. (from Equation (9-22b))}$$

Therefore, the lug tangs are not critical and the allowable joint load remains at 37900 pounds.

9.7   Lug and Bushing Strength Under Transverse Load

Transversely loaded lugs and bushings are checked in the same general manner as axially loaded lugs. The transversely loaded lug, however, is a more redundant structure than an axially loaded lug, and it has a more complicated failure mode. Figure 9-7 illustrates the different lug dimensions that are critical in determining the lug strength.
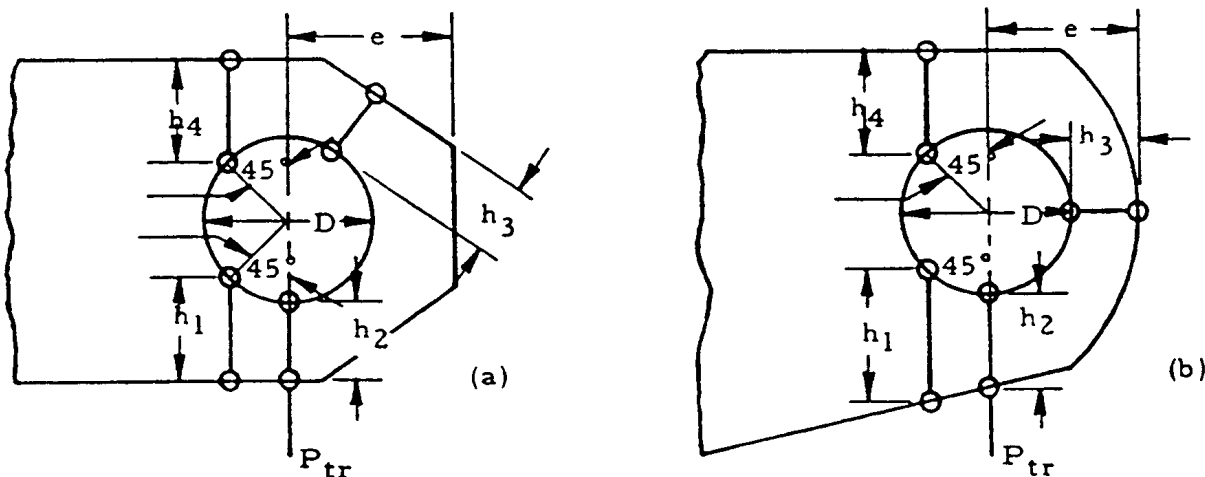
Figure 9-7.   Schematic of Lugs Under Transverse Loads

9.7.1   Lug Strength Under Transverse Load

The lug ultimate bearing stress (F_{bru_L}) is

$$F_{bru_L} = F_{tru} \, F_{tux} \qquad\qquad (9-28)$$

where K_{tru}, the transverse ultimate load coefficient, is obtained from Figure 9-8 as a function of the "effective" edge distance (h_{av}):

$$h_{av} = \frac{6}{3/h_1 + 1/h_2 + 1/h_3 + 1\,h/4}$$
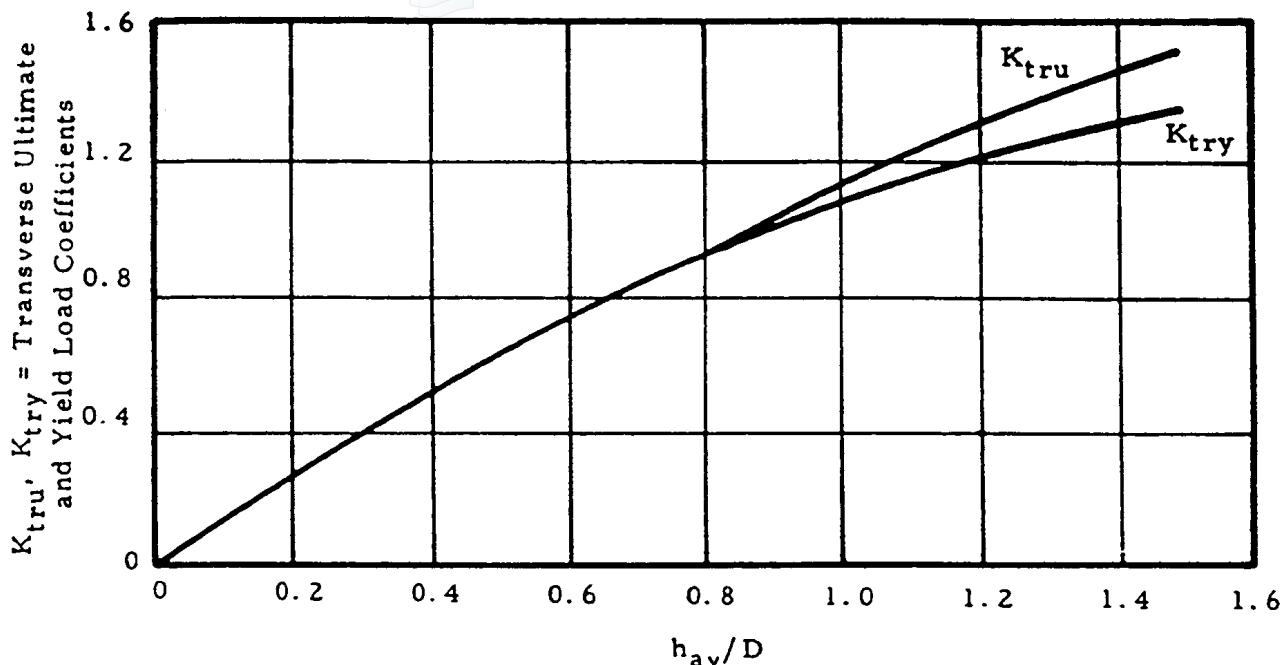
Figure 9-3

The effective edge distance can be found by using the nomograph in Figure 9-9. The nomograph is used by first connecting the h_1 and h_2 lines at the appropriate value of h_1 and h_2. The intersection with line A is noted. Next connect the h_3 and h_4 lines similarly, and note the B line intersection. Connecting the A and B line intersection gives the value of h_{av} to be read at the intersection with the h_{av} line. The different edge distances (h_1, h_2, h_3, h_4) indicate different critical regions in the lug, h_1 being the most critical. The distance h_3 is the smallest distance from the hole to the edge of the lug. If the lug is a concentric lug with parallel sides, h_{av}/D can be obtained directly from Figure 9-10 for any value of e/D. In concentric lugs, $h_1 = h_4$ and $h_2 = h_3$.

The lug yield bearing stress (F_{bry_L}) is

$$F_{bry_L} = K_{try} \ F_{tyx} \tag{9-29}$$

where K_{try}, the transverse yield load coefficient, is obtained from Figure 9-9.

The allowable lug transverse ultimate load (P_{tru_L}) is

$$P_{tru_L} = F_{br_L} \ Dt \ (\text{if } F_{tux} \leqq 1.304 \ F_{tyx}) \tag{9-30a}$$

$$P_{tru_L} = 1.304 \ F_{bry_L} \ Dt \ (\text{if } F_{tux} > 1.304 \ F_{tyx}) \tag{9-30b}$$

where F_{bru_L} and F_{bry_L} are obtained from Equations (9-28) and (9-29)).

9 - 21

EFFECTIVE EDGE DISTANCE

$$h_{av} = \frac{6}{3/h_1 + 1/h_2 + 1/h_3 + 1/h_4}$$
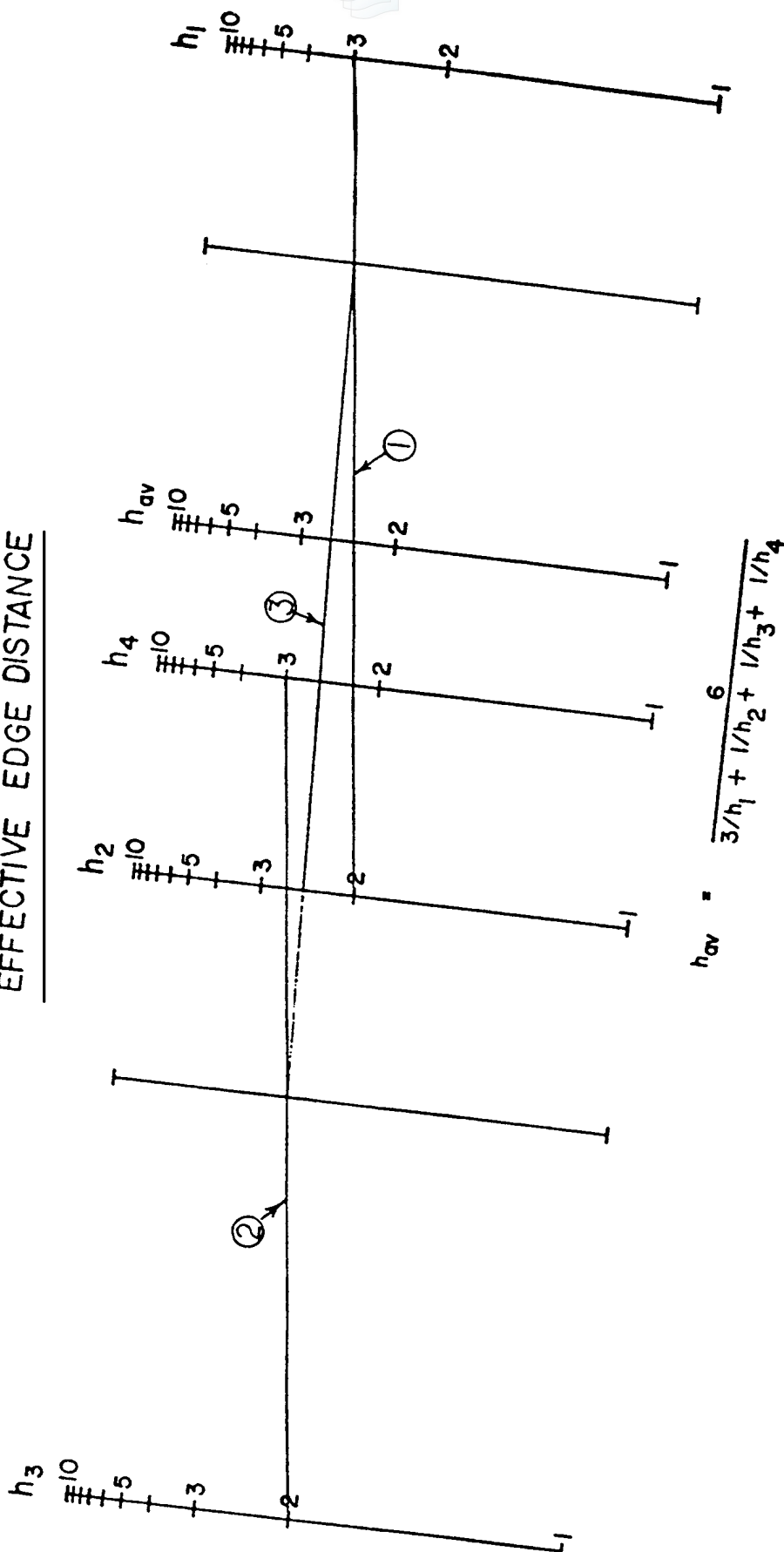
Figure 9-9 Nomograph for Effective Edge Distance
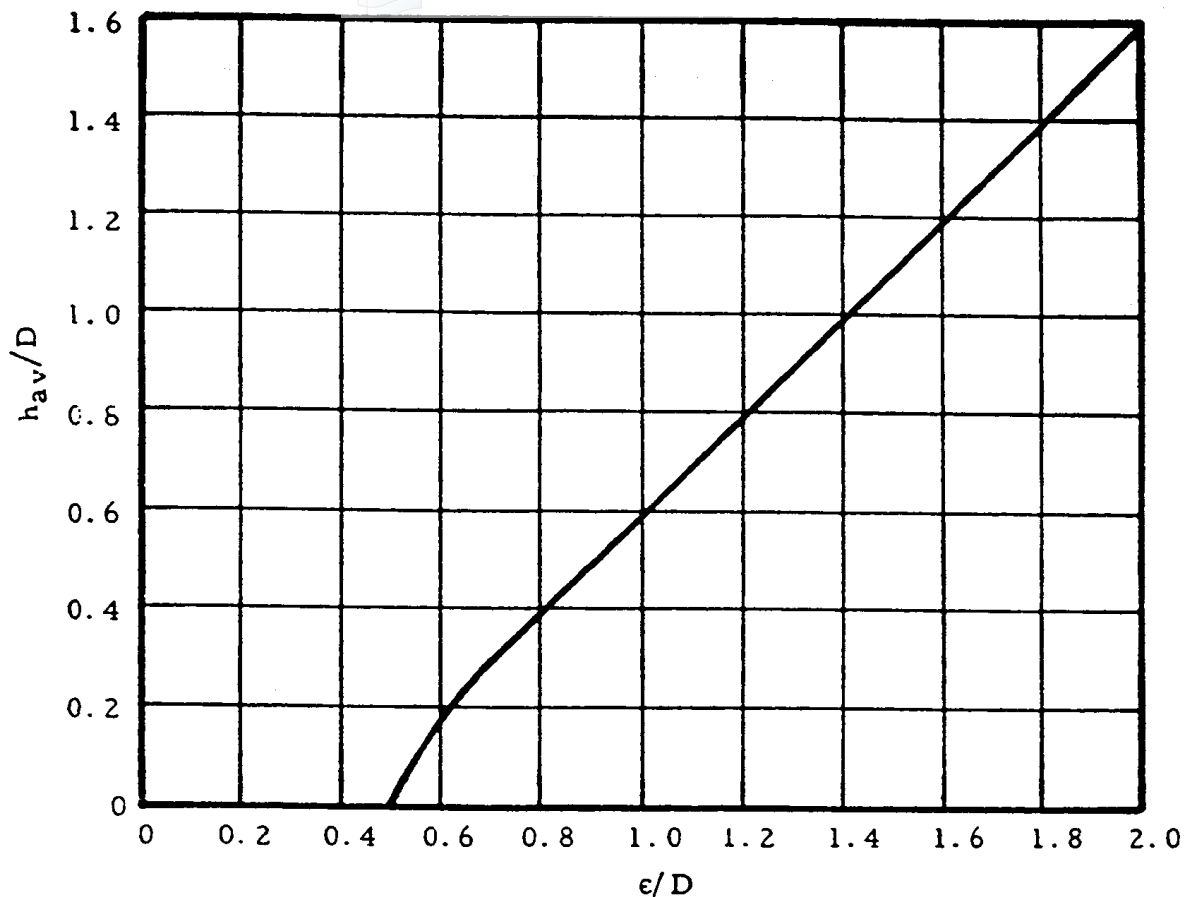
Figure 9-10.   Effective Edge Distance

If the lug is not of constant thickness, then A_{av}/A_{br} is substituted for h_{av}/D on the horizontal scale of the graph in Figure 9-8, where A_{br} is the lug bearing area, and

$$A_{av} = \frac{6}{3/A_1 + 1/A_2 + 1/A_3 + 1/A_4}$$

A_1, A_2, A_3, and A_4 are the areas of the sections defined by h_1, h_2, h_3, and h_4, respectively.

The values of K_{tru} and K_{try} corresponding to A_{av}/A_{br} are then obtained from the graph in Figure 9-8 and the allowable bearing stresses are obtained as before from Equations (9-28) and (9-29)).

9.7.2   Bushing Strength Under Transverse Load

The allowable bearing stress on the bushing is the same as that for the bushing in an axially loaded lug and is given by Equation (9-8).   The allowable bushing ultimate load (P_{tru_B}) is equal to P_{u_B} (Equation (9-9)).

9 - 23

9.8   Double Shear Joints Under Transverse Load

The strength calculations needed for double shear joint strength analysis are basically the same as those needed for axially loaded. Equations (9-11) through (9-19) can be used; however, the maximum lug bearing stresses at ultimate and yield loads must not exceed those given by Equations (9-28) and (9-29).

9.9   Single Shear Joints Under Transverse Load

The previous discussion on double shear joint applies to single shear joint strength analysis except the equations to be used are now Equations (9-23) through (9-27).

9.10   Lug and Bushing Strength Under Oblique Load

The analysis procedures used to check the strength of axially loaded lugs and of transversely loaded lugs are combined to analyze obliquely loaded lugs such as the one shown in Figure 9-11. These procedures apply only if α does not exceed 90°.
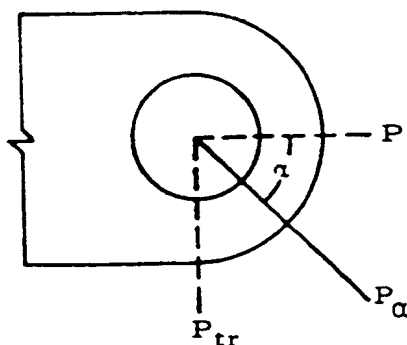
Figure 9-11.   Obliquely Loaded Lug

9.10.1   Lug Strength Under Oblique Load

The obliquely applied load (P_α) is resolved into an axial component ($P = P_\alpha \cos \alpha$) and a transverse component ($P_{tr} = P_\alpha \sin \alpha$). The allowable ultimate value of P_α is P_{α_L} and its axial and transverse components satisfy the following equation:

$$\left(\frac{P}{P_{u_L}}\right)^{1.6} + \left(\frac{P_{tr}}{P_{tru_L}}\right)^{1.6} = 1 \qquad (9\text{-}31)$$

where P_{u_L} is the strength of an axially loaded lug (Equation (9-7)) and P_{tru_L} is the strength of a transversely loaded lug (Equations (9-30a), (9-30b)). The allowable load curve defined by Equation (9-31) is plotted on the graph in Figure 9-12.
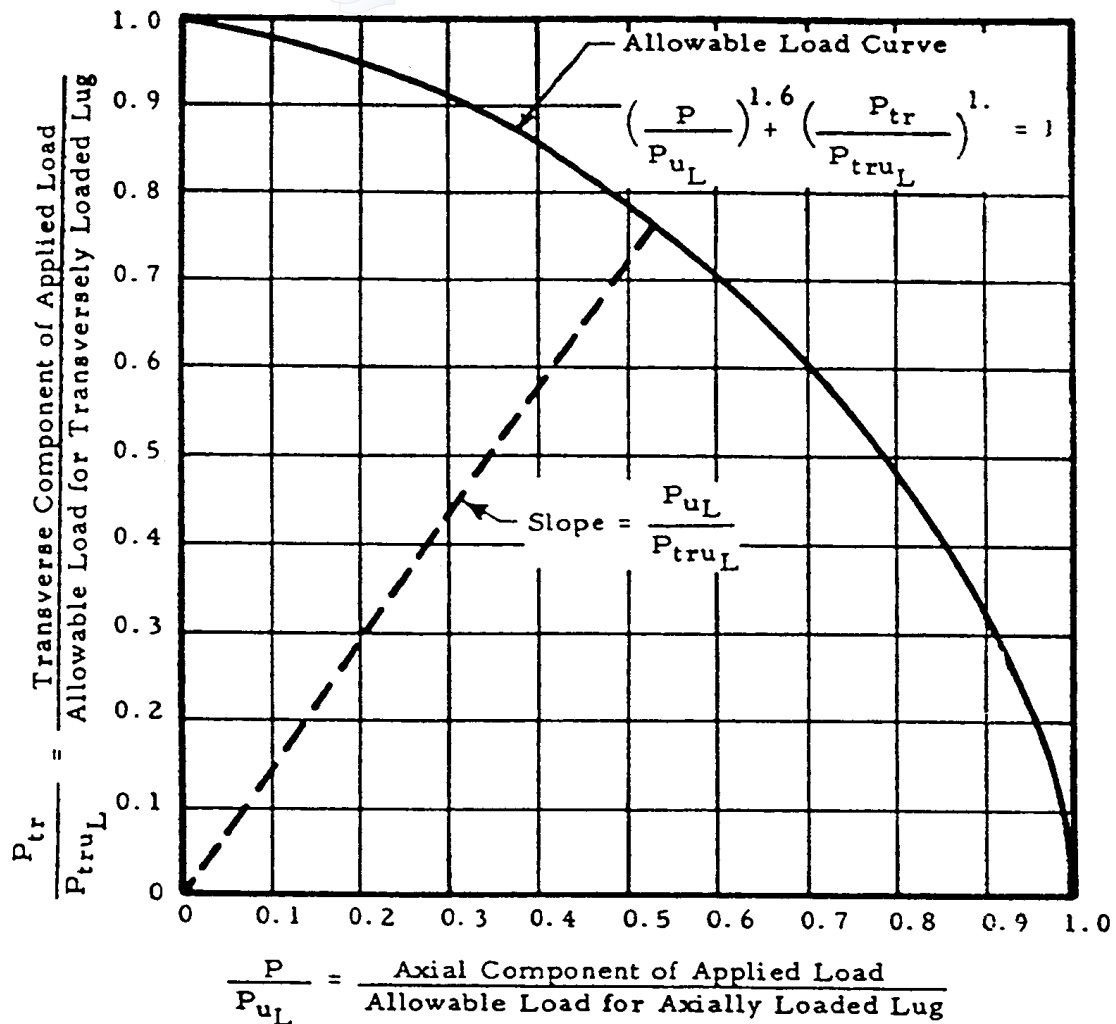
Figure 9-12. Allowable Load Curve

For any given value of α the allowable load (P_{α_t}) for a lug can be determined from the graph shown in Figure 9-12 by drawing a line from the origin with a slope equal to (P_{u_L}/P_{tru_L}). The intersection of this line with the allowable load curve (point 1 on the graph) indicates the allowable values of P/P_{u_L} and P_{tr}/P_{tru_L}, from which the axial and transverse components, P and P_{tr}, of the allowable load can be readily obtained.

9.10.2   Bushing Strength Under Oblique Load

The bushing strength calculations are identical to those for axial loading (Equations (9-8) and (9-9)).

9.11 Double Shear Joints Under Oblique Load

The strength calculations are basically the same as those for an axially loaded joint except that the maximum lug bearing stress at ultimate load must

9 - 25

not exceed P_{α_L}/Dt, where P_{α_L} is defined by Equation (9-31). Use Equations (9-11) through (9-19)).

9.12 Single Shear Joints Under Oblique Load

The previous discussion on double shear joints applies to single shear joint strength analysis except the equations to be used are now Equations (9-23) through (9-27).

9.13 Multiple Shear and Single Shear Connections

Lug-pin combinations having the geometry indicated in Figure 9-13 should be analyzed according to the following criteria:

(1) The load carried by each lug should be determined by distributing the total applied load P among the lugs as indicated in Figure 9-13, b being obtained in Table 9-2. This distribution is based on the assumption of plastic behavior (at ultimate load) of the lugs and elastic bending of the pin, and gives approximately zero bending deflection of the pin.

(2) The maximum shear load on the pin is given in Table 9-2.

(3) The maximum bending moment in the pin is given by the formulae

$$M = \frac{P_1 b}{2}$$ where b is given in Table 9-2.

These lugs of equal thickness t'

Two outer lugs of equal thickness not less than Ct' (See Table 9-2)

These lugs of equal thickness t"
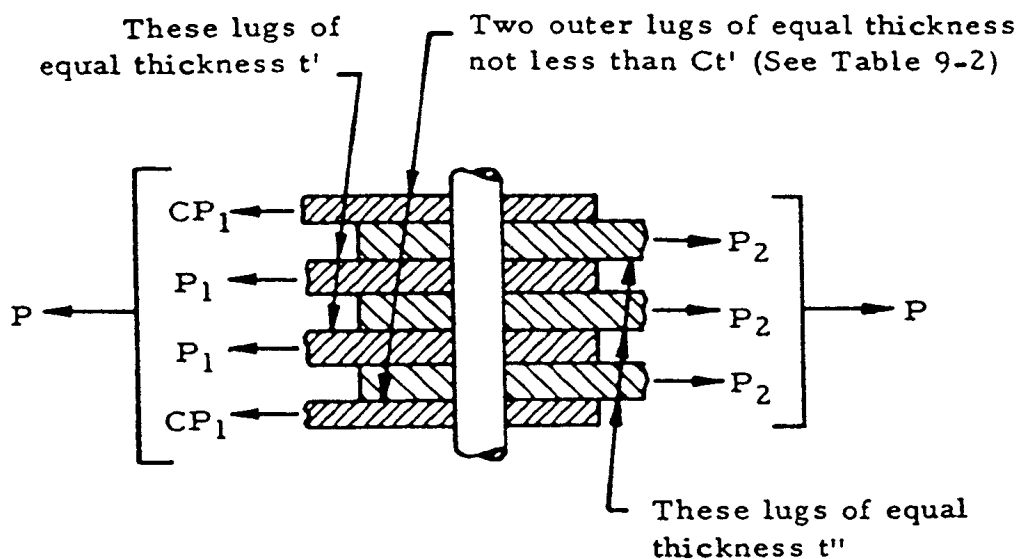
Figure 9-13. Schematic of Multiple Shear Joint in Tension

Total number of lugs including both sides	C	Pin Shear	b
5	.35	.50 P_1	$.28 \dfrac{t' + t''}{2}$
7	.40	.53 P_1	$.33 \dfrac{t' + t''}{2}$
9	.43	.54 P_1	$.37 \dfrac{t' + t''}{2}$
11	.44	.54 P_1	$.39 \dfrac{t' + t''}{2}$
∞	.50	.50 P_1	$.50 \dfrac{t' + t''}{2}$

9.14 Axially Loaded Lug Design

This section presents procedures for the optimized design of lugs, bushings and pin in a symmetrical, double-shear joint, such as shown in Figure 9-5, subjected to a static axial load (P). One design procedure applies to the case where the pin is critical in shear, the other to the case where the pin is critical in bending. A method is given to help determine which mode of pin failure is more likely, so that the appropriate design procedure will be used.

Portions of the design procedures may be useful in obtaining efficient designs for joints other than symmetrical, double-shear joints.

9.14.1   Axial Lug Design for Pin Failure

An indication of whether the pin in an optimized joint design is more likely to fail in shear or in bending can be obtained from the value of R (Equation (9-32)). If R is less than 1.0, the pin is likely to fail in shear and the design procedure for joints with pins critical in shear should be used to get an optimized design. If R is greater than 1.0, the pin is likely to be critical in bending and the design procedures for joints with pins critical in bending should be used.

$$ R = \frac{\pi F_{su_p}}{k_{b_p} F_{tu_p}} \left(\frac{F_{su_p}}{F_{br\,all\,1}} + \frac{F_{su_p}}{F_{br\,all\,2}} \right) \qquad (9\text{-}32) $$

where F_{su_p} and F_{tu_p} are the ultimate shear and ultimate tension stresses for the pin material, k_{b_p} is the plastic bending coefficient for the pin, and $F_{br\,all\,1}$

and $F_{br\,all_2}$ are allowable bearing stresses in the female and male lugs. The value of $F_{br\,all_1}$ can be approximated by the lowest of the following three values:

$$K\,F_{tux_1}\,\frac{D}{D_p}\;;\;1.304\,K\,F_{tyx_1}\,\frac{D}{D_p}\;;\;1.304\,F_{cy_{B_1}}$$

where F_{tux_1} and F_{tyx_1} are the cross-grain tensile ultimate and tensile yield stress for female lugs, $F_{cy_{B_1}}$ is the compressive yield stress of the bushings in the female lugs, and K is obtained from Figure 9-14. Assume $D = D_p$ if a better estimate cannot be made. $F_{br\,all_2}$ is approximated in a similar manner.
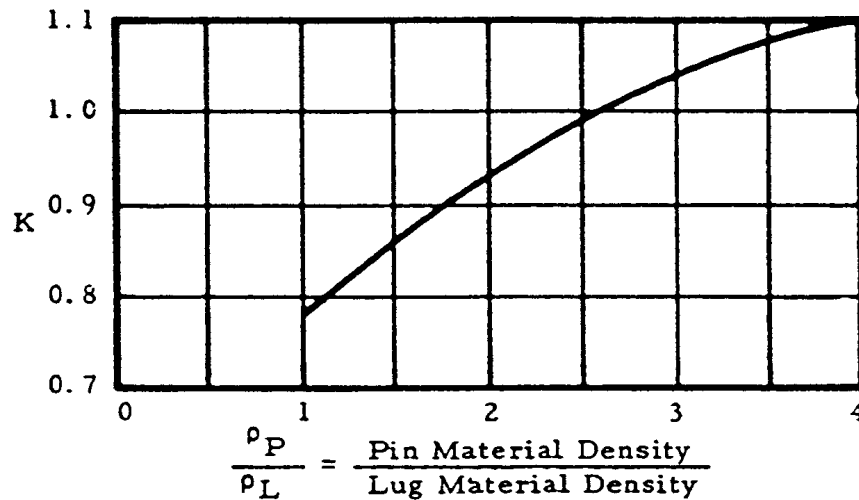
Figure 9-14. Allowable Bearing Coefficient

9.14.1.1 Axial Lug Design for Pin Failure in the Shearing Mode

Pin and Bushing Diameter

The minimum allowable diameter for a pin in double shear is

$$D_p = 0.798\sqrt{\frac{P}{F_{su_p}}} \tag{9-33}$$

The outside diameter of the bushing is $D = D_p + 2t_B$, where t_B is the bushing wall thickness.

Edge Distance Ratio (e/D)

The value of e/D that will minimize the combined lug and pin weight is obtained from Figure (9-15)(a) for the case where lug bearing failure and pin shear failure occur simultaneously. The lug is assumed not critical in net tension, and the bushing is assumed not critical in bearing.

9 - 28
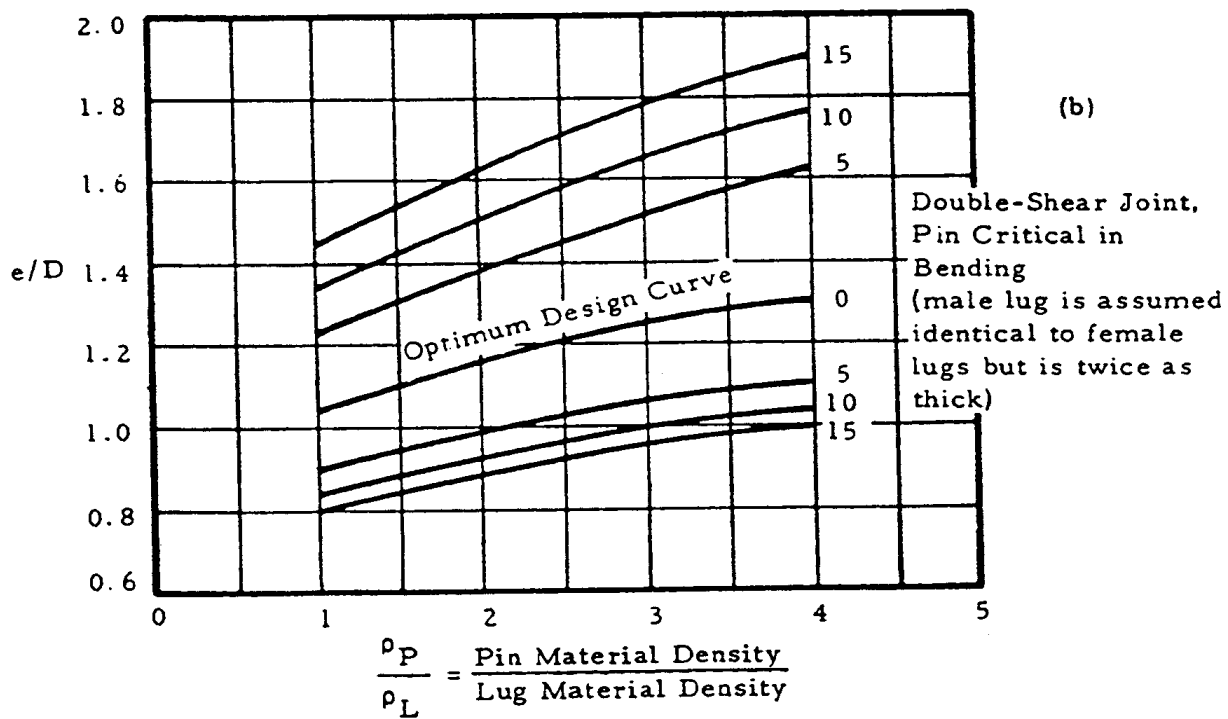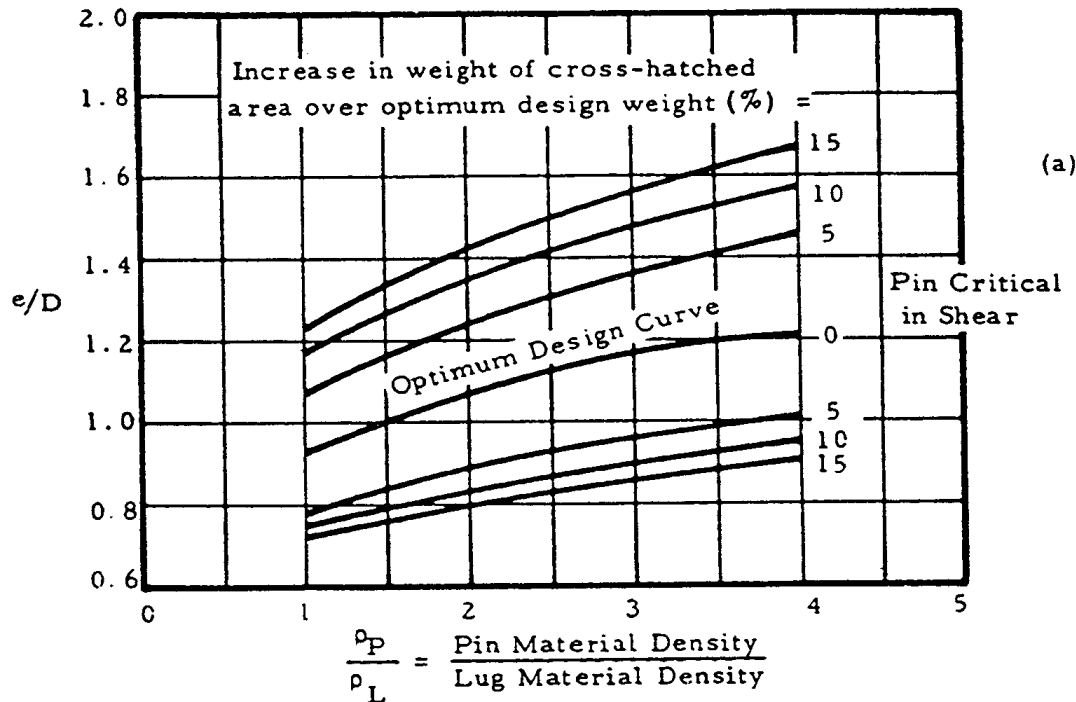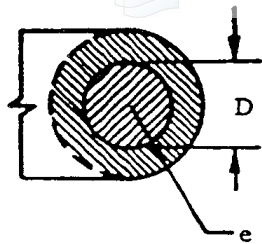
Figure 9-15.   Edge Distance Ratio

The curves in Figure 9-15 apply specifically to concentric lugs ($a = e - D/2$, and $w = 2e$), but they can be used for reasonably similar lugs.

Allowable Loads

The allowable loads for the different failure modes (lug bearing failure, lug net-tension failure, and bushing failure) are determined from Equations (9-3), (9-6), and (9-9) in terms of the (unknown) lug thickness. The lowest of these loads is critical.

Lug Thicknesses

The required male and female lug thicknesses are determined by equating the applied load in each lug to the critical failure load for the lug.

Pin Bending

To prevent bending failure of the pin before lug or bushing failure occurs in a uniformly loaded symmetrical double-shear joint, the required pin diameter is

$$D_p = \sqrt[3]{\frac{2.55\,P}{k_{b_p}\,F_{tu_p}}\left(t_1 + \frac{t_2}{2} + 2g\right)} \qquad (9\text{-}34)$$

where k_{b_p} is the plastic bending coefficient for the pin. If the value of D_p from Equation (9-34) is greater than that from Equation (9-33), the joint must be redesigned because the pin is critical in bending.

Reduced Edge Distance

If the allowable bushing load (Equation (9-9)) is less than the allowable lug load (Equation (9-3)), a reduced value of e, obtained by using the curve shown in Figure 9-16 for optimum e/D, will give a lighter joint in which lug bearing failure and bushing bearing failure will occur simultaneously. The previously calculated pin diameter and lug thicknesses are unchanged.

Reduced Lug Width

If the lug net-tension strength (Equation (9-6)) exceeds the bearing strength (Equation (9-3)), the net-section width can be reduced by the ratio of the bearing strength to the net-tension strength.

9.14.1.2 Axial Lug Design for Pin Failure in the Bending Mode

Pin and Bushing Diameters (First Approximation)

A first approximation to the optimum pin diameter is shown in Equation (9-35).

$$D_p = \sqrt[4]{\frac{1.273}{k_{b_p}} \left(\frac{P}{F_{tu_p}}\right)^2 \left(\frac{F_{tu_p}}{F_{t\,all_1}} + \frac{F_{tu_p}}{F_{t\,all_2}}\right)} \qquad (9\text{-}35)$$

where $F_{t\,all_1}$ is either F_{tux_1} or $1.304\,F_{tyx_1}$, whichever is smaller; and $F_{t\,all_2}$ is either F_{tux_2} or $1.304\,F_{tyx_2}$, whichever is smaller. This approximation becomes more accurate when there are no bushings and when there is no gap between lugs.

The first approximation to the outside diameter of the bushing is $D = D_p + 2t_B$.
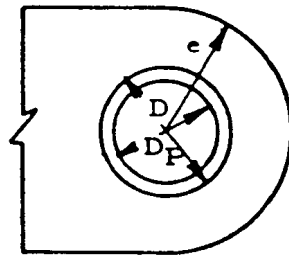
F_{br_B} = Allowable bushing ultimate bearing stress

F_{tux} = Lug material cross-grain ultimate tensile stress
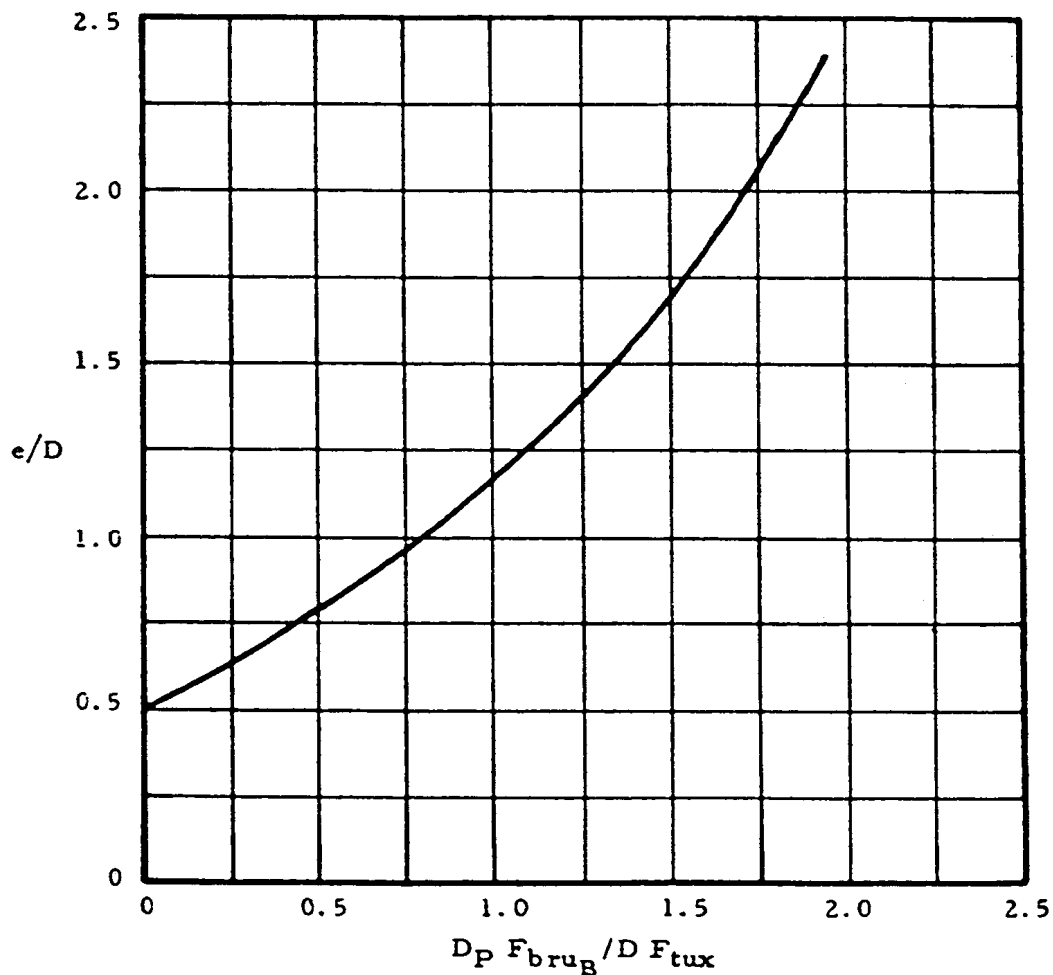
Figure 9-16. Edge Distance Ratio

Edge Distance Ratio (e/D)

The value of e/D that will minimize the combined lug and pin weight is obtained from Figure (9-15)(b) for the case of symmetrical double-shear joints in which lug bearing failure and pin bending failure occur simultaneously. The lug is assumed not critical in tension and the bushing is assumed not critical in bearing.

The curves apply specifically to concentric lugs (a = e - D/2, and w = 2e), but can be used for reasonably similar lugs.

Allowable Loads (First Approximation)

The allowable loads for the different failure modes (lug bearing failure, lug net-tension failure, and bushing failure) are determined from Equations (9-3), (9-6), and (9-9), in terms of the (unknown) lug thickness. The lowest of these loads is critical.

Lug Thicknesses (First Approximation)

The first approximation to the required male and female lug thicknesses are determined by equating the applied load in each lug to the lowest allowable load for the lug.

Pin Diameter (Second Approximation)

The second approximation to the pin diameter is obtained by substituting the first approximation lug thicknesses into Equation (9-34).

Final Pin and Bushing Diameters and Lug Thicknesses

The final optimum pin diameter is very closely approximated by

$$D_{p\ opt} = 1/3\ D_p\ (\text{Equation (9-35)}) + 2/3\ D_p\ (\text{Equation (9-34)}) \qquad (9\text{-}36)$$

An average value, however, is generally sufficient. If the final optimum value is not a standard pin diameter, choose the next larger standard pin and bushing.

The final lug thicknesses corresponding to the standard pin and bushing are then determined.

Pin Shear

The pin is checked for shear strength (Equation (9-33)).

9 - 32

Reduced Edge Distance

If the bushing bearing strength (Equation (9-9)) is less than the lug bearing strength (Equation (9-3)), a reduced value of e/D, obtained from the curve in Figure 9-16, will give a lighter joint. The pin diameter and lug thicknesses are unchanged.

Reduced Lug Width

If the lug net-tension strength (Equation (9-6)) exceeds the lug bearing strength (Equation (9-3)), the net-section width can be reduced by the ratio of the bearing strength to the net-tension strength.

9.14.1.3 Example of Axially Loaded Lug Design

Using the same materials for the lug, bushing and pin as mentioned in Section 9.6, and assuming the same allowable static load of 37900 pounds, a symmetrical double-shear joint will be designed to carry this load. A 0.10-inch gap is again assumed between the lugs. The bushing wall thickness is assumed to be 1/8 inch.

The lug will first be assumed to be concentric (a = e - D/2, and w = 2e) but the final minimum weight design will not necessarily be concentric.

Pin Failure Mode (Equation (9-32))

The pin is first checked to determine whether it will be critical in shear or bending, using Equation (9-32). Assuming $D = D_p$ as a first approximation, determine $F_{br\ all_1}$ and $F_{br\ all_2}$, using the graph in Figure 9-14 to determine K.

$$KF_{tux_1} = 1.02 \times 64000 = 65300 \text{ psi; } 1.304 \, KF_{tyx_1}$$

$$= 1.304 \times 1.02 \times 40000 = 53100 \text{ psi;}$$

$$1.304 \, F_{cy_{B_1}} = 1.304 \times 60000 = 78200 \text{ psi; therefore, } F_{br\ all_1} = 53100 \text{ psi}$$

$$KF_{tux_2} = 1.02 \times 77000 = 78500 \text{ psi; } 1.304 \, KF_{tyx_2}$$

$$= 1.304 \times 1.02 \times 66000 = 87900 \text{ psi}$$

$$1.304 \, F_{cy_{B_2}} = 1.304 \times 60000 = 78200 \text{ psi; therefore } F_{br\ all_2} = 78200 \text{ psi}$$

Therefore,

$$R = \frac{\pi \times 82000}{1.56 \times 125000} \times \left(\frac{82000}{53100} + \frac{82000}{78200} \right) = 3.4 \quad \text{(Equation (9-32))}$$

Therefore, the design procedure for pins critical in bending applies.

Pin and Bushing Diameters - First Approximation (Equation (9-35))

$$D_p = \sqrt[4]{\frac{1.273}{1.56} \times \left(\frac{37900}{125000} \right)^2 \times \left(\frac{125000}{52160} + \frac{125000}{77000} \right)} = 0.741 \text{ in.}$$

$$D = 0.741 + 2 \times 0.125 = 0.991 \text{ in.}$$

Edge Distance Ration (e/D)

The optimum value of e/D for both male and female lugs is 1.24 (Figure 9-15 (b)). Therefore a/D is 0.74 and w/D is 2.48 for a concentric lug (therefore, w = 2.46 in.).

Allowable Loads - Female Lugs and Bushings (First Approximation)

(a) Lug Bearing Strength (Equations (9-2a) and (9-36))

$$P_{bru_{L_1}} = 1.304 \times 1.46 \times 0.74 \times 40000 \times 0.991 \, t_1 = 55900 \, t_1 \text{ lbs.}$$

where K = 1.46 is obtained from Figure 9-2 for e/D = 1.24

(b) Lug Net-Section Tension Strength (Equations (9-5) and (9-6b))

K_{a_1} = 0.74 (obtained by interpolation from the graphs shown in Figure 9-9-4) for

$$\frac{D}{w} = 0.403; \qquad \frac{F_{ty}}{F_{tu}} = 0.625; \qquad \frac{F_{tu}}{E\epsilon_u} = 0.051$$

$$P_{nu_{L_1}} = 1.304 \times 40000 \times (2.46 - 0.991) \, t_1 = 56600 \, t_1 \text{ lbs.}$$

(c) Bushing Bearing Strength (Equation (9-9))

$$P_{u_{B_1}} = 1.304 \times 60000 \times 0.741 \, t_1 = 58000 \, t_1 \text{ lbs.}$$

Allowable Loads - Male Lug and Bushing (First Approximation)

(a) Lug Bearing Strength (Equations (9-1a) and (9-3a))

$$P_{bru_{L2}} = 1.46 \times 0.74 \times 77000 \times 0.991\, t_2 = 82500\, t_2 \text{ lbs.}$$

(b) <u>Lug Net-Section Tension Strength</u> (Equations (9-4) and (9-6a))

$K_{n2} = 0.88$ (obtained by interpolation from graphs shown in Figure 9-4) for

$$\frac{D}{w_2} = 0.403; \quad \frac{F_{ty}}{F_{tu}} = 0.857; \quad \frac{F_{tu}}{E\epsilon_u} = 0.125$$

$$P_{au_{L2}} = 0.88 \times 77000 \times (2.46 - 0.991)\, t_2 = 99500\, t_2 \text{ lbs.}$$

(c) <u>Bushing Bearing Strength</u> (Equation (9-9))

$$P_{u_{B2}} = 1.304 \times 60000 \times 0.741\, t_2 = 58000\, t_2 \text{ lbs.}$$

<u>Lug Thicknesses (First Approximation)</u>

$$t_1 = \frac{37900}{2 \times 55900} = 0.339 \text{ in.}; \quad t_2 = \frac{37900}{58000} = 0.654 \text{ in.}$$

<u>Pin Diameter - Second Approximation</u> (Equation (9-34))

$$D_p = \sqrt[3]{\frac{2.55 \times 37900}{1.56 \times 125000}}(0.339 + 0.327 + 0.200) = 0.755 \text{ in.}$$

$$D = 0.7555 + 2 \times 0.125 = 1.0005 \text{ in.}$$

<u>Final Pin and Bushing Diameter</u> (Equation (9-36))

$$D_{popt} = \frac{0.741}{2} + \frac{0.755}{2} = 0.748 \text{ in. (Use 0.750 inch pin)}$$

$$D = 0.750 + 2 \times 0.125 = 1.000 \text{ in.}$$

<u>Pin Shear</u> (Equation (9-33))

$$D_p = 0.798\sqrt{\frac{37900}{82000}} = 0.541 \text{ in.}$$

Therefore, the pin is not critical in shear.

<u>Final Lug Thicknesses</u>

$$t_1 = 0.339 \times \frac{0.991}{1.000} = 0.336 \text{ in.}$$

$$t_2 = 0.654 \times \frac{0.741}{0.750} = 0.646 \text{ in.}$$

Reduced Edge Distance

The lug tension strength (Equation (9-3)) exceeds the bushing strength (Equation (9-9)) for the male lug. Therefore, a reduced e/D can be obtained for the male lug shown in Figure 9-16.

$$\frac{D_p}{D} \frac{F_{bru_B}}{F_{tux}} = \frac{0.750}{1.000} \times \frac{1.304 \times 60000}{77000} = 0.762$$

Therefore, e/D = 0.97 (male lug)

Reduced Lug Width

The lug net-section tension strength (Equation (9-6)) exceeds the bearing strength (Equation (9-3)) for both the male and female lugs. Therefore, the widths can be reduced as follows:

$$w_1 = 1.00 + (2.48 - 1.00) \left(\frac{55900 \, t_1}{56600 \, t_1} \right) = 2.46 \text{ in.}$$

$$w_2 = 1.00 + (2.48 - 1.00) \left(\frac{82500 \, t_2}{99500 \, t_2} \right) = 2.23 \text{ in.}$$

Final Dimensions

$D_p = 0.750$ in.; $\quad D = 1.000$ in.

$t_1 = 0.336$ in.; $\quad e_1 = 1.24$ in.; $\quad w_1 = 2.46$ in.

$t_2 = 0.646$ in.; $\quad e_2 = 0.97$ in.; $\quad w_2 = 2.23$ in.

Since w_2 is larger than $2e_2$, the final male lug is not concentric.

9.15 Analysis of Lugs with Less Than 5 PCT Elongation

The procedures given through Section 9-14 for determining the static strength of lugs apply to lugs made from materials which have ultimate elongations, ϵ_u, of at least 5% in all directions in the plane of the lug. This section describes procedures for calculating reductions in strength for lugs made from materials which do not meet the elongation requirement. In addition to using these procedures, special consideration must be given to possible further loss in strength resulting from material defects when the short transverse gain direction of the lug material is in the plane of the lug.

The analysis procedures for lugs made from materials without defects but with less than 5% elongation are as follows:

9.15.1 Bearing Strength of Axially Loaded Lugs with Less Than 5 PCT Elongation

(1) Determine F_{ty}/F_{tu} and ϵ_y/ϵ_u, using values of F_{ty}, F_{tu}, ϵ_y and ϵ_u that correspond to the minimum value of ϵ_u in the plane of the lug.

(2) Determine the value of B, the ductility factor, from the graph shown in Figure 9-17.

(3) Determine a second value of B (denoted by $B_{.05}$) for the same values of F_{ty}, F_{tu}, and ϵ_y as before, but with $\epsilon_u = 0.05$.

(4) Multiply the bearing stress and bearing load allowables given by Equations (9-1a) through (9-3b) by $B/B_{.05}$ to obtain the corrected allowables.
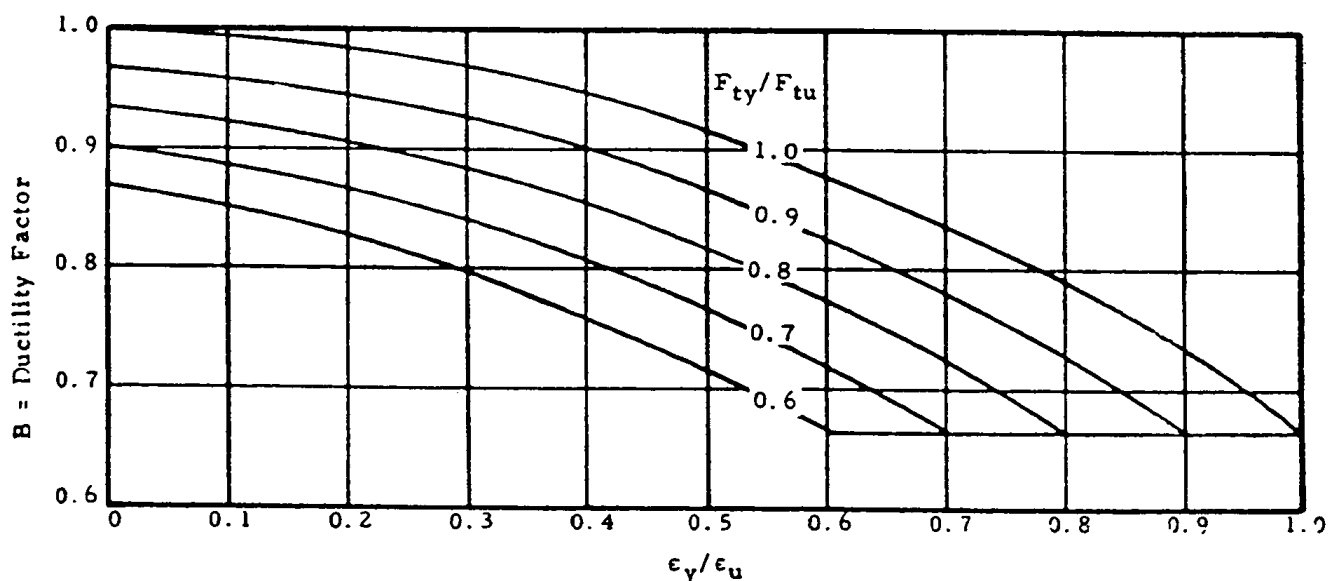
Figure 9-17. Ductility Factor

9.15.2 Net-Section Strength of Axially Loaded Lugs with Less Than 5 PCT Elongation

The procedure for determining net-section allowables is the same for all values of ϵ_u. The graphs in Figure 9-4 are used to obtain a value of K_n which is susbstituted in Equations (9-4) and (9-5). If the grain direction of the material is known, the values of F_{ty}, F_{tu}, and ϵ_u used in entering the graphs should correspond to the grain direction parallel to the load. Otherwise, use values corresponding to the minimum value of ϵ_u in the plane of the lug.

9.15.3 Strength of Lug Tangs in Axially Loaded Lugs with Less Than 5 PCT Elongation

The plastic bending coefficient for a rectangular cross section can be approximated by $k_{b_L} = 1.5B$, where B is obtained from Figure 9-17, in which y and u are the yield and ultimate strains of the lug tang material in the direction of loading. The maximum allowable value of k_{b_L} for a rectangle is 1.4.

9.15.4 Lug-Bushing Strength in Axially-Loaded Single-Shear Joint with Less Than 5 PCT Elongation

The values of k_{br_L} and k_{b_L} for rectangular cross sections are approximated by 1.5B, where B is determined from the graph as described in Figure 9-17. The maximum allowable values of k_{br_L} and k_{b_L} are 1.4.

9.15.5 Bearing Strength of Transversely Loaded Lugs with Less Than 5% Elongation (Equations (9-28) through (9-30b) in Section 9.7.1

The same procedure as that for the bearing strength of axially loaded lugs is used.

(1) Determine B and $B_{.05}$ as described for axially loaded lugs, where B corresponds to the minimum value of ϵ_u in the plane of the lug.

(2) Multiply the bearing stress and bearing load allowables given by Equations (9-28) through (9-30b) by $B/B_{0.5}$ to obtain the corrected allowables.

9.16 Stresses Due to Press Fit Bushings

Pressure between a lug and bushing assembly having negative clearance can be determined from consideration of the radial displacements. After assembly, the increase in inner radius of the ring (lug) plus the decrease in outer radius of the bushing equals the difference between the radii of the bushing and ring before assembly:

$$\delta = u_{ring} - u_{bushing} \tag{9-36}$$

where

δ = Difference between outer radius of bushing and inner radius of the ring.

u = Radial displacement, positive away from the axis of ring or bushing.

Radial displacement at the inner surface of a ring subjected to internal pressure p is

$$u = \frac{D_p}{E_{ring}} \left[\frac{C^2 + D^2}{C^2 - D^2} + \mu_{ring} \right] \qquad (9\text{-}37)$$

Radial displacement at the outer surface of a bushing subjected to external pressure p is

$$u = - \frac{B_p}{E_{bush.}} \left[\frac{B^2 + A^2}{B^2 - A^2} - \mu_{bush.} \right] \qquad (9\text{-}38)$$

where

A = Inner radius of bushing   D = Inner radius of ring (lug)
B = Outer radius of bushing   E = Modulus of elasticity
C = Outer radius of ring (lug) μ = Poisson's ratio

Substitute Equations (9-37) and (9-38) into Equation (9-36) and solve for p;

$$p = \frac{\delta}{\dfrac{D}{E_{ring}}\left(\dfrac{C^2 + D^2}{C^2 - D^2} + \mu_{ring}\right) + \dfrac{B}{E_{bush.}}\left(\dfrac{B^2 + A^2}{B^2 - A^2} - \mu_{bush.}\right)}$$

Maximum radial and tangential stresses for a ring subjected to internal pressure occur at the inner surface of the ring (lug).

$$F_r = -p \qquad F_t = p \left[\frac{C^2 + D^2}{C^2 - D^2} \right]$$

Positive sign indicates tension. The maximum shear stress at this point is

$$F_s = \frac{F_t - F_r}{2}$$

The maximum radial stress for a bushing subjected to external pressure occurs at the outer surface of the bushing is

$$F_r = -p$$

The maximum tangential stress for a bushing subjected to external pressure occurs at the inner surface of the bushing is

$$F_t = - \frac{2_{pB}^{\ 2}}{B^2 = A^2}$$

The allowable press fit stress may be based on:

(1)   Stress Corrosion. The maximum allowable press fit stress in
      magnesium alloys should not exceed 8000 psi. For all aluminum
      alloys the maximum press fit stress should not exceed 0.50 F_{ty}.

(2)   Static Fatigue. Static fatigue is the brittle fracture of metals
      under sustained loading, and in steel may result from several
      different phenomena, the most familiar of which is hydrogen
      embrittlement. Steel parts heat treated above 200 ksi, which
      by nature of their function or other considerations are exposed
      to hydrogen embrittlement, should be designed to an allowable
      press fit stress of 25% F_{tu}.

(3)   Ultimate Strength. Ultimate strength cannot be exceeded, but is
      not usually critical in a press fit application.

(4)   Fatigue Life. The hoop tension stresses resulting from the press
      fit of a bushing in a lug will reduce the stress range for oscillating
      loads, thereby improving fatigue life.

The presence of hard brittle coatings in holes that contain a press fit
bushing or bearing can cause premature failure by cracking of the coating
or by high press fit stresses caused by build-up of coating. Therefore,
Hardcoat or HAE coatings should not be used in holes that will subsequently
contain a press fit bushing or bearing.

Figures 9-18 and 9-19 permit determining the tangential stress, F_T,
for bushings pressed into aluminum rings. Figure 9-18 presents data for
general steel bushings, and Figure 9-19 presents data for the NAS 75 class
bushings. Figure 9-20 gives limits for maximum interference fits for steel
bushings in magnesium alloy rings.

9.17 Lug Fatigue Analysis

A method for determining the fatigue strength of 2024-T3 and 7075-T6
aluminum alloy lugs under axial loading is presented.

Figures 9-21 and 9-22 show the lug and the range of lug geometries
covered by the fatigue strength prediction method. Fatigue lives for lugs
having dimensional ratios falling outside the region shown should be corrobo-
rated by tests.

In this method the important fatigue parameters are k_1, k_2, and k_3
(see Figure 9-23).
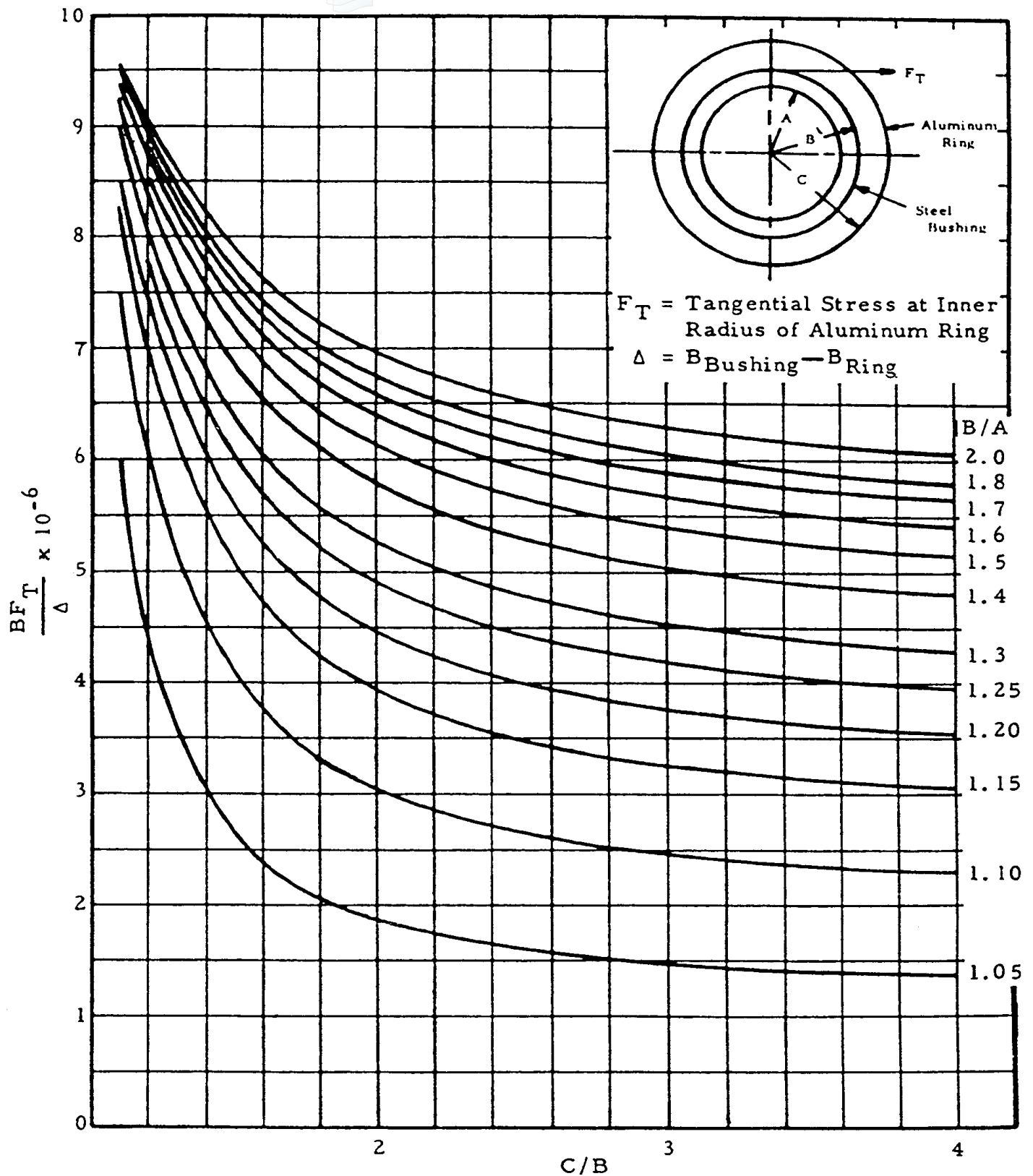
Figure 9-18. Tangential Stresses for Pressed Steel Bushings
in Aluminum Rings
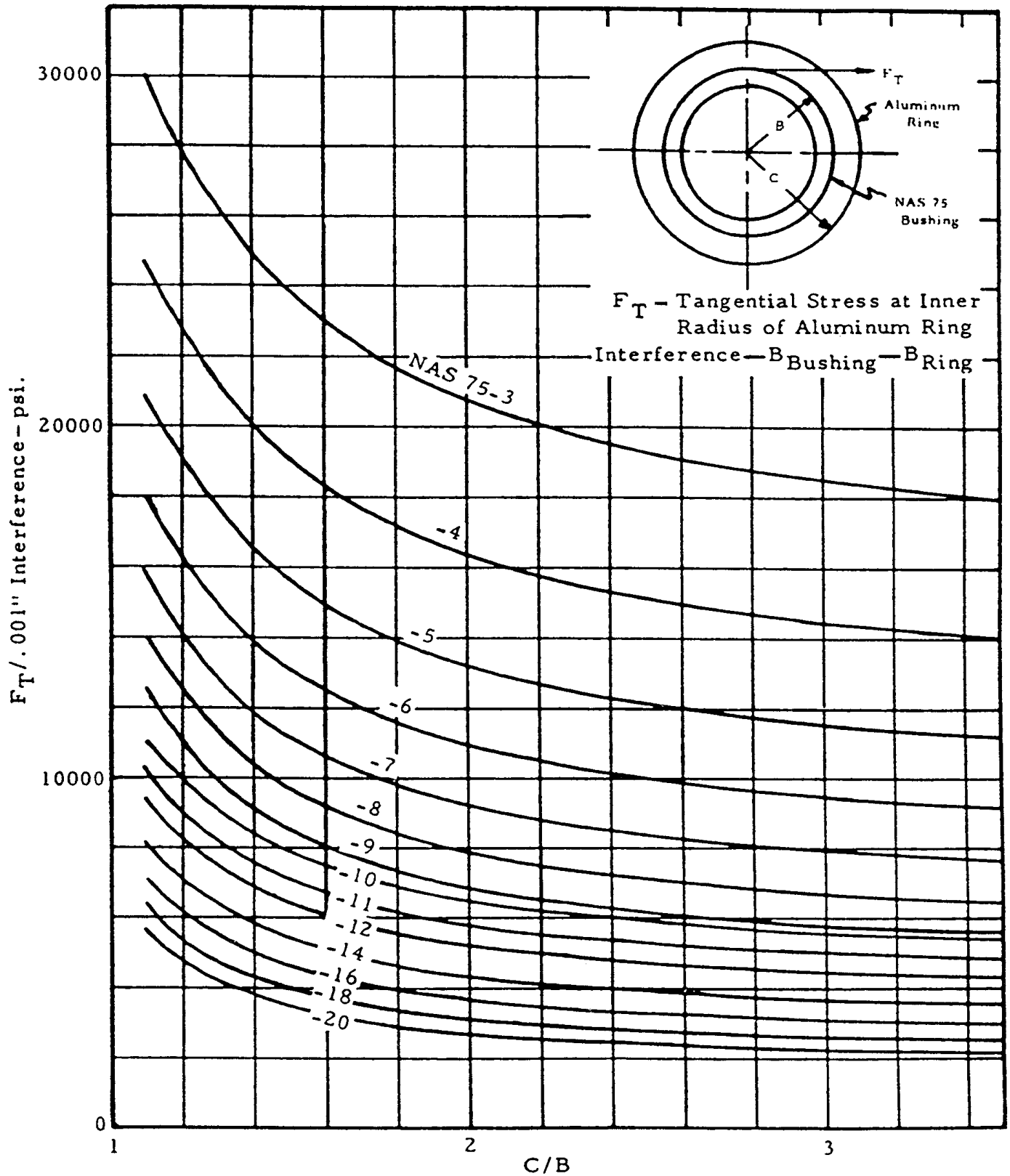
Figure 9-19.   Tangential Stresses for Pressed NAS 75 Bushings
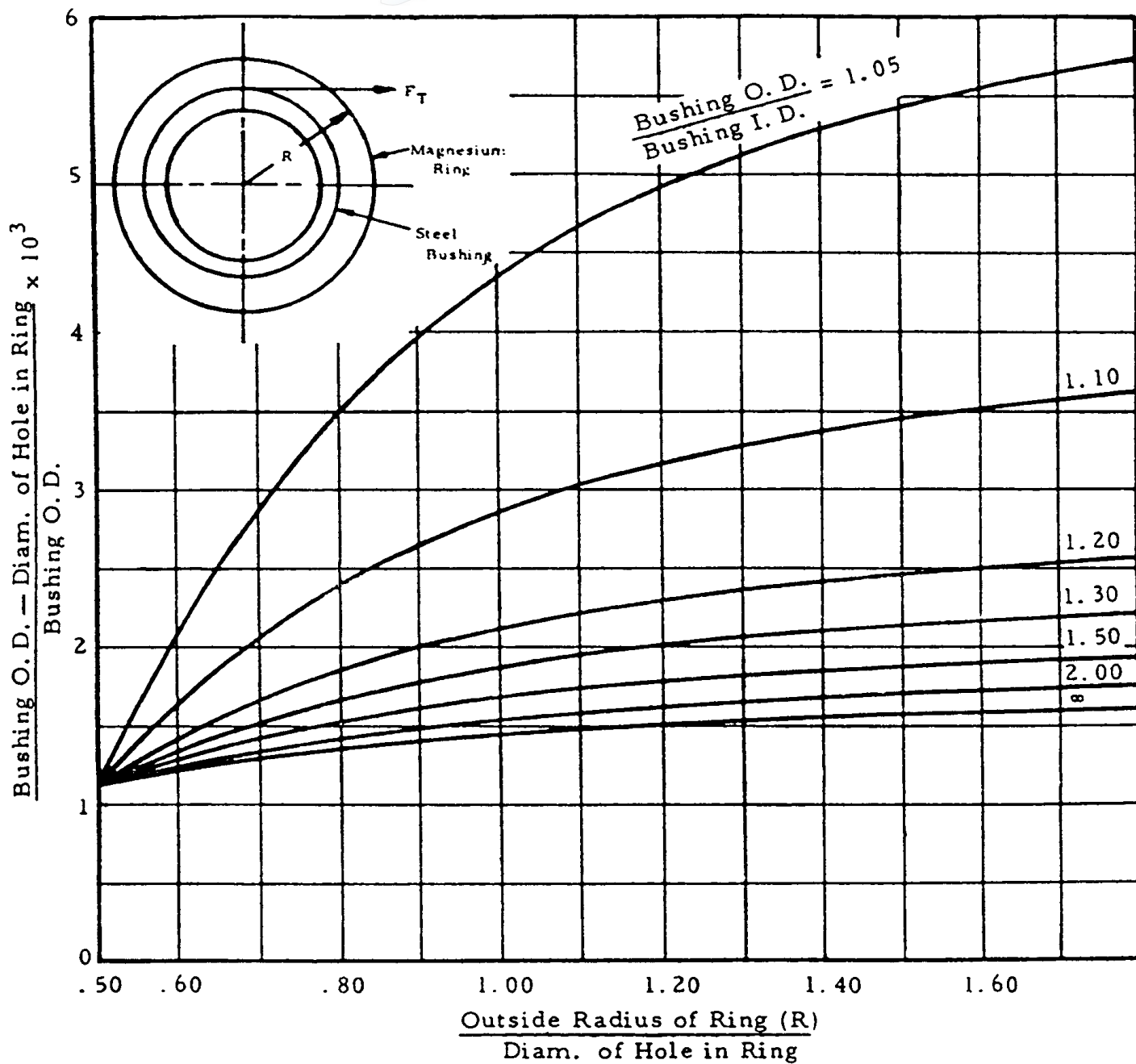
O. D. of the bushing is the after-plating diameter of the bushing.

The curves are based upon a maximum allowable interference tangential stress of 8000 psi.

Figure 9-20.   Maximum Interference Fits of Steel Bushings in Magnesium Alloy Rings
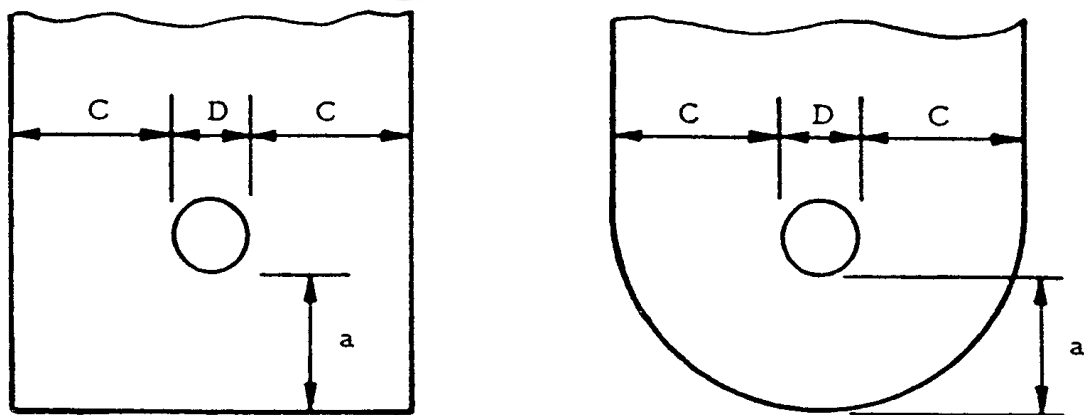
Figure 9-21. Lug Geometry for Fatigue Analysis
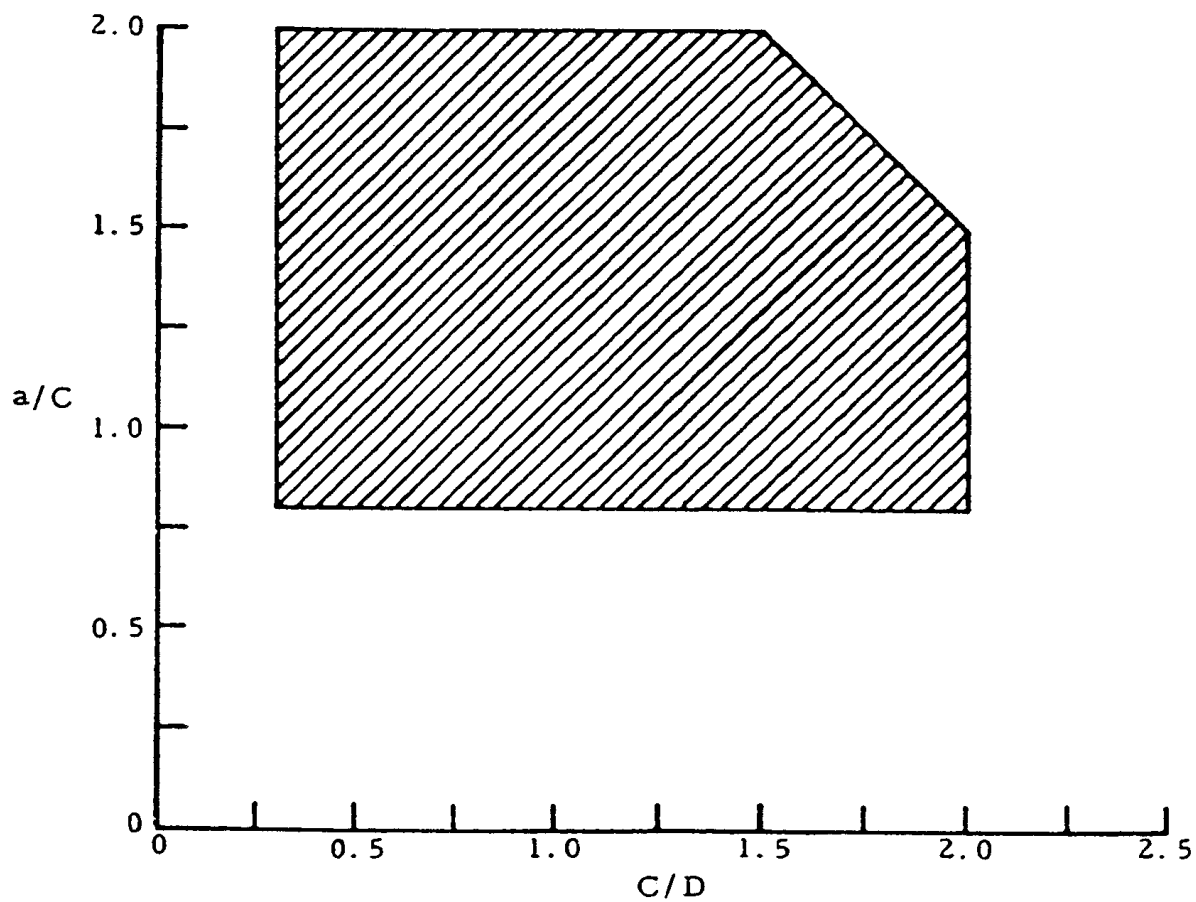
Figure 9-22. Region of Lug Geometries Covered by Fatigue
Prediction Method
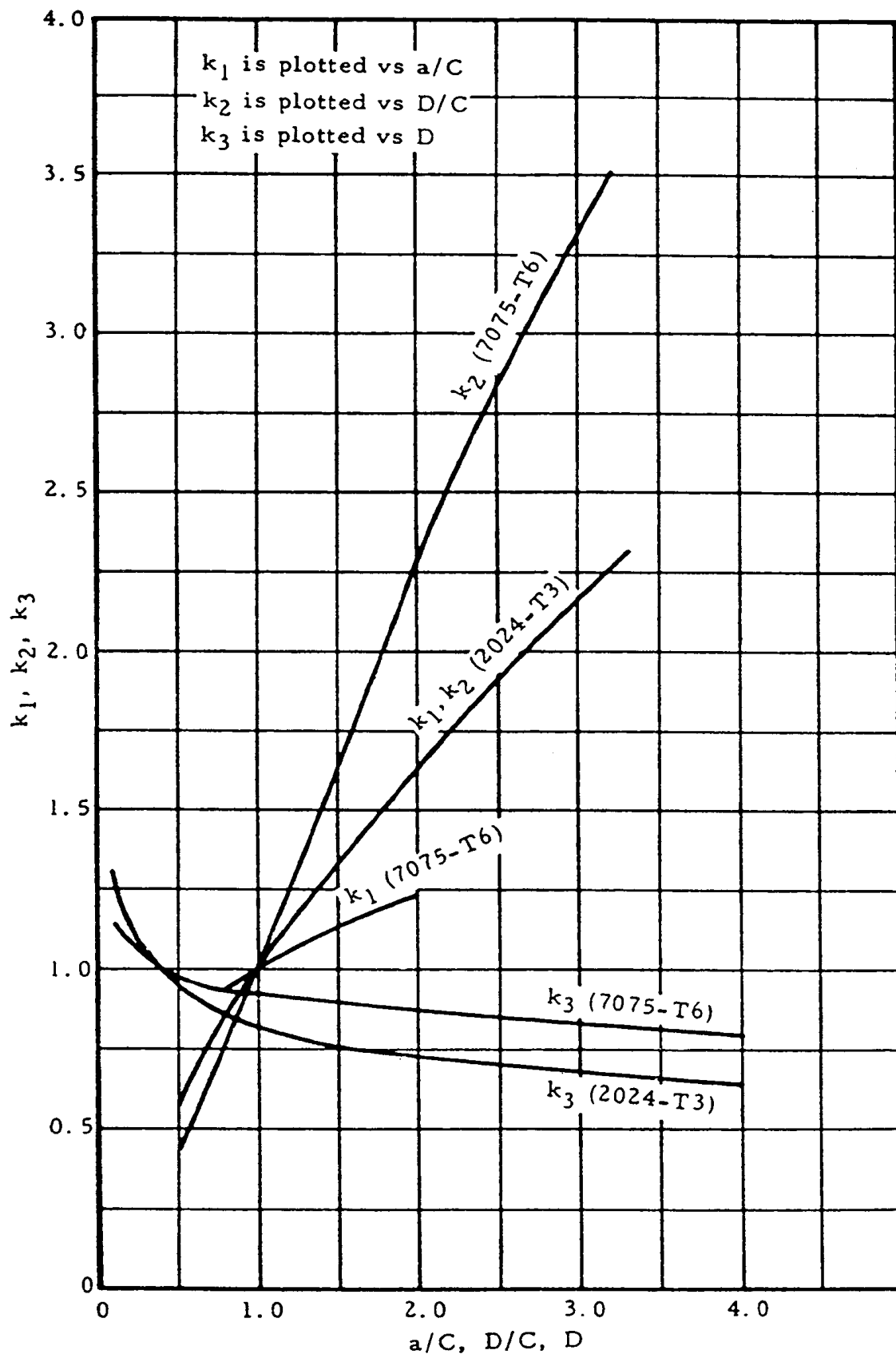
Figure 9-23. Parameters To Be Used in Figure 9-24 for Lug Fatigue Analysis

To find the allowable life knowing the applied stresses and lug dimensions, or to find the allowable stresses knowing the life, R value ($R = f_{min}/f_{max}$) and, lug dimensions, use the following procedure:

(1) Enter Figure 9-22 to check that the lug dimensional ratios fall within the region covered by the method. Enter Figure 9-23 and read k_1, k_2, and k_3; calculate the product $k_1k_2k_3$.

(2) Calculate the allowable net-tension static stress for the lug, F_{nu_L}, according to the method described in Section 9.3.2.

(3) Determine the value $0.4\ F_{nu_L}$. This is the alternating stress corresponding to a maximum stress value of $0.8\ F_{nu_L}$ when $f_{min} = 0$. $0.8\ F_{nu_L}$ was chosen as an average yield stress value for 2024 and 7075 aluminum alloy lugs.

(4) Using the value $0.4\ F_{nu_L}$ as an alternating stress, draw a straight line between the intersection of this value and the appropriate $k_1k_2k_3$ curve on Figures 9-24 or 9-25, and the point $0.5\ F_{nu_L}$ at 1 cycle. This extends the $k_1k_2k_3$ curve to cover the entire life range to static failure.

(5) Enter Figure 9-24 or 9-25 (lug fatigue curves for the case where R = 0) with $k_1k_2k_3$. For values of life, $N = 10^3$, 3×10^3, 10^4, etc., or any other convenient values, determine the corresponding values of f_a, the stress amplitude causing fatigue failure when R = 0.

(6) Plot the values of f_a found in Step 5 along the R = 0 line in a Goodman diagram such as shown in Figure 9-26 ($f_a = f_a$ when R = 0). The Goodman diagram shown in Figure 9-27 applies to a particular 7075-T6 lug for which $k_1k_2k_3 = 1.32$ (see example problem 1), but is typical of all such diagrams.

(7) Plot the allowable net-tension static stress found in Step 2 as f_m at the point (f_m, 0) of the Goodman diagram ($f_m = f_{max}$ when $f_a = 0$). For the case considered in Figure 9-26, this point is plotted as (f_m = 70,000 psi, f_a = 0).

(8) Connect the point plotted in Step 7 with each of the points plotted in Step 6 by straight lines. These are the constant life lines for the particular lug being analyzed. The Goodman diagram is now complete and may be used to determine a life for any given applied stresses, or to determine allowable stresses knowing the life and R value.
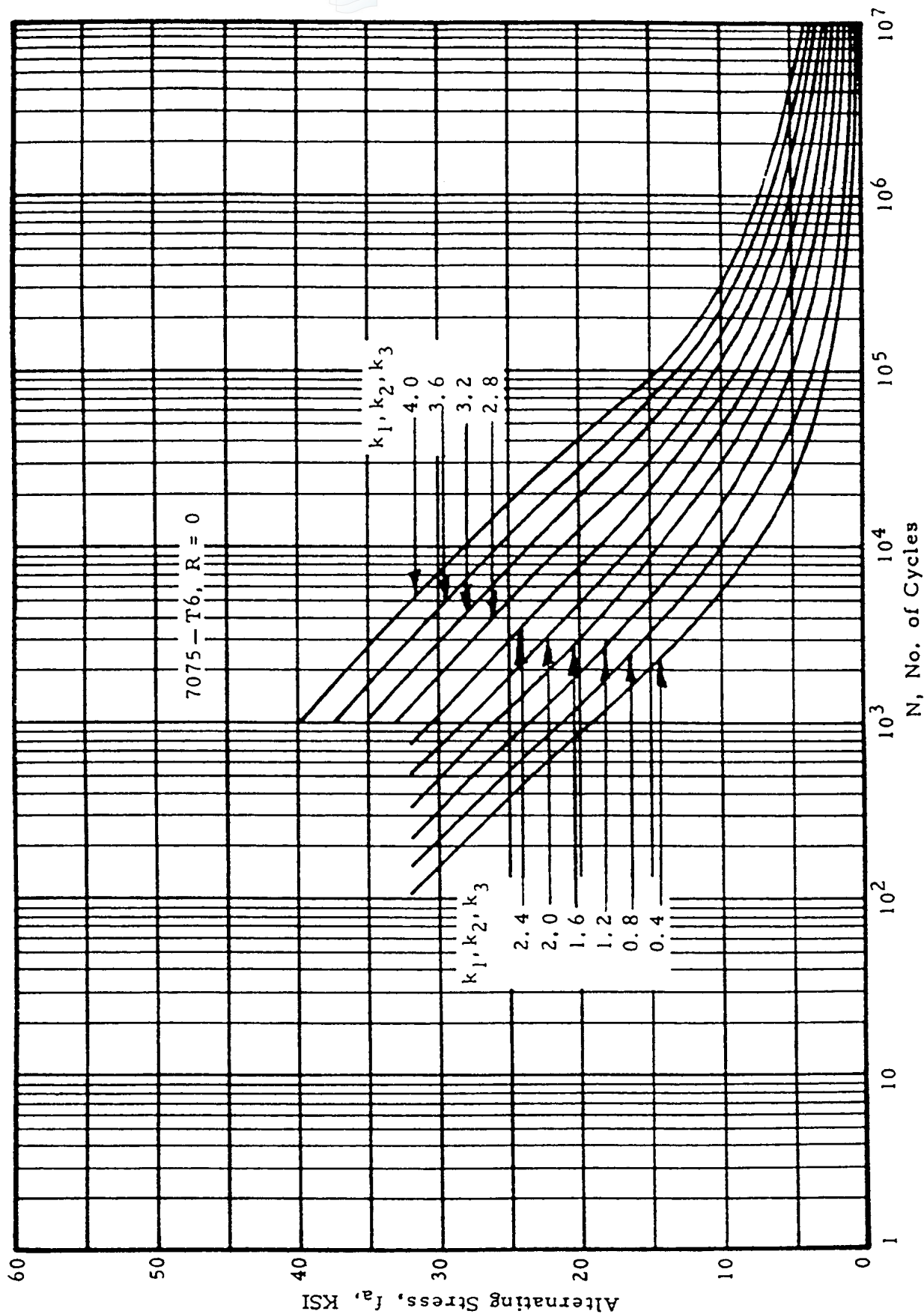
Figure 9-24. Fatigue Life Curves for Constant k_1, k_2, k_3 Values; 7075-T6, R = 0
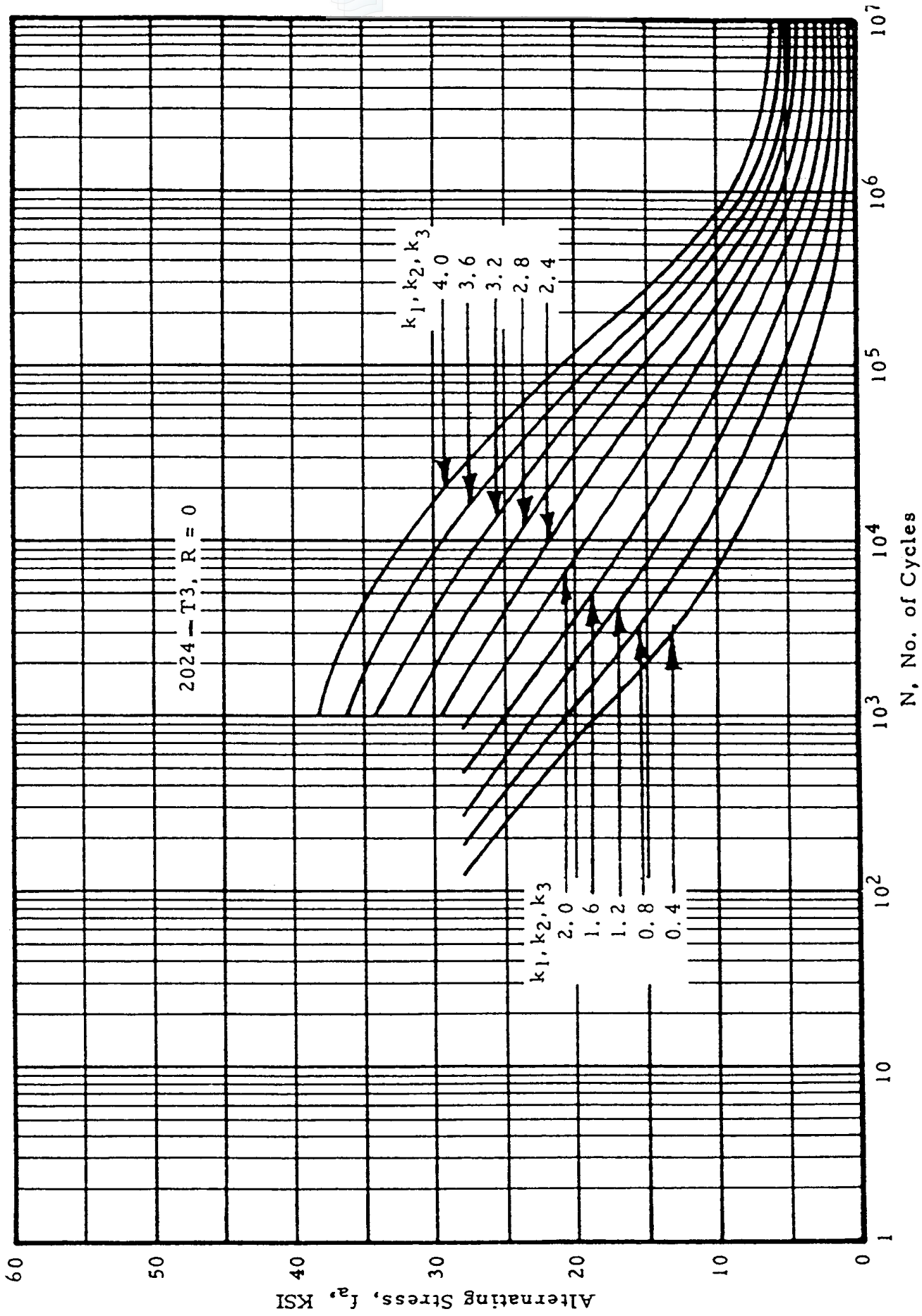
Figure 9-25. Fatigue Life Curves for Constant k_1, k_2, k_3 Values; 2024—T3, R = 0
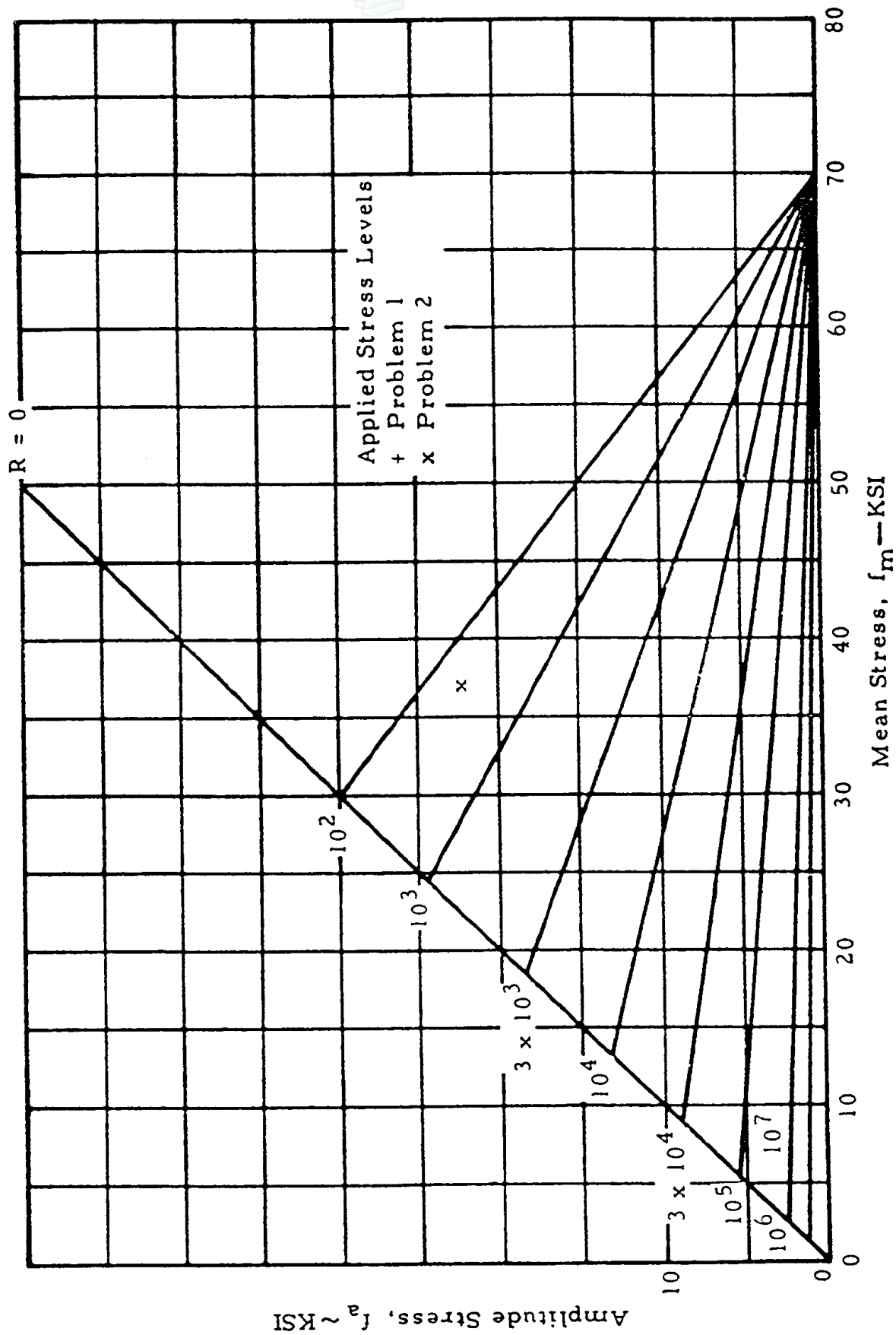
Figure 9-26. Goodman Diagram for Example Problems
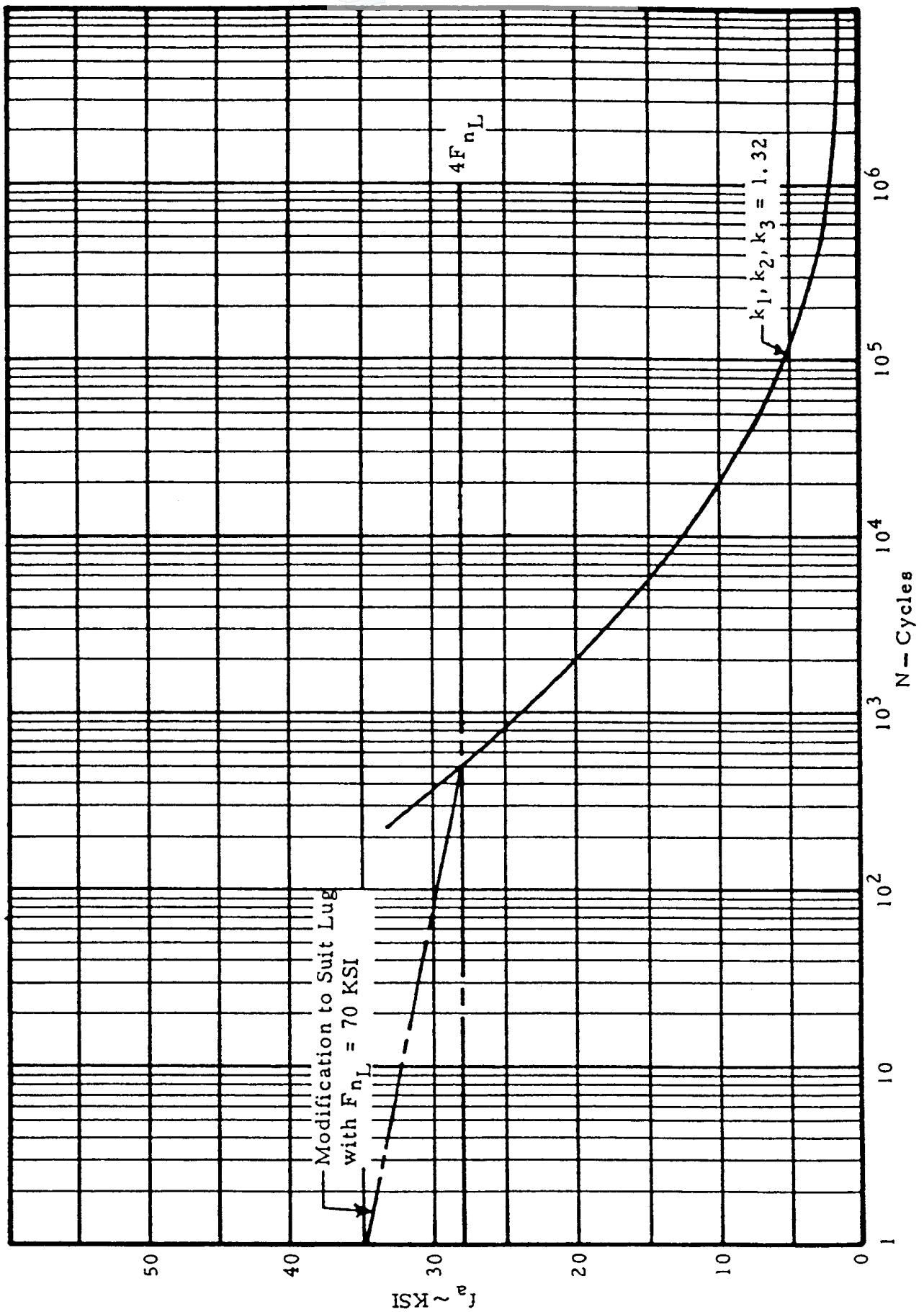
Figure 9-27. Modification to Curve $k_1, k_2, k_3 = 1.32$

9.18 Example Problem of Lug Fatigue Analysis

Given a concentric 7075-T6 aluminum lug as shown in Figure 9-21, with the following dimensions: a = 0.344 in, c = 0.3444 in, and D = 0.437 in. If the lug is subjected to a cycle axial load such that the maximum net-section stress is 27,000 psi and the minimum net section stress is 18,470 psi, find the fatigue life.

From the lug dimensions,

a/c = 1.0   c/D = 0.787   (D/c = 1.27)

(1) Figure 9-22 indicates that the lug may be analyzed using this method. From Figure 9-23,

$k_1 = 1.0$; $k_2 = 1.33$; $k_3 = 0.99$; $k_1k_2k_3 = 1.32$

(2) Calculate the allowable net-section tensile ultimate stress, F_{nu_L}, for Equation (9-4) in Section 9.3.2. For the given lug, $F_{nu_L} = 70,000$ psi.

(3) $0.4 F_{nu_L} = 0.4 \times 70,000 = 28,000$ psi.

(4) Draw a light pencil line on Figure 9-24 from the point ($f_a = 28,000$ psi on $k_1k_2k_3 = 1.32$) to the point ($f_a = 35,000$, N = 1 cycle) (This is illustrated, for clarity, on Figure 9-27).

(5) Enter Figure 9-24 and read values of f_a for various numbers of life cycles, using the line $k_1k_2k_3 = 1.32$. These numbers are as follows:

N	10^2	10^3	3×10^3	10^4	3×10^4	10^5	10^6	10^7
f_a	30KSI	24.5	18.8	13.5	8.88	5.70	2.34	1.30

(6) Plot the values of f_a along the R = 0 line of the Goodman diagram. (Refer to Figure 9-26.)

(7) Plot $F_{n_L} = 70,000$ psi, as f_a at the point (f_m, 0) of the Goodman diagram. (Refer to Figure 9-26.)

(8) Connect the points plotted in Step 6 with the point plotted in Step 7 by straight lines. The Goodman diagram is now complete.

9 - 51

(9) Enter the Goodman diagram with values of $f_a = \dfrac{27,700 - 18,470}{2} = $

4,615 psi and $f_m = \dfrac{27,700 + 18,470}{2} = 23,085$ psi, and read the

fatigue life, $N = 8 \times 10^4$ cycles, by interpolation (test results show $N = 8.6 \times 10^4$ cycles).

If the known quantities are life and R value, e.g., $N = 10^4$ cycles and $R = 0$, the allowable stresses can be obtained by using the same Goodman diagram. Enter the completed Goodman diagram at $R = 0$ and $N = 10^4$ cycles and read the amplitude and mean stresses (in this case $f_a = f_m = 13,500$ psi).

Only if the lug dimensions are changed, must a new Goodman diagram be drawn.

10. TRANSMISSION SHAFTING ANALYSIS

10.1 Introduction to Transmission Shaft Analysis

This section presents design methods for mechanical shafting. In this discussion, a shaft is defined as a rotating member, usually circular, which is used to transmit power. Although normal and shear stresses due to torsion and bending are the usual design case, axial loading may also be present and contribute to both normal and shear stresses. The design case must consider combined stresses.

The general design of shafts will be discussed with emphasis on circular sections, either solid or hollow.

10.2 Nomenclature Used in Transmission Shafting Analysis

The symbols used in this section are shown in Table 10-1.

TABLE 10-1

List of Symbols Used in Shaft Analysis

C	numerical constants	n	revolutions per minute
D, d	diameter	r	radius
E	modulus of elasticity	rpm	revolutions per minute
fpm	feet per minute	f	normal stress
F	force	f_e	endurance limit stress, reversed bending
G	modulus of elasticity in shear		
hp	horsepower	f_s	shearing stress
I	moment of inertia	f_{yp}	yield point stress, tension
J	polar moment of inertia	SAE	Society of Automotive Engineers
k	radius of gyration	T	torque
K	stress concentration factor, normal stress	V	velocity, feet per minute
		y	deflection
K_t	stress concentration factor, shear stress	α	column factor
		φ	(phi) angular deformation
l	length	ω	(omega) angular velocity, radians per second
M	bending moment		

10.3 Loadings on Circular Transmission Shafting

Transmission shafting is loaded by belts, chains, and gears which both receive power from prime movers and distribute it to accomplish desired results. Differences in the amount of power either added or subtracted at various points on the shaft result in torsion of the shaft. The driving forces and the driven resistances result in bending of the shaft and, for helical gearing, an axial loading is also produced. These loadings generate both normal and shear stresses in the shaft.

10 - 1

The torsion loading produces a maximum shear stress at the shaft surface calculated from

$$f_s = \frac{Tr}{J} \tag{10-1}$$

where the torque transmitted through the section is determined from the horsepower relation:

$$T = \frac{hp\,(63,000}{n} \tag{10-2}$$

The development of these relations can be found in standard texts.

The bending force produced by gears or chains is equal to the net driving force given by

$$F = \frac{T}{r} \tag{10-3}$$

where the radius of the gear or sprocket is used. Bending forces from belts must be obtained from the sum of the forces exerted on each side of the pulley. The usual method is to use the following relation:

$$F_1 + F_2 = C(F_1 - F_2) \tag{10-4}$$

where F_1 is the tension side force and F_2 is the slack side force. The quantity $(F_1 - F_2)$ is the net obtained from the horsepower equation. For flat belts, the value of C is between 2 and 3, depending upon conditions of installation. For V-belts, use C = 1.5.

The axial load produced from gearing must be obtained from considerations of the type of gear-tooth design used. It is beyond the scope of this section to elaborate on gear loadings. Suffice it to say that they must be considered.

The bending forces create normal stresses in the shaft given by

$$f = \frac{Mr}{I} \tag{10-5}$$

The axial forces create a normal stress

$$f = \alpha \frac{F}{A} \tag{10-6}$$

where α is the factor changing F/A into an equivalent column stress where F is compression and there is an appreciable length of unsupported shaft. The recommended values of α are given in the following relation:

$$\text{(for } \ell/k < 115) \qquad \alpha = \frac{1}{1 - 0.0044\,(\ell/k)} \qquad (10\text{-}7)$$

$$\text{for } \ell/k > 115) \qquad \alpha = \frac{f_y\,(\ell/k)^2}{C\,\pi^2\,E} \qquad (10\text{-}8)$$

$C = 1.0$ is used for hinged ends and $C = 2.25$ is used for fixed ends. For tensile axial loads and for short lengths in compression, $\alpha = 1.0$ is used.

10.4 Analysis of Combined Stresses in Transmission Shafting

The recommended method for design of ductile materials subjected to combined normal and shear stresses is that employing the maximum shear stress theory. This theory states that inelastic action begins when the shear stress equals the shearing limit of the material. The maximum shear stress at any section is given as follows:

$$f_{s_{max}} = \left[\, f_s^{\,2} + \left(\frac{f}{2}\right)^2 \,\right]^{\frac{1}{2}} \qquad (10\text{-}9)$$

where f_s and f are obtained from the relations given in Section 10.3. The value to be used for the design maximum shear stress, $f_{s_{max}}$, is discussed in the next section.

10.5 Design Stresses and Load Variations for Transmission Shafting

The design stress is obtained from the yield strength of the material to be used. However, it must be modified to account for various loading anomalies. The "Code of Design of Transmission Shafting," which has been published by the ASME as code B17c, 1927, gives the basic factors to be used in determining the design stresses, either normal or shear. According to this code, the basic design stress shall be:

Shear Design Stress
$$\begin{cases} f_s = 0.3 \text{ (tensile yield strength)} \\[4pt] \text{or} \\[4pt] f_s = 0.18 \text{ (tensile ultimate strength)} \end{cases}$$

Normal Design Stress
$$\begin{cases} f = 0.6 \text{ (tensile yield strength)} \\[4pt] \text{or} \\[4pt] f = 0.36 \text{ (tensile ultimate strength)} \end{cases}$$

10 - 3

The smaller of the two computed stresses is to be used. For combined stresses, as discussed in Section 10.4, the shear design stress is used. The code also applies a factor of 0.75 to the calculated design stress if the section being considered includes a keyway. It is noted that this is equivalent to a stress concentration factor of 1.33. Table 10-2 should also be consulted prior to making allowance for keyways. Although the code does not mention stress concentration factors further, they must be considered in any design.

Figures 10-1 through 10-5 give stress concentration factors to be applied to the design stress for various types of section discontinuities.
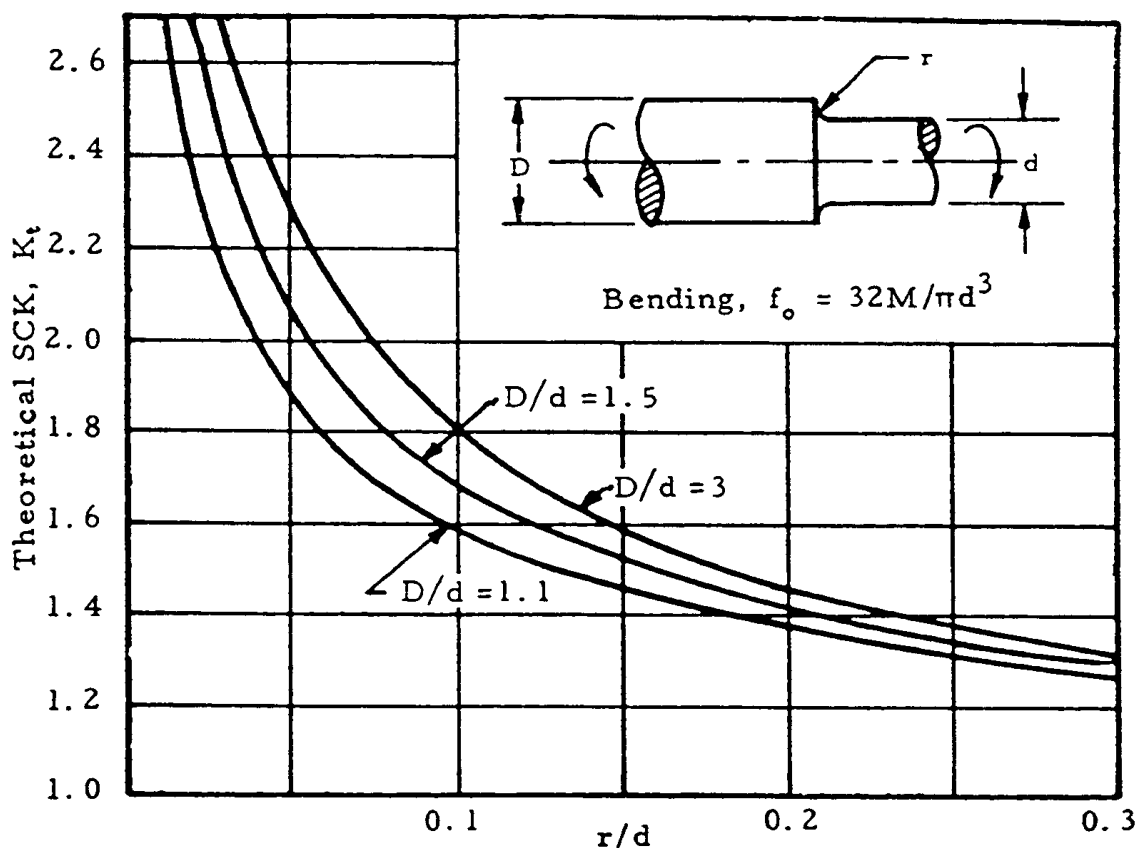
Figure 10-1. Stress Concentration Factor for Solid Shaft with Fillet
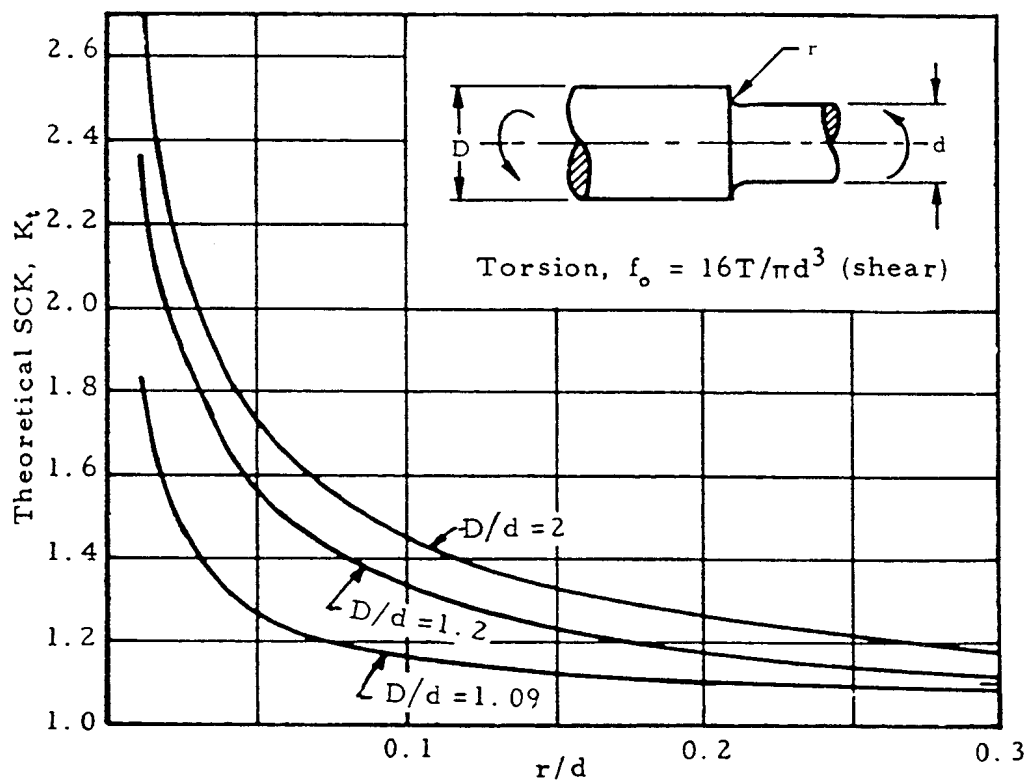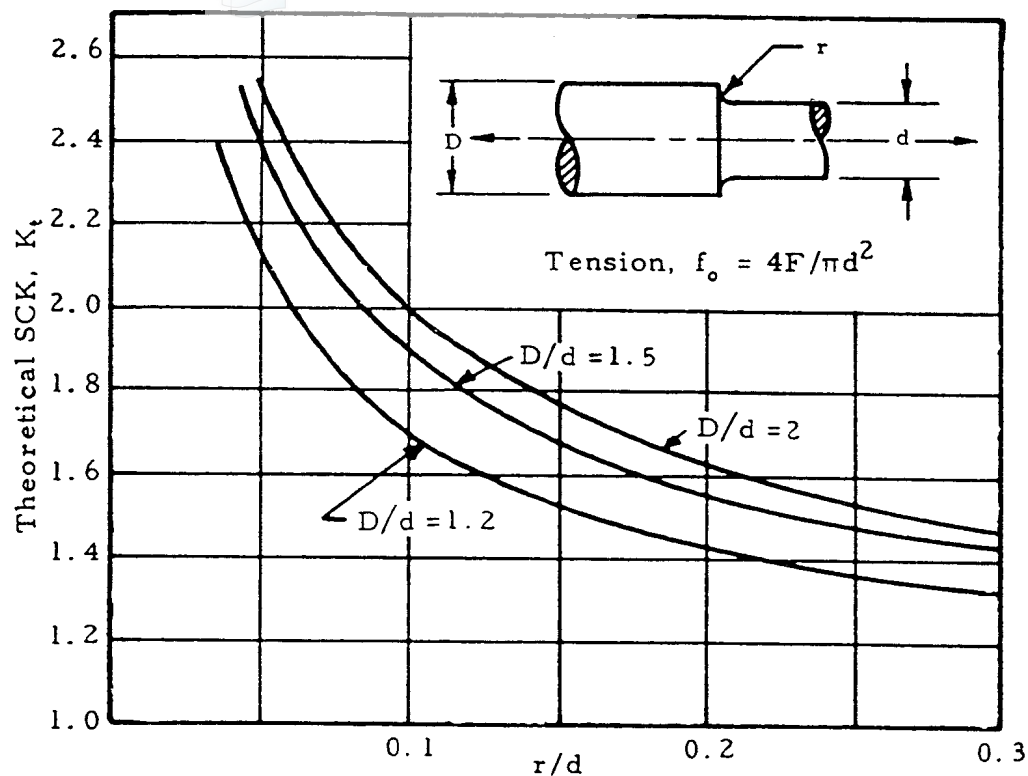
Figure 10-1. Stress Concentration Factor for Solid Shaft with Fillet (concluded)
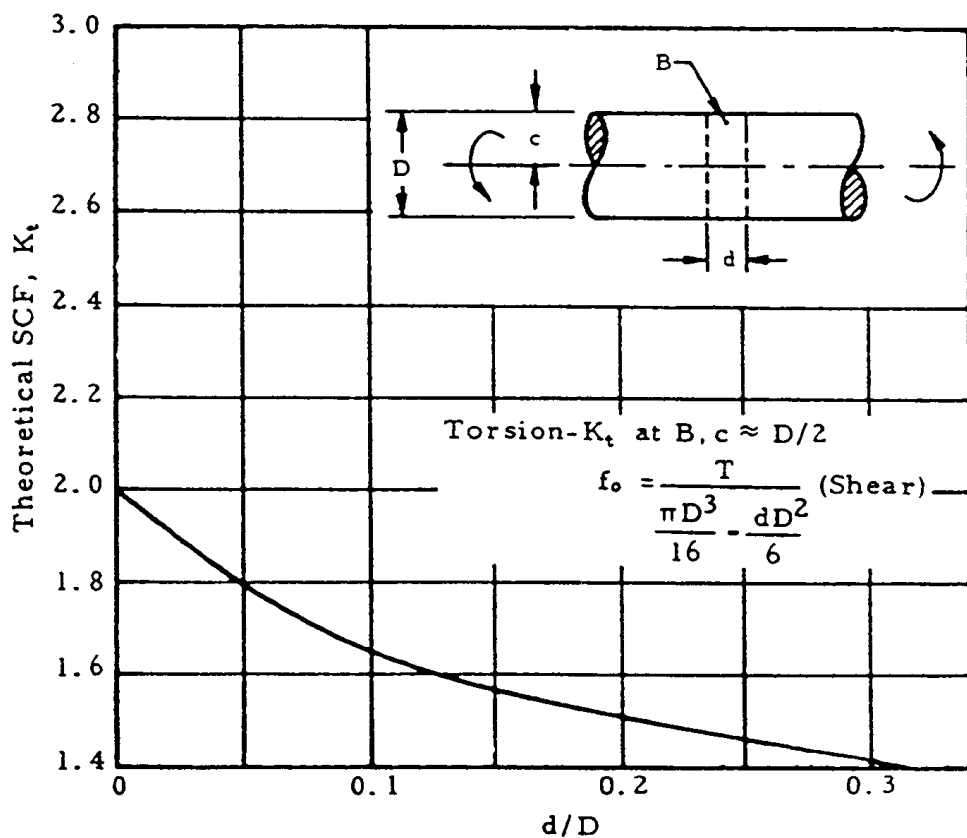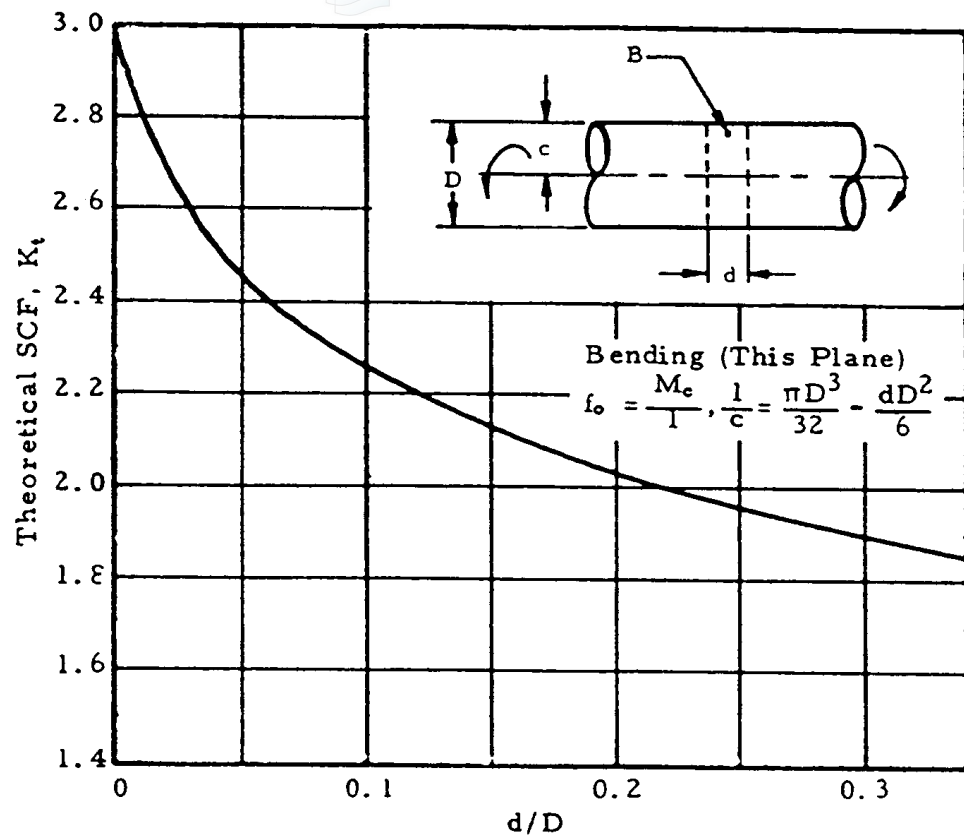
Figure 10-2. Stress Concentration Factor for Solid Shaft with Radial Hole
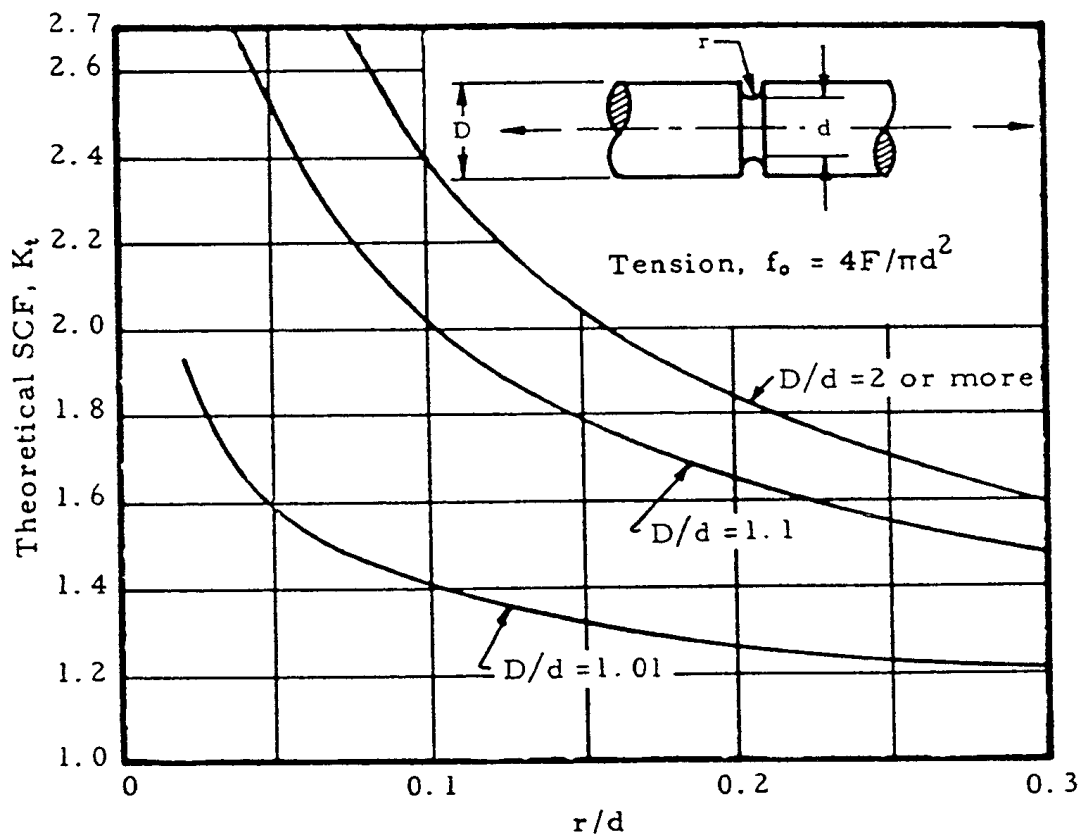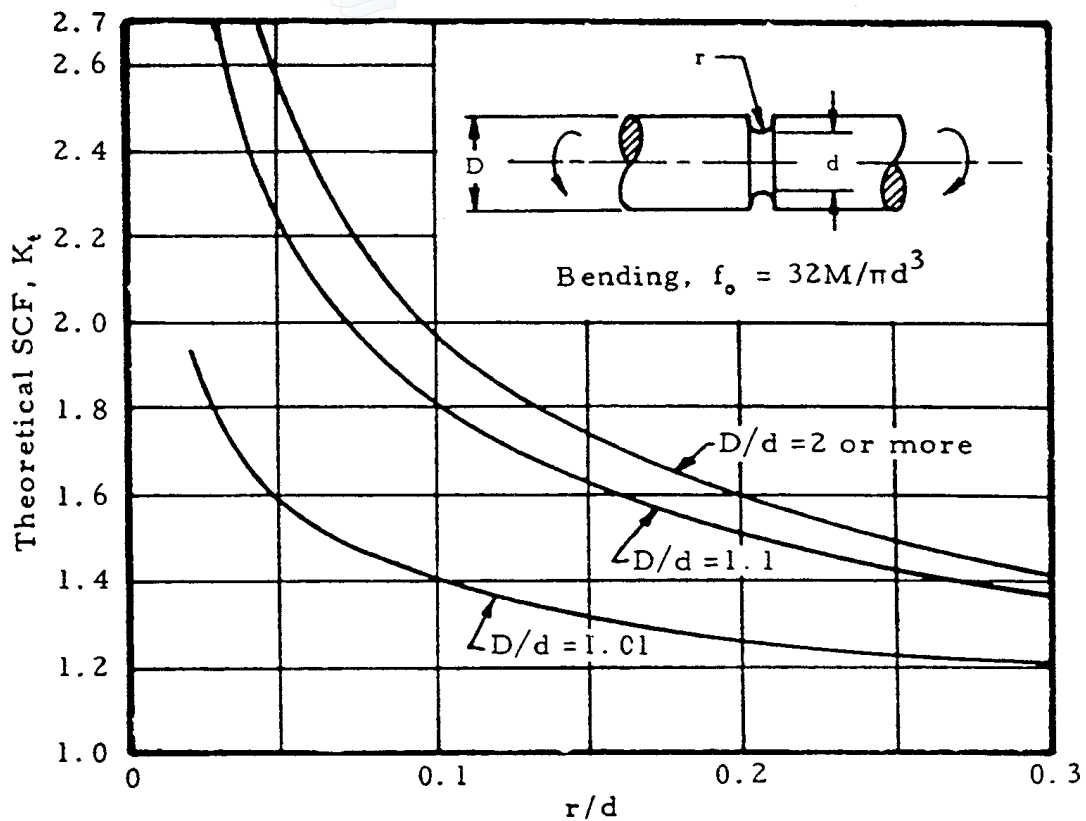
Figure 10-3. Stress Concentration Factor for Solid Shaft with Groove
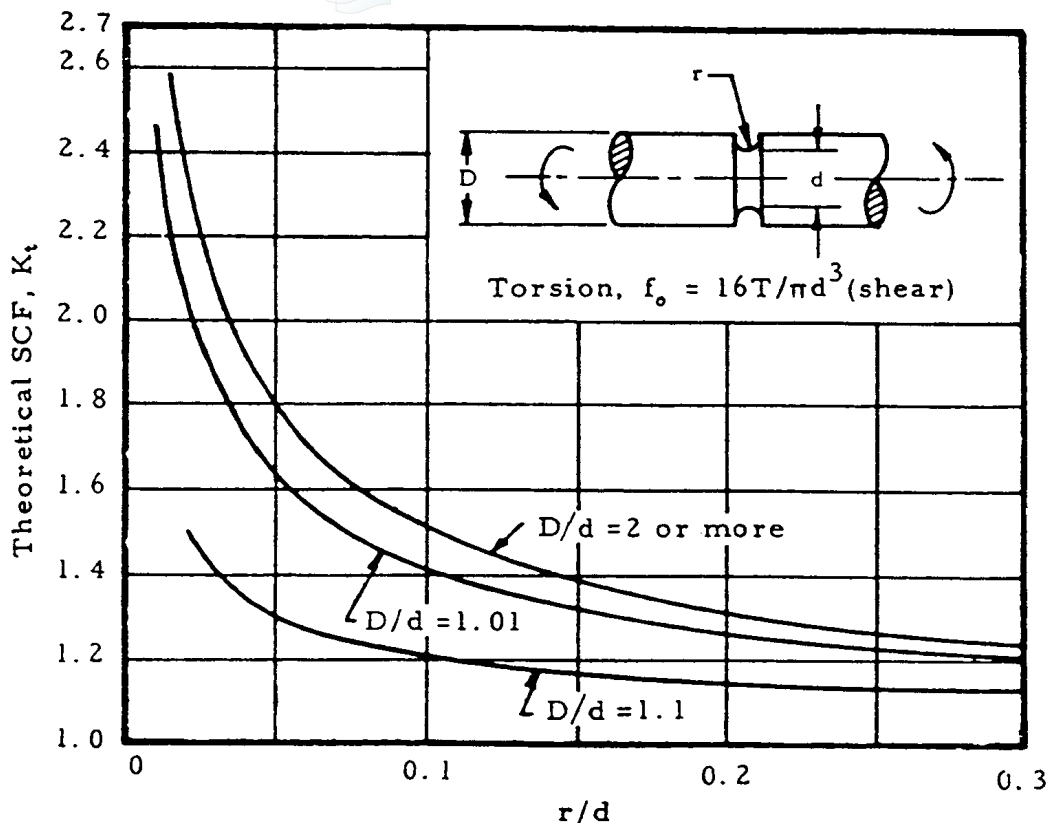
Figure 10-3. Stress Concentration Factor for Solid Shaft with Groove (concluded)
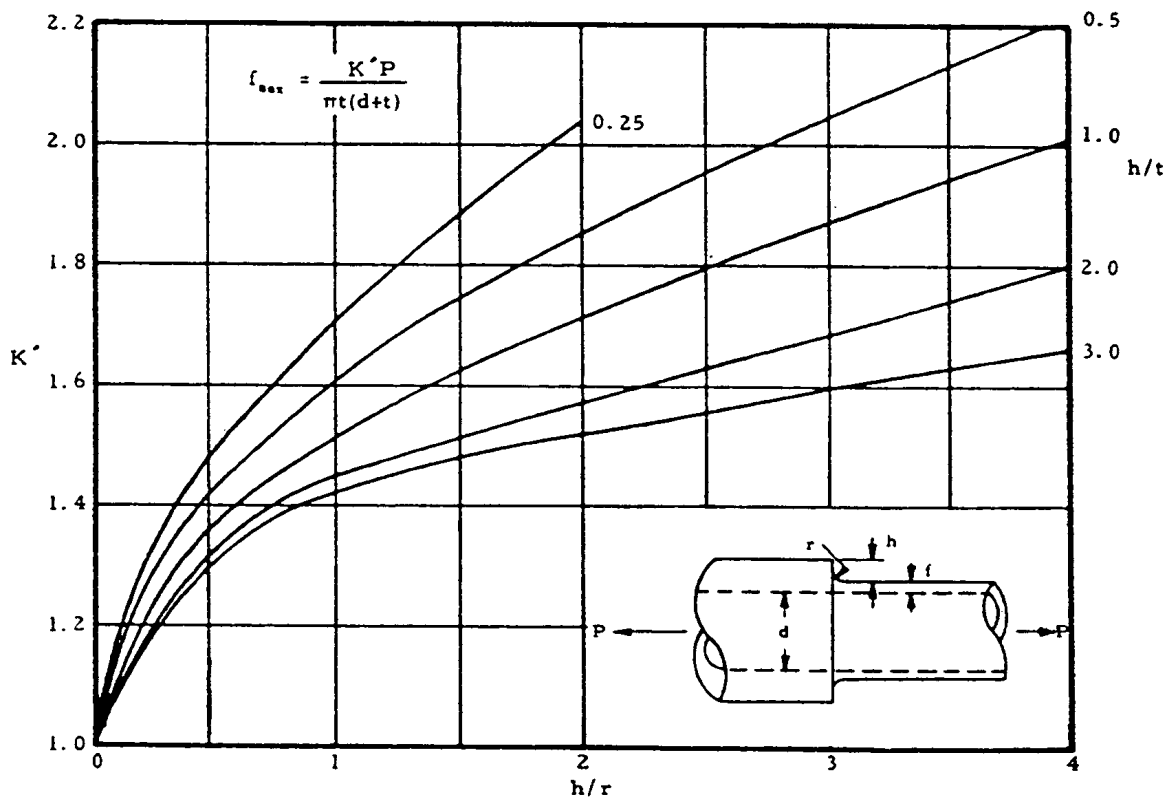
Note: The maximum stress occurs in the fillet close to the junction of the fillet with the small diameter.

Figure 10-4. Stress Concentration Factor for Hollow Shaft with Fillet

10 - 8

a. Shaft in Tension

$$f_{max} = \frac{4KP}{\pi (D_0^2 - D_1^2)}$$

$$f_{max} = \frac{16KT\, D_0}{\pi (D_0^4 - D_1^4)}$$
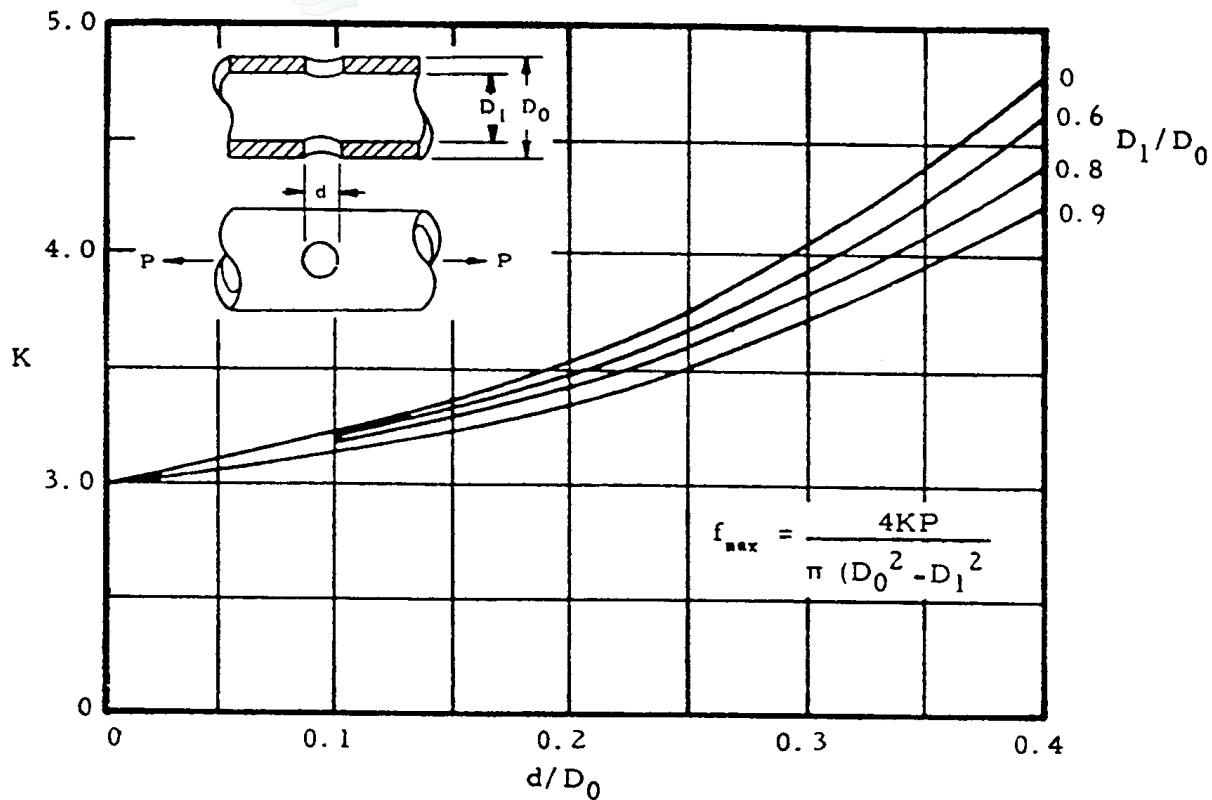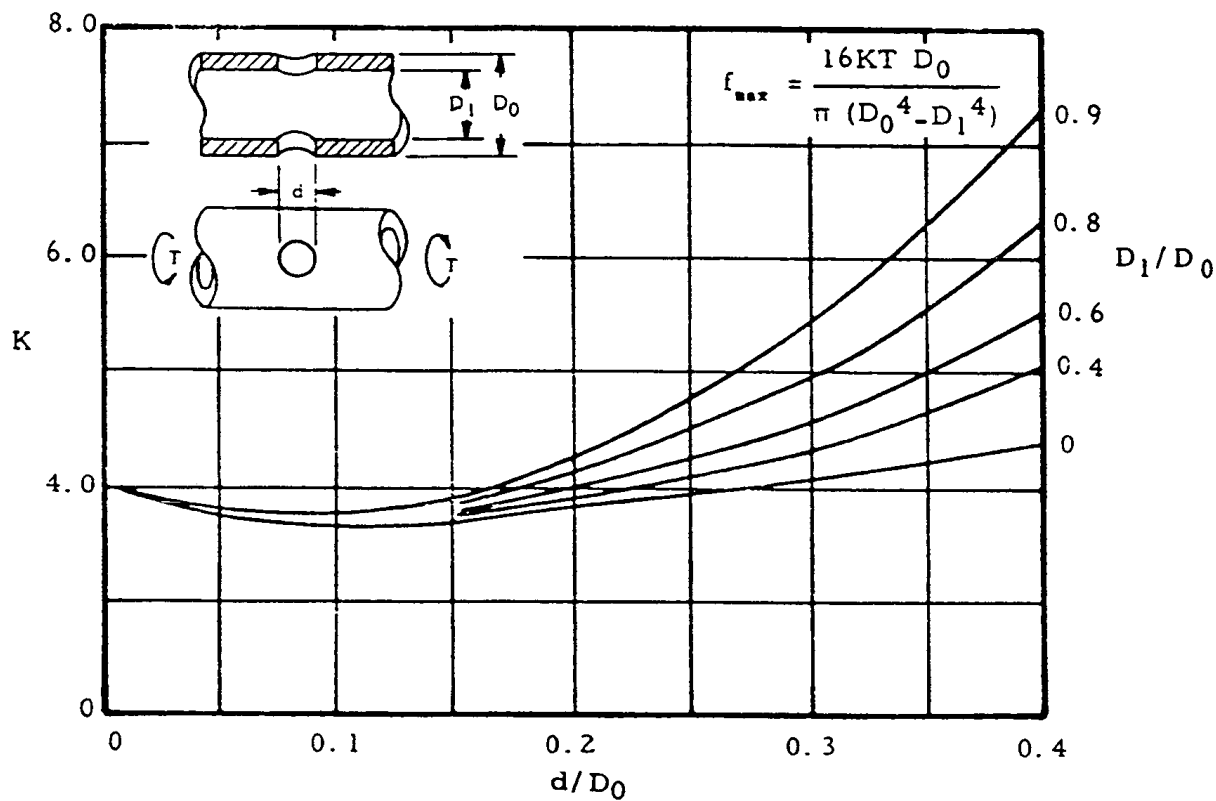
b. Shaft in Torsion

Figure 10-5.   Stress Concentration Factor for Hollow Shaft with Radial Hole
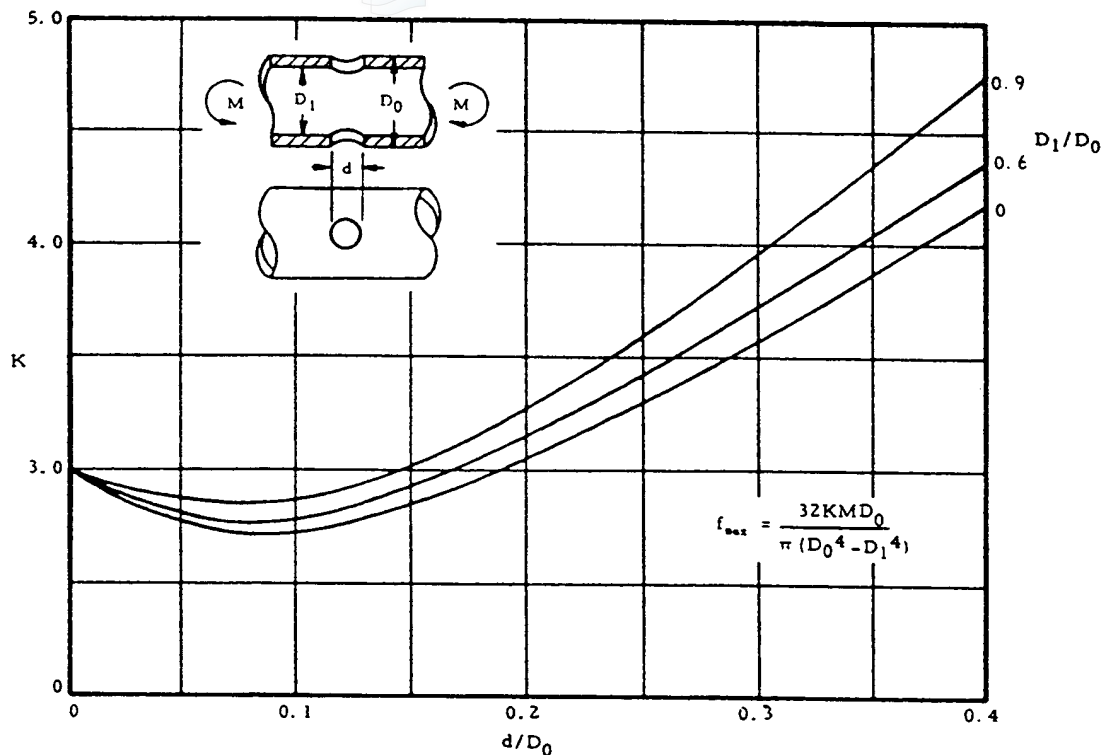
c. Shaft in Bendings

Figure 10-5.   Stress Concentration Factor for Hollow Shaft with Radial Hole (concluded)

Tables 10-2 and 10-3 give stress concentration factors to be applied to keyways and several screw thread types.   These are applied only if the section being analyzed includes either threads or a keyway.

TABLE 10-2

Values of Stress Concentration Factor for Keyways, K

Type of Keyway	Annealed		Hardened	
	Bending	Torsion	Bending	Torsion
Profile	1.6	1.3	2.0	1.6
Sled-Runner	1.3	1.3	1.6	1.6

TABLE 10-3

Values of Stress Concentration Factor for Screw Threads, K

Type of Thread	Annealed		Hardened	
	Rolled	Cut	Rolled	Cut
American National (square)	2.2	2.8	3.0	3.8
Whitworth, Unified St'd.	1.4	1.8	2.6	3.3
Dordelet	1.8	2.3	2.6	3.3

The code also recommends the application of a shock and fatigue factor to the computed torsional moment or bending moment. This factor accounts for the severity of the loading during stress reversals caused by the revolution of the shaft. Table 10-4 gives these factors for rotating shafts.

TABLE 10-4

Values of Shock and Fatigue Factors for Rotating Shafts
(from ASME Code)

Nature of Loading	K_z (bending)	K_s (torsion)
Gradually Applied or Steady	1.5	1.0
Suddenly Applied, minor	1.5 to 2.0	1.0 to 1.5
Suddenly Applied, heavy	2.0 to 3.0	1.5 to 3.0

10.6 Design Procedure for Circular Transmission Shafting

The recommended design procedure for circular shafts is as follows:

1) Define all loads on the shaft.
2) Determine the maximum torque and its location.
3) Determine the maximum bending moment and its location.
4) Determine the design stress.
5) Determine the shaft diameter at the critical diameter.
6) Check for shaft deflections.

A sample problem will illustrate the application of the above principles and the previous relations.

10.6.1 Sample Analysis of Circular Transmission Shafting

The loaded shaft illustrated in Figure 10-6 receives 20 hp at 300 rpm on pully B at a 45° angle from below. Gear C delivers 8 hp horizontally to the right, and gear E delivers 12 hp downward to the left at 30°. The shafting is to be cold-drawn C1035 with minimum values of tensile yield strength, f_y = 72,000 psi, and of tensile ultimate strength, f_u = 90,000 psi.
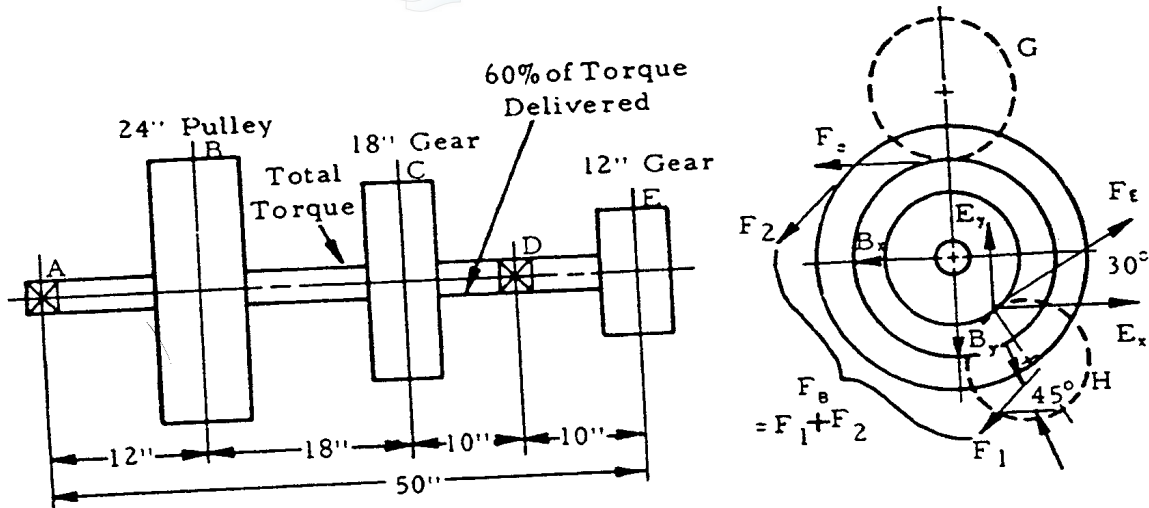
Figure 10-6. Drawing Illustrating a Loaded Shaft

The forces shown are those which are placed upon the shaft. The gearing loads do not consider the normal component. This is reasonable for $14\text{-}\frac{1}{2}°$ tooth design, but for higher pressure angles the side force should be included.

1) Define the loads.

The torques transmitted by the shaft are

$$T_B = \frac{63,000\ hp}{n} = \frac{(63,000)(20)}{300} = 4200\ in.\text{-}lbs \tag{10-10}$$

on shaft between B and C.

$$T_c = \frac{(63,000)(8)}{300} = 1680\ in.\text{-}lbs \tag{10-11}$$

taken off at C.

$$T_E = \frac{(63,000)(12)}{300} = 2520\ in.\text{-}lbs \tag{10-12}$$

on shaft between C and E.

The bending forces from the pulley is given by

$$F_B = 2(F_1 - F_2) = \frac{2T_B}{r_B} = \frac{2(4200)}{12} = 700\ lbs \tag{10-13}$$

The bending force from gear C is

$$F_c = \frac{T_c}{r_c} = \frac{1680}{9} = 187\ lbs \tag{10-14}$$

and from gear E, it is

$$F_E = \frac{T_E}{r_E} = \frac{2520}{6} = 420\ lbs \tag{10-15}$$

These applied loads are resolved into their vertical and horizontal components and the bearing reactions calculated. These reactions are found by summing moments and forces in the two planes. From these computations, the shear diagram shown in Figure 10-7 were constructed.

Horizontal Plane   Vertical Plane
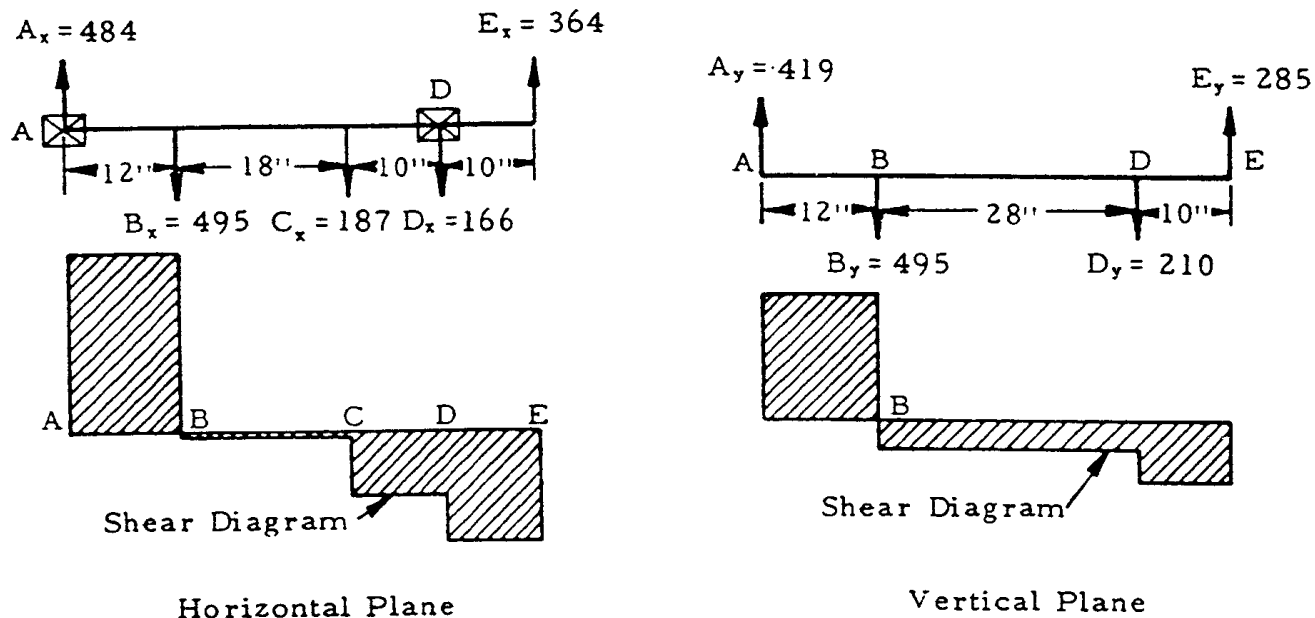
Figure 10-7. Drawing Illustrating Construction of Shear Diagrams

The maximum bending moment is located where the shear diagram crosses the axis. More complex loadings have several crossing points. Each should be investigated to find the maximum. For the present case, the maximum bending moment in the horizontal plane is

$$M_{B_x} = (12)(484) = 5810 \text{ in.-lbs} \qquad (10\text{-}16)$$

and in the vertical plane it is

$$M_{B_y} = (12)(419) = 5030 \text{ in.-lbs} \qquad (10\text{-}17)$$

Since both of these maximums are at the same place, at pulley B, this is the point of maximum moment for the shaft. It is given by

$$M_B = \left[(M_{B_x})^2 + (M_{B_y})^2 \right]^{\frac{1}{2}} \qquad (10\text{-}18)$$

$$M_B = \left[(5810)^2 + (5030)^2 \right]^{\frac{1}{2}} \qquad (10\text{-}19)$$

$$M_B = 7685 \text{ in.-lbs} \qquad (10\text{-}20)$$

It is observed that if the location of the maximum moments is not the same in each plane, both locations must be checked to find the maximum. It is also observed that for this example the maximum torque is also located at the same section.

The design stress is now determined. Based on the tensile yield strength, the shearing stress is

$$f_s = (0.3)(72,000) = 21,600 \text{ psi} \tag{10-21}$$

and based on tensile ultimate strength, it is

$$f_{s_{design}} = (0.18)(90,000) = 16,200 \text{ psi}. \tag{10-22}$$

Our design will be based on the smaller. An allowance for the keyway is now made. According to the code, 75% of the above stress is used. Thus,

$$f_{s_{design}} = (0.75)(16,200) = 12,150 \text{ psi} \tag{10-23}$$

The shock and vibration factors to be applied to the torque and moments for a gradually applied loading are $K_s = 1.0$ and $K_n = 1.5$; these are obtained from Table 10-4.

It is noted that if the section includes any other type of stress raiser such as a step in the shaft, a radial hole, or a groove, the appropriate stress concentration factors are to be applied to the design stress.

As this is a case of combined stress, the principle of maximum shear stress will be used for the design:

$$f_{s_{design}} = \left[f_s^2 + \left(\frac{f}{2} \right)^2 \right]^{\frac{1}{2}} \tag{10-24}$$

The shear stress f_s is due to the torque of 4200 in.-lbs and the normal stress f is due to the bending moment of 7685 in.-lbs.

Thus, based on the use of a solid circular shaft,

$$f_s = \frac{K_s T_c}{J} = \frac{16 K_s T}{\pi D^3} = \frac{(16)(1.0)(4200)}{\pi D^3} \tag{10-25}$$

$$f_x = \frac{K_n M_c}{I} = \frac{32 K_n M}{\pi D^3} = \frac{(32)(1.5)(7685)}{\pi D^3} \tag{10-26}$$

Substituting into Equation (10-24) the above quantities gives

$$12,150 = \left\{ \left[\frac{(16)(1.0)(4200)}{\pi D^3} \right]^2 + \left[\frac{(32)(1.5)(7685)}{2\pi D^3} \right]^2 \right\}^{\frac{1}{2}} \qquad (10\text{-}27)$$

Solving for D^3 gives

$$D^3 = \frac{16}{12.15\pi} \left\{ (4.2)^2 + [(1.5)(7.685)]^2 \right\}^{\frac{1}{2}} \qquad (10\text{-}28)$$

and

$$D = 1.726 \text{ in.} \qquad (10\text{-}29)$$

The closest size commercial shafting is 1-15/16 in. It is noted that commercial power transmission shafting is available in the following sizes:

$$\frac{15}{16}, \ 1\frac{3}{16}, \ 1\frac{7}{16}, \ 1\frac{11}{16}, \ 1\frac{15}{16}, \ 2\frac{3}{16}, \ 2\frac{7}{16}, \ 2\frac{15}{16}, \ 3\frac{7}{16}, \ 3\frac{15}{16}, \ 4\frac{7}{16},$$

$$4\frac{15}{16}, \ 5\frac{7}{16}, \ 5\frac{15}{16}, \ 6\frac{1}{2}, \ 7, \ 7\frac{1}{2}, \ 8$$

The use of standard sizes facilitates the selection of bearings, collars, couplings, and other hardware.

Machinery shafting, those used integrally in a machine, is available in the following sizes:

By 1/16 in. increments in this range	$\begin{cases} \text{1/2 to 1 in., tolerance of -0.002 in.} \\ \text{1-1/6 to 2 in., tolerance of -0.003 in.} \\ \text{2-1/6 to 2-1/2 in., tolerance of -0.004 in.} \end{cases}$
By 1/8 in. increments	2-5/8 to 4 in., tolerance of -0.004 in.
By 1/4 in. increments	4-1/4 to 6 in., tolerance of -0.005 in.
By 1/4 in. increments	6-1/4 to 8 in., tolerance of -0.006 in.

Returning to our example, the diameter of the shaft determined is based on strength considerations alone. As deflections are also a prime consideration, both angular and transverse deflections should be checked.

The torsional deflection of a shaft is given by

$$\varphi = \frac{T\ell}{GJ} \qquad (10\text{-}30)$$

10 - 15

where ℓ is the length of shaft between the point of application of the torque and the section being considered.

Although the example given was statically determinate, many situations encountered in practice are indeterminate. For these, the location of the maximum stress must be determined by methods of analysis for continuous beams: the area-moment method, the three-moment method, the method of superposition, and the moment-distribution method. The exposition of these methods is covered in the section of this manual devoted to beam analysis.

10.6.2. General Design Equation for Circular Transmission Shafting

A general design equation for circular shafts, both solid and hollow, can be developed on the basis of the recommended procedures. It is

$$D^3 = \frac{16}{f_s \pi (1-B^4)} \left\{ K_s^2 T^2 + \left[K_a M + \frac{\alpha FD (1 + B^2)}{8} \right]^2 \right\}^{\frac{1}{2}} \qquad (10-31)$$

where $B = D_i/D$ and D_i is the inside diameter of the hollow shaft. This equation requires several trials for solution because of the inclusion of the axial load F.

It is also pointed out that in the design of large-size shafting, the weight of the shaft and all pulleys and gears should be included in the design calculations.

11. BEARING STRESSES

11.1 Introduction to Bearing Stresses

The stresses developed when two elastic bodies are forced together are termed bearing stresses. They are localized on the surface of the material and may be very high due to the small areas in contact. The design information given in this section assumes either static loading or low velocity loading. The application to ball and roller antifriction bearings is not covered.

A brief discussion of bearing stresses in riveted joints is followed by a presentation of theoretically derived equations for the bearing stresses between various shapes in contact. An empirical treatment for the determination of allowable loads is also presented.

It is noted here that the design of ball and roller bearings is a very specialized area; however, their selections for various applications can be made based on data published by the various manufacturers.

11.2 Nomenclature for Bearing Stresses

a	=	1/2 the major diameter of an ellipse
c	=	1/2 the minor diameter of an ellipse
D	=	diameter
E	=	modulus of elasticity
F_{br}	=	allowable bearing load
F_{cp}	=	proportional limit in compression
F_{cy}	=	compressive yield stress
f_{br}	=	calculated bearing stress
f_{brc}	=	calculated compressive bearing stress
f_{brs}	=	calculated shear bearing stress
f_{brt}	=	calculated tensile bearing stress

$$K = \frac{8}{3} \frac{E_1 E_2}{E_2(1-\mu_1^2) + E_1(1-\mu_2^2)} \quad \text{for general case of two bodies in contact}$$

K_1, K_2, K_3	=	coefficients in Table 11-1
P	=	axial load
P_a	=	allowable axial load
R	=	minimum radius of curvature
R'	=	maximum radius of curvature
r	=	radius
r	=	cylindrical coordinate
t	=	thickness
t	=	width of rectangular area
w	=	load per length (lb/in)

w_a = allowable load per length (lb/in)

x, y = rectangular coordinates

Y = $\dfrac{4}{\dfrac{1}{R_1} + \dfrac{1}{R_2} + \dfrac{1}{R'_1} + \dfrac{1}{R'_2}}$ for general case of two bodies in contact

δ = deflection

θ = $\dfrac{1}{4} Y \left[\left(\dfrac{1}{R_1} - \dfrac{1}{R'_1} \right)^2 + \left(\dfrac{1}{R_2} - \dfrac{1}{R'_2} \right) \right.$

$\left. + 2 \left(\dfrac{1}{R_1} - \dfrac{1}{R'_1} \right) \left(\dfrac{1}{R_2} - \dfrac{1}{R'_2} \right) \cos 2\varphi \right]$

for general case of two bodies in contact

θ = cylindrical coordinate

u = Poisson's ratio

φ = angle shown in diagram for general case of two bodies in contact in Table 11-1

11.3 Bearing Stresses in Riveted Connections

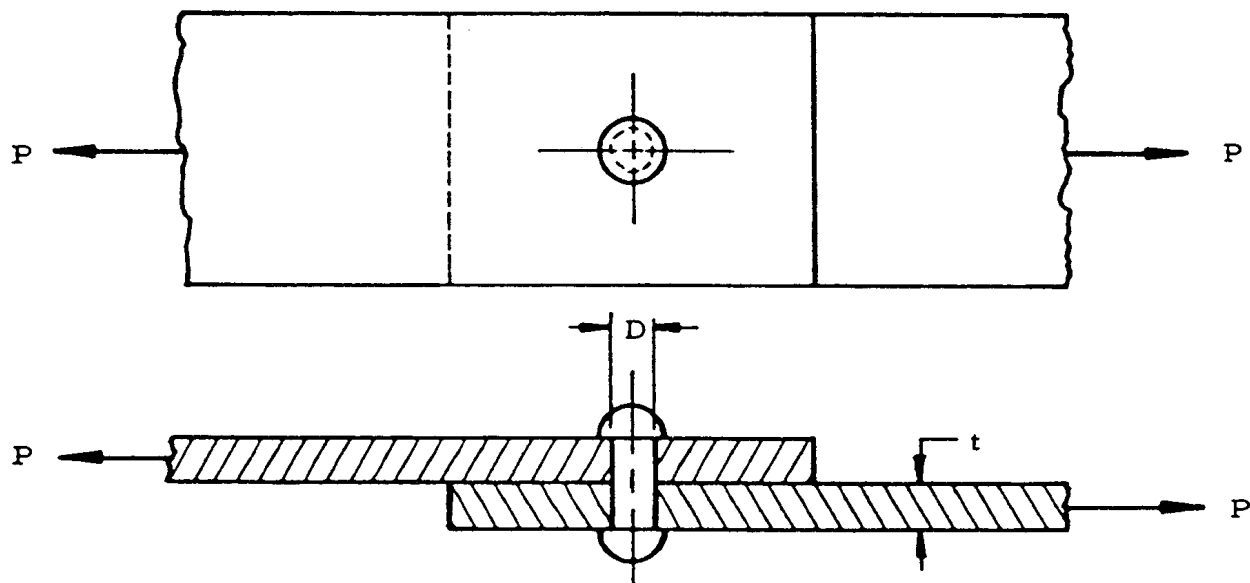Figure 11-1 shows a riveted connection between two plates.

Figure 11-1.   Riveted Connection

Excessive bearing stresses result in yielding of the plate, the rivet, or both.

The intensity of the bearing stress between the rivet and the hole is not constant but varies from zero at the edges to a maximum value directly in back of the rivet. The difficulty caused by considering a variable stress distribution may be avoided by the common practice of assuming the bearing stress to be uniformly distributed over the projected area of the rivet hole. The bearing stress is thus,

$$f_{br} = \frac{P}{Dt}$$

(11-1)

The allowable load is

$$P_a = F_{br} Dt$$

(11-2)

where F_{br} is the allowable bearing stress.

11.4 Sample Problem - Bearing Stresses in Riveted Connections

Given: The riveted plate in Figure 11-2

Find: The bearing stress between the rivets and the plate.

Solution: The load per rivet is 20,000/4 = 5,000 lb. From Equation (11-1),

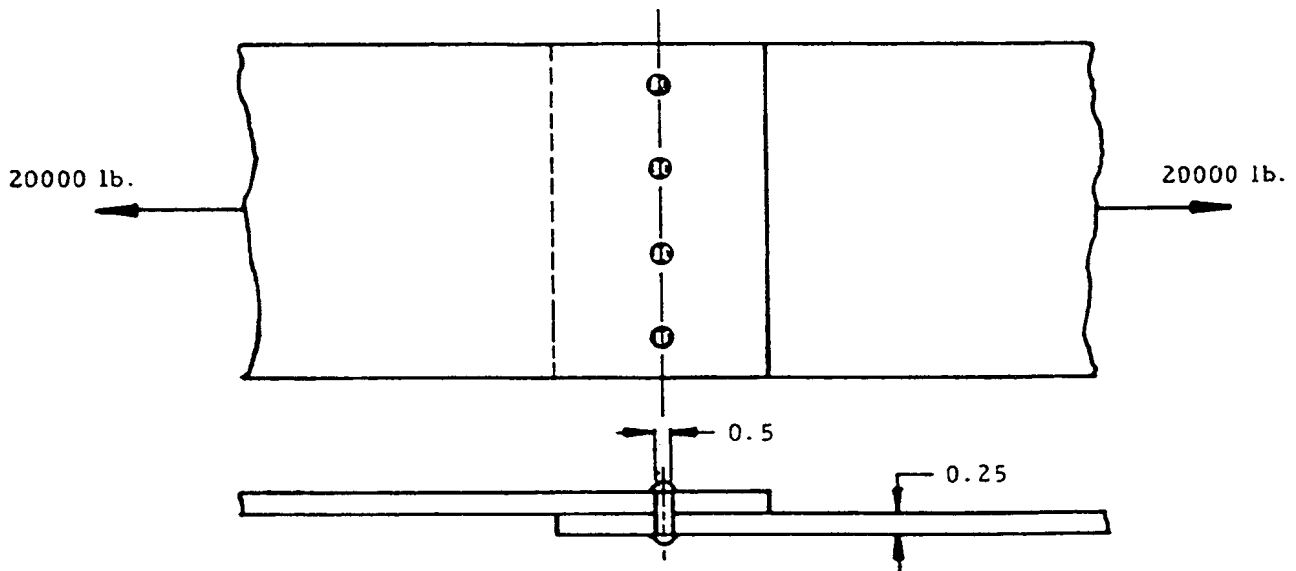$$f_{br} = \frac{P}{Dt} = \frac{5,000}{(0.5)(0.25)} = 40,000 \text{ psi}$$

Figure 11-2. Riveted Plate

11.5 Elastic Stresses and Deformation of Various Shapes in Contact

Table 11-1 treats the elastic stress and deformations produced by pressure between bodies of various forms. The first column of this table gives

11 - 3

the form of the bodies and the dimensions that describe them. The second column indicates the shape and size of the surface of contact between the two bodies as well as the combined deformation of the bodies, δ. The maximum compressive, tensile, and shear bending stresses (f_{brc}, f_{brt} and f_{brs}) are given in the third column of Table 11-1. The maximum compressive and tensile bearing stresses occur at the center of the surface of contact and at the edge of the surface of contact, respectively, and the maximum shear bearing stress occurs in the interiors of the compressed parts. The equations in Table 11-1 are based on the assumption that the length of the cylinder and the dimensions of the plate are infinite. For a very short cylinder or for a plate having a width of less than five or six times that of the contact area or a thickness of less than five or six times the depth to the point of maximum shear stress, the actual stresses may vary considerably from those given by the equation in Table 11-1.

Because of the very small area involved in what initially approximates a point or line contact, the stresses obtained from the equations in Table 11-1 are high even for light loads. However, since the stress is highly localized and triaxial, the stress intensity may be very high (above the yield point) without producing apparent damage. Since this is the case and the formulas in Table 11-1 hold only in the elastic range, the empirical formulas for allowable loads given in Section 11.7 are most useful for practical design. However, the formulas in Table 11-1 are useful as a guide to design, especially when empirical formulas are not available for a given case.

11.6 Sample Problem - Elastic Stress and Deformation of Cylinder on a Cylinder

Given: The cylinders shown in Figure 11-3.

Find: The contact surface, total deflection, and maximum compressive stress.

$$w = 30 \text{ lb/in.}$$

Steel, AISI 4130

$$E_1 = E_2 = E = 30 \times 10^6 \text{ psi}$$

$$\mu_1 = \mu_2 = 0.3$$

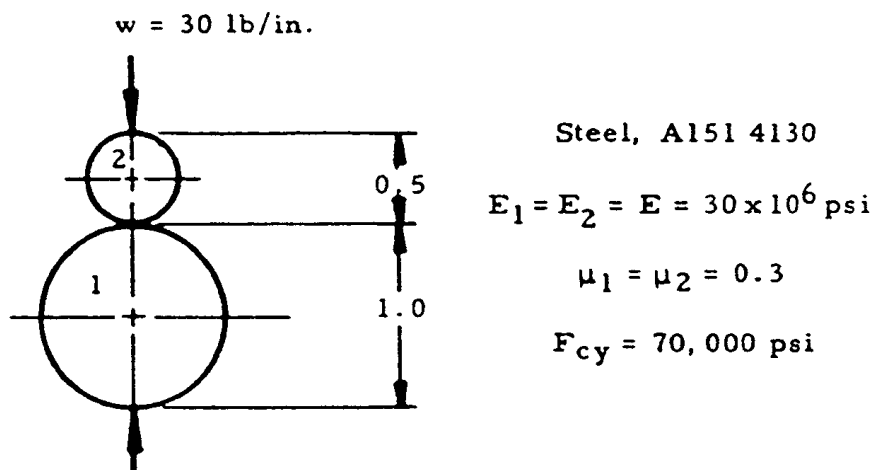$$F_{cy} = 70,000 \text{ psi}$$

Figure 11-3. Cylinders in Contact

<u>Solution:</u> From Table 11-1, the surface of contact between two cylinders with their axes parallel is a rectangular strip of width, b, given by

$$b = 1.6 \sqrt{\frac{w\, D_1 D_2}{D_1 + D_2} \left[\frac{1-\mu_1^2}{E_1} + \frac{1-\mu_2^2}{E_2} \right]}$$

In this case,

$$b = 1.6 \sqrt{\frac{30(1)(0.5)}{1+0.5} \left[\frac{1-0.3^2}{30 \times 10^6} + \frac{1-0.3^2}{30 \times 10^6} \right]} = 0.00125 \text{ in.}$$

The combined deflection of the cylinders is given by

$$\delta = \frac{2(1-\mu^2)w}{\pi E} \left(\frac{2}{3} + \log_e \frac{2D_1}{b} + \log_e \frac{2D_2}{b} \right)$$

if $E_1 = E_2 = E$ and $\mu_1 = \mu_2 = 0.3$, which is true for the given cylinders. Thus, in this case,

$$\delta = \frac{2(1-0.3^2)(30)}{\pi(30 \times 10^6)} \left(\frac{2}{3} + \log_e \frac{2(1)}{0.00125} + \log_e \frac{2(0.5)}{0.00125} \right) = 9.87 \times 10^{-6} \text{ in.}$$

From the third column of Table 11-1, the maximum compressive bearing stress between two parallel cylinders is

$$\text{Max } f_{brc} = 0.798 \sqrt{\frac{\dfrac{w(D_1 + D_2)}{D_1 D_2}}{\left[\dfrac{1-\mu_1^2}{E_1} + \dfrac{1-\mu_2^2}{E_2} \right]}}$$

In this case,

$$\text{Max } f_{brc} = 0.798 \sqrt{\frac{\dfrac{30(1+0.5)}{(1)(0.5)}}{\dfrac{1-0.3^2}{30 \times 10^6} + \dfrac{1-0.3^2}{30 \times 10^6}}} = 30,800 \text{ psi}$$

Thus, the cylinders will not yield and since Max $f_{brc} < F_{cy}$, the equations in Table 11-1 are valid.

TABLE 11-1

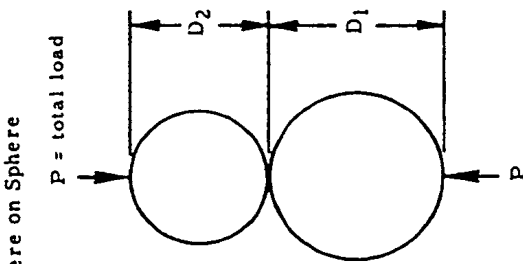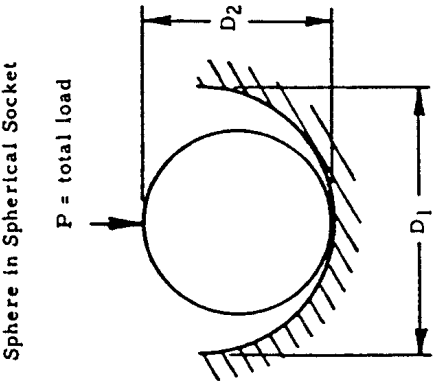## Formulas for Stress and Deformations Due to Pressure Between Elastic Bodies

Form of Contacting Bodies	Shape of Contact Surface and Combined Deformation	Maximum Bearing Stress
Sphere on Sphere P = total load 	$$r = 0.721 \sqrt[3]{P\left(\frac{D_1 D_2}{D_1 + D_2}\right)\left[\frac{1-\mu_1^2}{E_1} + \frac{1-\mu_2^2}{E_2}\right]}$$ $$\delta = 1.04 \sqrt[3]{\frac{P^2(D_1+D_2)}{D_1 D_2}\left(\frac{1-\mu_1^2}{E_1} + \frac{1-\mu_2^2}{E_2}\right)^2}$$	$$\text{Max } f_{brc} = 0.918 \sqrt[3]{\frac{P\left(\frac{D_1+D_2}{D_1 D_2}\right)^2}{\left[\frac{1-\mu_1^2}{E_1} + \frac{1-\mu_2^2}{E_2}\right]^2}}$$ If $E_1 = E_2 = E$ and $\mu_1 = \mu_2 = 0.3$, $$\text{Max } f_{brt} = 0.0820 \sqrt[3]{PE^2\left(\frac{D_1+D_2}{D_1 D_2}\right)^2}$$ and $$\text{Max } f_{brs} = 0.205 \sqrt[3]{PE^2\left(\frac{D_1+D_2}{D_1 D_2}\right)^2}$$
Sphere in Spherical Socket P = total load 	$$r = 0.721 \sqrt[3]{\frac{P D_1 D_2}{D_1 - D_2}\left[\frac{1-\mu_1^2}{E_1} , \frac{1-\mu_2^2}{E_2}\right]}$$ $$\delta = 1.04 \sqrt[3]{\frac{P^2(D_1-D_2)}{D_1 D_2}\left(\frac{1-\mu_1^2}{E_1} + \frac{1-\mu_2^2}{E_2}\right)^2}$$	$$\text{Max } f_{brc} = 0.918 \sqrt[3]{\frac{P\left(\frac{D_1 D_2}{D_1 D_2}\right)^2}{\left[\frac{1-\mu_1^2}{E_1} + \frac{1-\mu_2^2}{E_2}\right]^2}}$$ If $E_1 = E_2 = E$ and $\mu_1 = \mu_2 = 0.3$, $$\text{Max } f_{brt} = 0.0820 \sqrt[3]{PE^2\left(\frac{D_1 D_2}{D_1 D_2}\right)^2}$$ and $$\text{Max } f_{brs} = 0.205 \sqrt[3]{PE^2\left(\frac{D_1 D_2}{D_1 D_2}\right)^2}$$

TABLE 11-1

Formulas for Stress and Deformations Due to Pressure Between Elastic Bodies (Cont'd.)
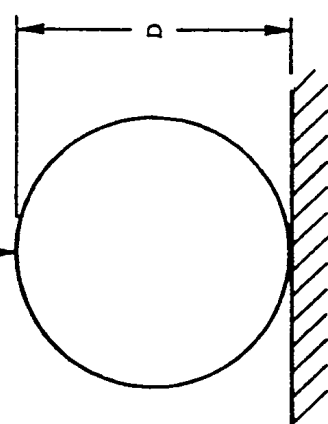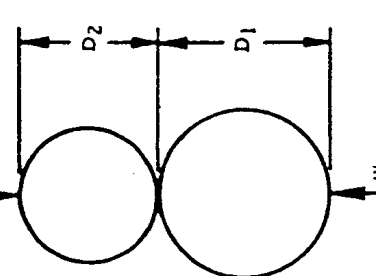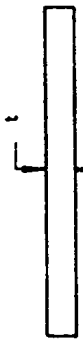
Form of Contacting Bodies	Shape of Contact Surface and Combined Deformation	Maximum Bearing Stress
Sphere on Flat Plate P = total load 	$$r = 0.721 \sqrt[3]{PD \left[\frac{1-\mu_1^2}{E_1} + \frac{1-\mu_2^2}{E_2}\right]}$$	$$\text{Max } f_{brc} = 0.918 \sqrt[3]{\dfrac{P}{D^2\left[\dfrac{1-\mu_1^2}{E_1} + \dfrac{1-\mu_2^2}{E_2}\right]^2}}$$ If $E_1 = E_2 = E$ and $\mu_1 = \mu_2 = 0.3$, $$\text{Max } f_{brt} = 0.0820 \sqrt[3]{\frac{PE^2}{D^2}}$$ and $$\text{Max } f_{brs} = 0.205 \sqrt[3]{\frac{PE^2}{D^2}}$$ at r/4 beneath the surface of the plate
Cylinder on Cylinder (Axes Parallel) w = load per linear inch 	$$t = 1.6 \sqrt{\frac{w D_1 D_2}{D_1 + D_2}\left[\frac{1-\mu_1^2}{E_1} + \frac{1-\mu_2^2}{E_2}\right]}$$ If $E_1 = E_2 = E$ and $\mu_1 = \mu_2 = 0.3$, $$\delta = \frac{2(1-\mu^2)w}{\pi E}\left(\frac{2}{3} + \log_e \frac{2D_1}{t} + \log_e \frac{2D_2}{t}\right)$$	$$\text{Max } f_{brc} = 0.798 \sqrt{\dfrac{\dfrac{w(D_1 + D_2)}{D_1 D_2}}{\dfrac{1-\mu_1^2}{E_1} + \dfrac{1-\mu_2^2}{E_2}}}$$

TABLE 11-1

Formulas for Stress and Deformations Due to Pressure Between Elastic Bodies (Cont'd.)
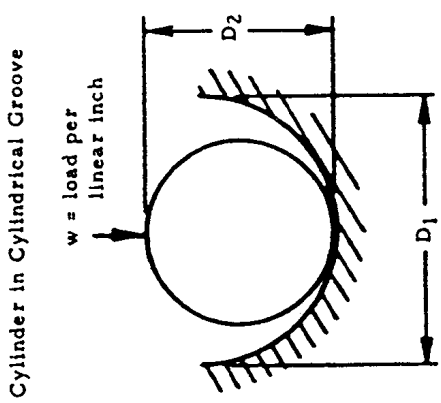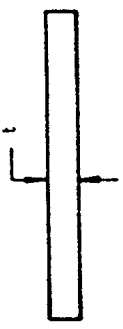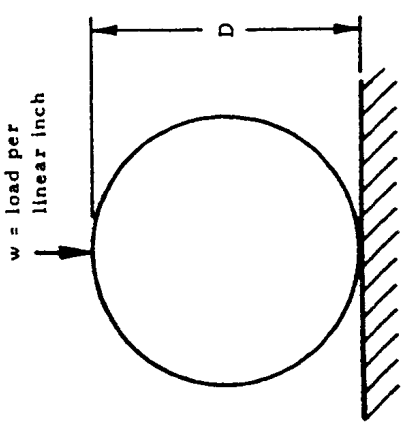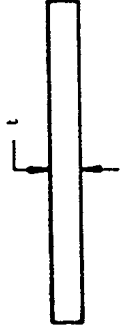
Form of Contacting Bodies	Shape of Contact Surface and Combined Deformation	Maximum Bearing Stress
Cylinder in Cylindrical Groove w = load per linear inch 	$$t = 1.6 \sqrt{\frac{w D_1 D_2}{D_1 - D_2}\left[\frac{1-\mu_1^2}{E_1} + \frac{1-\mu_2^2}{E_2}\right]}$$ If $E_1 = E_2 = E$ and $\mu_1 = \mu_2 = 0.3$, $$\delta = \frac{2(1-\mu^2)w}{E}\left(1 - 2\log_e \frac{b}{2}\right)$$	$$\text{Max } f_{brc} = 0.798 \sqrt{\frac{\dfrac{w(D_1 - D_2)}{D_1 D_2}}{\dfrac{1-\mu_1^2}{E_1} + \dfrac{1-\mu_2^2}{E_2}}}$$
Cylinder on Flat Plate w = load per linear inch 	$$t = 1.6 \sqrt{w D \left[\frac{1-\mu_1^2}{E_1} + \frac{1-\mu_2^2}{E_2}\right]}$$ If $E_1 = E_2 = E$ and $\mu_1 = \mu_2 = \mu$, the total compression of the cylinder between two plates is $$\Delta D = 4w\left(\frac{1-\mu^2}{\pi E}\right)\left(\frac{1}{3} + \log_e \frac{2D}{t}\right)$$	$$\text{Max } f_{brc} = 0.798 \sqrt{\frac{w}{D\left[\dfrac{1-\mu_1^2}{E_1} + \dfrac{1-\mu_2^2}{E_2}\right]}}$$ If $E_1 = E_2 = 30 \times 10^6$ psi and $\mu_1 = \mu_2 = 0.25$, $$f_{brs} = 958 \sqrt{\frac{w}{D}}$$ at a depth of 0.393t below the surface of the plate.

TABLE 11-1

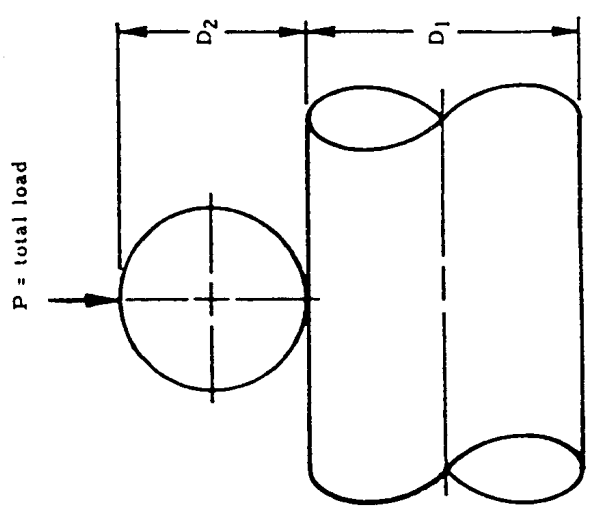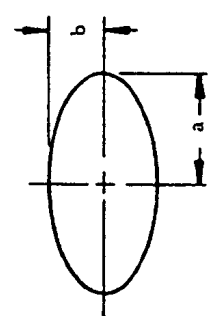### Formulas for Stress and Deformations Due to Pressure Between Elastic Bodies (Cont'd.)

Form of Contacting Bodies	Shape of Contact Surface and Combined Deformation	Maximum Bearing Stress
Cylinder on Cylinder (Axes at Right Angles) P = total load 	ellipse $a = K_1 \sqrt[3]{\dfrac{P D_1 D_2}{D_1 + D_2} \left[\dfrac{1-\mu_1^2}{E_1} + \dfrac{1-\mu_2^2}{E_2} \right]}$ $b = K_2 c$ $\delta = K_3 \sqrt[3]{P^2 \dfrac{\left(\dfrac{E_1}{1-\mu_1^2} + \dfrac{E_2}{1-\mu_2^2} \right)^2 \dfrac{(D_1+D_2)}{D_1 D_2}}{\ }}$ where K_1, K_2, and K_3 have values as follows:	Max $f_{brc} = \dfrac{1.5 \, P}{\pi a b}$ If $E_1 = E_2 = 30 \times 10^6$ psi , $\mu_1 = \mu_2 = 0.25$, and $1 < \dfrac{D_1}{D_2} < 8$, Max $f_{brs} = \dfrac{1175 \, O}{\left(\dfrac{D_1}{D_2} \right)^{0.271}} \sqrt[3]{\dfrac{4P}{D_2^2}}$

$\dfrac{D_1}{D_2}$	1	1-1/2	2	3
K_1	0.908	1.045	1.158	1.350
K_2	1	0.765	0.632	0.482
K_3	2.089	2.060	2.025	1.950

$\dfrac{D_1}{D_2}$	4	6	10
K_1	1.505	1.767	2.175
K_2	0.400	0.308	0.221
K_3	1.875	1.770	1.613

TABLE 11-1

Formulas for Stress and Deformations Due to Pressure Between Elastic Bodies (Cont'd.)

Form of Contacting Bodies	Shape of Contact Surface and Combined Deformation	Maximum Bearing Stress

Maximum Bearing Stress

$$\text{Max } f_{brc} = \frac{1.5\,P}{\pi ab}$$

where

$$a = K_1 \sqrt[3]{\frac{P\gamma}{K}}$$

and

$$b = K_2 \sqrt[3]{\frac{P\gamma}{K}}$$

Shape of Contact Surface and Combined Deformation

$$\delta = K_3 \sqrt[3]{\frac{P^2}{K^2\gamma}}$$

K_1, K_2, and K_3 are given in the following table, where

$$\theta = \arccos \frac{1}{4}\gamma \left[\left(\frac{1}{R_1} - \frac{1}{R'_1}\right)^2 + \left(\frac{1}{R_2} - \frac{1}{R'_2}\right)^2 + 2\left(\frac{1}{R_1} - \frac{1}{R'_1}\right)\left(\frac{1}{R_2} - \frac{1}{R'_2}\right)\cos 2\phi \right]^{1/2}$$

θ	0°	10°	20°	30°	35°	40°	45°	50°
K_1	∞	6.612	3.778	2.731	2.397	2.136	1.926	1.754
K_2	0	0.319	0.408	0.493	0.530	0.567	0.604	0.641
K_3	--	0.851	1.220	1.453	1.550	1.637	1.709	1.772

θ	55°	60°	65°	70°	75°	80°	85°	90°
K_1	1.611	1.486	1.378	1.284	1.202	1.128	1.061	1.00
K_2	0.678	0.717	0.759	0.802	0.846	0.893	0.944	1.00
K_3	1.828	1.875	1.912	1.944	1.967	1.985	1.996	2.00

Form of Contacting Bodies

General Case of Two Bodies in Contact (P = Total Load)

At point of contact, minimum and maximum radii of curvature are R_1 and R'_1 for Body 1 and R_2 and R'_2 for Body 2.

$$\gamma = \frac{4}{\dfrac{1}{R_1} + \dfrac{1}{R_2} + \dfrac{1}{R'_1} + \dfrac{1}{R'_2}}$$

$$K = \frac{8}{3}\,\frac{E_1 E_2}{E_2(1-\mu_1^2) + E_1(1-\mu_2^2)}$$

TABLE 11-1

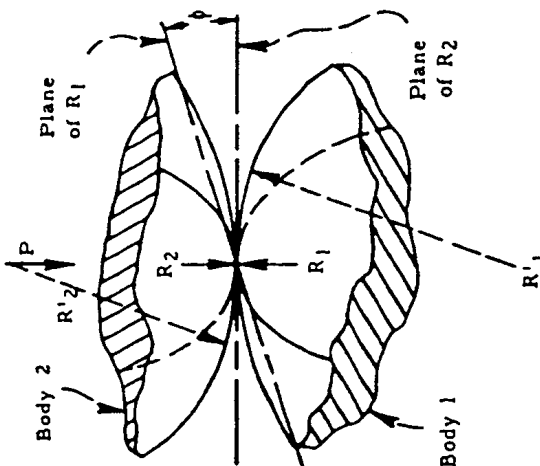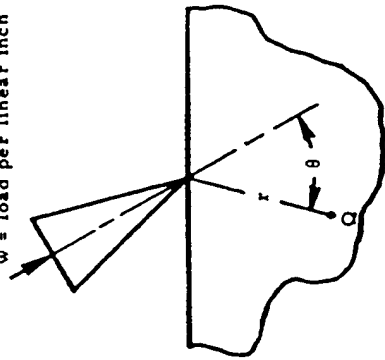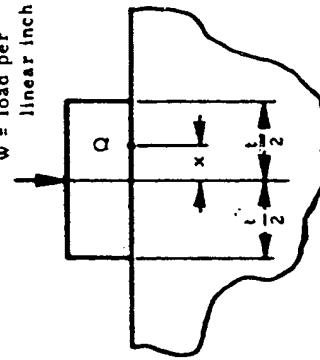Formulas for Stress and Deformations Due to Pressure Between Elastic Bodies (Cont'd.)
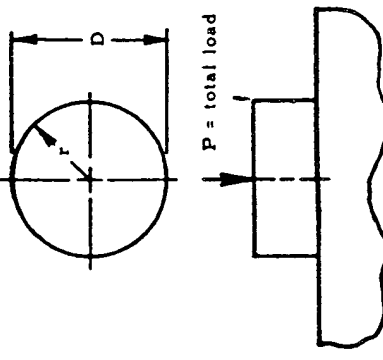
Form of Contacting Bodies	Shape of Contact Surface and Combined Deformation	Maximum Bearing Stress
Rigid Knife Edge on Plate w = load per linear inch		At any point Q, $$f_{brc} = \frac{2 w \cos \theta}{\pi r}$$
Rigid Block on Plate w = load per linear inch		At any point Q on surface of contact $$f_{brc} = \frac{w}{\pi \sqrt{\frac{t^2}{4} - x^2}}$$
Rigid Cylindrical Die on Plate P = total load	$$\delta = \frac{P(1-\mu^2)}{DE}$$	At any point on surface of contact $$f_{brc} = \frac{P}{\pi D \sqrt{\frac{D^2}{4} - r^2}}$$ Max $f_{brc} = \infty$ at edge

11.7 Empirical Treatment of Allowable Bearing Loads

Many tests have been made to determine the bearing strength of spheres and cylinders. However, it is difficult to interpret the results due to the lack of any satisfactory criterion for failure. Some permanent deformation is shown to be produced even for very small loads. This deformation increases progressively with increasing load, but there is no sharp break in the load-set curve. Thus, it is necessary to select some arbitrary criterion for the amount of plastic yielding that may be considered to represent failure. The circumstances of use determine the degree of permanent deflection necessary to make a part unfit for service.

The following sections present empirical formulas for the maximum allowable bearing loads for various shapes in contact.

11.7.1 Empirical Formulas for Allowable Bearing Loads of a Cylinder on a Flat Plate

Figure 11-4 shows a cylinder on a flat plate under a loading of w lb. per linear inch.
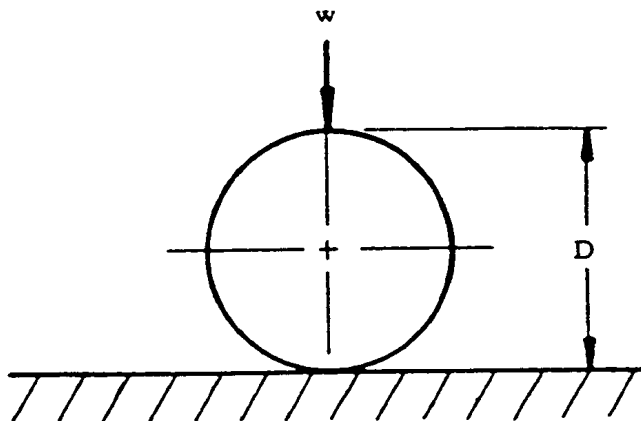

Figure 11-4. Cylinder on Flat Plate

Table 11-2 gives empirical formulas for the allowable load (w_a) for various diameters of steel cylinders on flat steel plates. It should be noted that there is little difference between failure under static conditions and that under slow rolling conditions if slipping does not occur. If slipping occurs, tests are necessary to obtain reliable information.

Although the allowable load (w_a) is dependent upon length for short cylinders, it is independent of length if the cylinders are longer than 6 inches. The last equation in Table 11-2 is based upon an elongation of 0.001 in./in. in the bearing plate.

TABLE 11-2

**Empirical Formulas for a Steel Cylinder
on a Flat Steel Plate**

Diameter	Loading Condition	Allowable Load (lb/in)
D < 25 in.	static	$w_a = \left(\dfrac{F_{cy} - 13000}{20000} \right) 600 \, D$
25 < D < 125 in.	static	$w_a = \left(\dfrac{F_{cy} - 13000)}{20000} \right) 3000 \sqrt{D}$
116 < D < 476 in.	slow rolling	$w_a = (18000 + 120 \, D) \left(\dfrac{F_{cy} - 13000}{23000} \right)$

11.7.2   **Empirical Formula for Allowable Bearing Load of Steel Spheres
in Contact**

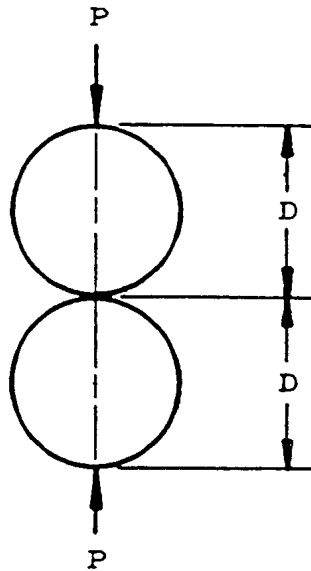Figure 11-5 shows two similar spheres in contact.

Figure 11-5.   Similar Spheres in Contact

The crushing load P is given by

$$P = 1960 \, (8D)^{1.75}$$

The test sphere used to derive this formula was steel of hardness 64 to 66
Rockwell C.

11 - 13